PROGRESS IN PATHOGEN IDENTIFICATION BASED ON MASS SPECTROMETRY

EDITED BY: Junping Peng, Yi-Wei Tang and Di Xiao
PUBLISHED IN: Frontiers in Cellular and Infection Microbiology

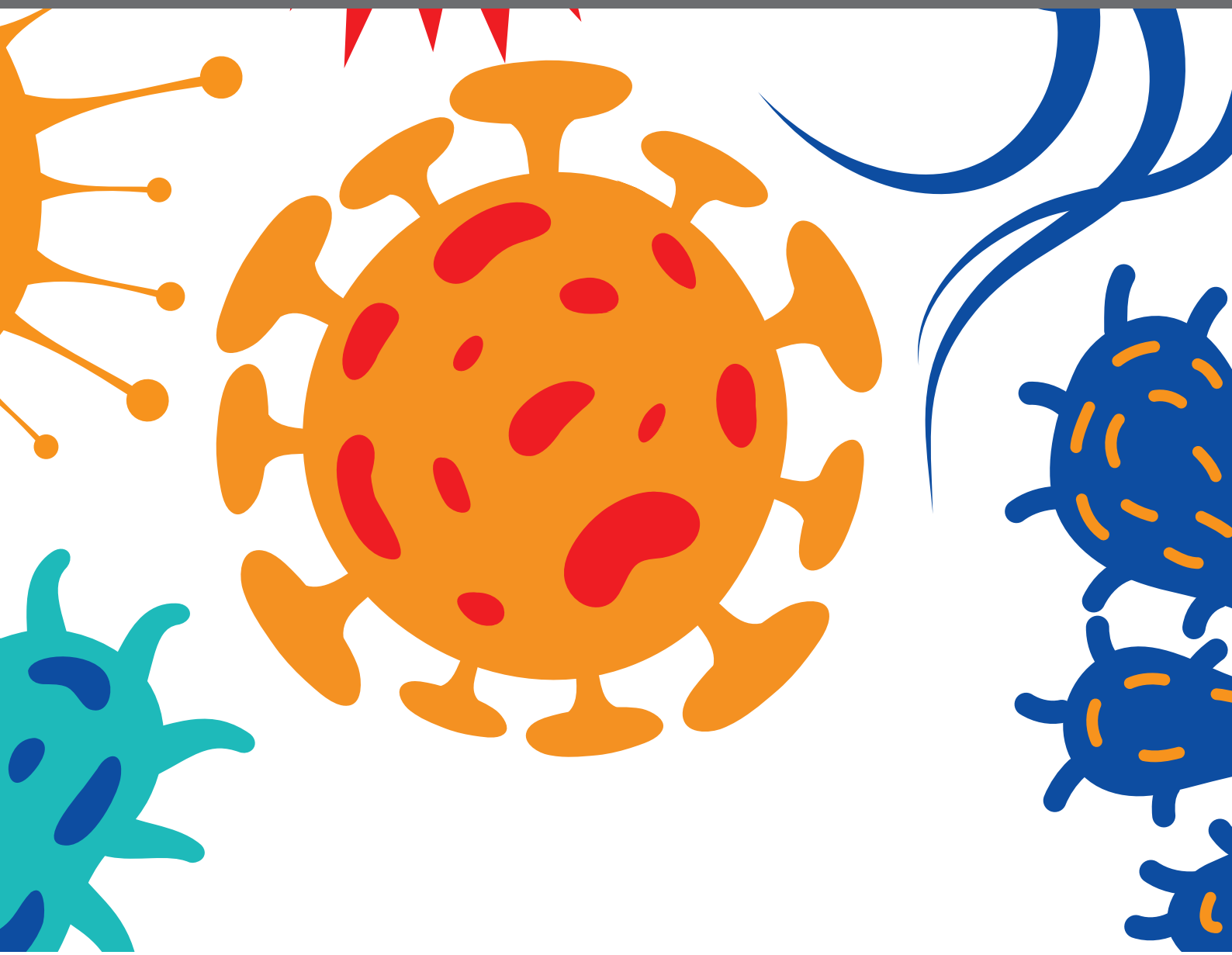

frontiers Research Topics

ISSN 1664-8714
ISBN 978-2-88974-454-1
DOI 10.3389/978-2-88974-454-1

About Frontiers

Frontiers is more than just an open-access publisher of scholarly articles: it is a pioneering approach to the world of academia, radically improving the way scholarly research is managed. The grand vision of Frontiers is a world where all people have an equal opportunity to seek, share and generate knowledge. Frontiers provides immediate and permanent online open access to all its publications, but this alone is not enough to realize our grand goals.

Frontiers Journal Series

The Frontiers Journal Series is a multi-tier and interdisciplinary set of open-access, online journals, promising a paradigm shift from the current review, selection and dissemination processes in academic publishing. All Frontiers journals are driven by researchers for researchers; therefore, they constitute a service to the scholarly community. At the same time, the Frontiers Journal Series operates on a revolutionary invention, the tiered publishing system, initially addressing specific communities of scholars, and gradually climbing up to broader public understanding, thus serving the interests of the lay society, too.

Dedication to Quality

Each Frontiers article is a landmark of the highest quality, thanks to genuinely collaborative interactions between authors and review editors, who include some of the world's best academicians. Research must be certified by peers before entering a stream of knowledge that may eventually reach the public - and shape society; therefore, Frontiers only applies the most rigorous and unbiased reviews.
Frontiers revolutionizes research publishing by freely delivering the most outstanding research, evaluated with no bias from both the academic and social point of view. By applying the most advanced information technologies, Frontiers is catapulting scholarly publishing into a new generation.

What are Frontiers Research Topics?

Frontiers Research Topics are very popular trademarks of the Frontiers Journals Series: they are collections of at least ten articles, all centered on a particular subject. With their unique mix of varied contributions from Original Research to Review Articles, Frontiers Research Topics unify the most influential researchers, the latest key findings and historical advances in a hot research area! Find out more on how to host your own Frontiers Research Topic or contribute to one as an author by contacting the Frontiers Editorial Office: frontiersin.org/about/contact

PROGRESS IN PATHOGEN IDENTIFICATION BASED ON MASS SPECTROMETRY

Topic Editors:
Junping Peng, Institute of Pathogen Biology (CAMS), China
Yi-Wei Tang, Cepheid (United States), United States
Di Xiao, National Institute for Communicable Disease Control and Prevention (China CDC), China

Citation: Peng, J., Tang, Y.-W., Xiao, D., eds. (2022). Progress in Pathogen Identification Based on Mass Spectrometry. Lausanne: Frontiers Media SA. doi: 10.3389/978-2-88974-454-1

Table of Contents

frontiers in Cellular and Infection Microbiology

EDITORIAL
published: 14 January 2022
doi: 10.3389/fcimb.2021.813133

Editorial: Progress in Pathogen Identification Based on Mass Spectrometry

Junping Peng[1,2]*, *Yi-Wei Tang*[3] and *Di Xiao*[4]

[1] National Health Commission (NHC) Key Laboratory of Systems Biology of Pathogens, Institute of Pathogen Biology, Chinese Academy of Medical Sciences & Peking Union Medical College, Beijing, China, [2] Key Laboratory of Respiratory Disease Pathogenomics, Chinese Academy of Medical Sciences and Peking Union Medical College, Beijing, China, [3] Department of Medical Affairs, Danaher Diagnostic Platform/Cepheid (China), New York, NY, United States, [4] State Key Laboratory of Infectious Disease Prevention and Control, Collaborative Innovation Center for Diagnosis and Treatment of Infectious Diseases, National Institute for Communicable Disease Control and Prevention, Chinese Center for Disease Control and Prevention, Beijing, China

Keywords: mass spectrometry, microbial identification, antimicrobial susceptibility testing, species differentiation, database

Editorial on the Research Topic

Progress in Pathogen Identification Based on Mass Spectrometry

OPEN ACCESS

Edited and reviewed by:
Nahed Ismail,
University of Illinois at Chicago, United States

***Correspondence:**
Junping Peng
pengjp@hotmail.com

Specialty section:
This article was submitted to Clinical Microbiology, a section of the journal Frontiers in Cellular and Infection Microbiology

Received: *11 November 2021*
Accepted: *27 December 2021*
Published: *14 January 2022*

Citation:
Peng J, Tang Y-W and Xiao D (2022) Editorial: Progress in Pathogen Identification Based on Mass Spectrometry. Front. Cell. Infect. Microbiol. 11:813133. doi: 10.3389/fcimb.2021.813133

The rapid identification of microbial pathogens is essential for the diagnosis and treatment of infectious diseases and the development of targeted prevention and treatment measures. The ubiquitous spread of novel infectious agents and multi-drug-resistant bacteria has generated a pressing need to develop rapid and reliable methods for microbial identification and antimicrobial susceptibility testing, which have previously relied on traditional culture-based methods that are time-consuming and labor-intensive. The potential utility of mass spectrometry (MS)-based techniques, including matrix-assisted laser desorption/ionization time-of-flight (MALDI-TOF) MS and liquid chromatography-tandem MS (LC-MS/MS), has been widely explored (Patel, 2015; Tran et al., 2015; Sandalakis et al., 2017; Oviano et al., 2018; Li et al., 2020). In the Research Topic of "Progress in Pathogen Identification Based on Mass Spectrometry", we covered the latest progresses of MS technologies in the field of pathogen biology. The Research Topic contains sixteen articles: thirteen reports of original research, two reviews, and one brief research report, covering various research directions from pathogen identification and procedure optimization, the analysis of antimicrobial resistance, to database extension.

Ten articles address the Research Topic of targeting proteins, lipids, or nucleic acids with MS-based methods to obtain stable, high abundance expression profiles. The profiles of the targeted bacteria or fungi are then compared with existing profiles in a database to identify strains at the genus or species level. Proper specimen preprocessing is the first key step in this procedure. Cuénod et al. optimized the factors associated with the spectral quality of MALDI-TOF MS in species identification, comparing the significant differences obtained by varying the sample preparation protocol, bacterial culture time, and the interval from calibration to detection. More specifically, to reduce the problems caused by the insufficient coverage of commercial databases and the deficiencies in the multi-step protein extraction procedure used in the routine identification of clinical filamentous fungi, Ning et al. developed two rapid protein extraction methods using focused

ultrasonication and zirconia-silica beads and built an in-house spectral library for the identification of filamentous fungi. That study reported the first use of zirconia-silica beads as a sample-processing method for building an in-house library of MALDI-TOF MS data. Another optimized protein extraction method was evaluated by Dai et al. These researchers combined density centrifugation and extra chemical lysis extraction to develop a rapid and simplified protocol for the direct identification of microorganisms in positive blood cultures. Like bacterial infections, fungal infections pose a major health burden, inducing superficial mycosis or organ disease, according to the invasion site. Baumbach et al. evaluated the reliability of MALDI-TOF MS for the identification of closely related zoophilic dermatophytes, and generated a score-oriented distance dendrogram. They compared the spectra obtained under two different growth conditions, i.e., liquid broth vs solid agar medium, which indicated that the use of liquid media for species identification or master spectra generation was not superior to the use of solid medium covered with filter paper. To establish an accurate and rapid identification method for *Candida auris* infection at the species level, De Carolis et al. developed a fast and reproducible MALDI-TOF MS assay and used the Bruker Daltonics Biotyper® database with *C. auris* spectrum profiles to generate a score-oriented dendrogram with a hierarchical cluster analysis. This allowed the classification of *Candida* isolates and non-*Candida* isolates according to species. In parallel research, they investigated the capacity of MS antifungal susceptibility testing (MS-AFST) to detect the susceptibility or resistance phenotypes of *C. auris* isolates, which is described in the next section. Some comparative studies have been based on different MALDI-TOF MS platforms or other proteomic analyses. Yi et al. evaluated the performance of Autof MS 1000 and Vitek MS in identifying closely related yeasts, including fourteen different species in five species complexes. The two commercial MALDI-TOF MS platforms differed in their identification capability: Autof MS 1000 showed a greater capacity for yeast identification, whereas Vitek MS was less accurate, mainly because the reference database of phylogenetically closely related yeast species was poor. In another comparative study, Kondori et al. used bottom-up proteomic approaches, LC-MS/MS, and species-specific peptide identification (shotgun proteotyping) to identify bacteria and fungi directly in a model system. The sensitivity and accuracy of the system in analyzing spiked negative blood samples and positive blood samples without further culture were compared with those of MALDI-TOF MS. This comparative study demonstrated that proteotyping-based methods, such as LC-MS, provided promising ways to detect infectious pathogens. This was confirmed in parallel by Bajaj et al. The structural diversity and species specificity of lipids and nucleic acids offer information that complements conventional protein-based MS approaches. Solntceva et al. reviewed the recent applications of MS-based lipidomics to the identification of microorganisms and the detection of antibiotic resistance. The latter is described below in detail. This review examines the future directions of MS in microbial lipidomics. Sun et al. combined MALDI-TOF MS with quantitative real-time PCR to determine the etiology of community-acquired pneumonia in the enrolled children and to identify the appropriate antibiotic therapy. That research is valuable for its provision of a comprehensive database of pathogens, including interrelated bacteria and viruses, and is extremely important in guiding antibiotic therapies based on etiology.

Antimicrobial resistance has evolved into a serious problem for public health, and rapid and accurate pathogen detection is essential for formulating effective programs of antibiotic treatment. MS-based techniques have opened another door in the field. Five articles are related in this Research Topic. Florio et al. provided a updated overview of the various methods based on MALDI-TOF MS that have been proposed, and provided well-referenced information on the antimicrobial resistance of clinically relevant bacteria. This included a method to assess β-lactamase activity by visualizing the hydrolysis of the β-lactam ring or the detection of biomarkers that correlate with drug-resistance. Wang et al. described proteins that were differentially expressed in drug-resistant and drug-susceptible *Acinetobacter baumannii* isolates, using label-free tandem mass tag labeling and a glycoproteomic analysis, to fully clarify the mechanism of antibiotic resistance. Similarly, Lu et al. investigated the failure of polymyxin B to affect *A. baumannii* by analyzing the whole membrane proteome of polymyxin-B-induced *A. baumannii* (ATCC 19606) with high resolution MS, using label-free quantitative and targeted proteome analyses to identify differentially expressed membrane proteins with nano-LC-MS/MS. In so doing, they developed a relatively rapid membrane protein extraction and preparation method. As mentioned above, Carolis et al. used a composite correlation index (CCI)-based proteomic approach to detect antifungal resistance in *Candida* species, developing a cost-effective and time-efficient method superior to conventional growth-based antifungal susceptibility testing. Similarly, Solntceva et al. confirmed the correlations between drug resistance and changes in membrane composition or the relative abundances of lipids. These studies demonstrated that several MS approaches, especially MALDI-TOF MS, provided auxiliary tools with excellent timelines and accuracy, which should allow clinicians to promptly select effective antimicrobial therapies for pathogen-based diseases.

Other researches based on the MS technology, such as database expansion and mechanism analyses, are also included. Bernhard et al. optimized sample pre-processing procedures, on the basis of which they created a set of publicly available references for the *Cryptococcus neoformans/gattii* species complexes for use with the MALDI Biotyper system. To examine the influence of growth media on toxin production or activity, Hille et al. used MALDI-TOF MS-based biomarker detection models to distinguish the presence or absence of secreted exotoxins in *Moraxella bovoculi* during incubation on different growth media, with or without calcium ions. Other mechanism-directed research conducted by Thorsing et al. investigated the development of effective vaccines against enterotoxigenic *Escherichia coli* (ETEC). The researchers used the MS-based method BEMAP (β-elimination of O-linked

carbohydrate modifications followed by the Michael addition of 2-aminoethyl phosphonic acid) and observed an important correlation between O-linked glycosylation and the relative immunogenicity of bacterial proteins. This finding constituted a proof of concept in considering ETEC proteins for inclusion in future broad-coverage subunit vaccine candidates.

In summary, these studies included in the Research Topic quantified the advantages and potential utility of MS in bacterial identification, the analysis of antimicrobial resistance, and database expansion, and provided a scientific basis for the timely formulation of therapy options and the further improvement of patient prognoses. Because MS is a continuously developing platform, attention should be paid to strengthen the comparative analysis of different systems, with multicenter verification, to expand and refine the clinical applications of MS-based methods in diagnostic microbiology.

AUTHOR CONTRIBUTIONS

JP was a guest associate editor of the Research Topic and wrote the paper text. Y-WT and DX were guest associate editors of the Research Topic and edited the text, respectively. All authors contributed to the article and approved the submitted version.

FUNDING

This research project is funded by the grants from the CAMS Innovation Fund for Medical Science (CIFMS, 2021-I2M-1-038).

ACKNOWLEDGMENTS

We thank the authors and reviewers for their outstanding contributions.

REFERENCES

Li, Y., Xiu, L., Liu, J., Zhang, C., Wang, F., Yin, Y., et al. (2020). A Multiplex Assay for Characterization of Antimicrobial Resistance in Neisseria Gonorrhoeae Using Multi-PCR Coupled With Mass Spectrometry. *J. Antimicrob. Chemother.* 75, 2817–2825. doi: 10.1093/jac/dkaa269

Oviano, M., Rodriguez-Sanchez, B., Gomara, M., Alcala, L., Zvezdanova, E., Ruiz, A., et al. (2018). Direct Identification of Clinical Pathogens From Liquid Culture Media by MALDI-TOF MS Analysis. *Clin. Microbiol. Infect.* 24, 624–629. doi: 10.1016/j.cmi.2017.09.010

Patel, R. (2015). MALDI-TOF MS for the Diagnosis of Infectious Diseases. *Clin. Chem.* 61, 100–111. doi: 10.1373/clinchem.2014.221770

Sandalakis, V., Goniotakis, I., Vranakis, I., Chochlakis, D., and Psaroulaki, A. (2017). Use of MALDI-TOF Mass Spectrometry in the Battle Against Bacterial Infectious Diseases: Recent Achievements and Future Perspectives. *Expert Rev. Proteomics* 14, 253–267. doi: 10.1080/14789450.2017.1282825

Tran, A., Alby, K., Kerr, A., Jones, M., and Gilligan, P. H. (2015). Cost Savings Realized by Implementation of Routine Microbiological Identification by Matrix-Assisted Laser Desorption Ionization-Time of Flight Mass Spectrometry. *J. Clin. Microbiol.* 53, 2473–2479. doi: 10.1128/JCM.00833-15

Conflict of Interest: The authors declare that the research was conducted in the absence of any commercial or financial relationships that could be construed as a potential conflict of interest.

Publisher's Note: All claims expressed in this article are solely those of the authors and do not necessarily represent those of their affiliated organizations, or those of the publisher, the editors and the reviewers. Any product that may be evaluated in this article, or claim that may be made by its manufacturer, is not guaranteed or endorsed by the publisher.

frontiers in Cellular and Infection Microbiology

MINI REVIEW
published: 11 November 2020
doi: 10.3389/fcimb.2020.572909

Detection of Antibiotic-Resistance by MALDI-TOF Mass Spectrometry: An Expanding Area

Walter Florio[1], *Lelio Baldeschi*[2], *Cosmeri Rizzato*[1], *Arianna Tavanti*[3], *Emilia Ghelardi*[1] *and Antonella Lupetti*[1]*

[1] *Dipartimento di Ricerca Traslazionale e delle Nuove Tecnologie in Medicina e Chirurgia, Università di Pisa, Pisa, Italy,*
[2] *Department of Ophthalmology, Université Catholique de Louvain, Cliniques Universitaires Saint-Luc, Brussels, Belgium,*
[3] *Dipartimento di Biologia, Università di Pisa, Pisa, Italy*

Several MALDI-TOF MS-based methods have been proposed for rapid detection of antimicrobial resistance. The most widely studied methods include assessment of β-lactamase activity by visualizing the hydrolysis of the β-lactam ring, detection of biomarkers responsible for or correlated with drug-resistance/non-susceptibility, and the comparison of proteomic profiles of bacteria incubated with or without antimicrobial drugs. Antimicrobial-resistance to a number of antibiotics belonging to different classes has been successfully tested by MALDI-TOF MS in a variety of clinically relevant bacterial species including members of *Enterobacteriaceae* family, non-fermenting Gram-negative bacteria, Gram-positive cocci, anaerobic bacteria and mycobacteria, opening this field to further clinically important developments. Early detection of drug-resistance by MALDI-TOF MS can be particularly helpful for clinicians to streamline the antibiotic therapy for a better outcome of patients with systemic infection, in all cases where a prompt and effective antibiotic treatment is essential to preserve organ function and/or patient survival.

Keywords: antimicrobial susceptibility testing, blood culture, rapid AST, microdroplet growth assay, MBT-ASTRA, MALDI-TOF, antimicrobial resistance

OPEN ACCESS

Edited by:
Yi-Wei Tang,
Cepheid, United States

Reviewed by:
Dalia Denapaite,
University of Trento, Italy
Shangshang Qin,
Zhengzhou University, China

***Correspondence:**
Antonella Lupetti
antonella.lupetti@med.unipi.it

Specialty section:
This article was submitted to Clinical Microbiology, a section of the journal Frontiers in Cellular and Infection Microbiology

Received: *15 June 2020*
Accepted: *22 September 2020*
Published: *11 November 2020*

Citation:
Florio W, Baldeschi L, Rizzato C, Tavanti A, Ghelardi E and Lupetti A (2020) Detection of Antibiotic-Resistance by MALDI-TOF Mass Spectrometry: An Expanding Area. Front. Cell. Infect. Microbiol. 10:572909. doi: 10.3389/fcimb.2020.572909

INTRODUCTION

The application of MALDI-TOF MS technology to clinical diagnostic microbiology has provided a new, accurate and robust tool allowing rapid and reliable microbial identification (Ferreira et al., 2011; Barnini et al., 2015; Tanaka et al., 2017; Florio et al., 2018a).

The widespread of multi-drug-resistant bacterial strains, especially in hospital settings, have generated a pressing need for the development of rapid and reliable methods for antimicrobial susceptibility testing (AST), and the potentials of MALDI-TOF MS to achieve this goal have been explored.

Multi-drug-resistance is a particularly dramatic problem in systemic infections (Palacios-Baena et al., 2017), and infections involving critical districts [e.g., eye and orbit, where timely administration of an effective therapy is fundamental for sparing organ specific functions or patient survival (Tsirouki et al., 2018; Choi et al., 2019)].

Therefore, a number of studies investigated the possibility to apply MALDI-TOF MS technology to rapid detection of antibiotic-resistance in bacterial pathogens isolated from bloodstream infections as well as to the detection of antimicrobial-resistance in pathogenic fungi (Florio et al., 2018b).

The present review provides (i) a synthetic, updated overview of the different proposed methods based on MALDI-TOF MS, mainly focusing on its most promising applications and (ii) rapid and accurate information regarding antimicrobial-resistance of clinically relevant bacteria.

ASSESSMENT OF β-LACTAMASE ACTIVITY BY MALDI-TOF MS

One of the first successful applications of MALDI-TOF MS to the detection of antibiotic-resistance (**Figure 1**) resulted from the observation that the hydrolysis of the β-lactam ring after exposure of β-lactam antibiotics to β-lactamase producing (aerobic and anaerobic) bacteria could be revealed in mass spectra by a decrease of the peak corresponding to the antibiotic and appearance of peaks representing its hydrolysis products (Burckhardt and Zimmermann, 2011; Hrabak et al., 2011; Johansson et al., 2014a,b; Jung et al., 2014b).

A protocol for detection of carbapenemase production by MALDI-TOF MS was developed in *Bacteroides fragilis* strains harboring the *cfiA* gene encoding for the carbapenemase (Johansson et al., 2014b). Hydrolysis of ertapenem was detected within 2.5 h only in *cfiA*-positive strains. The method was successfully applied to screen for carbapenemase activity directly from blood culture bottles inoculated with human blood and spiked with *B. fragilis* strains showing various ertapenem MICs (Johansson et al., 2014a), yielding the results in 3 h. Of interest, the logRQ values of spectra calculated by the software correlated with the MICs for positive strains.

To reduce time for detection of carbapenem-resistance in Gram-negative bacteria causing bloodstream infections, a MALDI-TOF MS-based assay was established by measuring the hydrolysis of imipenem in blood cultures (BCs) spiked with *Pseudomonas aeruginosa*, *Acinetobacter baumannii,* or *Enterobacteriaceae* producing different carbapenemases (Oviano et al., 2016). The analysis was performed using an MBT Compass STAR-BL module software (Bruker Daltonics), automatically providing a result (sensitivity or resistance) based on the degree of hydrolysis of the antibiotic. This assay, requiring a 30 min-incubation of bacteria with the antibiotic, showed 98% sensitivity and 100% specificity, both reaching 100% with a 60 min-incubation. These results have been confirmed in two large bacterial isolates collections in which the presence of carbapanemase genes was performed in accordance to CLSI method and by PCR (Akyar et al., 2019; Oviano et al., 2020). However, β-lactam resistance is detected only when it is mediated by β-lactamases, whereas the other mechanisms of resistance are not revealed, thus negative results should be confirmed by other assays.

IDENTIFICATION OF BIOMARKERS ASSOCIATED WITH DRUG-RESISTANCE

One of the proposed MALDI-TOF MS-based approaches to detect bacterial resistance to carbapenems relies on the identification of plasmids bearing bla_{KPC} carbapenemase genes (Lau et al., 2014). An extended-spectrum class C beta-lactamase from *A. baumannii*, belonging to the *Acinetobacter*-derived cephalosporinases (ADC) family, has been recently identified (m/z∼40,279) and evaluated as a possible biomarker for carbapenem-resistance. Among 51 carbapenem-resistant *A. baumannii* strains, 49 showed a signal at 40,279 ± 87 m/z, whereas four out of 15 carbapenem-susceptible strains showed a signal at the same m/z. The sensitivity and specificity were 96 and 73% in comparison to the microdilution imipenem susceptibility testing, which provides MIC determination (Chang et al., 2018).

Using the ClinProtTools analysis software (v3.0; Bruker Daltonics) to investigate possible differences between the protein patterns of KPC-producing and non-KPC-producing *K. pneumoniae* strains, an 11,109-Da peak was detected in the spectra of 30 out of 34 KPC producers, and it was absent in all non-KPC-producing isolates (Gaibani et al., 2016). Previous findings showed that the 11,109-Da peak is a cleavage product of a hypothetical protein named p019 (Lau et al., 2014). However, as p019 polypeptide was absent in a subset of *bla*KPC-harboring plasmids, negative results should be complemented by confirmatory tests.

The heterogeneous nature of methicillin-resistance in *Staphylococcus aureus* has hindered the possibility to classify methicillin-resistant *S. aureus* (MRSA) and methicillin-sensitive *S. aureus* (MSSA) into two clearly distinguishable groups based on clustering analysis of the spectral profiles of individual isolates (Wang et al., 2013). A partial success was achieved by establishing a method, which relies on the production of a phenol-soluble protein toxin (PSM-mec) by a subset of MRSA strains (Chatterjee et al., 2011), which is detectable by MALDI-TOF MS as a 2415 ± 2.00 m/z peak and may be present in up to half of MRSA isolates (Rhoads et al., 2016; Schuster et al., 2018). The PSM-mec peptide does not cause methicillin-resistance and its biological function is unknown, but its expression is associated with methicillin-resistance. The presence of the 2415 ± 2.00 m/z peak has been shown to predict *mecA* carriage in *S. aureus* with a specificity close to 100%. The software "MBT subtyping module" (Bruker Daltonics), has been developed to detect PSM-mec in the mass spectrum of *S. aureus* isolates, providing an indirect evidence of methicillin-resistance (**Figure 2**). Although the presence of PSM-mec is associated with methicillin-resistance also in coagulase-negative staphylococci (CoNS), the majority of those does not produce it (Schuster et al., 2018), thus being of limited usefulness to detect methicillin-resistant CoNS.

Identification of possible markers associated with drug-resistance by MALDI-TOF MS has been investigated also in anaerobes (Nagy et al., 2011) [e.g., *cfiA*-positive *B. fragilis* can be distinguished from *cfiA*-negative strains by a set of peak shifts in the interval 4,000–5,500 Da, using the MALDI Biotyper software (Bruker Daltonics)]. Two reference spectra were created, one specific for *cfiA*-negative and one for *cfiA*-positive strains. Subsequently, the possibility to screen for carbapenem-resistant *B. fragilis* strains directly from positive BCs was demonstrated by comparing ID-spectra of bacilli recovered from spiked BCs with *cfiA*-positive and *cfiA*-negative main spectra (Johansson et al., 2014a).

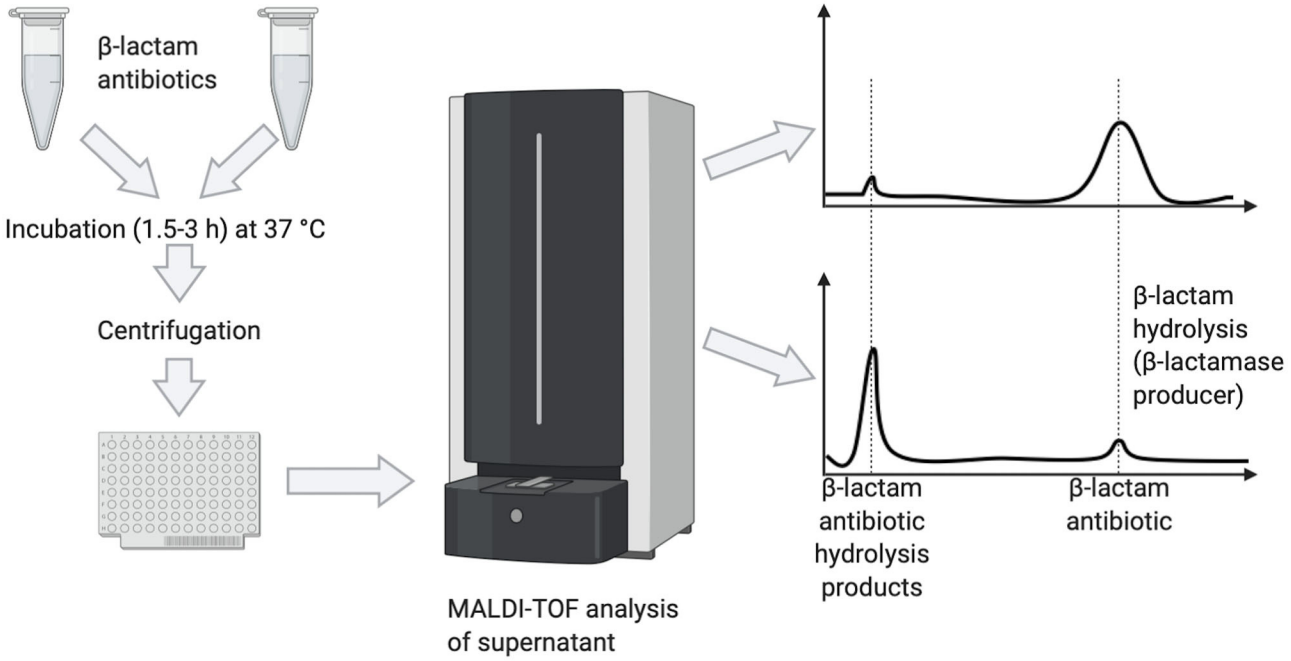

FIGURE 1 | Detection of β-lactamase producers by MALDI-TOF MS based on the hydrolysis of the target β-lactam antibiotic, as visualized by peak disappearance.

The increasing prevalence of extensively drug-resistant *P. aeruginosa* infections is due to the global spread of defined high-risk clones. Among them, ST175 is particularly frequent in Spain and France. A MALDI-TOF biomarker peak-based recognition model was evaluated in three collections from Spain and France. Spectra analysis revealed two biomarker-peaks (6,911 and 7,359 m/z) present in all ST175 strains, that most of the susceptible strains lacked. The peak 7,359 m/z was already associated with ST175 (Cabrolier et al., 2015) and the recognition of the second peak increased specificity to 97.8% (Mulet et al., 2019).

With another approach focusing on mass spectrometric analysis of membrane lipids, it was demonstrated that bacterial glycolipids possess species-specific characteristics allowing bacterial identification (Leung et al., 2017). Next, a lipid-extraction protocol was described (Liang et al., 2019) that reduces the identification time to <1 h. This method has been tested to detect antibiotic-resistance and to identify microbes, without requiring culture, using a library of the clinically relevant ESKAPE pathogens and colistin-resistant pathogens expressing the *mcr-1* gene in *trans*. Different biomarkers of resistance were found: *mcr-1*-containing *P. aeruginosa* strains showed a mass shift, 1,446–1,569 m/z, deriving by a PEtN (Δm/z 123) addition to lipid A. The 1,569 m/z ion was not observed in susceptible strains; while *K. pneumoniae* showed a modification of lipid A by AraN (Δm/z 131) attached on the terminal phosphate group of hexa-acetylated lipid A (1,824 m/z), resulting in a modified structure at 1,955 m/z; similarly mass spectrum from *Morganella morganii* with AraN-modified lipid A ions shifted from 1,796 to 1,927 m/z.

The above described methods are specific for one resistance mechanism, thus requiring confirmation of negative results, and have the advantage to use the routinely identification procedure without incubation with the antibiotic, followed by a different spectral analysis, except for the method of Leung, which does not require culture.

MALDI BIOTYPER-ANTIBIOTIC SUSCEPTIBILITY TEST RAPID ASSAY (MBT-ASTRA)

The MBT-ASTRA is a rapid method for detection of antibiotic-resistance based on a MALDI-TOF MS software tool that calculates and compares the area under the curves (AUCs) of spectra of bacteria either exposed or not to an antibiotic (Lange et al., 2014; Sparbier et al., 2016). The AUCs of the tested bacterial strain are compared to assess bacterial growth. If the microbial strain is susceptible, the AUC of the bacterial suspension with the antibiotic will be reduced compared to that without antibiotic, whereas with a resistant strain the AUCs with or without antibiotic will be comparable.

In principle, the MBT-ASTRA could be used for all classes of antibiotics and microbial species (Ceyssens et al., 2017). The ability of the MBT-ASTRA was evaluated to detect antimicrobial-resistance in a number of randomly selected clinical isolates of *Mycobacterium tuberculosis* and non-tuberculous mycobacteria (NTM). *M. tuberculosis* strains were tested for susceptibility to rifampin, isoniazid, linezolid, and ethambutol, and NTM to clarithromycin and rifabutin. The MBT-ASTRA measures

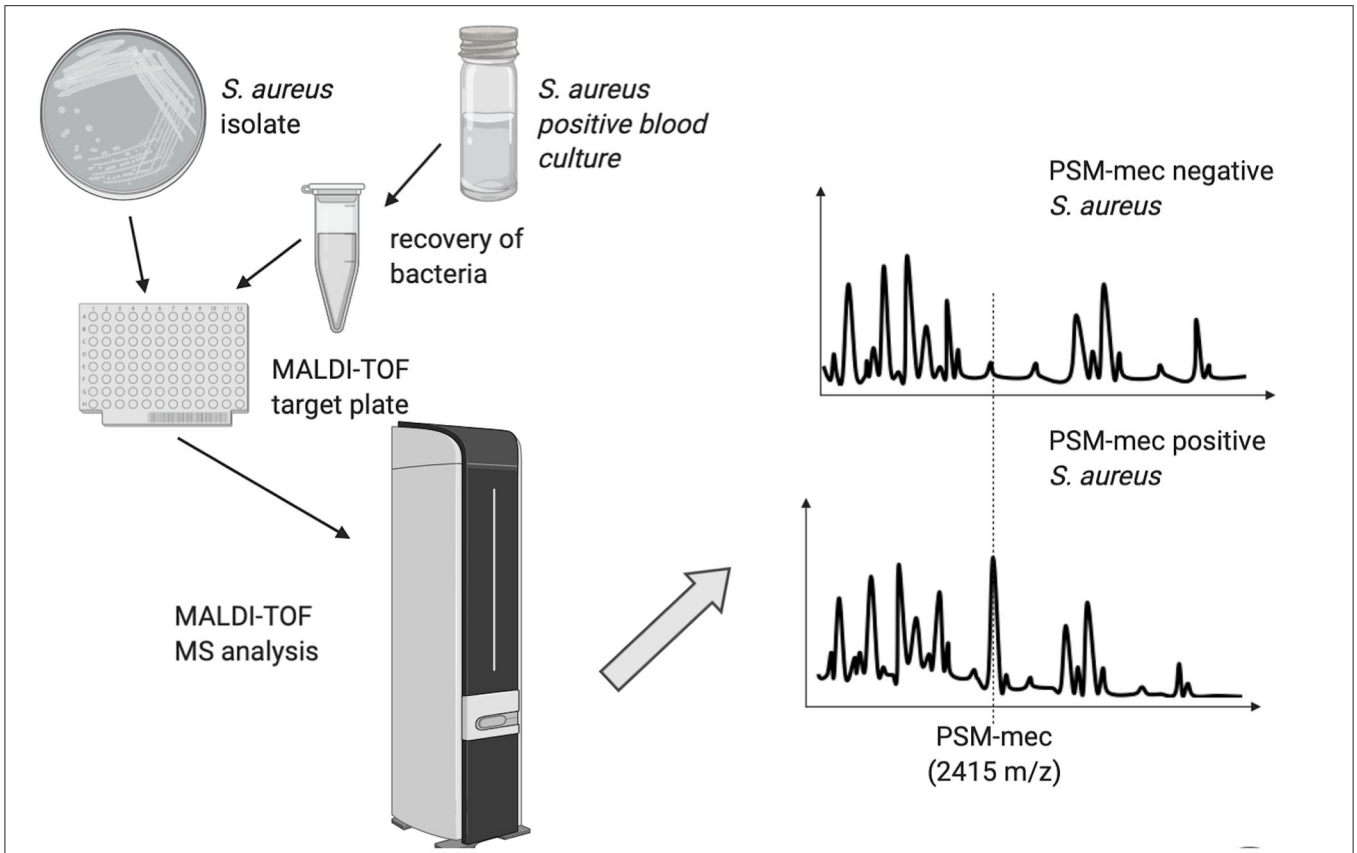

FIGURE 2 | Schematic representation of the MALDI-TOF MS method used to discriminate *Staphylococcus aureus* strains based on the presence of the PSM-mec peak.

bacterial biomass changes after addition of antimicrobial drugs. Using this method, the antimicrobial-resistance profiles of *M. tuberculosis* and NTM strains were correctly detected. However, the turnaround time was not shortened for *M. tuberculosis*, whereas for NTM was one week earlier.

The MBT-ASTRA approach was evaluated (Jung et al., 2014b) for detecting non-susceptibility against gentamicin and ciprofloxacin in BCs spiked with different *Enterobacteriaceae*, as well as against cefotaxime, piperacillin-tazobactam, and ciprofloxacin in monomicrobial BCs from patients with sepsis from Gram-negative bacteria. To detect non-susceptibility with the MBT-ASTRA method, antibiotics were tested at concentrations that were one dilution higher than the EUCAST susceptibility breakpoints. Overall, the results of microbial identification and susceptibility testing were obtained in ∼4 h. In experiments with spiked BCs, a clear separation between susceptible and non-susceptible isolates was obtained for gentamicin based on the observed median relative growth values. For ciprofloxacin, and piperacillin-tazobactam, a small number of isolates were misclassified as susceptible by the MBT-ASTRA mostly when MIC values were close to the antibiotic concentration used in the assay.

Overall, these results indicate that the MBT-ASTRA could be a promising approach for rapid AST of Gram-negative bacteria directly recovered from monomicrobial BCs, but also highlight the need to optimize the method, especially for correct classification of isolates with MIC values close to the breakpoint concentrations, and for some antibiotics.

The MBT-ASTRA was evaluated (Sauget et al., 2018) for rapid detection of amoxicillin- and cefotaxime-resistant *E. coli* isolates from positive BCs. An aliquot of the selected BCs was subcultured for 1 h in antibiotic-free liquid medium before recovery of bacteria and incubation with or without antibiotic, followed by analysis of spectra with the MBT-ASTRA software. Overall, the results of this susceptibility test were available within 4 h after BC positivity. Categorical agreement between the MBT ASTRA and the reference method was 97 and 83% for amoxicillin and cefotaxime, respectively. MBT-ASTRA correctly classified 95 and 84% of the amoxicillin- and cefotaxime-susceptible *E. coli* isolates, respectively, thus MBT-ASTRA may vary depending on the tested antibiotic.

The MBT-ASTRA was evaluated for AST of *B. fragilis* (Justesen et al., 2018), showing a clear difference of the relative growth between a susceptible (ATCC 25285) and a resistant (O18) strain exposed to clindamycin, meropenem, or

metronidazole. The accuracy of this method should be confirmed on clinical isolates.

Strength and limitation of this method will be discussed below.

ASSAYS BASED ON DETECTION OF PEAK SHIFT AFTER STABLE ISOTOPE-LABELING (MBT-RESIST)

Another proposed approach to determine drug-resistance in bacteria by MALDI-TOF MS is based on the use of non-radioactive isotope-labeled media (Demirev et al., 2013). Bacteria are grown, in parallel, in two different culture media, one containing ^{12}C, and the other one ^{13}C as carbon component. The mass spectrum of bacteria grown in antibiotic-containing isotope-labeled media is compared with the mass spectrum of the same strain grown in unlabeled media without antibiotic. Resistant bacteria can grow in the presence of the antibiotic incorporating ^{13}C in their polypeptides, which causes a shift of peaks to higher m/z in the mass spectrum.

To evaluate the applicability of the method discriminating MSSA from MRSA strains, culture media containing ^{13}C-labeled lysine were used to test oxacillin- and cefoxitin-resistant *S. aureus* clinical isolates (Sparbier et al., 2013). Bacteria were incubated for 3 h in three different conditions: ^{12}C-containing medium without antibiotic, ^{13}C-containing medium without antibiotic, and ^{13}C-containing medium with antibiotic. One out of 14 susceptible strains was misclassified as oxacillin-resistant, and three strains were misclassified regarding cefoxitin-susceptibility/resistance.

Next, peak shifts analysis after incubation for 3 h with either ^{13}C-^{15}N-labeled or unlabeled L-lysine was established to test meropenem-, tobramycin- and ciprofloxacin-resistant *P. aeruginosa* strains (Jung et al., 2014a). To optimize the assay, meropenem was added 30 min before addition of the stable isotope-labeled amino acid to the test tube, allowing the antibiotic to act. The results revealed concordant classification of susceptible and resistant strains with the reference method (Etest). Theoretically, this method as well as the MBT-ASTRA could be applied to all classes of antibiotics and microorganisms. Drawbacks of these two methods are (i) the incubation time required for microbial growth, (ii) the need to optimize experimental conditions for different isolate-antibiotic combinations, (iii) a correlation between an alteration of mass spectra and MIC values. For *Candida albicans*, the minimal profile change concentrations (MPCCs) [i.e., the minimum drug concentration at which an alteration of mass spectra can be detected, has been highly correlated with the MICs (Marinach et al., 2009)]. The main difference between MBT-ASTRA and MBT-Resist is that the latter requires three different growth conditions.

ANTIBIOTIC-RESISTANCE BY DIRECT-ON-TARGET MICRODROPLET GROWTH ASSAY (DOT-MGA)

An innovative method allowed the detection of antimicrobial-resistance/susceptibility of bacteria incubated with breakpoint concentrations of antibiotics directly on the target plate of MALDI-TOF MS (Idelevich et al., 2018a). The authors tested *K. pneumoniae* and *P. aeruginosa* for resistance to meropenem, but any microbial species and antimicrobial agent could be used, independently from the underlying resistance mechanisms. A 6 µl-incubation volume and optimal/minimum 4 and 5 h incubation times were established for *K. pneumoniae* and *P. aeruginosa*, respectively. In these experimental conditions, 100% sensitivity and specificity were reached for both microorganisms, and the rate of valid tests resulted 100% for *K. pneumoniae* and 83.3% for *P. aeruginosa*. Interestingly, the analysis of spectra after incubation with the antibiotic was performed using the MALDI Biotyper 3.1 software, routinely used for microbial identification.

In another study, the direct-on-target microdroplet growth assay was evaluated on positive BCs from blood samples spiked with meropenem-non-susceptible and meropenem-susceptible *Enterobacteriaceae* isolates (Idelevich et al., 2018b). The best performance was obtained by recovering bacteria from positive BCs, and after a 4 h-incubation of microdroplets with or without meropenem at the breakpoint concentration. In these conditions, 96.3% validity, 91.7% sensitivity, and 100% specificity were achieved.

Recently, a screening panel for detection of extended-spectrum β-lactamase (ESBL) and AmpC β-lactamase activity was developed employing the direct-on-target microdroplet growth assay (Correa-Martinez et al., 2019). The panel was validated on 50 clinical isolates including species of the *Enterobacteriaceae*, *Hafniaceae*, *Morganellaceae*, and *Yersiniaceae* families with different mechanisms of resistance (ESBL and/or AmpC) to third generation cephalosporins. The synergistic effect between four cephalosporins and ESBL (clavulanic acid) and/or AmpC (cloxacillin) β-lactamase inhibitors was evaluated to detect effective β-lactamase production. Incubation time of bacteria with or without β-lactamase inhibitors and/or antibiotics was optimized at 4 h. Compared to the PCR results, positive percent agreement values for ESBL, AmpC, and ESBL+AmpC resistance were 94.4, 94.4, and 100% and negative percent agreement values 100, 93.7, and 100%, respectively. The accuracy of the direct-on-target microdroplet growth assay resulted comparable to that of broth microdilution assay, with a time saving of about 14 h, and higher than combination disk tests.

Another MALDI-TOF MS-based method requires incubation of bacteria with different concentrations of antibiotic, recovery of microorganisms before MS analysis (Li et al., 2018) using the MALDI Biotyper 3.1 software. To evaluate the applicability of the method, meropenem-susceptible and meropenem-resistant *A. baumannii* clinical isolates were analyzed after a 4 h-incubation with different concentrations of antibiotic. The isolates were classified as resistant if identification was achieved with scores $\geq$1.7 after incubation with meropenem at the breakpoint concentration, and as susceptible if identification failed (scores $<$1.7). The authors recommend applying a threshold of 2 µg/mL for drug-resistance to lower the probability of very major errors (false susceptibility) due to insufficient bacterial growth in the presence of the antibiotic.

DISCUSSION

In this review, recent advances and newly proposed methods for rapid detection of antimicrobial-resistance in bacterial pathogens by MALDI-TOF MS have been summarized and discussed. Timeliness and accuracy of test results are crucial factors for clinicians to decide and promptly administer an effective and targeted antimicrobial therapy, especially in life-threatening infections or when crucial organs and functions, such as sight are at risk. Further research efforts will be made to refine and optimize MALDI-TOF MS-based assays to obtain accurate and reliable results in the shortest possible time. A major focus of future research in this field will be to achieve standardization of methods and simultaneous susceptibility testing of microbes to various classes of antimicrobials, because of the widespread of multi-drug-resistant microorganisms. So far, only two commercially available kits with software for automated interpretation of spectra have been authorized in Europe to detect or carbapenemase activity or resistance toward 3rd generation cephalosporins in clinical microbiology laboratories.

In conclusion, the possibility to detect peaks associated with drug-resistance directly in MALDI-TOF mass spectra of microbial isolates provides early, useful, though limited information that can help clinicians to streamline empirical antimicrobial therapy, as it is the case with some proposed markers for carbapenem-resistance.

The development of new analytical algorithms, automation of procedures, and optimization of assays are expected to expand and refine the clinical applications of MALDI-TOF MS in clinical diagnostic microbiology.

AUTHOR CONTRIBUTIONS

WF and AL contributed to the conception and design of the study. WF wrote the first draft of the manuscript. All authors contributed to manuscript revision, read, and approved the submitted version.

FUNDING

This research was supported by the PRIN 2017 grant prot. 20177J5Y3P from the Italian Ministry of Education, University and Research (MIUR).

ACKNOWLEDGMENTS

The authors wish to dedicate this work to WF, that passed away during the finalization of the manuscript.

REFERENCES

Akyar, I., Kaya Ayas, M., and Karatuna, O. (2019). Performance evaluation of MALDI-TOF MS MBT STAR-BL versus in-house carba NP testing for the rapid detection of carbapenemase activity in *Escherichia coli* and *Klebsiella pneumoniae* strains. *Microb. Drug Resist.* 25, 985–990. doi: 10.1089/mdr.2018.0355

Barnini, S., Ghelardi, E., Brucculeri, V., Morici, P., and Lupetti, A. (2015). Rapid and reliable identification of gram-negative bacteria and Gram-positive cocci by deposition of bacteria harvested from blood cultures onto the MALDI-TOF plate. *BMC Microbiol.* 15:124. doi: 10.1186/s12866-015-0459-8

Burckhardt, I., and Zimmermann, S. (2011). Using matrix-assisted laser desorption ionization-time of flight mass spectrometry to detect carbapenem resistance within 1 to 2.5 hours. *J. Clin. Microbiol.* 49, 3321–3324. doi: 10.1128/JCM.00287-11

Cabrolier, N., Sauget, M., Bertrand, X., and Hocquet, D. (2015). Matrix-assisted laser desorption ionization-time of flight mass spectrometry identifies *Pseudomonas aeruginosa* high-risk clones. *J. Clin. Microbiol.* 53, 1395–1398. doi: 10.1128/JCM.00210-15

Ceyssens, P. J., Soetaert, K., Timke, M., Van Den Bossche, A., Sparbier, K., De Cremer, K., et al. (2017). Matrix-assisted laser desorption ionization-time of flight mass spectrometry for combined species identification and drug sensitivity testing in mycobacteria. *J. Clin. Microbiol.* 55, 624–634. doi: 10.1128/JCM.02089-16

Chang, K. C., Chung, C. Y., Yeh, C. H., Hsu, K. H., Chin, Y. C., Huang, S. S., et al. (2018). Direct detection of carbapenemase-associated proteins of *Acinetobacter baumannii* using nanodiamonds coupled with matrix-assisted laser desorption/ionization time-of-flight mass spectrometry. *J. Microbiol. Methods* 147, 36–42. doi: 10.1016/j.mimet.2018.02.014

Chatterjee, S. S., Chen, L., Joo, H. S., Cheung, G. Y., Kreiswirth, B. N., and Otto, M. (2011). Distribution and regulation of the mobile genetic element-encoded phenol-soluble modulin PSM-mec in methicillin-resistant *Staphylococcus aureus*. *PLoS ONE* 6:e28781. doi: 10.1371/journal.pone.0028781

Choi, E. Y., Han, J. Y., Lee, H., Lee, S. C., Koh, H. J., Kim, S. S., et al. (2019). Impact of antibiotic resistance of pathogens and early vitrectomy on the prognosis of infectious endophthalmitis: a 10-years retrospective study. *Graefes Arch. Clin. Exp. Ophthalmol.* 257, 805–813. doi: 10.1007/s00417-019-04261-x

Correa-Martinez, C. L., Idelevich, E. A., Sparbier, K., Kostrzewa, M., and Becker, K. (2019). Rapid detection of extended-spectrum beta-lactamases (ESBL) and AmpC beta-lactamases in *Enterobacterales*: development of a screening panel using the MALDI-TOF MS-based direct-on-target microdroplet growth assay. *Front. Microbiol.* 10:13. doi: 10.3389/fmicb.2019.00013

Demirev, P. A., Hagan, N. S., Antoine, M. D., Lin, J. S., and Feldman, A. B. (2013). Establishing drug resistance in microorganisms by mass spectrometry. *J. Am. Soc. Mass. Spectrom.* 24, 1194–1201. doi: 10.1007/s13361-013-0609-x

Ferreira, L., Sanchez-Juanes, F., Porras-Guerra, I., Garcia-Garcia, M. I., Garcia-Sanchez, J. E., Gonzalez-Buitrago, J. M., et al. (2011). Microorganisms direct identification from blood culture by matrix-assisted laser desorption/ionization time-of-flight mass spectrometry. *Clin. Microbiol. Infect.* 17, 546–551. doi: 10.1111/j.1469-0691.2010.03257.x

Florio, W., Tavanti, A., Barnini, S., Ghelardi, E., and Lupetti, A. (2018a). Recent advances and ongoing challenges in the diagnosis of microbial infections by MALDI-TOF mass spectrometry. *Front. Microbiol.* 9:1097. doi: 10.3389/fmicb.2018.01097

Florio, W., Tavanti, A., Ghelardi, E., and Lupetti, A. (2018b). MALDI-TOF MS applications to the detection of antifungal resistance: state of the art and future perspectives. *Front. Microbiol.* 9:2577. doi: 10.3389/fmicb.2018.02577

Gaibani, P., Galea, A., Fagioni, M., Ambretti, S., Sambri, V., and Landini, M. P. (2016). Evaluation of matrix-assisted laser desorption ionization-time of flight mass spectrometry for identification of KPC-producing *Klebsiella pneumoniae*. *J. Clin. Microbiol.* 54, 2609–2613. doi: 10.1128/JCM.01242-16

Hrabak, J., Walkova, R., Studentova, V., Chudackova, E., and Bergerova, T. (2011). Carbapenemase activity detection by matrix-assisted laser desorption ionization-time of flight mass spectrometry. *J. Clin. Microbiol.* 49, 3222–3227. doi: 10.1128/JCM.00984-11

Idelevich, E. A., Sparbier, K., Kostrzewa, M., and Becker, K. (2018a). Rapid detection of antibiotic resistance by MALDI-TOF mass spectrometry using a novel direct-on-target microdroplet growth assay. *Clin. Microbiol. Infect.* 24, 738–743. doi: 10.1016/j.cmi.2017.10.016

Idelevich, E. A., Storck, L. M., Sparbier, K., Drews, O., Kostrzewa, M., and Becker, K. (2018b). Rapid direct susceptibility testing from positive blood cultures by the matrix-assisted laser desorption ionization-time of flight mass spectrometry-based direct-on-target microdroplet growth assay. *J. Clin. Microbiol.* 56, e00913–18. doi: 10.1128/JCM.00913-18

Johansson, A., Nagy, E., and Soki, J. (2014a). Instant screening and verification of carbapenemase activity in *Bacteroides fragilis* in positive blood culture, using matrix-assisted laser desorption ionization–time of flight mass spectrometry. *J. Med. Microbiol.* 63, 1105–1110. doi: 10.1099/jmm.0.075465-0

Johansson, A., Nagy, E., Soki, J., and ESGAI (ESCMID Study Group on Anaerobic Infections). (2014b). Detection of carbapenemase activities of *Bacteroides fragilis* strains with matrix-assisted laser desorption ionization–time of flight mass spectrometry (MALDI-TOF MS). *Anaerobe* 26, 49–52. doi: 10.1016/j.anaerobe.2014.01.006

Jung, J. S., Eberl, T., Sparbier, K., Lange, C., Kostrzewa, M., Schubert, S., et al. (2014a). Rapid detection of antibiotic resistance based on mass spectrometry and stable isotopes. *Eur. J. Clin. Microbiol. Infect. Dis.* 33, 949–955. doi: 10.1007/s10096-013-2031-5

Jung, J. S., Popp, C., Sparbier, K., Lange, C., Kostrzewa, M., and Schubert, S. (2014b). Evaluation of matrix-assisted laser desorption ionization-time of flight mass spectrometry for rapid detection of beta-lactam resistance in *Enterobacteriaceae* derived from blood cultures. *J. Clin. Microbiol.* 52, 924–930. doi: 10.1128/JCM.02691-13

Justesen, U. S., Acar, Z., Sydenham, T. V., and Johansson, A. (2018). Antimicrobial susceptibility testing of *Bacteroides fragilis* using the MALDI biotyper antibiotic susceptibility test rapid assay (MBT-ASTRA). *Anaerobe* 54, 236–239. doi: 10.1016/j.anaerobe.2018.02.007

Lange, C., Schubert, S., Jung, J., Kostrzewa, M., and Sparbier, K. (2014). Quantitative matrix-assisted laser desorption ionization-time of flight mass spectrometry for rapid resistance detection. *J. Clin. Microbiol.* 52, 4155–4162. doi: 10.1128/JCM.01872-14

Lau, A. F., Wang, H., Weingarten, R. A., Drake, S. K., Suffredini, A. F., Garfield, M. K., et al. (2014). A rapid matrix-assisted laser desorption ionization-time of flight mass spectrometry-based method for single-plasmid tracking in an outbreak of carbapenem-resistant *Enterobacteriaceae*. *J. Clin. Microbiol.* 52, 2804–2812. doi: 10.1128/JCM.00694-14

Leung, L. M., Fondrie, W. E., Doi, Y., Johnson, J. K., Strickland, D. K., Ernst, R. K., et al. (2017). Identification of the ESKAPE pathogens by mass spectrometric analysis of microbial membrane glycolipids. *Sci. Rep.* 7:6403. doi: 10.1038/s41598-017-04793-4

Li, M., Liu, M., Song, Q., Xiong, L., Chen, Z., Kang, M., et al. (2018). Rapid antimicrobial susceptibility testing by matrix-assisted laser desorption ionization-time of flight mass spectrometry using a qualitative method in *Acinetobacter baumannii* complex. *J. Microbiol. Methods* 153, 60–65. doi: 10.1016/j.mimet.2018.09.002

Liang, T., Leung, L. M., Opene, B., Fondrie, W. E., Lee, Y. I., Chandler, C. E., et al. (2019). Rapid microbial identification and antibiotic resistance detection by mass spectrometric analysis of membrane lipids. *Anal. Chem.* 91, 1286–1294. doi: 10.1021/acs.analchem.8b02611

Marinach, C., Alanio, A., Palous, M., Kwasek, S., Fekkar, A., Brossas, J.-Y., et al. (2009). MALDI-TOF MS-based drug susceptibility testing of pathogens: the example of *Candida albicans* and fluconazole. *Proteomics* 9, 4627–4631. doi: 10.1002/pmic.200900152

Mulet, X., Garcia, R., Gaya, M., and Oliver, A. (2019). O-antigen serotyping and MALDI-TOF, potentially useful tools for optimizing semi-empiric antipseudomonal treatments through the early detection of high-risk clones. *Eur. J. Clin. Microbiol. Infect. Dis.* 38, 541–544. doi: 10.1007/s10096-018-03457-z

Nagy, E., Becker, S., Soki, J., Urban, E., and Kostrzewa, M. (2011). Differentiation of division I (cfiA-negative) and division II (cfiA-positive) *Bacteroides fragilis* strains by matrix-assisted laser desorption/ionization time-of-flight mass spectrometry. *J. Med. Microbiol.* 60, 1584–1590. doi: 10.1099/jmm.0.031336-0

Oviano, M., Gato, E., and Bou, G. (2020). Rapid detection of KPC-producing enterobacterales susceptible to imipenem/relebactam by using the MALDI-TOF MS MBT STAR-carba IVD assay. *Front. Microbiol.* 11:328. doi: 10.3389/fmicb.2020.00328

Oviano, M., Sparbier, K., Barba, M. J., Kostrzewa, M., and Bou, G. (2016). Universal protocol for the rapid automated detection of carbapenem-resistant gram-negative bacilli directly from blood cultures by matrix-assisted laser desorption/ionisation time-of-flight mass spectrometry (MALDI-TOF/MS). *Int. J. Antimicrob. Agents* 48, 655–660. doi: 10.1016/j.ijantimicag.2016.08.024

Palacios-Baena, Z. R., Gutierrez-Gutierrez, B., De Cueto, M., Viale, P., Venditti, M., Hernandez-Torres, A., et al. (2017). Development and validation of the INCREMENT-ESBL predictive score for mortality in patients with bloodstream infections due to extended-spectrum-beta-lactamase-producing *Enterobacteriaceae*. *J. Antimicrob. Chemother.* 72, 906–913. doi: 10.1093/jac/dkw513

Rhoads, D. D., Wang, H., Karichu, J., and Richter, S. S. (2016). The presence of a single MALDI-TOF mass spectral peak predicts methicillin resistance in staphylococci. *Diagn. Microbiol. Infect. Dis.* 86, 257–261. doi: 10.1016/j.diagmicrobio.2016.08.001

Sauget, M., Bertrand, X., and Hocquet, D. (2018). Rapid antibiotic susceptibility testing on blood cultures using MALDI-TOF MS. *PLoS ONE* 13:e0205603. doi: 10.1371/journal.pone.0205603

Schuster, D., Josten, M., Janssen, K., Bodenstein, I., Albert, C., Schallenberg, A., et al. (2018). Detection of methicillin-resistant coagulase-negative staphylococci harboring the class A mec complex by MALDI-TOF mass spectrometry. *Int. J. Med. Microbiol.* 308, 522–526. doi: 10.1016/j.ijmm.2018.05.001

Sparbier, K., Lange, C., Jung, J., Wieser, A., Schubert, S., and Kostrzewa, M. (2013). MALDI biotyper-based rapid resistance detection by stable-isotope labeling. *J. Clin. Microbiol.* 51, 3741–3748. doi: 10.1128/JCM.01536-13

Sparbier, K., Schubert, S., and Kostrzewa, M. (2016). MBT-ASTRA: a suitable tool for fast antibiotic susceptibility testing? *Methods* 104, 48–54. doi: 10.1016/j.ymeth.2016.01.008

Tanaka, T., Oliveira, L. M. F., Ferreira, B. F. A., Kato, J. M., Rossi, F., Correa, K. L. G., et al. (2017). Bactec blood culture bottles allied to MALDI-TOF mass spectrometry: rapid etiologic diagnosis of bacterial endophthalmitis. *Diagn. Microbiol. Infect. Dis.* 88, 222–224. doi: 10.1016/j.diagmicrobio.2017.04.008

Tsirouki, T., Dastiridou, A. I., Ibanez Flores, N., Cerpa, J. C., Moschos, M. M., Brazitikos, P., et al. (2018). Orbital cellulitis. *Surv. Ophthalmol.* 63, 534–553. doi: 10.1016/j.survophthal.2017.12.001

Wang, Y. R., Chen, Q., Cui, S. H., and Li, F. Q. (2013). Characterization of *Staphylococcus aureus* isolated from clinical specimens by matrix assisted laser desorption/ionization time-of-flight mass spectrometry. *Biomed. Environ. Sci.* 26, 430–436. doi: 10.3967/0895-3988.2013.06.003

Conflict of Interest: The authors declare that the research was conducted in the absence of any commercial or financial relationships that could be construed as a potential conflict of interest.

frontiers in Cellular and Infection Microbiology

REVIEW
published: 04 February 2021
doi: 10.3389/fcimb.2020.621452

Detection of Species-Specific Lipids by Routine MALDI TOF Mass Spectrometry to Unlock the Challenges of Microbial Identification and Antimicrobial Susceptibility Testing

Vera Solntceva[1], *Markus Kostrzewa*[2] *and Gerald Larrouy-Maumus*[1]*

[1] MRC Centre for Molecular Bacteriology and Infection, Department of Life Sciences, Faculty of Natural Sciences, Imperial College London, London, United Kingdom, [2] Bruker Daltonik GmbH, Bremen, Germany

OPEN ACCESS

Edited by:
Di Xiao,
National Institute for Communicable Disease Control and Prevention (China CDC), China

Reviewed by:
Bryan Schmitt,
Indiana University Bloomington, United States
Simona Lobasso,
University of Bari Aldo Moro, Italy

***Correspondence:**
Gerald Larrouy-Maumus
g.larrouy-maumus@imperial.ac.uk

Specialty section:
This article was submitted to Clinical Microbiology, a section of the journal Frontiers in Cellular and Infection Microbiology

Received: 26 October 2020
Accepted: 18 December 2020
Published: 04 February 2021

Citation:
Solntceva V, Kostrzewa M and Larrouy-Maumus G (2021) Detection of Species-Specific Lipids by Routine MALDI TOF Mass Spectrometry to Unlock the Challenges of Microbial Identification and Antimicrobial Susceptibility Testing. Front. Cell. Infect. Microbiol. 10:621452. doi: 10.3389/fcimb.2020.621452

MALDI-TOF mass spectrometry has revolutionized clinical microbiology diagnostics by delivering accurate, fast, and reliable identification of microorganisms. It is conventionally based on the detection of intracellular molecules, mainly ribosomal proteins, for identification at the species-level and/or genus-level. Nevertheless, for some microorganisms (e.g., for mycobacteria) extensive protocols are necessary in order to extract intracellular proteins, and in some cases a protein-based approach cannot provide sufficient evidence to accurately identify the microorganisms within the same genus (e.g., *Shigella* sp. vs *E. coli* and the species of the *M. tuberculosis* complex). Consequently lipids, along with proteins are also molecules of interest. Lipids are ubiquitous, but their structural diversity delivers complementary information to the conventional protein-based clinical microbiology matrix-assisted laser desorption ionization time-of-flight (MALDI-TOF) based approaches currently used. Lipid modifications, such as the ones found on lipid A related to polymyxin resistance in Gram-negative pathogens (e.g., phosphoethanolamine and aminoarabinose), not only play a role in the detection of microorganisms by routine MALDI-TOF mass spectrometry but can also be used as a read-out of drug susceptibility. In this review, we will demonstrate that in combination with proteins, lipids are a game-changer in both the rapid detection of pathogens and the determination of their drug susceptibility using routine MALDI-TOF mass spectrometry systems.

Keywords: matrix-assisted laser desorption ionization, lipids, diagnostics, drug resistance, gram-negative, gram-positive, mycobacteria

INTRODUCTION

In recent years, matrix-assisted laser desorption ionization/time-of-flight (MALDI-TOF) mass spectrometry (MS) has revolutionized the field of microbiology (Clark et al., 2013; Singhal et al., 2015). MALDI-TOF MS provides rapid, accurate and cost-effective identification of a wide range of microbes based on protein signatures and requires only a single small colony for analysis (Croxatto et al., 2012). Development of commercial MALDI-TOF MS platforms capable of microbial identification and their subsequent approval for clinical use has made MALDI-TOF MS the standard routine identification tool in most diagnostic laboratories. Despite the advantages of MALDI-TOF MS, there are still several limitations to identification by protein profiling, such as the inability to differentiate closely related species and the laborious sample preparation required for some microorganisms.

In addition to proteins, lipids are also major cellular constituents. Lipids display high structural diversity and complexity, including species-specific characteristics which enable them to act as useful biomarkers for microbial identification. Although lipids have been used to characterize microorganisms since the 1960s (Abel et al., 1963; Moss and Lewis, 1967; Moss et al., 1980), the initial gas chromatography methods used for lipid analysis were time-consuming and unsuitable for clinical use. In the last decade, the popularity of microbial lipidomics has soared as novel methods of lipid analysis using MALDI-TOF MS have been developed (Cox et al., 2015; Larrouy-Maumus and Puzo, 2015; Leung et al., 2017). These methods can provide rapid and accurate microbial identification and differentiation and have the potential to address some of the challenges encountered by the proteomic approach and thereby complement them. Furthermore, analysis of lipids by MALDI-TOF MS is a promising tool for the detection of antibiotic resistance, particularly in the case of rapidly spreading resistance to polymyxins.

This review starts with a short overview of routine MALDI-TOF MS analysis and some of its current constraints, followed by the introduction of species-specific lipids and a brief history of lipid analysis for microbial identification. Afterwards, we will discuss the recent applications of mass-spectrometry based lipidomics for identification of microorganisms and detection of antibiotic resistance. We finish with an outlook toward the future directions for MALDI-TOF MS in microbial lipidomics.

PROTEIN-PROFILING BY MALDI-TOF FOR MICROBIAL IDENTIFICATION

In recent years, analysis of intracellular proteins signatures by MALDI-TOF MS has become a routine tool for the characterization of microorganisms (Croxatto et al., 2012; Angeletti and Ciccozzi, 2019; Bryson et al., 2019). Two commercial MALDI-TOF MS platforms, the MALDI Biotyper (Bruker Daltonics Inc.) and the VITEK MS (bioMérieux Inc.) - both recently approved by the FDA - are used in the majority of microbiology laboratories (Patel, 2015). For many microorganisms, these platforms enable high-throughput identification using simple sample preparation procedures and requiring only a single colony. Some microbes can be identified using direct cell profiling in which a colony is smeared on a MALDI target plate followed by the addition of a MALDI matrix that extracts the intracellular, mainly ribosomal, proteins (van Veen et al., 2010). For other microorganisms, including Gram-positive bacteria, a simple protocol of protein extraction using formic acid is sufficient prior to MALDI-TOF MS analysis (Bizzini et al., 2010; Alatoom et al., 2011).

Following sample processing, the protein mass spectra of an unknown isolate are acquired in the mass range of m/z 2,000 to m/z 20,000 in the positive ion mode. This range includes the ribosomal proteins that are present at high abundance in the cell. The mass spectra are then compared to a database that contains the profiles of known microbial species (Murray, 2012). As verified in numerous studies, MALDI-TOF MS provides highly accurate and reliable identification of a wide range of microorganisms (Cherkaoui et al., 2010; Carbonnelle et al., 2012; Wilson et al., 2017).

In addition to bacteria, MALDI-TOF MS is a valuable tool for the identification of fungal pathogens, particularly pathogenic yeasts (Buchan and Ledeboer, 2013). Many medically important yeast species, including *Candida* species and *Cryptococcus neoformans*, can be rapidly identified using simple on-plate extraction with formic acid (Theel et al., 2012; Westblade et al., 2013). MALDI-TOS MS identification of filamentous fungi can also be achieved but is not currently as successful as yeast typing due to the presence of robust cell walls and a lack of comprehensive fungal reference libraries (Becker et al., 2014; Wilkendorf et al., 2020).

Although protein profiling by MALDI-TOF MS is a valuable tool in microbiology, it has several constraints that will need to be addressed in the future. For microorganisms that are encased in complex, thick cell walls, laborious protein extraction procedures are required (Marklein et al., 2009; Rodriguez-Temporal et al., 2018; Kostrzewa et al., 2019). For example, a multistep method that involves heat inactivation and protein extraction is used for mycobacteria due to their robust cell walls and biosafety concerns (Wilen et al., 2015). According to the specimen preparation protocol described by El Khéchine et al., mycobacteria are first heat-inactivated for 1-hour at 95°C. Afterwards, mycobacterial cell walls are disrupted by vortex mixing with glass beads and the proteins are extracted using formic acid and acetonitrile (El Khechine et al., 2011). Labor-intensive protocols involving protein precipitation with ethanol and subsequent extraction with formic acid and acetonitrile are also used for yeasts to improve identification results (Bader, 2017).

Another major constraint of MALDI-TOF MS is a commonly encountered failure to differentiate some closely related species (Bizzini et al., 2010; Alcaide et al., 2018). For example, MALDI-TOF MS can fail to differentiate *Shigella* from *E. coli* (Martiny et al., 2012). These Gram-negative bacteria are very closely related and could genotypically be considered as the same

species, thus explaining the problems of differentiation using protein fingerprinting. Rapid discrimination between the two species is extremely important for infection control because *Shigella* species can cause shigellosis, an acute intestinal infection that is highly contagious. Enteroinvasive *E. coli* may trigger similar symptoms, but the disease is significantly less communicable (Niyogi, 2005). It also remains challenging to differentiate other closely related microorganisms such as the *Mycobacterium tuberculosis* complex which includes *M. africanum*, and the animal-adapted *M. caprae*, *M. bovis*, *M. microti*, *M. pinnipedii*, and *M. canettii*, or the *M. abscessus* complex which is composed of *M. abscessus* subsp. *abscessus*, *M. abscessus* subsp. *bolletii*, and *M. abscessus* subsp. *massiliense* (Saleeb et al., 2011; Nessar et al., 2012; Benwill and Wallace, 2014; Johnson and Odell, 2014; Angeletti et al., 2015; Bar-On et al., 2015). Other examples of erroneous identification of closely related species include *Streptococcus mitis* and *Streptococcus pneumoniae*, *Bordetella pertussis* and *Bordetella bronchiseptica*, *Klebsiella pneumoniae* and closely related species/subspecies, *Haemophilus influenzae* and *Haemophilus haemolyticus* and members of the *Enterobacter cloacae* complex (*Enterobacter cloacae*, *Enterobacter asburiae*, *Enterobacter hormaechei*, *Enterobacter kobei*, *Enterobacter ludwigii* and *Enterobacter nimipressuralis*, *Enterobacter. cloacae* and *Enterobacter hormaechei* (Stevenson et al., 2010; Frickmann et al., 2013; Angeletti et al., 2015; Schulthess et al., 2016; Rodrigues et al., 2017).

Consequently there is an ongoing need for the manufacturers of MALDI-TOF MS systems to continually update the databases and libraries with new reference spectra as new pathogens emerge innovative sample preparation improves microorganism identification. In addition to these commercial databases research laboratories can create custom reference spectra and expand existing databases with new microorganisms and applications. However, benchmarking against a reference method such as whole genome or 16S rRNA sequencing is required to ensure accurate identification and avoid misassignments.

LIPIDS AS SPECIES-SPECIFIC BIOMARKERS

Lipids are also a major functional and structural constituent of cells. and play important roles in membrane formation, cell signalling, energy storage and cell recognition (Hannun and Obeid, 2008; van Meer et al., 2008; Nakamura et al., 2014). To perform such diverse functions, cells contain a variety of lipid molecules that differ in the nature of the backbone and the headgroups, the number of fatty acids, and the chemical moieties they are modified with. Fatty acids themselves also vary in the length of the chain and the number of double bonds (Fahy et al., 2005). In combination with proteins, the diversity of lipids has the potential to make them useful biomarkers for microbial identification.

The differences in the cell wall structure and the membrane composition between Gram-positive and Gram-negative bacteria are well established, however, the lipid composition also varies among the species belonging to the same Gram type (Sohlenkamp and Geiger, 2016). In addition to common glycerophospholipids such as phosphatidylethanolamine and phosphatidylglycerol that are found in many organisms, bacteria possess species-specific lipids that display a high level of structural variability and are particularly useful for species differentiation. In Gram-negative bacteria, lipopolysaccharide (LPS) is a major structural component of the outer membrane. It is a glycolipid comprised of three parts: lipid A, a hydrophobic section of the molecule responsible for some aspects of toxicity of Gram-negative bacteria, the hydrophilic core oligosaccharide and the O antigen, a polysaccharide comprising the outermost domain of LPS (Raetz and Whitfield, 2002). The structure of LPS varies significantly among different species with the O antigen being the most diverse part of the molecule (Lerouge and Vanderleyden, 2002). The structure and composition of the O antigen can vary between strains of one species and has been used to assign serotypes of *Salmonella* and *E. coli* (Orskov and Orskov, 1992; Liu et al., 2014). Casabuono et al., reported on the structural characterization of lipid A from *Shigella flexneri* variant X, and discrete variants could serve to discriminate *Shigella* species from *E. coli* (Casabuono et al., 2012).

Gram-positive bacteria contain glycolipids, glucolipids and lipoteichoic acid (LTA), which is a typical constituent of the cell membrane (Reichmann and Grundling, 2011). LTA is defined as an alditol phosphate-containing polymer that is linked by a lipid anchor to the membrane. Based on chemical structure, there are five types of LTA (types I–V) (Percy and Grundling, 2014). Type I LTA is the most frequently encountered polymer found in many Gram-positive bacteria belonging to the phylum Firmicutes, including *B. subtilis*, *S. aureus* and *S. pyogenes* (Schneewind and Missiakas, 2014). Even though all type I LTA molecules have a common polyglycerol-phosphate backbone, variations of the core structure have been described in different species, particularly in the glycolipid anchor attaching the LTA to the membrane (Roethlisberger et al., 2000; Shiraishi et al., 2013). Type II and III LTA molecules, found in *Lactococcus garvieae* and *Clostridium innocuum*, respectively, contain repeat units of glycosylalditol-phosphate (Koch and Fischer, 1978). Type IV LTA is a complex molecule found in *S. pneumoniae* and some other *Streptococcus* species (Fischer, 1997).

In mycobacteria, several species-specific lipids have been described (Alberghina, 1976; Brennan and Nikaido, 1995; Ortalo-Magne et al., 1996; Ripoll et al., 2007; Batt et al., 2020). Mycolic acids are unique long-chain fatty acids that comprise the inner leaflet of the external mycomembrane in mycobacteria (Jackson, 2014). Mycolic acids display high structural diversity with variations observed in the chain length (60 to 90 carbon atoms), the level of unsaturation, and the chemical groups, such as ketones and methoxys (Marrakchi et al., 2014). This high level of diversity provides mycolic acids with species-specific characteristics making it possible to use them as taxonomic markers (Song et al., 2009). In addition to mycolic acids, other lipids are also found to be specific to particular species of mycobacteria. For example, sulfolipid 1 and polyacyltrehalose

are found exclusively in *M. tuberculosis*, while trehalose polyphleate is present in non-tuberculosis mycobacteria (NTM) species (Hatzios et al., 2009; Layre et al., 2011; Burbaud et al., 2016).

Glycolipids can also be used for the identification of fungi. Glycosylinositol-phosphorylceramides (GIPCs), which are a class of glycosphingolipids uniquely found in plant and fungal species, are particularly important biomarkers due to their high structural diversity (Fontaine et al., 2003; Costachel et al., 2005; Simenel et al., 2008; Saromi et al., 2020). GIPCs are major players in the establishment of infection in the vertebrate host by filamentous fungi such as *Aspergillus fumigatus* since they are involved in adhesion, signal transduction, modulation of the host immune response, and apoptosis (Toledo et al., 2007; Guimaraes et al., 2014; Fernandes et al., 2018). The conserved core structure of GIPCs consists of a ceramide moiety attached to a glucuronic acid-inositolphosphate group. Many diverse saccharides can be added to this core structure which generates complex glycan arrangements and results in significant structural variation among different fungal species (Cacas et al., 2012; Bure et al., 2014; Guimaraes et al., 2014).

As well as lipids from Gram-negative bacteria, Gram-positive bacteria, mycobacteria and filamentous fungi lipids, archaebacteria lipids have the potential to provide lipid-specific biomarkers. In contrast to glycerol-ester phospholipids from bacteria and filamentous fungi archaebacterial membranes are composed of isoprenoid and hydroisoprenoid hydrocarbons and isopranyl glycerol-ether lipids (De Rosa et al., 1986). Although these structures vary according to phenotypes (e.g., halophiles, methanogens, and thermophiles), these molecules are formed by condensation of glycerol or more complex polyols with isoprenoid alcohols containing 20, 25, or 40 carbon atoms (Woese et al., 1978; De Rosa et al., 1986). Indeed, due to their heterogeneity, these lipids have been proposed for the identification and classification of archaebacteria (Tornabene et al., 1980). They can therefore serve as chemical markers in combination with conventional 16S rRNA sequencing (McCartney et al., 2013; Sollai et al., 2019a; Sollai et al., 2019b).

As far as we are aware, routine identification of microorganisms by MALDI-TOF MS based on the identity and abundance of lipids has not been explored extensively to differentiate species and subspecies. This represents an exciting area which deserves more investigation.

HISTORY OF MICROBIAL LIPID ANALYSIS

Early attempts to utilize lipids for microbial identification were based on the analysis of fatty acids released from the microbial cells by chemical treatments and their subsequent analysis using either gas chromatography (GC) or gas chromatography mass spectrometry (GC/MS) (Abel et al., 1963; Moss and Lewis, 1967; Moss et al., 1980; Athalye et al., 1985; Kotilainen et al., 1991; Osterhout et al., 1991; Butler and Guthertz, 2001; Mosca et al., 2007). Both lipid and fatty acid composition varies among microbial species. Although most bacteria synthesize fatty acids that have chain lengths of 10 to 19 carbons, the relative abundance of each type of fatty acid varies among different species (O'Leary, 1962). Furthermore, some fatty acids are restricted to particular species such as the internally branched iso-fatty acids found in *Gaiella occulta* (Albuquerque et al., 2011). As a result of the quantitative differences in the fatty acid content and the presence of unusual or rare fatty acid types, the fatty acid profile of each species is distinctive which enables it to act a taxonomic marker.

The first evidence that bacteria can be identified based on their fatty acid composition was presented by Abel et al. in 1963. Their study employed gas chromatography to analyse the fatty acid composition of bacteria belonging to the family *Enterobacteriaceae* and some Gram-positive species (Abel et al., 1963). The major cellular fatty acids with chain lengths of 9 to 22 carbon atoms were extracted and trans-esterified into more volatile fatty acid methyl esters, followed by gas chromatographic analysis. The chromatographic profiles acquired were found to be distinct for each species which enabled bacterial characterization (Abel et al., 1963).

Subsequent studies have employed fatty acid analysis by gas chromatography for species-level identification of Gram-positive and Gram-negative bacterial species, mycobacteria and fungi (Jantzen et al., 1989; Veys et al., 1989; Marumo and Aoki, 1990; Kotilainen et al., 1991). Characterization was based on fatty acids with chain lengths between 9 and 20 carbon atoms, which represent the highly abundant fatty acids of phospholipids and glycolipids (Welch, 1991). Fatty acid analysis was particularly useful for identification of non-fermentative Gram-negative bacteria which are challenging to identify using conventional biochemical tests due to their relative un-reactivity (Veys et al., 1989; Wallace et al., 1990).

In 1991, efforts to automate and standardize the method were made which led to the introduction of the Sherlock Microbial Identification System (MIS). The MIS is an automated gas chromatographic system that identifies microorganisms based on the analysis of fatty acids that are between 9 and 20 carbons in length. The MIS automatically names and quantitates fatty acids enabling computerized identification of bacteria and fungi by comparing the fatty acid profile of the sample to profiles of known species in the database. It achieved a relatively high accuracy of identification for a range of microorganisms, including mycobacteria and non-fermentative Gram-negative bacteria (Osterhout et al., 1997; Mosca et al., 2007).

Despite the popularity of fatty acid analysis, this method has not reached clinical microbiology laboratories due to several limitations. The major drawback of gas chromatographic analysis of fatty acids is the time-consuming and laborious sample preparation. Before gas chromatography analysis, fatty acids are released by saponification and then methylated to generate fatty acid methyl ester (FAME) derivatives. FAMEs have increased volatility which facilitates their analysis by gas chromatography (Welch, 1991). This requires a multistep protocol which involves saponification of bacterial cells in sodium hydroxide, methylation with hydrochloric acid, lipid extraction and a wash at a basic pH. The procedure requires

sufficient technical expertise and typically takes several hours (Mosca et al., 2007). Another constraint of the method is how fatty acid composition varies depending on cell growth conditions such as temperature, medium composition and growth phase (Marr and Ingraham, 1962). To obtain a reproducible fatty acid profile, growth conditions must be standardized with great care, otherwise changes in fatty acid composition may lead to incorrect identification when the profile is compared to the reference database.

Analytical techniques including electrospray ionization (ESI) MS and Direct Analysis in Real Time (DART) MS have also been used as alternatives to GC-MS for fatty acid profiling (Song et al., 2009; Cody et al., 2015). However, attention largely shifted away from lipid analysis and those analysis techniques when MALDI platforms entered clinical laboratories and the proteomic approach became the most practical and rapid method of microbial identification.

LIPID-PROFILING BY MALDI-TOF FOR MICROBIAL IDENTIFICATION

MALDI-TOF MS is a powerful analytical tool with applications in microbiology not limited to protein profiling. Over the last decade many groups have developed MALDI-TOF routines for monitoring the degradation of antibiotics such as carbapenems and indicators of antibiotic resistance (Hrabak et al., 2011; Dortet et al., 2018c; Kostrzewa, 2018; Anantharajah et al., 2019; Huang et al., 2020). Several research groups have also employed MALDI-TOF MS for the analysis of lipid profiles from microorganisms (Cox et al., 2015; Larrouy-Maumus and Puzo, 2015; Leung et al., 2017; Liang et al., 2019).

Cox et al. developed a novel method of fatty acid analysis that uses CeO2-catalyzed fragmentation of lipids to produce fatty acids using the energy inherent to the MALDI laser (Cox et al., 2015). The conversion occurs *in situ* as the lipid extracts are added directly to the MALDI target plate spotted with CeO2. The technique, termed metal oxide laser ionization (MOLI) MS, obtained reproducible species- and strain-specific fatty acid profiles of isolates belonging to *Enterobacteriaceae*, *Acinetobacter* and *Listeria* genera. The accuracy of the method, validated by multivariate statistical methods, reached 100% for species-level classification and 98% for strain-level classification with only one strain being identified incorrectly. Particularly important for clinical microbiology, MOLI MS correctly identified the isolates of *Shigella*, the bacteria routinely classified by protein profiling as *E. coli* (Cox et al., 2015). A subsequent study that analyzed 50 *Staphylococcus* isolates including *S. aureus* strains and other species demonstrated a high accuracy of species- and strain-level identification (Saichek et al., 2016). Despite these initial promising results, this technology has not yet arrived in routine microbiology laboratories due to the constrains related to *in vitro* diagnostics, accessibility and implementation to such technology in clinical laboratories world-wide

Although fatty acids were traditionally used for microbial identification, analysis of whole lipids can be a more informative approach. Lipids are more complex molecules with greater scope for structural diversity and are therefore more suited to act as a chemical fingerprint for differentiation of microorganisms. A novel method of bacterial identification based on the analysis of glycolipids was recently developed by Leung et al. (2017). Glycolipids are a particularly diverse class of lipids due to the large variety of sugar modifications which enables them to generate species-specific mass spectral profiles. Furthermore, bacterial glycolipids are exclusive to bacterial cells and are not produced by mammals, which facilitates direct identification of bacteria from biological fluids. By analyzing the lipid extracts using MALDI-TOF MS, Leung and co-workers demonstrated that glycolipid mass spectra enabled differentiation of ESKAPE pathogens, a clinically relevant group of bacteria that have increased resistance to antibiotics. In addition, they employed the existing MALDI Biotyper software to construct a glycolipid library containing 50 microbial entries (Leung et al., 2017). This dataset was used in the subsequent machine learning study to identify *A. baumannii* and *K. pneumoniae* from polymicrobial mixtures, such as urinary tract infection specimens (Fondrie et al., 2018).

Traditionally, prior to MALDI-TOF MS analysis, lipid extraction is necessary. Leung et al. used a microextraction protocol developed by El Hamidi et al. which extracts glycolipids using hot ammonium isobutyrate (El Hamidi et al., 2005). Despite being efficient, this method is time-consuming and uses hazardous chemicals which limits its clinical utility. More recently, Liang et al. (2019) developed a novel method of lipid extraction in which sodium acetate buffer is added to the bacterial sample, followed by brief heating and organic solvent extraction. Using this method, bacterial identification can be completed in less than an hour making it a promising method for clinical diagnostics (Liang et al., 2019).

As mentioned previously, analysis of lipids or fatty acids required extraction of these molecules from the cells such as organic solvents extraction, partition and concentration (Bligh and Dyer, 1959; Maddi, 2019). Once extracted, those lipids could be analyzed by MALDI-TOF MS with the appropriate matrix to enable their ionization and desorption. For example, Angelini et al. have used 9-aminoacridine (9-AA), a matrix originally developed for the rapid analysis of glycerophospholipids, for direct analysis of lipid from extremely halophilic archaeon *Halobacterium salinarum* (Sun et al., 2008; Angelini et al., 2010). Prior to MALDI-TOF MS analysis, the lyophilized purple membrane of *H. salinarum* was finely ground with the dry 9-AA matrix and crushed in a mechanical die press. The resulting pellet was applied to the MALDI target and analyzed. This work showed that the 9-AA matrix enabled good ionization and easy detection of archaeal phospholipids and cardiolipins. The lipid profile generated using this method corresponded well to the MALDI-TOF MS profile obtained from the lipid extract of *H. salinarum*, demonstrating that it is possible to perform direct lipid analysis of intact lyophilized archaebacterial membranes, without the need for lipid extraction (Angelini et al., 2010).

9-AA matrix has also been utilized for lipid analysis of intact viruses (Vitale et al., 2013). Purified viral suspensions were

spotted on the MALDI target, followed by water evaporation and application of 9-AA matrix solution. The evaporated samples were then directly analyzed by MALDI-TOF MS. This method not only allowed the detection of the major lipids of these viruses, but also revealed novel details about the viral membrane composition, such as the presence of minor amount of phosphatidylcholine in PRD1 and φ6 bacteriophages (Vitale et al., 2013).

Another MALDI matrix, 1,8-bis(dimethylamino)naphthalene (DMAN), has also been utilized for lipid fingerprinting of intact Gram-positive *Lactobacillus sanfranciscensis* and *Lactobacillus planta-rum* strains (Calvano et al., 2011). The use of DMAN, which is a highly basic matrix, improves the detection of low molecular weight, less ionizable phospholipids, such as glycolipids and cardiolipins, in the negative ion mode due to the complete absence of matrix-related signals which can otherwise preclude lipid detection (Calvano et al., 2011).

However, a novel method developed by Larrouy-Maumus et al. enables direct MALDI-TOF MS analysis of lipids on intact microbes (Larrouy-Maumus and Puzo, 2015). A major advantage of this approach is a simple, rapid sample preparation that does not require any chemical treatment or purification prior to MALDI-TOF MS analysis. Heat-inactivated microorganisms are washed three times in double-distilled water and deposited on the MALDI target plate, followed by the specific MALDI matrix. The matrix consists of a 9:1 mixture of dihydroxybenzoic acid and 2-hydroxy-5-methoxybenzoic acid (super-DHB) solubilized in apolar solvent system (Larrouy-Maumus and Puzo, 2015; Larrouy-Maumus et al., 2016). The super-DHB matrix was chosen due to its versatility for the analysis of phospholipids and lipids (Schiller et al., 2007). Using this approach, microbial identification can be completed in less than 10 minutes on fewer than 1,000 bacteria making it a useful tool in the clinical laboratory (Gonzalo et al., 2020). To date, this method has been used to differentiate mycobacteria, filamentous fungi and detect lipid A from Gram-negative bacteria (Dortet et al., 2018a; Dortet et al., 2018b; Furniss et al., 2019; Dortet et al., 2020a; Dortet et al., 2020b; Furniss et al., 2020; Saromi et al., 2020). In the case of mycobacteria, (excluding uninterpretable results where 38/273 (14%) of isolates could not be assigned to either the Mtb or the NTM group, and 9 isolates (3%) were misidentified) this method not only achieves accurate identification with a sensitivity and specificity of 96.7% and 91.7%, respectively, but also represents a bio-safe alternative to conventional MALDI-TOF MS with minimal sample handling and preparation (Gonzalo et al., 2020).

LIPID MALDI FOR BACTERIAL DRUG SUSCEPTIBILITY

As antibiotic-resistant bacteria emerge worldwide, the timely detection of antibiotic resistance is critical for appropriate therapeutic management and effective infection control. One of the most promising applications of lipid-based MALDI-TOF MS analysis is the detection of colistin resistance. Colistin is one of the polymyxin antibiotics used as a last-resort therapy for treating multidrug-resistant Gram-negative bacterial infections (Poirel et al., 2017). Resistance to colistin most commonly arises from chemical modifications of the lipid A portion of LPS and can be mediated through chromosomal mutations or by the activity of plasmid-encoded mobile colistin resistance (MCR) genes. These modifications include addition of cationic groups such as 4-amino-4-deoxy-L-arabinose (L-Ara4N) or phosphoethanolamine (pETN) that reduce the binding of colistin to the positively charged LPS due to electrostatic repulsion (Jeannot et al., 2017). Analysis of bacterial lipids using MALDI-TOF MS represents a valuable tool for detecting colistin resistance as it can directly identify the lipid modifications.

A MALDI-TOF MS method that enables rapid detection of colistin resistance in intact bacteria was recently developed (Dortet et al., 2018a). This method, named the MALDIxin test, employs the simple sample preparation procedure developed by Larrouy-Maumus et al. in which intact bacteria or the bacterial lysate arising from mild-acid hydrolysis (acetic acid 1%) are mixed with the special matrix on the MALDI target plate, followed by MALDI-TOF MS analysis in the negative ion mode (Larrouy-Maumus et al., 2016; Dortet et al., 2018a; Dortet et al., 2018b; Furniss et al., 2019; Dortet et al., 2020b). The acquired mass spectra enable differentiation of colistin-susceptible and colistin-resistant strains based on the mass-to-charge (m/z) of the major lipid A peaks. The addition of pETN to a phosphate group at position 1 of lipid A results in an m/z +123 shift of the native lipid A-related peak, while L-Ara4N modification causes an m/z +131 shift. This test can also discriminate between chromosome- and MCR-mediated resistance as L-Ara4N modification is generally observed in strains with chromosome-encoded resistance, while pETN modification predominates in strains expressing MCR (Dortet et al., 2018a; Sun et al., 2018; Moffatt et al., 2019). The efficiency of the MALDIxin test has been demonstrated for clinically relevant *E. coli*, *A. baumannii*, *K. pneumoniae* and *S. enterica* species, achieving detection of colistin resistance in less than 15 minutes (Dortet et al., 2018a; Dortet et al., 2018b; Dortet et al., 2019; Dortet et al., 2020a). Furthermore, this method was recently adapted for the routine MALDI Biotyper Sirius system increasing its clinical utility (Furniss et al., 2019).

Analysis of cellular fatty acid composition might also be employed to detect antibiotic-resistant strains in particular species. A study by Saichek et al. utilized MOLI MS analysis of fatty acids to discriminate between methicillin-resistant *S. aureus* (MRSA) and methicillin-susceptible *S. aureus* (MSSA) strains (Saichek et al., 2016). The differences in fatty acid profiles were observed, with greater prevalence of odd-numbered fatty acids in MSSA isolates and higher abundance of even-numbered fatty acids in MRSA isolates, which enabled differentiation of methicillin-susceptible and -resistant strains. Particularly important for therapeutic management, this method can simultaneously identify bacterial strains and detect antibiotic resistance (Saichek et al., 2016).

In addition to the applications to polymyxins and *S. aureus* cited above, more generally, lipids profiling by MS systems has the potential to be used for broad antibiotics susceptibility

testing. For example, using MALDI coupled to high-resolution mass spectrometry named Fourier transform ion cyclotron resonance mass spectrometry (FT-ICR MS), Schenk and colleagues reported on the analogous distribution of altered fatty acids and glycerophospholipids, from *E. coli* strains, upon exposure to sublethal concentrations norfloxacin, an antibiotic that belongs to the class of fluoroquinolone antibiotics (Schenk et al., 2015). They concluded that variations of lipid content in the strain correspond to the extent of antibiotic resistance.

Indeed, that is supported by earlier work where significant alterations of fatty acid composition were observed in Gram-negative strains, such as *E. coli*, resistant to antibiotics such as tetracycline and polymyxins (Dunnick and O'Leary, 1970). The authors also reported on a correlation between the lipid content of Gram-positive *S. aureus* resistant to penicillin (Dunnick and O'Leary, 1970). Similar observations and correlations were also found for *Enterobacteriaceae*, such as *Serratia marcescens* (Chang et al., 1972; Suling and O'Leary, 1977).

However, further investigation is required to confirm the correlation between drug resistance, changes in membrane composition, and the relative abundance of different class of lipids, thus validating its use as an accurate and robust read-out of drug susceptibility routine MALDI-TOF MS system.

OUTLOOK AND AREAS FOR THE DEVELOPMENT OF LIPID-BASED MICROBIAL IDENTIFICATION

Adoption of lipidomics in clinical microbiology has lagged behind proteomic analysis due to the labor-intensive and time-consuming analytical methods initially available. However, novel methods of lipid analysis by MALDI-TOF MS have been developed in the last decade that can identify microorganisms with a speed and accuracy comparable to the routine MALDI-TOF MS analysis. Moreover, sample preparation has become significantly simpler and faster, particularly for lipid analysis of intact bacteria and filamentous fungi. Given these advances, lipid profiling has the potential to be employed alongside protein fingerprinting and may help to address some of the current constraints of MALDI-TOF MS, thereby further broadening its utility in clinical diagnostics and other routine microbiology applications. The workflow proposed in **Figure 1** would allow combination of lipid and protein analysis on the same MALDI target plate. This approach could accomplish several diagnostic goals in one analysis: the protein fingerprinting yields microbial identification at a species level while the lipid analysis can provide subspecies-level identification and detect antimicrobial susceptibility.

Although a considerable amount of progress has been made in optimizing sample preparation, further development of the bioinformatics resources is required to make the lipid analysis user-friendly in a clinical diagnostic setting, including the building of robust and accurate databases. Development of a representative lipid databases comparable in size and variety to the protein mass spectra libraries currently provided by commercial systems will improve the efficiency of microbial identification. Novel bioinformatic tools developed specifically for the analysis of lipid mass spectra such as the model-based spectral-library approach for matching mass spectra of glycolipids proposed by Ryu et al. will also advance identification (Ryu et al., 2019). A breakthrough in clinical microbiology diagnostics would be the ability to detect distinct

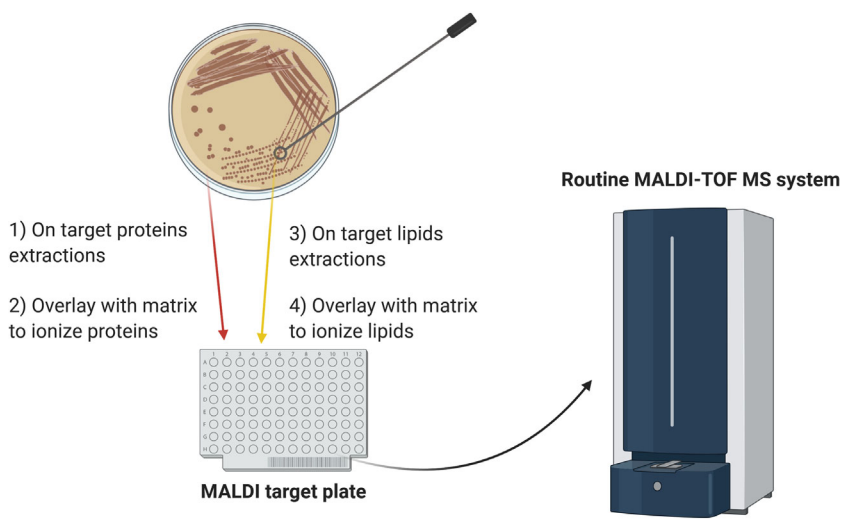

FIGURE 1 | Schematic diagram of the proposed workflow for combining lipid and protein MALDI-TOF MS analysis. For protein analysis, a colony is smeared on the target plate and overlaid with matrix. For analysis of lipid A, heat-inactivated microorganisms are submitted to mild-acid hydrolysis and the membranes resulting from this treatment are deposited on an adjacent position on the target plate, followed by matrix addition. Alternatively, for mycobacteria and filamentous fungi, heat-inactivated colonies are directly smeared on the target plate and overlaid with the appropriate matrix. The combined approach can yield species- and subspecies-level microbial identification and detect antibiotic resistance in one analysis.

microbial lipids directly from body fluids (e.g., serum, blood, and urine), thus avoiding the need for culture on agar plates or in liquid medium. Leung and colleagues attempted to address that challenge by spiking blood with *S. aureus* or *K. pneumoniae* B6 and recovering the bacteria by differential centrifugation to separate them from human cells. The lipids from the recovered bacteria were then extracted and analyzed by MALDI-TOF MS in the negative ion mode (Leung et al., 2017), and were able to get an excellent signal for 10^4 CFU of bacteria spiked in blood followed by 6 hours incubation. Although promising, the experimental manipulations required to enrich in bacteria would represent a hurdle for the rapid turn-over of samples in clinical microbiology laboratories. Being able to enrich microbial species-specific lipids from human or animal fluids, for veterinary applications, with limited sample preparation will be a gamechanger in rapid microbial diagnostics.

In future, lipid analysis may be extended to detect resistance to other antibiotics as well as colistin. Several papers report that antibiotic-resistant strains, such as rifampin-resistant *M. tuberculosis* and daptomycin-resistant *E. faecalis*, display altered lipid composition (Mishra et al., 2012; Lahiri et al., 2016). By detecting these alterations and their relative abundances, lipid profiling may be able to identify the resistant microorganisms, however, this would require a large-scale analysis of the lipid composition which is a highly complex task if done manually. To facilitate the data analysis, machine learning techniques should be developed to discriminate the mass spectra of antibiotic-resistant and -susceptible strains as has already been done in several studies employing protein-based MALDI-TOF MS analysis (Weis et al., 2020).

AUTHOR CONTRIBUTIONS

VS, GL-M, and MK conceived the review and wrote the manuscript. All authors contributed to the article and approved the submitted version.

FUNDING

This study was supported by the MRC Confidence in Concept Fund and the ISSF Wellcome Trust grant 105603/Z/14/Z (GL-M).

ACKNOWLEDGMENTS

We would like to thank Dr Brian Robertson (MRC-CMBI, Imperial College London) for careful reading of the manuscript.

REFERENCES

Abel, K., Deschmertzing, H., and Peterson, J. I. (1963). Classification of Microorganisms by Analysis of Chemical Composition. I. Feasibility of Utilizing Gas Chromatography. *J. Bacteriol.* 85, 1039–1044. doi: 10.1128/JB.85.5.1039-1044.1963

Alatoom, A. A., Cunningham, S. A., Ihde, S. M., Mandrekar, J., and Patel, R. (2011). Comparison of direct colony method versus extraction method for identification of gram-positive cocci by use of Bruker Biotyper matrix-assisted laser desorption ionization-time of flight mass spectrometry. *J. Clin. Microbiol.* 49 (8), 2868–2873. doi: 10.1128/JCM.00506-11

Alberghina, M. (1976). Relationship between lipid composition and antibiotic-resistance to isoniazid, streptomycin, p-aminosalicylic acid, ethambutol, rifampicin in mycobacteria. *Ital. J. Biochem.* 25 (2), 127–151.

Albuquerque, L., Franca, L., Rainey, F. A., Schumann, P., Nobre, M. F., and da Costa, M. S. (2011). Gaiella occulta gen. nov., sp. nov., a novel representative of a deep branching phylogenetic lineage within the class Actinobacteria and proposal of Gaiellaceae fam. nov. and Gaiellales ord. nov. *Syst. Appl. Microbiol.* 34 (8), 595–599. doi: 10.1016/j.syapm.2011.07.001

Alcaide, F., Amlerova, J., Bou, G., Ceyssens, P. J., Coll, P., Corcoran, D., et al. (2018). How to: identify non-tuberculous Mycobacterium species using MALDI-TOF mass spectrometry. *Clin. Microbiol. Infect.* 24 (6), 599–603. doi: 10.1016/j.cmi.2017.11.012

Anantharajah, A., Tossens, B., Olive, N., Kabamba-Mukadi, B., Rodriguez-Villalobos, H., and Verroken, A. (2019). Performance Evaluation of the MBT STAR((R))-Carba IVD Assay for the Detection of Carbapenemases With MALDI-TOF MS. *Front. Microbiol.* 10, 1413. doi: 10.3389/fmicb.2019.01413

Angeletti, S., and Ciccozzi, M. (2019). Matrix-assisted laser desorption ionization time-of-flight mass spectrometry in clinical microbiology: An updating review. *Infect. Genet. Evol.* 76, 104063. doi: 10.1016/j.meegid.2019.104063

Angeletti, S., Dicuonzo, G., Avola, A., Crea, F., Dedej, E., Vailati, F., et al. (2015). Viridans Group Streptococci clinical isolates: MALDI-TOF mass spectrometry versus gene sequence-based identification. *PloS One* 10 (3), e0120502. doi: 10.1371/journal.pone.0120502

Angelini, R., Babudri, F., Lobasso, S., and Corcelli, A. (2010). MALDI-TOF/MS analysis of archaebacterial lipids in lyophilized membranes dry-mixed with 9-aminoacridine. *J. Lipid Res.* 51 (9), 2818–2825. doi: 10.1194/jlr.D007328

Athalye, M., Noble, W. C., and Minnikin, D. E. (1985). Analysis of cellular fatty acids by gas chromatography as a tool in the identification of medically important coryneform bacteria. *J. Appl. Bacteriol.* 58 (5), 507–512. doi: 10.1111/j.1365-2672.1985.tb01491.x

Bader, O. (2017). Fungal Species Identification by MALDI-ToF Mass Spectrometry. *Methods Mol. Biol.* 1508, 323–337. doi: 10.1007/978-1-4939-6515-1_19

Bar-On, O., Mussaffi, H., Mei-Zahav, M., Prais, D., Steuer, G., Stafler, P., et al. (2015). Increasing nontuberculous mycobacteria infection in cystic fibrosis. *J. Cyst. Fibros.* 14 (1), 53–62. doi: 10.1016/j.jcf.2014.05.008

Batt, S. M., Minnikin, D. E., and Besra, G. S. (2020). The thick waxy coat of mycobacteria, a protective layer against antibiotics and the host's immune system. *Biochem. J.* 477 (10), 1983–2006. doi: 10.1042/BCJ20200194

Becker, P. T., de Bel, A., Martiny, D., Ranque, S., Piarroux, R., Cassagne, C., et al. (2014). Identification of filamentous fungi isolates by MALDI-TOF mass spectrometry: clinical evaluation of an extended reference spectra library. *Med. Mycol.* 52 (8), 826–834. doi: 10.1093/mmy/myu064

Benwill, J. L., and Wallace, R. J.Jr. (2014). Mycobacterium abscessus: challenges in diagnosis and treatment. *Curr. Opin. Infect. Dis.* 27 (6), 506–510. doi: 10.1097/QCO.0000000000000104

Bizzini, A., Durussel, C., Bille, J., Greub, G., and Prod'hom, G. (2010). Performance of matrix-assisted laser desorption ionization-time of flight mass spectrometry for identification of bacterial strains routinely isolated in a clinical microbiology laboratory. *J. Clin. Microbiol.* 48 (5), 1549–1554. doi: 10.1128/JCM.01794-09

Bligh, E. G., and Dyer, W. J. (1959). A rapid method of total lipid extraction and purification. *Can. J. Biochem. Physiol.* 37 (8), 911–917. doi: 10.1139/o59-099

Brennan, P. J., and Nikaido, H. (1995). The envelope of mycobacteria. *Annu. Rev. Biochem.* 64, 29–63. doi: 10.1146/annurev.bi.64.070195.000333

Bryson, A. L., Hill, E. M., and Doern, C. D. (2019). Matrix-Assisted Laser Desorption/Ionization Time-of-Flight: The Revolution in Progress. *Clin. Lab. Med.* 39 (3), 391–404. doi: 10.1016/j.cll.2019.05.010

Buchan, B. W., and Ledeboer, N. A. (2013). Advances in identification of clinical yeast isolates by use of matrix-assisted laser desorption ionization-time of flight mass spectrometry. *J. Clin. Microbiol.* 51 (5), 1359–1366. doi: 10.1128/JCM.03105-12

Burbaud, S., Laval, F., Lemassu, A., Daffe, M., Guilhot, C., and Chalut, C. (2016). Trehalose Polyphleates Are Produced by a Glycolipid Biosynthetic Pathway Conserved across Phylogenetically Distant Mycobacteria. *Cell Chem. Biol.* 23 (2), 278–289. doi: 10.1016/j.chembiol.2015.11.013

Bure, C., Cacas, J. L., Mongrand, S., and Schmitter, J. M. (2014). Characterization of glycosyl inositol phosphoryl ceramides from plants and fungi by mass spectrometry. *Anal. Bioanal. Chem.* 406 (4), 995–1010. doi: 10.1007/s00216-013-7130-8

Butler, W. R., and Guthertz, L. S. (2001). Mycolic acid analysis by high-performance liquid chromatography for identification of Mycobacterium species. *Clin. Microbiol. Rev.* 14 (4), 704–726, table of contents. doi: 10.1128/CMR.14.4.704-726.2001

Cacas, J. L., Furt, F., Le Guedard, M., Schmitter, J. M., Bure, C., Gerbeau-Pissot, P., et al. (2012). Lipids of plant membrane rafts. *Prog. Lipid Res.* 51 (3), 272–299. doi: 10.1016/j.plipres.2012.04.001

Calvano, C. D., Zambonin, C. G., and Palmisano, F. (2011). Lipid fingerprinting of gram-positive lactobacilli by intact–matrix-assisted laser desorption/ionization mass spectrometry using a proton sponge based matrix. *Rapid Commun. Mass. Spectrom.* 25 (12), 1757–1764. doi: 10.1002/rcm.5035

Carbonnelle, E., Grohs, P., Jacquier, H., Day, N., Tenza, S., Dewailly, A., et al. (2012). Robustness of two MALDI-TOF mass spectrometry systems for bacterial identification. *J. Microbiol. Methods* 89 (2), 133–136. doi: 10.1016/j.mimet.2012.03.003

Casabuono, A. C., van der Ploeg, C. A., Roge, A. D., Bruno, S. B., and Couto, A. S. (2012). Characterization of lipid A profiles from Shigella flexneri variant X lipopolysaccharide. *Rapid Commun. Mass. Spectrom.* 26 (17), 2011–2020. doi: 10.1002/rcm.6306

Chang, C. Y., Molar, R. E., and Tsang, J. C. (1972). Lipid content of antibiotic-resistant and -sensitive strains of Serratia marcescens. *Appl. Microbiol.* 24 (6), 972–976.

Cherkaoui, A., Hibbs, J., Emonet, S., Tangomo, M., Girard, M., Francois, P., et al. (2010). Comparison of two matrix-assisted laser desorption ionization-time of flight mass spectrometry methods with conventional phenotypic identification for routine identification of bacteria to the species level. *J. Clin. Microbiol.* 48 (4), 1169–1175. doi: 10.1128/JCM.01881-09

Clark, A. E., Kaleta, E. J., Arora, A., and Wolk, D. M. (2013). Matrix-assisted laser desorption ionization-time of flight mass spectrometry: a fundamental shift in the routine practice of clinical microbiology. *Clin. Microbiol. Rev.* 26 (3), 547–603. doi: 10.1128/CMR.00072-12

Cody, R. B., McAlpin, C. R., Cox, C. R., Jensen, K. R., and Voorhees, K. J. (2015). Identification of bacteria by fatty acid profiling with direct analysis in real time mass spectrometry. *Rapid Commun. Mass. Spectrom.* 29 (21), 2007–2012. doi: 10.1002/rcm.7309

Costachel, C., Coddeville, B., Latge, J. P., and Fontaine, T. (2005). Glycosylphosphatidylinositol-anchored fungal polysaccharide in Aspergillus fumigatus. *J. Biol. Chem.* 280 (48), 39835–39842. doi: 10.1074/jbc.M510163200

Cox, C. R., Jensen, K. R., Saichek, N. R., and Voorhees, K. J. (2015). Strain-level bacterial identification by CeO2-catalyzed MALDI-TOF MS fatty acid analysis and comparison to commercial protein-based methods. *Sci. Rep.* 5, 10470. doi: 10.1038/srep10470

Croxatto, A., Prod'hom, G., and Greub, G. (2012). Applications of MALDI-TOF mass spectrometry in clinical diagnostic microbiology. *FEMS Microbiol. Rev.* 36 (2), 380–407. doi: 10.1111/j.1574-6976.2011.00298.x

De Rosa, M., Gambacorta, A., and Gliozzi, A. (1986). Structure, biosynthesis, and physicochemical properties of archaebacterial lipids. *Microbiol. Rev.* 50 (1), 70–80.

Dortet, L., Bonnin, R. A., Pennisi, I., Gauthier, L., Jousset, A. B., Dabos, L., et al. (2018a). Rapid detection and discrimination of chromosome- and MCR-plasmid-mediated resistance to polymyxins by MALDI-TOF MS in Escherichia coli: the MALDIxin test. *J. Antimicrob. Chemother.* 73 (12), 3359–3367. doi: 10.1093/jac/dky330

Dortet, L., Potron, A., Bonnin, R. A., Plesiat, P., Naas, T., Filloux, A., et al. (2018b). Rapid detection of colistin resistance in Acinetobacter baumannii using MALDI-TOF-based lipidomics on intact bacteria. *Sci. Rep.* 8 (1), 16910. doi: 10.1038/s41598-018-35041-y

Dortet, L., Tande, D., de Briel, D., Bernabeu, S., Lasserre, C., Gregorowicz, G., et al. (2018c). MALDI-TOF for the rapid detection of carbapenemase-producing Enterobacteriaceae: comparison of the commercialized MBT STAR(R)-Carba IVD Kit with two in-house MALDI-TOF techniques and the RAPIDEC(R) CARBA NP. *J. Antimicrob. Chemother.* 73 (9), 2352–2359. doi: 10.1093/jac/dky209

Dortet, L., Broda, A., Bernabeu, S., Glupczynski, Y., Bogaerts, P., Bonnin, R., et al. (2019). Optimization of the MALDIxin test for the rapid identification of colistin resistance in Klebsiella pneumoniae using MALDI-TOF MS. *J. Antimicrob. Chemother.* 75 (1), 110–116. doi: 10.1093/jac/dkz405

Dortet, L., Bonnin, R. A., Le Hello, S., Fabre, L., Bonnet, R., Kostrzewa, M., et al. (2020a). Detection of Colistin Resistance in Salmonella enterica Using MALDIxin Test on the Routine MALDI Biotyper Sirius Mass Spectrometer. *Front. Microbiol.* 11, 1141. doi: 10.3389/fmicb.2020.01141

Dortet, L., Broda, A., Bernabeu, S., Glupczynski, Y., Bogaerts, P., Bonnin, R., et al. (2020b). Optimization of the MALDIxin test for the rapid identification of colistin resistance in Klebsiella pneumoniae using MALDI-TOF MS. *J. Antimicrob. Chemother.* 75 (1), 110–116. doi: 10.1093/jac/dkz405

Dunnick, J. K., and O'Leary, W. M. (1970). Correlation of bacteria lipid composition with antibiotic resistance. *J. Bacteriol.* 101 (3), 892–900. doi: 10.1128/JB.101.3.892-900.1970

El Hamidi, A., Tirsoaga, A., Novikov, A., Hussein, A., and Caroff, M. (2005). Microextraction of bacterial lipid A: easy and rapid method for mass spectrometric characterization. *J. Lipid Res.* 46 (8), 1773–1778. doi: 10.1194/jlr.D500014-JLR200

El Khechine, A., Couderc, C., Flaudrops, C., Raoult, D., and Drancourt, M. (2011). Matrix-assisted laser desorption/ionization time-of-flight mass spectrometry identification of mycobacteria in routine clinical practice. *PloS One* 6 (9), e24720. doi: 10.1371/journal.pone.0024720

Fahy, E., Subramaniam, S., Brown, H. A., Glass, C. K., Merrill, A. H.Jr., Murphy, R. C., et al. (2005). A comprehensive classification system for lipids. *J. Lipid Res.* 46 (5), 839–861. doi: 10.1194/jlr.E400004-JLR200

Fernandes, C. M., Goldman, G. H., and Del Poeta, M. (2018). Biological Roles Played by Sphingolipids in Dimorphic and Filamentous Fungi. *mBio* 9 (3). doi: 10.1128/mBio.00642-18

Fischer, W. (1997). Pneumococcal lipoteichoic and teichoic acid. *Microb. Drug Resist.* 3 (4), 309–325. doi: 10.1089/mdr.1997.3.309

Fondrie, W. E., Liang, T., Oyler, B. L., Leung, L. M., Ernst, R. K., Strickland, D. K., et al. (2018). Pathogen Identification Direct From Polymicrobial Specimens Using Membrane Glycolipids. *Sci. Rep.* 8 (1), 15857. doi: 10.1038/s41598-018-33681-8

Fontaine, T., Magnin, T., Melhert, A., Lamont, D., Latge, J. P., and Ferguson, M. A. (2003). Structures of the glycosylphosphatidylinositol membrane anchors from Aspergillus fumigatus membrane proteins. *Glycobiology* 13 (3), 169–177. doi: 10.1093/glycob/cwg004

Frickmann, H., Christner, M., Donat, M., Berger, A., Essig, A., Podbielski, A., et al. (2013). Rapid discrimination of Haemophilus influenzae, H. parainfluenzae, and H. haemolyticus by fluorescence in situ hybridization (FISH) and two matrix-assisted laser-desorption-ionization time-of-flight mass spectrometry (MALDI-TOF-MS) platforms. *PloS One* 8 (4), e63222. doi: 10.1371/journal.pone.0063222

Furniss, R. C. D., Dortet, L., Bolland, W., Drews, O., Sparbier, K., Bonnin, R. A., et al. (2019). Detection of Colistin Resistance in Escherichia coli by Use of the MALDI Biotyper Sirius Mass Spectrometry System. *J. Clin. Microbiol.* 57 (12). doi: 10.1128/JCM.01427-19

Furniss, R. C. D., Kostrzewa, M., Mavridou, D. A. I., and Larrouy-Maumus, G. (2020). The clue is in the lipid A: Rapid detection of colistin resistance. *PloS Pathog.* 16 (4), e1008331. doi: 10.1371/journal.ppat.1008331

Gonzalo, X., Broda, A., Drobniewski, F., and Larrouy-Maumus, G. (2020). Performance of lipid fingerprint-based MALDI-ToF for the diagnosis of mycobacterial infections. *Clin. Microbiol. Infect.* S1198–743(20):30510–3. doi: 10.1016/j.cmi.2020.08.027

Guimaraes, L. L., Toledo, M. S., Ferreira, F. A., Straus, A. H., and Takahashi, H. K. (2014). Structural diversity and biological significance of glycosphingolipids in pathogenic and opportunistic fungi. *Front. Cell Infect. Microbiol.* 4, 138. doi: 10.3389/fcimb.2014.00138

Hannun, Y. A., and Obeid, L. M. (2008). Principles of bioactive lipid signalling: lessons from sphingolipids. *Nat. Rev. Mol. Cell Biol.* 9 (2), 139–150. doi: 10.1038/nrm2329

Hatzios, S. K., Schelle, M. W., Holsclaw, C. M., Behrens, C. R., Botyanszki, Z., Lin, F. L., et al. (2009). PapA3 is an acyltransferase required for polyacyltrehalose biosynthesis in Mycobacterium tuberculosis. *J. Biol. Chem.* 284 (19), 12745–12751. doi: 10.1074/jbc.M809088200

Hrabak, J., Walkova, R., Studentova, V., Chudackova, E., and Bergerova, T. (2011). Carbapenemase activity detection by matrix-assisted laser desorption ionization-time of flight mass spectrometry. *J. Clin. Microbiol.* 49 (9), 3222–3227. doi: 10.1128/JCM.00984-11

Huang, T. S., Lee, S. S., Lee, C. C., and Chang, F. C. (2020). Detection of carbapenem-resistant Klebsiella pneumoniae on the basis of matrix-assisted laser desorption ionization time-of-flight mass spectrometry by using supervised machine learning approach. *PloS One* 15 (2), e0228459. doi: 10.1371/journal.pone.0228459

Jackson, M. (2014). The mycobacterial cell envelope-lipids. *Cold Spring Harb. Perspect. Med.* 4 (10). doi: 10.1101/cshperspect.a021105

Jantzen, E., Tangen, T., and Eng, J. (1989). Gas chromatography of mycobacterial fatty acids and alcohols: diagnostic applications. *APMIS* 97 (11), 1037–1045. doi: 10.1111/j.1699-0463.1989.tb00515.x

Jeannot, K., Bolard, A., and Plesiat, P. (2017). Resistance to polymyxins in Gram-negative organisms. *Int. J. Antimicrob. Agents* 49 (5), 526–535. doi: 10.1016/j.ijantimicag.2016.11.029

Johnson, M. M., and Odell, J. A. (2014). Nontuberculous mycobacterial pulmonary infections. *J. Thorac. Dis.* 6 (3), 210–220. doi: 10.3978/j.issn.2072-1439.2013.12.24

Koch, H. U., and Fischer, W. (1978). Acyldiglucosyldiacylglycerol-containing lipoteichoic acid with a poly(3-O-galabiosyl-2-O-galactosyl-sn-glycero-1-phosphate) chain from Streptococcus lactis Kiel 42172. *Biochemistry* 17 (24), 5275–5281.

Kostrzewa, M., Nagy, E., Schrottner, P., and Pranada, A. B. (2019). How MALDI-TOF mass spectrometry can aid the diagnosis of hard-to-identify pathogenic bacteria - the rare and the unknown. *Expert Rev. Mol. Diagn.* 19 (8), 667–682. doi: 10.1080/14737159.2019.1643238

Kostrzewa, M. (2018). Application of the MALDI Biotyper to clinical microbiology: progress and potential. *Expert Rev. Proteomics* 15 (3), 193–202. doi: 10.1080/14789450.2018.1438193

Kotilainen, P., Huovinen, P., and Eerola, E. (1991). Application of gas-liquid chromatographic analysis of cellular fatty acids for species identification and typing of coagulase-negative staphylococci. *J. Clin. Microbiol.* 29 (2), 315–322. doi: 10.1128/JCM.29.2.315-322.1991

Lahiri, N., Shah, R. R., Layre, E., Young, D., Ford, C., Murray, M. B., et al. (2016). Rifampin Resistance Mutations Are Associated with Broad Chemical Remodeling of Mycobacterium tuberculosis. *J. Biol. Chem.* 291 (27), 14248–14256. doi: 10.1074/jbc.M116.716704

Larrouy-Maumus, G., and Puzo, G. (2015). Mycobacterial envelope lipids fingerprint from direct MALDI-TOF MS analysis of intact bacilli. *Tuberculosis (Edinb.)* 95 (1), 75–85. doi: 10.1016/j.tube.2014.11.001

Larrouy-Maumus, G., Clements, A., Filloux, A., McCarthy, R. R., and Mostowy, S. (2016). Direct detection of lipid A on intact Gram-negative bacteria by MALDI-TOF mass spectrometry. *J. Microbiol. Methods* 120, 68–71. doi: 10.1016/j.mimet.2015.12.004

Layre, E., Paepe, D. C., Larrouy-Maumus, G., Vaubourgeix, J., Mundayoor, S., Lindner, B., et al. (2011). Deciphering sulfoglycolipids of Mycobacterium tuberculosis. *J. Lipid Res.* 52 (6), 1098–1110. doi: 10.1194/jlr.M013482

Lerouge, I., and Vanderleyden, J. (2002). O-antigen structural variation: mechanisms and possible roles in animal/plant-microbe interactions. *FEMS Microbiol. Rev.* 26 (1), 17–47. doi: 10.1111/j.1574-6976.2002.tb00597.x

Leung, L. M., Fondrie, W. E., Doi, Y., Johnson, J. K., Strickland, D. K., Ernst, R. K., et al. (2017). Identification of the ESKAPE pathogens by mass spectrometric analysis of microbial membrane glycolipids. *Sci. Rep.* 7 (1), 6403. doi: 10.1038/s41598-017-04793-4

Liang, T., Leung, L. M., Opene, B., Fondrie, W. E., Lee, Y. I., Chandler, C. E., et al. (2019). Rapid Microbial Identification and Antibiotic Resistance Detection by Mass Spectrometric Analysis of Membrane Lipids. *Anal. Chem.* 91 (2), 1286–1294. doi: 10.1021/acs.analchem.8b02611

Liu, B., Knirel, Y. A., Feng, L., Perepelov, A. V., Senchenkova, S. N., Reeves, P. R., et al. (2014). Structural diversity in Salmonella O antigens and its genetic basis. *FEMS Microbiol. Rev.* 38 (1), 56–89. doi: 10.1111/1574-6976.12034

Maddi, B. (2019). "Extraction Methods Used to Separate Lipids from Microbes," in *Microbial Lipid Production: Methods and Protocols*. Ed. V. Balan (New York, NY: Springer New York), 151–159.

Marklein, G., Josten, M., Klanke, U., Muller, E., Horre, R., Maier, T., et al. (2009). Matrix-assisted laser desorption ionization-time of flight mass spectrometry for fast and reliable identification of clinical yeast isolates. *J. Clin. Microbiol.* 47 (9), 2912–2917. doi: 10.1128/JCM.00389-09

Marr, A. G., and Ingraham, J. L. (1962). Effect of Temperature on the Composition of Fatty Acids in Escherichia Coli. *J. Bacteriol.* 84 (6), 1260–1267. doi: 10.1128/JB.84.6.1260-1267.1962

Marrakchi, H., Laneelle, M. A., and Daffe, M. (2014). Mycolic acids: structures, biosynthesis, and beyond. *Chem. Biol.* 21 (1), 67–85. doi: 10.1016/j.chembiol.2013.11.011

Martiny, D., Busson, L., Wybo, I., El Haj, R. A., Dediste, A., and Vandenberg, O. (2012). Comparison of the Microflex LT and Vitek MS systems for routine identification of bacteria by matrix-assisted laser desorption ionization-time of flight mass spectrometry. *J. Clin. Microbiol.* 50 (4), 1313–1325. doi: 10.1128/JCM.05971-11

Marumo, K., and Aoki, Y. (1990). Discriminant analysis of cellular fatty acids of Candida species, Torulopsis glabrata, and Cryptococcus neoformans determined by gas-liquid chromatography. *J. Clin. Microbiol.* 28 (7), 1509–1513. doi: 10.1128/JCM.28.7.1509-1513.1990

McCartney, C. A., Bull, I. D., and Dewhurst, R. J. (2013). Chemical markers for rumen methanogens and methanogenesis. *Animal* 7 Suppl 2, 409–417. doi: 10.1017/S1751731113000694

Mishra, A. K., Alves, J. E., Krumbach, K., Nigou, J., Castro, A. G., Geurtsen, J., et al. (2012). Differential arabinan capping of lipoarabinomannan modulates innate immune responses and impacts T helper cell differentiation. *J. Biol. Chem.* 287 (53), 44173–44183. doi: 10.1074/jbc.M112.402396

Moffatt, J. H., Harper, M., and Boyce, J. D. (2019). Mechanisms of Polymyxin Resistance. *Adv. Exp. Med. Biol.* 1145, 55–71. doi: 10.1007/978-3-030-16373-0_5

Mosca, A., Russo, F., Miragliotta, L., Iodice, M. A., and Miragliotta, G. (2007). Utility of gas chromatography for rapid identification of mycobacterial species frequently encountered in clinical laboratory. *J. Microbiol. Methods* 68 (2), 392–395. doi: 10.1016/j.mimet.2006.09.017

Moss, C. W., and Lewis, V. J. (1967). Characterization of clostridia by gas chromatography. I. Differentiation of species by cellular fatty acids. *Appl. Microbiol.* 15 (2), 390–397.

Moss, C. W., Dees, S. B., and Guerrant, G. O. (1980). Gas-liquid chromatography of bacterial fatty acids with a fused-silica capillary column. *J. Clin. Microbiol.* 12 (1), 127–130. doi: 10.1128/JCM.12.1.127-130.1980

Murray, P. R. (2012). What is new in clinical microbiology-microbial identification by MALDI-TOF mass spectrometry: a paper from the 2011 William Beaumont Hospital Symposium on molecular pathology. *J. Mol. Diagn.* 14 (5), 419–423. doi: 10.1016/j.jmoldx.2012.03.007

Nakamura, M. T., Yudell, B. E., and Loor, J. J. (2014). Regulation of energy metabolism by long-chain fatty acids. *Prog. Lipid Res.* 53, 124–144. doi: 10.1016/j.plipres.2013.12.001

Nessar, R., Cambau, E., Reyrat, J. M., Murray, A., and Gicquel, B. (2012). Mycobacterium abscessus: a new antibiotic nightmare. *J. Antimicrob. Chemother.* 67 (4), 810–818. doi: 10.1093/jac/dkr578

Niyogi, S. K. (2005). Shigellosis. *J. Microbiol.* 43 (2), 133–143.

O'Leary, W. M. (1962). The Fatty Acids of Bacteria. *Bacteriol. Rev.* 26 (4), 421–447.

Orskov, F., and Orskov, I. (1992). Escherichia coli serotyping and disease in man and animals. *Can. J. Microbiol.* 38 (7), 699–704.

Ortalo-Magne, A., Lemassu, A., Laneelle, M. A., Bardou, F., Silve, G., Gounon, P., et al. (1996). Identification of the surface-exposed lipids on the cell envelopes of Mycobacterium tuberculosis and other mycobacterial species. *J. Bacteriol.* 178 (2), 456–461. doi: 10.1128/jb.178.2.456-461.1996

Osterhout, G. J., Shull, V. H., and Dick, J. D. (1991). Identification of clinical isolates of gram-negative nonfermentative bacteria by an automated cellular fatty acid identification system. *J. Clin. Microbiol.* 29 (9), 1822–1830. doi: 10.1128/JCM.29.9.1822-1830.1991

Osterhout, D. J., Ebner, S., Xu, J., Ornitz, D. M., Zazanis, G. A., and McKinnon, R. D. (1997). Transplanted oligodendrocyte progenitor cells expressing a dominant-

negative FGF receptor transgene fail to migrate in vivo. *J. Neurosci.* 17 (23), 9122–9132.

Patel, R. (2015). MALDI-TOF MS for the diagnosis of infectious diseases. *Clin. Chem.* 61 (1), 100–111. doi: 10.1373/clinchem.2014.221770

Percy, M. G., and Grundling, A. (2014). Lipoteichoic acid synthesis and function in gram-positive bacteria. *Annu. Rev. Microbiol.* 68, 81–100. doi: 10.1146/annurev-micro-091213-112949

Poirel, L., Jayol, A., and Nordmann, P. (2017). Polymyxins: Antibacterial Activity, Susceptibility Testing, and Resistance Mechanisms Encoded by Plasmids or Chromosomes. *Clin. Microbiol. Rev.* 30 (2), 557–596. doi: 10.1128/CMR.00064-16

Raetz, C. R., and Whitfield, C. (2002). Lipopolysaccharide endotoxins. *Annu. Rev. Biochem.* 71, 635–700. doi: 10.1146/annurev.biochem.71.110601.135414

Reichmann, N. T., and Grundling, A. (2011). Location, synthesis and function of glycolipids and polyglycerolphosphate lipoteichoic acid in Gram-positive bacteria of the phylum Firmicutes. *FEMS Microbiol. Lett.* 319 (2), 97–105. doi: 10.1111/j.1574-6968.2011.02260.x

Ripoll, F., Deshayes, C., Pasek, S., Laval, F., Beretti, J. L., Biet, F., et al. (2007). Genomics of glycopeptidolipid biosynthesis in Mycobacterium abscessus and M. chelonae. *BMC Genomics* 8, 114. doi: 10.1186/1471-2164-8-114

Rodrigues, C., Novais, A., Sousa, C., Ramos, H., Coque, T. M., Canton, R., et al. (2017). Elucidating constraints for differentiation of major human Klebsiella pneumoniae clones using MALDI-TOF MS. *Eur. J. Clin. Microbiol. Infect. Dis.* 36 (2), 379–386. doi: 10.1007/s10096-016-2812-8

Rodriguez-Temporal, D., Perez-Risco, D., Struzka, E. A., Mas, M., and Alcaide, F. (2018). Evaluation of Two Protein Extraction Protocols Based on Freezing and Mechanical Disruption for Identifying Nontuberculous Mycobacteria by Matrix-Assisted Laser Desorption Ionization-Time of Flight Mass Spectrometry from Liquid and Solid Cultures. *J. Clin. Microbiol.* 56 (4). doi: 10.1128/JCM.01548-17

Roethlisberger, P., Iida-Tanaka, N., Hollemeyer, K., Heinzle, E., Ishizuka, I., and Fischer, W. (2000). Unique poly(glycerophosphate) lipoteichoic acid and the glycolipids of a Streptococcus sp. closely related to Streptococcus pneumoniae. *Eur. J. Biochem.* 267 (17), 5520–5530. doi: 10.1046/j.1432-1327.2000.01613.x

Ryu, S. Y., Wendt, G. A., Chandler, C. E., Ernst, R. K., and Goodlett, D. R. (2019). Model-Based Spectral Library Approach for Bacterial Identification via Membrane Glycolipids. *Anal. Chem.* 91 (17), 11482–11487. doi: 10.1021/acs.analchem.9b03340

Saichek, N. R., Cox, C. R., Kim, S., Harrington, P. B., Stambach, N. R., and Voorhees, K. J. (2016). Strain-level Staphylococcus differentiation by CeO2-metal oxide laser ionization mass spectrometry fatty acid profiling. *BMC Microbiol.* 16, 72. doi: 10.1186/s12866-016-0658-y

Saleeb, P. G., Drake, S. K., Murray, P. R., and Zelazny, A. M. (2011). Identification of mycobacteria in solid-culture media by matrix-assisted laser desorption ionization-time of flight mass spectrometry. *J. Clin. Microbiol.* 49 (5), 1790–1794. doi: 10.1128/JCM.02135-10

Saromi, K., England, P., Tang, W., Kostrzewa, M., Corran, A., Woscholski, R., et al. (2020). Rapid Glycosyl-Inositol-Phospho-Ceramides fingerprint from filamentous fungi pathogens using the MALDI Biotyper Sirius system. *Rapid Commun. Mass. Spectrom.* 34 (22), e8904. doi: 10.1002/rcm.8904

Schenk, E. R., Nau, F., Thompson, C. J., Tse-Dinh, Y. C., and Fernandez-Lima, F. (2015). Changes in lipid distribution in E. coli strains in response to norfloxacin. *J. Mass. Spectrom.* 50 (1), 88–94. doi: 10.1002/jms.3500

Schiller, J., Suss, R., Fuchs, B., Muller, M., Petkovic, M., Zschornig, O., et al. (2007). The suitability of different DHB isomers as matrices for the MALDI-TOF MS analysis of phospholipids: which isomer for what purpose? *Eur. Biophys. J.* 36 (4-5), 517–527. doi: 10.1007/s00249-006-0090-6

Schneewind, O., and Missiakas, D. (2014). Lipoteichoic acids, phosphate-containing polymers in the envelope of gram-positive bacteria. *J. Bacteriol.* 196 (6), 1133–1142. doi: 10.1128/JB.01155-13

Schulthess, B., Bloemberg, G. V., Zbinden, A., Mouttet, F., Zbinden, R., Bottger, E. C., et al. (2016). Evaluation of the Bruker MALDI Biotyper for Identification of Fastidious Gram-Negative Rods. *J. Clin. Microbiol.* 54 (3), 543–548. doi: 10.1128/JCM.03107-15

Shiraishi, T., Yokota, S., Morita, N., Fukiya, S., Tomita, S., Tanaka, N., et al. (2013). Characterization of a Lactobacillus gasseri JCM 1131T lipoteichoic acid with a novel glycolipid anchor structure. *Appl. Environ. Microbiol.* 79 (10), 3315–3318. doi: 10.1128/AEM.00243-13

Simenel, C., Coddeville, B., Delepierre, M., Latge, J. P., and Fontaine, T. (2008). Glycosylinositolphosphoceramides in Aspergillus fumigatus. *Glycobiology* 18 (1), 84–96. doi: 10.1093/glycob/cwm122

Singhal, N., Kumar, M., Kanaujia, P. K., and Virdi, J. S. (2015). MALDI-TOF mass spectrometry: an emerging technology for microbial identification and diagnosis. *Front. Microbiol.* 6:791:791. doi: 10.3389/fmicb.2015.00791

Sohlenkamp,, and Geiger, O. (2016). Bacterial membrane lipids: diversity in structures and pathways. *FEMS Microbiol. Rev.* 40 (1), 133–159. doi: 10.1093/femsre/fuv008

Sollai, M., Villanueva, L., Hopmans, E. C., Keil, R. G., and Sinninghe Damste, J. S. (2019a). Archaeal Sources of Intact Membrane Lipid Biomarkers in the Oxygen Deficient Zone of the Eastern Tropical South Pacific. *Front. Microbiol.* 10, 765. doi: 10.3389/fmicb.2019.00765

Sollai, M., Villanueva, L., Hopmans, E. C., Reichart, G. J., and Sinninghe Damste, J. S. (2019b). A combined lipidomic and 16S rRNA gene amplicon sequencing approach reveals archaeal sources of intact polar lipids in the stratified Black Sea water column. *Geobiology* 17 (1), 91–109. doi: 10.1111/gbi.12316

Song, S. H., Park, K. U., Lee, J. H., Kim, E. C., Kim, J. Q., and Song, J. (2009). Electrospray ionization-tandem mass spectrometry analysis of the mycolic acid profiles for the identification of common clinical isolates of mycobacterial species. *J. Microbiol. Methods* 77 (2), 165–177. doi: 10.1016/j.mimet.200901.023

Stevenson, L. G., Drake, S. K., and Murray, P. R. (2010). Rapid identification of bacteria in positive blood culture broths by matrix-assisted laser desorption ionization-time of flight mass spectrometry. *J. Clin. Microbiol.* 48 (2), 444–447. doi: 10.1128/JCM.01541-09

Suling, W. J., and O'Leary, W. M. (1977). Lipids of antibiotic-resistant and -susceptible members of the Enterobacteriaceae. *Can. J. Microbiol.* 23 (8), 1045–1051. doi: 10.1139/m77-156

Sun, G., Yang, K., Zhao, Z., Guan, S., Han, X., and Gross, R. W. (2008). Matrix-assisted laser desorption/ionization time-of-flight mass spectrometric analysis of cellular glycerophospholipids enabled by multiplexed solvent dependent analyte-matrix interactions. *Anal. Chem.* 80 (19), 7576–7585. doi: 10.1021/ac801200w

Sun, J., Zhang, H., Liu, Y. H., and Feng, Y. (2018). Towards Understanding MCR-like Colistin Resistance. *Trends Microbiol.* 26 (9), 794–808. doi: 10.1016/j.tim.2018.02.006

Theel, E. S., Schmitt, B. H., Hall, L., Cunningham, S. A., Walchak, R. C., Patel, R., et al. (2012). Formic acid-based direct, on-plate testing of yeast and Corynebacterium species by Bruker Biotyper matrix-assisted laser desorption ionization-time of flight mass spectrometry. *J. Clin. Microbiol.* 50 (9), 3093–3095. doi: 10.1128/JCM.01045-12

Toledo, M. S., Levery, S. B., Bennion, B., Guimaraes, L. L., Castle, S. A., Lindsey, R., et al. (2007). Analysis of glycosylinositol phosphorylceramides expressed by the opportunistic mycopathogen Aspergillus fumigatus. *J. Lipid Res.* 48 (8), 1801–1824. doi: 10.1194/jlr.M700149-JLR200

Tornabene, T. G., Lloyd, R. E., Holzer, G., and Oro, J. (1980). Lipids as a principle for the identification of archaebacteria. *Life Sci. Space Res.* 18, 109–121. doi: 10.1016/b978-0-08-024436-5.50016-0

van Meer, G., Voelker, D. R., and Feigenson, G. W. (2008). Membrane lipids: where they are and how they behave. *Nat. Rev. Mol. Cell Biol.* 9 (2), 112–124. doi: 10.1038/nrm2330

van Veen, S. Q., Claas, E. C., and Kuijper, E. J. (2010). High-throughput identification of bacteria and yeast by matrix-assisted laser desorption ionization-time of flight mass spectrometry in conventional medical microbiology laboratories. *J. Clin. Microbiol.* 48 (3), 900–907. doi: 10.1128/JCM.02071-09

Veys, A., Callewaert, W., Waelkens, E., and Van den Abbeele, K. (1989). Application of gas-liquid chromatography to the routine identification of nonfermenting gram-negative bacteria in clinical specimens. *J. Clin. Microbiol.* 27 (7), 1538–1542. doi: 10.1128/JCM.27.7.1538-1542.1989

Vitale, R., Roine, E., Bamford, D. H., and Corcelli, A. (2013). Lipid fingerprints of intact viruses by MALDI-TOF/mass spectrometry. *Biochim. Biophys. Acta* 1831 (4), 872–879. doi: 10.1016/j.bbalip.2013.01.011

Wallace, P. L., Hollis, D. G., Weaver, R. E., and Moss, C. W. (1990). Biochemical and chemical characterization of pink-pigmented oxidative bacteria. *J. Clin. Microbiol.* 28 (4), 689–693. doi: 10.1128/JCM.28.4.689-693.1990

Weis, C. V., Jutzeler, C. R., and Borgwardt, K. (2020). Machine learning for microbial identification and antimicrobial susceptibility testing on MALDI-

TOF mass spectra: a systematic review. *Clin. Microbiol. Infect.* 26 (10), 1310–1317. doi: 10.1016/j.cmi.2020.03.014

Welch, D. F. (1991). Applications of cellular fatty acid analysis. *Clin. Microbiol. Rev.* 4 (4), 422–438. doi: 10.1128/cmr.4.4.422

Westblade, L. F., Jennemann, R., Branda, J. A., Bythrow, M., Ferraro, M. J., Garner, O. B., et al. (2013). Multicenter study evaluating the Vitek MS system for identification of medically important yeasts. *J. Clin. Microbiol.* 51 (7), 2267–2272. doi: 10.1128/JCM.00680-13

Wilen, C. B., McMullen, A. R., and Burnham, C. A. (2015). Comparison of Sample Preparation Methods, Instrumentation Platforms, and Contemporary Commercial Databases for Identification of Clinically Relevant Mycobacteria by Matrix-Assisted Laser Desorption Ionization-Time of Flight Mass Spectrometry. *J. Clin. Microbiol.* 53 (7), 2308–2315. doi: 10.1128/JCM.00567-15

Wilkendorf, L. S., Bowles, E., Buil, J. B., van der Lee, H. A. L., Posteraro, B., Sanguinetti, M., et al. (2020). Update on Matrix-Assisted Laser Desorption Ionization-Time of Flight Mass Spectrometry Identification of Filamentous Fungi. *J. Clin. Microbiol.* 58 (12). doi: 10.1128/JCM.01263-20

Wilson, D. A., Young, S., Timm, K., Novak-Weekley, S., Marlowe, E. M., Madisen, N., et al. (2017). Multicenter Evaluation of the Bruker MALDI Biotyper CA System for the Identification of Clinically Important Bacteria and Yeasts. *Am. J. Clin. Pathol.* 147 (6), 623–631. doi: 10.1093/ajcp/aqw225

Woese, C. R., Magrum, L. J., and Fox, G. E. (1978). Archaebacteria. *J. Mol. Evol.* 11 (3), 245–251. doi: 10.1007/BF01734485

Conflict of Interest: GL-M is a co-inventor of the MALDIxin test for which a patent has been filed by Imperial Innovations. MK is an employee of Bruker, the manufacturer of the MALDI Biotyper system.

The remaining author declares that the research was conducted in the absence of any commercial or financial relationships that could be construed as a potential conflict of interest.

frontiers in Cellular and Infection Microbiology

ORIGINAL RESEARCH
published: 18 February 2021
doi: 10.3389/fcimb.2021.628828

Evaluation of Autof MS 1000 and Vitek MS MALDI-TOF MS System in Identification of Closely-Related Yeasts Causing Invasive Fungal Diseases

Qiaolian Yi[1†], Meng Xiao[1,2†], Xin Fan[3], Ge Zhang[1], Yang Yang[1], Jing-Jia Zhang[1], Si-Meng Duan[1], Jing-Wei Cheng[4], Ying Li[1], Meng-Lan Zhou[1], Shu-Ying Yu[1], Jing-Jing Huang[1], Xin-Fei Chen[1], Xin Hou[1], Fanrong Kong[5], Timothy Kudinha[6,7] and Ying-Chun Xu[1] on behalf of CHIF-NET study group*

[1] Department of Laboratory Medicine, and Beijing Key Laboratory for Mechanisms Research and Precision Diagnosis of Invasive Fungal Diseases, Peking Union Medical College Hospital, Chinese Academy of Medical Sciences, Beijing, China, [2] Graduate School, Peking Union Medical College, Beijing, China, [3] Department of Infectious Diseases and Clinical Microbiology, Beijing Chaoyang Hospital, Capital Medical University, Beijing, China, [4] Department of Laboratory Medicine, Beijing Friendship Hospital, Capital Medical University, Beijing, China, [5] Centre for Infectious Diseases and Microbiology Laboratory Services, Institute of Clinical Pathology and Medical Research, New South Wales Health Pathology, Westmead Hospital, The University of Sydney, Westmead, NSW, Australia, [6] Department of Clinical Laboratory, Charles Sturt University, Orange, NSW, Australia, [7] New South Wales Health Pathology, Regional and Rural, Orange Hospital, NSW, Australia

Matrix-assisted laser desorption ionization-time of flight mass spectrometry (MALDI-TOF MS) has been accepted as a rapid, accurate, and less labor-intensive method in the identification of microorganisms in clinical laboratories. However, there is limited data on systematic evaluation of its effectiveness in the identification of phylogenetically closely-related yeast species. In this study, we evaluated two commercially available MALDI-TOF systems, Autof MS 1000 and Vitek MS, for the identification of yeasts within closely-related species complexes. A total of 1,228 yeast isolates, representing 14 different species of five species complexes, including 479 of *Candida parapsilosis* complex, 323 of *Candida albicans* complex, 95 of *Candida glabrata* complex, 16 of *Candida haemulonii* complex (including two *Candida auris*), and 315 of *Cryptococcus neoformans* complex, collected under the National China Hospital Invasive Fungal Surveillance Net (CHIF-NET) program, were studied. Autof MS 1000 and Vitek MS systems correctly identified 99.2% and 89.2% of the isolates, with major error rate of 0.4% versus 1.6%, and minor error rate of 0.1% versus 3.5%, respectively. The proportion of isolates accurately identified by Autof MS 1000 and Vitek MS per each yeast complex, respectively, was as follows; *C. albicans* complex, 99.4% vs 96.3%; *C. parapsilosis* complex, 99.0% vs 79.1%; *C glabrata* complex, 98.9% vs 94.7%; *C. haemulonii* complex, 100% vs 93.8%; and *C. neoformans*, 99.4% vs 95.2%. Overall, Autof MS 1000 exhibited good capacity in yeast identification while Vitek MS had lower identification accuracy, especially in the identification of less common species within phylogenetically closely-related species complexes.

Keywords: MALDI-TOF MS, closely-related yeasts, invasive fungal diseases, Autof MS 1000, Vitek MS

OPEN ACCESS

Edited by:
Yi-Wei Tang,
Cepheid, United States

Reviewed by:
Bryan Schmitt,
Indiana University Bloomington, United States
Charles William Stratton,
Vanderbilt University Medical Center, United States

****Correspondence:***
Ying-Chun Xu
xycpumch@139.com

[†]These authors have contributed equally to this work

Specialty section:
This article was submitted to Clinical Microbiology, a section of the journal Frontiers in Cellular and Infection Microbiology

Received: *13 November 2020*
Accepted: *04 January 2021*
Published: *18 February 2021*

Citation:
Yi Q, Xiao M, Fan X, Zhang G, Yang Y, Zhang J-J, Duan S-M, Cheng J-W, Li Y, Zhou M-L, Yu S-Y, Huang J-J, Chen X-F, Hou X, Kong F, Kudinha T and Xu Y-C (2021) Evaluation of Autof MS 1000 and Vitek MS MALDI-TOF MS System in Identification of Closely-Related Yeasts Causing Invasive Fungal Diseases. Front. Cell. Infect. Microbiol. 11:628828. doi: 10.3389/fcimb.2021.628828

INTRODUCTION

Invasive fungal diseases (IFD) have become an emerging healthcare problem worldwide. It is associated with high rates of morbidity and mortality in immunocompromised individuals and critically ill patients (Miceli et al., 2011; Lockhart et al., 2017). Rapid, reliable, and species-specific diagnosis of fungal pathogens causing IFD is a prerequisite for cost-effective and successful therapy. However, some closely-related yeast species complexes are difficult to identify by conventional morphological or biochemical methods, and several of these cryptic species have distinct antifungal susceptibility profiles associated with specific clinical settings. These include *Candida parapsilosis sensu stricto*, *Candida metapsilosis*, *Candida orthopsilosis*, *Lodderomyces elongisporus* of the *C. parapsilosis* complex, *Candida albicans* and *Candida dubliniensis* of the *C. albicans* complex, *Candida glabrata sensu stricto*, *Candida nivariensis*, and *Candida bracarensis* of the *C. glabrata* complex, *Cryptococcus neoformans*, and *Cryptococcus gattii* of the *C. neoformans* complex, and finally, *Candida haemulonii*, *Candida duobushaemulonii*, and *Candida auris* of the *C. haemulonii* complex (also refered as multidrug-resistant [MDR] complex) (Muñoz et al., 2018).

Within less than a decade, the introduction of MALDI-TOF MS has enabled rapid and accurate identification of microorganisms including bacteria, mycobacteria, yeasts and filamentous fungi in clinical laboratories (Odds et al., 2007; Rychert et al., 2018) Autof MS 1000 (Autobio Diagnostics, Zhengzhou, China), a commercial MALDI-TOF MS system, has been available for routine pathogen identification in many clinical laboratories in China since 2018 (Wang et al., 2019). However, its performance and application in the identification of yeasts has not been fully evaluated. The purpose of this study was to evaluate the accuracy of Autof MS 1000 and Vitek MS in the identification of yeasts causing IFDs, especially for pathogens within closely-related species complexes.

MATERIALS AND METHODS

Yeast Isolates

A total of 1,228 yeast isolates causing IFDs, and collected from 57 hospitals in China during the period August 2016 to July 2017, under the CHIF-NET program, were studied. Isolates were initially inoculated on a chromogenic agar (Brilliance C., Oxoid Ltd., Hampshire, United Kingdom) then subcultured on Sabouraud dextrose agar (SDA), and incubated at 35°C for 24 to 48 h.

Sequencing-Based Identification

All isolates were identified by DNA sequencing of the internal transcribed spacer (ITS) region, which was considered the "gold standard". Primers ITS1 (5'-TCC GTA GGT GAA CCT GCG G-3') and ITS4 (5'-TCC TCC GCT TAT TGA TAT GC-3') were used to amplify the full-length ITS region. Amplification of the ITS region was carried out under the following conditions: denaturation at 94°C for 5 min, followed by 30 cycles of denaturation at 94°C for 30 s, annealing at 56°C for 90 s, and elongation at 72°C for 75 s, with a final extension step of 10 min at 72°C. Strain species identification was performed as described in a previous study (Wang et al., 2016).

Vitek MS Identification

A thin smear of a freshly cultured isolate was deposited onto a target plate, and 1 μl of formic acid (70%) was added. After air-drying, each spot was overlaid with 1 μl of α-cyano-4-hydroxycinnamic acid (HCCA) matrix (bioMérieux). The matrix was then allowed to dry at room air. *E.coli* ATCC 8739 was utilized as a calibrant and quality control strain per acquisition group on each slide. Measurement was then performed following the manufacturer's suggested setting using automated collecting spectra. Captured spectra were analyzed based on IVD database version 3.0. For data analysis, a "green frame" indicator with a reliability (probability) of between 60.0% and 99.9% indicated sufficient species level identification, and a "yellow triangle" indicator denoted low resolution. If no identification (NoID) was provided, the isolate was considered unidentified and presented as a "red circle".

Autof MS 1000 Identification

Autof MS 1000 is a new Chinese brand of MALDI-TOF MS platform for identification of micro-organisms which was approved for clinical use by China National Medical Products Administration in 2020. The operation process of this platform is similar to that of Vitek MS. A thin smear of a freshly cultured isolate was deposited onto a target plate, and 1 μl of formic acid (70%) was added. After air-drying, each spot was overlaid with 1 μl of α-cyano-4-hydroxycinnamic acid (HCCA) matrix. But without a fixed calibration point, Autof MS 1000 system runs identification immediately after sampling. The database (Autof Acquirer Version V2.0.18) contains 14,125 microbial strains comprising 4,226 species, 360 of which are fungal species. Results were interpreted based on the log score value of the first best match following manufacturer's instructions as follows: 0.0≤score<6.0, not reliable identification; 6.0≤score<9.0, genus-level reliable identification and probable species-level identification; score≥9.0 species-level reliable identification.

Criteria for Identification and Discrepant Analysis

In the case of discrepant results or no identification result for one or both methods, the result of ITS sequencing was considered the final correct identification. A major error (ME) in identification by each of the methods studied (compared to the gold standard ITS) was defined as the incorrect genus identification ("no identification" not included). A minor error (MIE) was defined as the correct genus identification with incorrect species identification.

RESULTS

Correct Identification by Vitek MS and Autof MS 1000

A total of 1,228 isolates representing 14 different yeast species within five closely-related species complexes (ie. *C. albicans*

complex, *C. parapsilosis* complex, *C. glabrata* complex, *C. haemulonii* complex and *C. neoformans* complex), were evaluated in this study. Out of these isolates, 1,218 (99.2%) were correctly identified to species level by the Autof MS 1000 system, while 1,095 (89.2%) were correctly identified by Vitek MS (**Table 1**).

A majority (96.3%, 311/323) of *C. albicans* complex isolates were correctly identified to the species level by Vitek MS. For Autof MS 1000, the identification accuracy rate for *C. albicans* complex isolates was 99.4% (321/323). For *C. glabrata* complex isolates, 98.9% (94/95) were correctly identified to the species level by Autof MS 1000, which was higher than that of Vitek MS at 94.7% (90/95). For *C. parapsilosis* complex, 79.1% (379/479) of the isolates were correctly identified to species level by Vitek MS, which was much less than that of Autof MS 1000 at 99.0% (474/479). For *C. neoformans* complex, 95.2% (300/315) were correctly identified to the species level by Vitek MS while for Autof MS 1000, 99.4% (313/315) were correctly identified to species level (**Table 1**).

Comparison of "No Identification" Results

Four isolates (0.3%) yielded "no identification" result by Autos MS 1000, and 70 (5.7%) by Vitek MS (**Table 1**).

For species included in both systems' identification databases, there were two (2/3, 66.6%) *C. nivariensis* isolates and 31 (31/64, 48.4%) of *C. metapsilosis* that were not identified by Vitek MS, which was a direct opposite to Autof MS 1000 which correctly identified both species. There were 5 (5/10, 50.0%) *C. gattii* isolates that were unidentified by Vitek MS.

In addition, *C. bracarensis* (n=1) was correctly identified by Autof MS 1000, but unidentified by Vitek MS as this species is not included in the Vitek MS database IVD 3.0.

Misidentifications by Vitek MS and Autof MS 1000

Autof MS 1000 identification results of five isolates (0.4%) were defined as major error while for Vitek MS it was for 20 isolates (1.6%) (**Table 2**). Only one identification result from an isolate was defined as a minor error for Autof MS 1000, while for Vitek MS, there were 43 (3.5%) isolates whose identification results were considered minor errors. One *C. nivariensis* (n=3) isolate was misidentified as *C. glabrata*; in addition, among *C. metapsilosis* (n=64) isolates, the identification results of five isolates were considered as ME, and 25 as MIE by Vitek MS. For *C. gattii* (n=10) there was one identification result that was considered as MIE by Autof MS 1000, and two by Vitek MS.

DISCUSSION

Accurate identification of pathogens is important to ensure accurate diagnosis of diseases and subsequent proper treatment of the condition. As a newly licensed MALDI-TOF MS platform, few comparisons have been done between Autof MS 1000 and other systems. Recent studies have evaluated the performance of Autof MS 1000 in the identification of *Bacteroides fragilis* group isolates (Wang et al., 2019) and clinically relevant filamentous fungi (Sun et al., 2020). In this study, we evaluated the performance of MALDI-TOF MS systems, Autof MS 1000 and Vitek MS, in the identification of closely-related yeast species causing IFDs, using ITS sequencing as the reference method. Previous studies have shown that the accuracy for yeast identification ranges from 76.5% to 96.2% for Vitek MS (Wang et al., 2016). In this study, performance of Vitek MS in the identification of yeasts showed an overall accuracy of 89.2%.

TABLE 1 | Results of matrix-assisted laser desorption ionization-time of flight mass spectrometry (MALDI-TOF MS) identification by Autof MS 1000 and Vitek MS.

Organism defined by ITS sequencing (no. of isolates)	Autof MS 1000								Vitek MS							
	Agree		ME		MIE		No ID		Agree		ME		MIE		No ID	
C. parapsilosis complex (n=479)	474	99.0%	2	0.4%	0	0.0%	3	0.6%	379	79.1%	9	1.9%	40	8.4%	51	10.6%
C. parapsilosis (384)	380	99.0%	1	0.3%	0	0.0%	3	0.8%	366	95.3%	3	0.8%	0	0.0%	15	3.9%
C. metapsilosis (64)	64	100.0%	0	0.0%	0	0.0%	0	0.0%	3	4.7%	5	7.8%	25	39.1%	31	48.4%
C. orthopsilosis (26)	25	96.2%	1	3.8%	0	0.0%	0	0.0%	6	23.1%	1	3.8%	15	57.7%	4	15.4%
L. elongisporus (5)	5	100.0%	0	0.0%	0	0.0%	0	0.0%	4	80.0%	0	0.0%	0	0.0%	1	20.0%
C. albicans complex (n=323)	321	99.4%	2	0.6%	0	0.0%	0	0.0%	311	96.3%	8	2.5%	0	0.0%	4	1.2%
C. albicans (322)	320	99.4%	2	0.6%	0	0.0%	0	0.0%	310	96.3%	8	2.5%	0	0.0%	4	1.2%
C. dubliniensis (1)	1	100.0%	0	0.0%	0	0.0%	0	0.0%	1	100.0%	0	0.0%	0	0.0%	0	0.0%
C. neoformans complex (n=315)	313	99.4%	0	0.0%	1	0.3%	1	0.3%	300	95.2%	2	0.6%	2	0.6%	11	3.5%
C. neoformans (305)	304	99.7%	0	0.0%	0	0.0%	1	0.3%	297	97.4%	2	0.7%	0	0.0%	6	2.0%
C. gattii (10)	9	90.0%	0	0.0%	1	10.0%	0	0.0%	3	30.0%	0	0.0%	2	20.0%	5	50.0%
C. glabrata complex (n=95)	94	98.9%	1	1.1%	0	0.0%	0	0.0%	90	94.7%	1	1.1%	1	1.1%	3	3.2%
C. glabrata (91)	90	98.9%	1	1.1%	0	0.0%	0	0.0%	90	98.9%	1	1.1%	0	0.0%	0	0.0%
C. nivariensis (3)	3	100.0%	0	0.0%	0	0.0%	0	0.0%	0	0.0%	0	0.0%	1	33.3%	2	66.7%
*C. bracarensis** (1)	1	100.0%	0	0.0%	0	0.0%	0	0.0%	0	0.0%	0	0.0%	0	0.0%	1	100.0%
C. haemulonii complex (n=16)	16	100.0%	0	0.0%	0	0.0%	0	0.0%	15	93.8%	0	0.0%	0	0.0%	1	6.3%
C. haemulonii (11)	11	100.0%	0	0.0%	0	0.0%	0	0.0%	11	100.0%	0	0.0%	0	0.0%	0	0.0%
C. duobushaemulonii (3)	3	100.0%	0	0.0%	0	0.0%	0	0.0%	2	66.7%	0	0.0%	0	0.0%	1	33.3%
C. auris (2)	2	100.0%	0	0.0%	0	0.0%	0	0.0%	2	100.0%	0	0.0%	0	0.0%	0	0.0%
Total (1228)	1218	99.2%	5	0.4%	1	0.1%	4	0.3%	1095	89.2%	20	1.6%	43	3.5%	70	5.7%

ITS, internal transcribed spacer region; ME, major error; MIE, minor error; No ID, no identification.
**Candida bracarensis was not included in database IVD 3.0 of Vitek MS system.*

TABLE 2 | Misidentification and "no identification" results by two systems.

Species by ITS sequencing	Autof MS 1000	Vitek MS
C. parapsilosis complex (n=479)		
C. parapsilosis (384)	No ID (3) *C. guilliermondii* (1)	No ID (15) *C. albicans* (2) *C. pelliculosa* (1)
C. orthopsilosis (26)	*C. albicans* (1)	No ID (4) *C. parapsilosis* (15) *C. albicans* (1)
C. metapsilosis (64)	0	No ID (32) *C. parapsilosis* (15) *C. orthopsilosis* (5) *C. pelliculosa* (1) *C. pulcherrima* (2) *C. laurentii* (1) *L. elongisporus* (4) *P. italicum* (1)
L. elongisporus (5)	0	No ID (1)
C. glabrata complex (n=95)		
C. glabrata (91)	*C. guilliermondii* (1)	*C. parapsilosis* (1)
C. nivariensis (3)	0	No ID (2) *C. glabrata* (1)
C. bracarensis (1)	0	No ID (1)
C. albicans complex (n=323)		
C. albicans (322)	*C. parapsilosis* (1) *C. tropicalis* (1)	No ID (4) *C. utilis* (4) *C. parapsilosis* (1) *C. tropicalis* (1) *C. glabrata/C. tropicalis/C. famata* (1) *C. tropicalis/C. dubliniensis* (1)
C. dubliniensis (1)	0	0
C. neoformans complex (n=315)		
C. neoformans (305)	No ID (1)	No ID (6) *C. tropicalis* (1) *C. parapsilosis* (1)
C. gattii (10)	*C. neoformans* (1)	No ID (5) *C. neoformans* (2)
C. haemulonii complex (n=16)		
C. duobushaemulonii (3)	0	No ID (1)
C. haemulonii (11)	0	0
C. auris (2)	0	0

Misidentifications or no identifications were more likely to occur in less-common species within each species complexes. In comparison, Autof MS 1000 system exhibited higher identification accuracy in all species complexes (>98% for all species with overall accuracy of 99.2%).

C. albicans is the most frequent cause of superficial and systemic candidiasis. Before the introduction of further genetic studies, its closely related species, *C. dubliniensis*, was commonly misidentified as *C. albicans* (Sullivan et al., 1995). However, unlike *C. albicans*, *C. dubliniensis* causes fewer cases of systemic candidiasis (Odds et al., 2007). In the present study, both Vitek MS and Autof MS 1000 correctly identified >96% of *C. albicans* isolates, and correctly assigned *C. dubliniensis* to species-level.

C. parapsilosis has become the second to fourth most prevalent *Candida* species worldwide, and even surpasses *C. albicans* in some geographic regions (Harrington et al., 2017; Tóth et al., 2019; Xiao et al., 2020). Before the introduction of molecular tests and further biochemical investigations, *C. orthopsilosis*, and *C. metapsilosis* used to be classified into the *C. parapsilosis* complex (Tavanti et al., 2005). In addition, *L. elongisporus*, which may be misidentified as *C. parapsilosis* by conviential methods, remains underestimated in its clinical significance (Lockhart et al., 2008; Al-Obaid et al., 2018). However, the incidence, pathogenicity, and drug resistance of species within the *C. parapsilosis* complex has been shown to be different (Neji et al., 2017; Xiao et al., 2020). Overall, there was a significant difference in the performance of Autof MS 1000 (99.0%) and Vitek MS (79.1%) in assigning *C. parapsilosis* complex isolates to the correct species-level. Of note, Vitek MS system exhibited significant limitations in correctly identifying *C. orthopsilosis* (accuracy 23.1%) and *C. metapsilosis* (accuracy 4.7%), while Autof MS 1000 correctly identified all 64 *C. metapsilosis* and 96.2% of *C. orthopsilosis* isolates.

C. glabrata has emerged as the second most common cause of invasive candidiasis in the United States (Pfaller and Diekema, 2007), while in China it ranks fourth among clinically invasive yeast infections (Xiao et al., 2015). Its phylogenetically related species, *C. nivariensis* and *C. bracarensis*, were previously identified as *C. glabrata* by routine identification methods (Alcoba-Flórez et al., 2005; Correia et al., 2006). However their clinical significance and epidemiological role in candidiasis is different (Bishop et al., 2008). In this study, both systems correctly identified 98.9% of *C. glabrata* isolates. Autof MS 1000 system correctly identified all three *C. nivariensis* and one *C. bracarensis* isolates. However, no *C. nivariensis* or *C. bracarensis* isolates were correctly identified by Vitek MS. Of note, *C. bracarensis* is not included in the Vitek MS database IVD 3.0.

The basidiomycetous yeasts of the *C. neoformans-C. gattii* species complex are the causative agents of cryptococcosis with different pathogenicity (Samarasinghe and Xu, 2018). *C. neoformans* is more common in AIDS patients, whereas infections caused by *C. gattii* are more often reported in immunocompetent patients (Kwon-Chung et al., 2015). Previously, conventional L-canavanine glycine bromothymol blue (CGB) agar was used to distinguish the two species (Chen et al., 2014). In this study, Vitek MS and Autof MS 1000 correctly assigned 97.4% and 99.7% of *C. neoformans* isolates to species level, respectively. However, in 10 C. *gattii* isolates, the Vitek MS came up with a " no identification" result in three isolates and misidentified two isolates as *C. neoformans*. In contrast, Autof MS 1000 accurately identified 90% of the *C. gattii* isolates with only one isolate misidentified as *C. neoformans*.

C. auris has recently drawn much attention clinically due to its multidrug resistant characteristics and fast spread worldwide (Spivak and Hanson, 2018). *C. auris*, and its closely-related species *C. haemulonii*, *C. duobushaemulonii*, and *C. pseudohaemulonii*, are difficult to identify using standard laboratory methods (Muñoz et al., 2018). In the identification

of this species complex, both Autof MS 1000 and Vitek MS performed well, with only one isolate of *C. duobushaemulonii* not identified by Vitek MS.

The principle of MALDI-TOF MS in microbial identification is based on using scoring algorithms to match analyzed spectra with reference spectra (Freiwald and Sauer, 2009; Jang and Kim, 2018). Regardless of the instruments used, distinct algorithms in the same platform result in different identification reports (Panagea et al., 2015; Leyer et al., 2017). For Autof MS 1000, just like MALDI BioTyper (Bruker, Billerica, MA), the database is based on an isolate-specific references approach, while for Vitek MS, it is based on a taxonomical group-specific approach (Cassagne et al., 2016). In this study, Autof MS 1000 performed better than Vitek MS in the identification of closely-related yeasts causing invasive fungal diseases. We suppose that differences in reference spectral databases and scoring algorithms of these two platforms may contribute to the performance discrepancies.

Our study has some limitations. We only evaluated the systems' performance on closely-related yeast species commonly seen in patients, it is not clear whether similar results would have been obtained on other yeast and filamentous fungal species. On the other hand, Vitek MS v3.0 System has shown its excellent accuracy for the identification of filamentous fungi (Rychert et al., 2018). Therefore, further investigations are needed for validating the performance of Autof MS 1000 (compared to other widely-used MALDI-TOF MS systems), in the identifitication of a broader range of bacterial and fungal species.

CONCLUSION

MALDI-TOF MS has previously proven to be valuable in the routine identification of yeast species. In this study, Autof MS 1000 exhibited higher identification accuracy than Vitek MS system in the identification of yeast isolates within different species complexes. The identification capacity of Vitek MS, especially in identifying less-common species within phylogenetically closely-related species complexes, still needs to be improved.

DATA AVAILABILITY STATEMENT

The raw data supporting the conclusions of this article will be made available by the authors, without undue reservation.

AUTHOR CONTRIBUTIONS

QY processed the experimental data, performed the analysis, drafted the manuscript, designed the tables, and revised the manuscript. MX, the main conceptual ideas and proof outline, performed the analysis and revised the manuscript. XF, GZ, YY, J-JZ, and S-MD contributed to sample preparation, performed MALDI-TOF MS identification. J-WC, YL, M-LZ, S-YY, J-JH, X-FC, and XH carried out the experiments, performed 16S rDNA sequencing identification. FK, TK, and Y-CX revised the manuscript, and Y-CX was involved in planning and supervised the work. All authors contributed to the article and approved the submitted version.

FUNDING

This work was supported by a National Major Science and Technology Project (grant number 2018ZX10712001); Beijing Hospitals Authority Youth Programe (QML20190301); the Natural Science Foundation of China (81802042, 81971979, 81802049); Beijing Nova Program (Z201100006820127); Outstanding Young Talents Cultivation Program in Dongcheng District (2018 grant to MX); Beijing Key Clinical Specialty for Laboratory Medicine - Excellent Project (No. ZK201000).

ACKNOWLEDGMENTS

We would like to acknowledge the co-principal investigators in the 57 hospitals participating in the China Hospital Invasive Fungal Surveillance Net (CHIF-NET) program for offering the yeast isolates. They are: (1) Zhang Qiang-Qiang, Huashan Hospital, Fudan University; (2) Liu Yun, Shanghai Changhai Hospital; (3) Xu Ying-Chun, Peking Union Medical College Hospital, Chinese Academy of Medical Sciences; (4) Chu Yun-Zhuo, First Hospital of China Medical University; (5) Liao Kang, the First Affiliated Hospital of Zhongshan University; (6) Sun Zi-Yong, Tongji Hospital, Tongji Medical College Huazhong University of Science & Technology; (7) Yu Hua, Sichuan Academy of Medical Sciences & Sichuan Provincial People's Hospital; (8) Liu Peng-Peng, Affiliated Hospital of Medical College, Qingdao University; (9) Hu Xin-Lan, Fujian Provincial Hospital; (10) Kong Hai-Shen, Sir Run Run Shaw Hospital School of Medicine, Zhejiang University; (11) Mei Ya-Ning, Jiangsu Province People's Hospital; (12) Li Qing-Feng, Public Health Clinical Medical Center of Chengdu; (13) Luo Yan-Ping, the General Hospital of PLA; (14) Meng Ling, Second Affiliated Hospital of Lanzhou University; (15) Kang Mei, Department of Laboratory Medicine, West China Hospital, Sichuan University; (16) Liu Zhi-Yong, Southwest Hospital Affiliated the Third Military Medical University; (17) Yu Yun-Song, Sir Run Run Shaw Hospital; (18) Jia Wei, The General Hospital Affiliated to Ningxia Medical University; (19) Pan Yu-Hong, Fujian Medical University Union Hospital; (20) Xi Hai-Yan, General Hospital of Nanjing Military Area Command; (21) Hu Zhi-Dong, General Hospital of Tianjin Medical University; (22) Fei Ying, The Affiliated Hospital of Guiyang Medical College; (23) Wang Shan-Mei, Henan Provincial People's Hospital; (24) Zhang Li-Ping, the First Affiliated Hospital of Chongqing Medical Hospital; (25) Yang Bin, First Affiliated

Hospital of Fujian Medical University; (26) Liu Wen-En, Xiangya Hospital Central South University; (27) Li Yi-Min, The First Affiliated Hospital of Guangzhou Medical Collage; (28) Liang Jia-Yin, The Third Hospital Attached to Zhongshan University; (29) Huang Jian-Sheng, Central Hospital of Lishui City; (30) Ma Ling, Union Hospital Tongji Medical College of Huazhong University of Science and Technology; (31) Xu Xiu-Li, Xining Hospital, Fourth Military Medical University; (32) Yang Yin-Mei, Guangzhou First People's Hospital Nansha Hospital; (33) Wu Jin-Ying, The Affiliated Yantai Yuhuangding Hospital of Qingdao University; (34) Shan Bin, the First Affiliated Hospital, Kunming Medical University; (35) Li Ruo-Yu, Peking University First Hospital; (36) Zhang Qing, Third Affiliated Hospital of Wenzhou Medical College; (37) Cao Wei, The Second Xiangya Hospital of Central South University; (38) Lu Wei-Ping, Daping Hospital, The Third Affiliated Hospital of Third Military Medical University; (39) Zhang Rong, the Second Affiliated Hospital of Zhejiang University School of Medicine; (40) Zhang Jian-Lei, Tianjin First Centre Hospital; (41) Lei Jin-E, the First Affiliated Hospital of Xi'an Jiaotong University; (42) Ma Xiao-Ling, the First Affiliated Hospital of University of Science and Technology of China; (43) Wang Shu-Feng, First Hospital of Shanxi Medical University; (44) Liang Hong-Jie, the First Affiliated Hospital of Guangxi Medical University; (45) Zhou Ting-Yin, Shanghai Changzheng Hospital; (46) Chen Xiang-Yang, People's Hospital of Zhengzhou; (47) Li Juan, People's Hospital of Xinjiang Uygur Autonomous Region; (48) Jin Yan, Shandong Provincial Hospital; (49) Ha Xiao-Qin, General Hospital of Lanzhou Military Region; (50) Ji Ping, the First Hospital of Xinjiang Medical University; (51) Yu Su-Fei, Taizhou Hospital of Zhejiang Province; (52) Wang Xiao-Ning, the First Hospital of Jilin University; (53) Gu Yi-Hai, 3201 Hospitals of Hanzhong; (54) Wang Hai-Bin, First Affiliated Hospital of PLA General Hospital; (55) Zhang Xian-Feng, The First Affiliated Hospital of Suzhou; (56) Kang Jian-Bang, The Second Hospital of Shanxi Medical University; (57) Xiao Qun, the 94th Hospital of Chinese People's Liberation Army.

REFERENCES

Alcoba-Flórez, J., Méndez-Álvarez, S., Cano, J., Guarro, J., Pérez-Roth, E., and Del Pilar Arévalo, M. (2005). Phenotypic and molecular characterization of Candida nivariensis sp. nov., a possible new opportunistic fungus. *J. Clin. Microbiol.* 43, 4107–4111. doi: 10.1128/JCM.43.8.4107-4111.2005

Al-Obaid, K., Ahmad, S., Joseph, L., and Khan, Z. (2018). Lodderomyces elongisporus: a bloodstream pathogen of greater clinical significance. *New Microbes New Infect.* 26, 20–24. doi: 10.1016/j.nmni.2018.07.004

Bishop, J. A., Chase, N., Magill, S. S., Kurtzman, C. P., Fiandaca, M. J., and Merz, W. G. (2008). Candida bracarensis detected among isolates of Candida glabrata by peptide nucleic acid fluorescence in situ hybridization: Susceptibility data and documentation of presumed infection. *J. Clin. Microbiol.* 46, 443–446. doi: 10.1128/JCM.01986-07

Cassagne, C., Normand, A. C., L'Ollivier, C., Ranque, S., and Piarroux, R. (2016). Performance of MALDI-TOF MS platforms for fungal identification. *Mycoses* 59, 678–690. doi: 10.1111/myc.12506

Chen, S. C., Meyer, W., and Sorrell, C. (2014). Cryptococcus gattii Infections. *Cryptococcus Gattii Infect.* 27, 980–1024. doi: 10.1128/CMR.00126-13

Correia, A., Sampaio, P., James, S., and Pais, C. (2006). Candida bracarensis sp. nov., a novel anamorphic yeast species phenotypically similar to Candida glabrata. *Int. J. Syst. Evol. Microbiol.* 56, 313–317. doi: 10.1099/ijs.0.64076-0

Freiwald, A., and Sauer, S. (2009). Phylogenetic classification and identification of bacteria by mass spectrometry. *Nat. Protoc.* 4, 732–742. doi: 10.1038/nprot.2009.37

Harrington, R., Kindermann, S. L., Hou, Q., Taylor, R. J., Azie, N., and Horn, D. L. (2017). Candidemia and invasive candidiasis among hospitalized neonates and pediatric patients. *Curr. Med. Res. Opin.* 33, 1803–1812. doi: 10.1080/03007995.2017.1354824

Jang, K. S., and Kim, Y. H. (2018). Rapid and robust MALDI-TOF MS techniques for microbial identification: a brief overview of their diverse applications. *J. Microbiol.* 56, 209–216. doi: 10.1007/s12275-018-7457-0

Kwon-Chung, K. J., Fraser, J. A., Doering, T. Á. L., Wang, Z. A., Janbon, G., Idnurm, A., et al. (2015). Cryptococcus neoformans and Cryptococcus gattii, the etiologic agents of cryptococcosis. *Cold Spring Harb. Perspect. Med.* 4, a019760. doi: 10.1101/cshperspect.a019760

Leyer, C., Gregorowicz, G., Mougari, F., Raskine, L., Cambau, E., and De Briel, D. (2017). Comparison of saramis 4.12 and IVD 3.0 vitek MS matrix-assisted laser desorption ionization-time of flight mass spectrometry for identification of mycobacteria from solid and liquid culture media. *J. Clin. Microbiol.* 55, 2045–2054. doi: 10.1128/JCM.00006-17

Lockhart, S. R., Messer, S. A., Pfaller, M. A., and Diekema, D. J. (2008). Lodderomyces elongisporus masquerading as Candida parapsilosis as a cause of bloodstream infections. *J. Clin. Microbiol.* 46, 374–376. doi: 10.1128/JCM.01790-07

Lockhart, S. R., Etienne, K. A., Vallabhaneni, S., Farooqi, J., Chowdhary, A., Govender, N. P., et al. (2017). Simultaneous emergence of multidrug-resistant candida auris on 3 continents confirmed by whole-genome sequencing and epidemiological analyses. *Clin. Infect. Dis.* 64, 134–140. doi: 10.1093/cid/ciw691

Miceli, M. H., Díaz, J. A., and Lee, S. A. (2011). Emerging opportunistic yeast infections. *Lancet Infect. Dis.* 11, 142–151. doi: 10.1016/S1473-3099(10)70218-8

Muñoz, J. F., Gade, L., Chow, N. A., Loparev, V. N., Juieng, P., Berkow, E. L., et al. (2018). Genomic insights into multidrug-resistance, mating and virulence in Candida auris and related emerging species. *Nat. Commun.* 9. doi: 10.1038/s41467-018-07779-6

Neji, S., Hadrich, I., Trabelsi, H., Abbes, S., Cheikhrouhou, F., Sellami, H., et al. (2017). Virulence factors, antifungal susceptibility and molecular mechanisms of azole resistance among Candida parapsilosis complex isolates recovered from clinical specimens. *J. Biomed. Sci.* 24, 1–16. doi: 10.1186/s12929-017-0376-2

Odds, F. C., Hanson, M. F., Davidson, A. D., Jacobsen, M. D., Wright, P., Whyte, J. A., et al. (2007). One year prospective survey of Candida bloodstream infections in Scotland. *J. Med. Microbiol.* 56, 1066–1075. doi: 10.1099/jmm.0.47239-0

Panagea, T., Pincus, D. H., Grogono, D., Jones, M., Bryant, J., Parkhill, J., et al. (2015). Mycobacterium abscessus complex identification with matrix-assisted laser desorption ionization - Time of flight mass spectrometry. *J. Clin. Microbiol.* 53, 2355–2358. doi: 10.1128/JCM.00494-15

Pfaller, M. A., and Diekema, D. J. (2007). Epidemiology of invasive candidiasis: A persistent public health problem. *Clin. Microbiol. Rev.* 20, 133–163. doi: 10.1128/CMR.00029-06

Rychert, J., Slechta, E. S., Barker, A. P., Miranda, E., Babady, N. E., Tang, Y. W., et al. (2018). Multicenter Evaluation of the Vitek MS v3.0 System for the Identification of Filamentous Fungi. *J. Clin. Microbiol.* 56, 1–11. doi: 10.1128/JCM.01353-17

Samarasinghe, H., and Xu, J. (2018). Hybrids and hybridization in the Cryptococcus neoformans and Cryptococcus gattii species complexes. *Infect. Genet. Evol.* 66, 245–255. doi: 10.1016/j.meegid.2018.10.011

Spivak, E. S., and Hanson, K. E. (2018). Candida auris: an Emerging Fungal Pathogen. *J. Clin. Microbiol.* 56, 1–10. doi: 10.1128/JCM.01588-17

Sullivan, D. J., Westerneng, T. J., Haynes, K. A., Bennett, D. E., and Coleman, D. C. (1995). Candida dubliniensis sp. nov.: phenotypic and molecular characterization of a novel species associated with oral candidosis in HIV-infected individuals. *Microbiology* 141, 1507–1521. doi: 10.1099/13500872-141-7-1507

Sun, Y., Guo, J., Chen, R., Hu, L., Xia, Q., Wu, W., et al. (2020). Multicenter evaluation of three different MALDI-TOF MS systems for identification of clinically relevant filamentous fungi. *Med. Mycol.* 59, 1–6. doi: 10.1093/mmy/myaa037

Tavanti, A., Davidson, A. D., Gow, N. A. R., Maiden, M. C. J., and Odds, F. C. (2005). Candida orthopsilosis and Candida metapsilosis spp. nov. to replace Candida parapsilosis groups II and III. *J. Clin. Microbiol.* 43, 284–292. doi: 10.1128/JCM.43.1.284-292.2005

Tóth, R., Nosek, J., Mora-Montes, H. M., Gabaldon, T., Bliss, J. M., Nosanchuk, J. D., et al. (2019). Candida parapsilosis: From genes to the bedside. *Clin. Microbiol. Rev.* 32, 1–38. doi: 10.1128/CMR.00111-18

Wang, H., Fan, Y. Y., Kudinha, T., Xu, Z. P., Xiao, M., Zhang, L., et al. (2016). A Comprehensive Evaluation of the Bruker Biotyper MS and Vitek MS Matrix-Assisted Laser Desorption Ionization-Time of Flight Mass Spectrometry Systems for Identification of Yeasts, Part of the National China Hospital Invasive Fungal Surveillance Net (CHIF). *J. Clin. Microbiol.* 54, 1376–1380. doi: 10.1128/JCM.00162-16

Wang, Y., Chen, X. F., Xie, X. L., Xiao, M., Yang, Y., Zhang, G., et al. (2019). Evaluation of VITEK MS, Clin-ToF-II MS, Autof MS 1000 and VITEK 2 ANC card for identification of Bacteroides fragilis group isolates and antimicrobial susceptibilities of these isolates in a Chinese university hospital. *J. Microbiol. Immunol. Infect.* 52, 456–464. doi: 10.1016/j.jmii.2018.12.009

Xiao, M., Fan, X., Chen, S. C. A., Wang, H., Sun, Z. Y., Liao, K., et al. (2015). Antifungal susceptibilities of Candida glabrata species complex, Candida krusei, Candida parapsilosis species complex and Candida tropicalis causing invasive candidiasis in China: 3 year national surveillance. *J. Antimicrob. Chemother.* 70, 802–810. doi: 10.1093/jac/dku460

Xiao, M., Chen, S. C. A., Kong, F., Xu, X. L., Yan, L., Kong, H. S., et al. (2020). Distribution and Antifungal Susceptibility of Candida Species Causing Candidemia in China: An Update From the CHIF-NET Study. *J. Infect. Dis.* 221, S139–S147. doi: 10.1093/infdis/jiz573

Conflict of Interest: The authors declare that the research was conducted in the absence of any commercial or financial relationships that could be construed as a potential conflict of interest.

frontiers in Cellular and Infection Microbiology

ORIGINAL RESEARCH
published: 24 February 2021
doi: 10.3389/fcimb.2021.625430

Proteomic Analyses of *Acinetobacter baumannii* Clinical Isolates to Identify Drug Resistant Mechanism

Ping Wang[1], Ren-Qing Li[2], Lei Wang[3], Wen-Tao Yang[3], Qing-Hua Zou[1] and Di Xiao[3]**

[1] Department of Microbiology, School of Basic Medical Sciences, Peking University Health Science Center, Beijing, China, [2] Institute for Control of Infectious Diseases and Endemic Diseases, Beijing Center for Disease Prevention and Control, Beijing, China, [3] State Key Laboratory of Infectious Disease Prevention and Control, Collaborative Innovation Center for Diagnosis and Treatment of Infectious Diseases, National Institute for Communicable Disease Control and Prevention, Chinese Center for Disease Control and Prevention, Beijing, China

Acinetobacter baumannii is one of the main causes of nosocomial infections. Increasing numbers of multidrug-resistant *Acinetobacter baumannii* cases have been reported in recent years, but its antibiotic resistance mechanism remains unclear. We studied 9 multidrug-resistant (MDR) and 10 drug-susceptible *Acinetobacter baumannii* clinical isolates using Label free, TMT labeling approach and glycoproteomics analysis to identify proteins related to drug resistance. Our results showed that 164 proteins exhibited different expressions between MDR and drug-susceptible isolates. These differential proteins can be classified into six groups: a. proteins related to antibiotic resistance, b. membrane proteins, membrane transporters and proteins related to membrane formation, c. Stress response-related proteins, d. proteins related to gene expression and protein translation, e. metabolism-related proteins, f. proteins with unknown function or other functions containing biofilm formation and virulence. In addition, we verified seven proteins at the transcription level in eight clinical isolates by using quantitative RT-PCR. Results showed that four of the selected proteins have positive correlations with the protein level. This study provided an insight into the mechanism of antibiotic resistance of multidrug-resistant *Acinetobacter baumannii*.

Keywords: ***Acinetobacter baumannii*, antibiotic resistance, proteomic, TMT, label free, glycopeptides**

OPEN ACCESS

Edited by:
Yang Zhang,
University of Pennsylvania,
United States

Reviewed by:
Israa M. S. Al-Kadmy,
Al-Mustansiriya University, Iraq
Hao Zhang,
University of Pennsylvania,
United States
Jie Chen,
University of Pennsylvania,
United States
Sutthirat Sitthisak,
Naresuan University, Thailand

****Correspondence:***
Di Xiao
xiaodi@icdc.cn
Qing-Hua Zou
zouqinghua@bjmu.edu.cn

Specialty section:
This article was submitted to Clinical Microbiology, a section of the journal Frontiers in Cellular and Infection Microbiology

Received: *03 November 2020*
Accepted: *11 January 2021*
Published: *24 February 2021*

Citation:
Wang P, Li R-Q, Wang L, Yang W-T, Zou Q-H and Xiao D (2021) Proteomic Analyses of Acinetobacter baumannii Clinical Isolates to Identify Drug Resistant Mechanism. Front. Cell. Infect. Microbiol. 11:625430. doi: 10.3389/fcimb.2021.625430

Abbreviations: MDR, multidrug-resistant; TMT, tandem mass tag; TEAB, triethyl ammonium bicarbonate; HCD, higher energy collisional dissociation; PPI, protein-protein interaction; DEP, differential expressed proteins; GO, Gene Ontology; MBL, metal β-lactamase; PBP, penicillin binding proteins; BAM, β Barrel Outer Membrane Protein; Omp, Outer membrane protein; RHD, Rhodanese-Like Domain; SOD, Superoxide dismutase; Usp, Universal stress protein.

HIGHLIGHTS

1) 164 proteins exhibited different expressions between drug-resistant isolates and drug-susceptible isolates.
2) Classifying six groups of differential expressed proteins between drug-resistant isolates and drug-susceptible isolates.
3) A specifically expressed polysaccharide on the S21 site of adenylate kinase was found in most MDR strains.

INTRODUCTION

Nosocomial infections caused by multidrug-resistant (MDR) bacteria strains are a serious problem worldwide in decades. *Acinetobacter baumannii* has become one of the most common species that cause nosocomial infections and healthcare-associated infections such as bacteremia, pneumonia, meningitis, skin and wound infections, and urinary tract infection due to its strong biofilm formation ability and the ability to resist nutrient deprivation and antibiotics (Dijkshoorn et al., 2007; Shin and Park, 2015; Mujawar et al., 2019). The traditional first-line treatment of *A. baumannii* uses carbapenem antibiotics such as imipenem, but since the early 1990s, there have been reports of outbreaks caused by imipenem-resistant *A. baumannii* (Tankovic et al., 1994). Other therapeutic antibiotics include aminoglycosides, sulbactam, polymyxin and tigecycline, etc., and combined antibiotics are also being used. However, studies have shown that MDR strains which are resistant to different antibiotics are reported commonly (Li et al., 2006; Peleg et al., 2007; Göttig et al., 2014; Al-Kadmy et al., 2020). Whether for developing new drugs or making full use of old drugs to treat infections caused by MDR strains, it is necessary to fully understand the antibiotic resistance mechanism. A full understanding of the resistance mechanism is critical to improve the eradication rate of *A. baumannii*. Studies have shown that the antibiotics resistant mechanism mainly includes the modification of the target site, inactivation or modification of the drugs by producing enzymes such as β-lactamases, the activation of the efflux pump and the changes of the membrane structure and permeability of bacteria (Dijkshoorn et al., 2007; Zarrilli et al., 2013; Lee et al., 2017; Ramirez et al., 2020).

Genomics and proteomics studies can explore the expression of genes or proteins under various conditions thus to help understand the different mechanisms of bacteria drug resistance. At present, there have been extensive researches on *A. baumannii* through proteomic analysis to explore the relevant mechanisms of drug resistance, drought tolerance, biofilm formation, virulence, and nutrient regulation (Kwon et al., 2009; Shin et al., 2009; Nwugo et al., 2011; Long et al., 2013; Gayoso et al., 2014; Scribano et al., 2019). Researches on drug resistance of *A. baumannii* have studied the differences of a single strain pre and after the induction of resistance (Fernández-Reyes et al., 2009; Hood et al., 2010; Hua et al., 2017) or under different culture conditions (Yun et al., 2011; De Silva et al., 2018), or the difference between susceptible strains and resistant strains (Siroy et al., 2006; Vashist et al., 2010; Li et al., 2015; Wang et al., 2016). However, the researches usually analyze only one or two strains and focused only on a certain antibiotic. Different proteomics methods have their advantages and disadvantages. Using more than one proteomics method can complement each other and enhance the reproducibility and effectiveness of proteomics (Tiwari and Tiwari, 2014). In addition, protein glycosylation is an important means of protein modification, and different glycosylation modifications are critical to protein function (Ahmad Izaham and Scott, 2020). In this study, we intend to use the approach of label free and tandem mass tag (TMT) labeling-based proteomics and glycoproteomes to analyze the different proteins between MDR and drug-susceptible *A. baumannii* to fully clarify the mechanism of the antibiotic resistance.

MATERIALS AND METHODS

Bacteria Strains

Nineteen *A. baumannii* clinical strains (9 MDR and 10 susceptible isolates) were isolated from different patients in the second affiliated hospital of Nanchang University, China, during 2011–2019. The isolates were identified by VITEK-2 compact system and 16S ribosomal DNA identification. The 16S ribosomal DNA were amplified with the primer (16s-PCRF and 16s-PCRR) showed in **Supplementary Table 1**. The fragments were sequenced and blasted in NCBI non-redundant database for species identification. Antibiotic susceptibility of the following antibiotics were tested by Kirby–Bauer test (KB-test): β-lactam antibiotics [piperacillin, ceftazidime, ceftriaxone, cefotaxime, cefepime, imipenem, Unasyn (ampicillin/sulbactam), and Tazocilin (piperacillin/tazobactam)], aminoglycoside (gentamicin and tobramycin), tetracyclines (minocycline and tigecycline), polymyxin B, fluoroquinolone (levofloxacin, Ciprofloxacin), and paediatric compound sulfamethoxazole tablets. Data of these isolates are shown in **Supplementary Table 2**.

Protein Extraction

The experiment process is shown in **Figure 1**. All the isolates were cultured in LB broth at 37°C with shaking until $OD_{600\ nm}$ of 0.7–0.8 reached. The cells were collected and lysed by 8M urea in 50 mM triethyl ammonium bicarbonate (TEAB) and ultrasonic breakage for 20 s. The protein samples were collected *via* centrifugation at 16,000×g for 10 min at 4°C. The protein concentration of the supernatant was determined using BCA Protein Assay Kit (Thermo-Fisher Scientific).

Trypsin Digestions and Peptides Purification

The proteins were reduced by incubation with TCEP (200 mM) at 55°C for 1 h and alkylated by incubation with iodoacetamide (IAA, 375 mM, Thermo Scientific) for 30 min in dark at room temperature. TEAB (100 mM) was used to adjust the urea concentration of less than 1M in all the protein samples, and then the proteins were digested to peptides using trypsin (Promega) at a trypsin/protein ratio of 1:50 (w/w) overnight at 37°C. The generated tryptic peptides were dried by speed

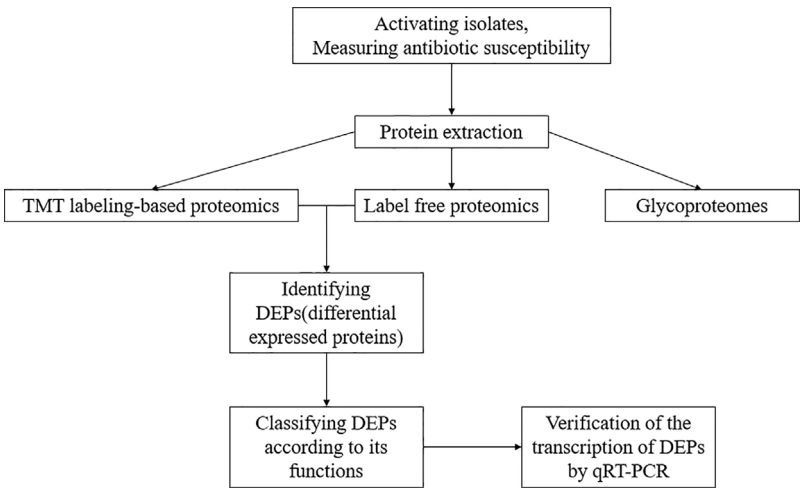

FIGURE 1 | The experiment process of this study.

vacuum at 4°C and desalted with C18 Spin column. For TMT labeling, the resultant peptide mixture of 10 isolates were labeled using TMT reagent kit (Thermo Scientific, USA) as resistant strain-127 isobaric tag and susceptible strain-126 isobaric tag (Chen et al., 2014). The combinations are as follows: A151 and A9, A159 and A11, A160 and A21, A161 and A90, A162 and A132.

Nano-HPLC-MS/MS Analysis

The samples were reconstituted in 0.1% formic acid (FA) and separated on a NanoAcquity Ultra Performance Liquid Chromatography (UPLC) system (EASY-nLC 1000, Thermo Scientific). Afterward, the samples were fitted with a nanoAcquity Symmetry C18 trap column (100 μm × 2 cm, NanoViper C18, 5 μm, 100Å) and an analytical column (75 μm × 15 cm, NanoViper C18, 3 μm, 100Å). The mobile phase A was 100:0.1 HPLC grade water/FA, and mobile phase B was 100:0.1 ACN/FA. Each sample was loaded on the trapping column with a flow rate of 2.0 μl/min, followed by separation on the analytical column using a 100 min 3%–35% mobile phase B linear gradient at a flow rate of 0.8 μl/min. Retention Time Calibration Mixture (Thermo Scientific) was used to optimize LC and MS parameters and was used to monitor the stability of the system.

The analytical column was coupled to a high-resolution Q-Exactive Plus mass spectrometer (Thermo Fisher Scientific, San Jose, CA) using a nano-electrospray ion source, which was operated in positive ion mode. The source was operated at 2.0 kV with transfer-capillary temperature maintained at 250°C and S-Lens RF level set at 60. MS spectra were obtained by scanning over the range m/z 350–2000. Mass spectra were acquired in the Orbitrap mass analyzer with 1 microscan per spectrum for both MS and MS/MS. Resolving power for MS and MS/MS were set at 70,000 and 17,500, respectively. Tandem MS data were acquired in parallel with MS, on the top 20 most abundant multiply charged precursors, with higher energy collisional dissociation (HCD) at normalized collision energy of 30V. Precursors were isolated using a 2.0 m/z window and dynamic exclusion of 60 s was enabled during precursor selection. The data were determined twice.

Proteome Data Analysis

For TMT labeling, Proteome Discoverer (version 1.4, Thermo Scientific, USA) was used to search the UniProtKB/Swiss-Prot database. The parameters were set as follows: integration tolerance, 20 ppm; precursor mass tolerance, 10 ppm; fragment mass tolerance, 0.02 Da. Dynamic modification Oxidation/+15.99 Da and carbamidomethyl/+57.02 Da) were set as dynamic and static modifications. Proteins that were differentially expressed were determined by peptide identifications with 95% confidence interval. Meanwhile, TMT signal analyses showed at least two-fold change in abundance, and its P value was <0.05 in unpaired Student's t-test.

For Label free, peptide identification and label free relative quantification analysis were carried out using Peaks Studio 8.5 software (Bioinformatics Solutions Inc., Waterloo, ON, Canada). Using *A. baumannii* UniProtKB database (326,258 sequences, downloaded in June 2019). Input parameters: 20 ppm precursor mass tolerance, 0.02 Da fragment mass tolerance. The false discovery rates for protein and peptides were set at a maximum of 1%.

Only those protein groups which passed the filter are displayed in the protein profile heatmap. The relative protein abundance is represented as a heat map of the representative proteins of each protein group. The representative proteins are clustered if they exhibit a similar expression trend across the samples.

Intact Glycopeptide Enrichment *via* Hydrophilic Interaction Liquid Chromatography (HILIC)

Glycopeptides in the samples were enriched by HILIC (The Nest Group, Inc.). Briefly, the tryptic and desalted peptides were

resuspended in 80% ACN. The appropriate amounts of HILIC particle in 80% ACN were placed in Pierce spin columns (Thermo Scientific) and equilibrated three times using 80% ACN, which was followed by sample loading three times and washing two times with 80% ACN. Then, glycopeptides bound to the HILIC column were eluted three times with 100 µl of 0.1% TFA. The samples were dried by a SpeedVac and stored at −80°C until analysis.

The analytical column was coupled to a high-resolution Q-Exactive Plus mass spectrometer (Thermo Fisher Scientific, San Jose, CA) with a nano electrospray ion source operated in positive ion mode. The source was operated at 2.0 kV with the transfer capillary temperature maintained at 250°C and the S-lens RF level set at 60. MS spectra were obtained by scanning over an m/z range of 350–2000. Mass spectra in both MS and MS/MS were acquired in an Orbitrap mass analyzer with 1 microscan per spectrum. The resolving power for MS and MS/MS was set at 70,000 and 17,500, respectively. Tandem MS data on the top 20 most abundant multiply charged precursors were acquired in parallel with MS data, with higher energy collisional dissociation (HCD) at a normalized collision energy of 30 V. Precursors were isolated using a 2.0 m/z window, and dynamic exclusion of 60 s was enabled during precursor selection.

Database searches were performed using Byonic software (v2.13.17, Protein Metrics, Inc.). The following parameters were set for the search: cleavage sites, RK; cleavage side, C-terminal; digestion specificity, fully specific; missed cleavages, 2; precursor mass tolerance, 10 ppm; fragmentation type, QTOF/HCD; fragment mass tolerance, 0.02 Da, and protein false discovery rate (FDR), 1% FDR (or 20 reverse counts). All the other settings were set at their default values.

Byonic scores reflect the absolute quality of the peptide-spectrum match and not the relative quality compared to other candidate peptides. The Byonic score ranges from 0 to approximately 1,000, with 300 being a good score, 400 a very good score, and peptide-spectrum matches with scores over 500 almost certainly correct. The DeltaMod value indicates whether modifications are confidently localized; DeltaMod values over 10 indicate a high likelihood that all modification placements are correct. Therefore, a score over 300, a DeltaMod value over 10, a q-value < 0.05, and an FDR < 0.1% were set as thresholds in this study. Systematic and comprehensive analyses of specific glycopeptides, glycoforms, and glycosylation sites related to our samples from all the proteins identified by Byonic were carried out.

Bioinformatics Analysis

To further understand the functions of differential expressed proteins (DEP) between drug-resistant and drug-susceptible *A. baumannii* isolates, The DEPs were further submitted to NCBI (National Center for Biotechnology Information) and Uniprot (https://www.uniprot.org/) for GO enrichment analysis (statistically significant differences of GO terms were defined by $P < 0.05$), KOBAS 2.0 (KEGG Orthology Based Annotation System; http://kobas.cbi.pku.edu.cn/home.do) for KEGG pathway analysis and STRING database (https://string-db.org/) for protein-protein interaction (PPI) analysis. The subcellular localization and the specific information of the DEPs were identified by pSORTb version 3.0.2 (https://www.psort.org/psortb/) and Pubmed, respectively. The potential glycosylation sites were output from NetOGlyc 4.0 Server (http://www.cbs.dtu.dk/services/NetOGlyc/).

RNA Extraction and Real-Time Quantitative Polymerase Chain Reaction (qRT-PCR)

Eight *A. baumannii* clinical isolates (four resistant strains and four susceptible strains) from the same hospital (data shown in **Supplementary Table 3**) were used to determine the transcription of seven kinds of DEPs: Aminoglycoside (3') phosphotransferase AphA1 or APH (3')-Ia (AFV53106), Beta-lactamase AmpC (AFA35105/AFA35107), Outer membrane protein assembly factor BamD (WP_000056810), MFS transporter (RSR57702), ABC transporter (AXV52620), HlyD membrane-fusion protein of T1SS (ENV25944), and Elongation factor Tu (KLT84190). Primers are listed in **Supplementary Table 1**. All isolates were grown overnight at 37°C in LB broth, and sub-cultured 1/100 into fresh LB broth for 4 h. RNA extraction was performed using RNAprep Pure Kit (TianGen). The extracted RNA was reversed to cDNA using the All-in-One^{TM} First-Strand cDNA Synthesis Kit (TaKara). Then qRT-PCR were performed using the 2*SYBR Green qPCR Master Mix (Low Rox). The CT value was obtained by using the 7500 Fast DX instrument, *rpoB* was used as the internal parameter. The normalized relative expression levels of the target genes were calculated by the comparative cycle threshold ($2^{-\Delta\Delta CT}$). The data obtained were analyzed and plotted with Graphpad prism version 5.0. Error bars represent the SDs. Significant differences were defined by $P < 0.05$ (*), $P < 0.01$(**), and $P < 0.001$(***).

RESULTS AND DISCUSSION

Proteomics analysis uses non-targeted research to directly detect the expression of a large number of proteins. In this study, we used TMT labeling-based proteomics, label-free proteomics, and glycoproteomics to analyze the differentially expressed proteins between 9 MDR and 10 drug-susceptible *A.baumannii* isolates. All MDR strains are resistant to Cefepime, imipenem, gentamicin, tobramycin, levofloxacin, ciprofloxacin, and paediatric compound sulfamethoxazole. Drug-susceptible isolates are only non-susceptible to penicillins and cephalosporins of the eight antimicrobial categories listed in **Supplementary Table 2**.

Analysis of TMT Labeling-Based Proteomics

For the TMT labeling-based proteomics, we randomly selected 10 isolates (5 MDR and 5 drug-susceptible) and made them into 5 drug-resistant and drug-susceptible pairs. Each pair was subjected to two biological replicates. The MDR isolates and drug-susceptible isolates were labelled by 127 and 126 reagent, respectively. In the first pair, 2,270 and 2,730 proteins were found in two biological iterations, and a total of 3,884 proteins were identified. In the second pair, 2,050 and 2,061 proteins were

found respectively, and a total of 3,150 proteins were found. In the third pair, 2,695 and 2,200 proteins were found, and a total of 3,782 proteins were found. In the fourth pair, 1,953 and 1,874 proteins were found, and a total of 2,977 proteins were identified. In the fifth pair, 2,021 and 1,927 proteins were found, and a total of 3,051 proteins were found. In order to conduct an overall analysis, we finally selected 127/126 ≥ 2 and ≤0.5 data for analysis. As seen in **Supplementary Table 4**, a total of 70 proteins were obtained with the same expression trend in more than 4 pairs, among which there were 23 kinds of proteins with the same expression trend in 5 pairs. The relative molecular mass of the protein is between 6 and 118 kda, a larger proportion is between 10 and 50kda, and the isoelectric point is between 4.42 and 11.12. 58 up-regulated proteins (127/126 ≥ 2) and 12 down-regulated proteins (127/126 ≤ 0.5) were expressed in MDR isolates. Gene Ontology (GO) analysis can classify genes to different groups according to their functions. Based on the GO annotation analysis, the proteins were classified into three categories: molecular function, cellular component, and biological process. GO analysis with the largest number of proteins involved were shown in **Figure 2**, up-regulated proteins are classified into 20 molecular function related proteins, 11 cellular component related proteins, and 14 biological process related proteins; downregulated proteins are classified into 7 molecular function related proteins, 3 cellular component related proteins, and 5 biological process related proteins. The DEPs of MDR and drug-susceptible isolates focused on catalytic activity and binding. There are 22 KEGG pathways involved in the down-regulated proteins, most of which are involved in metabolic pathways; 39 KEGG pathways are involved in the up-regulated proteins, which are mostly involved in metabolic pathways, carbon metabolism, and biosynthesis of amino acids (**Supplementary Figure 1**). The PPI net showed the interactions of the 59 proteins. The average node degree is 2.78 and the interaction of ribosomal-related proteins is relatively dense (**Supplementary Figure 2**).

Analysis of Label Free Proteomics

We analyzed 10 drug-susceptible isolates and 9 MDR isolates by label free proteomics and obtained 102 proteins that are all present in more than 8 resistant isolates and only in 1 or less susceptible isolate (**Supplementary Table 5**). The number of proteins involved in molecular function, cellular component, and biological process are 52, 20, and 33, respectively (**Figure 3**). DEPs mainly focused on catalytic activity, binding, cellular process, metabolic process, and cellular anatomical entity. A total of 48 KEGG pathways (input numbers) were involved in Metabolic pathways (28), Carbon metabolism (11), Biosynthesis of amino acids (10), Glycine, serine and threonine metabolism (7), Valine, leucine and isoleucine degradation (6), Cysteine and methionine metabolism (6), Glyoxylate and dicarboxylate metabolism (5), etc. (**Supplementary Figure 3**). The PPI network diagram showed a total of 87 protein interactions, with an average node degree of 0.437 (**Supplementary Figure 4**). The heat map of similar expressed proteins showed differences in the expression of resistant isolates and susceptible isolates, differences in strains would also lead to different expression levels of some proteins in different bacteria (**Figure 4**).

Different Expressed Proteins (DEPs) in Drug-Resistant Isolates vs. Drug-Susceptible Isolates

The results from TMT labeling-based proteomics and label free proteomics were combined and we found a total of 164 DEPs. The subcellular localizations of these DEPs were mainly in the cytoplasm, the proteins up-regulated or identified by label free proteomics mainly on the periplasmic or outer membrane of the cell (**Figure 5**). We further classified the proteins into six groups with different functions. According to this classification, there were 12, 20, 22, 14, 60, and 37 differentially expressed proteins of A, B, C, D, E, and F group, respectively. As following:

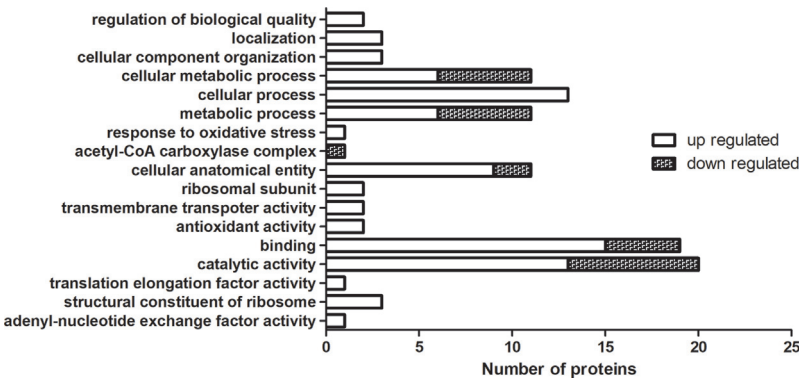

FIGURE 2 | GO enrichment analysis of DEPs in TMT-labeling proteomics. The MDR isolates and drug-susceptible isolates were labelled by 127 and 126 reagent. Up-regulated and down-regulated means 127/126 ≥ 2 and ≤0.5, respectively. Each column represented the number of proteins involved in GO annotation analysis of DEPs in TMT-labeling proteomics. Statistically significant differences of GO terms were defined by $P < 0.05$.

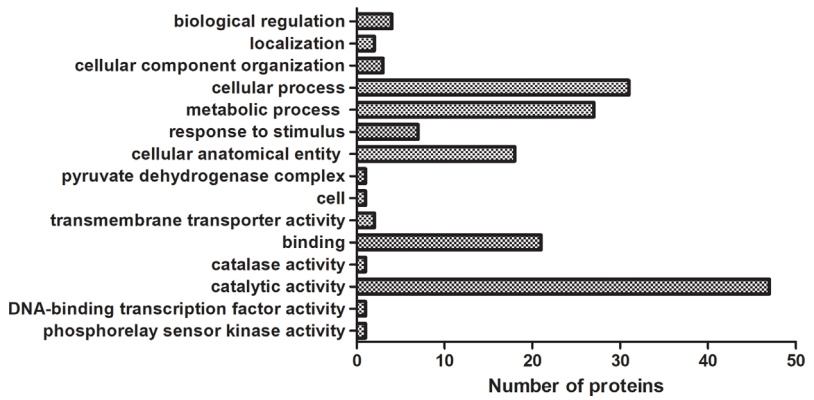

FIGURE 3 | GO enrichment analysis of DEPs in label free proteomics. The proteins in label free proteomics are all present in more than 8 resistant isolates and only in 1 or less susceptible isolate. Each column represented the number of proteins involved in GO annotation analysis of DEPs in label free proteomics. Statistically significant differences of GO terms were defined by $P < 0.05$.

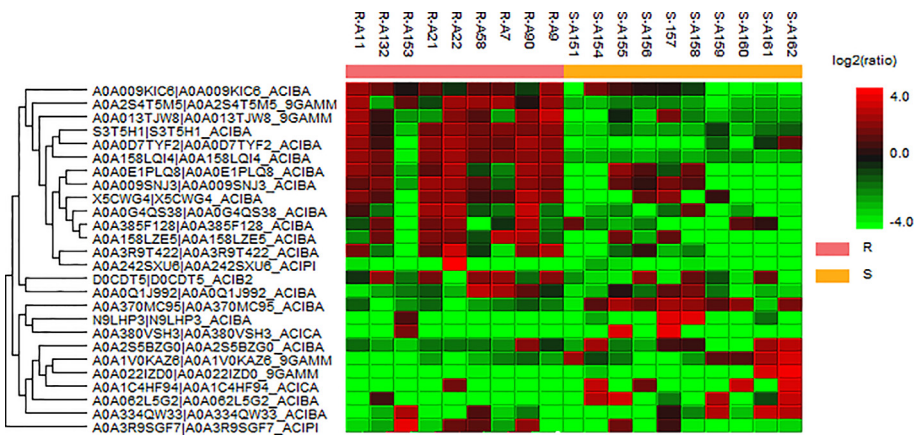

FIGURE 4 | Heat map of the representative proteins of each isolate. "R" means drug-resistant isolates and "S" means drug-susceptible isolates. The representative proteins identified from label free proteomics are clustered if they exhibit a similar expression trend across the samples. The hierarchical clustering is generated using neighbor joining algorithm with a Euclidean distance similarity measurement of the log2 ratios of the abundance of each sample relative to the average abundance.

Proteins Related to Antibiotic Resistance

In this study, we found 12 proteins more abundant in the MDR isolates classified to group a (**Table 1**). These 12 proteins belong to a variety of known antibiotic resistance proteins, such as beta-lactamases and aminoglycoside phosphotransferase. The resistance of *Acinetobacter* to β-lactam is mainly due to the synthesis and enzymatic degradation of the species-specific β-lactamase, all four types of β-lactamases have been identified in *A. baumannii* (Lee et al., 2017), and the analysis of 23 MDR *A. baumannii* clinical isolates in Taiwan has shown that all *A. baumannii* can encode AmpC cephalosporins (Lin et al., 2011). OXA-23 and OXA-72 belong to class D β-lactamases (Donald et al., 2000; Evans and Amyes, 2014). Metal-dependent hydrolases such as metal β-lactamase (MBL) are zinc-dependent hydrolases that can cleave the β-lactam bond of most β-lactam antibiotics (Parimelzaghan et al., 2016; Kwapien et al., 2017). In this study, both metal-dependent hydrolase-related proteins and β-lactamase-related proteins were up-regulated in MDR isolates. The resistance of *Acinetobacter* to aminoglycoside antibiotics is mainly through N-acetylation, adenylation or O-phosphorylation modification to inactivate aminoglycosides (Seward et al., 1998; Shakil et al., 2008). AphA1b is one of the modifying enzymes involved in aminoglycoside resistance (Nigro et al., 2011). In this study, it is uniquely expressed in MDR isolates, which can explain its prevalence to tobramycin, gentamicin, and other aminoglycoside antibiotics. DacD (D-alanyl-D-alanine carboxypeptidase) belongs to penicillin binding proteins (PBPs) (Spidlova et al., 2018), also called PBP6b in *A. baumannii*, which is involved in the metabolism of peptidoglycans (Cayô et al., 2011). In addition,

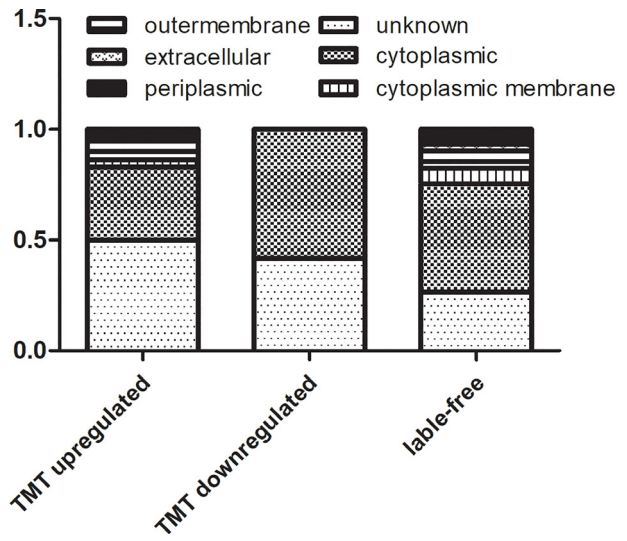

FIGURE 5 | The subcellular localization of DEPs in TMT-labeling proteomics and label free proteomics.

studies have found that Cell division protein ZapA is related to the resistance of β-lactam antibiotics (Knight et al., 2016). These proteins are all up-regulated in the drug-resistant isolates in this study.

Membrane Proteins, Membrane Transporters, and Proteins Related to Membrane Formation

The second category contains of 20 DEPs (**Table 2**) including 1 down-regulated protein and 19 up-regulated proteins. Thioredoxin, which is a member of the thioredoxin superfamily, is involved in the virulence of bacteria and also related to the expression of genes related to the ABC transport system (May et al., 2019). This protein is shown to be down-regulated in our results which are consistent with the literature. The upregulated proteins in this group include proteins that play a key role in the formation of the outer membrane, proteins related to maintaining the integrity of the outer membrane, pump proteins, and outer membrane proteins: β Barrel Outer Membrane Protein (BAM) is related to bacterial nutrient acquisition, protein secretion, signal transduction and bacterial survival, and drug resistance (Sikora et al., 2018). Porin has been shown to play an important role in the resistance mechanism (Lee et al., 2017). Lipoprotein can act as a fusion protein to promote the complete biogenesis of the cell membrane (Melly et al., 2019). Studies have found that lipoproteins are upregulated in MDR *A. baumannii* strains (Chopra et al., 2013). SurA is a periplasmic chaperone protein involved in the folding of outer membrane porins, and is closely related to the integrity of the outer membrane (Bell et al., 2018). The alpha/beta hydrolase folding superfamily is a class of hydrolase enzymes involved in lipid metabolism, cell membrane maintenance, virulence, efflux, and metabolism of cell (Johnson, 2017). Outer membrane protein A (OmpA) is the outer membrane protein of bacteria, which is related to the efflux pump and drug resistance of bacteria (Kwon et al., 2017). The expression of OmpW is down-regulated in carbapenem-resistant strains, and its down-regulation can make PBPs unavailable (Tiwari et al., 2012). Study have also found that OmpW has a higher expressed in MDR strains (Chopra et al., 2013). The outer membrane protein CarO is associated with carbapenem drug resistance (Xiao et al., 2016). The multicomponent efflux pump system is widely present in bacteria and it can make bacteria resistant to antibiotics by pumping out antibiotics. Six superfamily of resistant pumps have been identified in *A. baumannii*: major facilitator superfamily (MFS), resistance nodulation division (RND), multidrug and toxic compound extrusion (MATE), small multidrug resistance (SMR), ATP-binding cassette (ABC), and proteobacterial antimicrobial compound efflux (PACE) (Pérez-Varela et al., 2019). In our study, we found that both ABC transporter, MFS transporter, and RND transporter were up-regulated. MFS efflux pump and ABC transporter have been found to be associated with quinolone

TABLE 1 | Proteins related to antibiotic resistance.

Genbank accession	Uniprot accession	Subcellular localization	Protein name	Classification
TPU58603	A0A335ECA6	Unknown	Beta-lactamase OXA-23	TMT up-regulated & Label-free
AJZ68886	A0A0D5W3B6	Unknown	Carbapenem-hydrolyzing beta-lactamase OXA-72 (Fragment)	Label-free
AFI94694	A0A454ATR7	Unknown	D-alanyl-D-alanine carboxypeptidase	Label-free
EEY77424	D0S1V7	Periplasmic	Beta-lactamase	Label-free
ALY01035	A0A0E4HMD5	Periplasmic	Beta-lactamase	Label-free
AFV53106	K4P0R4	Cytoplasmic Membrane	Aminoglycoside (3') phosphotransferase AphA1 or APH (3')-Ia	Label-free
EOQ64883	R8Y658	Periplasmic	Beta-lactamase	Label-free
ADX04518	A0A335L319	Unknown	Metal-dependent hydrolase of the aminoacylase-2/carboxypeptidase-Z family	Label-free
VAX45430	A0A0A8XI29	Unknown	Cell division protein ZapA	Label-free
ANA37603	A0A334SNB2	Cytoplasmic	Zn-dependent hydrolase	Label-free
AFA35105	A7Y416	Periplasmic	Beta-lactamase	Label-free
AFA35107	A7Y413	Periplasmic	Beta-lactamase	Label-free

TABLE 2 | Proteins related to membrane proteins, membrane transporters, and membrane formation.

Genbank accession	Uniprot accession	Subcellular localization	Protein name	Classification
OIG07664	A0A1S2FR42	Cytoplasmic	Thioredoxin (Fragment)	TMT down-regulated
WP_000056810	A0A009Q2E5	Outer Membrane	Outer membrane protein assembly factor BamD	TMT up-regulated & Label-free
EXC53439	A0A009SK97	Cytoplasmic Membrane	Ubiquinol oxidase subunit 2	TMT up-regulated
CAP01694	B0VSC6	Outer Membrane	Putative lipoprotein	TMT up-regulated
EXC52624	A0A009SI69	Unknown	Chaperone SurA	TMT up-regulated
PZM13340	A0A3F3MK29	Outer Membrane	OmpA family protein	TMT up-regulated
SSU67456	A0A334ZIV7	Unknown	Surface antigen	TMT up-regulated
KCY23168	A0A062IZ25	Outer Membrane	Porin subfamily protein	TMT up-regulated & Label-free
EXC51784	A0A009TK41	Outer Membrane	Peptidoglycan-associated protein	TMT up-regulated
RSR57702	A0A3R9S2V0	Cytoplasmic Membrane	MFS transporter (Fragment)	TMT up-regulated
AXV52620	A0A2P1B3I7	Periplasmic	ABC transporter, phosphonate, periplasmic substrate-binding family protein	TMT up-regulated
EXB00312	A0A009H862	Outer Membrane	OmpW family protein	Label-free
ENV25944	A0A158LU97	Cytoplasmic Membrane	Uncharacterized protein(HlyD membrane-fusion protein of T1SS; cl25633)	Label-free
AFX97596	K7Z0V1	Cytoplasmic Membrane	Kinase sensor (AdeS)	Label-free
ABR18859	A0A2Z5ZA15	Outer Membrane	Carbapenem-associated resistance outer membrane protein (Fragment)	Label-free
SSM96339	A0A333EPN9	Unknown	Putative surface antigen	Label-free
KCY66385	A0A062MBU0	Extracellular	Type I secretion C-terminal target domain protein	Label-free
OTL21614	A0A241YRY7	Cytoplasmic Membrane	Efflux transporter periplasmic adaptor subunit (Fragment)	Label-free
AFI94256	A0A454ASL3	Outer Membrane	Outer membrane protein/ peptidoglycan-associated (Lipo) protein	Label-free
WP_024436048	A0A009T321	Outer Membrane	Outer membrane protein assembly factor BamA	Label-free

resistance and beta lactam resistance (Correia et al., 2016; Xiao et al., 2016; Lari et al., 2018; Pérez-Varela et al., 2018). T1SS is formed by HlyB (ABC transporter), HlyD (membrane fusion protein), and TolC (outer membrane). Its C-terminal can carry a secretion signal, and the deletion of the C-terminal will cause secretion blocked (Holland et al., 2016). In our study, both the C-terminal target domain and the hypothetical protein F962_01862 encoding HlyD were up-regulated.

Stress Response-Related Proteins

We found there were 22 stress response-related proteins differentially expressed between MDR and drug-susceptible isolates (**Table 3**), among them, the expression of Antibiotic biosynthesis monooxygenase which can oxidize and inactivate antibiotics (Minerdi et al., 2016; Koteva et al., 2018) is interestingly down-regulated. The expression of heat shock proteins and acid shock proteins were upregulated. Heat shock protein is generally used as a molecular chaperone or protease to repair damaged proteins, and its expression increases during stress response such as antibiotic induction. Bacteria with heat shock proteins induced are more resistant to antibiotic environments (Cardoso et al., 2010). Acid shock protein can improve the acid resistance of bacteria (Villarreal et al., 2000). Other proteins related to the stress response and resistance to environment were also upregulated as following: Trigger factor (TF) can play a key role as a molecular chaperone, also related to the resistance to the external environment (Lee et al., 2009). Heavy metal-associated (HMA) domain proteins can give bacteria the ability to resist high metal environments (Maynaud et al., 2014). Rhodanese-Like Domain (RHD) Protein participates in biological processes such as sulfur metabolism and environmental adaptability (Cipollone et al., 2007). Superoxide dismutase (SOD) can effectively catalyze the conversion of superoxide free radicals and protect bacteria from reactive oxygen. It has been shown to be related to the oxidative stress response of *Acinetobacter baumannii* and its resistance to antibiotics (Heindorf et al., 2014). Catalase catalyzes the degradation of hydrogen peroxide and is closely related to the defense of bacteria against related environments (Sun et al., 2016). Universal stress protein (Usp) helps bacteria adapt to oxidative stress, high temperature, pH, etc. (Elhosseiny et al., 2015). Aldehyde dehydrogenase (AldA) is related to a variety of metabolic processes such as redox regulation of bacteria, and can participate in environmental stress defense such as hypochlorite stress (Imber et al., 2018). Cysteine synthase CysK can be used to synthesize cysteine (Bogicevic et al., 2016), and cysteine related products are important molecules required for the oxidative stress response of bacteria (Hicks and Mullholland, 2018).

TABLE 3 | Stress response-related proteins.

Genbank accession	Uniprot accession	Subcellular localization	Protein name	Classification
KRI51357	A0A0R0RLL9	Unknown	Antibiotic biosynthesis monooxygenase	TMT down-regulated
AFI96375	A0A454AYE3	Unknown	Heat shock protein	TMT up-regulated & Label-free
EXC53193	A0A009SJR6	Cytoplasmic	Trigger factor	TMT up-regulated
ANA38542	A0A0D7TYF2	Cytoplasmic	Chaperone protein DnaK	TMT up-regulated
EXC50791	A0A009T8J5	Unknown	Heavy-metal-associated domain protein	TMT up-regulated
EXC53824	A0A009SLH6	Unknown	Rhodanese-like domain protein	TMT up-regulated
EXA83425	A0A009GB49	Periplasmic	Superoxide dismutase (Fragment)	TMT up-regulated
EXC50244	A0A009SB62	Cytoplasmic	Protein GrpE	TMT up-regulated
PHQ01889	A0A2G1TI69	Cytoplasmic	Catalase	TMT up-regulated
AFI95883	A0A454AX51	Cytoplasmic	Catalase	TMT up-regulated & Label-free
RSR19198	A0A3R9SYU8	Unknown	Universal stress protein (Fragment)	TMT up-regulated
AUT38163	A0A2I8CT30	Cytoplasmic	Aldehyde dehydrogenase	Label-free
EXA83546	A0A009FVR3	Cytoplasmic	Peptidase M16 inactive domain protein	Label-free
ANA36730	A0A0D5YN58	Cytoplasmic	Cysteine synthase	Label-free
POZ07170	A0A0M3FGT4	Cytoplasmic	Chaperone protein HchA	Label-free
OTL46319	A0A241YVG9	Cytoplasmic	NAD(P)H-quinone oxidoreductase (Fragment)	Label-free
AFI94331	A0A454ASQ3	Cytoplasmic	Putative NAD(P)H quinone oxidoreductase, PIG3 family	Label-free
PAM75163	A0A237TK91	Cytoplasmic	Protease	Label-free
SSU69655	A0A335SV40	Periplasmic	Acid shock protein	Label-free
EXB32044	A0A009KMD8	Cytoplasmic	Chaperone protein HscA homolog	Label-free
RSR52999	A0A429MNG9	Unknown	Response regulator (Fragment)	Label-free
KCY73957	A0A062N321	Unknown	Antitoxin	Label-free

NAD(P)H-quinone oxidoreductase participates in quinone detoxification and helps bacteria to survive under adverse conditions (Ryan et al., 2014), which is also related to resistance to oxidative stress (Kishko et al., 2012). Bacterial proteases play an important role in the survival, stress response, and pathogenicity of bacteria (Culp and Wright, 2017). Isochorismatase family protein is related to serum resistance in *A. baumannii* (Jacobs et al., 2010). Response regulators are related to the tolerance to dehydration and resistance to oxidative stress (Farrow et al., 2018). The toxin antitoxin system also regulates the response of SOS stress (Fernández-García et al., 2016).These proteins all showed upregulated or unique expressed in MDR isolates in this study. The upregulated expression of these stress proteins that resist the external environment may promote the resistance of bacteria by making the resistance of bacteria more stable.

Proteins Related to Gene Expression and Protein Translation

The forth group is proteins that have important functions for gene expression and protein translation or modification (**Table 4**). The expression of Serine hydroxymethyltransferase in this class is down-regulated. This protein is an iron inhibitory protein and can bind to mRNA to control gene expression and participate in the overall bacterial response (Nwugo et al., 2011). Up-regulated proteins includes enolase, DNA breaking-rejoining elements, ribosomal proteins, elongation factor Tu (EF-Tu), ribonuclease E (RNase), Valyl-tRNA synthetase, NusA, and long-chain fatty acid transport proteins. Enolase can play a central role in RNA processing (Krucinska et al., 2019). DNA breaking-rejoining enzymes play an important role in the transmission of genetic elements (Van Houdt et al., 2012). The ribosomal protein S4 RpsD is related to the assembly of ribosomes (Olsson and Isaksson, 1979).

TABLE 4 | Proteins related to gene expression and protein translation.

Genbank accession	Uniprot accession	Subcellular localization	Protein name	Classification
EXH77350	A0A140QTL6	Cytoplasmic	Serine hydroxymethyltransferase	TMT down-regulated
PAM68667	A0A334GYE2	Cytoplasmic	Enolase	TMT up-regulated
PAM68199	A0A270N7U1	Unknown	DNA breaking-rejoining protein	TMT up-regulated
EXC51028	A0A009SW10	Cytoplasmic	30S ribosomal protein	TMT up-regulated
WP_001273421	A0A454AZ45	Cytoplasmic	50S ribosomal protein L25	TMT up-regulated
KLT84190	A0A0J0ZQ10	Cytoplasmic	Elongation factor Tu (Fragment)	TMT up-regulated
EXC51023	A0A009SW05	Cytoplasmic	50S ribosomal protein L15	TMT up-regulated
EXC51011	A0A009T933	Cytoplasmic	50S ribosomal protein L16	TMT up-regulated
ANA36598	A0A0B9WR03	Cytoplasmic	Ribonuclease E	Label-free
EXB30595	A0A009KIU0	Cytoplasmic	Valine–tRNA ligase	Label-free
ANA37581	A0A0D8GW25	Unknown	Nucleoid-associated protein	Label-free
WP_000532247	A0A454B0H3	Cytoplasmic	Transcription termination/antitermination protein NusA	Label-free
KHO17349	A0A0B2XPD2	Unknown	Long-chain fatty acid transporter	Label-free
SSS41843	A0A334Z5E6	Unknown	Long-chain fatty acid transport protein	Label-free

The 50S ribosomal proteins L15 and L16 are important translation proteins (McNicholas et al., 2001; Dutton et al., 2016). EF-Tu is also related to protein translation and can interact with a variety of proteins to perform different biological functions (Premkumar et al., 2014). EF-Tu and ribosomal protein can help the production of bacterial protein, and some study have found them upregulated in carbapenem-resistant strains (Tiwari et al., 2012). RNase can perform different processing on RNA to regulate gene expression (Mardle et al., 2019). Valyl-tRNA synthetase is responsible for the aminoacylation of tRNA (Heck and Hatfield, 1988). Nucleoid-associated proteins play an important role in concentrating DNA and regulating gene expression (Lee and Marians, 2013). Transcription termination/antitermination protein NusA can bind to RNA polymerase or nascent RNA to influence transcription (Qayyum et al., 2016). Long-chain fatty acid transport proteins are involved in the transport of fatty acids and can affect intracellular signal transduction and gene expression (Dirusso and Black, 2004).These proteins may help the expression of drug resistance-related proteins by influencing the progress of gene expression or protein translation.

Metabolism-Related Proteins

The largest category contains 60 DEPs expressed differently between the MDR isolates and drug-susceptible isolates. These proteins are mainly related to metabolism (**Supplementary Table 6**). This group includes seven downregulated proteins, which are Serine hydroxymethyltransferase, NADH-quinone oxidoreductase, Malate dehydrogenase, Non-heme chloroperoxidase, 3,4-dihydroxy-2-butanone 4-phosphate synthase, Ketol-acid reductoisomerase [NADP (+)] and Acetyl-coenzyme A carboxylase carboxyl transferase subunit beta. They participate in the biosynthesis of serine, tetrahydrofolate, nitropyrrolidin, branched-chain amino acids, and fatty acids which are related to cellular processes such as bacterial respiration and TCA cycle (Shin et al., 2009; Nwugo et al., 2011; Deris et al., 2014; Reddy et al., 2014; Krishna et al., 2019). Among them, Malate dehydrogenase, which is upregulated in bacterial biofilm state (Shin et al., 2009), and the expression of it in carbapenem-resistant *A.baumannii* was up-regulated, the researcher hypothesis that it contributes to energy production and can improve the survival rate of bacteria (Tiwari et al., 2012). In our results, the protein is down-regulated. We speculate this may be due to strain differences. There are 53 up-regulated or uniquely expressed proteins in MDR strains, which are involved in lipid metabolism (Jang et al., 2008; Gu et al., 2019), amino acid metabolism (Stancik et al., 2002; Bezsudnova et al., 2017), TCA cycle (Corregido et al., 2019), purine anabolic metabolism (Spurr et al., 2012), pyruvate metabolism (Song et al., 2010), fatty acid metabolism (Nishimaki-Mogami et al., 1987), intracellular electron transfer of bacteria (López Rivero et al., 2019), nutrition and energy acquisition (Drewke et al., 1996), and other metabolic processes. In addition, the heavy metal associated (HMA) domain protein which is closely related to the utilization and metabolism of metal ions such as copper ions and zinc ions (Furukawa et al., 2018) is also up-regulated.

Proteins With Unknown Function or Other Functions Containing Biofilm Formation and Virulence

The final category F includes proteins with unknown functions or other functions besides the other five groups such as virulence or biofilm formation (**Supplementary Table 7**). Studies have found that the resistance of bacteria to disinfectants and antibacterial agents will be greatly increased after the formation of biofilms (Høiby et al., 2010) and the resistance of *A. baumannii* that produces biofilms is significantly higher than that of bacteria that cannot produce biofilms (Gurung et al., 2013). The mechanisms of biofilm formation causing resistance include delaying the penetration of antibacterial agents into bacteria, causing changes in the growth rate of membrane-forming microorganisms, and upregulating efflux pumps and other physiological metabolic differences (Donlan and Costerton, 2002; Kentache et al., 2017). Our study also found the proteins related to biofilm formation expressed more in drug-resistance isolates. For example, flagellin which is involved in the formation of bacterial flagella and the fimbriae assembly protein FilF are both related to bacterial biofilm formation (Karatan and Watnick, 2009). Histidine kinase and esterase members are also involved in the formation of biofilms (Chen et al., 2017; Larsen and Johnson, 2019). They both are upregulated in our study. A comparison of drug-resistant clinical strains and susceptible clinical strains found that drug-resistant clinical strains contain more virulence factors such as FilF, GroEL, and hemagglutinin-like protein (Li et al., 2015). In our study another type of up-regulated protein is mainly related to the virulence of bacteria. For example, hemolysin is one of the virulence factors of bacteria and is closely related to the pathogenicity of bacteria (Bhakdi et al., 1988). Cupin family protein is a superfamily of proteins with multiple functions such as metalloenzymes, sugar binding, and pathogenicity (Sim et al., 2016). Several hypothetical proteins are also up-regulated in MDR strains. Among them, putative septicolysin, cholesterol-dependent cytolysin family, and related proteins are generally virulence factors produced by bacteria (Lukoyanova et al., 2016). Other uncharacterized proteins are also upregulated. It is worth noting that an undefined protein is a member of LysM domain/BON superfamily protein. The unknown functional protein of LysM domain/BON superfamily protein was detected in both upregulated and downregulated proteins. A previous study found that a 16 kDa protein of LysM domain/BON superfamily protein detected in the outer membrane protein of susceptible *Klebsiella pneumoniae* (Kádár et al., 2017). Another study found that it may be related to the stress response of *Klebsiella pneumoniae* to Carbapenem (Khan et al., 2017). However, its specific function is unknown and deserves further study.

Analysis of Glycoproteomes

Studies have found that O-glycosylation mechanism is widespread in *A.baumannii*, and it is closely related to the virulence and biofilm formation ability of the bacteria (Iwashkiw et al., 2012; Kinsella et al., 2015), but its association with drug resistance was rarely reported. Other post-translational modifications such as phosphorylation and acetylation have been shown to be related to

drug resistance (Kentache et al., 2016). Our study aimed to identify the different glycosylation between the MDR and drug-susceptible strains. A total of 77 glycoproteins were found in the 9 MDR isolates and 97 glycoproteins were found in the 10 drug-susceptible isolates. MDR strains had 10 specifically expressed polysaccharides, and drug-susceptible strains had 30 specifically expressed polysaccharides (**Supplementary Table 8**). The specifically expressed polysaccharides found in MDR strain contain chaperone protein DnaK and phosphoenolpyruvate carboxykinase which both are essential for metabolism and survival (**Supplementary Table 9**). By further analysis, we found a polysaccharide form of HexNAc(2)Hex(2)Fuc(1) on the S21 (OGlycan/876.3223) site of adenylate kinase (the product of *adk*) is present in six MDR isolates and not exist in any drug-susceptible isolates. NetOGlyc predicts an additional glycosylation site at site 129 that is more likely to carry O-GalNAc modifications in this protein. The adenylate kinase is related to energy metabolism (Shin and Park, 2015). There is a study showed that the main mechanism of multidrug resistance is the increased activity of adenosine triphosphate (ATP)-dependent drug efflux transporters (Wen et al., 2018). Therefore, we speculate that glycosylation of adenylate kinase is closely related to the metabolism of bacteria, which may enhance the bacteria's metabolic ability and efflux ability to enhance their drug resistance.

Transcription Level of 7 DEPs by qRT-PCR

To verify the results from proteomics, we randomly chose another eight *A.baumannii* isolates from the same hospital to identify the transcription level of 7 DEPs: Aminoglycoside (3') phosphotransferase AphA1 or APH (3')-Ia (AFV53106), Beta-lactamase AmpC (AFA35105/AFA35107), Outer membrane protein assembly factor BamD (WP_000056810), MFS transporter (RSR57702), ABC transporter (AXV52620), HlyD membrane-fusion protein of T1SS (ENV25944), and Elongation factor Tu (KLT84190). Our results (**Figure 6**) showed that the transcription levels of AFV53106, AF135105, AXV52620, and ENV25944 in MDR isolates have a higher trend than that of drug-susceptible isolates, which is consistent with the results of proteomics. However, the transcription levels of WP_000056810, RSR57702 and KLT84190 in MDR isolates and susceptible isolates showed no difference. Previous studies have also found disparity between the protein levels and transcription levels of certain genes. This may be due to protein expression and post-translational modifications. In general, the verification of other MDR strains and drug-sensitive strains showed consistency with the proteomic results, indicating that the protein obtained in our results is closely related to the resistance mechanism of *A.baumannii*.

In conclusion, our study found that in MDR strains, a large number of membrane proteins and membrane formation and efflux-related proteins, metabolism-related proteins, stress response-related proteins, and proteins involved in gene expression regulation and protein translation are all upregulated, and glycosylation of adenosine triphosphate is unique in MDR strains. Through the study of the mechanism

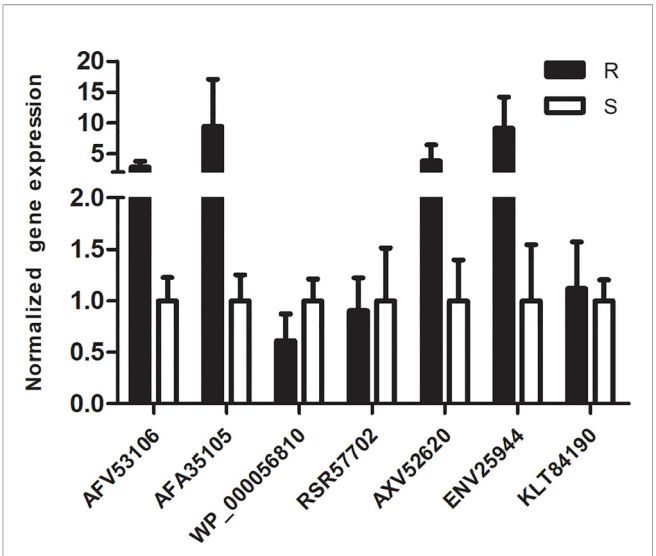

FIGURE 6 | qRT-PCR analysis of 7 representative proteins: The normalized expression level (2-ΔΔct) of 7 DEPs genes of the resistant isolates and susceptible isolates were tested by qRT-PCR. *rpoB* was used as the internal parameter. Error bars represent the SDs.

of multidrug resistance of *A.baumannii*, treatment can be adopted for its resistance mechanism to improve the success rate of treatment of *A.baumannii* infection, such as using engineered endolysin to degrade bacterial peptidoglycan to replace carbapenem drugs (Lee et al., 2017) or add certain compounds that can increase the energy production of bacteria and enhance the permeability of their cell membranes during antibiotic treatment to promote the therapeutic effect of antibiotics (Shin and Park, 2015). The development of vaccines against drug-resistant-related proteins is also another effective strategy to solve drug-resistant bacterial infections (Mujawar et al., 2019). This study uses plenty of isolates for comparative and comprehensive analysis, however, because these isolates were isolated from the same hospital and might have similar genetic phenotypes, we still need further study like expanding sample sources or sequencing these isolates to found the genetic mechanism. In addition, the specific mechanism of how DEPs-related genes influence drug resistance still needs to be further studied and explored using auxiliary methods such as gene knockout to support the results of proteomics.

DATA AVAILABILITY STATEMENT

The datasets presented in this study can be found in online repositories. The names of the repository/repositories and accession number(s) can be found in the article/**Supplementary Material**.

AUTHOR CONTRIBUTIONS

DX and Q-HZ conceived and designed the study. PW and R-QL analyzed the data. LW and W-TY performed experiments. PW

and Q-HZ wrote the manuscript. All authors contributed to the article and approved the submitted version.

FUNDING

This work was supported by The Major Infectious Diseases AIDS and Viral Hepatitis Prevention and Control Technology Major Projects (Grant No. 2018ZX10712001-006012 and Grand No. 2018ZX10733402-003002).

SUPPLEMENTARY MATERIAL

The Supplementary Material for this article can be found online at: https://www.frontiersin.org/articles/10.3389/fcimb.2021.625430/full#supplementary-material

REFERENCES

Ahmad Izaham, A. R., and Scott, N. E. (2020). Open Database Searching Enables the Identification and Comparison of Bacterial Glycoproteomes without Defining Glycan Compositions Prior to Searching. *Mol. Cell Proteomics* 19 (9), 1561–1574. doi: 10.1074/mcp.TIR120.002100

Al-Kadmy, I. M. S., Ibrahim, S. A., Al-Saryi, N., Aziz, S. N., Besinis, A., and Hetta, H. F. (2020). Prevalence of Genes Involved in Colistin Resistance in Acinetobacter baumannii: First Report from Iraq. *Microb. Drug Resist.* 26 (6), 616–622. doi: 10.1089/mdr.2019.0243

Bell, E. W., Zheng, E. J., and Ryno, L. M. (2018). Identification of inhibitors of the E. coli chaperone SurA using in silico and in vitro techniques. *Bioorg. Med. Chem. Lett.* 28 (22), 3540–3548. doi: 10.1016/j.bmcl.2018.09.034

Bezsudnova, E. Y., Boyko, K. M., and Popov, V. O. (2017). Properties of Bacterial and Archaeal Branched-Chain Amino Acid Aminotransferases. *Biochemistry (Mosc)* 82 (13), 1572–1591. doi: 10.1134/s0006297917130028

Bhakdi, S., Mackman, N., Menestrina, G., Gray, L., Hugo, F., Seeger, W., et al. (1988). The hemolysin of Escherichia coli. *Eur. J. Epidemiol.* 4 (2), 135–143. doi: 10.1007/bf00144740

Bogicevic, B., Berthoud, H., Portmann, R., Bavan, T., Meile, L., and Irmler, S. (2016). Cysteine biosynthesis in Lactobacillus casei: identification and characterization of a serine acetyltransferase. *FEMS Microbiol. Lett.* 363 (4), fnw012. doi: 10.1093/femsle/fnw012

Cardoso, K., Gandra, R. F., Wisniewski, E. S., Osaku, C. A., Kadowaki, M. K., Felipach-Neto, V., et al. (2010). DnaK and GroEL are induced in response to antibiotic and heat shock in Acinetobacter baumannii. *J. Med. Microbiol.* 59 (Pt 9), 1061–1068. doi: 10.1099/jmm.0.020339-0

Cayô, R., Rodríguez, M. C., Espinal, P., Fernández-Cuenca, F., Ocampo-Sosa, A. A., Pascual, A., et al. (2011). Analysis of genes encoding penicillin-binding proteins in clinical isolates of Acinetobacter baumannii. *Antimicrob. Agents Chemother.* 55 (12), 5907–5913. doi: 10.1128/aac.00459-11

Chen, C., Xiao, D., Zhou, W., Shi, Q., Zhang, H. F., Zhang, J., et al. (2014). Global protein differential expression profiling of cerebrospinal fluid samples pooled from Chinese sporadic CJD and non-CJD patients. *Mol. Neurobiol.* 49 (1), 290–302. doi: 10.1007/s12035-013-8519-2

Chen, R., Lv, R., Xiao, L., Wang, M., Du, Z., Tan, Y., et al. (2017). A1S_2811, a CheA/Y-like hybrid two-component regulator from Acinetobacter baumannii ATCC17978, is involved in surface motility and biofilm formation in this bacterium. *Microbiologyopen* 6 (5), e510. doi: 10.1002/mbo3.510

Chopra, S., Ramkissoon, K., and Anderson, D. C. (2013). A systematic quantitative proteomic examination of multidrug resistance in Acinetobacter baumannii. *J. Proteomics* 84, 17–39. doi: 10.1016/j.jprot.2013.03.008

Cipollone, R., Ascenzi, P., and Visca, P. (2007). Common themes and variations in the rhodanese superfamily. *IUBMB Life* 59 (2), 51–59. doi: 10.1080/15216540701206859

Corregido, M. C., Asención Diez, M. D., Iglesias, A., and Piattoni, C. V. (2019). New pieces to the carbon metabolism puzzle of Nitrosomonas europaea: Kinetic characterization of glyceraldehyde-3 phosphate and succinate semialdehyde dehydrogenases. *Biochimie* 158, 238–245. doi: 10.1016/j.biochi.2019.01.013

Correia, S., Hébraud, M., Chafsey, I., Chambon, C., Viala, D., Torres, C., et al. (2016). Impacts of experimentally induced and clinically acquired quinolone resistance on the membrane and intracellular subproteomes of Salmonella Typhimurium DT104B. *J. Proteomics* 145, 46–59. doi: 10.1016/j.jprot.2016.04.001

Culp, E., and Wright, G. D. (2017). Bacterial proteases, untapped antimicrobial drug targets. *J. Antibiot. (Tokyo)* 70 (4), 366–377. doi: 10.1038/ja.2016.138

De Silva, P. M., Chong, P., Fernando, D. M., Westmacott, G., and Kumar, A. (2018). Effect of Incubation Temperature on Antibiotic Resistance and Virulence Factors of Acinetobacter baumannii ATCC 17978. *Antimicrob. Agents Chemother.* 62 (1), e01514-17. doi: 10.1128/aac.01514-17

Deris, Z. Z., Akter, J., Sivanesan, S., Roberts, K. D., Thompson, P. E., Nation, R. L., et al. (2014). A secondary mode of action of polymyxins against Gram-negative bacteria involves the inhibition of NADH-quinone oxidoreductase activity. *J. Antibiot. (Tokyo)* 67 (2), 147–151. doi: 10.1038/ja.2013.111

Dijkshoorn, L., Nemec, A., and Seifert, H. (2007). An increasing threat in hospitals: multidrug-resistant Acinetobacter baumannii. *Nat. Rev. Microbiol.* 5 (12), 939–951. doi: 10.1038/nrmicro1789

Dirusso, C. C., and Black, P. N. (2004). Bacterial long chain fatty acid transport: gateway to a fatty acid-responsive signaling system. *J. Biol. Chem.* 279 (48), 49563–49566. doi: 10.1074/jbc.R400026200

Donald, H. M., Scaife, W., Amyes, S. G., and Young, H. K. (2000). Sequence analysis of ARI-1, a novel OXA beta-lactamase, responsible for imipenem resistance in Acinetobacter baumannii 6B92. *Antimicrob. Agents Chemother.* 44 (1), 196–199. doi: 10.1128/aac.44.1.196-199.2000

Donlan, R. M., and Costerton, J. W. (2002). Biofilms: survival mechanisms of clinically relevant microorganisms. *Clin. Microbiol. Rev.* 15 (2), 167–193. doi: 10.1128/cmr.15.2.167-193.2002

Drewke, C., Klein, M., Clade, D., Arenz, A., Müller, R., and Leistner, E. (1996). 4-O-phosphoryl-L-threonine, a substrate of the pdxC(serC) gene product involved in vitamin B6 biosynthesis. *FEBS Lett.* 390 (2), 179–182. doi: 10.1016/0014-5793(96)00652-7

Dutton, L. C., Paszkiewicz, K. H., Silverman, R. J., Splatt, P. R., Shaw, S., Nobbs, A. H., et al. (2016). Transcriptional landscape of trans-kingdom communication between Candida albicans and Streptococcus gordonii. *Mol. Oral. Microbiol.* 31 (2), 136–161. doi: 10.1111/omi.12111

Elhosseiny, N. M., Amin, M. A., Yassin, A. S., and Attia, A. S. (2015). Acinetobacter baumannii universal stress protein A plays a pivotal role in stress response and is essential for pneumonia and sepsis pathogenesis. *Int. J. Med. Microbiol.* 305 (1), 114–123. doi: 10.1016/j.ijmm.2014.11.008

Evans, B. A., and Amyes, S. G. (2014). OXA β-lactamases. *Clin. Microbiol. Rev.* 27 (2), 241–263. doi: 10.1128/cmr.00117-13

Farrow, J. M. III., Wells, G., and Pesci, E. C. (2018). Desiccation tolerance in Acinetobacter baumannii is mediated by the two-component response regulator BfmR. *PloS One* 13 (10), e0205638. doi: 10.1371/journal.pone.0205638

Fernández-García, L., Blasco, L., Lopez, M., Bou, G., García-Contreras, R., Wood, T., et al. (2016). Toxin-Antitoxin Systems in Clinical Pathogens. *Toxins (Basel)* 8 (7), 227. doi: 10.3390/toxins8070227

Fernández-Reyes, M., Rodríguez-Falcón, M., Chiva, C., Pachón, J., Andreu, D., and Rivas, L. (2009). The cost of resistance to colistin in Acinetobacter baumannii: a proteomic perspective. *Proteomics* 9 (6), 1632–1645. doi: 10.1002/pmic.200800434

Furukawa, Y., Lim, C., Tosha, T., Yoshida, K., Hagai, T., Akiyama, S., et al. (2018). Identification of a novel zinc-binding protein, C1orf123, as an interactor with a heavy metal-associated domain. *PloS One* 13 (9), e0204355. doi: 10.1371/journal.pone.0204355

Gayoso, C. M., Mateos, J., Méndez, J. A., Fernández-Puente, P., Rumbo, C., Tomás, M., et al. (2014). Molecular mechanisms involved in the response to desiccation stress and persistence in Acinetobacter baumannii. *J. Proteome Res.* 13 (2), 460–476. doi: 10.1021/pr400603f

Göttig, S., Gruber, T. M., Higgins, P. G., Wachsmuth, M., Seifert, H., and Kempf, V. A. (2014). Detection of pan drug-resistant Acinetobacter baumannii in Germany. *J. Antimicrob. Chemother.* 69 (9), 2578–2579. doi: 10.1093/jac/dku170

Gu, Q., Yuan, Q., Zhao, D., Huang, J., Hsiang, T., Wei, Y., et al. (2019). Acetyl-coenzyme A synthetase gene ChAcs1 is essential for lipid metabolism, carbon utilization and virulence of the hemibiotrophic fungus Colletotrichum higginsianum. *Mol. Plant Pathol.* 20 (1), 107–123. doi: 10.1111/mpp.12743

Gurung, J., Khyriem, A. B., Banik, A., Lyngdoh, W. V., Choudhury, B., and Bhattacharyya, P. (2013). Association of biofilm production with multidrug resistance among clinical isolates of Acinetobacter baumannii and Pseudomonas aeruginosa from intensive care unit. *Indian J. Crit. Care Med.* 17 (4), 214–218. doi: 10.4103/0972-5229.118416

Heck, J. D., and Hatfield, G. W. (1988). Valyl-tRNA synthetase gene of Escherichia coli K12. Primary structure and homology within a family of aminoacyl-TRNA synthetases. *J. Biol. Chem.* 263 (2), 868–877. doi: 10.1016/S0021-9258(19)35434-1

Heindorf, M., Kadari, M., Heider, C., Skiebe, E., and Wilharm, G. (2014). Impact of Acinetobacter baumannii superoxide dismutase on motility, virulence, oxidative stress resistance and susceptibility to antibiotics. *PloS One* 9 (7), e101033. doi: 10.1371/journal.pone.0101033

Hicks, J. L., and Mullholland, C. V. (2018). Cysteine biosynthesis in Neisseria species. *Microbiology (Reading)* 164 (12), 1471–1480. doi: 10.1099/mic.0.000728

Høiby, N., Bjarnsholt, T., Givskov, M., Molin, S., and Ciofu, O. (2010). Antibiotic resistance of bacterial biofilms. *Int. J. Antimicrob. Agents* 35 (4), 322–332. doi: 10.1016/j.ijantimicag.2009.12.011

Holland, I. B., Peherstorfer, S., Kanonenberg, K., Lenders, M., Reimann, S., and Schmitt, L. (2016). Type I Protein Secretion-Deceptively Simple yet with a Wide Range of Mechanistic Variability across the Family. *EcoSal Plus* 7 (1). doi: 10.1128/ecosalplus.ESP-0019-2015

Hood, M. I., Jacobs, A. C., Sayood, K., Dunman, P. M., and Skaar, E. P. (2010). Acinetobacter baumannii increases tolerance to antibiotics in response to monovalent cations. *Antimicrob. Agents Chemother.* 54 (3), 1029–1041. doi: 10.1128/aac.00963-09

Hua, X., Liu, L., Fang, Y., Shi, Q., Li, X., Chen, Q., et al. (2017). Colistin Resistance in Acinetobacter baumannii MDR-ZJ06 Revealed by a Multiomics Approach. *Front. Cell Infect. Microbiol.* 7:45:45. doi: 10.3389/fcimb.2017.00045

Imber, M., Loi, V. V., Reznikov, S., Fritsch, V. N., Pietrzyk-Brzezinska, A. J., Prehn, J., et al. (2018). The aldehyde dehydrogenase AldA contributes to the hypochlorite defense and is redox-controlled by protein S-bacillithiolation in Staphylococcus aureus. *Redox Biol.* 15, 557–568. doi: 10.1016/j.redox.2018.02.001

Iwashkiw, J. A., Seper, A., Weber, B. S., Scott, N. E., Vinogradov, E., Stratilo, C., et al. (2012). Identification of a general O-linked protein glycosylation system in Acinetobacter baumannii and its role in virulence and biofilm formation. *PloS Pathog.* 8 (6), e1002758. doi: 10.1371/journal.ppat.1002758

Jacobs, A. C., Hood, I., Boyd, K. L., Olson, P. D., Morrison, J. M., Carson, S., et al. (2010). Inactivation of phospholipase D diminishes Acinetobacter baumannii pathogenesis. *Infect. Immun.* 78 (5), 1952–1962. doi: 10.1128/iai.00889-09

Jang, H. J., Chang, M. W., Toghrol, F., and Bentley, W. E. (2008). Microarray analysis of toxicogenomic effects of triclosan on Staphylococcus aureus. *Appl. Microbiol. Biotechnol.* 78 (4), 695–707. doi: 10.1007/s00253-008-1349-x

Johnson, G. (2017). The α/β Hydrolase Fold Proteins of Mycobacterium tuberculosis, with Reference to their Contribution to Virulence. *Curr. Protein Pept. Sci.* 18 (3), 190–210. doi: 10.2174/1389203717666160729093515

Kádár, B., Kocsis, B., Tóth, Á., Kristóf, K., Felső, P., Kocsis, B., et al. (2017). Colistin resistance associated with outer membrane protein change in Klebsiella pneumoniae and Enterobacter asburiae. *Acta Microbiol. Immunol. Hung.* 64 (2), 217–227. doi: 10.1556/030.64.2017.017

Karatan, E., and Watnick, P. (2009). Signals, regulatory networks, and materials that build and break bacterial biofilms. *Microbiol. Mol. Biol. Rev.* 73 (2), 310–347. doi: 10.1128/mmbr.00041-08

Kentache, T., Jouenne, T., Dé, E., and Hardouin, J. (2016). Proteomic characterization of Nα- and Nε-acetylation in Acinetobacter baumannii. *J. Proteomics* 144, 148–158. doi: 10.1016/j.jprot.2016.05.021

Kentache, T., Ben Abdelkrim, A., Jouenne, T., Dé, E., and Hardouin, J. (2017). Global Dynamic Proteome Study of a Pellicle-forming Acinetobacter baumannii Strain. *Mol. Cell Proteomics* 16 (1), 100–112. doi: 10.1074/mcp.M116.061044

Khan, A., Sharma, D., Faheem, M., Bisht, D., and Khan, A. U. (2017). Proteomic analysis of a carbapenem-resistant Klebsiella pneumoniae strain in response to meropenem stress. *J. Glob. Antimicrob. Resist.* 8, 172–178. doi: 10.1016/j.jgar.2016.12.010

Kinsella, R. L., Scott, N. E., and Feldman, M. F. (2015). Clinical implications of glycoproteomics for Acinetobacter baumannii. *Expert Rev. Proteomics* 12 (1), 1–3. doi: 10.1586/14789450.2015.987756

Kishko, I., Harish, B., Zayats, V., Reha, D., Tenner, B., Beri, D., et al. (2012). Biphasic kinetic behavior of E. coli WrbA, an FMN-dependent NAD(P)H: quinone oxidoreductase. *PloS One* 7 (8), e43902. doi: 10.1371/journal.pone.0043902

Knight, D., Dimitrova, D. D., Rudin, S. D., Bonomo, R. A., and Rather, P. N. (2016). Mutations Decreasing Intrinsic β-Lactam Resistance Are Linked to Cell Division in the Nosocomial Pathogen Acinetobacter baumannii. *Antimicrob. Agents Chemother.* 60 (6), 3751–3758. doi: 10.1128/aac.00361-16

Koteva, K., Cox, G., Kelso, J. K., Surette, M. D., Zubyk, H. L., Ejim, L., et al. (2018). Rox, a Rifamycin Resistance Enzyme with an Unprecedented Mechanism of Action. *Cell Chem. Biol.* 25 (4), 403–412.e405. doi: 10.1016/j.chembiol.2018.01.009

Krishna, V. S., Zheng, S., Rekha, E. M., Guddat, L. W., and Sriram, D. (2019). Discovery and evaluation of novel Mycobacterium tuberculosis ketol-acid reductoisomerase inhibitors as therapeutic drug leads. *J. Comput. Aided Mol. Des.* 33 (3), 357–366. doi: 10.1007/s10822-019-00184-1

Krucinska, J., Falcone, E., Erlandsen, H., Hazeen, A., Lombardo, M. N., Estrada, A., et al. (2019). Structural and Functional Studies of Bacterial Enolase, a Potential Target against Gram-Negative Pathogens. *Biochemistry* 58 (9), 1188–1197. doi: 10.1021/acs.biochem.8b01298

Kwapien, K., Damergi, M., Nader, S., El Khoury, L., Hobaika, Z., Maroun, R. G., et al. (2017). Calibration of 1,2,4-Triazole-3-Thione, an Original Zn-Binding Group of Metallo-β-Lactamase Inhibitors. Validation of a Polarizable MM/MD Potential by Quantum Chemistry. *J. Phys. Chem. B* 121 (26), 6295–6312. doi: 10.1021/acs.jpcb.7b01053

Kwon, S. O., Gho, Y. S., Lee, J. C., and Kim, S. I. (2009). Proteome analysis of outer membrane vesicles from a clinical Acinetobacter baumannii isolate. *FEMS Microbiol. Lett.* 297 (2), 150–156. doi: 10.1111/j.1574-6968.2009.01669.x

Kwon, H. I., Kim, S., Oh, M. H., Na, S. H., Kim, Y. J., Jeon, Y. H., et al. (2017). Outer membrane protein A contributes to antimicrobial resistance of Acinetobacter baumannii through the OmpA-like domain. *J. Antimicrob. Chemother.* 72 (11), 3012–3015. doi: 10.1093/jac/dkx257

Lari, A. R., Ardebili, A., and Hashemi, A. (2018). AdeR-AdeS mutations & overexpression of the AdeABC efflux system in ciprofloxacin-resistant Acinetobacter baumannii clinical isolates. *Indian J. Med. Res.* 147 (4), 413–421. doi: 10.4103/ijmr.IJMR_644_16

Larsen, E. M., and Johnson, R. J. (2019). Microbial esterases and ester prodrugs: An unlikely marriage for combating antibiotic resistance. *Drug Dev. Res.* 80 (1), 33–47. doi: 10.1002/ddr.21468

Lee, C., and Marians, K. J. (2013). Characterization of the nucleoid-associated protein YejK. *J. Biol. Chem.* 288 (44), 31503–31516. doi: 10.1074/jbc.M113.494237

Lee, K., Choi, H., and Im, H. (2009). Identification and expression of the tig gene coding for trigger factor from psychrophilic bacteria with no information of genome sequence available. *Curr. Microbiol.* 59 (2), 160–166. doi: 10.1007/s00284-009-9412-0

Lee, C. R., Lee, J. H., Park, M., Park, K. S., Bae, I. K., Kim, Y. B., et al. (2017). Biology of Acinetobacter baumannii: Pathogenesis, Antibiotic Resistance Mechanisms, and Prospective Treatment Options. *Front. Cell Infect. Microbiol.* 7:55:55. doi: 10.3389/fcimb.2017.00055

Li, J., Rayner, C. R., Nation, R. L., Owen, R. J., Spelman, D., Tan, K. E., et al. (2006). Heteroresistance to colistin in multidrug-resistant Acinetobacter baumannii. *Antimicrob. Agents Chemother.* 50 (9), 2946–2950. doi: 10.1128/aac.00103-06

Li, Z. T., Zhang, R. L., Bi, X. G., Xu, L., Fan, M., Xie, D., et al. (2015). Outer membrane vesicles isolated from two clinical Acinetobacter baumannii strains exhibit different toxicity and proteome characteristics. *Microb. Pathog.* 81, 46–52. doi: 10.1016/j.micpath.2015.03.009

Lin, M. F., Chang, K. C., Lan, C. Y., Chou, J., Kuo, J. W., Chang, C. K., et al. (2011). Molecular epidemiology and antimicrobial resistance determinants of multidrug-resistant Acinetobacter baumannii in five proximal hospitals in Taiwan. *Jpn. J. Infect. Dis.* 64 (3), 222–227. doi: 10.1258/ijsa.2010.010389

Long, Q., Huang, C., Liao, P., and Xie, J. (2013). Proteomic insights into Acinetobacter baumannii drug resistance and pathogenesis. *Crit. Rev. Eukaryot. Gene Expr.* 23 (3), 227–255. doi: 10.1615/critreveukaryotgeneexpr.2013007266

López Rivero, A. S., Rossi, M. A., Ceccarelli, E. A., and Catalano-Dupuy, D. L. (2019). A bacterial 2[4Fe4S] ferredoxin as redox partner of the plastidic-type ferredoxin-NADP(+) reductase from Leptospira interrogans. *Biochim. Biophys. Acta Gen. Subj.* 1863 (4), 651–660. doi: 10.1016/j.bbagen.2019.01.004

Lukoyanova, N., Hoogenboom, B. W., and Saibil, H. R. (2016). The membrane attack complex, perforin and cholesterol-dependent cytolysin superfamily of pore-forming proteins. *J. Cell Sci.* 129 (11), 2125–2133. doi: 10.1242/jcs.182741

Mardle, C. E., Shakespeare, T. J., Butt, L. E., Goddard, L. R., Gowers, D. M., Atkins, H. S., et al. (2019). A structural and biochemical comparison of Ribonuclease E homologues from pathogenic bacteria highlights species-specific properties. *Sci. Rep.* 9 (1), 7952. doi: 10.1038/s41598-019-44385-y

May, H. C., Yu, J. J., Zhang, H., Wang, Y., Cap, A. P., Chambers, J. P., et al. (2019). Thioredoxin-A is a virulence factor and mediator of the type IV pilus system in Acinetobacter baumannii. *PloS One* 14 (7), e0218505. doi: 10.1371/journal.pone.0218505

Maynaud, G., Brunel, B., Yashiro, E., Mergeay, M., Cleyet-Marel, J. C., and Le Quéré, A. (2014). CadA of Mesorhizobium metallidurans isolated from a zinc-rich mining soil is a P(IB-2)-type ATPase involved in cadmium and zinc resistance. *Res. Microbiol.* 165 (3), 175–189. doi: 10.1016/j.resmic.2014.02.001

McNicholas, P. M., Mann, P. A., Najarian, D. J., Miesel, L., Hare, R. S., and Black, T. A. (2001). Effects of mutations in ribosomal protein L16 on susceptibility and accumulation of evernimicin. *Antimicrob. Agents Chemother.* 45 (1), 79–83. doi: 10.1128/aac.45.1.79-83.2001

Melly, G. C., Stokas, H., Dunaj, J. L., Hsu, F. F., Rajavel, M., Su, C. C., et al. (2019). Structural and functional evidence that lipoprotein LpqN supports cell envelope biogenesis in Mycobacterium tuberculosis. *J. Biol. Chem.* 294 (43), 15711–15723. doi: 10.1074/jbc.RA119.008781

Minerdi, D., Zgrablic, I., Castrignanò, S., Catucci, G., Medana, C., Terlizzi, M. E., et al. (2016). Escherichia coli Overexpressing a Baeyer-Villiger Monooxygenase from Acinetobacter radioresistens Becomes Resistant to Imipenem. *Antimicrob. Agents Chemother.* 60 (1), 64–74. doi: 10.1128/aac.01088-15

Mujawar, S., Mishra, R., Pawar, S., Gatherer, D., and Lahiri, C. (2019). Delineating the Plausible Molecular Vaccine Candidates and Drug Targets of Multidrug-Resistant Acinetobacter baumannii. *Front. Cell Infect. Microbiol.* 9:203:203. doi: 10.3389/fcimb.2019.00203

Nigro, S. J., Post, V., and Hall, R. M. (2011). Aminoglycoside resistance in multiply antibiotic-resistant Acinetobacter baumannii belonging to global clone 2 from Australian hospitals. *J. Antimicrob. Chemother.* 66 (7), 1504–1509. doi: 10.1093/jac/dkr163

Nishimaki-Mogami, T., Yamanaka, H., and Mizugaki, M. (1987). Involvement of the fatty acid oxidation complex in acetyl-CoA-dependent chain elongation of fatty acids in Escherichia coli. *J. Biochem.* 102 (2), 427–432. doi: 10.1093/oxfordjournals.jbchem.a122070

Nwugo, C. C., Gaddy, J. A., Zimbler, D. L., and Actis, L. A. (2011). Deciphering the iron response in Acinetobacter baumannii: A proteomics approach. *J. Proteomics* 74 (1), 44–58. doi: 10.1016/j.jprot.2010.07.010

Olsson, M. O., and Isaksson, L. A. (1979). Analysis of rpsD mutations in Escherichia coli. I. Comparison of mutants with various alterations in ribosomal protein S4. *Mol. Gen. Genet.* 169 (3), 251–257. doi: 10.1007/bf00382271

Parimelzaghan, A., Anbarasu, A., and Ramaiah, S. (2016). Gene Network Analysis of Metallo Beta Lactamase Family Proteins Indicates the Role of Gene Partners in Antibiotic Resistance and Reveals Important Drug Targets. *J. Cell Biochem.* 117 (6), 1330–1339. doi: 10.1002/jcb.25422

Peleg, A. Y., Potoski, B. A., Rea, R., Adams, J., Sethi, J., Capitano, B., et al. (2007). Acinetobacter baumannii bloodstream infection while receiving tigecycline: a cautionary report. *J. Antimicrob. Chemother.* 59 (1), 128–131. doi: 10.1093/jac/dkl441

Pérez-Varela, M., Corral, J., Aranda, J., and Barbé, J. (2018). Functional Characterization of AbaQ, a Novel Efflux Pump Mediating Quinolone Resistance in Acinetobacter baumannii. *Antimicrob. Agents Chemother.* 62 (9), e00906-18. doi: 10.1128/aac.00906-18

Pérez-Varela, M., Corral, J., Aranda, J., and Barbé, J. (2019). Roles of Efflux Pumps from Different Superfamilies in the Surface-Associated Motility and Virulence of Acinetobacter baumannii ATCC 17978. *Antimicrob. Agents Chemother.* 63 (3), e02190-18. doi: 10.1128/aac.02190-18

Premkumar, L., Kurth, F., Duprez, W., Grøftehauge, M. K., King, G. J., Halili, M. A., et al. (2014). Structure of the Acinetobacter baumannii dithiol oxidase DsbA bound to elongation factor EF-Tu reveals a novel protein interaction site. *J. Biol. Chem.* 289 (29), 19869–19880. doi: 10.1074/jbc.M114.571737

Qayyum, M. Z., Dey, D., and Sen, R. (2016). Transcription Elongation Factor NusA Is a General Antagonist of Rho-dependent Termination in Escherichia coli. *J. Biol. Chem.* 291 (15), 8090–8108. doi: 10.1074/jbc.M115.701268

Ramirez, M. S., Bonomo, R. A., and Tolmasky, M. E. (2020). Carbapenemases: Transforming Acinetobacter baumannii into a Yet More Dangerous Menace. *Biomolecules* 10 (5), 720. doi: 10.3390/biom10050720

Reddy, M. C., Breda, A., Bruning, J. B., Sherekar, M., Valluru, S., Thurman, C., et al. (2014). Structure, activity, and inhibition of the Carboxyltransferase β-subunit of acetyl coenzyme A carboxylase (AccD6) from Mycobacterium tuberculosis. *Antimicrob. Agents Chemother.* 58 (10), 6122–6132. doi: 10.1128/aac.02574-13

Ryan, A., Kaplan, E., Nebel, J. C., Polycarpou, E., Crescente, V., Lowe, E., et al. (2014). Identification of NAD(P)H quinone oxidoreductase activity in azoreductases from P. aeruginosa: azoreductases and NAD(P)H quinone oxidoreductases belong to the same FMN-dependent superfamily of enzymes. *PloS One* 9 (6), e98551. doi: 10.1371/journal.pone.0098551

Scribano, D., Marzano, V., Levi Mortera, S., Sarshar, M., Vernocchi, P., Zagaglia, C., et al. (2019). Insights into the Periplasmic Proteins of Acinetobacter baumannii AB5075 and the Impact of Imipenem Exposure: A Proteomic Approach. *Int. J. Mol. Sci.* 20 (14), 3451. doi: 10.3390/ijms20143451

Seward, R. J., Lambert, T., and Towner, K. J. (1998). Molecular epidemiology of aminoglycoside resistance in Acinetobacter spp. *J. Med. Microbiol.* 47 (5), 455–462. doi: 10.1099/00222615-47-5-455

Shakil, S., Khan, R., Zarrilli, R., and Khan, A. U. (2008). Aminoglycosides versus bacteria–a description of the action, resistance mechanism, and nosocomial battleground. *J. BioMed. Sci.* 15 (1), 5–14. doi: 10.1007/s11373-007-9194-y

Shin, B., and Park, W. (2015). Synergistic Effect of Oleanolic Acid on Aminoglycoside Antibiotics against Acinetobacter baumannii. *PloS One* 10 (9), e0137751. doi: 10.1371/journal.pone.0137751

Shin, J. H., Lee, H. W., Kim, S. M., and Kim, J. (2009). Proteomic analysis of Acinetobacter baumannii in biofilm and planktonic growth mode. *J. Microbiol.* 47 (6), 728–735. doi: 10.1007/s12275-009-0158-y

Sikora, A. E., Wierzbicki, I. H., Zielke, R. A., Ryner, R. F., Korotkov, K. V., Buchanan, S. K., et al. (2018). Structural and functional insights into the role of BamD and BamE within the β-barrel assembly machinery in Neisseria gonorrhoeae. *J. Biol. Chem.* 293 (4), 1106–1119. doi: 10.1074/jbc.RA117.000437

Sim, D. W., Kim, J. H., Kim, H. Y., Jang, J. H., Lee, W. C., Kim, E. H., et al. (2016). Structural identification of the lipopolysaccharide-binding capability of a cupin-family protein from Helicobacter pylori. *FEBS Lett.* 590 (17), 2997–3004. doi: 10.1002/1873-3468.12332

Siroy, A., Cosette, P., Seyer, D., Lemaître-Guillier, C., Vallenet, D., Van Dorsselaer, A., et al. (2006). Global comparison of the membrane subproteomes between a multidrug-resistant Acinetobacter baumannii strain and a reference strain. *J. Proteome Res.* 5 (12), 3385–3398. doi: 10.1021/pr060372s

Song, J., Park, Y. H., Nemeria, N. S., Kale, S., Kakalis, L., and Jordan, F. (2010). Nuclear magnetic resonance evidence for the role of the flexible regions of the E1 component of the pyruvate dehydrogenase complex from gram-negative bacteria. *J. Biol. Chem.* 285 (7), 4680–4694. doi: 10.1074/jbc.M109.082842

Spidlova, P., Stojkova, P., Dankova, V., Senitkova, I., Santic, M., Pinkas, D., et al. (2018). Francisella tularensis D-Ala D-Ala Carboxypeptidase DacD Is Involved in Intracellular Replication and It Is Necessary for Bacterial Cell Wall Integrity. *Front. Cell Infect. Microbiol.* 8:111:111. doi: 10.3389/fcimb.2018.00111

Spurr, I. B., Birts, C. N., Cuda, F., Benkovic, S. J., Blaydes, J. P., and Tavassoli, A. (2012). Targeting tumour proliferation with a small-molecule inhibitor of AICAR transformylase homodimerization. *Chembiochem* 13 (11), 1628–1634. doi: 10.1002/cbic.201200279

Stancik, L. M., Stancik, D. M., Schmidt, B., Barnhart, D. M., Yoncheva, Y. N., and Slonczewski, J. L. (2002). pH-dependent expression of periplasmic proteins and amino acid catabolism in Escherichia coli. *J. Bacteriol.* 184 (15), 4246–4258. doi: 10.1128/jb.184.15.4246-4258.2002

Sun, D., Crowell, S. A., Harding, C. M., De Silva, P. M., Harrison, A., Fernando, D. M., et al. (2016). KatG and KatE confer Acinetobacter resistance to hydrogen peroxide but sensitize bacteria to killing by phagocytic respiratory burst. *Life Sci.* 148, 31–40. doi: 10.1016/j.lfs.2016.02.015

Tankovic, J., Legrand, P., De Gatines, G., Chemineau, V., Brun-Buisson, C., and Duval, J. (1994). Characterization of a hospital outbreak of imipenem-resistant Acinetobacter baumannii by phenotypic and genotypic typing methods. *J. Clin. Microbiol.* 32 (11), 2677–2681. doi: 10.1128/jcm.32.11.2677-2681.1994

Tiwari, V., and Tiwari, M. (2014). Quantitative proteomics to study carbapenem resistance in Acinetobacter baumannii. *Front. Microbiol.* 5:512:512. doi: 10.3389/fmicb.2014.00512

Tiwari, V., Vashistt, J., Kapil, A., and Moganty, R. R. (2012). Comparative proteomics of inner membrane fraction from carbapenem-resistant Acinetobacter baumannii with a reference strain. *PloS One* 7 (6), e39451. doi: 10.1371/journal.pone.0039451

Van Houdt, R., Leplae, R., Lima-Mendez, G., Mergeay, M., and Toussaint, A. (2012). Towards a more accurate annotation of tyrosine-based site-specific recombinases in bacterial genomes. *Mob. DNA* 3 (1):6. doi: 10.1186/1759-8753-3-6

Vashist, J., Tiwari, V., Kapil, A., and Rajeswari, M. R. (2010). Quantitative profiling and identification of outer membrane proteins of beta-lactam resistant strain of Acinetobacter baumannii. *J. Proteome Res.* 9 (2), 1121–1128. doi: 10.1021/pr9011188

Villarreal, L., Heredia, N. L., and García, S. (2000). Changes in protein synthesis and acid tolerance in Clostridium perfringens type A in response to acid shock. *Int. Microbiol.* 3 (2), 113–116.

Wang, J., Zhang, J., Fu, Q., Guo, S., Ta, L., and Sun, P. (2016). Proteomic Analyses Uncover the Mechanisms Underlying Antibiotic Resistance Differences among Three Acinetobacter baumannii Isolates. *J. Mol. Microbiol. Biotechnol.* 26 (6), 401–409. doi: 10.1159/000447454

Wen, S. H., Su, S. C., Liou, B. H., Lin, C. H., and Lee, K. R. (2018). Sulbactam-enhanced cytotoxicity of doxorubicin in breast cancer cells. *Cancer Cell Int.* 18, 128. doi: 10.1186/s12935-018-0625-9

Xiao, S. Z., Chu, H. Q., Han, L. Z., Zhang, Z. M., Li, B., Zhao, L., et al. (2016). Resistant mechanisms and molecular epidemiology of imipenem-resistant Acinetobacter baumannii. *Mol. Med. Rep.* 14 (3), 2483–2488. doi: 10.3892/mmr.2016.5538

Yun, S. H., Choi, C. W., Kwon, S. O., Park, G. W., Cho, K., Kwon, K. H., et al. (2011). Quantitative proteomic analysis of cell wall and plasma membrane fractions from multidrug-resistant Acinetobacter baumannii. *J. Proteome Res.* 10 (2), 459–469. doi: 10.1021/pr101012s

Zarrilli, R., Pournaras, S., Giannouli, M., and Tsakris, A. (2013). Global evolution of multidrug-resistant Acinetobacter baumannii clonal lineages. *Int. J. Antimicrob. Agents* 41 (1), 11–19. doi: 10.1016/j.ijantimicag.2012.09.008

Conflict of Interest: The authors declare that the research was conducted in the absence of any commercial or financial relationships that could be construed as a potential conflict of interest.

frontiers in Cellular and Infection Microbiology

ORIGINAL RESEARCH
published: 11 March 2021
doi: 10.3389/fcimb.2021.632679

Evaluation of a Rapid and Simplified Protocol for Direct Identification of Microorganisms From Positive Blood Cultures by Using Matrix Assisted Laser Desorption Ionization Time-of-Flight Mass Spectrometry (MALDI-TOF MS)

*Yufeng Dai[1], Xinyi Xu[1], Xue Yan[2], Daming Li[1], Wei Cao[1], Lingli Tang[1,3], Min Hu[1,3] and Chuanhao Jiang[1,3]**

[1] Department of Laboratory Medicine, The Second Xiangya Hospital, Central South University, Changsha, China, [2] Center for Experimental Medicine, The Third Xiangya Hospital, Central South University, Changsha, China, [3] Clinical Molecular Diagnostic Center of Hunan Province, The Second Xiangya Hospital, Central South University, Changsha, China

Early and rapid identification of microorganisms is critical for reducing the mortality rate caused by bloodstream infections (BSIs). The accuracy and feasibility of directly identifying pathogens in positive blood cultures by matrix assisted laser desorption ionization time-of-flight mass spectrometry (MALDI-TOF MS) has been intensely confirmed. In this study, we combined density centrifugation and extra chemical lysis-extraction to develop an optimized method in the blood culture process, which significantly improved the effectiveness of direct identification by MALDI-TOF MS. The accuracy was evaluated by 2,032 positive blood culture samples (115 species of microorganism). The overall MALDI-TOF MS based identification rate with scores ≥ 1.700 was 87.60%. 94.06% of gram-negative bacteria were identified consistently to the genus level, followed by anaerobes (93.33%), gram-positive bacteria (84.46%), and fungi (60.87%). This protocol could obtain results within 10–20 min at a cost of less than $0.1 per sample, which saved up to 24 h in identifying 87.60% of the microorganism from positive blood cultures. This rapid and simplified protocol facilitates the direct identification of microorganism in positive blood cultures, and exhibits the advantages of cost-effective, time-saving, and easy-to-use. It could provide the causative organism of the patient to clinicians in time for targeted treatment and reduce mortality.

Keywords: bloodstream infections, blood culture, MALDI-TOF MS, direct identification, optimized protocol

OPEN ACCESS

Edited by:
Yi-Wei Tang,
Cepheid, United States

Reviewed by:
Krisztina M. Papp-Wallace,
Louis Stokes Cleveland VA Medical Center, United States
Charles William Stratton,
Vanderbilt University Medical Center, United States

***Correspondence:**
Chuanhao Jiang
jiangchuanhao@csu.edu.cn

Specialty section:
This article was submitted to Clinical Microbiology, a section of the journal Frontiers in Cellular and Infection Microbiology

Received: *23 November 2020*
Accepted: *16 February 2021*
Published: *11 March 2021*

Citation:
Dai Y, Xu X, Yan X, Li D, Cao W, Tang L, Hu M and Jiang C (2021) Evaluation of a Rapid and Simplified Protocol for Direct Identification of Microorganisms From Positive Blood Cultures by Using Matrix Assisted Laser Desorption Ionization Time-of-Flight Mass Spectrometry (MALDI-TOF MS). Front. Cell. Infect. Microbiol. 11:632679. doi: 10.3389/fcimb.2021.632679

INTRODUCTION

Bloodstream infections (BSIs) are the major cause of sepsis-related morbidity and mortality in hospitalized patients worldwide (Kumar et al., 2006; Tabah et al., 2012; Mortality and Causes of Death, 2015). The 58.3% of the nosocomial BSIs in the intensive care unit (ICU) were caused by gram-negative bacteria, 32.8% by gram-positive bacteria, 7.8% by fungi, and 1.2% by obligate anaerobes (Tabah et al., 2012). The mortality rate of sepsis-related hypotensive patients is increasing at a rate of 7.6% per hour (Kumar et al., 2006). Hence, rapid identification of the causative organism is crucial for the clinical treatment of BSIs and decreasing mortality.

Blood culture remains the reference standard for the diagnosis of BSIs (Peker et al., 2018). The traditional identification process requires culture broth from the positive blood culture bottles to be streaked on solid media and incubated for 18–24 h. The pure colonies were obtained from those subculture media for subsequent pathogen identification and antimicrobial sensitivity testing (AST). Although this traditional method is useful for routine identification of general organisms, it is challenging for fastidious bacteria such as anaerobes (Dubourg and Raoult, 2016). Moreover, the long turn-around time (TAT) would greatly depreciate its value as a rapid diagnostic method.

Matrix-assisted laser desorption ionization–time-of-flight mass spectrometry (MALDI-TOF MS) combines the MALDI source and the TOF mass. It can identify bacteria based on comparing the protein profiles of bacteria with standard profiles of known bacteria in a database (Angeletti, 2017). MALDI-TOF MS has been proved to be a high-throughput and efficient microbial identification system, which improves the reliability of microbial identification and reduces the complexity of operation (Martin, 2012; Gorton et al., 2014; Doern and Butler-Wu, 2016; Hou et al., 2019). It has been widely utilized in clinical microbiology laboratories, especially for conventional identification of pure colony cultured on solid mediums and direct identification of microorganism in blood cultures. Although notable efforts have been made, the existing methods are still relatively time-consuming and laborious, which limits the clinical application of MALDI-TOF MS in rapid diagnosis (Gorton et al., 2014; Jakovljev and Bergh, 2015; Robinson and Ussher, 2016). Also, nonbacterial proteins in blood culture broth disturb the analysis of microbial proteome profiles during direct identification. Therefore, a rapid and effective preprocessing method to eliminate interference proteins while also concentrating the bacterial is still explored. It could facilitate the widespread application of MALDI-TOF MS for the direct identification of microorganisms from blood cultures (Di Gaudio et al., 2018; Scohy et al., 2018).

This study aims to develop a relatively cost-effective and simplified protocol to directly identify microorganisms from positive blood cultures with high reliability. We optimized the previous pretreatment protocol, and prospectively assessed the performance of this protocol by comparing it with the conventional culture-dependent identification method. The complete workflow was shown in **Figure 1**. Our protocol would contribute to promptly provide causative organism of patients to clinicians for appropriate antimicrobial therapy promptly and reduce mortality.

MATERIALS AND METHODS

Sample Collection

2,081 blood culture bottles were detected positive from the Second Xiangya Hospital of Central South University between October 2018 to October 2019. 32 of the positive cultures failed to grow on subculturing, and 17 were polymicrobial. Those samples were excluded from the study. For patients with

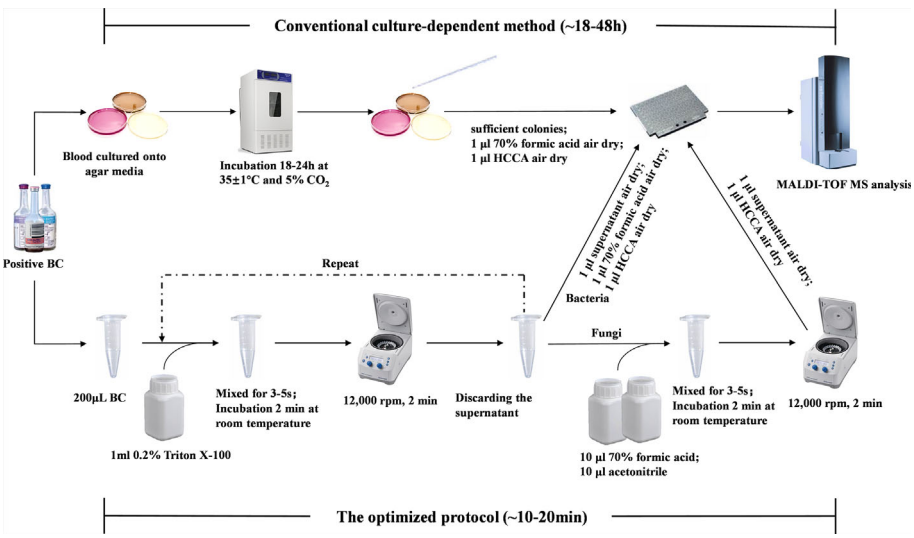

FIGURE 1 | Workflow of direct identification in positive blood cultures using MALDI-TOF MS.

multiple blood cultures simultaneously, only the blood culture that was first reported to be positive was used for further experiments to avoid repetition. Finally, the remaining 2,032 monomicrobial blood cultures, belonging to 1,870 adult patients and 162 pediatric patients, were included in the study. This study has been approved by the research and ethics committee of the Second Xiangya Hospital of Central South University. All patients are anonymized and no results were used in patient management. Therefore, no informed consent was required.

Blood Culture Processing

Blood was taken with aseptic technique, directly inoculated into aerobic (BD BACTEC Plus Aerobic/F) and anaerobic culture vials (BD BACTEC Lytic/10 Anaerobic/F), or peds culture vials (BD BACTEC Peds Plus/F culture vials) (Becton Dickinson & Co, BD, Shanghai, China). Each adult patient needed an Aerobic and an anaerobic culture vials, the Peds vials were used only for pediatric patients. All blood culture bottles were loaded onto the BD BACTEC FX instrument (Becton Dickinson, Franklin Lakes, NJ, USA).

Conventional Culture-Dependent Identification Method

Upon signaling positive, the blood culture broth was analyzed by Gram stain and cultured onto a blood agar plate (BIOIVT, Zhengzhou, China) and/or obligate anaerobic agar plate (BIOIVT, Zhengzhou, China), and incubated in 5%CO_2 at 35 ± 1°C for 18 to 24 h (Thermo Fisher Scientific, USA). Whenever Gram stain indicated the presence of fungi, the sample was additionally subcultured on SDA agar plate (BIOIVT, Zhengzhou, China) and incubated at 37°C for 48 h. Following incubation, a sterile, disposable inoculation loop was used to transfer sufficient colonies of a pure culture from those subculture media to a 96-spot polished steel target plate (Bruker Daltonics, Bremen, Germany) for MALDI-TOF MS analysis.

Lysis and Centrifugation

The blood culture bottle was vigorously shaken to ensure homogeneous mixing. 200 µl blood culture broth were harvested from positive blood culture and added into a 1.5 ml Eppendorf tube. 1 ml solution of Triton X-100 (Solarbio Biotech, Beijing, China) at a concentration of 0.2% were added. The mixture was vortexed briefly and then incubated at room temperature for 2 min. Following centrifuged at 12,000 rpm for 2 min, the supernatant was discarded, and a further 1 ml of 0.2% Triton X-100 was added before a second cycle of vortexing and centrifugation. The supernatant was discarded again, and the upper liquid was carefully removed to retain the white precipitation. Then, one loop of the white precipitation was picked out by a sterile, disposable inoculation loop and deposited onto a 96-spot polished steel target plate for MALDI-TOF MS analysis.

Extra Extraction for Fungi

The precipitation obtained in the previous step was re-suspended in 10 µl of 70% formic acid (Sigma-Aldrich, Shanghai, China). The mix was vortexed for 5 s and then incubated at room temperature for 2 min. Ten microliters of acetonitrile (Sigma-Aldrich) was added before a second cycle of vortexing and centrifugation. Finally, 1 µl of the supernatant was deposited onto a 96-spot polished steel target plate for MALDI-TOF MS analysis.

MALDI-TOF MS

After drying the bacterial pellet on a MALDI-TOF MS target plate at room temperature, 1 µl of 70% formic acid (70% v/v) was added to each spot and air-dried (fungal pellets after an extra extraction could skip this step). Lastly, 1 µl of alpha-cyano-4-hydroxycinnamic acid (HCCA) matrix solution was placed onto each spot and then air-dried for MALDI-TOF analysis.

Bruker LT Microflex MALDI-TOF MS (Bruker, Daltonics, Germany), Bruker Biotyper 2.3 system software, and Bruker database 5989 were adopted to read the target plates. The mass spectrometer was calibrated using a Bruker BTS (bacterial test standard) spot: *Escherichia coli* and three internal control spots: *Escherichia coli* ATCC 25922, *Staphylococcus aureus* ATCC 25923, and *Candida albicans* ATCC 90028. After analysis with Microflex LT, Biotyper software calculated a similarity score [log (score)] by comparing the protein spectra of each spot with the database spectra. Ten scores per spot could be obtained, ranging from a higher to lower probability of valid identification. According to the manufacturer's instructions, a score ≥2.000 indicates identification to the species level, a score between 1.700 and 1.999 indicates identification to the genus level, and a score <1.700 indicates no reliable identification. The inconsistent identification between the conventional culture-dependent method and optimized protocol was further characterized by 16S rRNA gene sequencing at the reference laboratory.

RESULTS

In this study, a total of 2,032 positive blood cultures [57.48% (1,168/2,032) aerobic blood culture vials, 34.55% (702/2,032) anaerobic blood culture vials, and 7.97% (162/2,032) Peds blood culture vials] were collected after excluding 32 bacteria-free blood cultures and 17 polymicrobial blood cultures (**Figure 2A**). All samples were classified based on the identification of the conventional culture-dependent method. 48.03% (976/2,032) strains were gram-negative bacteria, 43.7% (888/2,032) strains were gram-positive bacteria, 6.79% (138/2,032) strains were fungi, and 1.48% (30/2,032) strains were anaerobes (**Figure 2B**). The 115 different microbial species were isolated, and the effectiveness of the optimized method was evaluated by comparing with the conventional culture-dependent method under different log(score) threshold (**Table 1**). Without considering the cut-off value, the total coincidence rate of direct identification was 97.39% (1,979/2,032) compared to the conventional method. When setting the cut-off threshold to 1.700, the coincidence rate was 87.60% (1,780/2,032). More precisely, we identified 94.06% (918/976) gram-negative bacteria, 93.33% (28/30) anaerobes, 84.46% (750/888) gram-

positive bacteria, and 60.87% (84/138) fungi to the genus level (**Figure 3A** and **Table 2**). The most common isolates from BSIs in this study were *Escherichia coli* (18.21%, 370/2,032), *Klebsiella pneumoniae* (10.53%, 214/2,032), and *Staphylococcus aureus* (10.29%, 209/2,032), which had high concordance rates of 98.92% (366/370), 97.66% (209/214), and 97.61% (204/209) respectively. The identification rates of different culture bottles were similar. The Peds blood culture bottles (88.27%, 143/162) had an excellent identification rate, followed by aerobic blood culture bottles (86.56%, 1,011/1,168), and anaerobic blood culture bottles (86.48%, 607/702) (**Figure 3B**).

With the optimized protocol, 94.06% (918/976) gram-negative isolates were identified with a score ≥1.700. A lower percentage was reached to the species level, which is 68.95% (673/976). There were 721 *Enterobacterales* strains in total, and 96.81% (698/721) were identified with scores higher than 1.700. *Nonfermenting gram-negative bacilli*, mainly consists of *Acinetobacter*, *Pseudomonas*, and *Stenotrophomonas*, also had a high compliance rate with the results obtained from the conventional phenotypic identification, which is 89.07% (163/183) (**Figure 3C**).

For 888 gram-positive organisms, the scores of 84.46% (750/888) isolates ≥1.700. There are 88.91% (521/586) *Staphylococcus* were identified to the genus level. A score ≥1.700 was obtained for 97.61% (204/209) of *Staphylococcus aureus*. The 121 isolates of *Streptococcus* exhibited 71.18% (121/170) concordance with the results of conventional laboratory culture-dependent identification. *Streptococcus anginosus, Streptococcus sanguinis*, and *Streptococcus gordonii* showed high confidence identification rates, which were 96.15% (25/26), 95.65% (22/23), and 94.44% (17/18) respectively. Also, *Enterococcus* presented excellent identification with 92.31% (60/65) to the genus level. *Enterococcus faecium* and *Enterococcus faecalis* were correctly identified with 95.12% (39/41) and 94.74% (18/19) with scores higher than 1.700 (**Figure 3D**).

Among the fungi, 84 out of 138 samples (60.87%) were able to be identified at the genus level with the optimized protocol. There were seven different species of fungi that had been identified in our study. After extra lysis, *Candida tropicalis* had a concordance rate of 80.95% (34/42) with scores higher than 1.700, and 74.36% (29/39) *Candida parapsilosis* was identified to genes level. Low concordance rate was associated with *Candida albicans* (33.33%, 11/33) and *Candida glabrata* (30%, 6/20).

Seven species of anaerobic bacteria were included in our study. 93.33% (28/30) anaerobic bacteria were secured to the genus level. All of our 21 strains of gram-negative anaerobes were successfully identified to the genus level. Only two strains of gram-positive anaerobes failed to obtain reliable results. One (of two) *Propionibacterium acnes* got a score of 1.659, nearly to 1.700. One (of four) *Clostridium innocuum* got a score under 1.400.

The pretreatment time including lytic, washing, and re-suspension bacteria is about 10 min, and the identification time for MALDI-TOF MS analysis is about 2 min. Hence, only 12 min is needed for this protocol. For the identification of fungi, due to the requirement for additional extraction steps, the sample processing time is about 10 min longer than that of bacteria.

DISCUSSION

We described a rapid and simplified protocol for direct identification of microorganisms from positive blood cultures with MALDI-TOF MS in this study. The efficacy of the protocol was validated with 2032 isolates. *Enterobacterales* (96.81%), *Enterococcus* (92.31%), *Nonfermenting bacilli* (89.07%), *Staphylococcus* (88.91%), and other general organisms causing BSIs were excellently identified. It is worth noting that, compared to existing methods, including similar lysis and centrifugation approach, our protocol shows superiority. The identification success rates of our method are similar to more complicated methods but higher than most of the nonmodified methods (**Table S1**) (Campigotto et al., 2018; Lin et al., 2018; Pan et al., 2018; Tsuchida et al., 2018; Azrad et al., 2019). We noticed that Simon's research group has used the lysis and centrifugation method for blood culture broth extraction. Among 632 blood cultures, they reached a concordance rate of 80% with the conventional method when the log (score) threshold was ≥1.500 (Simon et al., 2019). However, they didn't include fungi in their work. Unlike Simon's work, we have developed an effective extra extraction process for fungi, which is the

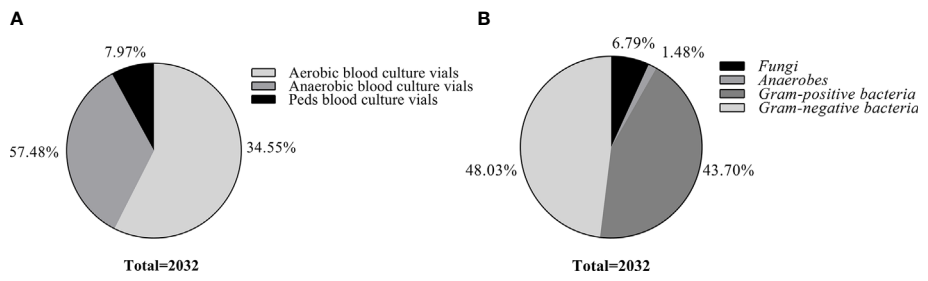

FIGURE 2 | Distribution of blood culture vials and different microbial groups identified by conventional culture-dependent method. **(A).** Distribution of blood culture vials used in this study. **(B).** Distribution of different microbial groups identified by conventional culture-dependent method.

TABLE 1 | Consistency rate of the conventional culture-dependent method and the optimized method for identifying positive blood cultures by MALDI-TOF MS (n = 2032).

Microorganisms	Conventional method (no. of isolates)	Direct method				Mis-identification (%)
		No. (%) log(score) of:				
		Score ≥2.000	Score ≥1.700	Score ≥1.400	Score <1.400	
Gram-positive bacteria	888	436 (49.10)	750 (84.46)	849 (95.61)	8 (0.90)	31 (3.49)
Staphylococcus	586	346 (59.04)	521 (88.91)	564 (96.25)	7 (1.19)	15 (2.56)
Staphylococcus aureus	209	174 (83.25)	204 (97.61)	206 (98.56)	1 (0.48)	2 (0.96)
Staphylococcus auricularis	1		1 (100.00)	1 (100.00)		
Staphylococcus capitis	33	17 (51.52)	29 (87.88)	29 (87.88)	3 (9.09)	1 (3.03)
Staphylococcus caprae	1	1 (100.00)	1 (100.00)	1 (100.00)		
Staphylococcus cohnii	2					2 (100.00)
Staphylococcus epidermidis	159	59 (37.11)	138 (86.79)	153 (96.23)	1 (0.63)	5 (3.14)
Staphylococcus equorum	1	1 (100.00)	1 (100.00)	1 (100.00)		
Staphylococcus haemolyticus	43	9 (20.93)	29 (67.44)	41 (95.35)	1 (2.33)	1 (2.33)
Staphylococcus hominis	117	76 (64.96)	108 (92.31)	116 (99.15)		1 (0.85)
Staphylococcus intermedius	2					2 (100.00)
Staphylococcus lentus	1					1 (100.00)
Staphylococcus lugdunensis	10	7 (70.00)	7 (70.00)	9 (90.00)	1 (10.00)	
Staphylococcus pettenkoferi	1	1 (100.00)	1 (100.00)	1 (100.00)		
Staphylococcus saprophyticus	3			3 (100.00)		
Staphylococcus sciuri	1			1 (100.00)		
Staphylococcus warneri	2	1 (50.00)	2 (100.00)	2 (100.00)		
Streptococcus	170	24 (14.12)	121 (71.18)	156 (91.76)		14 (8.24)
Streptococcus acidominimus	1		1 (100.00)	1 (100.00)		
Streptococcus agalactiae	7	1 (14.29)	5 (71.43)	7 (100.00)		
Streptococcus anginosus	26	4 (15.38)	25 (96.15)	25 (96.15)		1 (3.85)
Streptococcus constellatus	7		7 (100.00)	7 (100.00)		
Streptococcus cristatus	1		1 (100.00)	1 (100.00)		
Streptococcus dysgalactiae	8		7 (87.50)	7 (87.50)		1 (12.50)
Streptococcus gordonii	18	2 (11.11)	17 (94.44)	18 (100.00)		
Streptococcus mitis/oralis	38	12 (31.58)	20 (52.63)	28 (73.68)		10 (26.32)
Streptococcus pneumoniae	14	2 (14.29)	11 (78.57)	14 (100.00)		
Streptococcus pyogenes	1		1 (100.00)	1 (100.00)		
Streptococcus salivarius	6	3 (50.00)	4 (66.67)	5 (83.33)		1 (16.67)
Streptococcus sanguinis	23		22 (95.65)	22 (95.65)		1 (4.35)
Streptococcus sinensis	16			16 (100.00)		
Streptococcus vestibularis	4			4 (100.00)		
Enterococcus	65	38 (58.46)	60 (92.31)	64 (98.46)	1 (1.54)	
Enterococcus avium	1		1 (100.00)	1 (100.00)		
Enterococcus casseliflavus	2		1 (50.00)	2 (100.00)		
Enterococcus faecalis	19	15 (78.95)	18 (94.74)	19 (100.00)		
Enterococcus faecium	41	23 (56.10)	39 (95.12)	40 (97.56)	1 (2.44)	
Enterococcus gallinarum	2		1 (50.00)	2 (100.00)		
Others	67	28 (41.79)	48 (71.64)	56 (97.01)		2 (2.99)
Abiotrophia defectiva	12		4 (33.33)	12 (100.00)		
Arthrobacter polymorpha	1			1 (100.00)		
Bacillus cereus	2	2 (100.00)	2 (100.00)	2 (100.00)		
Bacillus subtilis	1	1 (100.00)	1 (100.00)	1 (100.00)		
Brevibacterium casei	2	2 (100.00)	2 (100.00)	2 (100.00)		
Corynebacterium aurimucosum	1		1 (100.00)	1 (100.00)		
Corynebacterium diphtheroides	2					2 (100.00)
Corynebacterium glucuronolyticum	1		1 (100.00)	1 (100.00)		
Corynebacterium jeikeium	1			1 (100.00)		
Corynebacterium mucifaciens	5	3 (60.00)	4 (80.00)	5 (100.00)		
Corynebacterium striatum	6	2 (33.33)	3 (50.00)	6 (100.00)		
Granulicatella adiacens	11	6 (54.55)	10 (90.91)	11 (100.00)		
Lactococcus garvieae	1	1 (100.00)	1 (100.00)	1 (100.00)		
Leifsonia aquatica	1	1 (100.00)	1 (100.00)	1 (100.00)		
Listeria monocytogenes	9	6 (66.67)	9 (100.00)	9 (100.00)		
Micrococcus luteus	7	3 (42.86)	5 (71.43)	7 (100.00)		
Mycobacterium avium	1		1 (100.00)	1 (100.00)		
Rothia mucilaginosa	3	1 (33.33)	3 (100.00)	3 (100.00)		
Gram-negative bacteria	976	673 (68.95)	918 (94.06)	950 (97.34)	4 (0.41)	22 (2.25)

(Continued)

TABLE 1 | Continued

Microorganisms	Conventional method (no. of isolates)	Direct method				Mis-identification (%)
		No. (%) log(score) of:				
		Score ≥2.000	Score ≥1.700	Score ≥1.400	Score <1.400	
Enterobacterales	721	535 (74.20)	698 (96.81)	712 (98.75)	2 (0.28)	7 (0.97)
Citrobacter braakii	2	1 (50.00)	2 (100.00)	2 (100.00)		
Citrobacter freundii	8	7 (87.50)	8 (100.00)	8 (100.00)		
Citrobacter koseri	5	4 (80.00)	5 (100.00)	5 (100.00)		
Enterobacter aerogenes	13	10 (76.92)	12 (92.31)	13 (100.00)		
Enterobacter agglomerans	4	1 (25.00)	3 (75.00)	4 (100.00)		
Enterobacter asburiae	6	2 (33.33)	5 (83.33)	6 (100.00)		
Enterobacter cloacae	28	17 (60.71)	23 (82.14)	23 (82.14)		5 (17.86)
Enterobacter Kobei	3	1 (33.33)	2 (66.67)	2 (66.67)	1 (33.33)	
Escherichia coli	370	281(75.95)	366 (98.92)	369 (99.73)	1 (0.27)	
Escherichia fergusonii	1		1 (100.00)	1 (100.00)		
Klebsiella oxytoca	14	9 (64.29)	12 (85.71)	12 (85.71)		2 (14.29)
Klebsiella planticola	1	1 (100.00)	1 (100.00)	1 (100.00)		
Klebsiella pneumoniae	214	177 (82.71)	209 (97.66)	214 (100.00)		
Morganella morganii	4	2 (50.00)	4 (100.00)	4 (100.00)		
Proteus mirabilis	9	6 (66.67)	8 (88.89)	9 (100.00)		
Salmonella SP	7	3 (42.86)	7 (100.00)	7 (100.00)		
Serratia marcescens	32	13 (40.63)	30 (93.75)	32 (100.00)		
Others	255	138 (54.12)	220 (86.27)	238 (93.33)	2 (0.78)	15 (5.88)
Acinetobacter baumannii	64	42 (65.63)	53 (82.81)	54 (84.38)		10 (15.63)
Acinetobacter johnsonii	1		1 (100.00)	1 (100.00)		
Acinetobacter junii	3	2 (66.67)	3 (100.00)	3 (100.00)		
Acinetobacter lwoffii	1					1 (100.00)
Aeromonas caviae	2		2 (100.00)	2 (100.00)		
Aeromonas hydrophila	4	2 (50.00)	4 (100.00)	4 (100.00)		
Brucella	7	5 (71.43)	7 (100.00)	7 (100.00)		
Burkholderia cepacia	7	5 (71.43)	6 (85.71)	6 (85.71)		1 (14.29)
Burkholderia gladioli	1	1 (100.00)	1 (100.00)	1 (100.00)		
Chryseobacterium hominis	1		1 (100.00)	1 (100.00)		
Chryseobacterium indologenes	1	1 (100.00)	1 (100.00)	1 (100.00)		
Cupriavidus gilardii	9	8 (88.89)	8 (88.89)	8 (88.89)	1 (11.11)	
Delftia acidovorans	1	1 (100.00)	1 (100.00)	1 (100.00)		
Dialister	2			2 (100.00)		
Haemophilus influenzae	4	2 (50.00)	4 (100.00)	4 (100.00)		
Haemophilus parainfluenzae	4	0.00		4 (100.00)		
Kluyvera ascorbata	4	2 (50.00)	4 (100.00)	4 (100.00)		
Moraxella nonliquefaciens	1		1 (100.00)	1 (100.00)		
Neisseria elongata ssp elongata	1			1 (100.00)		
Neisseria flavescens	1	1 (100.00)	1 (100.00)	1 (100.00)		
Ochrobactrum anthropi	7	1 (14.29)	4 (57.14)	6 (85.71)		1 (14.29)
Ochrobactrum gallinifaecis	1		1 (100.00)	1 (100.00)		
Plesiomonas shigelloides	4	2 (50.00)	4 (100.00)	4 (100.00)		
Pseudomonas aeruginosa	62	49 (79.03)	60 (96.77)	61 (98.39)	1 (1.61)	
Pseudomonas alcaligenes	1	1 (100.00)	1 (100.00)	1 (100.00)		
Ralstonia mannitolilytica	1		1 (100.00)	1 (100.00)		
Ralstonia pickettii	7	1 (14.29)	4 (57.14)	5 (71.43)		2 (28.57)
Rhizobium radiobacter	1	1 (100.00)	1 (100.00)	1 (100.00)		
Sphingomonas paucimobilis	1	1 (100.00)	1 (100.00)	1 (100.00)		
Stenotrophomonas maltophilia	51	10 (19.61)	45 (88.24)	51 (100.00)		
Fungi	138	12 (8.70)	84 (60.87)	128 (92.75)	10 (7.25)	
Candida albicans	33	1 (3.03)	11 (33.33)	28 (84.85)	5 (15.15)	
Candida glabrata	20	2 (10.00)	6 (30.00)	17 (85.00)	3 (15.00)	
Candida parapsilosis	39		29 (74.36)	38 (97.44)	1 (2.56)	
Candida tropicalis	42	8 (19.05)	34 (80.95)	41 (97.62)	1 (2.38)	
Pichia norvegensis	1		1 (100.00)	1 (100.00)		
Saccharomyces cerevisiae	1	1 (100.00)	1 (100.00)	1 (100.00)		
Trichosporon asahii	2		2 (100.00)	2 (100.00)		
Anaerobic bacteria	30	15 (50.00)	28 (93.33)	29 (96.67)	1 (3.33)	
Anaerobiospirillum succiniciproducens	2		2 (100.00)	2 (100.00)		

(Continued)

TABLE 1 | Continued

Microorganisms	Conventional method (no. of isolates)	Direct method				Mis-identification (%)
		No. (%) log(score) of:				
		Score ≥2.000	Score ≥1.700	Score ≥1.400	Score <1.400	
Bacteroides fragilis	13	4 (30.77)	13 (100.00)	13 (100.00)		
Clostridium clostridiiform	3	3 (100.00)	3 (100.00)	3 (100.00)		
Clostridium innocuum	4	2 (50.00)	3 (75.00)	3 (75.00)	1 (25.00)	
Prevotella bivia	5	5 (100.00)	5 (100.00)	5 (100.00)		
Prevotella buccae	1	1 (100.00)	1 (100.00)	1 (100.00)		
Propionibacterium acnes	2		1 (50.00)	2 (100.00)		
Total	2,032	1,136 (55.91)	1,780 (87.60)	1,956 (96.26)	23 (1.13)	53 (2.61)

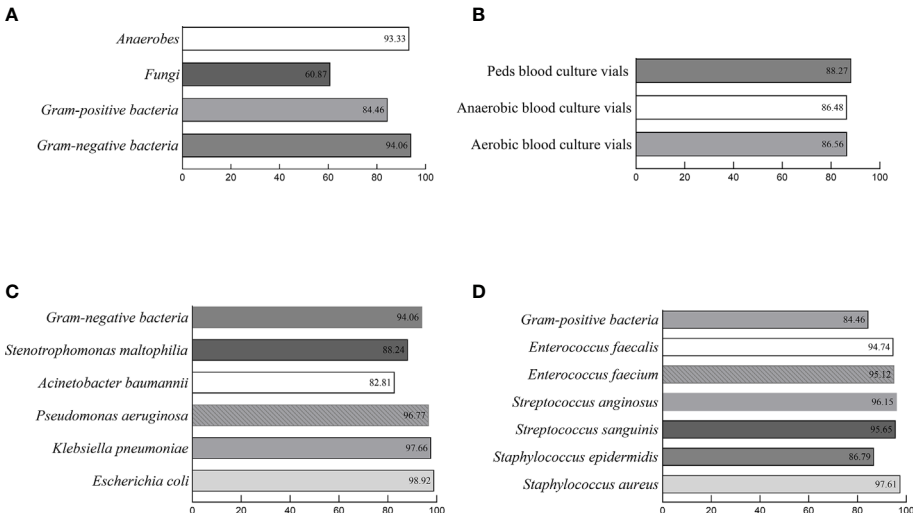

FIGURE 3 | Consistency rates of the optimized protocol for direct identification of microorganisms from positive blood cultures with the conventional method. **(A).** The percentages of concordant results were 93.33%/60.87%/84.46%/94.06%, respectively for Fungi, Anaerobes, Gram-positive bacteria, and Gram-negative bacteria with a log(score) of ≥1.700. **(B).** The percentages of concordant results were 88.27%/86.48%/86.56%, respectively for Peds/Anaerobic/Aerobic blood culture vials with a log(score) of ≥1.700. **(C).** The percentages of concordant results were 88.24%/82.81%/96.77%/97.66%/98.92%, respectively for general gram-negative bacteria *Stenotrophomonas maltophilia*, *Acinetobacter baumannii*, *Pseudomonas aeruginosa*, *Klebsiella pneumonia*, and *Escherichia coli* with a log(score) of ≥1.700. **(D).** The percentages of concordant results were 94.74%/95.12%/96.15%/95.65%/86.79%/97.61%, respectively for general gram- positive bacteria *Enterococcus faecalis*, *Enterococcus faecium*, *Streptococcus anginosus*, *Streptococcus sanguini*, *Staphylococcus epidermidis*, and *Staphylococcus aureus* with a log(score) of ≥1.700.

TABLE 2 | The percentage of concordant results between direct identification and conventional method among 2,032 monomicrobial blood cultures.

Group of Microorganism	Conventional method (no. of isolates)	Direct method		
		No. (%) log(score) of:		
		Score ≥2.000	Score ≥1.700	Score ≥1.400
Gram-positive bacteria	888	49.10%	84.46%	95.61%
Gram-negative bacteria	976	68.95%	94.06%	97.34%
Fungi	138	8.70%	60.87%	92.75%
Anaerobic bacteria	30	50%	93.33%	96.67%
Total	2,032	55.91%	87.60%	96.26%

contribution of our work. Besides, our protocol remarkably shortened the duration of the processing, and less amount of broth is needed (**Table S2**) (Loonen et al., 2012; Robinson and Ussher, 2016; Yonetani et al., 2016; Caspar et al., 2017). It is also easier to be integrated into clinical laboratories because it is economic and requires fewer personnel.

The species identification success rate of gram-negative aerobes was generally high. However, we noticed that five (of 28) strains of *Enterobacter cloacae* were incorrectly identified as *Enterobacter hormaechei*, which is in line with the previous study (Juiz et al., 2012). Meanwhile, the 10 discordant results of *Acinetobacter baumannii* consisted of six *Acinetobacter nosocomialis* and four *Acinetobacter pittii*. Several studies have reported that MALDI-TOF MS had defects in the species-level

identification of *Acinetobacter spp* as well as *Enterobacter spp*, because their species are similar in phenotype and protein profile (Turton et al., 2010; Lee et al., 2011; Juiz et al., 2012; Jeong et al., 2016).

The consistency rate of our protocol with the conventional method for gram-positive bacteria (84.46%) is still lower than for gram-negative bacteria (94.06%). The thicker peptidoglycan cell walls of gram-positive bacteria can render these bacteria more resistant to cleavage than their gram-negative counterparts, resulting in poor MALDI-TOF MS profiles (Risch et al., 2010; Clark et al., 2013). Nine of ten mis-identified *Streptococcus mitis/oralis* were erroneously identified as *Streptococcus pneumoniae* in our study. Like other protocols, it is difficult to distinguish *Streptococcus pneumoniae* with *Streptococcus mitis/oralis*, which are closely related species of viridans group *Streptococcus* (VGS) (Yonetani et al., 2016; Simon et al., 2019). VGS have the similar 16sRNA and a close compose of protein (Yonetani et al., 2016). Although the ability of MALDI-TOF MS for identifying VGS into species-level remains controversial, the accuracy for identification to the group level was generally acceptable (Loonen et al., 2012; Su et al., 2018). Additional biochemical tests, such as bile solubility test and optochin susceptibility test could be utilized to help to discriminate *Streptococcus pneumoniae* from *Streptococcus mitis/oralis*.

What's more, we have been able to successfully identify 60% of fungi from blood cultures with extra extraction, which is higher than some studies (Vecchione et al., 2018; Azrad et al., 2019; Wu et al., 2019). It has been reported that the cut-off value could be lowered down to 1.400 without compromising accuracy (Lagace-Wiens et al., 2012; Saffert et al., 2012; Simon et al., 2019). When the cut-off value was not taken into account, all results of fungal samples obtained from our protocol were successfully matched with the results from the conventional method. As reported, the thick cell wall of fungi is one of the predominant reasons that hinder the identification (Prod'hom et al., 2010). The results obtained from this study indicated that extra lysis helps disturb the cell wall and liberate intracellular proteins. We noticed that some results of fungal samples with a score ≤1.700 obtained ten correct results after analyzed by Microflex LT, but with low bacterial load. Insufficient biomass of proteins would make it hard to obtain peaks of sufficient intensity for MS analysis (De Bruyne et al., 2011).

Due to its stringent cultivation requirements, anaerobes are difficult to be cultured and identified in clinical laboratories by conventional approaches. It should be noticed that the correct identification of anaerobes by our method was 93.33% (28/30), indicating that this method is reliable for directly identifying anaerobes.

The seven strains of *Brucella* could not be successfully tested at first because the Species database that the manufacturer provided did not contain the *Brucella* strains. After introducing the spectra of respective *Brucella* into the database, all tested *Brucella* were explicitly identified at the genus level using our protocol. Therefore, optimizing the libraries of information and perfecting the database is useful to improve the identification accuracy of MALDI-TOF MS (Veloo et al., 2018; Li et al., 2019).

This study provides supporting evidence for the direct identification of microorganisms from positive blood cultures by using MALDI-TOF MS, but there are several limitations. A larger-scale test is needed to obtain more accurate information. Although more than 2,000 isolates were included in this study, the sample sizes of fastidious bacteria, fungi, and anaerobes were relatively small. Besides, this protocol has been only tested in one clinical microbiology laboratory, the repeatability and reproducibility of the protocol need to be assessed. The strict and systematic training for operators should be conducted to eliminate the operative difference and reduce analytical errors (Li et al., 2019; Luethy and Johnson, 2019).

Our further study may focus on creating more user-defined databases, directly antimicrobial susceptibility testing, and detecting virulence factors. All of those studies will facilitate the continuing research on the clinical application of MALDI-TOF MS.

In conclusion, this easy-to-use and cost-effective protocol can accurately identify 87.60% of microorganisms from blood cultures in 20 min. It could remarkably shorten the TAT of BSIs diagnosis and reduce morbidity and mortality of patients.

DATA AVAILABILITY STATEMENT

The original contributions presented in the study are included in the article/**Supplementary Material**. Further inquiries can be directed to the corresponding author.

AUTHOR CONTRIBUTIONS

CJ and YD conceptualized and designed the research. CJ, YD, XX, and DL performed the experiments. CJ, YD, XY, WC, LT, and MH carried out the data analysis. CJ and YD wrote the manuscript. All authors contributed to the article and approved the submitted version.

FUNDING

This work was supported by the National Nature Science Foundation of China (81701577) and the Natural Science Foundation of Hunan Province of China (2018JJ2559).

SUPPLEMENTARY MATERIAL

The Supplementary Material for this article can be found online at: https://www.frontiersin.org/articles/10.3389/fcimb.2021.632679/full#supplementary-material

REFERENCES

Angeletti, S. (2017). Matrix assisted laser desorption time of flight mass spectrometry (MALDI-TOF MS) in clinical microbiology. *J. Microbiol. Methods* 138, 20–29. doi: 10.1016/j.mimet.2016.09.003

Azrad, M., Keness, Y., Nitzan, O., Pastukh, N., Tkhawkho, L., Freidus, V., et al. (2019). Cheap and rapid in-house method for direct identification of positive blood cultures by MALDI-TOF MS technology. *BMC Infect. Dis.* 19, 72. doi: 10.1186/s12879-019-3709-9

Campigotto, A., Goneau, L., and Matukas, L. M. (2018). Direct identification and antimicrobial susceptibility testing of microorganisms from positive blood cultures following isolation by lysis-centrifugation. *Diagn. Microbiol. Infect. Dis.* 92, 189–193. doi: 10.1016/j.diagmicrobio.2018.06.010

Caspar, Y., Garnaud, C., Raykova, M., Bailly, S., Bidart, M., and Maubon, D. (2017). Superiority of SDS lysis over saponin lysis for direct bacterial identification from positive blood culture bottle by MALDI-TOF MS. *Proteomics Clin. Appl.* 11, 5–6. doi: 10.1002/prca.201600131

Clark, A. E., Kaleta, E. J., Arora, A., and Wolk, D. M. (2013). Matrix-assisted laser desorption ionization-time of flight mass spectrometry: a fundamental shift in the routine practice of clinical microbiology. *Clin. Microbiol. Rev.* 26, 547–603. doi: 10.1128/CMR.00072-12

De Bruyne, K., Slabbinck, B., Waegeman, W., Vauterin, P., De Baets, B., and Vandamme, P. (2011). Bacterial species identification from MALDI-TOF mass spectra through data analysis and machine learning. *Syst. Appl. Microbiol.* 34, 20–29. doi: 10.1016/j.syapm.2010.11.003

Di Gaudio, F., Indelicato, S., Indelicato, S., Tricoli, M. R., Stampone, G., and Bongiorno, D. (2018). Improvement of a rapid direct blood culture microbial identification protocol using MALDI-TOF MS and performance comparison with SepsiTyper kit. *J. Microbiol. Methods* 155, 1–7. doi: 10.1016/j.mimet.2018.10.015

Doern, C. D., and Butler-Wu, S. M. (2016). Emerging and Future Applications of Matrix-Assisted Laser Desorption Ionization Time-of-Flight (MALDI-TOF) Mass Spectrometry in the Clinical Microbiology Laboratory: A Report of the Association for Molecular Pathology. *J. Mol. Diagn.* 18, 789–802. doi: 10.1016/j.jmoldx.2016.07.007

Dubourg, G., and Raoult, D. (2016). Emerging methodologies for pathogen identification in positive blood culture testing. *Expert Rev. Mol. Diagn.* 16, 97–111. doi: 10.1586/14737159.2016.1112274

Gorton, R. L., Seaton, S., Ramnarain, P., Mchugh, T. D., and Kibbler, C. C. (2014). Evaluation of a short, on-plate formic acid extraction method for matrix-assisted laser desorption ionization-time of flight mass spectrometry-based identification of clinically relevant yeast isolates. *J. Clin. Microbiol.* 52, 1253–1255. doi: 10.1128/JCM.03489-13

Hou, T. Y., Chiang-Ni, C., and Teng, S. H. (2019). Current status of MALDI-TOF mass spectrometry in clinical microbiology. *J. Food Drug Anal.* 27, 404–414. doi: 10.1016/j.jfda.2019.01.001

Jakovljev, A., and Bergh, K. (2015). Development of a rapid and simplified protocol for direct bacterial identification from positive blood cultures by using matrix assisted laser desorption ionization time-of- flight mass spectrometry. *BMC Microbiol.* 15, 258. doi: 10.1186/s12866-015-0594-2

Jeong, S., Hong, J. S., Kim, J. O., Kim, K. H., Lee, W., Bae, I. K., et al. (2016). Identification of Acinetobacter Species Using Matrix-Assisted Laser Desorption Ionization-Time of Flight Mass Spectrometry. *Ann. Lab. Med.* 36, 325–334. doi: 10.3343/alm.2016.36.4.325

Juiz, P. M., Almela, M., Melcion, C., Campo, I., Esteban, C., Pitart, C., et al. (2012). A comparative study of two different methods of sample preparation for positive blood cultures for the rapid identification of bacteria using MALDI-TOF MS. *Eur. J. Clin. Microbiol. Infect. Dis.* 31, 1353–1358. doi: 10.1007/s10096-011-1449-x

Kumar, A., Roberts, D., Wood, K. E., Light, B., Parrillo, J. E., Sharma, S., et al. (2006). Duration of hypotension before initiation of effective antimicrobial therapy is the critical determinant of survival in human septic shock. *Crit. Care Med.* 34, 1589–1596. doi: 10.1097/01.CCM.0000217961.75225.E9

Lagace-Wiens, P. R., Adam, H. J., Karlowsky, J. A., Nichol, K. A., Pang, P. F., Guenther, J., et al. (2012). Identification of blood culture isolates directly from positive blood cultures by use of matrix-assisted laser desorption ionization-time of flight mass spectrometry and a commercial extraction system: analysis of performance, cost, and turnaround time. *J. Clin. Microbiol.* 50, 3324–3328. doi: 10.1128/JCM.01479-12

Lee, K., Yong, D., Jeong, S. H., and Chong, Y. (2011). Multidrug-resistant Acinetobacter spp.: increasingly problematic nosocomial pathogens. *Yonsei Med. J.* 52, 879–891. doi: 10.3349/ymj.2011.52.6.879

Li, Y., Shan, M., Zhu, Z., Mao, X., Yan, M., Chen, Y., et al. (2019). Application of MALDI-TOF MS to rapid identification of anaerobic bacteria. *BMC Infect. Dis.* 19, 941. doi: 10.1186/s12879-019-4584-0

Lin, J. F., Ge, M. C., Liu, T. P., Chang, S. C., and Lu, J. J. (2018). A simple method for rapid microbial identification from positive monomicrobial blood culture bottles through matrix-assisted laser desorption ionization time-of-flight mass spectrometry. *J. Microbiol. Immunol. Infect.* 51, 659–665. doi: 10.1016/j.jmii.2017.03.005

Loonen, A. J., Jansz, A. R., Stalpers, J., Wolffs, P. F., and Van Den Brule, A. J. (2012). An evaluation of three processing methods and the effect of reduced culture times for faster direct identification of pathogens from BacT/ALERT blood cultures by MALDI-TOF MS. *Eur. J. Clin. Microbiol. Infect. Dis.* 31, 1575–1583. doi: 10.1007/s10096-011-1480-y

Luethy, P. M., and Johnson, J. K. (2019). The Use of Matrix-Assisted Laser Desorption/Ionization Time-of-Flight Mass Spectrometry (MALDI-TOF MS) for the Identification of Pathogens Causing Sepsis. *J. Appl. Lab. Med.* 3, 675–685. doi: 10.1373/jalm.2018.027318

Martin, G. S. (2012). Sepsis, severe sepsis and septic shock: changes in incidence, pathogens and outcomes. *Expert Rev. Anti Infect. Ther.* 10, 701–706. doi: 10.1586/eri.12.50

Mortality, G. B. D., and Causes of Death, C. (2015). Global, regional, and national age-sex specific all-cause and cause-specific mortality for 240 causes of deat-2013: a systematic analysis for the Global Burden of Disease Study 2013. *Lancet* 385, 117–171. doi: 10.1016/S0140-6736(14)61682-2

Pan, H. W., Li, W., Li, R. G., Li, Y., Zhang, Y., and Sun, E. H. (2018). Simple Sample Preparation Method for Direct Microbial Identification and Susceptibility Testing From Positive Blood Cultures. *Front. Microbiol.* 9:481. doi: 10.3389/fmicb.2018.00481

Peker, N., Couto, N., Sinha, B., Rossen, J. J. C. M., Microbiology, I.T.O.P.O.T.E.S.O.C., and Diseases, I. (2018). Diagnosis of bloodstream infections from positive blood cultures and directly from blood samples: recent developments in molecular approaches. *Clin. Microbiol. Infect.* 24, 944–955. doi: 10.1016/j.cmi.2018.05.007

Prod'hom, G., Bizzini, A., Durussel, C., Bille, J., and Greub, G. (2010). Matrix-assisted laser desorption ionization-time of flight mass spectrometry for direct bacterial identification from positive blood culture pellets. *J. Clin. Microbiol.* 48, 1481–1483. doi: 10.1128/JCM.01780-09

Risch, M., Radjenovic, D., Han, J. N., Wydler, M., Nydegger, U., and Risch, L. (2010). Comparison of MALDI TOF with conventional identification of clinically relevant bacteria. *Swiss Med. Wkly* 140, w13095. doi: 10.4414/smw.2010.13095

Robinson, A. M., and Ussher, J. E. (2016). Preparation of positive blood cultures for direct MALDI-ToF MS identification. *J. Microbiol. Methods* 127, 74–76. doi: 10.1016/j.mimet.2016.05.026

Saffert, R. T., Cunningham, S. A., Mandrekar, J., and Patel, R. (2012). Comparison of three preparatory methods for detection of bacteremia by MALDI-TOF mass spectrometry. *Diagn. Microbiol. Infect. Dis.* 73, 21–26. doi: 10.1016/j.diagmicrobio.2012.01.010

Scohy, A., Noel, A., Boeras, A., Brassinne, L., Laurent, T., Rodriguez-Villalobos, H., et al. (2018). Evaluation of the Bruker(R) MBT Sepsityper IVD module for the identification of polymicrobial blood cultures with MALDI-TOF MS. *Eur. J. Clin. Microbiol. Infect. Dis.* 37, 2145–2152. doi: 10.1007/s10096-018-3351-2

Simon, L., Ughetto, E., Gaudart, A., Degand, N., Lotte, R., and Ruimy, R. (2019). Direct Identification of 80 Percent of Bacteria from Blood Culture Bottles by Matrix-Assisted Laser Desorption Ionization-Time of Flight Mass Spectrometry Using a 10-Minute Extraction Protocol. *J. Clin. Microbiol.* 57, e01278–18. doi: 10.1128/JCM.01278-18

Su, T. Y., Lee, M. H., Huang, C. T., Liu, T. P., and Lu, J. J. (2018). The clinical impact of patients with bloodstream infection with different groups of Viridans group streptococci by using matrix-assisted laser desorption ionization-time of flight mass spectrometry (MALDI-TOF MS). *Med. (Baltimore)* 97, e13607. doi: 10.1097/MD.0000000000013607

Tabah, A., Koulenti, D., Laupland, K., Misset, B., Valles, J., Bruzzi De Carvalho, F., et al. (2012). Characteristics and determinants of outcome of hospital-acquired bloodstream infections in intensive care units: the EUROBACT International Cohort Study. *Intensive Care Med.* 38, 1930–1945. doi: 10.1007/s00134-012-2695-9

Tsuchida, S., Murata, S., Miyabe, A., Satoh, M., Takiwaki, M., Matsushita, K., et al. (2018). An improved in-house lysis-filtration protocol for bacterial identification from positive blood culture bottles with high identification rates by MALDI-TOF MS. *J. Microbiol. Methods* 148, 40–45. doi: 10.1016/j.mimet.2018.03.014

Turton, J. F., Shah, J., Ozongwu, C., and Pike, R. (2010). Incidence of Acinetobacter species other than A. baumannii among clinical isolates of Acinetobacter: evidence for emerging species. *J. Clin. Microbiol.* 48, 1445–1449. doi: 10.1128/JCM.02467-09

Vecchione, A., Florio, W., Celandroni, F., Barnini, S., Lupetti, A., and Ghelardi, E. (2018). A Rapid Procedure for Identification and Antifungal Susceptibility Testing of Yeasts From Positive Blood Cultures. *Front. Microbiol.* 9, 2400. doi: 10.3389/fmicb.2018.02400

Veloo, A. C. M., Jean-Pierre, H., Justesen, U. S., Morris, T., Urban, E., Wybo, I., et al. (2018). Validation of MALDI-TOF MS Biotyper database optimized for anaerobic bacteria: The ENRIA project. *Anaerobe* 54, 224–230. doi: 10.1016/j.anaerobe.2018.03.007

Wu, S., Xu, J., Qiu, C., Xu, L., Chen, Q., and Wang, X. (2019). Direct antimicrobial susceptibility tests of bacteria and yeasts from positive blood cultures by using serum separator gel tubes and MALDI-TOF MS. *J. Microbiol. Methods* 157, 16–20. doi: 10.1016/j.mimet.2018.12.011

Yonetani, S., Ohnishi, H., Ohkusu, K., Matsumoto, T., and Watanabe, T. (2016). Direct identification of microorganisms from positive blood cultures by MALDI-TOF MS using an in-house saponin method. *Int. J. Infect. Dis.* 52, 37–42. doi: 10.1016/j.ijid.2016.09.014

Conflict of Interest: The authors declare that the research was conducted in the absence of any commercial or financial relationships that could be construed as a potential conflict of interest.

frontiers in Cellular and Infection Microbiology

ORIGINAL RESEARCH
published: 16 March 2021
doi: 10.3389/fcimb.2021.632647

MALDI-TOF MS Biomarker Detection Models to Distinguish RTX Toxin Phenotypes of *Moraxella bovoculi* Strains Are Enhanced Using Calcium Chloride Supplemented Agar

Matthew M. Hille[1], *Michael L. Clawson*[2], *Aaron M. Dickey*[2], *Justin H. Lowery*[1] *and John Dustin Loy*[1]*

[1] School of Veterinary Medicine and Biomedical Sciences, Institute for Agriculture and Natural Resources, University of Nebraska-Lincoln, Lincoln, NE, United States, [2] U.S. Meat Animal Research Center, United States Department of Agriculture, Agricultural Research Service, Clay Center, NE, United States

OPEN ACCESS

Edited by:
Di Xiao,
National Institute for Communicable Disease Control and Prevention (China CDC), China

Reviewed by:
Grazieli Maboni,
University of Georgia, United States
Michael John Calcutt,
University of Missouri, United States

***Correspondence:**
John Dustin Loy
jdloy@unl.edu

Specialty section:
This article was submitted to Clinical Microbiology, a section of the journal Frontiers in Cellular and Infection Microbiology

Received: 23 November 2020
Accepted: 01 March 2021
Published: 16 March 2021

Citation:
Hille MM, Clawson ML, Dickey AM, Lowery JH and Loy JD (2021) MALDI-TOF MS Biomarker Detection Models to Distinguish RTX Toxin Phenotypes of Moraxella bovoculi Strains Are Enhanced Using Calcium Chloride Supplemented Agar. Front. Cell. Infect. Microbiol. 11:632647. doi: 10.3389/fcimb.2021.632647

Moraxella bovoculi is the bacterium most often cultured from ocular lesions of cattle with infectious bovine keratoconjunctivitis, also known as bovine pinkeye. Some strains of *M. bovoculi* contain operons encoding for a repeats-in-toxin (RTX) toxin, which is a known virulence factor of multiple veterinary pathogens. We explored the utility of MALDI-TOF MS and biomarker detection models to classify the presence or absence of an RTX phenotype in *M. bovoculi*. Ninety strains that had undergone whole genome sequencing were classified by the presence or absence of complete RTX operons and confirmed with a visual assessment of hemolysis on blood agar. Strains were grown on Tryptic Soy Agar (TSA) with 5% sheep blood, TSA with 5% bovine blood that was supplemented with 10% fetal bovine serum, 10 mmol/L$CaCl_2$, or both. The formulations were designed to determine the influence of growth media on toxin production or activity, as calcium ions are required for toxin secretion and activity. Mass spectra were obtained for strains grown on each agar formulation and biomarker models were developed using ClinProTools 3.0 software. The most accurate model was developed using spectra from strains grown on TSA with 5% bovine blood and supplemented with $CaCl_2$, which had a sensitivity and specificity of 93.3% and 73.3%, respectively, regarding RTX phenotype classification. The same biomarker model algorithm developed from strains grown on TSA with 5% sheep blood had a substantially lower sensitivity and specificity of 68.0% and 52.0%, respectively. Our results indicate that MALDI-TOF MS biomarker models can accurately classify strains of *M. bovoculi* regarding the presence or absence of RTX toxin operons and that agar media modifications improve the accuracy of these models.

Keywords: MALDI-TOF MS, *Moraxella bovoculi*, infectious bovine keratoconjunctivitis, biomarker model, RTX toxin, Moraxella bovis

INTRODUCTION

Infectious bovine keratoconjunctivitis (IBK) is the most common ocular disease in cattle (Brown et al., 1998). IBK has a substantial economic impact including costs associated with treatment as well as decreased weight gain in affected animals and impacts animal welfare by causing pain and blindness (Killinger et al., 1977; Dewell et al., 2014). *Moraxella bovis* (*M. bovis*) is the only bacterium that has reproduced IBK-like lesions in a variety of experimental models (Henson and Grumbles, 1960; Aikman et al., 1985). Other bacteria are often associated with IBK, but so far none have produced disease experimentally. The most notable and frequently isolated of these associated bacteria is *Moraxella bovoculi* (Angelos et al., 2007b). While *M. bovoculi* has been unsuccessful at inducing IBK experimentally (Gould et al., 2013), it is more frequently isolated from IBK lesions when compared to *M. bovis*, using both aerobic culture and molecular detection techniques (Loy and Brodersen, 2014; Zheng et al., 2019). Despite the lack of proven causation for *M.* bovoculi in IBK to date, in 2017 the USDA approved the first conditionally licensed *M. bovoculi* based vaccine product to be marketed for the prevention of IBK (USDA CVM code: 2A77.00, Addison Biological Laboratory). Recently, whole genome sequencing of *M. bovoculi* has revealed a large degree of diversity within the species that led to the characterization of two distinct genotypes (genotype 1 and genotype 2) separated by over 23,000 single nucleotide polymorphisms (Dickey et al., 2018). To date, only genotype 1 *M. bovoculi* have been isolated from IBK lesions while both genotypes have been recovered from animals without clinical signs.

Strains of *M. bovis* have been shown to produce an exotoxin belonging to the repeats-in-toxin (RTX) class of exotoxins that is cytopathic to bovine erythrocytes and neutrophils (Clinkenbeard and Thiessen, 1991; Angelos et al., 2001). In *M. bovis*, this RTX toxin, encoded by *mbxA* within an operon, is often referred to by several names including cytolysin, hemolysin, or cytotoxin. RTX toxins are known virulence factors in a variety of veterinary pathogens, including species within the family *Pasteurellacea* (Linhartova et al., 2018). A well-studied example of this is the leukotoxin produced by *Mannheimia haemolytica* (Frey, 2019). These RTX toxins are secreted in a calcium-dependent manner *via* a type I secretion system (T1SS) responsible for translocating the toxin from the cytosol to the exterior (Linhartova et al., 2018) Like *M. bovis*, some *M. bovoculi* strains also contain a complete RTX operon that produces an RTX toxin, cytotoxin A encoded by *mbvA* (Angelos et al., 2007a). Like *mbxA* produced by *M. bovis, mbvA* of *M. bovoculi* is responsible for hemolytic and lytic activity on bovine cells (Cerny et al., 2006; Angelos et al., 2007b). Within *M. bovoculi*, only the disease associated genotype 1 strains have been shown to possess the RTX operon, although not all do (Dickey et al., 2018). Besides RTX toxins, both *M. bovis* and *M. bovoculi* express a type IV pilus, a known virulence factor in other bacterial pathogens (Angelos et al., 2021). These similar potential virulence factors between the two *Moraxella* species highlight the relevance of continued investigation into the diversity within *M. bovoculi* and how this diversity may impact IBK pathogenesis.

Matrix-assisted laser desorption/ionization time-of-flight mass spectrometry (MALDI-TOF MS) is an approach that is increasingly being applied to the identification of prokaryotes and eukaryotes. (Seng et al., 2009; Clark et al., 2013; Khot and Fisher, 2013; Karger et al., 2019). MALDI-TOF MS has replaced or supplemented more traditional biochemical identification methods as it is faster and increasingly more accurate as databases become mature. Using spectrum profiles generated from MALDI-TOF MS, biomarker models have been developed that are capable of differentiating subspecies and genotypes within a given bacterial species (Loy and Clawson, 2017; Mani et al., 2017; Perez-Sancho et al., 2018). Recently, a MALDI-TOF biomarker model was developed that accurately distinguishes *M. bovoculi* genotypes 1 and 2 (Hille et al., 2020). This model allows for the screening of strains for potential disease associated genotypes without the need for genome sequencing.

Genotype 1 *M. bovoculi* strains isolated from IBK associated eyes have been found with a higher frequency of the RTX operon than those isolated from unaffected eyes (Dickey et al., 2018). While it can be suspected based on a hemolytic phenotype, confirming the presence or absence of an RTX operon requires PCR or genomic sequencing (Angelos et al., 2003). In this study we evaluated the utility of MALDI-TOF MS biomarker models to accurately classify *M. bovoculi* strains regarding the presence or absence of an RTX operon among strains that had previously undergone whole genome sequencing and thus whose RTX operon status was known. Such a model would allow for an additional screening tool to characterize strains more likely to represent disease associated strains.

In addition to traditional tryptic soy agar (TSA) with 5% sheep blood agar culture conditions, we also compared biomarker model accuracies using three additional growth agar formulations to determine if agar formulation could improve model accuracy. The hemolytic activity of hemolysin produced by *M. bovis* has been shown to decrease when extracellular calcium is rendered unavailable (Clinkenbeard and Thiessen, 1991; Billson et al., 2000). Calcium has also been shown to promote efficient post translational modification and excretion of RTX toxins from the cell *via* the T1SS in *Bordetella pertussis* (Bumba et al., 2016). We hypothesized calcium may be a limiting factor in the production of RTX for *M. bovoculi* using the traditional culture conditions. Additionally, in the authors' experience, *Moraxella* sp. isolated from cattle grow subjectively better on agar that utilizes bovine red blood cells vs traditional sheep's blood agar.

METHODS

Bacterial Strains

The 90 *M. bovoculi* strains used in this study had previously been identified to the species level using both PCR and MALDI-TOF MS techniques as previously described (Loy and Brodersen, 2014; Robbins et al., 2018). The strains also underwent whole genome sequencing which enabled characterization to the genotype level as well as the presence or absence of an RTX operon element (Dickey et al., 2018). Included were 45 genotype 1,

RTX negative and 45 genotype 1, RTX positive strains obtained from a total of 18 different states within the US (**Table 1**). Hemolytic activity on blood agar containing 5% sheep blood was confirmed for all RTX positive strains and was absent in all RTX negative strains. All 90 strains were used in the models developed from TSA with 5% sheep erythrocytes and a subset of 70 strains were used in the models developed from TSA with 5% bovine erythrocytes.

Culture Conditions

From a library of frozen stocks, *M. bovoculi* strains were plated on either TSA(Becton, Dickinson & Company, Sparks, MD) with 5% sheep blood (Remel, Lenexa, KS) or TSA with 5% defibrinated bovine blood (Colorado Serum Company, Denver, CO). Additionally, the agars using bovine blood were supplemented with either 10% fetal bovine serum (Colorado Serum Company), 10 mmol/L $CaCl_2$ (Fisher Scientific, Waltham, MA), or both. After the strains were plated they were incubated in 5% CO_2 at 37° C for 24 hours prior to being passed once on the same agar formulation for an additional 24 hours prior to MALDI-TOF MS analysis.

MALDI-TOF MS

MALDI-TOF MS spectra were obtained for each of the strains listed in **Table 1** according to the manufacturer's recommendation using the formic acid-ethanol extraction method that has previously been described (Khot et al., 2012; Hille et al., 2020). Spectra were collected on a linear MALDI-TOF MS (Bruker microflex, Bruker Daltonik, Billerica, MA) using settings and calibrations as described previously (Hille et al., 2020). For the sheep's blood media models, strains were spotted three times on the target plate and analyzed once for each spot well resulting in three spectra per strain. For the bovine blood models, the strains were spotted five times each and analyzed twice per well resulting in 10 spectra per strain. This yielded a total of 970 unique spectra being analyzed for this study.

Biomarker Models

ClinProTools 3.0 software (Bruker Daltonik) was used to analyze the spectra for the presence of RTX phenotype specific, discriminatory peaks. To develop biomarker models, three spectra classification algorithms were used that included support vector machine (SVM), genetic algorithm (GA), and quick classifier (QC) methods. *M. bovoculi* strains were randomly assigned to separate groups according to RTX status to develop the biomarker models which included model generation, model validation, and model classify groups (**Table 1**). Spectra from the model generation groups were input into ClinProTools 3.0 software (Bruker Daltonik) according to their known RTX status to develop the models. The model validation step used spectra that were input with the RTX status known to the software as a test of accuracy of the developed models. Finally, the classification step involved inputting spectra with RTX status unknown to the software and allowing the models to classify them. The accuracy of the models to classify spectra was then calculated manually based on individual spectra as well as

TABLE 1 | The biomarker model group, RTX status, and state of origin for the 90 *M. bovoculi* strains used in this study.

Group	Strain Number	RTX +/-	State
Model Generation	57909	–	Nebraska
	58026	–	Oklahoma
	58036	–	Iowa
	58058	–	Nebraska
	58065	–	Indiana
	58079	–	Kansas
	58094	–	Nebraska
	58122	–	Nebraska
	60479	–	Nebraska
	68507	–	Nebraska
	57851	+	Montana
	57855	+	Ohio
	57904	+	California
	57917	+	Nebraska
	57922	+	Indiana
	58001	+	Montana
	58015	+	Illinois
	58027	+	Virginia
	58080	+	Minnesota
	58119	+	Nebraska
Model Validation	57861	–	South Dakota
	57876	–	Nebraska
	57923	–	Minnesota
	58034	–	Nebraska
	58054	–	Kansas
	58075	–	Nebraska
	58090	–	Illinois
	60476	–	Nebraska
	68485	–	Nebraska
	68511	–	Nebraska
	57860	+	Iowa
	57870	+	Nebraska
	57884	+	Indiana
	57891	+	Wisconsin
	57993	+	Nebraska
	58030	+	Kansas
	58035	+	Illinois
	58053	+	Montana
	58063	+	Minnesota
	58088	+	Minnesota
Model Classify	57881	–	Nebraska
	57883	–	Nebraska
	58028	–	South Dakota
	58047	–	Virginia
	58067	–	Nebraska
	58086	–	Virginia
	58123	–	Iowa
	60481	–	Nebraska
	68486	–	Nebraska
	68512	–	Nebraska
	68513	–	Nebraska
	68542	–	Nebraska
	68552	–	Nebraska
	68554	–	Nebraska
	68555	–	Nebraska
	58029*	–	Wisconsin
	58037*	–	Nebraska
	58044*	–	Oklahoma
	58055*	–	Kansas
	58091*	–	Nebraska
	58108*	–	Nebraska
	60478*	–	Nebraska

(Continued)

TABLE 1 | Continued

Group	Strain Number	RTX +/-	State
	68528*	–	Nebraska
	68529*	–	Nebraska
	68541*	–	Nebraska
	57854	+	Nebraska
	57863	+	Indiana
	57865	+	Nebraska
	57879	+	Oklahoma
	57894	+	Kansas
	57903	+	California
	57905	+	Iowa
	57906	+	Montana
	57918	+	North Dakota
	57919	+	Washington
	58009	+	Montana
	58016	+	Illinois
	58039	+	Kansas
	58097	+	South Carolina
	58101	+	Ohio
	57857*	+	Texas
	57871*	+	Nebraska
	57873*	+	Nebraska
	57878*	+	Nebraska
	57887*	+	Wisconsin
	57892*	+	Indiana
	57894*	+	Kansas
	58010*	+	Tennessee
	58011*	+	Illinois
	58069*	+	Nebraska

All strains were used in the development of models using TSA + 5% sheep erythrocytes. Strain numbers with an asterisk signify strains omitted from the TSA + 5% bovine erythrocyte model development portion of this study.

using the majority classification from a strain's spectra profile. When the study was expanded to assess different agar formulations, the number of isolates used in the model classification groups was reduced by 10 for each genotype to minimize the extra culture time and computational power required to do the study yet still allow for accuracy comparisons across all models. The isolates removed were chosen at random and resulted in a total of 70 isolates being used for the bovine blood agar portion of the study as opposed to the 90 isolates used in the sheep blood agar portion. When a model classified half of the spectra from a given strain as RTX – and half of the spectra as RTX +, this was counted as an incorrect classification by the model. Sensitivity, specificity, negative predictive value, and positive predictive value were also calculated manually using the genomic sequencing RTX classification as the gold standard.

RESULTS

TSA + 5% Sheep Blood SVM Model

The SVM method proved the most accurate for this study overall and is the focus of the remainder of the paper. The parameters and accuracy of all models developed in this study across all culture conditions and biomarker model development methods are included as **supplementary material** (**Supplementary Table 1**). The SVM model developed using TSA + 5% sheep blood yielded individual spectra classification accuracies of 50.7% for RTX – strains and 66.6% for RTX + strains (**Table 2**). In terms of the presence or absence of RTX, these statistics would correlate to specificity and sensitivity, respectively, when interpreting the model result as a diagnostic assay. When all spectra for an individual strain were classified, and the majority model classification was used for the final strain phenotype interpretation, these accuracy values increased slightly to 52% for RTX -, and 68% for RTX + strains. This equates to a negative predictive value of 61.9% and a positive predictive value of 58.6% when using the majority classification.

TSA + 5% Bovine Blood + 10 mmol $CaCl_2$ SVM Model

We tested the same MALDI-TOF MS biomarker model development methods using strains grown on TSA + 5% bovine blood supplemented with either 10% fetal bovine serum (FBS), 10 mmol/L $CaCl_2$, or both. The addition of $CaCl_2$ alone to the bovine blood agar resulted in the most accurate model (**Table 2**). The two most common peaks incorporated into the models in this study had m/z values of at or very near 3971 and 7530 (**Supplementary Table 1**). Using these peaks, when we examine 2-dimensional plots within ClinProTools 3.0, the different culture conditions show more defined clustering and less overlap in the spectra of strains grown on bovine blood plates with $CaCl_2$ when compared to those grown on the sheep blood plates (**Figure 2**). The models developed incorporating FBS are summarized in the **Supplementary Material** (**Supplementary Table 1**). Using the bovine blood agar and 10 mmol/L $CaCl_2$, the specificity and sensitivity increased to 73.3% and 93.3% respectively (**Table 2**). Additionally, the negative predictive value and positive predictive value increased to 91.7% and 77.8%

TABLE 2 | Accuracy of SVM models developed in this study using TSA + 5% sheep blood and TSA + 5% bovine blood supplemented with $CaCl_2$.

Culture Conditions	TSA + 5% sheep rbc	TSA + 5% bovine rbc + 10 mmol/L $CaCl_2$
Recognition	100%	100%
Cross Validation	91.69%	99.23%
RTX – External Validation	23.3%	67%
RTX + External Validation	83.3%	83%
RTX – Classify per spectra	50.7%	67.3%
RTX + Classify per spectra	66.6%	90%
RTX - Classify majority spectra	52%	73.3%
RTX + Classify majority spectra	68%	93.3%
NPV: Classify majority spectra	61.9%	91.7%
PPV: Classify majority spectra	58.6%	77.8%

NPV, negative predictive value; PPV, positive predictive value.

respectively. All the $CaCl_2$ supplemented bovine blood plates displayed subjectively larger colonies with a more visually prominent zone of hemolysis suggesting either an overall increase in RTX production per bacterial cell, an increase in RTX hemolytic activity, an increase in cellular division, or a combination of the three (**Figure 1**). The most discriminatory peaks incorporated into the models in this study often had subtle differences between RTX groups that were not always easily discernible by visually examining the spectra alone, regardless of the agar formulation used (**Figure 3**).

DISCUSSION

Here we have described a group of biomarker models developed using ClinProTools 3.0 software that are capable of correctly phenotyping most *M. bovoculi* genotype 1 strains for RTX. Across all models, the RTX phenotype specificity ranged from 26.7% - 86.7% while the sensitivity ranged from 46.7% - 93.3%. The most accurate model overall was the SVM model developed using strains grown on TSA + 5% bovine blood supplemented with 10 mmol/L $CaCl_2$, which had a specificity and sensitivity of

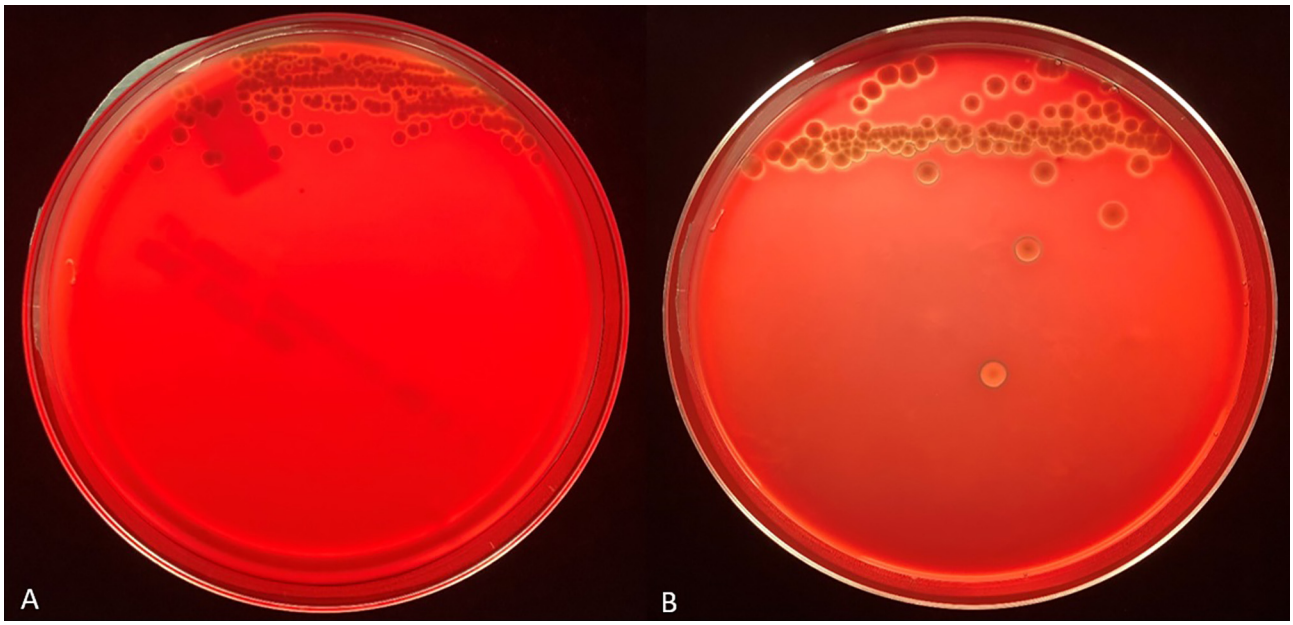

FIGURE 1 | Representative backlit blood agar plates streaked with strain #57905 after 48 hours incubation in 5% CO_2 at 37°C on TSA with 5% sheep blood **(A)** and TSA with 5% bovine blood and 10 mmol/L $CaCl_2$ **(B)**. Care was taken to ensure the thickness of the bovine blood agar within the petri dish was like that of the commercial sheep blood agar.

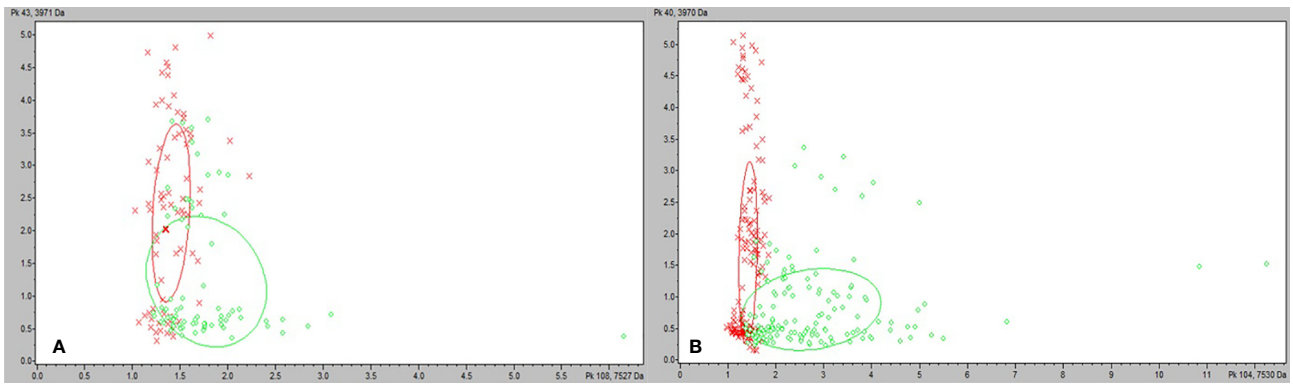

FIGURE 2 | ClinProTools 3.0 2-D plots incorporating the two most common and highest weighted peaks in the study. **(A)** *M. bovoculi* strains grown on TSA + 5% sheep blood. **(B)** *M. bovoculi* strains grown on TSA + 5% bovine blood with 10 mmol/L $CaCl_2$. Red X: RTX – strains. Green circle: RTX + strains.

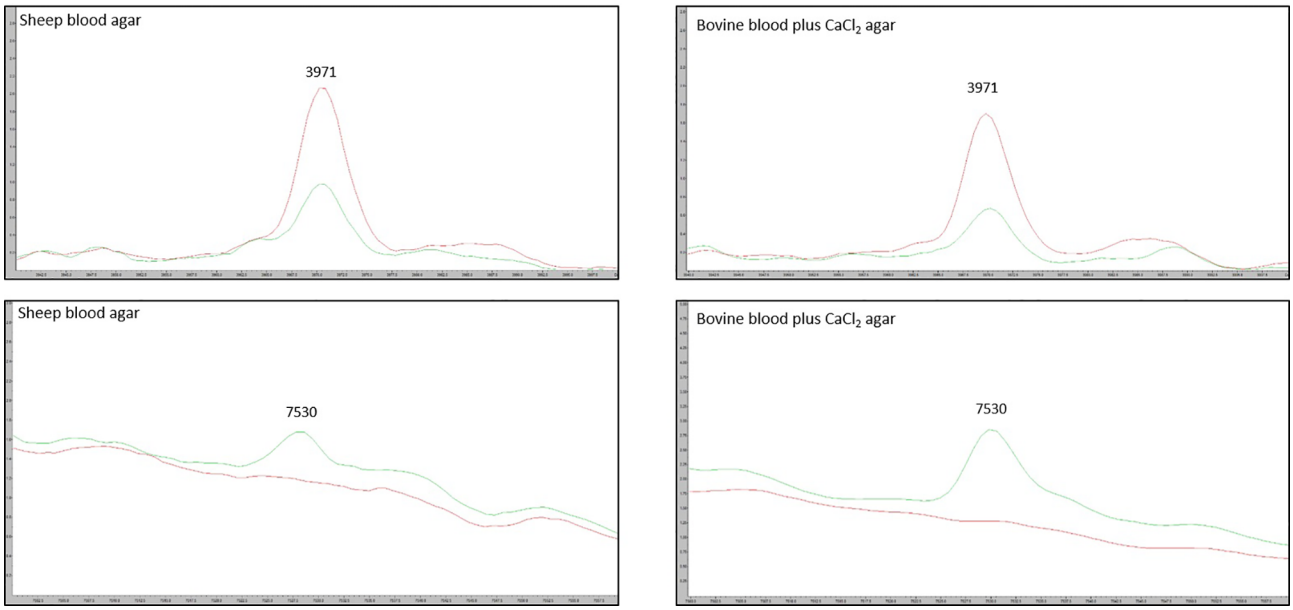

FIGURE 3 | Spectra of the two most discriminatory peaks 3971 m/z and 7530 m/z, compared between the sheep blood agar and bovine blood agar plus $CaCl_2$ formulations. Red line: average RTX – spectra for the group of model classify strains. Green line: average RTX + spectra for the group of model classify strains.

73.3% and 93.3% respectively. Regardless of the biomarker model algorithm used, the usage of agar incorporating bovine blood and $CaCl_2$ substantially outperformed sheep blood agar. Since secretion of RTX toxins utilizes a calcium-dependent T1SS, the extra calcium may result in an overall increase in RTX production, although confirming this would require more investigation and was outside the scope of this study. Additionally, mammalian erythrocytes vary in the composition of their membranes (de and Van Deenen, 1961), and the species of erythrocyte has shown to affect activity of other toxins (Bhakdi et al., 1984). This increase in hemolysis may increase nutrient or other factor availability that enhances model performance.

MALDI-TOF MS biomarker models often highlight discriminatory peaks between groups of spectra that are different enough in their m/z value that they can be discerned even without the use of computer models. For instance, within *M. bovoculi* a strong peak at 9057 m/z is specific for genotype 1 whereas a peak at 6550 m/z is specific for genotype 2 (Hille et al., 2020). Having strong discriminatory peaks such as these allows those without ClinProTools 3.0 software to differentiate groups by manually examining spectra. This was not the case for the current study and highlights the need for biomarker models and their algorithmic approach to analysis when spectra peak differences may be subtle between groups.

The SVM model developed in this study using bovine blood agar and $CaCl_2$ provides an efficient method of RTX phenotyping for *M. bovoculi* without the need for PCR or genomic sequencing. A negative predictive value of 91.7% means that RTX – strains can be classified accordingly with acceptable accuracy. While the importance of RTX toxins in the pathogenesis of IBK is not fully known, they are regarded as likely important virulence factors and RTX + strains are overrepresented in cases of IBK (Angelos et al., 2007a; Dickey et al., 2018). The ability to classify RTX – strains in this manner may prove beneficial in the formulation of autogenous vaccines for IBK as this will allow vaccine manufacturers to eliminate any RTX – strains from consideration and include only strains that are more likely to represent disease associated, RTX + strains within the vaccine formulation. With hemolysis shown to be RTX mediated in *M. bovis*, an RTX phenotyping MALDI-TOF MS biomarker model for *M. bovis* analogous to the one described here for *M. bovoculi*, would provide the same utility for vaccine formulations that choose to include *M. bovis*. Developing an *M. bovis* model would benefit from a library of sequenced *M. bovis* isolates whose RTX status is defined, unless hemolytic activity alone was used to assume RTX status. Here, we focused solely on *M. bovoculi* given our in-house library of previously sequenced isolates in order to examine the biomarker phenotyping proof-of-concept since the known presence of RTX components allowed us to avoid using hemolysis alone to classify RTX presence. In addition to its relevance to IBK, this study also serves as a blueprint of methods and proof-of-concept for utilizing MALDI-TOF MS spectra and biomarker models to distinguish strains of bacteria based on their ability to produce secreted exotoxins. Such methods could prove beneficial in differentiating other bacterial pathogens of both humans and animals that possess secreted exotoxins as virulence factors. Beyond being a proof-of-concept, the methods described here also reduce the time required to classify a *M. bovoculi* isolate by RTX status based solely on hemolysis. The gross appearance of

hemolysis is often not readily apparent until 48 hours of growth while the MALDI-TOF MS biomarkers models we developed here use colonies that were grown for only 24 hours.

A major limitation for this study is the inability to assure only a single variable, in this case RTX presence or absence, differentiates the groups of isolates. It is possible that some of the peaks incorporated into the models developed here represent isolate components unrelated to RTX itself. We have mitigated the likelihood of this limitation affecting the overall study interpretation by: 1) utilizing only genotype 1 strains for the entire study, and 2) incorporating a large number of isolates and spectra within each group, and 3) utilizing geographically diverse populations of isolates for both RTX status groups.

DATA AVAILABILITY STATEMENT

The original contributions presented in the study are included in the article/**Supplementary Material**. Further inquiries can be directed to the corresponding author.

AUTHOR CONTRIBUTIONS

MH performed MALDI-TOF analysis, developed the biomarker models, wrote the original manuscript draft and edited the manuscript. MC and AD performed genomic sequencing analysis on the bacterial strains and edited the manuscript. JHL performed MALDI-TOF analysis. JDL conceptualized the study, supervised the project, and edited the manuscript. All authors contributed to the article and approved the submitted version.

FUNDING

This project was funded by the Nebraska Experiment Station with funds from the Animal Health and Disease Research (section 1433) capacity funding program (accession 1017646) through the USDA National Institute of Food and Agriculture. The use of product and company names is necessary to accurately report the methods and results; however, the United States Department of Agriculture (USDA) neither guarantees nor warrants the standard of the products, and the use of names by the USDA implies no approval of the product to the exclusion of others that may also be suitable. The USDA is an equal opportunity provider and employer.

ACKNOWLEDGMENTS

The authors would like to thank the faculty and staff of the Nebraska Veterinary Diagnostic Center.

SUPPLEMENTARY MATERIAL

The Supplementary Material for this article can be found online at: https://www.frontiersin.org/articles/10.3389/fcimb.2021.632647/full#supplementary-material

REFERENCES

Aikman, J. G., Allan, E. M., and Selman, I. E. (1985). Experimental production of infectious bovine keratoconjunctivitis. *Vet. Rec.* 117, 234–239. doi: 10.1136/vr.117.10.234

Angelos, J. A., Hess, J. F., and George, L. W. (2001). Cloning and characterization of a Moraxella bovis cytotoxin gene. *Am. J. Vet. Res.* 62, 1222–1228. doi: 10.2460/ajvr.2001.62.1222

Angelos, J. A., Hess, J. F., and George, L. W. (2003). An RTX operon in hemolytic Moraxella bovis is absent from nonhemolytic strains. *Vet. Microbiol.* 92, 363–377. doi: 10.1016/S0378-1135(02)00410-8

Angelos, J. A., Ball, L. M., and Hess, J. F. (2007a). Identification and characterization of complete RTX operons in Moraxella bovoculi and Moraxella ovis. *Vet. Microbiol.* 125, 73–79. doi: 10.1016/j.vetmic.2007.05.009

Angelos, J. A., Spinks, P. Q., Ball, L. M., and George, L. W. (2007b). Moraxella bovoculi sp. nov., isolated from calves with infectious bovine keratoconjunctivitis. *Int. J. Syst. Evol. Microbiol.* 57, 789–795. doi: 10.1099/ijs.0.64333-0

Angelos, J. A., Clothier, K. A., Agulto, R. L., Mandzyuk, B., and Tryland, M. (2021). Relatedness of type IV pilin PilA amongst geographically diverse Moraxella bovoculi isolated from cattle with infectious bovine keratoconjunctivitis. *JMed Microbiol.* 70. doi: 10.1099/jmm.0.001293

Bhakdi, S., Muhly, M., and Füssle, R. (1984). Correlation between toxin binding and hemolytic activity in membrane damage by staphylococcal alpha-toxin. *Infect. Immun.* 46, 318–323. doi: 10.1128/IAI.46.2.318-323.1984

Billson, F. M., Harbour, C., Michalski, W. P., Tennent, J. M., Egerton, J. R., and Hodgson, J. L. (2000). Characterization of hemolysin of Moraxella bovis using a hemolysis-neutralizing monoclonal antibody. *Infect. Immun.* 68, 3469–3474. doi: 10.1128/IAI.68.6.3469-3474.2000

Brown, M. H., Brightman, A. H., Fenwick, B. W., and Rider, M. A. (1998). Infectious bovine keratoconjunctivitis: a review. *J. Vet. Intern. Med.* 12, 259–266. doi: 10.1111/j.1939-1676.1998.tb02120.x

Bumba, L., Masin, J., Macek, P., Wald, T., Motlova, L., Bibova, I., et al. (2016). Calcium-Driven Folding of RTX Domain β-Rolls Ratchets Translocation of RTX Proteins through Type I Secretion Ducts. *Mol. Cell.* 62, 47–62. doi: 10.1016/j.molcel.2016.03.018

Cerny, H. E., Rogers, D. G., Gray, J. T., Smith, D. R., and Hinkley, S. (2006). Effects of Moraxella (Branhamella) ovis culture filtrates on bovine erythrocytes, peripheral mononuclear cells, and corneal epithelial cells. *J. Clin. Microbiol.* 44, 772–776. doi: 10.1128/JCM.44.3.772-776.2006

Clark, A. E., Kaleta, E. J., Arora, A., and Wolk, D. M. (2013). Matrix-assisted laser desorption ionization-time of flight mass spectrometry: a fundamental shift in the routine practice of clinical microbiology. *Clin. Microbiol. Rev.* 26, 547–603. doi: 10.1128/CMR.00072-12

Clinkenbeard, K. D., and Thiessen, A. E. (1991). Mechanism of action of Moraxella bovis hemolysin. *Infect. Immun.* 59, 1148–1152. doi: 10.1128/IAI.59.3.1148-1152.1991

De Gier, J., and Van Deenen, L. (1961). Some lipid characteristics of red cell membranes of various animal species. *Biochim. Biophys. Acta* 49, 286–296. doi: 10.1016/0006-3002(61)90128-7

Dewell, R. D., Millman, S. T., Gould, S. A., Tofflemire, K. L., Whitley, R. D., Parsons, R. L., et al. (2014). Evaluating approaches to measuring ocular pain in bovine calves with corneal scarification and infectious bovine keratoconjunctivitis–associated corneal ulcerations. *J. Anim. Sci.* 92, 1161–1172. doi: 10.2527/jas.2013-7264

Dickey, A. M., Schuller, G., Loy, J. D., and Clawson, M. L. (2018). Whole genome sequencing of Moraxella bovoculi reveals high genetic diversity and evidence

for interspecies recombination at multiple loci. *PloS One* 13, e0209113. doi: 10.1371/journal.pone.0209113

Frey, J. (2019). RTX Toxins of Animal Pathogens and Their Role as Antigens in Vaccines and Diagnostics. *Toxins (Basel)* 10, 11. doi: 10.3390/toxins11120719

Gould, S., Dewell, R., Tofflemire, K., Whitley, R. D., Millman, S. T., Opriessnig, T., et al. (2013). Randomized blinded challenge study to assess association between Moraxella bovoculi and Infectious Bovine Keratoconjunctivitis in dairy calves. *Vet. Microbiol.* 164, 108–115. doi: 10.1016/j.vetmic.2013.01.038

Henson, J. B., and Grumbles, L. C. (1960). Infectious bovine keratoconjunctivitis. I. Etiology. *Am. J. Vet. Res.* 21, 761–766.

Hille, M., Dickey, A., Robbins, K., Clawson, M. L., and Loy, J. D. (2020). Rapid differentiation of Moraxella bovoculi genotypes 1 and 2 using MALDI-TOF mass spectrometry profiles. *J. Microbiol. Methods* 173, 105942. doi: 10.1016/j.mimet.2020.105942

Karger, A., Bettin, B., Gethmann, J. M., and Klaus, C. (2019). Whole animal matrix-assisted laser desorption/ionization time-of-flight (MALDI-TOF) mass spectrometry of ticks - Are spectra of Ixodes ricinus nymphs influenced by environmental, spatial, and temporal factors? *PloS One* 14, e0210590. doi: 10.1371/journal.pone.0210590

Khot, P. D., and Fisher, M. A. (2013). Novel approach for differentiating Shigella species and Escherichia coli by matrix-assisted laser desorption ionization-time of flight mass spectrometry. *J. Clin. Microbiol.* 51, 3711–3716. doi: 10.1128/JCM.01526-13

Khot, P. D., Couturier, M. R., Wilson, A., Croft, A., and Fisher, M. A. (2012). Optimization of matrix-assisted laser desorption ionization-time of flight mass spectrometry analysis for bacterial identification. *J. Clin. Microbiol.* 50, 3845–3852. doi: 10.1128/JCM.00626-12

Killinger, A. H., Valentine, D., Mansfield, M. E., Ricketts, G. E., Cmarik, G. F., Neumann, A. H., et al. (1977). Economic impact of infectious bovine keratoconjunctivitis in beef calves. *Vet. Med. Small Anim. Clin.* 72, 618–620.

Linhartova, I., Osicka, R., Bumba, L., Masin, J., and Sebo, P. (2018). "Repeats-in-Toxin (RTX) Toxins: A Review," in *Microbial Toxins* (Dordrecht: Springer Netherlands), 353–381.

Loy, J. D., and Brodersen, B. W. (2014). Moraxella spp. isolated from field outbreaks of infectious bovine keratoconjunctivitis: a retrospective study of case submissions from 2010 to 2013. *J. Vet. Diagn. Invest.* 26, 761–768. doi: 10.1177/1040638714551403

Loy, J. D., and Clawson, M. L. (2017). Rapid typing of Mannheimia haemolytica major genotypes 1 and 2 using MALDI-TOF mass spectrometry. *J. Microbiol. Methods* 136, 30–33. doi: 10.1016/j.mimet.2017.03.002

Mani, R. J., Thachil, A. J., and Ramachandran, A. (2017). Discrimination of Streptococcus equi subsp. equi and Streptococcus equi subsp. zooepidemicus using matrix-assisted laser desorption/ionization time-of-flight mass spectrometry. *J. Vet. Diagn. Invest.* 29, 622–627. doi: 10.1177/1040638717702687

Perez-Sancho, M., Vela, A. I., Horcajo, P., Ugarte-Ruiz, M., Dominguez, L., Fernandez-Garayzabal, J. F., et al. (2018). Rapid differentiation of Staphylococcus aureus subspecies based on MALDI-TOF MS profiles. *J. Vet. Diagn. Invest.* 30, 813–820. doi: 10.1177/1040638718805537

Robbins, K., Dickey, A. M., Clawson, M. L., and Loy, J. D. (2018). Matrix-assisted laser desorption/ionization time-of-flight mass spectrometry identification of Moraxella bovoculi and Moraxella bovis isolates from cattle. *J. Vet. Diagn. Invest.* 30, 739–742. doi: 10.1177/1040638718789725

Seng, P., Drancourt, M., Gouriet, F., La Scola, B., Fournier, P. E., Rolain, J. M., et al. (2009). Ongoing revolution in bacteriology: routine identification of bacteria by matrix-assisted laser desorption ionization time-of-flight mass spectrometry. *Clin. Infect. Dis.* 49, 543–551. doi: 10.1086/600885

Zheng, W., Porter, E., Noll, L., Stoy, C., Lu, N., Wang, Y., et al. (2019). A multiplex real-time PCR assay for the detection and differentiation of five bovine pinkeye pathogens. *J. Microbiol. Methods* 160, 87–92. doi: 10.1016/j.mimet.2019.03.024

Conflict of Interest: The authors declare that the research was conducted in the absence of any commercial or financial relationships that could be construed as a potential conflict of interest.

frontiers in Cellular and Infection Microbiology

ORIGINAL RESEARCH
published: 16 March 2021
doi: 10.3389/fcimb.2021.645049

Are We Ready for Nosocomial *Candida auris* Infections? Rapid Identification and Antifungal Resistance Detection Using MALDI-TOF Mass Spectrometry May Be the Answer

Elena De Carolis[1], *Federica Marchionni*[1], *Marilisa La Rosa*[1], *Jacques F. Meis*[2,3], *Anuradha Chowdhary*[4], *Brunella Posteraro*[5] *and Maurizio Sanguinetti*[1,5]*

[1] *Dipartimento di Scienze di Laboratorio e Infettivologiche, Fondazione Policlinico Universitario A. Gemelli IRCCS, Rome, Italy,* [2] *Department of Medical Microbiology and Infectious Diseases, Canisius Wilhelmina Hospital, Nijmegen, Netherlands,* [3] *Centre of Expertise in Mycology, Radboudumc/Canisius Wilhelmina Hospital, Nijmegen, Netherlands,* [4] *Vallabhbhai Patel Chest Institute, Department of Medical Mycology, University of Delhi, Delhi, India,* [5] *Dipartimento di Scienze Biotecnologiche di Base, Cliniche Intensivologiche e Perioperatorie, Università Cattolica del Sacro Cuore, Rome, Italy*

The occurrence of multidrug-resistant *Candida auris* isolates and the increased mortality associated with invasive infections or outbreaks due to this *Candida* species have been reported in many healthcare settings. Therefore, accurate and rapid identification at the species level of clinical *C. auris* isolates as well as their timely differentiation as susceptible or resistant to antifungal drugs is mandatory. Aims of the present study were to implement the MALDI-TOF mass spectrometry (MS) Bruker Daltonics Biotyper® database with *C. auris* spectrum profiles and to develop a fast and reproducible MS assay for detecting anidulafungin (AFG) resistance in *C. auris* isolates. After creation of main *C. auris* spectra, a score-oriented dendrogram was generated from hierarchical cluster analysis, including spectra of isolates from *C. auris* and other *Candida* (*C. glabrata*, *C. guilliermondii*, *C. haemulonii*, *C. lusitaniae*, and *C. parapsilosis*) or non-*Candida* (*Rhodotorula glutinis*) species. Cluster analysis allowed to group and classify the isolates according to their species designation. Then, a three-hour incubation antifungal susceptibility testing (AFST) assay was developed. Spectra obtained at null, intermediate, or maximum AFG concentrations were used to create composite correlation index matrices for eighteen *C. auris* isolates included in the study. All six resistant *C. auris* isolates were detected as resistant whereas 11 of 12 susceptible *C. auris* isolates were detected as susceptible by the MS-AFST assay. In conclusion, our MS-based assay offers the possibility of rapidly diagnosing and appropriately treating patients with *C. auris* infection.

Keywords: *Candida auris*, 3-hour MS-AFST, multidrug resistance, anidulafungin, new emerging pathogen, rapid identification and susceptibility testing

OPEN ACCESS

Edited by:
Di Xiao,
National Institute for Communicable Disease Control and Prevention (China CDC), China

Reviewed by:
Ferry Hagen,
Westerdijk Fungal Biodiversity Institute, Netherlands
Bryan Schmitt,
Indiana University Bloomington, United States

***Correspondence:**
Maurizio Sanguinetti
maurizio.sanguinetti@policlinicogemelli.it

Specialty section:
This article was submitted to Clinical Microbiology, a section of the journal Frontiers in Cellular and Infection Microbiology

Received: *22 December 2020*
Accepted: *22 February 2021*
Published: *16 March 2021*

Citation:
De Carolis E, Marchionni F, La Rosa M, Meis JF, Chowdhary A, Posteraro B and Sanguinetti M (2021) Are We Ready for Nosocomial Candida auris *Infections? Rapid Identification and Antifungal Resistance Detection Using MALDI-TOF Mass Spectrometry May Be the Answer. Front. Cell. Infect. Microbiol. 11:645049. doi: 10.3389/fcimb.2021.645049*

INTRODUCTION

The fungal pathogen *Candida auris* has emerged over a decade ago in East Asia and, since then, multidrug-resistant *C. auris* isolates causing nosocomial outbreaks have been isolated in many countries worldwide (Du et al., 2020). This is alarming because bloodstream infections caused by *C. auris* have been associated with a 30 to 60% rate of infection-related mortality (Chowdhary et al., 2017). To cope with the healthcare issues arisen from this emerging pathogen, species-level identification of *C. auris* isolates and their differentiation as susceptible or resistant to the commonly used antifungals agents became mandatory. However, biochemical/enzymatic identification methods are time-consuming and, in the beginning, misidentified *C. auris* (Kathuria et al., 2015); whereas MALDI-TOF mass spectrometry (MS) based identification was not optimal (Buil et al., 2019) until when MALDI-TOF MS databases were enriched with *C. auris* specific mass spectrum profiles (Girard et al., 2016; Bao et al., 2018). Of course, molecular methods such as *C. auris* colony-specific PCR and DNA sequencing (Kordalewska et al., 2017; Valentin et al., 2018) are efficient but less rapid than those based on the MALDI-TOF MS analysis.

While defined CLSI or EUCAST minimum inhibitory concentration (MIC) breakpoints for *C. auris* susceptibility are unavailable to date (Kordalewska and Perlin, 2019), tentative MIC breakpoints have been proposed (Lockhart et al., 2017). Nonetheless, 99% of *C. auris* isolates studied by Arendrup et al. had high MIC values to fluconazole while occasionally retaining full susceptibility to other triazole antifungal agents (Arendrup et al., 2017). Regarding echinocandins or amphotericin B, resistance rates are variable, being 7% and 10 to 35%, respectively, whereas acquired resistance to echinocandins has been associated with the presence of S639F orS639P mutations in the glucan-synthase encoding gene *FKS1*, which is the target of echinocandins (Kordalewska et al., 2018). While echinocandins are regarded as first-line treatment for *C. auris* infections, echinocandin-resistant isolates of *C. auris* may occur in patients during antifungal treatment (Park et al., 2019; Novak et al., 2020), calling for repeated susceptibility testing in order to monitor possible therapeutic failures.

Consistent with these observations, we implemented the MALDI Biotyper® database (Bruker Daltonics, Bremen, Germany) with mass spectrum profiles from *C. auris* isolates, and we developed a fast and reproducible MALDI-TOF MS based assay to detect resistance to the echinocandin anidulafungin in *C. auris* isolates.

MATERIALS AND METHODS

Study Isolates

The *C. auris* isolates used in this study were clinical clade I isolates that are part of a collection at the Centre of Expertise in Mycology, Nijmegen, The Netherlands. Additionally, a single *C. auris* isolate that was derived from the first diagnosed case of candidemia in Central Italy was also studied. In total, eight isolates that were confirmed to be *C. auris* by PCR and sequencing of the ribosomal DNA internal transcribed spacer (ITS) region were submitted to protein extraction according to a previously developed MALDI-TOF MS protocol (De Carolis et al., 2014). Briefly, yeast cells were suspended in 10% formic acid and then vortexed; one µL of lysate was placed on the MALDI target plate to obtain 12 technical replicates, which were overlaid each with one µL of absolute ethanol before allowing co-crystallization with the α-cyano-4-hydroxycinnamic acid matrix (Bruker Daltonics). A total of ≥5000 laser shots were used to generate a main spectrum profile (MSP) for each isolate, which was then added to the Bruker MALDI Biotyper® database. Isolates were also submitted to antifungal susceptibility testing (AFST), which was performed using a MALDI-TOF MS based assay (see below).

MALDI-TOF MS Identification Analysis

The MALDI-TOF MS analysis on *C. auris* isolates was undertaken with a Microflex LT mass spectrometer, by which spectra were recorded in the positive linear mode within a 2000–20000 Da range. A bacterial test standard (BTS255343; Bruker Daltonics) was used for the instrument calibration. Preliminarily, the Bruker Biotyper® database (version 7.0; 7311 entries), which contains only three MSP profiles of *C. auris*, did not allow reliable identification (i.e., log (score) values were lower than 2.0, which is the manufacturer-recommended cutoff level for MALDI-TOF MS species-level identification) of the isolates included in the study. Then, MSP profiles from the isolates were obtained and added to the Bruker Biotyper® database—this resulted into an extended MALDI database—following Bruker Daltonics standard operating procedures (https://spectra.folkhalsomyndigheten.se). Accordingly, isolates' protein extracts were prepared submitting each isolate—which grew on Sabouraud dextrose agar for 48 h at 37°C—to the aforementioned fast formic-acid extraction procedure. High-quality mass spectra from different spots for each isolate were analyzed by the MALDI BioTyper® software, and used to create a MSP for each isolate. After MSP creation, using the integrated statistical tool Matlab 7.1 (The MathWorks Inc.; Natick, MA, USA), a hierarchical cluster analysis was performed to generate a score-oriented dendrogram, which included MSP profiles from *C. auris* isolates together with those from isolates of other *Candida* (*C. glabrata*, *C. guilliermondii*, *C. haemulonii*, *C. lusitaniae*, and *C. parapsilosis*) or non-*Candida* (*Rhodotorula glutinis*) species.

Then, mass spectrum profiles from 18 challenge isolates were analyzed in duplicate, automatically acquired, and matched against those of the extended MALDI database to allow species-level identification, for which the highest log(score) value from any match was reported. Finally, the challenge isolates were matched against an updated Bruker Biotyper® database (version 9.0; which includes nine *C. auris* isolates), as well as against the Bruker-CDC merged MicrobeNet database (version 9978; https://microbenet.cdc.gov/).

MALDI-TOF MS Antifungal-Resistance Detection Analysis

According to our previous studies (De Carolis et al., 2012; Vella et al., 2013; Vella et al., 2017), selected *C. auris* isolates were exposed to serial AFG concentrations (i.e., ranging from 0.06 to

512 μg/mL) and to a null concentration (0 μg/mL) for 3 h at 37°C. The spectrum obtained at each concentration was matched against those at the two extreme concentrations, i.e., null (0 μg/mL) and maximum (512 μg/mL), respectively. Values resulting from the composite correlation index (CCI) matrices derived from the spectra indicated a clear diversity between the spectra when values were near 0 and high similarity between the spectra when values were around 1. These experiments allowed to find a breakpoint AFG concentration, which was used in a subsequent assay. For each isolate, two technical and three biological replicates were analyzed for both the preliminary experiments and the assays illustrated below. Briefly, *C. auris* cells (1×10^7 CFU/mL, as determined by cell counting) were exposed to AFG concentrations of 64 μg/mL (maximum), 0.06 μg/mL (breakpoint), and 0 μg/mL (null) for 3 hours at 37°C under agitation (300 rpm) in RPMI-1640 medium (supplemented with L-glutamine and sodium bicarbonate; R8758; Merck, Rome, Italy). Cells were centrifuged and the pellet washed twice with deionized water before the resuspension in 10% formic acid. The *C. auris* isolates profiles obtained at null, intermediate, or maximum AFG concentrations were used to create CCI matrices within the range 3000–8000 Da (15 intervals) using the MALDI Biotyper 3.1 software (De Carolis et al., 2012).

As previously reported, we matched each "breakpoint" spectrum against the spectrum at the maximum concentration or the spectrum at the null concentration of AFG. Then, isolates were classified as susceptible or resistant to AFG when the CCI value obtained matching the breakpoint spectrum with the "maximum" spectrum was higher or lower than the spectrum obtained matching the breakpoint spectrum with the "null" spectrum, respectively. The CCI ratios were calculated dividing the CCI_{max} by the CCI_{null}, and a *C. auris* isolate was categorized as susceptible if the CCI_{max}/CCI_{null} ratio was >1 or as resistant if the CCI_{max}/CCI_{null} ratio was <1. Results of the mass spectrometry AFST (MS-AFST) were compared with the MIC values obtained using the commercial AFST method Sensititre YeastOne (Thermo Scientific, Italy), which was an adaptation of the CLSI M27-A3 broth microdilution standard (CLSI, 2008). The tentative MIC breakpoints (expressed as μg/mL) above mentioned were used as criteria to interpret AFST results.

RESULTS AND DISCUSSION

As of November 2019, we identified in our hospital a bloodstream infection due to *C. auris*, which represented the first case of invasive *C. auris* infection detected in Central Italy where the hospital is located. *Ad hoc* extending the MALDI Bruker Biotyper® database version 7.1 with MSPs from *C. auris* isolates enabled us to identify the bloodstream *Candida* pathogen as *C. auris*, which yielded a MALDI log(score) of 2.230. Using the extended database as well as the Bruker-CDC merged database (data not shown), we were able to obtain reliable species-level identification (log(score) values, >2.0) for 18 C. *auris* isolates from clade I. Particularly for *C. auris*, phenotypic identification methods such as VITEK 2 YST, API 20C, or BD Phoenix systems as well as the fully automated MicroScan system fail to provide accurate identification at the species level. As shown in this and in other studies (Delavy et al., 2019), older versions of commercially available MALDI-TOF MS databases proved to be unable to identify *C. auris*. To corroborate our findings, we investigated the relatedness among 20 MSPs obtained from eight isolates of *C. auris* and two isolates each of *C. glabrata*, *C. guilliermondii*, *C. haemulonii*, *C. lusitaniae*, *C. parapsilosis*, and *Rhodotorula glutinis*. **Figure 1** shows the score-oriented dendrogram resulting from the hierarchical cluster analysis used for this investigation. Based on correlation distance values, all the *C. auris* isolates grouped in a separate branch of the dendrogram according to their species designation.

In parallel, we investigated the capability of an MS-AFST assay to detect susceptibility or resistance phenotypes for 18 C. *auris* isolates exposed to 64 μg/mL, 0.06 μg/mL, or 0 μg/mL concentrations of AFG, respectively, for three hours at 37°C (**Figure 2**). Although MALDI-TOF MS-based AFST assays have already been developed for several antifungal drugs and *Candida* species, including *C. auris* (Delavy et al., 2019; Vatanshenassan et al., 2019), we defined the optimal AFG concentrations for use with *C. auris*. Details of our MS-AFST assay are shown in **Figure 3**, where the relationship between *C. auris* mass spectra acquired at the indicated AFG concentrations was visualized in a matrix (heat map) of CCI values and the relative MALDI-TOF MS profiles are reported for a susceptible and resistant *C. auris* isolate.

According to MIC interpretive criteria, *C. auris* isolates were identified as susceptible or resistant to AFG, respectively. As shown in **Table 1**, we found that the MS-AFST assay correctly classified 6 (100%) of 6 resistant isolates and 11 (91.7%) of 12 susceptible isolates, as determined by the Sensititre YeastOne (herein used as the reference method) and published tentative echinocandin breakpoints (Lockhart et al., 2017). Note that one *C. auris* isolate that had an intermediate AFG susceptibility (MIC value, 1 μg/mL) was classified as resistant by the AFST-MS assay. Although *C. auris* isolates displaying a wild-type *FKS1* hot spot 1 (HS1) genotype are relatively frequent (Chowdhary et al., 2018), we noted that two of six resistant isolates (with elevated AFG MICs) harbored the S639F mutation in the *FKS1* HS1 region. Very recently, Sharma et al. (2020) investigated a possible role for upregulated chitin or cell-wall stress response genes in echinocandin-resistant and -intermediate C. *auris* isolates. Despite being beyond the study's scope, it would have been interesting to investigate whether the *C. auris* isolate showing intermediate susceptibility by the Sensititre YeastOne method but resistance with the MS-AFST assay could have any altered expression in specific genes related to AFG-susceptible or -resistant phenotypes. Conversely, we did not exclude the hypothesis that an additional single-nucleotide polymorphism (i.e., outside HS1 region) might have attenuated the otherwise resistant phenotype in that isolate.

Our study has some limitations. The data set is somewhat limited not only by the size—which is understandable considering that *C. auris* is not a ubiquitous pathogen—but also by the geographic restriction—which is understandable

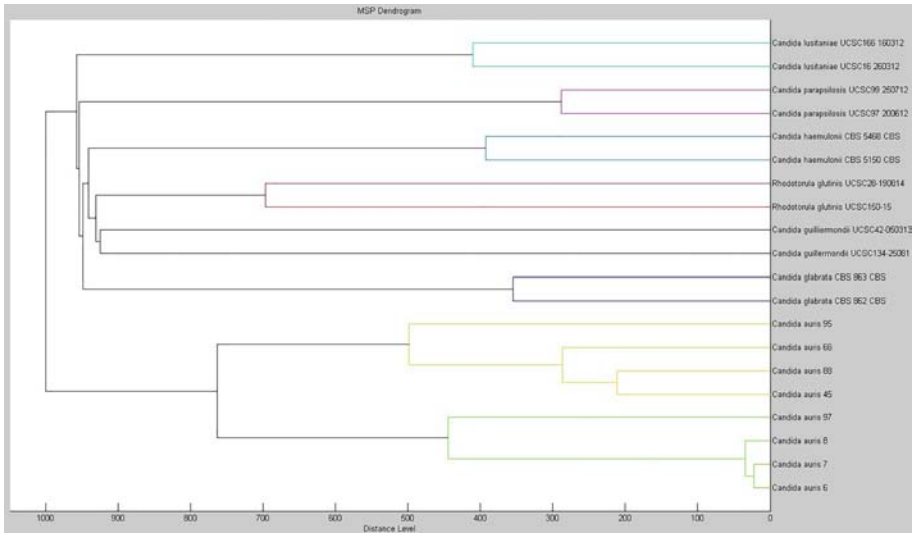

FIGURE 1 | Dendrogram created with the MSPs from eight isolates of *C. auris* and from two isolates each of *C. glabrata*, *C. guilliermondii*, *C. haemulonii*, *C. lusitaniae*, *C. parapsilosis*, and *Rhodotorula glutinis*. The distance values are normalized to the maximum value of 1000.

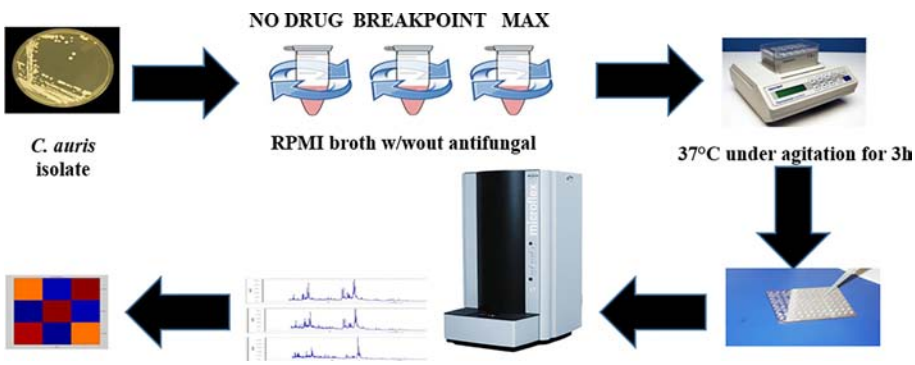

FIGURE 2 | MS-AFST assay for resistance detection in *C. auris*. Shown is the workflow that includes an incubation with AFG at 37°C for 3 hours, followed by a generation of mass spectrum profiles that are visualized in a CCI matrix (heat map).

considering that *C. auris* isolates used by us represented clade I. Thus, it is not surprising that our isolates gave MALDI-TOF MS identification (log)scores of <2.0 when challenged with the Bruker Biotyper® database containing three isolates (version 7.0) or nine isolates (version 9.0). Likewise, it is not surprising that extending the Bruker Biotyper® database with the MSPs from eight *C. auris* isolates, which had the same geographic origin as those being challenged, resulted in higher (log)scores—three *C. auris* isolates in the database version 7.0 were from Korea or Japan. Additionally, we generated MSPs from *C. auris* isolates using the same formic-acid based extraction method as that used to prepare mass spectra from the isolates being identified. Taken together, our experimental situation was such that we did not consider to lower MALDI-TOF MS (log)scores below 2.0 (i.e., to ≥1.7) for species-level identification, which is instead the strategy applied in many laboratories that perform identifications for *Candida*, *Aspergillus*, or difficult-to-identify bacteria. Particularly for filamentous fungi including *Aspergillus*, this strategy was shown to significantly increase the rate of accurate species-level identifications while not increasing the number of misidentifications even when cryptic *Aspergillus* species were tested (Wilkendorf et al., 2020).

Our study adds support to the successfully applied CCI-based proteomic approaches for antifungal resistance detection in *Candida* species, which offer the advantage to considerably reduce the time to result (three hours in our study) compared

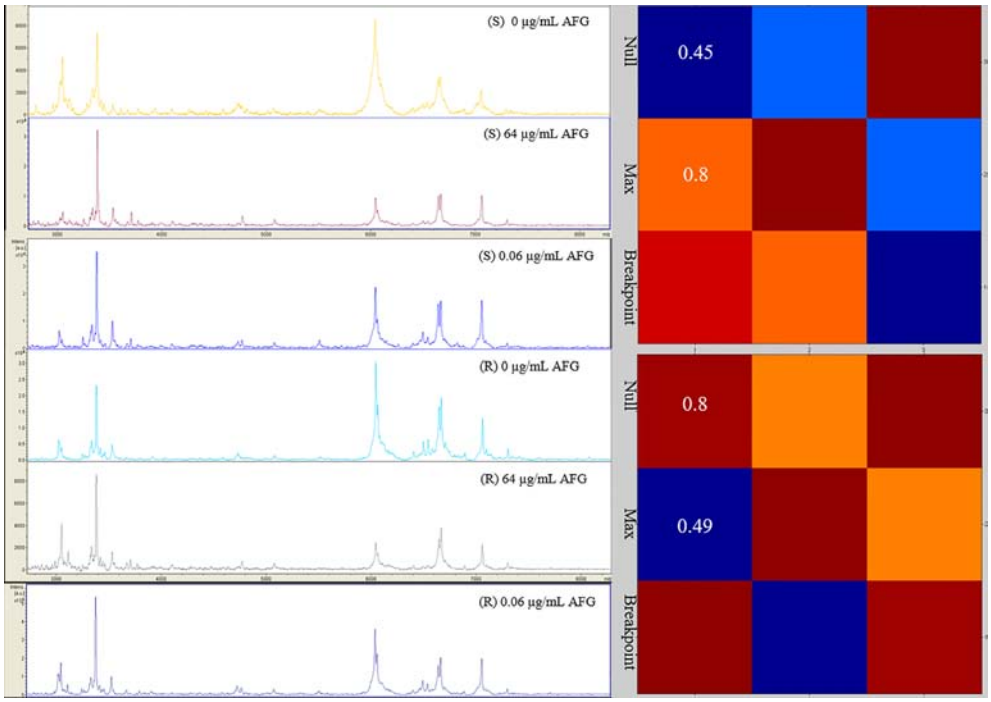

FIGURE 3 | Raw mass spectra of susceptible (n = 1) and resistant (n = 1) *C. auris* isolates incubated at the null, maximum, or breakpoint concentration of AFG. In the heat map, hot colors denote similar spectra whereas cold colors denote dissimilar spectra. CCI values are reported accordingly.

TABLE 1 | MS-AFST categorization of wild-type (WT) or non-WT *C. auris* isolates tested against anidulafungin.

Isolate designation	*FKS1* phenotype	Anidulafungin susceptibility testing					
		CLSI		MS-AFST	CCI ratio	CCI_{null}	CCI_{max}
		MIC (µg/mL)	Category				
10.05.12.66	S639F	≥4	R	R	0.97	1.00	0.97
					0.95	1.00	0.95
					0.30	1.00	0.30
10.05.12.62	S639F	≥4	R	R	0.74	0.92	0.68
					0.69	0.80	0.55
					0.50	1.00	0.50
10.05.12.57	WT	≥4	R	R	0.58	0.81	0.47
					0.66	0.71	0.47
					0.66	0.73	0.48
10.05.12.59	WT	0.125	S	S	1.83	0.48	0.88
					1.78	0.45	0.80
					2.60	0.35	0.91
10.05.18.95	WT	≥4	R	R	0.85	0.97	0.82
					0.91	0.99	0.90
					0.92	0.37	0.34
10.05.12.45	WT	≥4	R	R	0.23	0.97	0.22
					0.80	1.00	0.80
					0.61	0.80	0.49
10.05.12.88	WT	1	S	R	0.83	0.60	0.50
					0.86	0.80	0.69
					0.73	0.81	0.59
10.05.18.97	WT	≥4	R	R	0.89	0.96	0.85
					0.95	0.95	0.90
					0.93	0.98	0.91
10.03.10.64	WT	0.06	S	S	5.45	0.11	0.60
					5.50	0.14	0.77

(Continued)

TABLE 1 | Continued

Isolate designation	*FKS1* phenotype	Anidulafungin susceptibility testing					
		CLSI		MS-AFST	CCI ratio	CCI_{null}	CCI_{max}
		MIC (μg/mL)	Category				
					1.30	0.70	0.91
10.03.10.63	WT	0.125	S	S	2.50	0.30	0.75
					2.75	0.20	0.55
					2.21	0.38	0.84
10.03.11.62	WT	0.125	S	S	2.21	0.39	0.86
					3.67	0.15	0.55
					2.57	0.21	0.54
10.08.12.28	WT	0.25	S	S	1.09	0.87	0.95
					1.44	0.55	0.79
					1.09	0.57	0.62
10.08.12.29	WT	0.25	S	S	0.99	0.84	0.83
					1.52	0.50	0.76
					1.11	0.35	0.39
10.05.15.49	WT	0.125	S	S	1.15	0.75	0.86
					1.38	0.13	0.18
					1.07	0.71	0.77
10.08.16.39	WT	0.125	S	S	1.05	0.19	0.20
					1.69	0.49	0.83
					1.86	0.37	0.69
10.08.12.66	WT	0.125	S	S	5.66	0.09	0.51
					5.10	0.10	0.51
					1.13	0.69	0.78
10.11.02.11	WT	0.06	S	S	1.01	0.95	0.96
					1.09	0.69	0.44
					1.10	0.59	0.65
10.08.12.39	WT	0.125	S	S	1.03	0.79	0.81
					0.98	0.81	0.79
					1.07	0.57	0.61

R, resistant; S, susceptible.

with conventional AFST methods (Delavy et al., 2019; Roberto et al., 2020). In addition to being a cost-effective method (few euro-cents per run), our MS-AFST assay differs from the growth-based MALDI Biotyper antibiotic (antifungal) susceptibility test rapid assay (MBT-ASTRA) recently developed for rapid detection of AFG-resistant *C. glabrata* and *C. auris* isolates (Vatanshenassan et al., 2018; Vatanshenassan et al., 2019). In particular, our assay can be even successful with poorly growing isolates, thereby avoiding the need to set an isolate-dependent growth cutoff. However, further studies are necessary to ascertain the usefulness of MALDI-TOF MS based assays for the management of outbreaks sustained by multidrug-resistant *C. auris* isolates in the hospital setting.

DATA AVAILABILITY STATEMENT

The original contributions presented in the study are included in the article/supplementary material. Further inquiries can be directed to the corresponding author.

AUTHOR CONTRIBUTIONS

EC developed the theory, analyzed the data and wrote the manuscript with support from BP and MS. FM and MR carried out the experiment. JM and AC provided critical feedback. All authors contributed to the article and approved the submitted version.

REFERENCES

Arendrup, M. C., Prakash, A., Meletiadis, J., Sharma, C., and Chowdhary, A. (2017). Comparison of EUCAST and CLSI reference microdilution MICs of eight antifungal compounds for *Candida auris* and associated tentative epidemiological cutoff values. *Antimicrob. Agents Chemother.* 61, e00485–e004 7. doi: 10.1128/AAC.00485-17

Bao, J. R., Master, R. N., Azad, K. N., Schwab, D. A., Clark, R. B., Jones, R. S., et al. (2018). Rapid, accurate identification of *Candida auris* by using a novel matrix-assisted laser desorption ionization-time of flight mass spectrometry (MALDI-TOF MS) database (library). *J. Clin. Microbiol.* 56, e01700–e01717. doi: 10.1128/JCM.01700-17

Buil, J. B., van der Lee, H. A. L., Curfs-Breuker, I., Verweij, P. E., and Meis, J. F. (2019). External quality assessment evaluating the ability of Dutch clinical microbiological laboratories to identify *Candida auris*. *J. Fungi* 5, 94. doi: 10.3390/jof5040094

Chowdhary, A., Sharma, C., and Meis, J. F. (2017). *Candida auris*: a rapidly emerging cause of hospital-acquired multidrug-resistant fungal infections globally. *PloS Pathog.* 13, e1006290. doi: 10.1371/journal.ppat.1006290

Chowdhary, A., Prakash, A., Sharma, C., Kordalewska, M., Kumar, A., Sarma, S., et al. (2018). A multicentre study of antifungal susceptibility patterns among

350 *Candida auris* isolates(2009–17) in India: role of the *ERG11* and *FKS1* genes in azole and echinocandin resistance. *J. Antimicrob. Chemother.* 73, 891–899. doi: 10.1093/jac/dkx480

CLSI (2008). *M27-A3 reference method for broth dilution antifungal susceptibility testing of yeasts; approved standard. 3rd* (Wayne PA: Clinical and Laboratory Standards Institute).

De Carolis, E., Vella, A., Florio, A. R., Posteraro, P., Perlin, D. S., Sanguinetti, M., et al. (2012). Use of matrix-assisted laser desorption ionization-time of flight mass spectrometry for caspofungin susceptibility testing of *Candida* and *Aspergillus* species. *J. Clin. Microbiol.* 50, 2479–2483. doi: 10.1128/JCM.00224-12

De Carolis, E., Vella, A., Vaccaro, L., Torelli, R., Posteraro, P., Ricciardi, W., et al. (2014). Development and validation of an in-house database for matrix-assisted laser desorption ionization-time of flight mass spectrometry-based yeast identification using a fast protein extraction procedure. *J. Clin. Microbiol.* 52, 1453–1458. doi: 10.1128/JCM.03355-13

pDelavy, M., Dos Santos, A. R., Heiman, C. M., and Coste, A. T. (2019). Investigating antifungal susceptibility in *Candida* species with MALDI-TOF MS-based assays. *Front. Cell. Infect. Microbiol.* 9, 19. doi: 10.3389/fcimb.2019.00019

Du, H., Bing, J., Hu, T., Ennis, C. L., Nobile, C. J., and Huang, G. (2020). *Candida auris*: epidemiology, biology, antifungal resistance, and virulence. *PloS Pathog.* 16, e1008921. doi: 10.1371/journal.ppat.1008921

Girard, V., Mailler, S., Chetry, M., Vidal, C., Durand, G., van Belkum, A., et al. (2016). Identification and typing of the emerging pathogen *Candida auris* by matrix-assisted laser desorption ionisation time of flight mass spectrometry. *Mycoses* 59, 535–538. doi: 10.1111/myc.12519

Kathuria, S., Singh, P. K., Sharma, C., Prakash, A., Masih, A., Kumar, A., et al. (2015). Multidrug-resistant *Candida auris* misidentified as *Candida haemulonii*: characterization by matrix-assisted laser desorption ionization-time of flight mass spectrometry and DNA sequencing and its antifungal susceptibility profile variability by Vitek 2, CLSI broth microdilution, and Etest method. *J. Clin. Microbiol.* 53, 1823–1830. doi: 10.1128/JCM.00367-15

Kordalewska, M., Zhao, Y., Lockhart, S. R., Chowdhary, A., Berrio, I., and Perlin, D. S. (2017). Rapid and accurate molecular identification of the emerging multidrug resistant pathogen *Candida auris*. *J. Clin. Microbiol.* 55, 2445–2452. doi: 10.1128/JCM.00630-17

Kordalewska, M., Lee, A., Park, S., Berrio, I., Chowdhary, A., Zhao, Y., et al. (2018). Understanding echinocandin resistance in the emerging pathogen *Candida auris*. *Antimicrob. Agents Chemother.* 62, e00238–e00218. doi: 10.1128/AAC.00238-18

Kordalewska, M., and Perlin, D. S. (2019). Identification of drug resistant *Candida auris*. *Front. Microbiol.* 10, 1918. doi: 10.3389/fmicb.2019.01918

Lockhart, S. R., Etienne, K. A., Vallabhaneni, S., Farooqi, J., Chowdhary, A., Govender, N. P., et al. (2017). Simultaneous emergence of multidrug-resistant *Candida auris* on 3 continents confirmed by whole-genome sequencing and epidemiological analyses. *Clin. Infect. Dis.* 64, 134–140. doi: 10.1093/cid/ciw691

Novak, A. R., Bradley, M. E., Kiser, T. H., and Mueller, S. W. (2020). Azole-resistant *Aspergillus* and echinocandin-resistant *Candida* – What are the treatment options? *Curr. Fungal Infect. Rep.* 14, 141–152. doi: 10.1007/s12281-020-00379-2

Park, J. Y., Bradley, N., Brooks, S., Burney, S., and Wassner, C. (2019). Management of patients with *Candida auris* fungemia at community hospital, Brooklyn, New York, US–2018. *Emerg. Infect. Dis.* 25, 601–602. doi: 10.3201/eid2503.180927

Roberto, A., Xavier, D. E., Vidal, E. E., Vidal, C., Neves, R. P., and Lima-Neto, R. G. (2020). Rapid detection of echinocandins resistance by MALDI-TOF MS in *Candida parapsilosis* complex. *Microorganisms* 8, 109. doi: 10.3390/microorganisms8010109

Sharma, D., Paul, R. A., Chakrabarti, A., Bhattacharya, S., Soman, R., Shankarnarayan, S. A., et al. (2020). Caspofungin resistance in *Candida auris* due to mutations in *Fks*1 with adjunctive role of chitin and key cell wall stress response pathway genes. *bioRxiv*. doi: 10.1101/2020.07.09.196600

Valentin, E., Tormo-Mas, M. A., Eraso, E., Pemán, J., and de Groot, P. (2018). Molecular identification of *Candida auris* by PCR amplification of species-specific GPI protein-encoding genes. *Int. J. Med. Microbiol.* 308, 812–818. doi: 10.1016/j.ijmm.2018.06.014

Vatanshenassan, M., Boekhout, T., Lass-Flörl, C., Lackner, M., Schubert, S., Kostrzewa, M., et al. (2018). MBT ASTRA: proof-of-concept for a rapid MALDI-TOF MS based method to detect caspofungin resistance in *Candida albicans* and *Candida glabrata*. *J. Clin. Microbiol.* 56, e00420–e00418. doi: 10.1128/JCM.00420-18

Vatanshenassan, M., Boekhout, T., Meis, J. F., Berman, J., Chowdhary, A., Ben-Ami, R., et al. (2019). *Candida auris* identification and rapid antifungal susceptibility testing against echinocandins by MALDI-TOF MS. *Front. Cell. Infect. Microbiol.* 9, 20. doi: 10.3389/fcimb.2019.00020

Vella, A., De Carolis, E., Vaccaro, L., Posteraro, P., Perlin, D. S., Kostrzewa, M., et al. (2013). Rapid antifungal susceptibility testing by matrix-assisted laser desorption ionization-time of flight mass spectrometry analysis. *J. Clin. Microbiol.* 51, 2964–2969. doi: 10.1128/JCM.00903-13

Vella, A., De Carolis, E., Mello, E., Perlin, D. S., Sanglard, D., Sanguinetti, M., et al. (2017). Potential use of MALDI-ToF mass spectrometry for rapid detection of antifungal resistance in the human pathogen *Candida glabrata*. *Sci. Rep.* 7, 9099. doi: 10.1038/s41598-017-09329-4

Wilkendorf, L. S., Bowles, E., Buil, J. B., van der Lee, H. A. L., Posteraro, B., Sanguinetti, M., et al. (2020). Update on matrix-assisted laser desorption ionization-time of flight mass spectrometry identification of filamentous fungi. *J. Clin. Microbiol.* 58, e01263–e01220. doi: 10.1128/JCM.01263-20

Conflict of Interest: The authors declare that the research was conducted in the absence of any commercial or financial relationships that could be construed as a potential conflict of interest.

frontiers in Cellular and Infection Microbiology

ORIGINAL RESEARCH
published: 16 March 2021
doi: 10.3389/fcimb.2021.646648

Factors Associated With MALDI-TOF Mass Spectral Quality of Species Identification in Clinical Routine Diagnostics

Aline Cuénod[1,2]*, *Frédéric Foucault*[3], *Valentin Pflüger*[3] and *Adrian Egli*[1,2]

[1] Applied Microbiology Research, Department of Biomedicine, University of Basel, Basel, Switzerland, [2] Division of Clinical Bacteriology and Mycology, University Hospital Basel, Basel, Switzerland, [3] Mabritec AG, Riehen, Switzerland

Background: An accurate and timely identification of bacterial species is critical in clinical diagnostics. Species identification allows a potential first adaptation of empiric antibiotic treatments before the resistance profile is available. Matrix assisted Laser Desorption Ionization Time of Flight mass spectrometry (MALDI-TOF MS) is a widely used method for bacterial species identification. However, important challenges in species identification remain. These arise from (i) incomplete databases, (ii) close relatedness of species of interest, and (iii) spectral quality, which is currently vaguely defined.

Methods: We selected 47 clinically relevant bacterial isolates from 39 species, which can be challenging to identify by MALDI-TOF MS. We measured these isolates under various analytical conditions on two MALDI-TOF MS systems. First, we identified spectral features, which were associated with correct species identification in three different databases. Considering these features, we then systematically compared spectra produced with three different sample preparation protocols. In addition, we varied quantities of bacterial colony material applied and bacterial colony age.

Results: We identified (i) the number of ribosomal marker peaks detected, (ii) the median relative intensity of ribosomal marker peaks, (iii) the sum of the intensity of all detected peaks, (iv) a high measurement precision, and (v) reproducibility of peaks to act as good proxies of spectral quality. We found that using formic acid, measuring bacterial colonies at a young age, and frequently calibrating the MALDI-TOF MS device increase mass spectral quality. We further observed significant differences in spectral quality between different bacterial taxa and optimal measurement conditions vary per taxon.

Conclusion: We identified and applied quality measures for MALDI-TOF MS and optimized spectral quality in routine settings. Phylogenetic marker peaks can be reproducibly detected and provide an increased resolution and the ability to distinguish between challenging species such as those within the *Enterobacter cloacae* complex, *Burkholderia cepacia* complex, or viridans streptococci.

Keywords: MALDI-TOF mass spectrometry, quality control, standardisation, species identification, microbial diagnostics

OPEN ACCESS

Edited by:
Yi-Wei Tang,
Cepheid, United States

Reviewed by:
Bryan Schmitt,
Indiana University Bloomington, United States
Krisztina M. Papp-Wallace,
Louis Stokes Cleveland VA Medical Center, United States

***Correspondence:**
Aline Cuénod
aline.cuenod@stud.unibas.ch

Specialty section:
This article was submitted to Clinical Microbiology, a section of the journal Frontiers in Cellular and Infection Microbiology

Received: *27 December 2020*
Accepted: *01 February 2021*
Published: *16 March 2021*

Citation:
Cuénod A, Foucault F, Pflüger V and Egli A (2021) Factors Associated With MALDI-TOF Mass Spectral Quality of Species Identification in Clinical Routine Diagnostics. Front. Cell. Infect. Microbiol. 11:646648. doi: 10.3389/fcimb.2021.646648

INTRODUCTION

Matrix assisted Laser Desorption Ionization Time of Flight mass spectrometry (MALDI-TOF MS) has revolutionised microbial diagnostics. Due to its minimal hands-on and turnaround time, low costs, and high accuracy it has become the method of choice for bacterial species identification in clinical diagnostics (Angeletti and Ciccozzi, 2019; Rodríguez-Sánchez et al., 2019). Multiple studies have highlighted the potential of MALDI-TOF MS to identify virulent or resistant bacterial sub-lineages within a species (Wolters et al., 2011; Christner et al., 2014). Despite these potential applications, important challenges remain for routine diagnostics, such as the inability to properly differentiate clinically relevant taxonomic groups, such as the species within the *Burkholderia cepacia* complex (Fehlberg et al., 2013), the *K. pneumoniae* complex (Dinkelacker et al., 2018) or viridans streptococci (Angeletti et al., 2015). Challenges in species identification arise from (i) incomplete databases, (ii) close relatedness of the bacterial species of interest, and (iii) poor spectral quality.

Species identification through commonly used MALDI-TOF MS systems is based on the comparison of unknown spectra to reference spectra databases through pattern matching. MALDI-TOF mass spectra consist of peaks from highly abundant, intracellular proteins including ribosomal subunit proteins, which are present in high copy numbers in replicating bacterial cells (Fenselau and Demirev, 2001; Ryzhov and Fenselau, 2001). With the abundance of bacterial whole genome sequences, reference databases comprising predicted ribosomal subunit masses have become an alternative to pattern based microbial identification in MALDI-TOF MS. The mass of ribosomal subunits can be directly calculated from genomic sequences, as they are relatively conserved and rarely post-translationally modified. Their potential to serve as MALDI-TOF MS biomarkers has been applied to clinically relevant phylogenetic groups (Hotta et al., 2010; Ziegler et al., 2015; Rothen et al., 2019), and multiple databases using marker masses predicted from genomic data are now available (Kassim et al., 2017; Ojima-Kato et al., 2017; Tomachewski et al., 2018). A ribosomal marker based approach has successfully been applied to distinguish between subspecies and clonal complexes within species such as *Streptococcus agalactiae* and *Escherichia coli* (Matsumura et al., 2014; Lafolie et al., 2015; Rothen et al., 2019).

When MALDI-TOF MS was first applied for microbial species identification (Anhalt and Fenselau, 1975) and in its first years in routine diagnostics, samples were processed using a protein extraction protocol (Patel, 2015). However, as high accuracies in species identification have been reported using a much simpler procedure, applying bacterial colonies directly onto the MALDI-TOF MS target plate has become the standard sample preparation protocol in routine diagnostics (Bizzini et al., 2010; van Veen et al., 2010). Although the Clinical and Laboratory Standard Institute (Pennsylvania, USA) has published a guideline on bacterial identification by MALDI-TOF MS (Branda et al., 2017), the definition criteria of spectral quality remain vague. Many diagnostic laboratories have developed their own Standard Operating Procedures for sample preparation and interpretation of species identification by MALDI-TOF MS. Currently it is already well established that MALDI-TOF mass spectral quality is influenced by the amount of bacterial colony material added to the target plate, the age of the bacterial colony, as well as the sample preparation protocol used (Alatoom et al., 2011; Croxatto et al., 2012; Veloo et al., 2014). However, there is a clear lack of an optimal and standardised sample preparation and data analysis workflow. Criteria defining the spectral quality will help to compare differences in preparation and analytical workflows. Closing this gap will substantially increase the reproducible detection of phylogenetic marker peaks in MALDI-TOF mass spectra acquired and thereby improve species identification in routine diagnostics.

The purpose of this study is to (i) identify quantitative spectral features suitable to define spectral quality, (ii) compare the influence of sample preparation protocols for bacterial identification by MALDI-TOF MS, and (iii) raise awareness for the potential of an increased resolution of MALDI-TOF MS for subtyping and associated limitations.

We have selected 47 clinically relevant bacterial isolates from 39 species and measured these under various conditions on two different MALDI-TOF MS systems. First, we identified spectral features, which positively correlate with correct species identification. Considering these, we systematically compared spectral quality produced with different sample protocols, with varying amounts of bacterial colony material applied, and with varying bacterial colony age.

MATERIALS AND METHODS

Bacterial Isolates

We selected 47 clinically relevant bacterial isolates from public and in-house strain collections. The included 39 species can be challenging to identify using MALDI-TOF MS, either because intracellular proteins cannot be ionised easily due to cell wall composition (e.g. *Corynebacterium* spp.), or because of their close relatedness to another bacterial species (e.g. *Klebsiella oxytoca/Klebsiella michiganensis*; *Shigella/Escherichia coli*).

The bacterial isolates were assigned to 8 phylogenetic groups (**Table 1**). For the strains in each group, we expect both comparable spectral features (e.g. total number of peaks detected) and lysis characteristics, respectively. For the evaluation of species identification, the group '*Streptococcus*' was further split up into 'viridans streptococci' and 'other streptococci' as the former group are of special interest in clinical routine diagnostics.

Whole Genome Sequencing

Isolates were grown on Columbia 5% Sheep Blood Agar (bioMérieux, Marcy-l'Étoile, France) and DNA was extracted using the QIACube with the QIAamp DNA Mini Kit (QIAGEN, Hilden, Germany). After quality control of the DNA by Tapestation (Agilent, Santa Clara, USA), tagmentation libraries were generated as described by the manufacturer (Nextera Flex kit, Illumina, San Diego, USA). The genomes were sequenced

TABLE 1 | Strains included in this study.

#	Species	Strain collection	Internal strain number	Group	NCBI/ENA Accession Number
01	*Klebsiella pneumoniae*	in-house	602149-19	*Enterobacteriaceae*	SAMN16951201
02	*Klebsiella oxytoca*	in-house	708776-17	*Enterobacteriaceae*	SAMN12212273
03	*Klebsiella grimontii*	in-house	132656-17	*Enterobacteriaceae*	SAMN12212117
04	*Klebsiella michiganensis*	in-house	401065-17	*Enterobacteriaceae*	SAMN12212153
05	*Klebsiella aerogenes*	in-house	717657-17	*Enterobacteriaceae*	SAMN12212322
06	*Klebsiella variicola*	in-house	717892-17	*Enterobacteriaceae*	SAMN12212293
09	*Escherichia coli*	in-house	807627-2-16	*Enterobacteriaceae*	SAMN16951202
10	*Escherichia coli*	in-house	807628-3-16	*Enterobacteriaceae*	SAMN16951203
11	*Escherichia coli*	in-house	804255-13	*Enterobacteriaceae*	SAMN16951204
12	*Escherichia coli*	in-house	805237-12	*Enterobacteriaceae*	SAMN16951205
13	*Shigella flexneri*	in-house	300666-18	*Enterobacteriaceae*	SAMN16951206
14	*Shigella flexneri*	in-house	301552-18	*Enterobacteriaceae*	SAMN16951207
15	*Shigella sonnei*	commercial	DSMZ-5570	*Enterobacteriaceae*	SAMN16951208
16	*Shigella sonnei*	in-house	301974-17	*Enterobacteriaceae*	SAMEA104430192
35	*Enterobacter sichuanensis*	in-house	403902-15	*Enterobacteriaceae*	SAMN16951209
36	*Enterobacter hormaechei*	commercial	ATCC-49162	*Enterobacteriaceae*	SAMN16951210
37	*Enterobacter asburiae*	commercial	ATCC-35956	*Enterobacteriaceae*	SAMN16951211
38	*Enterobacter ludwigii*	commercial	DSMZ-15213	*Enterobacteriaceae*	SAMN16951212
07	*Listeria monocytogenes*	in-house	107373-13	*Listeria*	SAMN16951213
08	*Listeria monocytogenes*	in-house	O1910-17	*Listeria*	SAMN16951214
17	*Burkholderia cepacia*	in-house	208050-16	*Burkholderia*	SAMN16951215
18	*Burkholderia contaminans*	in-house	O-13	*Burkholderia*	SAMEA54114418
19	*Burkholderia multivorans*	in-house	O-10	*Burkholderia*	SAMEA54118168
20	*Burkholderia cenocepacia*	in-house	O-3	*Burkholderia*	SAMEA54110668
21	*Bordetella bronchiseptica*	in-house	502474-16	*Bordetella*	SAMN16951216
22	*Bordetella pertussis*	commercial	ATCC-9797	*Bordetella*	SAMN16951217
23	*Bordetella parapertussis*	commercial	ATCC-53893	*Bordetella*	SAMN16951218
24	*Streptococcus pneumoniae*	in-house	144265-17	*Streptococcus*	SAMN16951219
25	*Streptococcus infantis*	in-house	131226-17	*Streptococcus*	SAMN16951220
26	*Streptococcus gordonii*	commercial	ATCC-33399	*Streptococcus*	SAMN16951221
27	*Streptococcus gallolyticus*	in-house	PRA0000041	*Streptococcus*	SAMN16951222
28	*Streptococcus lutetiensis*	commercial	DSMZ-15350-TS	*Streptococcus*	SAMN16951223
29	*Streptococcus pseudopneumoniae*	in-house	610886-17	*Streptococcus*	SAMN16951224
30	*Streptococcus equinus*	commercial	ATCC-9812	*Streptococcus*	SAMN16951225
31	*Streptococcus dysgalactiae*	in-house	STO0000159	*Streptococcus*	SAMN16951226
32	*Streptococcus dysgalactiae*	in-house	602125-13	*Streptococcus*	SAMN16951227
39	*Staphylococcus aureus*	in-house	351358-18	*Staphylococcus*	SAMN16951228
40	*Staphylococcus schweitzeri*	commercial	DSM-28300-TS	*Staphylococcus*	SAMN16951229
41	*Staphylococcus argenteus*	commercial	DSMZ-28299-TS	*Staphylococcus*	SAMN16951230
42	*Corynebacterium amycolatum*	commercial	ATCC-700206	*Actinobacteria*	SAMN16951231
43	*Corynebacterium urealyticum*	commercial	DSMZ-7109	*Actinobacteria*	SAMN16951232
44	*Gardnerella vaginalis*	commercial	ATCC-14018	*Actinobacteria*	SAMN16951233
45	*Winkia neuii*	in-house	STO0000012	*Actinobacteria*	SAMN16951234
46	*Actinomyces israelii*	commercial	ATCC-10048	*Actinobacteria*	SAMN16951235
47	*Pasteurella multocida*	commercial	ATCC-11039	Gram negative Anaerobes	SAMN16951236
33	*Bacteroides fragilis*	in-house	609216-11	Gram negative Anaerobes	SAMN16951237
34	*Bacteroides fragilis*	in-house	600609-16	Gram negative Anaerobes	SAMN16951238

Strains were either retrieved from in-house or commercial strain collections. Strains which are assigned the same 'Group' are expected to respond similarly to varying sample protocols, quantities of bacterial colony material applied and varying bacterial colony age.

under 24x multiplexing using a paired end 150 base pairs V3 reaction kit on an Illumina NextSeq500 instrument (Illumina) reaching an average coverage of approximately 60-fold for all isolates. The resulting raw reads were and assembled using Spades (v3.13) (Bankevich et al., 2012) *via* Unicycler (v0.3.0b) (Wick et al., 2017) using default settings. All accession numbers can be found in **Table 1**. Species identification of all strains was performed by comparing genomic sequences to bacterial type strains using Average Nucleotide Identity (ANIm) (Richter and Rosselló-Móra, 2009) and *via* the TrueBac ID database (Ha et al., 2019). For strains of the genus Bordetella we used ribosomal Multi-Locus Sequence Typing for additional confirmation of the species identity (Jolley et al., 2012).

In Silico Prediction of Ribosomal Subunit Protein Masses From WGS Data

The molecular weight of 56 ribosomal subunits were predicted as previously described (Ziegler et al., 2015; Rothen et al., 2019). Briefly, tblastn (v 2.2.31+) was used to extract the amino acid sequences of 56 ribosomal subunits from whole genome assemblies. The most frequent post translational modifications (Arnold and Reilly, 1999), specifically N-terminal methionine

loss (Frottin et al., 2006) and methylation, were considered for subsequent prediction of the monoisotopic molecular weights of the ribosomal subunit proteins. For the ribosomal subunit protein L33, we added 15 Daltons to the predicted molecular weight for the genera *Enterobacter*, *Escherichia*, *Shigella*, *Klebsiella* and *Pasteurella*, accounting for a single methylation of these proteins.

Spectra Quality Variables

All scripts used in the course of this study can be accessed *via* GitHub (https://github.com/appliedmicrobiologyresearch/MALDI-TOF-mass-spectral-quality-study).

We queried each spectrum for the following features: (i) number of peaks, (ii) peak with the highest m/z value, (iii) m/z value of the peak at the 90th percentile, (iv) fraction of peaks with a m/z value > 10,000, and (v) sum of the intensity of all detected peaks. As the highest peak often corresponds to technical artefacts, we included the m/z value of the peak at the 90th percentile for further analysis.

Furthermore, we queried each spectrum for the presence and intensity of ribosomal marker peaks predicted from the genomic sequence of the respective strain using an 800 ppm error range. If multiple peaks were detected in this error range, the one with the highest intensity and lower measurement error was considered for further analysis. Bacterial strains encode variable number of ribosomal markers in the mass range of 2,000–20,000 Da. We therefore normalised the number of detected marker peaks by dividing through the number of predicted ribosomal marker peaks in the MALDI-TOF MS mass range, when comparing between the bacterial taxa.

To quantify the measurement error, we calculated the mean distance between predicted and detected m/z value of ribosomal marker peaks for each spectrum. In order to estimate reproducibility, we calculated the 'fraction of reproducibly detected peaks'. We defined this as the number of peaks, which were detected in at least three out of four technical replicates using a bin size of 800 ppm, divided by the number of peaks in each spectrum. A more detailed and graphical explanation of the MALDI-TOF mass spectral features analysed in this study can be found in **Supplementary Methods 1**.

Further, we evaluate which of the above MALDI-TOF mass spectral features are good proxies for spectra quality and are associated with a correct species identification. We compared spectra for which the correct species was identified to spectra where the correct species could not be identified. Spectra for which the correct species could not be identified included spectra with wrong species being identified and spectra for which no species identification was possible. Henceforward, we will refer to these collectively as 'incorrectly identified spectra'. We performed this analysis exclusively on species which are covered by all three databases included in this study (**Supplementary Table S1**) and excluded empty spectra.

In order to assess how spectra quality impacts species identification accuracy, we included spectra acquired using the 'direct smear', the '25% formic acid (FA) overlay' or the 'simple protein extraction' method (see section 'Variation of sample preparation' for details) of the *Enterobacter cloacae complex* (*Enterobacter hormaechei*, *Enterobacter asburiae* and *Enterobacter ludwigii*), the *Burkholderia cepacia complex* (*Burkholderia contaminans*, *Burkholderia multivorans* and *Burkholderia cenocepacia*), and viridans streptococci (*Streptococcus pneumoniae* and *Streptococcus pseudopneumoniae*). We assigned these spectra to three intensity levels, by dividing the sum of the intensities of all detected peaks in three equal parts per group.

MALDI-TOF MS Spectra Acquisition

All MALDI-TOF mass spectra acquired for this study can be accessed *via* the Open Science Foundation (https://osf.io/ksz7r/). The bacterial isolates were cultured from Microbank^{TM} freezing beads (Pro-lab Diagnostics, Toronto, Canada) onto 5% Sheep Blood agar plates (bioMérieux, Marcy-l'Étoile, France) and subcultured before MALDI-TOF mass spectra acquisition. Strains were incubated under aerobic conditions at 37°C except for strains of the species *Bacterioides fragilis, Actinomyces israelii*, and *Winkia neuii*, which were incubated under anaerobic conditions using a whitley A95 anaerobic workstation (Don Whitley Scientific Limited, Bingley, United Kingdom). Strains of the species *Streptococcus pneumoniae*, *Bordetella pertussis*, and *Bordetella parapertussis* were incubated under 5% enriched CO_2 conditions. All mass spectra were acquired on reusable steel target plates [MBT Biotarget 96 (Bruker Daltonics, Bremen, Germany) and steel target plates (Industrietechnik mab AG, Basel, Switzerland)].

Variation of Sample Preparation

We cultured the bacterial strains as described above. We prepared the strains under three different short protocols, all of which are frequently used in microbial diagnostics: (i) 'Direct smear' method: using a plastic inoculation needle, we transferred bacterial colonies onto a steel target plate and overlaid each spot with 1 µl α-Cyano-4-hydroxycinnamic (CHAC) matrix (Sigma-Aldrich, St. Louis, USA) and left it to air dry completely before MALDI-TOF MS measurements. (ii) '25% FA overlay': using a plastic inoculation needle, we transferred bacterial colonies onto a steel target plate and overlaid each spot with 1 µl of 25% formic acid (Sigma-Aldrich, St. Louis, USA) and left it to air dry completely before applying 1 µl of CHAC matrix onto each spot. The target plates were left to air dry completely before MALDI-TOF MS measurements. (iii) 'Simple protein extraction': we transferred a heaped 1 µl inoculation loop of bacterial colony material into 1 ml PBS, rigorously vortexed, and centrifuged for 5 min at 17,000 x g. We removed the supernatant and added 30 µl 70% formic acid and dissolved the pellet by pipetting up and down. 30 µl acetonitrile (Sigma-Aldrich, St. Louis, USA) were added and the mixture was vortexed before centrifuging for 5 minutes at 17,000 x g. Next, 5 µl of the supernatant were mixed with 25 µl of CHAC matrix before spotting onto the steel target plate.

We performed measurements as quadruplicate on a Bruker microflex LT/LS 'smart' (Bruker Daltonics, Bremen, Germany) and a Shimadzu Axima Confidence (Shimadzu, Kyoto, Japan) MALDI-TOF MS device as technical replicates and repeated on three different days with fresh subcultures as biological replicates.

Variation of Bacterial Colony Age

We grew the strains over 1, 2, 3, 4, 5 or 6 nights before preparing them for measurement using the '25% FA overlay' method described above. Each overnight culture corresponds to 18 - 24 hours of incubation time. We performed measurements as quadruplicate on a Bruker microflex LT/LS 'smart' and a Shimadzu Axima Confidence MALDI-TOF MS device.

Variation of Bacterial Colony Material Quantity

The amount of bacteria transferred onto the MALDI-TOF MS steel target plate has been shown to impact spectral quality (Branda et al., 2017). The direct transfer of bacteria onto a steel target plate is difficult to standardise. We therefore decided to measure bacterial suspensions at different dilutions to assess the impact of the amount of bacterial colony material measured on mass spectral quality. We randomly selected the following two strains per phylogenetic group for this experiment: *Enterobacteriaceae:* #07, #08*; Listeria:* #09, #10; *Burkholderia:* #17, #19; *Bordetella:* #21, #23; *Streptococcus:* #26, #27; *Staphylococcus:* #39, #40; *Actinobacteria*: #45, #46; Gram negative anaerobes: #33, #34.

We transferred a heaped 1 µl inoculation loop of bacterial colony material into 200 µl of TMA (1x) buffer (Sigma-Aldrich, St. Louis, USA). Next, 5 µl of the bacterial mixture was diluted in 25 µl of CHAC matrix (1:5 dilution) and spotted onto the target plates. 5 µl of the suspension were transferred into a new tube containing 25 µl CHAC matrix (1:25 dilution). We continued the serial dilution up to a factor of 1:15,625. As the majority of measurements with 1:3,125 and 1:15,625 dilutions yielded empty spectra, these were excluded from further analysis. We measured quadruplicates on two MALDI-TOF MS devices as technical replicates and repeated on three different days as biological replicates.

Variation of Time After Calibration to Assess the Impact on Measurement Precision

We performed the measurements on two microflex biotyper devices (LH/LS and LH/LS 'smart'). Both devices were calibrated using the Bacterial Test Standard (BTS, Part.-Nr. 8255343, Bruker Daltonics, Bremen, Germany) and steel target plates (Bruker Daltonics, Bremen, Germany).

We used an *E. coli* strain from our strain collection (*E. coli* 805237-12) for these measurements as strains of this species generally yield rich spectra using routine sample preparation. We transferred bacteria onto a steel target plate, overlaid with 1 µl 70% FA, left to air dry completely before applying 1 µl CHAC matrix. Each measurement was performed in quadruplicate on two different target plates and MALDI-TOF MS devices as technical replicates and repeated by picking three different colonies as biological replicates. Spectra were acquired on days 1-7 after calibration on the same target plate which was used for calibration. BTS was measured on the row A of the target plate, measurements on day 1-7 after calibration were measured on rows B, C, D, E, F, G and H, respectively. Both MALDI-TOF MS devices where used for microbial species identification in routine diagnostics over the duration of this experiment with a median of 39 (Interquartile range (IQR): [32, 51]) and 137 (IQR: [123, 173]) of routine measurements per day on the microflex biotyper LH/LS and the microflex biotyper LH/LS 'smart', respectively.

MALDI-TOF MS Spectra Processing

In order to be most comparable to spectra acquired and processed in microbial routine diagnostic, we picked the peaks using default settings by the softwares included in the microflex Biotyper or the Axima Confidence system. Spectra acquired on microflex Biotyper devices were exported as 'fid' files and peak picking was performed in the flexAnalyses software (v3.4) and exported as '.txt' files. Spectra acquired on the Axima Confidence devices were exported as '.mzXml' files. These do already exclusively contain m/z values and intensities of picked peaks and were converted to '.txt' files. We subsequently exclusively worked with the intensity and m/z value of these picked peaks, and did not consider further peak characteristics such as the resolution or the signal to noise ratio of a peak.

We excluded spectra as contaminations for which the identified genus did not match the genus identified by ANIm. Strain 17 and strain 20 are missing in one out of three repetitions of the 'simple protein extraction' protocol, strain 32 is missing from day 6 of the and of strain 46 only three technical replicates were acquired on the Axima Confidence device using the 'direct smear' method.

Species Identification

Each spectrum acquired on a Bruker device was compared to the MALDI Biotyper database (MALDI Biotyper Compass Library, Revision E (Vers. 8.0, 7854 MSP, RUO)) included in the flexControl Software v3 (Bruker Daltonics, Bremen, Germany). Spectra acquired on the Axima Confidence device were analyzed with the VitekMS database (bioMérieux, Marcy-l'Étoile, France) (v3.2). Furthermore, we compared each spectrum to a ribosomal marker based database (PAPMID™ (Kassim et al., 2017), Mabritec AG, Riehen, Switzerland). In this study, we used this marker based approach as a subtyping module and each spectrum was compared only to a subset of bacterial species. Spectra of the species *Escherichia coli*, *Shigella flexneri*, *Shigella sonnei*, *Streptococcus gordonii*, *Streptococcus gallolyticus*, *Streptococcus lutetiensis*, *Streptococcus equinus*, *Streptococcus dysgalactiae, Corynebacterium amycolatum, Corynebacterium urealyticum, Gardnerella vaginalis, Winkia neuii, Actinomyces israelii, Pasteurella multocida*, and *Bacteroides fragilis* were compared to databases including mass profiles of the respective bacterial family. Spectra of the closely related *Klebsiella* spp., *Enterobacter cloacae complex, Listeria* spp., *Burkholderia cepacia complex, Bordetella* spp., *Staphylococcus aureus complex*, and viridans streptococci were identified using marker based subtyping modules exclusively including the species of the respective phylogenetic complex. Henceforward, species identification by these subtyping modules and using PAPMID™ database, both based on the detection of ribosomal marker peaks will be referred to as PAPMID™.

The MALDI Biotyper system classifies species identification according to log scores: mass spectra yielding a log score above 2.0 are assigned the label 'highly confidence identification', whereas spectra with a log score between 1.7 and 2.0 are assigned 'low confidence identification'. Spectra with a log score lower than 1.7 are assigned 'no organism identification possible'. For each spectrum with a log score above 1.7, we evaluated whether the species assigned by the MALDI Biotyper database corresponds to the true species identity determined by whole genome sequence analysis and ANIm. For species with a log score ≥ 2.0 we furthermore evaluated, how many species were assigned a log score ≥2.0.

Similar to the MALDI Biotyper database, the VitekMS database assigns scores to each species classification. Furthermore, each species identification is assigned a *Confidence level* [%] and a *Type of identification*, which is either 'Single Choice' or 'Low Discrimination' and indicates whether the species identification was unambiguous or whether the database could not unambiguously discriminate between two or more species entries. Identifications with an assigned probability, lower than a probability threshold (60%) are not assigned an unambiguous species label. In this situation, due to low confidence values, the Type of identification 'No Identification' or 'Low Discrimination' is assigned. For spectra with a Type of identification other than 'No Identification', we evaluated the Type of Identification and whether the assigned species corresponds to the true species identity of the measured strains.

We compared all spectra in our dataset to a ribosomal marker based database (PAPMID™). Marker based species identification tools such as the PAPMID™ database assign scores which correspond to the number of ribosomal marker peaks detected. The bacterial species is assigned for which most marker masses could be detected in a mass spectrum.

If a spectrum matches a maximal number of marker masses for multiple profiles of the same species, an unambiguous single species identification is assigned. If a spectrum matches an equal maximal number of marker masses from different species, multiple species are assigned ('multi-species Identification'). Species identifications with fewer marker peaks detected than the taxon-specific identification threshold, are assigned the label 'No identification possible'. The taxon specific thresholds used in this study were 20 for the species of the *Enterobacter cloacae complex*, 15 for *Klebsiella* spp. and *Escherichia coli/Shigella*, 7 for the species within the *S. aureus* complex, and 10 for all other phylogenetic groups included in this study.

Statistical Analysis

We used paired Wilcoxon rank tests when comparing spectra acquired from the same strains under different conditions. We excluded spectra of strains which were missing in one of the sets of interest. We used unpaired wilcoxon rank tests when comparing spectra acquired from different strains, e.g. when comparing between different phylogenetic groups or between correctly and incorrectly identified spectra.

When reporting comparisons in the running text, we refer to spectra acquired on the microflex Biotyper if not explicitly stated otherwise and use the nomenclature 'median (lower bound of the IQR, upper bound of the IQR)', throughout the study. Results and summary plots for spectra acquired on the Axima Confidence system can be found in the supplement.

We report the exact p-values when these are > 0.0001 and report use '****' for p-values < 0.0001. All analysis was performed in R (4.0.3) using the ggpubr (4.0) package.

RESULTS

Defining MALDI-TOF Mass Spectral Quality

In order to investigate spectral quality of the different datasets, we first assessed which spectral features are associated with a correct species identification with all databases and therefore suitable as quantitative measures for spectral quality. The spectra analysed here include a range of mass spectral quality, and were acquired using all different sample preparation protocols examined in this study and for the species included in three databases (MALDI Biotyper, VitekMS, PAPMID™) (**Supplementary Table S1**).

Five spectral features are good proxies for the correct species identification. In correctly identified spectra (i.e. high spectral quality) over all phylogenetic groups we found an increase in the number of ribosomal marker peaks detected (median = 22 IQR = (18, 25) (same nomenclature used throughout the paper) vs. 13 (6, 20)), their median relative intensity (1.27 (1.02, 1.65) vs. 1.00 (0.77, 1.27)), the sum of the intensity of all detected peaks (1.69×10^6 mV (0.97×10^6 mV, 2.39×10^6 mV) vs. 0.90×10^6 mV (0.27×10^6 mV, 1.62×10^6 mV)) and a decrease in the measurement error (249 ppm (186 ppm, 338 ppm) vs. (289 ppm (213 ppm, 388 ppm)) (all p-values < 0.0001) when compared to incorrectly identified spectra (**Figure 1** and **Supplementary Figures S1** and **S2**). In order to account for reproducibility, we included the fraction of reproducibly detected peaks between technical replicates as fifth quality measure. These five features were henceforth used to evaluate the spectral quality in the dataset.

When comparing correctly to incorrectly identified spectra we observed, over all phylogenetic groups, a small increase in total number of peaks (173 (146, 203) vs. 163 (128, 206), p-value < 0.0001)). However, when comparing within each phylogenetic group, and especially for spectra acquired on the microflex Biotyper, we did not observe a beneficial effect of an increased total number of peaks (**Supplementary Figure S1**). Therefore, we did not include the number of peaks as a quality measure. The fraction of peaks > 10'000 Da (30.5% (23.0%, 38.2%) vs. 31.6% (18.1%, 42.4%), p-value = 0.91) and the m/z value at the 90th percentile (15,323 Da (13,304 Da, 16,128 Da) vs. 15,387 Da (11,394 Da, 16,264 Da), p-value = 0.07) were comparable between correctly and incorrectly identified spectra, respectively.

In the following, we evaluated which sample preparation yielded highest quality spectra, over all phylogenetic groups, for unknown samples and within each phylogenetic group separately.

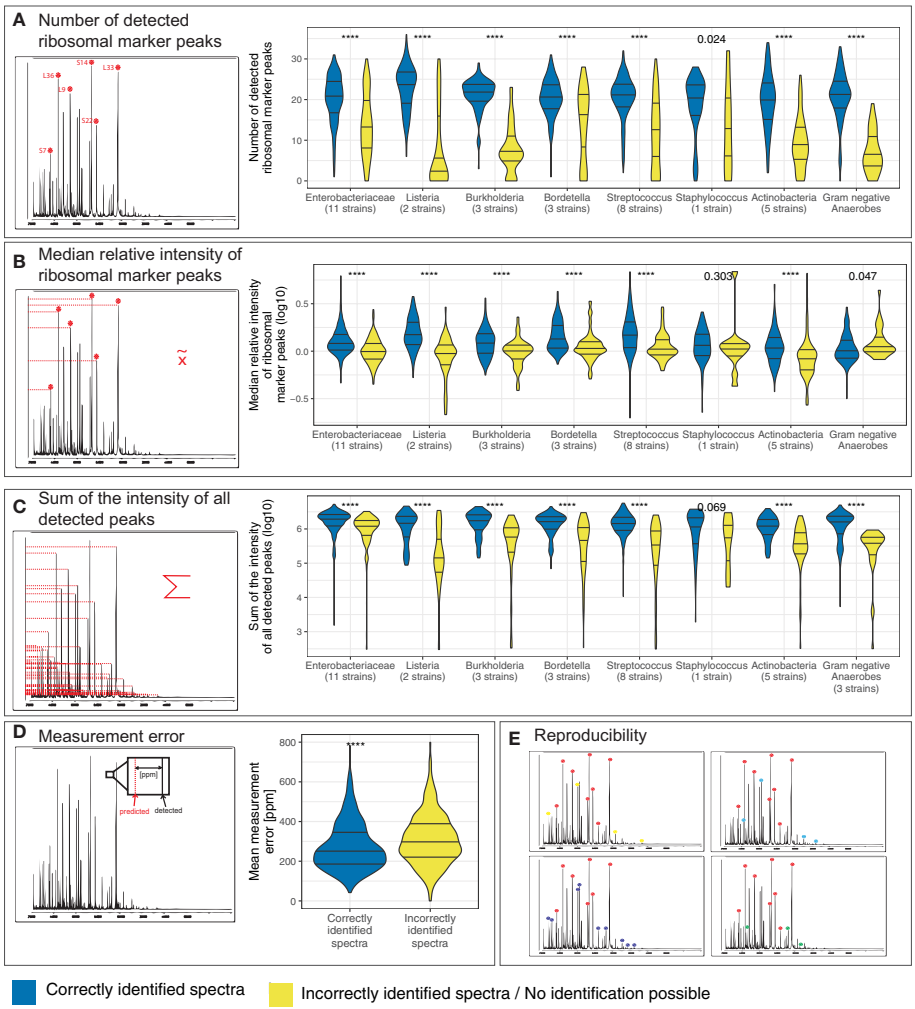

FIGURE 1 | Spectra features compared between correctly and incorrectly identified spectra per phylogenetic group. Species identification was performed by the MALDI Biotyper database and spectra were acquired on a microflex Biotyper. **(A)** the number of detected ribosomal marker peaks, **(B)** the median relative intensity of these, **(C)** the sum of intensity of all detected peaks, **(D)** measurement error and **(E)** reproducibility i.e. number of peaks detected in three out of four technical replicates divided by the total number of peaks in a spectrum. ****p-value < 0.0001.

Mass Spectral Quality Improvement With Different Sample Preparation Methods

In order to identify the best sample preparation, we first tested three different protocols. Over all phylogenetic groups, we found the '25% FA overlay' method yielded the highest spectral quality.

We observed the median relative intensity of ribosomal marker peaks (1.49 (1.14, 1.91) vs. 1.27 (0.97, 1.73), p-value = 0.025), the sum of the intensity of all detected peaks (2.16×10^6 mV (1.53×10^6 mV, 2.73×10^6 mV) vs. 1.80×10^6 mV (1.22×10^6 mV, 2.36×10^6 mV)) and the fraction of reproducibly detected peaks (74.0% (66.0%, 80.1%) vs. 69.5%, (59.7%, 77.7%)) to be higher for spectra acquired under the '25% FA overlay' method compared to the 'smear' method (p-values < 0.0001). Furthermore, we observed less variation when comparing the number of ribosomal marker peaks detected (22 (19, 25) vs. 22 (16, 25)) for spectra acquired under the '25% FA overlay' method compared to the 'smear' method.

Spectra acquired with the 'simple protein extraction' method yielded overall lower values for these measures ('median relative intensity of the ribosomal marker peaks detected': 1.17 (1.03, 1.37); 'sum of the intensity of all detected peaks': 1.22×10^6 mV, (0.74×10^6 mV, 2.14×10^6 mV); 'number of ribosomal marker peaks detected': 19 (12, 23)) when compared to spectra acquired under the 'smear' method (p-values < 0.0001), except for the fraction of reproducibly detected peaks, where we observed higher values for spectra acquired under the 'simple protein extraction' (73.7%, (65.3%, 82.2)) when compared to spectra acquired under the 'smear' method (p-value < 0.0001). The accuracy of identification by PAPMID™ generally follows quality measures, with the highest fraction of correctly

identified spectra under the '25% FA overlay method' (**Figures 1**, **Supplementary Figure S3**).

Increased Bacterial Age Decreased Spectral Quality

In order to assess how the age of a bacterial colony influences mass spectral quality, we measured the strains in our dataset after varying incubation time. We found a younger bacterial colony to be associated with a higher mass spectral quality. Increasing colony age had a negative impact on spectral quality with less ribosomal marker peaks detected (19.5 (17, 22) vs. 22 (20, 24)) and with a lower relative intensity (1.24 (0.96, 1.75) vs. 1.65 (1.34, 2.12)), and a lower fraction of reproducibly detected peaks (69.5% (64.8%, 74.6%) vs. 71.2% (64.6%, 77.6%)) after three days when compared one day incubation time (p-values < 0.0001) (**Figure 2**).

The accuracy of identification by PAPMID™ generally follows quality measures, with an increasing number of spectra not being identified, and decreasing spectral quality over the time period.

The Amount of Bacterial Colony Material Applied Has a Significant Impact on Spectral Quality

In order to identify the best preparation procedure, we tested varying concentrations of the bacterial sample applied to the steel target plate.

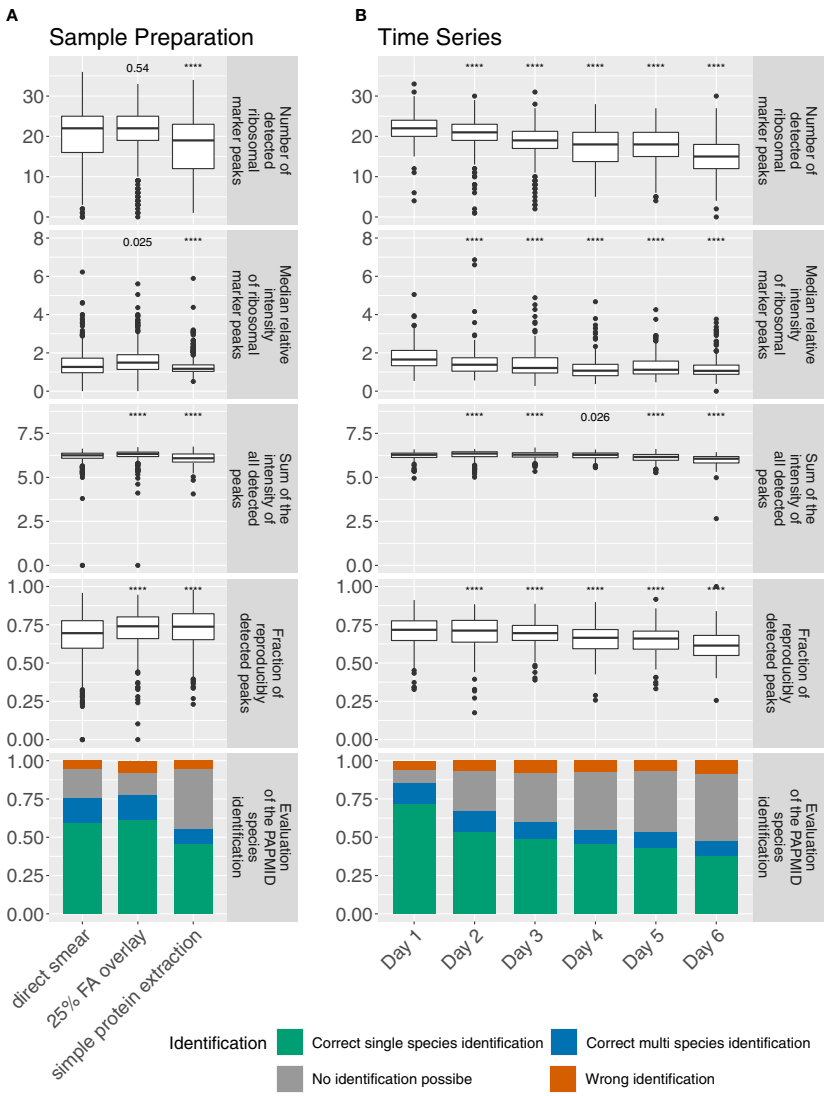

FIGURE 2 | **(A)** Comparison of different sample preparation protocols across all 47 bacterial isolates, (including 3 biological replicates and 4 technical replicates for each strain and protocol) and **(B)** age of the bacterial colony (47 bacterial isolates, 4 technical replicates for each strain and day) for spectra acquired on a microflex Biotyper MALDI-TOF MS system. '****'p-value < 0.0001.

Over all phylogenetic groups, we found that diluting the bacterial sample 1:5 did not decrease the number of ribosomal marker peaks detected (22.5 (14, 26) vs. 22 (19, 24)), nor the fraction of reproducibly detected peaks (75.2% (65.0%, 81.4%) vs. 72.4% (65.0%, 80.1%)) when compared to spectra acquired under the '25% FA overlay' method (**Figure 3**).

However, we observed a decreased median intensity of the ribosomal marker peaks (1.06, (0.94, 1.21) vs. 1.53 (1.16, 2.02)) and a decreased sum of the intensity of all detected peaks (1.17×10^6 mV (0.50×10^6 mV, 1.92×10^6 mV) vs. 2.15×10^6 mV (1.53×10^6 mV, 2.64×10^6 mV)) for 1:5 diluted samples when compared to samples processed using the '25% FA overlay' method (p-values < 0.0001).

Diluting bacterial colony material 1:25 or more generally decreased mass spectral quality ('number of ribosomal marker peaks detected': 21 (8.75, 24); 'median intensity of the ribosomal marker peaks: 1.07 (0.95, 1.29); 'sum of the intensity of all detected peaks': 0.51×10^6 mV, (0.16×10^6 mV, 0.85×10^6 mV)). However, we found taxon specific effects e.g. with *Burkholderia* yielding highest quality spectra with the highest number of ribosomal marker peaks detected with an additional dilution to 1:25 (**Supplementary Figures S5** and **S6**).

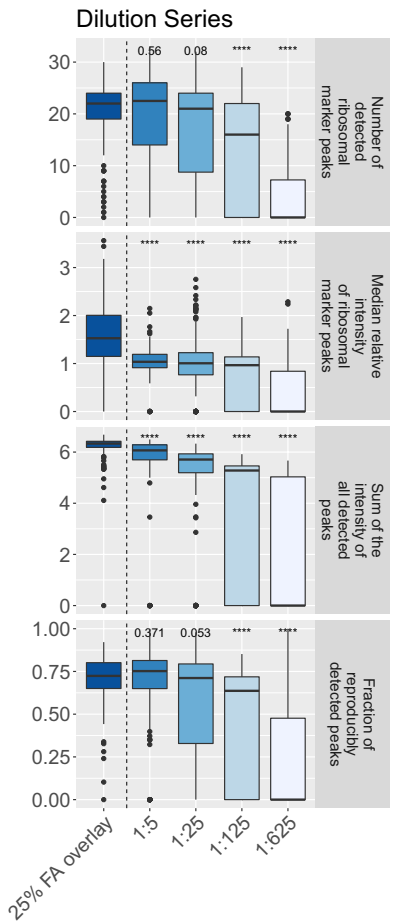

FIGURE 3 | Comparison of the amount of bacterial colony material applied onto a steel target plate for spectral quality (16 bacterial isolates, 3 biological and 4 technical replicates per dilution and strain). Spectra were acquired on a microflex Biotyper MALDI-TOF MS system. '****'p-value < 0.0001.

Calibration Is Crucial

All MALDI-TOF MS were externally calibrated in a routine setting and the effect of calibration has been previously investigated (Mitchell et al., 2015). Here, we tested the impact of time between calibration and the measurement on measurement precision. We found that the measurement error increased with time after calibration, (Day 1: 194 ppm (166 ppm, 235 ppm) vs. Day 7: 296 ppm (236 ppm, 379 ppm)) (p-value < 0.0001) (**Figure 4**).

Major Differences in Spectra Quality Between Bacterial Taxa

Testing whether the mass spectral quality is sufficient for spectra acquired with the '25% FA overlay' method for all bacterial taxa, we found important differences (**Figure 5**, **Supplementary Figure S7**). *Enterobacteriaceae* was the biggest family in our dataset (18 strains) and strains within this family generally yielded rich MALDI-TOF mass spectra with a high fraction of ribosomal marker peaks detected 57.1%, (50.0%, 61.9%)). For statistical analyses, we used *Enterobacteriaceae* as a reference group (**Figure 5**, **Supplementary Figure S7**). On both MALDI-TOF MS systems, we found Gram positive bacteria generally yielded lower quality spectra than the Gram negative strains, with a lower fraction of ribosomal marker peaks detected (46.1% (34.7%, 53.6%) vs. 55.0% (50.0%, 61.9%), a lower sum of the intensity of all detected peaks (1.64×10^6 mV (1.11×10^6 mV, 2.39×10^6 mV) vs. 2.38×10^6 (1.91×10^6 mV, 3.05×10^6 mV)) and a lower fraction of reproducibly detected peaks (66.7% (60.2%, 73.9%) vs. 77.7% (72.0%, 82.8%)) (p-values < 0.0001). *Actinobacteria* and streptococci other than viridans streptococci yielded lowest quality MALDI-TOF mass spectra

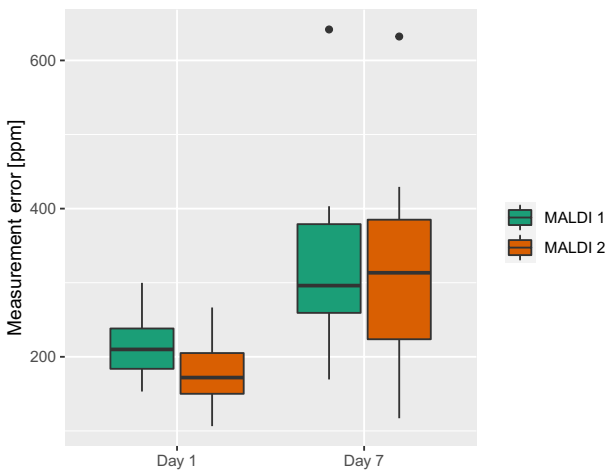

FIGURE 4 | Measurement error for Day 1 and Day 7 after calibration (1 bacterial isolate, 3 biological and 4 technical replicates per day).

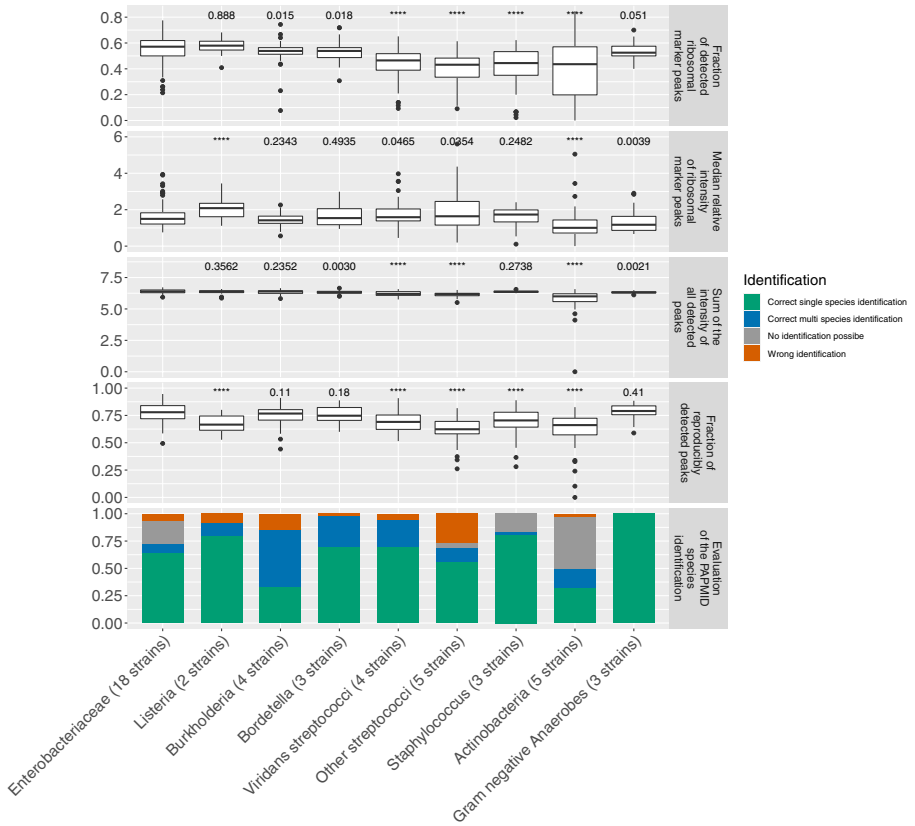

FIGURE 5 | MALDI-TOF mass spectra features and species identification of spectra acquired with the '25% FA overlay' method and after one day of incubation on a microflex Biotyper (3 biological and 4 technical replicates per strain). '****'p-value < 0.0001.

with the lowest fraction of ribosomal marker peaks detected (43.6% (19.8% - 57.1%), 43.2% (33.5% - 48.3%), respectively) and the lowest fraction of reproducibly detected peaks (66.1% (57.2% - 72.4%), 62.3% (58.2% - 69.5%), respectively).

Among the generally lower performing Gram positive bacteria and against the general trend, we detected the highest median fraction of detected ribosomal marker peaks for *Listeria* (58.0% (54.5% - 61.4%)), whereas Gram negative anaerobes yielded the highest fraction of reproducibly detected peaks (79.0%, (75.6% - 83.7%)).

Differences Between MALDI-TOF MS Databases

In order to evaluate different available databases we compared spectra acquired on the microflex Biotyper to the MALDI Biotyper database (MALDI Biotyper Compass Library, Revision E (Vers. 8.0, 7854 MSP, RUO)) and spectra acquired on the Axima Confidence system to the VitekMS database (v3.2) for species identification. All spectra compared were acquired under the '25% FA overlay' method. Please note that, while spectra were compared to the entire latter two databases for species identification, they were compared only to a subset of entries or subtyping modules of the PAPMID™ database.

Neither the MALDI Biotyper nor the VitekMS database cover all species included in this study (**Supplementary Table S1**). Spectra of strains belonging to species missing in these databases are often wrongly identified as closely related species represented in the database (**Figure 6**). The MALDI Biotyper database covers more species represented in our strain collection than the VitekMS DB (**Supplementary Table S1**) and more often results in a correct species assignment (**Figure 6**). However, comparison of spectra to MALDI Biotyper databases can lead to ambiguous results with multiple species yielding Scores > 2.0.

We observed the biggest difference between the MALDI Biotyper and the VitekMS database for *Staphylococcus* spectra, including spectra of the species *S. aureus*, *S. argenteus* and *S. schweitzeri*, with correctly identified species in 94.4% of spectra using the MALDI Biotyper database compared to 30.6% using the VitekMS database.

Species identification by the PAPMID™ yielded more often correct single species identification for spectra acquired on the

Axima Confidence device than for spectra acquired on the microflex Biotyper device.

Increased Mass Spectral Quality Increased Species Identification Accuracy

In order to understand the impact of mass spectral quality on species identification accuracy in more detail we looked at three species complexes, namely the *Burkholderia cepacia complex*, viridans streptococci and the *Enterobacter cloacae complex*, and exclusively considering species which are covered by all three databases examined in this study. We split the spectra of these three complexes into three equal groups according to the sum of the intensity of all detected peaks in each spectrum, using this as a universally applicable proxy for spectral quality. We observed that with increasing intensity, the number of detected ribosomal marker peaks, their median relative intensity, the reproducibility and measurement precision increase, suggesting that these quality features are correlated.

Importantly, we found a larger fraction of correctly identified species with a higher confidence level (MALDI Biotyper log score) with increasing spectral quality (**Figure 7** and **Supplementary Figure S19**). As an exception, we observed within the *Enterobacter cloacae complex*, an increase of incorrectly identified spectra using the MALDI Biotyper database with an increasing spectral quality.

Taxon-Specific Sample Preparation for Highest Spectral Quality

Following the inherent differences in mass spectral quality between the phylogenetic groups (**Figure 5**) we hypothesise taxon-specific improvement of spectral quality when using different sample preparation, quantity, and age of the bacterial colony. In order to assess these we have compared the sample preparation conditions evaluated in this study, for each group separately (**Supplementary Figures S5, S6, S8–S16**). Here, we suggest optimized taxon-specific sample preparation and handling protocols in order to achieve optimal spectral quality. We summarised the optimal sample preparation and bacterial colony age per group which yielded good quality spectra (**Table 2**).

TABLE 2 | Optimal sample protocol and bacterial age summarised per phylogenetic group.

Group	Protocol	Day
Enterobacteriaceae	25% FA overlay	Day 1
Listeria	25% FA overlay/Dilute 1:5	Day 1/2/3/4
Burkholderia	Dilute 1:25	Day 2
Bordetella	25% FA overlay/Dilute 1:5	Day 1/2
Streptococcus	Simple protein extraction	Day 1/2/3/4/5
Staphylococcus	Dilute 1:5/Simple protein extraction	Day 1/2
Actinobacteria	Simple protein extraction	Day 1
Gram - Anaerobes	Dilute 1:5	Day 1/2

DISCUSSION

In this study we determined MALDI-TOF mass spectra quality features, associated with correct identification and showed that these features can be increased in routine diagnostics by adapting sample preparations protocols.

Comparing the spectra quality yielded by varying sample preparations we found that over all phylogenetic groups and for unknown samples, measuring bacterial samples at a young age and overlaying the sample with 25% formic acid yielded the best quality spectra. As *Enterobacteriaceae* was the biggest group in our dataset, it had the strongest influence on the optimal sample preparation protocols when we analysed all strains congruently. Nonetheless, also when analyzing the impact of different sample preparation protocols for each group separately, the '25% FA overlay' method was amongst the best performing methods for most phylogenetic groups and with little hands-on time.

Over all phylogenetic groups, we observe the highest mass spectral quality after one overnight culture, followed by a decrease in mass spectral quality with increasing bacterial colony age. However, slower growing bacteria might require a longer incubation time before sufficient bacterial material can be transferred onto a target plate and before entering a phase of exponential growth, where ribosomal proteins are highly abundant (Fenselau and Demirev, 2001).

We find that, over all phylogenetic groups, diluting the bacterial sample 1:5 does not decrease mass spectral quality and a dilution step can in fact increase the spectral quality for certain taxa.

Overlaying the bacterial colony material with 25% formic acid does not increase spectral quality for all phylogenetic groups and can in fact often be omitted, and these samples can be prepared using the 'direct smear' method when the taxon of an isolate is known. On the other hand, not all phylogenetic groups yielded good-quality spectra even when overlaying the sample with 25% formic acid, most notably *Actinobacteria*. Here, a 'simple protein extraction' might be required to detect intracellular proteins (Alatoom et al., 2011).

Summarizing our sample preparation experiments, we encourage laboratories working in routine diagnostics to measure unknown microorganisms after one night of growth, with little bacterial colony material, and overlaying each spot with 25% formic acid. If the spectra acquired using this protocol do not yield satisfying identification results, we furthermore propose the application of taxon-specific protocols. These can also be used to obtain optimal quality mass spectra for subtyping.

To define mass spectral quality, we analysed several spectral features among which we identified the following five as best proxies: (i) number of ribosomal marker peaks detected, (ii) median relative intensity of ribosomal marker peaks, (iii) sum of the intensity of all detected peaks, (iv) measurement precision, and (v) reproducibility of all peaks. The first four were increased in spectra which were correctly identified with all three databases when compared to incorrectly identified spectra. The effect of these features is more pronounced when spectra are acquired on the Axima confidence than on the microflex Biotyper. Incorrectly identified Axima Confidence spectra appear to be signal poor with a low total number of peaks (**Supplementary**

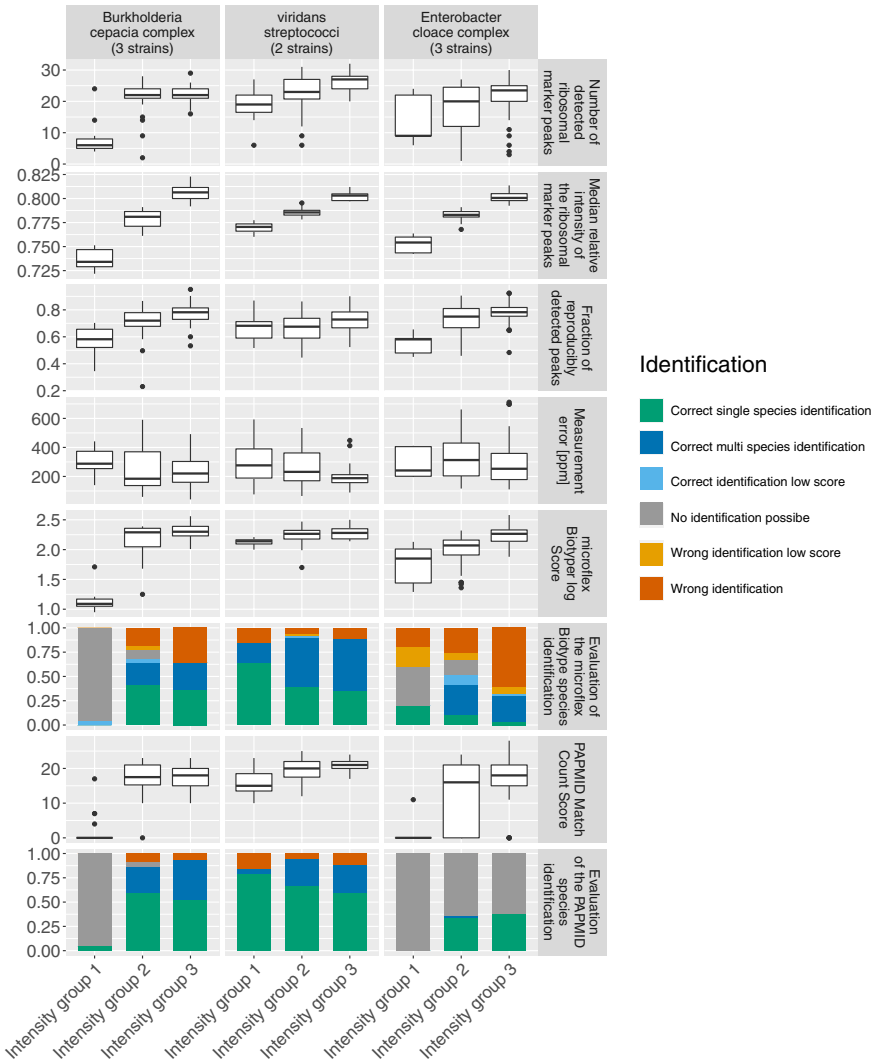

FIGURE 7 | Spectra quality features and evaluation of species identifications grouped by the sum of the intensity of all detected peaks. Spectra acquired on the microflex LT/LH 'smart'. Color Code: green: correct single species identification; dark blue: correct identification, multiple species above threshold; light blue: correct identification, MALDI Biotyper log score < 2; grey: no identification possible, yellow: wrong species identified, low security (MALDI Biotyper log score < 2), red: wrong species identified, high security (MALDI Biotyper log score > 2 and single species identification using a marker based approach).

Figure S2). Incorrectly identified microflex Biotyper spectra can harbour a high number of peaks, but are sparse in ribosomal marker masses and sum of the intensity of all detected peaks, which suggests that these spectra are noisy (**Supplementary Figure S1**). This is also reflected in the higher number of false positive hits in ribosomal marker masses leading to a higher fraction of wrongly identified microflex Biotyper spectra than Axima Confidence spectra when compared to the PAPMID™ database. As hardware settings, such as the tension of the detector, might affect the total number of peaks, it remains unclear whether the observed trends hold true for all microflex Biotyper devices. A study involving multiple devices is required to assess this question.

When using the '25% FA overlay' method, we found a median of 74.0% of peaks reproducibly detected in technical replicates of the same sample (**Figure 2**). This measure assesses the reproducibility of picked peaks with which we decided to work with, as they are the bases for species identification. This measure of reproducibility is different from the pearson correlation, comparing the shapes of two or more spectra (Zhang et al., 2014; Oberle et al., 2016). A reproducible detection of 75% of the picked peaks in a spectrum with 100 peaks, would mean that 75 peaks were detected in at least 3 out of 4 technical replicates of the same measurement. By using optimal sample preparation methods, we can increase the number of reproducibly detected peaks. These reproducibly detectable peaks could potentially be used as marker peaks, additional to ribosomal subunit masses and for spectra identification, further increasing the resolution of this method.

We observed the measurement error to increase with increasing time after calibration and therefore advise for frequent calibration of MALDI-TOF MS devices.

Microbiology taxonomy is in flux and many bacterial species have been newly described or have changed the genus in recent years (Janda, 2020). It is hardly possible for any diagnostic database to be up to date at every moment in time. We would like to emphasise that we have included strains in this study which pose difficulties for bacterial species identification and that bacterial species identification by MALDI-TOF MS is highly accurate in routine diagnostics (Croxatto et al., 2012). The challenges posed by the species included in this study are known and also clearly communicated by the MALDI-TOF MS manufacturers by e.g. displaying a warning message indicating which species cannot, or not reliably be distinguished from one another.

As the MALDI Biotyper database covers more of the species included in this study than the VitekMS database, spectral assignment from this database more often results in a correct species identification (**Figure 6**). This is most remarkable for spectra of the *S. aureus* complex, where the MALDI Biotyper database includes all three species (*S. aureus*, *S. argenteus* and *S. schweitzeri*), whereas the VitekMS database lists only *S. aureus* (**Supplementary Table S1**). However, interpreting the MALDI Biotyper species identification is not always trivial as multiple species can yield a log score > 2, which is used as a threshold for the assignment 'highly confidence identification'.

Importantly, we have shown that an increased spectra quality can increase the accuracy of species identifications by all three databases. However, against the general trend, the number of incorrectly identified spectra increases with increasing spectra quality for species of the *Enterobacter cloacae complex* analysed with the MALDI Biotyper database. A possible explanation could be the MALDI Biotyper database frequently assigning the more frequent sister species *E. cloacae sensu stricto*.

We find *Actinobacteria* yielding the lowest spectra quality of all phylogenetic groups analysed in this study. When comparing spectra of this group to the PAPMID™ database we find less often correctly identified spectra, compared to the other phylogenetic groups. For *Actinobacteria* only few ribosomal marker peaks can be detected, which makes distinction solely based on these, difficult. For this group, species identification using a pattern matching approach, applied by the MALDI Biotyper and the VitekMS database, more often yielded correct results. As it remains unclear which proteins form the basis of this species identification and how these vary between closely related species, it is possible that discrimination between closely related species might be challenging within *Actinobacteria* using a pattern matching approach.

MALDI-TOF mass spectra quality might be influenced by factors not considered in this study including: (i) hardware factors such as the age and intensity of the laser; (ii) the type of MALDI-TOF MS target plates and matrix used; (iii) culturing variables such as the agar media used or the atmosphere in which bacterial isolates are grown; (iv) spectra acquisition settings such as the number of laser shots applied and spectra averaged per measurement and (v) factors considering technical knowledge on acquiring MALDI-TOF mass spectra including regular training of staff and quality control of MALDI-TOF MS measurements. In order to assess and standardise MALDI-TOF mass spectral quality in routine diagnostics, a broader study comparing spectra acquired in multiple laboratories by different personnel is required.

The reliable detection of marker peaks in clinical routine would allow for higher resolution typing based on MALDI-TOF mass spectra, also distinguishing between closely related species e.g. within the *Klebsiella pneumoniae complex*, the *Staphylococcus aureus complex* and within viridans streptococci. An effective standardisation in culture conditions and spectra quality assessment might help the automation process of colony picking and mass spectral acquisition. Using a marker based approach for identification, we can congruently query spectra acquired on different MALDI-TOF MS systems around the world. Using the potential of routinely generated MALDI-TOF MS data for sublineage detection would open up new avenues of disease control by tracing the spread of important sub-lineages in real time with little additional effort.

DATA AVAILABILITY STATEMENT

The datasets presented in this study can be found in online repositories. The names of the repository/repositories and accession number(s) can be found in the article/**Supplementary Material**.

AUTHOR CONTRIBUTIONS

AC, AE, and VP designed and planned the study. AC conducted the experiments. AC, FF, and VP performed bioinformatic analysis. AC, AE, FF, and VP critically reviewed the manuscript. All authors contributed to the article and approved the submitted version.

FUNDING

This study was supported by a "Personalized Health" at ETHZ (D-BSSE) and University of Basel grant (PMB-03-17) and a Doc.Mobility Fellowship by the Swiss National Science Foundation (P1BSP3-184342).

ACKNOWLEDGMENTS

We thank Roxanne Mouchet (Mabritec AG, Riehen Switzerland), Doris Hohler (University Hospital of Basel) for excellent technical assistance in acquiring the MALDI-TOF mass spectra and culturing the strains and species identification using a marker based approach. We want to thank Dr. Tim Roloff, Magdalena

Schneider, Christine Kiessling, Elisabeth Schultheiss, Rosa-Maria Vesco, and Clarisse Straub (all University Hospital of Basel) for the DNA extraction, library preparations and sequencing of the bacterial isolates. We would like to thank Dr. Florian Geier and Dr. Robert Ivanek (Department for Biomedicine, University of Basel) for consultancy considering the statistical analyses. Further, we would like to thank Dr. Martin Welker (bioMérieux, Marcy-l'Étoile, France) for providing us access to the VitekMS database and technical consultancy as well as Ilona Mossbrugger (Bruker Daltonics, Bremen, Germany) for technical consultancy. We thank Dr. Vladimira Hinic, Dr. Helena Seth-Smith, Dr. Kirstine Kobberøe Søgaard (all University Hospital of Basel), Dr. Samuel Lüdin (Mabritec AG) and Vincent Somerville (University of Lausanne) for carefully reading the manuscript and giving valuable feedback. Calculations were performed at sciCORE (http://scicore.unibas.ch/) scientific computing center at University of Basel, the support from the sciCORE team for the analysis is greatly appreciated.

SUPPLEMENTARY MATERIAL

The Supplementary Material for this article can be found online at: https://www.frontiersin.org/articles/10.3389/fcimb.2021.646648/full#supplementary-material

REFERENCES

Alatoom, A. A., Cunningham, S. A., Ihde, S. M., Mandrekar, J., and Patel, R. (2011). Comparison of Direct Colony Method versus Extraction Method for Identification of Gram-Positive Cocci by Use of Bruker Biotyper Matrix-Assisted Laser Desorption Ionization–Time of Flight Mass Spectrometry. *J. Clin. Microbiol.* 49 (8), 2868–2873. doi: 10.1128/JCM.00506-11

Angeletti, S., and Ciccozzi, M. (2019). Matrix-Assisted Laser Desorption Ionization Time-of-Flight Mass Spectrometry in Clinical Microbiology: An Updating Review. *Infect. Genet. Evol.* 76 (December):104063. doi: 10.1016/j.meegid.2019.104063

Angeletti, S., Dicuonzo, G., Avola, A., Crea, F., Dedej, E., Vailati, F., et al. (2015). Viridans Group Streptococci Clinical Isolates: MALDI-TOF Mass Spectrometry versus Gene Sequence-Based Identification. *PloS One* 10 (3), e0120502. doi: 10.1371/journal.pone.0120502

Anhalt, J. P., and Fenselau, C. (1975). Identification of Bacteria Using Mass Spectrometry. *Anal. Chem.* 47 (2), 219–255. doi: 10.1021/ac60352a007

Arnold, R. J., and Reilly, J. P. (1999). Observation of Escherichia Coli Ribosomal Proteins and Their Posttranslational Modifications by Mass Spectrometry. *Anal. Biochem.* 269 (1), 105–112. doi: 10.1006/abio.1998.3077

Bankevich, A., Nurk, S., Antipov, D., Alexey, A., Dvorkin, G. M., Kulikov, A. S., et al. (2012). SPAdes: A New Genome Assembly Algorithm and Its Applications to Single-Cell Sequencing. *J. Comput. Biol.* 19 (5), 455–477. doi: 10.1089/cmb.2012.0021

Bizzini, A., Durussel, C., Bille, J., Greub, G., and Prod'hom, G. (2010). Performance of Matrix-Assisted Laser Desorption Ionization-Time of Flight Mass Spectrometry for Identification of Bacterial Strains Routinely Isolated in a Clinical Microbiology Laboratory. *J. Clin. Microbiol.* 48 (5), 1549–1554. doi: 10.1128/JCM.01794-09

Branda, J. A., Fritsche, T. R., Burnham, C.-A., Butler-Wu, S., Doern, C., Doing, K. M., et al. (2017). M58- Methods for the Identification of Cultured Microorganisms Using Matrix-Assisted Laser Desorption/Ionization Time-of-Flight Mass Spectrometry.

Christner, M., Trusch, M., Rohde, H., Kwiatkowski, M., Schlüter, H., Wolters, M., et al. (2014). Rapid MALDI-TOF Mass Spectrometry Strain Typing during a Large Outbreak of Shiga-Toxigenic Escherichia Coli. *PloS One* 9 (7), e1019245. doi: 10.1371/journal.pone.0101924

Croxatto, A., Prod'hom, G., and Greub, G. (2012). Applications of MALDI-TOF Mass Spectrometry in Clinical Diagnostic Microbiology. *FEMS Microbiol. Rev.* 36 (2), 380–407. doi: 10.1111/j.1574-6976.2011.00298.x

Dinkelacker, A. G., Vogt, S., Oberhettinger, P., Mauder, N., Rau, J., Kostrzewa, M., et al. (2018). Typing and Species Identification of Clinical Klebsiella Isolates by Fourier Transform Infrared Spectroscopy and Matrix-Assisted Laser Desorption Ionization–Time of Flight Mass Spectrometry. *J. Clin. Microbiol.* 56 (11), e00843-18. doi: 10.1128/JCM.00843-18

Fehlberg, L. C. C., Andrade, L. H. S., Assis, D. M., Pereira, R. H. V., Gales, A. C., and Marques, E. A. (2013). Performance of MALDI-ToF MS for Species Identification of Burkholderia Cepacia Complex Clinical Isolates. *Diagn. Microbiol. Infect. Dis.* 77 (2), 126–128. doi: 10.1016/j.diagmicrobio.2013.06.011

Fenselau, C., and Demirev, P. A. (2001). Characterization of Intact Microorganisms by MALDI Mass Spectrometry. *Mass Spectrom. Rev.* 20 (4), 157–171. doi: 10.1002/mas.10004

Frottin, F, Martinez, A., Peynot, P., Mitra, S., Holz, R. C., Giglione, C., et al. (2006). The Proteomics of N-Terminal Methionine Cleavage. *Mol. Cell. Proteomics* 5 (12), 2336–2349. doi: 10.1074/mcp.M600225-MCP200

Ha, S.-M., Kim, C. K., Roh, J., Byun, J.-H., Yang, S.-J., Choi, S.-B., et al. (2019). Application of the Whole Genome-Based Bacterial Identification System, TrueBac ID, Using Clinical Isolates That Were Not Identified With Three Matrix-Assisted Laser Desorption/Ionization Time-of-Flight Mass Spectrometry (MALDI-TOF MS) Systems. *Ann. Lab. Med.* 39 (6), 530–3655. doi: 10.3343/alm.2019.39.6.530

Hotta, Y., Teramoto, K., Sato, H., Yoshikawa, H., Hosoda, A., and Tamura, H. (2010). Classification of Genus Pseudomonas by MALDI-TOF MS Based on Ribosomal Protein Coding in S10–spc–alpha Operon at Strain Level. *J. Proteome Res.* 9 (12), 6722–6728. doi: 10.1021/pr100868d

Janda, J.M. (2020). Proposed Nomenclature or Classification Changes for Bacteria of Medical Importance: Taxonomic Update 5. *Diagn. Microbiol. Infect. Dis.* 97 (3), 1150475. doi: 10.1016/j.diagmicrobio.2020.115047

Jolley, K. A., Bliss, C. M., Bennett, J. S., Bratcher, H. B., Brehony, C., Colles, F. M., et al. (2012). Ribosomal Multilocus Sequence Typing: Universal Characterization of Bacteria from Domain to Strain. *Microbiology* 158 (4), 1005–1015. doi: 10.1099/mic.0.055459-0

Kassim, A., Pflüger, V., Premji, Z., Daubenberger, C., and Revathi, G. (2017). Comparison of Biomarker Based Matrix Assisted Laser Desorption Ionization-Time of Flight Mass Spectrometry (MALDI-TOF MS) and Conventional Methods in the Identification of Clinically Relevant Bacteria and Yeast. *BMC Microbiol* 17, 128. doi: 10.1186/s12866-017-1037-z. 17(May).

Lafolie, J., Sauget, M., Cabrolier, N., Hocquet, D., and Bertrand, X. (2015). Detection of Escherichia Coli Sequence Type 131 by Matrix-Assisted Laser Desorption Ionization Time-of-Flight Mass Spectrometry: Implications for Infection Control Policies? *J. Hosp. Infect.* 90 (3), 208–212. doi: 10.1016/j.jhin.2014.12.022

Matsumura, Y., Yamamoto, M., Nagao, M., Tanaka, M., Machida, K., Ito, Y., et al. (2014). Detection of Extended-Spectrum-β-Lactamase-Producing Escherichia Coli ST131 and ST405 Clonal Groups by Matrix-Assisted Laser Desorption Ionization–Time of Flight Mass Spectrometry. *J. Clin. Microbiol.* 52 (4), 1034–1040. doi: 10.1128/JCM.03196-13

Mitchell, M., Mali, S., King, C. C., and Bark, S. J. (2015). Enhancing MALDI Time-Of-Flight Mass Spectrometer Performance through Spectrum Averaging. *PloS One* 10 (3), e0120932. doi: 10.1371/journal.pone.0120932

Oberle, M., Wohlwend, N., Jonas, D., Maurer, F. P., Jost, G., Tschudin-Sutter, S., et al. (2016). The Technical and Biological Reproducibility of Matrix-Assisted Laser Desorption Ionization-Time of Flight Mass Spectrometry (MALDI-TOF MS) Based Typing: Employment of Bioinformatics in a Multicenter Study. *PloS One* 11 (10), e0164260. doi: 10.1371/journal.pone.0164260

Ojima-Kato, T., Yamamoto, N., Nagai, S., Shima, K., Akiyama, Y., Ota, J., et al. (2017). Application of Proteotyping Strain Solution™ Ver. 2 Software and Theoretically Calculated Mass Database in MALDI-TOF MS Typing of *Salmonella* Serotype. *Appl. Microbiol. Biotechnol.* 101 (23–24), 8557–8569. doi: 10.1007/s00253-017-8563-3

Patel, R. (2015). MALDI-TOF MS for the Diagnosis of Infectious Diseases. *Clin. Chem.* 61 (1), 100–111. doi: 10.1373/clinchem.2014.221770

Richter, M., and Rosselló-Móra, R. (2009). Shifting the Genomic Gold Standard for the Prokaryotic Species Definition. *Proc. Natl. Acad. Sci. U. S. A.* 106 (45), 19126–19131. doi: 10.1073/pnas.0906412106

Rodríguez-Sánchez, B., Cercenado, E., Coste, A. T., and Greub, G. (2019). Review of the Impact of MALDI-TOF MS in Public Health and Hospital Hygien. *Eurosurveillance* 24 (4), 1800193. doi: 10.2807/1560-7917.ES.2019.24.4.1800193

Rothen, J., Pothier, J. F., Foucault, F., Blom, J., Nanayakkara, D., Li, C., et al. (2019). Subspecies Typing of Streptococcus Agalactiae Based on Ribosomal Subunit Protein Mass Variation by MALDI-TOF MS. *Front. Microbiol.* 10, 471. doi: 10.3389/fmicb.2019.00471

Ryzhov, V., and Fenselau, C. (2001). Characterization of the Protein Subset Desorbed by MALDI from Whole Bacterial Cells. *Anal. Chem.* 73 (4), 746–750. doi: 10.1021/ac0008791

Tomachewski, D., Galvão, C. W., de Campos Júnior, A., Margarete Guimarães, A., Ferreira da Rocha, J. C., and Etto, R. M. (2018). Ribopeaks: A Web Tool for Bacterial Classification through m/z Data from Ribosomal Proteins. *Bioinf. (Oxford England)* 34 (17), 3058–3060. doi: 10.1093/bioinformatics/bty215

van Veen, S. Q., Claas, E. C. J., and Kuijper, E. (2010). High-Throughput Identification of Bacteria and Yeast by Matrix-Assisted Laser Desorption Ionization-Time of Flight Mass Spectrometry in Conventional Medical Microbiology Laboratories. *J. Clin. Microbiol.* 48 (3), 900–907. doi: 10.1128/JCM.02071-09

Veloo, A. C. M., Elgersma, P. E., Friedrich, A. W., Nagy, E., and van Winkelhoff, A. J. (2014). Influence of Incubation Time, Sample Preparation and Exposure to Oxygen on the Quality of the MALDI-TOF MS Spectrum of Anaerobic Bacteria. *Clin. Microbiol. Infect.* 20 (12), O1091–O1097. doi: 10.1111/1469-0691.12644

Wick, R. R., Judd, L. M., Gorrie, C. L., and Holt, K. E. (2017). Unicycler: Resolving Bacterial Genome Assemblies from Short and Long Sequencing Reads. *PloS Comput. Biol.* 13 (6), e1005595. doi: 10.1371/journal.pcbi.1005595

Wolters, M., Rohde, H., Maier, T., Belmar-Campos, C., Franke, G., Scherpe, S., et al. (2011). MALDI-TOF MS Fingerprinting Allows for Discrimination of Major Methicillin-Resistant Staphylococcus Aureus Lineages. *Int. J. Med. Microbiol.* 301 (1), 64–68. doi: 10.1016/j.ijmm.2010.06.002

Zhang, L., Borror, C. M., and Sandrin, T. R. (2014). A Designed Experiments Approach to Optimization of Automated Data Acquisition during Characterization of Bacteria with MALDI-TOF Mass Spectrometry. *PloS One* 9 (3), e92720. doi: 10.1371/journal.pone.0092720

Ziegler, D., Pothier, J. F., Ardley, J., Fossou, R. K., Pflüger, V., de Meyer, S., et al. (2015). Ribosomal Protein Biomarkers Provide Root Nodule Bacterial Identification by MALDI-TOF MS. *Appl. Microbiol. Biotechnol.* 99 (13), 5547–5562. doi: 10.1007/s00253-015-6515-3

Conflict of Interest: VP and FF are employed by Mabritec AG.

The remaining authors declare that the research was conducted in the absence of any commercial or financial relationships that could be construed as a potential conflict of interest.

frontiers in Cellular and Infection Microbiology

ORIGINAL RESEARCH
published: 19 April 2021
doi: 10.3389/fcimb.2021.634382

CryptoType – Public Datasets for MALDI-TOF-MS Based Differentiation of *Cryptococcus neoformans/gattii* Complexes

Mareike Bernhard[1], Navaporn Worasilchai[2†], Mourine Kangogo[3], Christine Bii[4], Wioleta J. Trzaska[5], Michael Weig[1], Uwe Groß[1], Ariya Chindamporn[2] and Oliver Bader[1]*

[1] Institute for Medical Microbiology, University Medical Center Göttingen, Göttingen, Germany, [2] Department of Microbiology, Faculty of Medicine, Chulalongkorn University, Bangkok, Thailand, [3] Department of Medical Microbiology, Jomo Kenyatta University of Agriculture and Technology, Nairobi, Kenya, [4] Center for Microbiology Research, Mycology Laboratory, Kenya Medical Research Institute, Nairobi, Kenya, [5] School of Biosciences, Institute of Microbiology and Infection, University of Birmingham, Birmingham, United Kingdom

Yeasts of the *Cryptococcus neoformans/gattii* species complexes are human pathogens mostly in immune compromised individuals, and can cause infections from dermal lesions to fungal meningitis. Differences in virulence and antifungal drug susceptibility of species in these complexes indicate the value of full differentiation to species level in diagnostic procedures. MALDI-TOF MS has been reported to sufficiently discriminate these species. Here, we sought to re-evaluate sample pre-processing procedures and create a set of publicly available references for use with the MALDI Biotyper system. Peak content using four different pre-processing protocols was assessed, and database entries for 13 reference strains created. These were evaluated against a collection of 153 clinical isolates, typed by conventional means. The use of decapsulating protocols or mechanical disruption did not sufficiently increase the information content to justify the extra hands-on-time. Using the set of 13 reference entries created with the standard formic acid extraction, we were able to correctly classify 143/153 (93.5%) of our test isolates. The majority of the remaining ten isolates still gave correct top matches; only two isolates did not give reproducible identifications. This indicates that the log score cut-off can be lowered also in this context. Ease to identify cryptococcal isolates to the species level is improved by the workflow evaluated here. The database references are freely available from https://github.com/oliverbader/BioTyper-libraries for incorporation into local diagnostic systems.

Keywords: MALDI-TOF MS, identification, capsule, *Cryptococcus neoformans* complex, *Cryptococcus gattii* complex

OPEN ACCESS

Edited by:
Di Xiao,
National Institute for Communicable Disease Control and Prevention (China CDC), China

Reviewed by:
Bryan Schmitt,
Indiana University Bloomington, United States
Volker Rickerts,
Robert Koch Institute (RKI), Germany

***Correspondence:**
Oliver Bader
oliver.bader@med.uni-goettingen.de

†Present address:
Navaporn Worasilchai, Department of Transfusion Medicine and Clinical Microbiology, Faculty of Allied Health Sciences, Chulalongkorn University, Bangkok, Thailand

Specialty section:
This article was submitted to Clinical Microbiology, a section of the journal Frontiers in Cellular and Infection Microbiology

Received: *27 November 2020*
Accepted: *30 March 2021*
Published: *19 April 2021*

Citation:
Bernhard M, Worasilchai N, Kangogo M, Bii C, Trzaska WJ, Weig M, Groß U, Chindamporn A and Bader O (2021) CryptoType – Public Datasets for MALDI-TOF-MS Based Differentiation of Cryptococcus neoformans/gattii Complexes. Front. Cell. Infect. Microbiol. 11:634382. doi: 10.3389/fcimb.2021.634382

INTRODUCTION

The group of basidiomycetous yeast of the *Cryptococcus neoformans/gattii* complexes hosts a variety of human pathogenic species, causing infections from skin lesions to fatal meningitis [reviewed in (Kronstad et al., 2011)]. This mainly contributes to morbidity and mortality in patients with underlying immune deficiencies (e.g. HIV), but can also affect immunocompetent hosts. Species of the *C. neoformans/gattii* complexes are readily found in the environment, living, for example, on eucalyptus tree bark, and bird droppings.

The most prominent diagnostic feature of these species are the large capsules of most isolates [reviewed in (O'Meara and Alspaugh, 2012)], which can easily be visualized by, e.g., displacement of India ink stain. India ink does not penetrate the capsule and thus creates a halo around the cells visible in microscopy. The polysaccharides shed from the cell also give rise to efficient and specific serologic tests of cryptococcal infections through serum detection of galactomannan.

Species in this complex have traditionally been divided into four serotypes based on antigenicity of the capsule, forming three varieties: *C. neoformans* var. *grubii* (serotype A), var. *gattii* (serotypes B and C), and var. *neoformans* (serotype D). They are also able to form inter-species hybrids leading to, e.g., an AD serotype (Boekhout et al., 2001). Several genetic methods are available to stratify the different serotypes into further molecular types (Meyer et al., 2003) and characterize hybrid strains. Recently, it has been proposed to formally raise the non-hybrid molecular types to species level (Kwon-Chung et al., 2002; Hagen et al., 2015) and a fifth *C. gattii* lineage has recently been described (Farrer et al., 2019) from environmental and animal specimen.

In clinical samples from Europe most frequently serotype A is found, mainly from immunocompromised patients, e.g. those suffering from AIDS (Kronstad et al., 2011). Highly virulent isolates usually stem from the *C. gattii* complex, which also readily infect immuno-competent hosts. Differences in mean antifungal susceptibility between closely related molecular types have been reported (Trilles et al., 2012; Cogliati et al., 2018; Lee et al., 2019) and *in vitro* differences in cytokine responses (Herkert et al., 2018). Some molecular types, mainly VGII and VGIII, are more prone to be involved in outbreak scenarios (Kidd et al., 2004; Carriconde et al., 2011; Springer et al., 2014). A major difference between *C. neoformans* and *C. gattii* groups is the lack of growth inside macrophages among *C. gattii* isolates, with the notable exception of such outbreak lineages (Voelz et al., 2014).

Together this underlines the benefit of methods easily discriminating between the major molecular types, not only in clinical contexts, but also for epidemiological studies which so far rely on laborious genetic typing [e.g. our own work (Tangwattanachuleeporn et al., 2013; Kangogo et al., 2015; Worasilchai et al., 2017) or others (Fang et al., 2020; Jin et al., 2020)]. MALDI-TOF MS has been established over the past years as a widely used clinical species identification tool and has been shown to be able to discriminate between the seven known molecular types within the *C. neoformans/gattii* complexes (McTaggart et al., 2011; Firacative et al., 2012; Posteraro et al., 2012; Hagen et al., 2015). For *C. gatti* and *C. deuterogatii* differential mass peaks have been described (Jin et al., 2020).

However, this has not been implemented in diagnostic systems, which remain at the point where only *C. neoformans* var. *neoformans/grubii* vs. *C. gattii* complexes can be identified. In part, this may be due to the observation that false species designations above the significance threshold can be observed (Posteraro et al., 2012), and reflect the complexity introduced by hybrid formation between the different linages.

In this study, we created a publicly available MALDI Biotyper database reference ("main spectrum projections", MSPs) set from 13 type strains of seven recognized non-hybrid subtypes in the *Cryptococcus neoformans/gattii* complexes. Their performance using different preprocessing protocols is evaluated on a set of characterized isolates.

MATERIALS AND METHODS

Yeast Strains and Culture Conditions, Chemicals

For long-term storage, *Cryptococcus* isolates were kept at -70°C in cryobank stocks (Mast Diagnostica, Reinfeld, Germany). After thawing, strains were propagated on Sabouraud's (SAB) agar slants supplemented with 0.5% peptone (casein), 0.5% peptone (meat), and 2% glucose. Before sample preparation, strains were cultivated on SAB agar overnight at 30°C.

For the purpose of text clarity, only the species nomenclature according to Hagen et al. (Hagen et al., 2015) is adopted from here. As references, thirteen strains of the CBS collection (Westerdijk Fungal Biodiversity Institute) were used: three *C. neoformans* (CBS 8710 (molecular type VNI), CBS 10084 (VNII), CBS 10085(VNI)), two *C. deneoformans* (CBS 6900 and CBS 10079 (VNIV)), two *C. gattii* (CBS 6289,and CBS 10078, VGI), two *C. deuterogattii* (CBS 10082, and CBS 10514, VGII) two *C. bacillisporus* (CBS 6955 and CBS 10081, VGIII), one *C. tetragattii* (CBS 10101, VGIV), and *C. decagattii* (CBS 11687, VGIV).

A test set of 153 isolates was assembled from previously characterized collections. This included all Thai strains from Worasilchai et al. (2017), augmented with rare species isolates from Kenya (Kangogo et al., 2015) and the Birmingham laboratory collection, which include strain from various studies [e.g. (Voelz et al., 2014)]. All isolates were typed either previously (Kangogo et al., 2015; Worasilchai et al., 2017) or specifically for the purpose of this study using the *URA5*-RFLP method. The final set contained n=96 *C. neoformans*, n=6 *C. deneoformans*, n=5 *C. gattii*, n=18 *C. bacillisporus*, n=20 *C. deuterogattii*, and n=8 *C. tetragattii* isolates. A negative control group was assembled from mass spectra randomly chosen from those obtained during bacterial (n=86) of fungal (n=403) routine diagnostics.

URA5-RFLP

Restriction fragment length polymorphisms were performed as described previously (Kangogo et al., 2015; Worasilchai et al., 2017). Briefly, genomic DNA was extracted from cells using phenol/chloroform and the *URA5* gene was amplified using

URA5 forward (5-ATGTCCTCCCAAGCCCTCGACTCCG-3) and SJ01 reverse (5-TTAAGACCTCTGAACACCGTACTC-3) primers (Meyer et al., 2003). The amplicons obtained were either simultaneously digested with HhaI (20 U/µl) and Sau96I (10 U/µl) or StuI (10 U/µl) alone for 8 hours (all from New England Biolabs). The digestion products were purified using a PCR clean-up kit (NucleoSpin, Macherey-Nagel, Düren, Germany) and visualized on a 3% agarose gel.

MALDI-TOF MS Preprocessing Protocols

For regular harvest and formic acid-extraction [preprocessing protocol (A) (Bader, 2017)], cells were taken from agar plates by scraping approximately a 1µl loop full of cells and re-suspending them in 300 µl water. 700 µl absolute ethanol was added to a final concentration of 70% (v/v) and vortexes. Cells were spun down at 8500x*g* for 5 min, the supernatant completely discarded and the cells lysed first with 50 µl 70% (v/v) formic acid, and 50 µl pure acetonitrile. Modifications to this protocol tested were for preprocessing protocol (B) that cells were collected in 300 µl 5% (v/v) $DMSO_{ad}$, for preprocessing protocol (C) that DMSO was included in the 70% ethanol washing step to a final volume of 5% (v/v), and for preprocessing protocol (D) that cells were collected in 300 µl water already including an equivalent of ~100 µl glass beads (0.5 mm diameter, Roth, Karlsruhe, Germany). Here, cells were mechanically disrupted in a FP120 fast prep machine (Bio101, Thermo Savant) at setting 4, for 30 sec during the formic acid step.

Generation of MALDI Biotyper Database References

MSP references for the MALDI Biotyper were generated according to the manufacturer's guidelines (Kostrzewa and Maier, 2017), using preprocessing protocol A. Spectra from 24 individual spots were gathered on a freshly calibrated (BTS reference standard) Autoflex III system (Bruker Daltonics, Bremen, Germany) using the automated acquisition mode of the Biotyper 3.1. Spectra were processed using the inbuilt MSP generation method, using the standard parameters.

RESULTS AND DISCUSSION

Method Optimization

The literature reports that both, removal of cryptococcal capsule can (Thomaz et al., 2016) or does not (Hagen et al., 2015) positively influence spectrum quality. Since the capsule material is soluble in DMSO, we devised pre-processing protocols that would deplete the capsule prior to the regular formic acid/acetonitrile extraction protocol. Both pre-processing protocols, B (**Figures 1A, B**) and C (not shown), efficiently removed capsules in all strains. However, subsequent measurement of mass spectra did not reveal any additional mass signals, or major differences in spectrum quality (**Figure 1C**).

Next, we tested if mechanical disruption of the cells yielded more informative spectra using mechanical disruption (preprocessing protocol D). Indeed, mass spectra recorded from mechanically disrupted cells resulted in more evenly distributed peak intensities across the major mass signals. However, no additional mass signals of high intensity were found (**Figure 1D**).

In our hands removal of the capsule did not result in spectra with higher information content, at any time. Mechanical disruption did reveal some additional masses, but in favor of the lower hands-on-time the original pre-processing protocol A was subsequently used for MSP creation and testing.

Creation of Single Species MSPs

Next, we created MSPs for 13 reference strains encompassing seven molecular types of the *C. neoformans/gattii* complexes (Meyer et al., 2003; Hagen et al., 2015), using the standard extraction procedure (pre-processing protocol A). Cluster analysis of the MSPs generated suggested sufficient distance to clearly distinguish between *C. neoformans* complex molecular types VNIV (*C. deneoformans*) and VNI/II, and possibly also between VNI and VNII themselves, but less so among molecular types within the *C. gattii* complex (**Figure 2**).

Identification Performance

Mass spectra for all test isolates were obtained using preprocessing protocol A. Were MALDI-TOF results using the new MSP set deviated from previous data, *URA5*-RFLP typing was repeated as the gold standard (**Figure 3A**). All but two deviations could be resolved (see below). To discriminate between *C. tetragattii* and potential *C. decagattii* strains, we sequenced the *URA5*-amplicon obtained from CBS 11687 (*C. decagattii*, deposited at Genebank under the accession number MH605184) and compared it to the respective sequence of CBS 10101 (*C. tetragattii*, gene bank accession AY973155). Restriction with StuI was found, and experimentally confirmed, to discriminate the two species (**Figure 3B**). However, there were no further *C. decagattii* isolates among our strains. *C. decagattii* remains a rare species, and only a single isolate of this molecular type (CBS 11687) was available for this study, which was already included in the reference set. Therefore, the final test collection encompassed only six of the seven species used for generation of references.

From the test collection, we were able to correctly identify 143/153 (93.5%) of the isolates on species-level using duplicate spots, with the top log score ≥ 2.000 (**Figure 3C**), as recommended by the manufacturer. Of the remaining ten isolates, eight still gave correct species matches at scores between 1.700 and 1.999, considered only genus-level by the manufacturer. Among the negative control set, there were no results higher than a log score of 1.300, indicating no false positives are to be expected under routine diagnostic conditions (**Figure 3C**). Inconsistent identifications were only observed for two *C. tetragattii* isolates where repetitively top matches of different spots of the same preparation were *C. tetragattii, C. gattii*, or *C. deuterogattii*, all at values above 1.999.

Because of this, and the close relations found during cluster analysis (**Figure 2**), we also inspected the log score difference from the correct to the highest scoring false match for each spot (**Figure 3D**) for those tests where a second species matched above the significance threshold. Only 3% of all tested spots (14 out of 428) matched a second MSP with a log score >1.999. As expected from the cluster analysis, these "best false" second matches were found only among species in the *C. gattii*

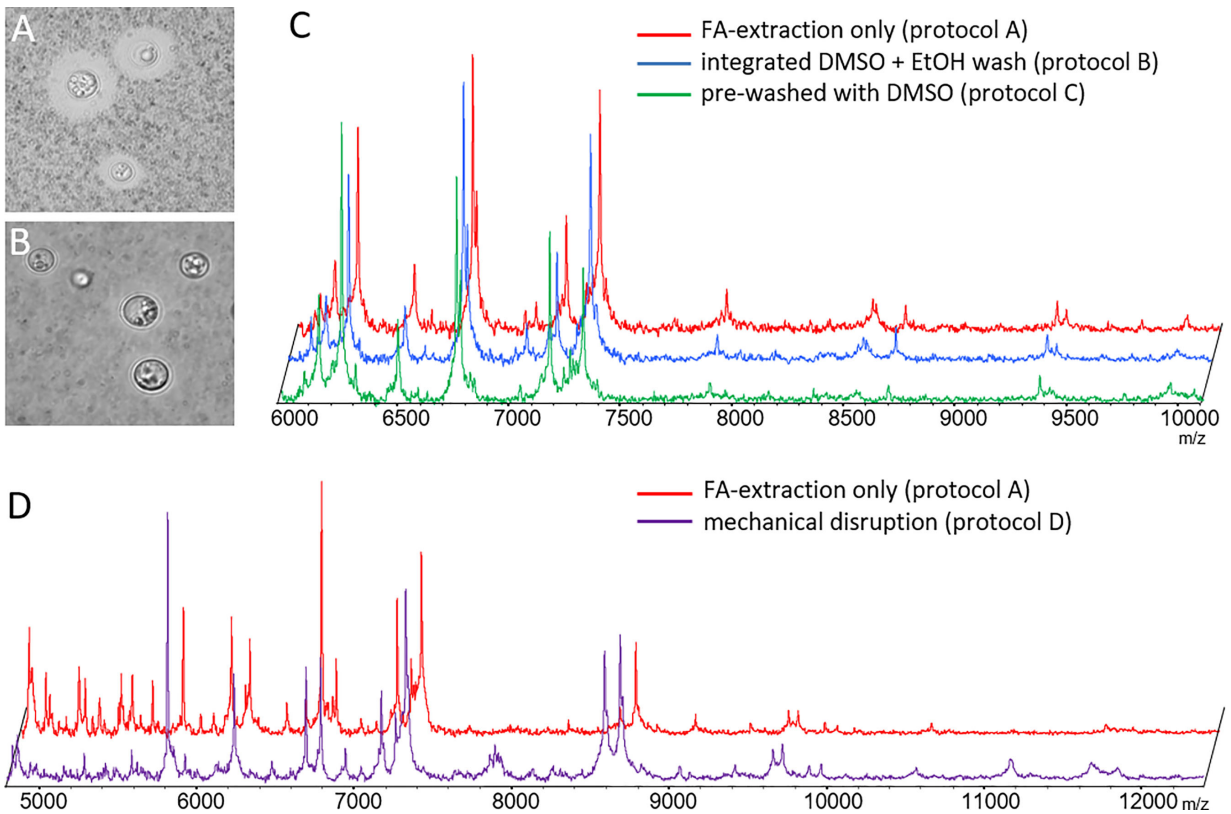

FIGURE 1 | Optimization of sample pre-processing procedures. Phase contrast microscopy of ink-stained cryptococcal cells **(A)** without and **(B)** with DMSO treatment depleting capsular material (protocol B). **(C)** Spectra obtained from de-capsulated cells by protocols B and C were not different from those generated by formic acid extraction alone. **(D)** Spectra obtained from mechanically disrupted cells (protocol D) had similar masses, but differed in relative signal intensity for some, as compared to those obtained by formic acid extraction. Example results shown here for CBS 10485 are valid for all isolates. Signal intensities on y-axes in panels **(C, D)** mainly rely on number of spectra gathered in sum buffer. Spectra have been manually re-scaled on the y-axis for better visual comparison between different experimental conditions, and scaling has been omitted to reflect this fact.

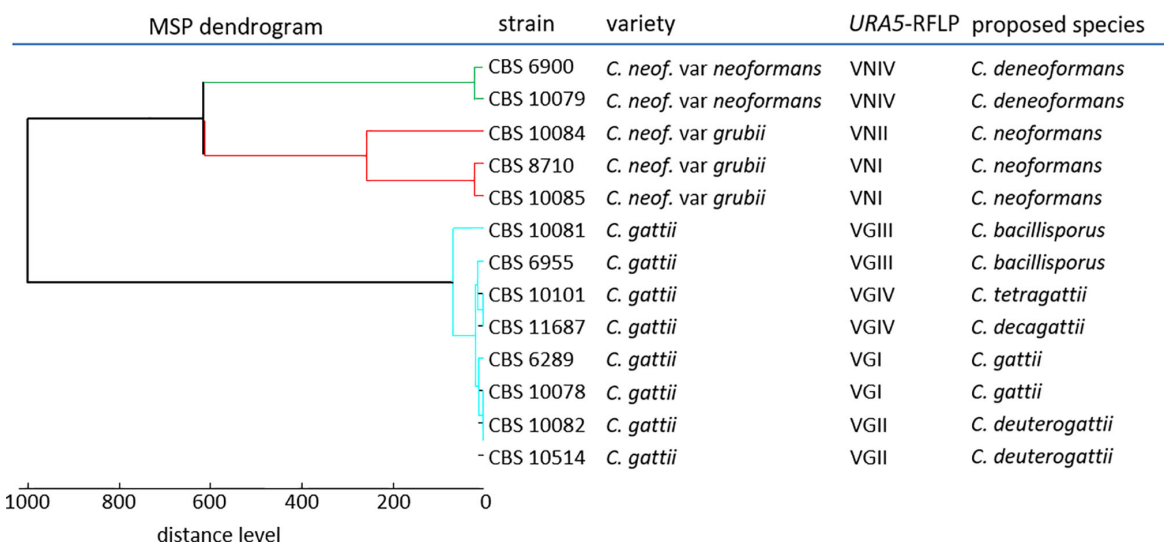

FIGURE 2 | Dendrogram reference MSPs.

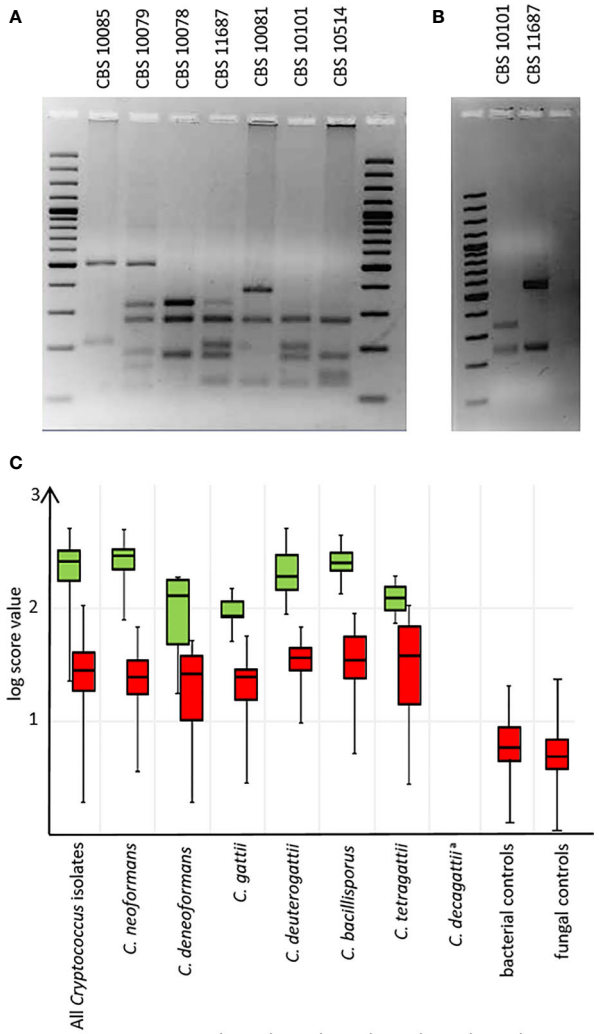

D

	N=	*C. neoformans*	*C. deneoformans*	*C. gattii*	*C. deuterogattii*	*C. bacillisporus*	*C. tetragattii*	*C. decagattii*
C. neoformans	96		1%	98%	1%	0%	0%	0%
C. deneoformans	6	0%		92%	0%	8%	0%	0%
C. gattii	5	0%	32%		24%	12%	28%	4%
C. deuterogattii	20	3%	4%	22%		20%	39%	0%
C. bacillisporus	18	2%	0%	0%	22%		41%	35%
C. tetragattii	8	0%	0%	17%	17%	44%		22%
C. decagattii	0 [a]	N/A	N/A	N/A	N/A	N/A	N/A	

[a] no isoates of *C. decagattii* available for testing

FIGURE 3 | *URA5*-RFLPs. **(A)** *URA5*-RFLP patterns of control isolates. **(B)** CBS10101 (*C. tetragattii*) and CBS 11687 (*C. decagattii*) can be differentiated by digesting the *URA5*-amplicon with StuI. **(C)** log-score values stratified by species/*URA5*-RFLP and matching type. Green: scores of correct matches, red: highest scoring incorrect matches. **(D)** Pairwise percentages of highest scoring *in*correct matches. [a] *C. decagattii* was not present among testing isolates, as the only strain available for this study was already used to create the MSP reference.

complex. This was the case for three *C. bacillisporus* isolates giving a second best match with *C. decagattii*, with a log score difference between 0.1 to 0.4. In addition to the two inconsistent *C. tetragattii* isolates discussed above, one additional *C. tetragattii* isolate also gave a second best match with *C. decagattii*. The score values for both matches were near 2.000. The close relationships of the different species will likely also have implications on properly identifying hybrid isolates.

CONCLUSION

Cryptococcal typing and species identification is complicated by the ongoing discovery of new species (Farrer et al., 2019), and the formation of inter-species hybrids (Hagen et al., 2015). Nevertheless, our data confirms that proper routine identification of clinically relevant non-hybrid *C. neoformans/gattii* complex molecular types using MALDI-TOF is possible with the current algorithms and standard workflows. In our hands, the only exception was distinguishing the rarer types *C. tetragattii* and *C. decagattii*, which was not sufficiently possible. This may be due to the fact, that only low numbers of isolates of these linages were available for testing.

The MSP sets generated in this study are freely available from https://github.com/oliverbader/BioTyper-libraries for use with the molecular type- (Meyer et al., 2003) or the species nomenclatures (Hagen et al., 2015).

DATA AVAILABILITY STATEMENT

The datasets presented in this study can be found in online repositories. The names of the repository/repositories and accession number(s) can be found in the article.

AUTHOR CONTRIBUTIONS

Performed experiments: MB, NW, MK, OB. Contributed typed strains: NW, MK, CB, WT, AC. Wrote the manuscript: MB, AC, OB. Prepared the revision: MB, OB. Supervised the study: MW, UG, AC, OB. All authors contributed to the article and approved the submitted version.

FUNDING

This study received funding from Thai-German mobility scheme "CryptoType" to AC and OB (grant number 01DP13001). Article publishing fees were covered by the Open-Access-publications funds of the Universitätsmedizin Göttingen.

ACKNOWLEDGMENTS

The authors would like to thank Agnieszka Goretzki for expert technical assistance. This study was mainly funded by the Thai-German mobility scheme "CryptoType" to AC and OB.

REFERENCES

Bader, O. (2017). Fungal Species Identification by MALDI-ToF Mass Spectrometry. *Methods Mol. Biol.* 1508, 323–337. doi: 10.1007/978-1-4939-6515-1_19

Boekhout, T., Theelen, B., Diaz, M., Fell, J. W., Hop, W. C., Abeln, E. C., et al. (2001). Hybrid genotypes in the pathogenic yeast *Cryptococcus neoformans*. *Microbiology* 147, 891–907. doi: 10.1099/00221287-147-4-891

Carriconde, F., Gilgado, F., Arthur, I., Ellis, D., Malik, R., Van De Wiele, N., et al. (2011). Clonality and alpha-a recombination in the Australian *Cryptococcus gattii* VGII population–an emerging outbreak in Australia. *PloS One* 6, e16936. doi: 10.1371/journal.pone.0016936

Cogliati, M., Prigitano, A., Esposto, M. C., Romano, L., Grancini, A., Zani, A., et al. (2018). Epidemiological trends of cryptococcosis in Italy: Molecular typing and susceptibility pattern of *Cryptococcus neoformans* isolates collected during a 20-year period. *Med. Mycol.* 56, 963–971. doi: 10.1093/mmy/myx152

Fang, L. F., Zhang, P. P., Wang, J., Yang, Q., and Qu, T. T. (2020). Clinical and microbiological characteristics of cryptococcosis at an university hospital in China from 2013 to 2017. *Braz. J. Infect. Dis.* 24, 7–12. doi: 10.1016/j.bjid.2019.11.004

Farrer, R. A., Chang, M., Davis, M. J., Van Dorp, L., Yang, D. H., Shea, T., et al. (2019). A New Lineage of Cryptococcus gattii (VGV) Discovered in the Central Zambezian Miombo Woodlands. *mBio* 10 (6), e02306-19. doi: 10.1128/mBio.02306-19

Firacative, C., Trilles, L., and Meyer, W. (2012). MALDI-TOF MS enables the rapid identification of the major molecular types within the *Cryptococcus neoformans*/*C. gattii* species complex. *PloS One* 7, e37566. doi: 10.1371/journal.pone.0037566

Hagen, F., Khayhan, K., Theelen, B., Kolecka, A., Polacheck, I., Sionov, E., et al. (2015). Recognition of seven species in the *Cryptococcus gattii*/*Cryptococcus neoformans* species complex. *Fungal Genet. Biol.* 78, 16–48. doi: 10.1016/j.fgb.2015.02.009

Herkert, P. F., Dos Santos, J. C., Hagen, F., Ribeiro-Dias, F., Queiroz-Telles, F., Netea, M. G., et al. (2018). Differential In Vitro Cytokine Induction by the Species of *Cryptococcus gattii* Complex. *Infect. Immun.* 86 (4), e00958-17. doi: 10.1128/IAI.00958-17

Jin, L., Cao, J. R., Xue, X. Y., Wu, H., Wang, L. F., Guo, L., et al. (2020). Clinical and microbiological characteristics of Cryptococcus gattii isolated from 7 hospitals in China. *BMC Microbiol.* 20, 73. doi: 10.1186/s12866-020-01752-4

Kangogo, M., Bader, O., Boga, H., Wanyoike, W., Folba, C., Worasilchai, N., et al. (2015). Molecular types of *Cryptococcus gattii*/*Cryptococcus neoformans* species complex from clinical and environmental sources in Nairobi, Kenya. *Mycoses* 58, 665–670. doi: 10.1111/myc.12411

Kidd, S. E., Hagen, F., Tscharke, R. L., Huynh, M., Bartlett, K. H., Fyfe, M., et al. (2004). A rare genotype of *Cryptococcus gattii* caused the cryptococcosis outbreak on Vancouver Island (British Columbia, Canada). *Proc. Natl. Acad. Sci. U.S.A.* 101, 17258–17263. doi: 10.1073/pnas.0402981101

Kostrzewa, M., and Maier, T. (2017). "Criteria for Development of MALDI-TOF Mass Spectral Database," in *MALDI-TOF and Tandem MS for Clinical Microbiology*, *one ed.* Eds. H. N. Shah and S. E. Garbia (Hoboken, New Jersey: John Wiley & Sons Ltd), 39–54.

Kronstad, J. W., Attarian, R., Cadieux, B., Choi, J., D'souza, C. A., Griffiths, E. J., et al. (2011). Expanding fungal pathogenesis: *Cryptococcus* breaks out of the opportunistic box. *Nat. Rev. Microbiol.* 9, 193–203. doi: 10.1038/nrmicro2522

Kwon-Chung, K. L., Boekhout, T., Fell, J. W., and Diaz, M. (2002). Proposal to conserve the name *Cryptococcus gattii* against *C. hondurianus* and *C. bacillisporus* (Basidiomycota, Hymenomycetes, Tremenomycetidae). *Taxon* 51, 804–806. doi: 10.2307/1555045

Lee, G. A., Arthur, I., Merritt, A., and Leung, M. (2019). Molecular types of *Cryptococcus neoformans* and *Cryptococcus gattii in* Western Australia and correlation with antifungal susceptibility. *Med. Mycol.* 57 (8), 1004–1010. doi: 10.1093/mmy/myy161

McTaggart, L. R., Lei, E., Richardson, S. E., Hoang, L., Fothergill, A., and Zhang, S. X. (2011). Rapid identification of *Cryptococcus neoformans* and *Cryptococcus gattii* by matrix-assisted laser desorption ionization-time of flight mass spectrometry. *J. Clin. Microbiol.* 49, 3050–3053. doi: 10.1128/JCM.00651-11

Meyer, W., Castaneda, A., Jackson, S., Huynh, M., Castaneda, E.Iberoamerican Cryptococcal Study Group (2003). Molecular typing of IberoAmerican *Cryptococcus neoformans* isolates. *Emerg. Infect. Dis.* 9, 189–195. doi: 10.3201/eid0902.020246

O'Meara, T. R., and Alspaugh, J. A. (2012). The *Cryptococcus neoformans* capsule: a sword and a shield. *Clin. Microbiol. Rev.* 25, 387–408. doi: 10.1128/CMR.00001-12

Posteraro, B., Vella, A., Cogliati, M., De Carolis, E., Florio, A. R., Posteraro, P., et al. (2012). Matrix-Assisted Laser Desorption Ionization-Time of Flight Mass Spectrometry-Based Method for Discrimination between Molecular Types of *Cryptococcus neoformans* and *Cryptococcus gattii*. *J. Clin. Microbiol.* 50, 2472–2476. doi: 10.1128/JCM.00737-12

Springer, D. J., Billmyre, R. B., Filler, E. E., Voelz, K., Pursall, R., Mieczkowski, P. A., et al. (2014). *Cryptococcus gattii* VGIII isolates causing infections in HIV/AIDS patients in Southern California: identification of the local environmental source as arboreal. *PloS Pathog.* 10, e1004285. doi: 10.1371/journal.ppat.1004285

Tangwattanachuleeporn, M., Somparn, P., Poolpol, K., Gross, U., Weig, M., and Bader, O. (2013). Prevalence and Antifungal Susceptibility of *Cryptococcus neoformans* Isolated from Pigeon Excreta in Chon Buri Province, Eastern Thailand. *Med. Mycol. J.* 54, 303–307. doi: 10.3314/mmj.54.303

Thomaz, D. Y., Grenfell, R. C., Vidal, M. S., Giudice, M. C., Del Negro, G. M., Juliano, L., et al. (2016). Does the Capsule Interfere with Performance of Matrix-Assisted Laser Desorption Ionization-Time of Flight Mass Spectrometry for Identification of *Cryptococcus neoformans* and *Cryptococcus gattii*? *J. Clin. Microbiol.* 54, 474–477. doi: 10.1128/JCM.02635-15

Trilles, L., Meyer, W., Wanke, B., Guarro, J., and Lazera, M. (2012). Correlation of antifungal susceptibility and molecular type within the *Cryptococcus neoformans*/*C. gattii* species complex. *Med. Mycol.* 50, 328–332. doi: 10.3109/13693786.2011.602126

Voelz, K., Johnston, S. A., Smith, L. M., Hall, R. A., Idnurm, A., and May, R. C. (2014). 'Division of labour' in response to host oxidative burst drives a fatal *Cryptococcus gattii* outbreak. *Nat. Commun.* 5, 5194. doi: 10.1038/ncomms6194

Worasilchai, N., Tangwattanachuleeporn, M., Meesilpavikkai, K., Folba, C., Kangogo, M., Gross, U., et al. (2017). Diversity and Antifungal Drug Susceptibility of *Cryptococcus* Isolates in Thailand. *Med. Mycol.* 55, 680–685. doi: 10.1093/mmy/myw130.

Conflict of Interest: The authors declare that the research was conducted in the absence of any commercial or financial relationships that could be construed as a potential conflict of interest.

frontiers in Cellular and Infection Microbiology

ORIGINAL RESEARCH
published: 28 April 2021
doi: 10.3389/fcimb.2021.631681

Identification of Zoophilic Dermatophytes Using MALDI-TOF Mass Spectrometry

Christina-Marie Baumbach[1], Stefanie Müller[1], Maximilian Reuschel[2], Silke Uhrlaß[3], Pietro Nenoff[3], Christoph Georg Baums[1] and Wieland Schrödl[1]*

[1] Institute of Bacteriology and Mycology, Centre of Infectious Diseases, Faculty of Veterinary Medicine, Leipzig University, Leipzig, Germany, [2] Clinic for Small Mammals, Reptiles and Birds, University of Veterinary Medicine Hannover, Foundation, Hannover, Germany, [3] Laboratory for Medical Microbiology, Mölbis, Germany

OPEN ACCESS

Edited by:
Yi-Wei Tang, Cepheid, United States

Reviewed by:
Dhiraj Kumar Singh, Southwest National Primate Research Center (SNPRC), United States
Yinggai Song, Peking University First Hospital, China

***Correspondence:**
Christoph Georg Baums christoph.baums@vetmed.uni-leipzig.de

Specialty section:
This article was submitted to Clinical Microbiology, a section of the journal Frontiers in Cellular and Infection Microbiology

Received: *20 November 2020*
Accepted: *14 April 2021*
Published: *28 April 2021*

Citation:
Baumbach C-M, Müller S, Reuschel M, Uhrlaß S, Nenoff P, Baums CG and Schrödl W (2021) Identification of Zoophilic Dermatophytes Using MALDI-TOF Mass Spectrometry. Front. Cell. Infect. Microbiol. 11:631681. doi: 10.3389/fcimb.2021.631681

Dermatophytoses represent a major health burden in animals and man. Zoophilic dermatophytes usually show a high specificity to their original animal host but a zoonotic transmission is increasingly recorded. In humans, these infections elicit highly inflammatory skin lesions requiring prolonged therapy even in the immunocompetent patient. The correct identification of the causative agent is often crucial to initiate a targeted and effective therapy. To that end, matrix assisted laser desorption ionization time-of-flight mass spectrometry (MALDI-TOF MS) represents a promising tool. The objective of this study was to evaluate the reliability of species identification of zoophilic dermatophytes using MALDI-TOF MS. The investigation of isolates from veterinary clinical samples suspicious of dermatophytoses suggests a good MALDI-TOF MS based identification of the most common zoophilic dermatophyte *Microsporum canis*. *Trichophyton (T.)* spp. usually achieved scores only around the cutoff value for secure species identification because of a small number of reference spectra. Moreover, these results need to be interpreted with caution due to the close taxonomic relationship of dermatophytes being reflected in very similar spectra. In our study, the analysis of 50 clinical samples of hedgehogs revealed no correct identification using the provided databases, nor for zoophilic neither for geophilic causative agents. After DNA sequencing, adaptation of sample processing and an individual extension of the in-house database, acceptable identification scores were achieved (*T. erinacei* and *Arthroderma* spp., respectively). A score-oriented distance dendrogram revealed clustering of geophilic isolates of four different species of the genus *Arthroderma* and underlined the close relationship of the important zoophilic agents *T. erinacei, T. verrucosum* and *T. benhamiae* by forming a subclade within a larger cluster including different dermatophytes. Taken together, MALDI-TOF MS proofed suitable for the identification of zoophilic dermatophytes provided fresh cultures are used and the reference library was previously extended with spectra of laboratory-relevant species.

Performing independent molecular methods, such as sequencing, is strongly recommended to substantiate the findings from morphologic and MALDI-TOF MS analyses, especially for uncommon causative agents.

Keywords: dermatophytoses, zoonoses, hedgehog, zoophilic, geophilic, *Trichophyton*, *Microsporum*, *Trichophyton erinacei*

INTRODUCTION

Dermatophytoses are common worldwide and represent a growing health concern for human patients, companion animals and livestock alike (Chermette et al., 2008; Havlickova et al., 2008). These superficial infections of skin and its appendages (hair, nail, fur, spines, hoofs, claws etc.) are often caused by dermatophytes, which are able to invade the aforementioned host structures and digest the tough, fibrous proteins forming their structural framework. They belong to three main genera, i.e. *Epidermophyton (E.)*, *Microsporum (M.)* and *Trichophyton (T.)*, and are categorized as anthropophilic, zoophilic and geophilic according to their preferential habitat and evolutionary adaptation to humans, animals and soil, respectively (Weitzman and Summerbell, 1995). About 40 species are of clinical relevance in human and veterinary medicine nowadays (Ferguson and Fuller, 2017).

Zoophilic dermatophytes are animal pathogens that often exhibit a strong host specificity but also a notable zoonotic potential. Human infections with zoophiles (and also geophiles) are highly inflammatory, contagious and the patients frequently need systemic and long-lasting treatments (Weitzman and Summerbell, 1995; Havlickova et al., 2008). Especially children and adolescents are affected due to close contact to household pets, e.g. cats and guinea pigs, that are often asymptomatic carriers (Chermette et al., 2008; Nenoff et al., 2014a).

Routine diagnostic identification of dermatophytosis-causing agents continues to be mostly accomplished by macroscopic and microscopic examination of mycological cultures, i.e. mycelia, fruiting bodies and characteristic conidia. This approach is time-consuming and requires expert knowledge due to remarkable morphological similarities between the different species (Nenoff et al., 2013). On the other hand, DNA sequencing, which is considered the "gold standard" for species identification, is laborious and resource-expensive (Nenoff et al., 2013; Heireman et al., 2020). Moreover, nucleic acid sequence comparison relies on public, not necessarily validated databases that also need to be interpreted cautiously because of non-standardized preparation methods and the ongoing renaming and reclassification of dermatophytes (Abarca et al., 2017).

On the contrary, the identification of microorganisms based on matrix assisted laser desorption ionization time-of-flight mass spectrometry (MALDI-TOF MS), particularly of bacteria and yeasts, is considered simple, fast and reliable. However, for clinically relevant filamentous fungi, and especially dermatophytes, the thus-far established sample preparation methods need extensive adaptations since growth requirements and sample processing are more elaborate in these species (van Veen et al., 2010; Carbonnelle et al., 2011; Juiz et al., 2012; Biswas and Rolain, 2013; L'Ollivier and Ranque, 2017).

Here, we examined the reliability of MALDI-TOF MS for the identification of closely related zoophilic dermatophytes. Furthermore, we compared the spectra obtained from growth in two different conditions, i.e. liquid broth vs. solid agar media. Finally, we describe a cohort of samples from our veterinary clinical practice where the extension of the reference database was crucial to identify the uncommon causative agents involved.

MATERIAL AND METHODS

Sampling and Fungal Culture

Clinical specimens of suspected dermatophytoses were routinely sampled according to a modified McKenzie Brush technique (Mackenzie, 1963). After a rough disinfection, the margins of lesions were brushed with sterile tooth brushes and hair/spines and skin scales were transferred to Sabouraud-Dextrose (2%; SDA; Sifin Diagnostics GmbH, Berlin, Germany) or modified dermatophyte agar plates (MDA; Sifin; containing 0.4 mg/ml cycloheximide). SDA and MDA were supplemented with 0.05 mg/ml gentamicin-sulfate, 0.05 mg/ml chlortetracycline and 0.1 mg/ml chloramphenicol). The plates were incubated for one to two weeks at 28°C (in suspicion of *T. verrucosum*: 37°C); selected isolates are shown in **Figure 1**. Species identity of pure subcultures was assessed by macroscopic and microscopic examination, sequencing and/or MALDI-TOF MS measurements (see below).

The herein described dermatophyte isolates of wild hedgehogs (*Erinaceus europaeus)* were obtained after submission of the animals to the clinic showing a poor general health condition or injuries from accidents (asymptomatic and symptomatic for dermatophytoses; sampled in 2018 by the Clinic for Small Mammals, Reptiles and Birds, University of Veterinary Medicine Hannover, Hannover, Germany). Sampling ensued from recently deceased or –if medically indicated- euthanized animals as described above (approval by an animal ethics committee not needed).

Species Identification by DNA Sequencing and Creation of an ITS-Based Dendrogram

Sequencing of the *internal transcribed spacer* region (ITS) of the rDNA with a subsequent similarity search using the Basic Local Alignment Search Tool (BLASTn; https://blast.ncbi.nlm.nih.gov/Blast) was conducted to confirm species identity.

Therefore, total DNA from pure fungal cultures was extracted using the QIAmp® DNA Mini Kit (Qiagen, Hilden, Germany) according to the manufacturer's instructions with an additional

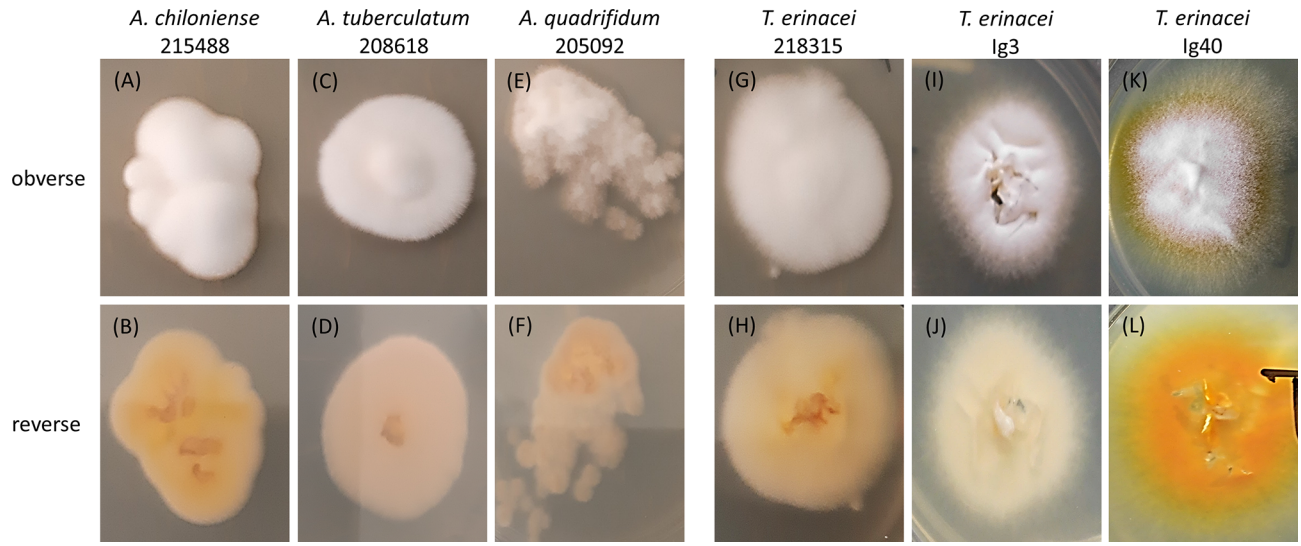

FIGURE 1 | Photographs of the colony morphology of selected *Arthroderma (A.)* spp. **(A–F)** and *Trichophyton (T.) erinacei* cultures **(G–L)** isolated from symptomatic and asymptomatic hedgehogs. Cultures were grown on Sabouraud-Dextrose agar (2%) at 28°C for 3d, species identity was confirmed by sequencing of the ITS region of fungal rDNA. The first column shows the typical morphology of *A. chiloniense* with a white, fluffy obverse **(A)** and a beige to yellow reverse **(B)**. *T. erinacei* 218315 **(G, H)** showed a very similar appearance rendering those two isolates hardly distinguishable solely by the assessment of phenotypic traits. The typical colony morphology of *T. erinacei* is depicted in **(K)** (obverse: white to yellow, granular) and **(L)** (reverse: yellow to bright orange). Intermediate, rather untypical morphologies (fluffy, folded, elevated in the center) with varying color shades from white to cream to beige are seen with other *Arthroderma* spp. and *T. erinacei* isolates.

overnight Proteinase K digestion at 56°C. Amplification of the ITS region by PCR was carried out essentially as described in Sharma et al. (2006) using the universal primers V9G (5′ TTACGTCCCTGCCCTTTGTA3′) and LSU266 (5′ GCATTCCCAAACAACTCGACTC3′) (Sharma et al., 2006). Sanger sequencing was performed by Microsynth Seqlab GmbH (Goettingen, Germany).

The obtained sequences were edited using the Chromas 2.6.6 software (Technelysium, South Brisbane, Australia); alignment and phylogenetic analyses were conducted in MEGA X (Kumar et al., 2018) using the Maximum Likelihood method and the Tamura-Nei model (Tamura and Nei, 1993). The percentage of trees in which the associated taxa clustered together is indicated next to the branches (1000 replicates). Values of ≥ 70% represent a robust clade support, values between 70% and 50% are considered moderate and ≤ 50% poor. Initial trees for the heuristic search were obtained automatically by applying Neighbor-Join and BioNJ algorithms to a matrix of pairwise distances estimated using the Maximum Composite Likelihood (MCL) approach, and then selecting the topology with the superior log likelihood value. The tree is drawn to scale with branch lengths measured in the number of substitutions per site and shown in **Figure 2**. The analysis involved 37 nucleotide sequences with a total of 1208 positions in the final dataset including the dermatophytes isolated during this study and during veterinary diagnostics, human-derived isolates from the clinical routine of the Laboratory of Medical Microbiology (with informed patient consent) and sequences derived from the NCBI database.

All fungal isolates obtained during this study are available at the German Collection of Microorganisms and Cell Cultures GmbH (DSMZ, Braunschweig, Germany; see **Table 1** for the detailed assignment of isolates to culture collection identifiers). The corresponding ITS sequences of the *T. erinacei*-isolates were deposited in the NCBI BLASTn database (see **Table 1** for acc. no.), for *Arthroderma* spp., these are in preparation.

MALDI-TOF MS Measurements

MALDI-TOF MS analyses were carried out using a MALDI Biotyper™ MBT™ smart instrument (Bruker Daltonik GmbH, Bremen, Germany) and the internal libraries "BDAL" (8468 MSPs, 2969 species; 12/09/2019) and "Filamentous Fungi" (577 MSPs, 180 species; 12/09/2019). Samples for MS measurements were prepared according to the standard operating procedure (SOP) of the manufacturer following a modified extended direct transfer or the extraction sample preparation method (SOP 1867813 "Cultivation and Sample Preparation for Filamentous Fungi"; Bruker Daltonik GmbH) and deposited on a polished steel target (MSP 96, cat. no. 8280800, Bruker Daltonik GmbH). The minor modification consisted of a 2min incubation of fungal material in 70% formic acid in a 1.5ml reaction tube and vigorous pipetting before transferring 1µl of the supernatant to the target (rather than the successive application of "front mycelium" and formic acid to the same target spot). The target was subsequently loaded into the MS instrument and measurements were carried out in linear positive-ion mode within a mass range of 2-20kDa using the MBT_AutoX_FilFungi settings in the FlexControl software (version 3.4.204.10, Bruker Daltonik GmbH).

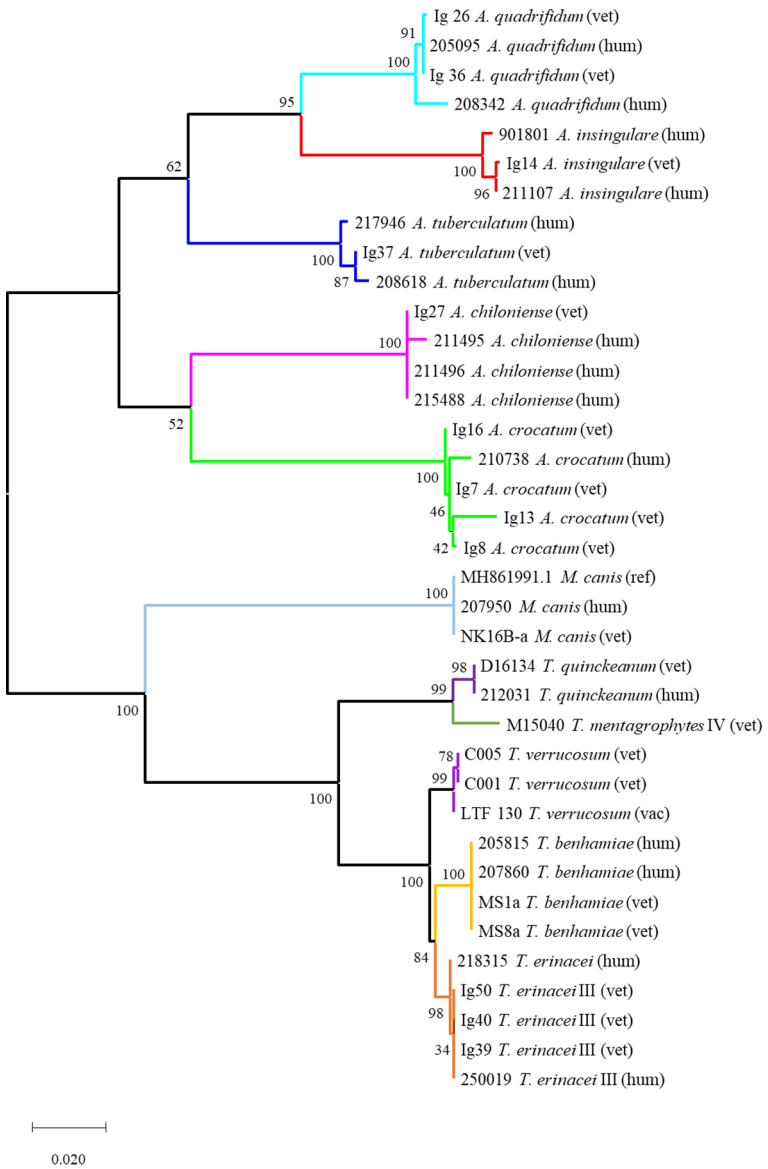

FIGURE 2 | Phylogenetic tree based on fungal rDNA ITS sequences for the investigated dermatophyte isolates (Tamura-Nei-model, Neighbor-Join and BioNJ algorithms, MCL approach, 1000 replicates). The tree is drawn to scale with branch lengths measured in the number of substitutions per site and indicated support values; the analysis involved 37 nucleotide sequences including the dermatophytes isolated during this study and from veterinary routine diagnostics (vet; vac refers to a vaccine strain used in bovine practice), human-derived isolates from the Laboratory of Medical Microbiology (hum) and sequences derived from the NCBI database. Generally, each dermatophyte species forms an own subclade with mostly very robust support; the different origins of isolation (vet vs. hum) are not reflected. The tree comprises two main clades: the upper one contains all geophiles, i.e. all *Arthroderma* spp.; the lower one all isolates of the genera *Trichophyton* and *Microsporum*. The latter form individual subclades in this lower clade; the very closely related species *T. benhamiae* and *T. erinacei* as well as *T. mentagrophytes* and *T. quinckeanum* are separated in distinct subclades.

Additional settings included: ion source 1 voltage: 20kV, ion source 2 voltage: 18.3kV, lens: 6kV, linear detector: 2694V. LogScore values (scores) from 0 (no similarity) to 3 (perfect match) were automatically calculated against the entries of the above-mentioned internal libraries. The manufacturer recommends cutoff values of ≥ 1.7 and ≥ 2.0 for a probable/secure identification at genus- and species-level, respectively. Additionally, we considered 5 to 10 of the next best hits in the identification score matching chart given by the software and their corresponding scores for final species determination.

Creation of Master Spectra (MSP) and a Score-Oriented Distance Dendrogram

For the creation of own MSPs, fungi were grown on one of the above-mentioned solid agar media covered with a sterilized filter paper (filter circle, Ø 70 mm, type 1573, Schleicher & Schuell,

now Whatman; **Figure 3**) or in liquid Sabouraud-2% Dextrose-broth according to SOP 1867813 (section 5.3 "Liquid Cultivation Sample Preparation Procedure"; Bruker Daltonik GmbH). Note that for "Liquid Cultivation", an incubation no longer than 1-2d in the respective culture broth is strongly recommended by the manufacturer; however, on solid media, dermatophyte growth is considerably slower and more time is usually needed to obtain sufficient fungal material from direct specimens for species identification.

Samples from both growth conditions (solid vs. liquid) were prepared for MS measurements following the extraction sample preparation procedure described in the above-mentioned SOP, i.e. washing fungal material in HPLC-grade water and ethanol and a subsequent formic acid/acetonitrile treatment. After the last centrifugation step, each of at least 12 spots of an MBT Biotarget 96 (cat. no. 1840375; Bruker Daltonik GmbH) was covered with 1µl of this solution. The spots were air dried and finally overlaid with 1µl of saturated α-cyano-4-hydroxy cinnamic acid solution (HCCA matrix; Bruker Daltonik GmbH) for co-crystallization. The bacterial test standard (BTS, cat. no. 8255343; Bruker Daltonik GmbH) provided by the manufacturer was added to the Biotarget 96 as the calibration standard and positive control.

MS measurements were carried out using the MBT_AutoX_FilFungi settings in the FlexControl software (see above). Each spot was measured twice to obtain at least 24 raw spectra of each sample; selected raw spectra from different isolates and growth conditions are shown in **Figure 4**.

The subsequent quality control of these raw spectra for MSP creation was performed using the FlexAnalysis software (version 3.4.79.0; Bruker Daltonik GmbH) and included baseline correction, smoothing and peak filtering. MSPs were created by combining the remaining raw spectra that fulfilled the quality requirements using the "MSP creation" function of the MBT Compass Explorer software (Bruker Daltonik GmbH). Afterwards, they were scored by the "Start Identification" function (MBT Compass Explorer; Bruker Daltonik GmbH) through comparison to the above-mentioned libraries and own library-entries after MSP creation.

A score-oriented distance dendrogram based on the mass spectrometric data of MSPs (intensity [arbitrary units]/mass-to-charge-ratio) was generated to identify similarities and clusters of the fungi isolated during this study and during routine human and veterinary diagnostics (Distance Measure Correlation mode, MBT Compass Explorer, Bruker Daltonik GmbH; **Figure 5**).

RESULTS

ITS-Based Identification and Phylogenetic Analysis of Dermatophytes

From the cohort of 50 hedgehog-samples of suspected dermatophytoses, 17 samples (34%) gave rise to fungal colonies on SDA or MDA and were subjected to species identification by MALDI-TOF MS and ITS sequencing. None of these cultures were identified using MALDI-TOF MS in the first place (samples were read but not identified; note: in 2018/2019, the above-mentioned internal libraries "BDAL" and "Filamentous Fungi" did not contain MSP of the later identified species). Due to uncharacteristic macro- and micromorphologies as exemplified in **Figure 1**, an unambiguous identification by phenotypic traits was also not possible. Therefore, species identity was analyzed by PCR, ITS sequencing and similarity searches revealing the most common causative agent of hedgehog-dermatophytosis, namely *T. erinacei* (n = 8; 16% of the total sample size), and five different *Arthroderma* spp. (n = 9; 18%) being rare geophiles (*Arthroderma (A.) crocatum*, *A. quadrifidum*, *A. insingulare*, *A. tuberculatum*, *A. chiloniense*; **Table 1**).

A dendrogram based on these ITS sequences was compiled to show similarities between the analyzed dermatophytes (**Figure 2**). Generally, each species formed an own subclade. Different origins of isolation, i.e. human-derived (hum) or from veterinary practice (vet – veterinary; vac - vaccine strain) were not reflected. The tree comprised two main clades: the upper one contained all *Arthroderma* spp., the lower one all isolates of the genera *Trichophyton* and *Microsporum*. The latter formed individual subclades in the lower main clade. *T. benhamiae* and *T. erinacei* as well as *T. mentagrophytes* and *T. quinckeanum* were separated in distinct subclades. Overall, the ITS-based dendrogram is in agreement with reliable identification. However, in the case of species identification with the genus *Arthroderma* this

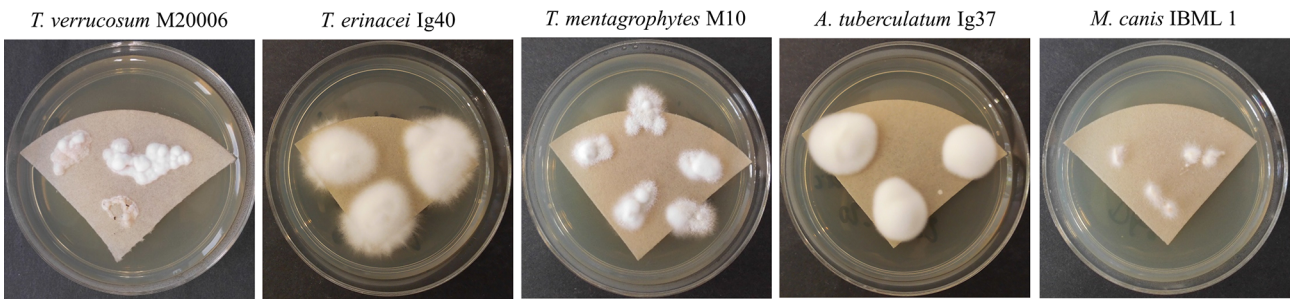

FIGURE 3 | Sabouraud-Dextrose agar (2%) covered with a sterilized filter paper promoted fungal growth successfully and facilitated sampling of merely fungal material for MALDI-TOF MS analysis. Different *Trichophyton (T.), Arthroderma (A.) and Microsporum (M.)* isolates are exemplarily shown after an incubation time of 5d at 28°C (*T. verrucosum:* 37°C). Species identity was confirmed by sequencing of the ITS region of fungal rDNA.

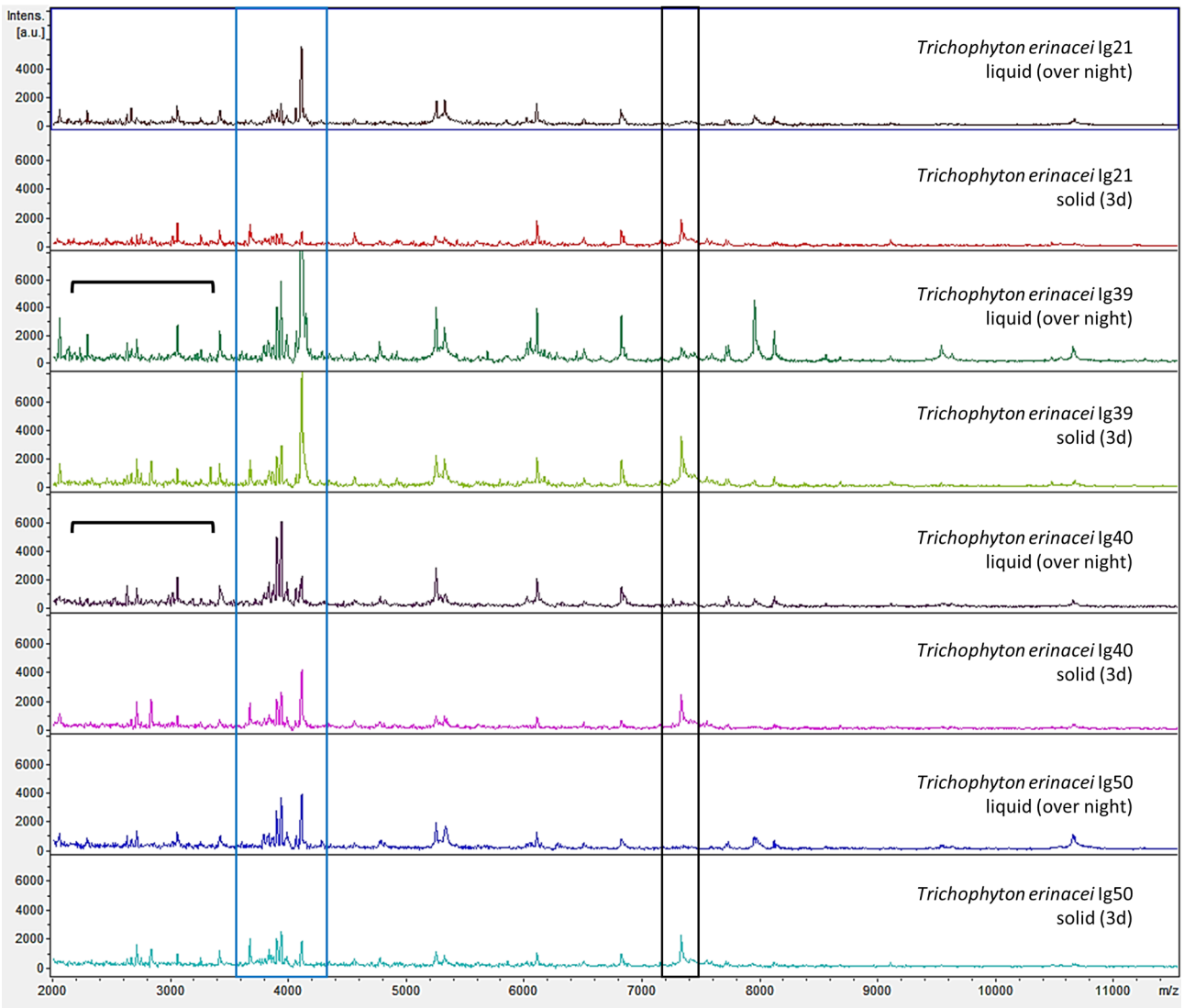

FIGURE 4 | Examples of mass spectrometric profiles (raw spectra) of different *Trichophyton (T.) erinacei*-isolates cultured in liquid Sabouraud-2% Dextrose-broth over-night with gentle rotation at room temperature (liquid, over-night) and on solid agar plates for 3d at 28°C (solid, 3d) are shown. Species identity was confirmed by sequencing of the ITS region of fungal rDNA. Overall, the mass spectrometric profiles were very similar for both cultivation methods. For some isolates grown in liquid media, more and/or more intense peaks were observed in the lower mass range (indicated by the black parenthesis). On the other hand, a peak at around 7300 m/z (black box) was predominantly found in solid cultures. However, a cluster of peaks around 4000 m/z (blue box) seems somewhat species specific for *T. erinacei* since it was found in most examined isolates regardless of the cultivation method.

identification relies only on ITS sequences deposited in the NCBI database.

MALDI-TOF MS Identification of Dermatophytes

Based on the sequencing results, MSPs of all of the above-mentioned 17 cultures were created and deposited in the in-house library to facilitate future identification. We obtained best quality raw spectra from the double-measurement of at least 12 replicates of the same protein extraction (at least 24 raw spectra) rather than triplicate measurements of 8 replicates (as recommended by the manufacturer). More measurements per spot lead to less identical raw spectra that would less likely pass quality control. Moreover, with our method using less measurements per spot, the manufacturer-recommended minimal number of raw spectra for the creation of reliable MSPs (n = 20) was usually obtained.

During further analyses, multiple measurements of cultures gave rise to spectra of varying quality and to variable scores. To find out whether the poorer scores resulted from different culture conditions (solid vs. liquid) or incubation periods (over-night vs. several days), selected dermatophyte isolates were cultured with both methods and measured after different incubation times (**Supplementary Table 1**). The cultivation on solid media was conducted using the above-mentioned filter papers to reduce

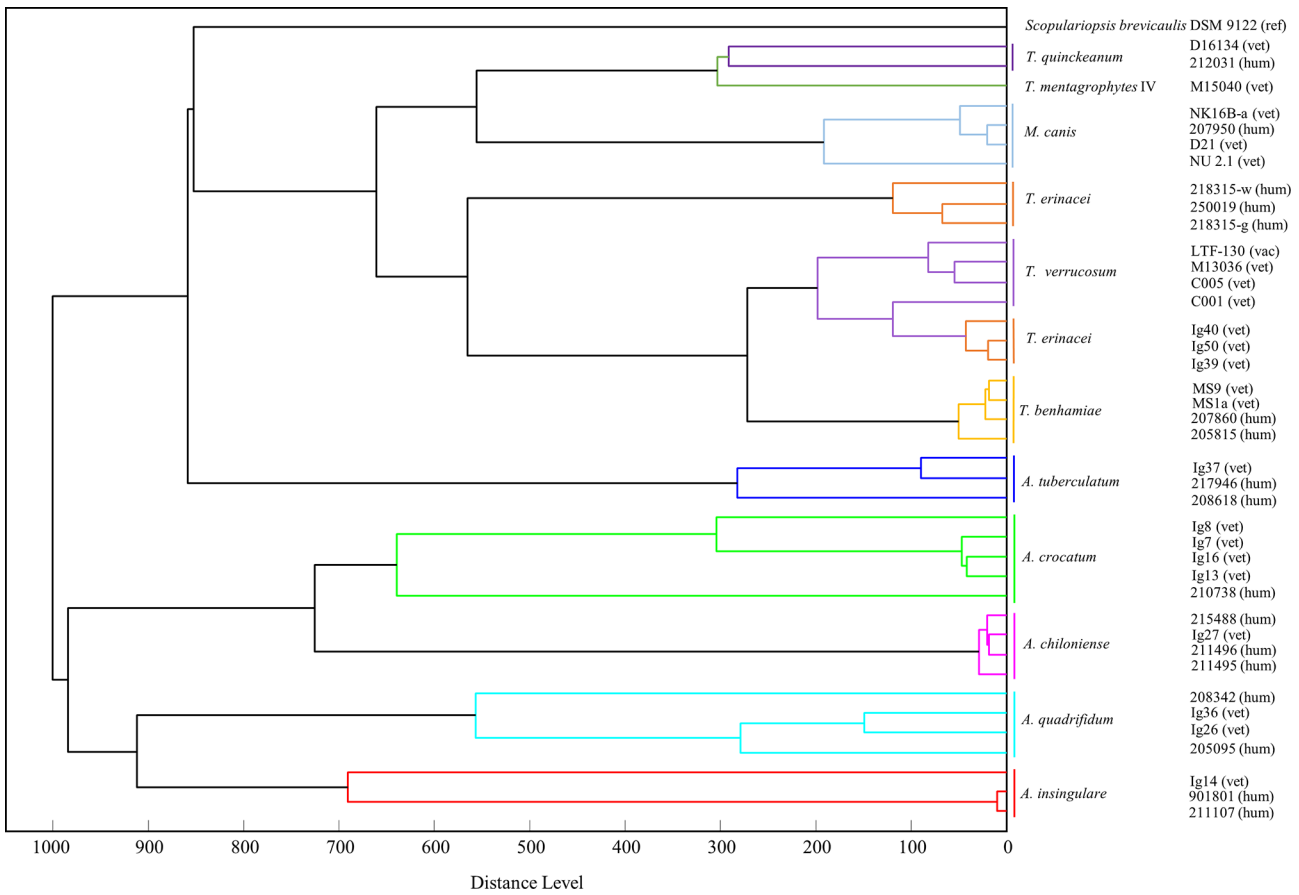

FIGURE 5 | A score-oriented distance dendrogram based on the mass spectrometric data (MSP) was generated to identify similarities and clusters of closely related zoophilic and geophilic dermatophytes (Distance Measure Correlation mode, MBT Compass Explorer, Bruker Daltonik GmbH). Isolates of *Trichophyton (T.) erinacei, Arthroderma (A.)* spp. as well as others from the genera *Trichophyton* and *Microsporum*, respectively, from animal (vet, vac) and human patients (hum) were included (ref - reference, derived from NCBI database). The different species cluster in two main clades: the lower one comprises geophilic isolates only, i.e. *A. insingulare, A. quadrifidum, A. chiloniense* and *A. crocatum*. The isolates of *A. tuberculatum* group into the upper clade but therein in the lowest position, i.e. closest to the other *Arthroderma* spp. The upper clade further comprises the *Trichophyton* spp. and the *M. canis*-isolates (and *S. brevicaulis*). All *T. erinacei, T. verrucosum* and *T. benhamiae*-isolates form one subclade indicating their close relation. Species identity was previously confirmed by sequencing of the ITS region of fungal rDNA.

contamination of the spectra by agar traces. Noteworthy, fresh subcultures were investigated which generally show faster initial growth in comparison to primary cultures of clinical samples. Using the afore-mentioned Bruker libraries only, some of the tested dermatophyte species were not identified correctly, e.g. *T. verrucosum* or *T. benhamiae*, and often with scores at or below the cutoff value for "probable genus identification" recommended by the manufacturer (≤ 1.7). Liquid cultures mostly obtained higher scores compared to time-matched solid cultures (**Supplementary Table 1**). On the other hand, *M. canis* was identified correctly with the internal Bruker libraries after growth of subcultures up to 5d using solid and liquid media (**Supplementary Table 1**). However, *T. verrucosum* IBML C005 was misidentified as *T. erinacei* with scores above 2 using the Bruker database after cultivation on solid medium (not recommended by Bruker; **Supplementary Table 1**).

Applying the in-house library, a "secure genus identification, probable species identification" with scores ≥ 2.0 was usually computed for all cultures of *T. verrucosum*, *T. benhamiae*, *T. erinacei* and *M. canis* grown in liquid and on solid media likewise, provided relatively fresh cultures (up to 5d of growth) were used and time- and cultivation-matched MSPs were included prior (**Supplementary Table 1**). Older cultures were more often attributed with poorer scores or not identified at all although the most elaborate procedure of sample preparation for MALDI-TOF MS measurements (i.e. extraction) was performed (data not shown).

Comparing the three different procedures for sample preparation recommended by the manufacturer (direct transfer vs. extended direct transfer vs. extraction), generally, we found the extraction method for dermatophytes most successful and hence implemented it for all MALDI-TOF MS measurements for daily diagnostics. Direct and extended direct transfer with the addition of formic acid to the sample on the target plate mostly lead to "no peaks" and repeated measurements; the modified extended direct transfer method as described above often yielded

TABLE 1 | Identification of dermatophytes isolated from skin and spine samples of hedgehogs *(Erinaceus europaeus)* by PCR and sequencing of the *internal transcribed spacer* (ITS) region of fungal rDNA.

Date of Report	Lab-No.	Species[a]	Highest Similarity to NCBI entry (acc. no., culture collection identifier)[b]	Percent identity	Culture Collection Identifier (NCBI acc. no. of ITS sequence)[c]
07/08/2018	250030 (lg1)	*T. erinacei*	MH860764 CBS 511.73	99.83%	DSM 109030 MN961146
07/08/2018	250031 (lg3)	*T. erinacei*	MH860764 CBS 511.73	99.83%	DSM 108356 MN961147
04/16/2019	600135 (lg7)	*A. crocatum*	LR746284 CCF 5207	99.41%	DSM 109743
04/16/2019	250171 (lg8)	*A. crocatum*	LR746284 CCF 5207	99.85%	DSM 109028
04/16/2019	600136 (lg13)	*A. crocatum*	LR746284 CCF 5207	98.08%	DSM 109753
01/02/2019	250170 (lg14)	*A. insingulare*	NR_144885 CBS 521.71	98.86%	DSM 109197
04/16/2019	600137 (lg16)	*A. crocatum*	LR746284 CCF 5207	99.26%	DSM 109752
01/24/2019	600006 (lg18)	*T. erinacei*	MH860764 CBS 511.73	99.83%	DSM 109203 MN974534
01/24/2019	600007 (lg20)	*T. erinacei*	MH860764 CBS 511.73	99.83%	DSM 109202 MN974535
01/24/2019	600008 (lg21)	*T. erinacei*	MH860764 CBS 511.73	99.83%	DSM 109201 MN974536
01/02/2019	250172 (lg26)	*A. quadrifidum*	LR746285 CCF 5792	99.84%	DSM 109172
01/02/2019	250173 (lg27)	*A. chiloniense*	LT992885 CBS 144073	99.89%	DSM 109029
01/02/2019	250169 (lg36)	*A. quadrifidum*	LR746285 CCF 5792	100.00%	DSM 109171
01/02/2019	250174 (lg37)	*A. tuberculatum*	NR_077140 CBS 473.77	99.06%	DSM 109027
01/24/2019	600009 (lg39)	*T. erinacei*	MH860764 CBS 511.73	99.83%	DSM 109200 MN974537
01/24/2019	600010 (lg40)	*T. erinacei*	MH860764 CBS 511.73	99.83%	DSM 109199 MN974539
01/24/2019	600011(lg50)	*T. erinacei*	MH860764 CBS 511.73	99.83%	DSM 109198 MN974538

[a]*Species identity was deduced from sequencing the ITS region of fungal rDNA and similarity searches using the Basic Local Alignment Search Tool for nucleotide sequences (BLASTn; NCBI).*

[b]*Accession numbers (acc. no.) of most similar sequences; CBS – Culture Collection of fungi and yeasts; Utrecht, The Netherlands; CCF, Culture Collection of Fungi; Prague, Czech Republic.*

[c]*All isolates of this study were subsequently deposited in the German Collection of Microorganisms and Cell Cultures GmbH (DSMZ, Braunschweig, Germany) and thoroughly sequenced for deposition in the NCBI BLASTn database.*

correct species identification but sometimes slightly poorer scores than the extraction procedure (data not shown).

Taking a closer look at the raw spectra of some *T. erinacei*-isolates of the current study, liquid cultivation resulted in more and/or more intense peaks, particularly in the lower mass range up to 4000 m/z (**Figure 4**, *T. erinacei* Ig39 (liquid, over-night) and *T. erinacei* Ig40 (liquid, over-night), black parentheses). However, that was not seen uniformly for all tested isolates of this particular species. On the other hand, a cluster of peaks around 4000 m/z seems somewhat species specific since this arrangement was seen in most examined isolates (**Figure 4**, blue box). Interestingly, spectra resulting from cultures grown on solid media exhibited a peak at around 7300 m/z which was not seen in spectra derived from liquid cultures (**Figure 4**, black box).

In summary, growth time and culture condition have an influence on individual raw spectra but not so much on computed scores and species identification if relatively fresh cultures are analyzed.

Distance Dendrogram Based on MALDI-TOF MS

For similarity and cluster analyses, MSPs were used to generate a score-oriented distance dendrogram that is depicted in **Figure 5**. Some of the current isolates of *T. erinacei* and *Arthroderma* spp. (all marked with "Ig", **Figure 5**) as well as other closely related *Trichophyton* spp. and *M. canis*-isolates from animal and human patients were included in this analysis. *Scopulariopsis (S.) brevicaulis* was chosen as presumed outgroup. The species cluster in two main groups of which the lower one comprises geophilic isolates only, i.e. *A. insingulare, A. quadrifidum, A. chiloniense* and *A. crocatum*. The isolates of *A. tuberculatum* group into the upper clade but therein in the lowest position, i.e. closest to the other *Arthroderma* spp. Apart from that, the upper clade consists of different *Trichophyton* spp., the *M. canis*-isolates and *S. brevicaulis*. All *T. erinacei, T. verrucosum* and *T. benhamiae*-isolates form one subclade indicating their close relation.

DISCUSSION

MALDI-TOF MS previously proofed a rapid, accurate and reliable method for the identification of microorganisms in clinical settings and basic research. In the last years, the spectrum of species that are readily identifiable increased substantially due to technical refinements, methodological adaptations and constant extension of reference databases (Cassagne et al., 2016). Here, we can report of a good MALDI-TOF MS performance for the identification of the most common zoophilic dermatophyte *M. canis* (Nenoff et al., 2014b). However, when it comes to less frequent or uncommon causative agents, MALDI-TOF MS still reaches its limits quickly due to incomplete reference data bases (Croxatto et al., 2012; Biswas and Rolain, 2013; Sacheli et al., 2020).

Recollecting from our recent routine laboratory diagnostics, of the zoophilic dermatophytes only *M. canis* was identified reliably with trustworthy scores (n = 10, score ≥ 2.0) and identical next best hits using the provided libraries (BDAL, Filamentous Fungi, Bruker Daltonik GmbH). Supposedly, the high number of deposited spectra of different *M. canis*-isolates (n = 11; 11/20/2020) enables this fast and correct identification. For *T. erinacei*, the most common causative agent of dermatophytoses in hedgehogs, the latter was difficult probably because as few as two reference spectra were only recently introduced to the Bruker libraries.

Within the Bruker MALDI-TOF MS system, the libraries are based on an isolate-specific reference approach in which spectral data are computed from replicates of the same isolate. Different references are not linked and do not influence each other as opposed to the taxonomical group-specific approach pursued by other systems, e.g. Axima@Saramis (Shimadzu/AnagnosTec, Duisburg, Germany) and Vitek MS (bioMérieux, Marcy-l′étoile, France). Although this isolate-specific approach relies on the correct species identification prior to deposition in the library, it enables the entry of new, customized references immensely, which is a huge advantage in speeding up routine workflows (Cassagne et al., 2016). After creation of MSPs of the above-mentioned *T. erinacei*-isolates and deposition in the in-house library, identification of such samples became a lot more successful. A designated, larger test cohort comprising among others different zoophilic dermatophytes not used for MSP creation will be assessed in the near future to confirm the reliability of the in-house library in a broader context.

Interestingly, although the Bruker databases comprised quite a few spectra of the genus *Arthroderma*, our samples were not identified in the first place; only DNA sequencing provided full account of the different *Arthroderma* spp. Dermatophytoses is often asymptomatic in hedgehogs (66% in our cohort) but if spines are affected and ultimately lost, it may also be lethal and demands special medical attention including the correct identification of disease-causing agents (Weishaupt et al., 2014; Abarca et al., 2017). Moreover, since pet-hedgehogs have increased in popularity, the transmission of *T. erinacei*-infections to humans is also increasingly reported (Abarca et al., 2017; Gebauer et al., 2018; Kargl et al., 2018; Wiegand et al., 2019). The genus *Arthroderma* comprises anthropophilic, zoophilic and geophilic species as well (de Hoog et al., 2017), rendering a zoonotic transmission and human infection also highly likely.

We ascribe the unexpected multitude of dermatophyte species isolated from the hedgehogs in our study to their way of life. However, the high prevalence in this cohort of animals might also be related to their poor health status.

Critical factors for MALDI-TOF MS-based dermatophyte identification include cultural features (media, incubation time) and sample preparation (method, matrix) as well as dermatophyte (species resolution, taxonomy) and mass spectrometer/system characteristics (instrument, library; L'Ollivier and Ranque, 2017).

Concerning the media used, although one might expect different protein expression profiles of dermatophytes grown on different media as a thigmotropic or nutritional response to certain environmental conditions, many studies describe no or negligible effects of different media compositions on the MALDI-TOF-MS identification performance (Theel et al., 2011; L'Ollivier et al., 2013; Bartosch et al., 2018). However, to the best of our knowledge, this is the first study describing the comparison of solid vs. liquid media formulations.

In our study, the usage of liquid media for species identification and/or MSP generation did not prove superior to solid media covered with a filter paper. Spectra obtained from both growth conditions were equally well identified using the in-house library and, hence, the more fastidious liquid culture method was not pursued further. This is mainly due to handling inquiries during sample preparation, e.g. even multiple centrifugation steps did not ensure complete removal of culture media and washing buffer. Also, for some isolates no growth was observed even after a prolonged incubation time. We agree furthermore with our colleagues that 1) contaminations are not as easily identified in liquid cultures and 2) this procedure seems inconvenient to be integrated into a routine workflow for fast diagnostics (Lau et al., 2019; Sacheli et al., 2020). Indeed, for some isolates more and/or more intense peaks/spectrum were obtained which might result in a higher specificity for MSP creation but this was not seen generally. In accordance with others, our study proves that cultures grown on solid media also produce high-quality spectra and good identification scores (Respinis et al., 2014; Sacheli et al., 2020). The filter paper ensured neat sampling of merely fungal material without protraction of agar and proved a fast and cost-effective alternative to other commercially available growth media provided with a membrane, as e.g. ID-fungi plates (IDFP; Conidia, Quincieux, France). Indeed, these plates were described to promote faster growth of filamentous fungi due to an optimized composition and pH (Heireman et al., 2020) but we did not notice any growth difficulties with the isolates tested during our study. Even *T. verrucosum*, which is especially slow growing and demanding (Kane and Smitka, 1978), could be harvested unproblematically already after a few days of cultivation. Nevertheless, IDFP might represent an alternative for otherwise fastidious isolates with special nutritional requirements.

Regarding the incubation time of dermatophyte cultures, in accordance with others we observed better identification scores with younger cultures (over-night in liquid broth or up to 5d on solid media; L'Ollivier et al., 2013). We attribute this to the fact that all entries in the relevant Bruker libraries are established using cultures handled according to the "Liquid Cultivation Procedure", i.e. only over-night-incubation probably leading to more similar protein expression profiles to younger cultures (pers. comm. with Bruker Daltonik GmbH). The reliable identification after such short incubation times - before characteristic morphological traits of fungi are displayed - is one of the main advantages of MALDI-TOF MS (L'Ollivier et al., 2013). Interestingly, others report of higher identification rates with older cultures (up to 14d of incubation) which might be explained with the production of secondary metabolites that are usually only found in mature cultures (Coulibaly et al., 2011; Packeu et al., 2014). We therefore recommend to include cultures of the relevant species of different incubation times into one's own library to circumvent these complications.

Both dendrograms, i.e. based on ITS-sequences and on MSP data, support the often-described close relation of dermatophytes altogether and within the different genera (de Hoog et al., 2017).

Two main clades are formed in both trees separating geophilic and zoophilic dermatophyte species almost completely. In the MALDI-TOF MS dendrogram, the majority of the geophilic species cluster in the lower clade; the *A. tuberculatum*-isolates are located directly next to this clade and, in terms of subclades, separated from the zoophilic species. In the ITS-dendrogram, the separation between geophiles and zoophiles is even sharper with both groups forming distinct subclades.

Here, furthermore, each species forms its own subclade; this is also seen in the MALDI-TOF MS dendrogram apart from *T. verrucosum* with one isolate clustering together with the veterinary *T. erinacei*-isolates. However, the nested arrangement of *T. erinacei*, *T. verrucosum* and *T. benhamiae* together in one subcluster in the MSP-dendrogram underlines their close interspecies-relation which is not only seen in other proteome analyses (Bartosch et al, 2018) but also reported in other genomic studies (Gräser et al., 2008; Baumbach et al., 2020). Furthermore, the latter is also supported by the current ITS-tree in which these three species form one common subclade as well.

T. mentagrophytes forms a subclade with *T. quinckeanum* in both trees; the latter was only recently separated from the *T. mentagrophytes*-complex and classified as an independent species rather than a variant (Uhrlaß et al., 2018).

Interestingly, their seems to be a close relation to *M. canis* as well since the latter isolates are found in close proximity to *T. mentagrophytes* and *T. quinckeanum* in both trees.

In the MALDI-TOF MS dendrogram, the *T. erinacei*-isolates subcluster according to the host they were isolated from, i.e. all veterinary and all human isolates form distinct subclades. Also, *A. insingulare* and *A. crocatum* show this separation according to the origin of isolation. This phenomenon is not observed in the current ITS-dendrogram and was also not seen in a previous study with *T. benhamiae*-isolates derived from human patients and infected guinea pigs (Baumbach et al., 2020). However, for *T. erinacei* this may be explained with the different geographical sampling sites of these isolates (human: Central Germany; hedgehog: Hannover area).

The overall distribution and organization in common subclades among the *Arthroderma*-isolates is very similar in both dendrograms: *A. chiloniense* and *A. crocatum* form a common subclade as well as *A. insingulare* and *A. quadrifidum*; as mentioned before, the *A. tuberculatum*-isolates are somewhat separated from the other *Arthroderma* spp. Brasch et al. identified a rather remote position for *A. quadrifidum* and, furthermore, quite a distance between the former and *A. insingulare* in another ITS-based phylogenetic analysis but they included only one isolate of each investigated species (Brasch et al., 2019). However, similar to the zoophilic dermatophyte, the interspecific sequence divergence in the genus *Arthroderma* does not exceed 2% (Brasch et al., 2019).

Although *S. brevicaulis* is a mold of the *Microascus* genus, it was grouped into one of the main clades of the MSP-dendrogram and not as a real outgroup. *S. brevicaulis* is regularly isolated from nail infections and, hence, typically associated with mold-related onychomycosis; keratinolytic activities are well reported (Issakainen et al., 2007; Macura and Skóra, 2015). Although the majority of the extracted proteins for MALDI-TOF MS are ribosomal proteins rather than secreted proteases, this similar lifestyle compared to dermatophytes may explain the position of *S. brevicaulis* in the dendrogram.

In conclusion, our results suggest that MALDI-TOF MS is a suitable method for the identification and differentiation of zoophilic dermatophytes provided that the reference library is supplemented with laboratory-relevant species, underrepresented and uncommon taxa, and sufficient isolates per species to circumvent the observed intraspecies diversity and cultivation variations (Theel et al., 2011; Croxatto et al., 2012; Respinis et al., 2013; L'Ollivier and Ranque, 2017).To further improve identification rates, we recommend taking the list of the next best hits from the mass spectrometer identification score matching chart into consideration to conclude secured results. Furthermore, combination with ITS sequencing is advisable in critical cases.

DATA AVAILABILITY STATEMENT

The datasets presented in this study can be found in online repositories. The names of the repository/repositories and accession number(s) can be found below: https://www.ncbi.nlm.nih.gov/genbank/, MN961146-961147; MN974534-974539.

ETHICS STATEMENT

Ethical review and approval was not required for the animal study because the herein described isolates of wild hedgehogs were obtained from samples taken after submission of the animals to the clinic showing a poor general health condition or injuries after accidents (*Erinaceus europaeus*, asymptomatic and symptomatic; sampled in 2018 by the Clinic for Small Mammals, Reptiles and Birds, University of Veterinary Medicine Hannover, Hannover,

Germany). Sampling ensued from recently deceased or –if medically indicated- euthanized animals (approval by an animal ethics committee not needed).

AUTHOR CONTRIBUTIONS

C-MB: fungal culture, data analysis, writing of original and revised draft, creation of figures. SM: fungal culture, MALDI-TOF MS measurements, creation of MSPs and score-oriented dendrogram, data analysis. MR: conceptualization of the study, sampling. PN: species identification by PCR and sequencing, supervision and administration. SU: fungal culture, species identification by PCR, sequencing and creation of ITS-based dendrogram, deposition of cultures and sequences in the DSMZ and NCBI BLASTn database, respectively. CB: conceptualization, supervision and administration. WS: conceptualization and experimental design, supervision and administration, optimization of fungal culture, MSP creation, data analysis. All authors contributed to the article and approved the submitted version.

FUNDING

Self-funded study. The authors acknowledge support from the German Research Foundation (DFG) and Leipzig University within the program of Open Access Publishing.

ACKNOWLEDGMENTS

We are grateful for the comprehensive technical and software support of Bruker Daltonik GmbH.

SUPPLEMENTARY MATERIAL

The Supplementary Material for this article can be found online at: https://www.frontiersin.org/articles/10.3389/fcimb.2021.631681/full#supplementary-material

REFERENCES

Abarca, M. L., Castellá, G., Martorell, J., and Cabañes, F. J. (2017). *Trichophyton erinacei* in Pet Hedgehogs in Spain: Occurrence and Revision of Its Taxonomic Status. *Med. Mycol.* 55 (2), 164–172. doi: 10.1093/mmy/myw057

Bartosch, T., Heydel, T., Uhrlaß, S., Nenoff, P., Müller, H., Baums, C. G., et al. (2018). MALDI-TOF MS Analysis of Bovine and Zoonotic Trichophyton Verrucosum Isolates Reveals a Distinct Peak and Cluster Formation of a Subgroup With *Trichophyton benhamiae*. *Med. Mycol.* 56 (5), 602–609. doi: 10.1093/mmy/myx084

Baumbach, C. M., Michler, J. K., Nenoff, P., Uhrlaß, S., and Schrödl, W. (2020). Visualising Virulence Factors: *Trichophyton benhamiaes* Subtilisins Demonstrated in a Guinea Pig Skin Ex Vivo Model. *Mycoses* 63 (9), 970–978. doi: 10.1111/myc.13136

Biswas, S., and Rolain, J.-M. (2013). Use of MALDI-TOF Mass Spectrometry for Identification of Bacteria That are Difficult to Culture. *J. Microbiol. Methods* 92 (1), 14–24. doi: 10.1016/j.mimet.2012.10.014

Brasch, J., Beck-Jendroschek, V., Voss, K., Yurkov, A., and Gräser, Y. (2019). *Arthroderma chiloniense* sp. nov. Isolated From Human Stratum Corneum: Description of a New Arthroderma Species. *Mycoses* 62, 73–80. doi: 10.1111/myc.12850

Carbonnelle, E., Mesquita, C., Bille, E., Day, N., Dauphin, B., Beretti, J.-L., et al. (2011). MALDI-TOF Mass Spectrometry Tools for Bacterial Identification in Clinical Microbiology Laboratory. *Clin. Biochem.* 44 (1), 104–109. doi: 10.1016/j.clinbiochem.2010.06.017

Cassagne, C., Normand, A.-C., L'Ollivier, C., Ranque, S., and Piarroux, R. (2016). Performance of MALDI-TOF MS Platforms for Fungal Identification. *Mycoses* 59 (11), 678–690. doi: 10.1111/myc.12506

Chermette, R., Ferreiro, L., and Guillot, J. (2008). Dermatophytoses in Animals. *Mycopathologia* 166 (5-6), 385–405. doi: 10.1007/s11046-008-9102-7

Coulibaly, O., Marinach-Patrice, C., Cassagne, C., Piarroux, R., Mazier, D., and Ranque, S. (2011). *Pseudallescheria/Scedosporium Complex* Species Identification by Matrix-Assisted Laser Desorption Ionization Time-of-Flight Mass Spectrometry. *Med. Mycol* 49 (6), 621–626.

Croxatto, A., Prod'hom, G., and Greub, G. (2012). Applications of MALDI-TOF Mass Spectrometry in Clinical Diagnostic Microbiology. *FEMS Microbiol. Rev.* 36 (2), 380–407. doi: 10.1111/j.1574-6976.2011.00298.x

de Hoog, G. S., Dukik, K., Monod, M., Packeu, A., Stubbe, D., Hendrickx, M., et al. (2017). Toward a Novel Multilocus Phylogenetic Taxonomy for the Dermatophytes. *Mycopathologia* 182 (1-2), 5–31. doi: 10.1007/s11046-016-0073-9

Ferguson, L., and Fuller, L. C. (2017). Spectrum and Burden of Dermatophytes in Children. *J. Infection* 74, S54–S60. doi: 10.1016/S0163-4453(17)30192-5

Gebauer, S., Uhrlass, S., Koch, D., Krüger, C., Rahmig, N., Hipler, U.-C., et al. (2018). Painful Circumscribed Bullous Dermatosis of the Left Hand After Contact With African Four-Toed Hedgehogs. *JDDG* 16 (6), 787–790. doi: 10.1111/ddg.13536

Gräser, Y., Scott, J., and Summerbell, R. (2008). The New Species Concept in Dermatophytes—a Polyphasic Approach. *Mycopathologia* 166 (5), 239. doi: 10.1007/s11046-008-9099-y

Havlickova, B., Czaika, V. A., and Friedrich, M. (2008). Epidemiological Trends in Skin Mycoses Worldwide. *Mycoses* 51 (Suppl 4), 2–15. doi: 10.1111/j.1439-0507.2008.01606.x

Heireman, L., Patteet, S., and Steyaert, S. (2020). Performance of the New ID-Fungi Plate Using Two Types of Reference Libraries (Bruker and MSI) to Identify Fungi With the Bruker MALDI Biotyper. *Med. Mycol* 58 (7), 946–957. doi: 10.1093/mmy/myz138

Issakainen, J., Heikkilä, H., Vainio, E., Koukila-Kähkölä, P., Castren, M., Liimatainen, O., et al. (2007). Occurrence of *Scopulariopsis* and *Scedosporium* in Nails and Keratinous Skin. a 5-Year Retrospective Multi-Center Study. *Med. Mycol* 45 (3), 201–209.

Juiz, P. M., Almela, M., Melción, C., Campo, I., Esteban, C., Pitart, C., et al. (2012). A Comparative Study of Two Different Methods of Sample Preparation for Positive Blood Cultures for the Rapid Identification of Bacteria Using MALDI-TOF MS. *Eur. J. Clin. Microbiol. Infect. Dis.* 31 (7), 1353–1358. doi: 10.1007/s10096-011-1449-x

Kane, J., and Smitka, C. (1978). Early Detection and Identification of *Trichophyton verrucosum*. *J. Clin. Microbiol.* 8 (6), 740–747.

Kargl, A., Kosse, B., Uhrlaß, S., Koch, D., Krüger, C., Eckert, K., et al. (2018). gelpilze in Einer Münchner Hautarztpraxis: Fallbeschreibungen Und Übersicht. *Hautarzt* 69 (7), 576–585. doi: 10.1007/s00105-018-4134-5

Kumar, S., Stecher, G., Li, M., Kyaz, C., and Tamura, K. (2018). Mega X: Evolutionary Genetics Analysis Across Computing Platforms. *Mol. Biol. Evol.* 35, 1547–1549. doi: 10.1093/molbev/msy096

Lau, A. F., Walchak, R. C., Miller, H. B., Slechta, E. S., Kamboj, K., Riebe, K., et al. (2019). Multicenter Study Demonstrates Standardization Requirements for Mold Identification by MALDI-TOF MS. *Front. Microbiol.* 10, 2098. doi: 10.3389/fmicb.2019.02098

L'Ollivier, C., Cassagne, C., Normand, A.-C., Bouchara, J.-P., Contet-Audonneau, N., Hendrickx, M., et al. (2013). a MALDI-TOF MS Procedure for Clinical Dermatophyte Species Identification in the Routine Laboratory. *Med. Mycol.* 51 (7), 713–720. doi: 10.3109/13693786.2013.781691

L'Ollivier, C., and Ranque, S. (2017). Maldi-Tof-Based Dermatophyte Identification. *Mycopathologia* 182 (1–2), 183–192. doi: 10.1007/s11046-016-0080-x

Mackenzie, D. W. R. (1963). "Hairbrush Diagnosis" in Detection and Eradication of Non-Fluorescent Scalp Ringworm. *BMJ* 2 (5353), 363–365.

Macura, A. B., and Skóra, M. (2015). 21-Year Retrospective Study of the Prevalence of Scopulariopsis Brevicaulis in Patients Suspected of Superficial Mycoses. *Postepy Dermatol. Alergol.* 32 (3), 189–194. doi: 10.5114/pdia.2014.40965

Nenoff, P., Erhard, M., Simon, J. C., Muylowa, G. K., Herrmann, J., Rataj, W., et al. (2013). MALDI-TOF Mass Spectrometry - a Rapid Method for the Identification of Dermatophyte Species. *Med. Mycol.* 51 (1), 17–24. doi: 10.3109/13693786.2012.685186

Nenoff, P., Krüger, C., Ginter-Hanselmayer, G., and Tietz, H.-J. (2014b). Mycology - an Update. Part 1: Dermatomycoses: Causative Agents, Epidemiology and Pathogenesis. *JDDG* 12 (3), 188–212.

Nenoff, P., Uhrlaß, S., Krüger, C., Erhard, M., Hipler, U.-C., Seyfarth, F., et al. (2014a). Trichophyton Species of *Arthroderma benhamiae* - a New Infectious Agent in Dermatology. *JDDG* 12 (7), 571–581.

Packeu, A., Bel, A., l'Ollivier, C., Ranque, S., Detandt, M., and Hendrickx, M. (2014). Fast and Accurate Identification of Dermatophytes by Matrix-Assisted Laser Desorption Ionization-Time of Flight Mass Spectrometry: Validation in the Clinical Laboratory. *J. Clin. Microbiol.* 52 (9), 3440–3443. doi: 10.1128/JCM.01428-14

Respinis, S., Monnin, V., Girard, V., Welker, M., Arsac, M., Cellière, B., et al. (2014). Matrix-Assisted Laser Desorption Ionization-Time of Flight (MALDI-TOF) Mass Spectrometry Using the Vitek MS System for Rapid and Accurate Identification of Dermatophytes on Solid Cultures. *J. Clin. Microbiol.* 52 (12), 4286–4292. doi: 10.1128/JCM.02199-14

Respinis, S., Tonolla, M., Pranghofer, S., Petrini, L., Petrini, O., and Bosshard, P. P. (2013). Identification of Dermatophytes by Matrix-Assisted Laser Desorption/Ionization Time-of-Flight Mass Spectrometry. *Med. Mycol* 51 (5), 514–521. doi: 10.3109/13693786.2012.746476

Sacheli, R., Henri, A.-S., Seidel, L., Ernst, M., Darfouf, R., Adjetey, C., et al. (2020). Evaluation of the New Id-Fungi Plates From Conidia for MALDI-TOF MS Identification of Filamentous Fungi and Comparison With Conventional Methods as Identification Tool for Dermatophytes From Nails, Hair and Skin Samples. *Mycoses* 63 (10), 1115–1127. doi: 10.1111/myc.13156

Sharma, R., Rajak, R. C., Pandey, A. K., and Gräser, Y. (2006). Internal Transcribed Spacer (ITS) of Rdna of Appendaged and Non-Appendaged Strains of Microsporum Gypseum Reveals Microsporum Appendiculatum as Its Synonym. *Antonie Van Leeuwenhoek* 89 (1), 197–202. doi: 10.1007/s10482-005-9018-x

Tamura, K., and Nei, M. (1993). Estimation of the Number of Nucleotide Substitutions in the Control Region of Mitochondrial DNA in Humans and Chimpanzees. *Mol. Biol. Evol.* 10, 512–526.

Theel, E. S., Hall, L., Mandrekar, J., and Wengenack, N. L. (2011). Dermatophyte Identification Using Matrix-Assisted Laser Desorption Ionization-Time of Flight Mass Spectrometry. *J. Clin. Microbiol.* 49 (12), 4067–4071. doi: 10.1128/JCM.01280-11

Uhrlaß, S., Schroedl, W., Mehlhorn, C., Krüger, C., Hubka, V., Maier, T., et al. (2018). Molecular Epidemiology of *Trichophyton quinckeanum* - a Zoophilic Dermatophyte on the Rise. *JDDG* 16 (1), 21–32. doi: 10.1111/ddg.13408

van Veen, S. Q., Claas, E. C. J., and Kuijper, E. J. (2010). High-Throughput Identification of Bacteria and Yeast by Matrix-Assisted Laser Desorption Ionization-Time of Flight Mass Spectrometry in Conventional Medical Microbiology Laboratories. *J. Clin. Microbiol.* 48 (3), 900–907. doi: 10.1128/JCM.02071-09

Weishaupt, J., Kolb-Mäurer, A., Lempert, S., Nenoff, P., Uhrlaß, S., Hamm, H., et al. (2014). A Different Kind of Hedgehog Pathway: Tinea Manus Due to *Trichophyton erinacei* Transmitted by an African Pygmy Hedgehog (Atelerix Albiventris). *Mycoses* 57 (2), 125–127. doi: 10.1111/myc.12113

Weitzman, I., and Summerbell, R. C. (1995). The Dermatophytes. *Clin. Microbiol. Rev.* 8 (2), 240–259. doi: 10.1128/CMR.8.2.240

Wiegand, C., Burmester, A., Tittelbach, J., Darr-Foit, S., Goetze, S., Elsner, P., et al. (2019). Dermatophytosen, Verursacht Durch Seltene Anthropophile Und Zoophile Erreger. *Hautarzt* 70 (8), 561–574. doi: 10.1007/s00105-019-4429-1

Conflict of Interest: The authors declare that the research was conducted in the absence of any commercial or financial relationships that could be construed as a potential conflict of interest.

frontiers in Cellular and Infection Microbiology

ORIGINAL RESEARCH
published: 22 June 2021
doi: 10.3389/fcimb.2021.656880

Accurate Identification of Closely Related *Mycobacterium tuberculosis* Complex Species by High Resolution Tandem Mass Spectrometry

Amol O. Bajaj[1*], *Suraj Saraswat*[1†], *Juha E. A. Knuuttila*[2], *Joanna Freeke*[3,4], *J. Benjamin Stielow*[3,4] *and Adam P. Barker*[1*]

[1] Research & Development, Associated Regional and University Pathologists, Inc. (ARUP) Institute for Clinical and Experimental Pathology, Salt Lake City, UT, United States, [2] Research & Development, Thermo Fisher Scientific, Helsinki-Vantaa, Finland, [3] Centre for Infectious Diseases, Radboud University Medical Center (UMC), Nijmegen, Netherlands, [4] Research & Development, Thermo Fisher Scientific, Landsmeer, Netherlands

OPEN ACCESS

Edited by:
Di Xiao,
National Institute for Communicable Disease Control and Prevention (China CDC), China

Reviewed by:
Motlatso Tiny Hlokwe, Onderstepoort Veterinary Institute (ARC-SA), South Africa
Keyvan Tadayon, Razi Vaccine and Serum Research Institute, Iran

***Correspondence:**
Adam P. Barker
adam.barker@aruplab.com
Amol O. Bajaj
amol.bajaj@aruplab.com

†Present address:
Suraj Saraswat, Pivotal group, Attribute Sciences, Amgen, Thousand Oaks, CA, United States

Specialty section:
This article was submitted to Clinical Microbiology, a section of the journal Frontiers in Cellular and Infection Microbiology

Received: *21 January 2021*
Accepted: *07 May 2021*
Published: *22 June 2021*

Citation:
Bajaj AO, Saraswat S, Knuuttila JEA, Freeke J, Stielow JB and Barker AP (2021) Accurate Identification of Closely Related Mycobacterium tuberculosis Complex Species by High Resolution Tandem Mass Spectrometry. Front. Cell. Infect. Microbiol. 11:656880. doi: 10.3389/fcimb.2021.656880

Rapid and accurate differentiation of *Mycobacterium tuberculosis* complex (*MTBC*) species from other mycobacterium is essential for appropriate therapeutic management, timely intervention for infection control and initiation of appropriate health care measures. However, routine clinical characterization methods for *Mycobacterium tuberculosis* (*Mtb*) species remain both, time consuming and labor intensive. In the present study, an innovative liquid Chromatography-Mass Spectrometry method for the identification of clinically most relevant *Mycobacterium tuberculosis* complex species is tested using a model set of mycobacterium strains. The methodology is based on protein profiling of *Mycobacterium tuberculosis* complex isolates, which are used as markers of differentiation. To test the resolving power, speed, and accuracy of the method, four ATCC type strains and 37 recent clinical isolates of closely related species were analyzed using this new approach. Using different deconvolution algorithms, we detected hundreds of individual protein masses, with a subpopulation of these functioning as species-specific markers. This assay identified 216, 260, 222, and 201 proteoforms for *M. tuberculosis* ATCC 27294™, *M. microti* ATCC 19422™, *M. africanum* ATCC 25420™, and *M. bovis* ATCC 19210™ respectively. All clinical strains were identified to the correct species with a mean of 95% accuracy. Our study successfully demonstrates applicability of this novel mass spectrometric approach to identify clinically relevant *Mycobacterium tuberculosis* complex species that are very closely related and difficult to differentiate with currently existing methods. Here, we present the first proof-of-principle study employing a fast mass spectrometry-based method to identify the clinically most prevalent species within the *Mycobacterium tuberculosis* species complex.

Keywords: mass spectrometry, species delimitation, clinical mycobacteriology, *Mycobacterium tuberculosis*, clinical diagnostics

INTRODUCTION

Mycobacterium tuberculosis is responsible for one of the most devastating and chronic infectious diseases known to science and is an important and formidable human pathogen that has claimed nearly 1.2 million lives in 2019 (Andersen and Brennan, 1994). Approximately 10 million people were infected in 2019 and the pathogen can persist in a hidden form if undiagnosed for a long period of time within the human host (Bloom and Murray, 1992; WHO, 2020). Almost 10% of an infected population will progress to disease (active tuberculosis) following a latent period (from weeks to decades) (Bloom and Murray, 1992). Multidrug-resistant tuberculosis has recently emerged (MDR-TB) and represents an enormous challenge to the public health system worldwide. Worldwide in 2019, close to half a million people developed rifampicin-resistant TB (RR-TB), of which 78% had multidrug-resistant TB (MDR-TB). The three countries with the largest share of the global burden were India (27%), China (14%) and the Russian Federation (8%) (WHO, 2020). The largest increase seen globally in the number of nontuberculosis mycobacterial (NTM) and *MTBC* infections was observed in patients who had already contracted the human immunodeficiency virus (HIV).

Mycobacterium tuberculosis complex encompasses a group of organisms of paramount clinical relevance that cause tuberculosis (TB) in humans and animals. TB in humans is caused mainly by *M. tuberculosis* comprising an enormous diversity of genetic lineages (e.g. including its formerly known *M. africanum*) but also by other members of *MTBC*. Zoonotic TB is caused by its less well understood animal-associated subspecies *M. bovis*, *M. canetti, M. caprae*, *M. pinnipedii*, *M. suricattae*, *M. orygis*, *M. microti*, and *M. mungi* (Gagneux and Small, 2007; Alexander et al., 2010; Gupta et al., 2018; Riojas et al., 2018; Lipworth et al., 2019). However, not all zoonotic *MTBC* species are nomenclatural validly published and *MTBC* taxonomy has been under constant scientific revision, with future changes being expected. Despite their genetically close relationship, they differ in epidemiology, pathogenicity, geographical range, host preference, and severity of tuberculosis disease in humans. Genetically, all members of this complex are highly conserved, possessing 99.9% similarity at the nucleotide level and identical 16S rRNA sequences (Peters et al., 2020). *M. tuberculosis* species, the most common pathogens in humans, can be further divided into genetic groups that also show differences in their levels of virulence, immunogenicity, and geographical distributions (Gagneux and Small, 2007). *M. bovis* BCG is one of the most common *MTBC* organisms found in clinical laboratory and is used to treat bladder cancer (DeGeorge et al., 2017; Larsen et al., 2020). *M. bovis* BCG is one of the most commonly administered vaccines and its complications include disseminated BCG disease which is rare but increasingly reported in immunodeficient children (Hesseling et al., 2007; Ritz et al., 2009). It is clinically important to differentiate *MTBC* members from other mycobacterium species considering the differences in resistance and treatment response rate to antibiotics (Scorpio and Zhang, 1996). The ability to distinguish between strict human and zoonotic tuberculosis and to trace source exposure during epidemiological studies is critical for the infection control process (Djelouadji et al., 2008).

Characterization of the proteome of *MTBC* is essential for differentiation at the species level with the proposed approach. It has been shown that during infection some expressed proteins vary during different stages of infection while others are present during the entire infection (Mehaffy et al., 2012). Some of the *Mtb* secreted proteins are essential for pathogenesis of the disease and can be potential targets for vaccine development (Brock et al., 2001). For example MtbHU (a small dimeric nucleoid-associated protein), HspX/14-kDa (α-crystalline homologue), the molecular chaperone GroEL2, and bacterioferritin (BfrB) are essential for growth and pathogenesis of *Mtb* and can serve as target for treatment (Bhowmick et al., 2014). Any delay in correct diagnosis and treatment may lead to sepsis and emergence of resistance to available drugs, this can be one of the driving forces for the search of new drugs that will take years or decades to develop. There are many known mechanisms of resistance such as possible mutations of the *pncA* and *rpoB* gene, hydrophobic and waxy cell wall composition, slow growth rate while dormant, capacity to suppress the host immune response, and an efficient efflux pump system (Scorpio and Zhang, 1996; Somoskovi et al., 2001; de Steenwinkel et al., 2010; Louw et al., 2011). Outside of these known resistance pathways there may be many unknown resistance mechanisms which need to be explored as well. Therefore, a rapid and accurate differentiation of closely related pathogens is crucial. However, most of the recent methods that are based on phenotypes, biochemical characteristics, nucleic acids, and molecular systems (Somoskovi et al., 2008) for *MTBC* species differentiation and identification have suboptimal diagnostic performance. In addition, next generation sequencing is laborious to perform (Hughes et al., 2012). Even MALDI-TOF, which has revolutionized the clinical microbiology identification of mycobacterium (Mather et al., 2014), could not discriminate *MTBC* species (particularly as IVD cleared test) (Chen et al., 2013; Lévesque et al., 2015).

In addition to the need of a more discerning assay, it is also essential to have a pre-analytical method to render the microbes non-viable. A unique incubation with pre-incubation solution (Thermo Fisher Scientific, proprietary) followed by rigorous mixing in buffered solution method was developed for inactivation of *MTBC* to overcome shortcomings of other inactivation methods such as heat treatment (Doig et al., 2002), exposure to lethal irradiation (Murdoch et al., 2012), multiple centrifugation and washing steps etc. In this study, we utilize micro (nano) flow liquid chromatography-mass spectrometry (LC-MS) to separate proteins from microbial extracts and analyze them in a high-resolution accurate mass (HRAM) orbitrap mass spectrometer. We used a workflow consisting of cell sonication, solid-phase extraction (SPE) purification, mass spectrometry, and computational algorithms to achieve our high identification accuracy for these organisms. The goal of the present study was to provide a proof-of-principle experiment employing

orbitrap LC-MS for discrimination of mycobacterium species. This is the first study in which differentiation of the *MTBC* at a species level is achieved by employing a mass spectrometry driven approach with the potential to discriminate all types of closely related *Mtb* pathogens.

MATERIALS AND METHODS

Strain Selection and Reference Identifications

Mycobacterium strains belonging to the species *M. africanum* (*syn. M. tuberculosis; Genetic lineage*), *M. tuberculosis*, *M. bovis*, *M. bovis* BCG and *M. microti* being of paramount clinical relevance were selected as representatives for the *Mycobacterium tuberculosis* complex). Although *M. canetti*, *M. caprae*, *M. orygis*, *M. suricattae*, *M. pinnipedii*, and *M. mungi* also form the *MTBC*, we excluded them in this study due occurrence as causative agents of rare zoonotic human TB infections and their partially unclarified taxonomic status. Key objective to this study was providing an initial proof-of-principle towards the diagnostic potential of our novel LC-MS assay only. Taxonomic anchors were defined by ATCC type material and selected for the subsequent analysis (*M. tuberculosis* ATCC 27294™, *M. microti* ATCC 19422™, *M. africanum* ATCC 25420™, and *M. bovis* ATCC 19210™ (Note: This type strain appears to be *M. bovis BCG* by ARUP internal PCR based validation). In addition, 37 recent US clinical isolates obtained by Associated Regional and University Pathologists (ARUP) laboratories (7 clinical isolate strains of *M africanum*, 10 *M. tuberculosis*, 10 *M. bovis* and 10 *M. bovis* BCG) were analyzed in order to assess assay robustness. ATCC type material was obtained pre-identified in accordance with ATCC identifications procedures; all other recent clinical isolates were identified by quantitative (real-time) PCR and meltcurve analysis with a multiplex probe set to obtain a reference identification (Pounder et al., 2010) prior to LC-MS data acquisition. All strains of recent clinical origin were collected throughout the year 2019 at ARUP laboratories, with no additional metadata being available (double blinded clinical identifiers).

Chemicals and Reagents

Optima LC-MS grade Water (H_2O), Optima LC-MS grade acetonitrile (ACN), and Optima LC-MS grade formic acid (FA) were purchased from Fisher Scientific (Fair Lawn, NJ).

Sample Preparation

Preparation of Whole Cell Extracts (WCE) for *M. tuberculosis* Complex Species

ATCC strains and clinical isolates of *M. tuberculosis* complex were cultured on 7H11 agar plates for approximately 18-24 days in a CO2 incubator maintained at 37°C in a BSL3 laboratory. A 1 μL loopful of colonies was transferred into sonication vials (Thermo Fisher Scientific, proprietary). Subsequently the pre-incubation solution containing alcohol (Thermo Fisher Scientific, proprietary) was added to the cells at room temperature (RT, 20-25°C) and following a short centrifugation step (12,000 x g for 2 minutes at RT) the supernatant was discarded and then the pellet was suspended into 100 μL of incubation solution containing formic acid and acetonitrile (Thermo Fisher Scientific, proprietary). The cell lysate were incubated for 20 minutes (vortexed once at the 10-minute mark for 2 seconds), followed by sonication for one minute at 50% amplitude. Cells were diluted with 100 μL dilution buffer containing acetonitrile (Thermo Fisher Scientific, proprietary) and centrifuged for 5 minutes at 12,000 × g at RT. The supernatant was collected in low protein binding (LBE) Eppendorf tubes and stored at -80°C if not immediately used for LC-MS analysis.

RP4H SPE Protocol

The whole cell extract (WCE) was diluted with SPE buffer-1 (Thermo Fisher Scientific, proprietary) before Solid-Phase Extraction (SPE) cleanup. Reverse Phase monolith (RP4H) SPE tips (Thermo Fisher Scientific, proprietary) were placed in 96 well-plate and conditioned and equilibrated with 50 μL proprietary SPE buffer-2 (Thermo Fisher Scientific, proprietary), respectively. A centrifuge (Laboratory centrifuge 4-15C, Thermo Fisher, Osterode, Germany) capable of handling two 96 well-plates was used for centrifugation at 2000 × g for 2 minutes at RT. Diluted WCE (50 μL) was loaded into the SPE tips and centrifuged. The tips were washed with 50 μL of proprietary SPE buffer-3 and placed in liquid chromatography (modified Easy-1000, Thermo Fisher Scientific, proprietary) autosampler plate for further online elution and mass spectrometric analysis. Blanks were treated as negative controls and were prepared in a similar way as described above, instead of cell lysate water was added to the SPE tips.

LC-MS Analysis

All experiments were performed on a micro flow Liquid chromatography-Mass spectrometry (LC-MS) system. The liquid chromatography (LC) system was connected to a Q Exactive™ HF Orbitrap™ mass spectrometer (Thermo Fisher Scientific, San Jose, CA). Mobile phase A consisted of 0.2% FA, 10% ACN in H2O and mobile phase B consisted of 0.2% FA in ACN. Elution was done using gradient elution where after flow stabilization at 4 μL/min for 2%B, percent of B was increased to 33% B in 5 min. The LC and mass spectrometer were controlled by Xcalibur software version 3.0 (Thermo Fisher Scientific). The mass spectrometer was operated in positive electrospray ionization (+ ESI) mode. The general mass spectrometric conditions were: The spray voltage was set at 2.0 kV. The capillary temperature was 325°C and S-lens RF level was set to 65. The maximum injection time was 200 millisecond and 40 microscans were used. Automatic Gain Control (AGC) target was 3e6, resolution was 120,000 for MS. Intact protein MS mode was used with trapping gas pressure set to 0.2 and C-trap charge detection was set OFF. Mass analysis of proteins was performed in the range from 450 to 2000 m/z for full scan mode.

Data Processing and Species Identification

The raw data was deconvoluted (proprietary algorithm) in real time to monoisotopic masses (i.e. list of proteoforms).

Subsequently, the data was processed with in-house algorithms for building of the database and identification of mycobacterium species. The individual data acquisition and processing steps are depicted in **Figure 1**. Each strain in the analysis was measured in two technical replicates for database construction and subsequent species prediction. Each ATCC strain in the analysis was also analyzed in six replicates (two technical replicates from three biological replicates) for the estimation of technical reproducibility of the sample processing and measurement.

Processing of the mass spectra was performed by Thermo Fisher proprietary software to deconvolute spectra in *m*/*z* space into monoisotopic protein masses between 5 and 40 kDa. Measured monoisotopic masses from each measurement were mass aligned to construct a list of consensus markers. One-way ANOVA was used to select top 200 consensus markers that have the most predictive value for the differentiation of the species. Species prediction was accomplished by a Thermo Fisher Scientific proprietary distance-based clustering algorithm. The robustness of species prediction was simulated by leave-one-out iterations where each sample was tested against a database constructed without data for the same strain (training and test dataset). The data will be made available on reasonable request.

RESULTS

Inference and Determination of LC-MS Proteome Patterns

To verify whether different *MTBC* species show unique MS spectrum profiles, the masses of the deconvoluted proteoforms from each species were aligned to construct a list of consensus markers (clustering of monoisotopic masses). Subsequently, we could depict common (shared) proteoforms from deconvoluted spectrum profiles in order to determine visually common and non-common proteoforms (**Figure 2**). Unique masses per species were those masses present in all or most replicates of a given species and predominantly absent from replicates from other species. To verify whether different *MTBC* strains show similar mass spectral profiles, we analyzed 37 clinical isolates of *MTBC* with the depicted LC-MS analysis workflow (**Figure 1**). Consistent with the mass spectrum profiles obtained from the ATCC type strains, all clinical isolates exhibited a similar pattern (data not shown), which comprises common proteoforms ranging from 5 to 40 kDa. Accordingly, similar elution profiles and identified proteins, result in consistent species-specific proteome patterns.

Differentiation of MTBC Species

We next evaluated whether the MS spectrum profile and common proteoforms obtained from different species within *MTBC* can differentiate the species within the complex. Based on the different expression of species-specific protein profiles (unique masses), we developed species-specific databases capable of rapidly differentiating *MTBC* at species level with very high identification accuracy.

As represented by the clustered monoisotopic masses which were visually depicted as heatmap in **Figure 2**, the unique protein signatures are successfully able to differentiate *M. bovis* and *M. bovis* BCG from other taxa of the *MTBC* in individual distinct monophyletic clusters. Similarly, *M. tuberculosis* and its genetic lineage syn. *M. africanum* as well *M. microti* are monophyletically differentiated based on unique protein profiles. The results of the mass clustering were in accordance with the alternative identification obtained by qPCR meltcurve analysis as described above under material and methods. However, a single *M. tuberculosis* isolates was falsely clustered

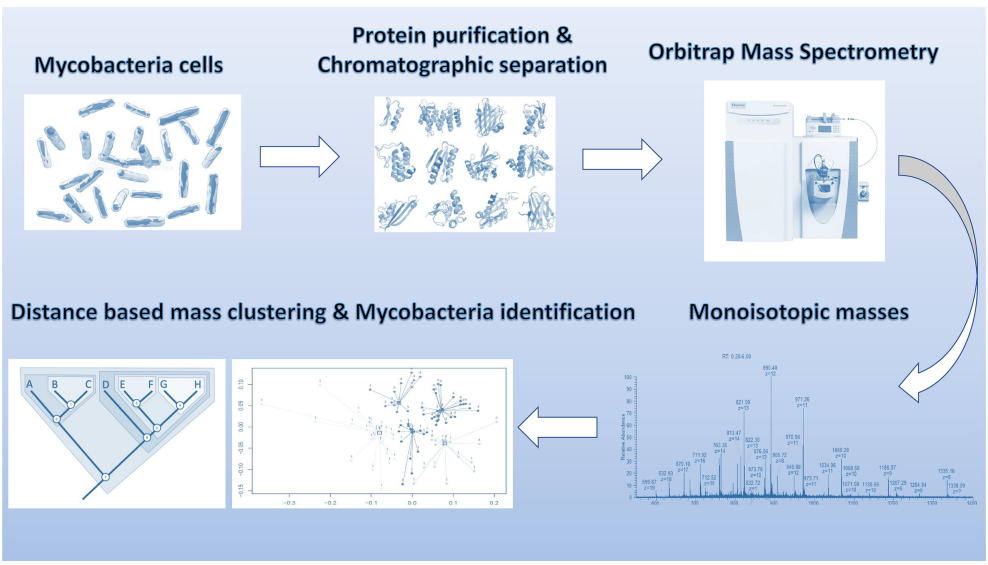

FIGURE 1 | Schematic overview of sample processing, data acquisition and analysis steps employed in stepwise analysis of LC-MS Orbitrap data.

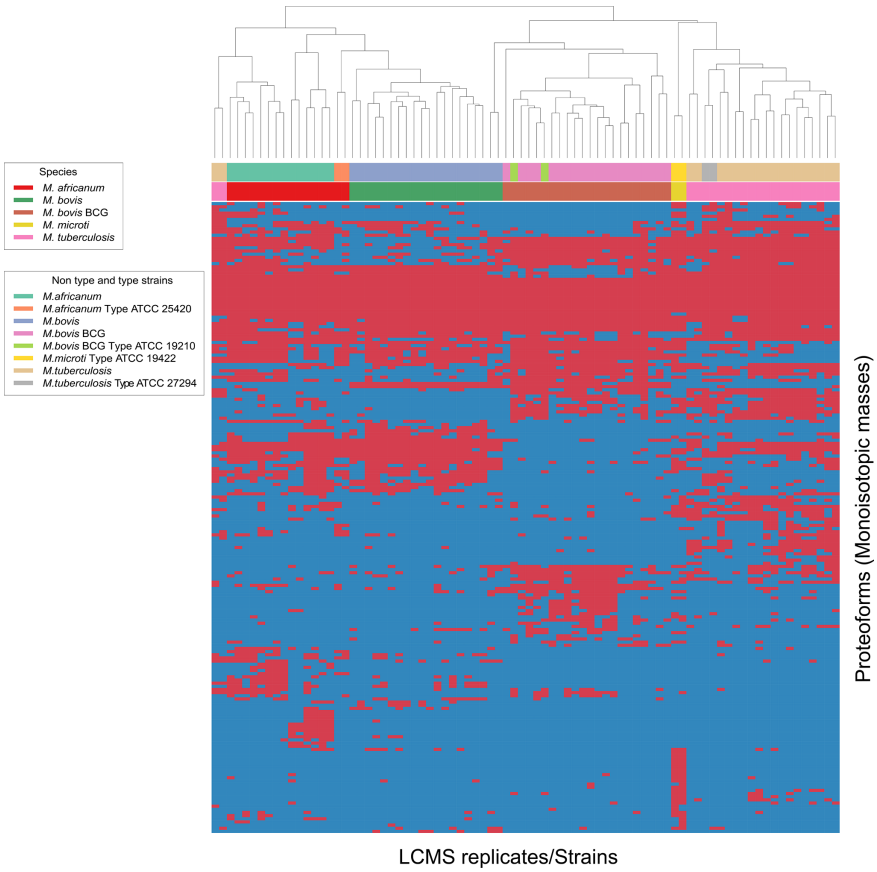

FIGURE 2 | Heat map generated for all 4 species analyzed indicating top-200 discriminatory proteoforms. Horizontal bar on top, indicates the color assignment for the type and non-type strains used in the study, horizontal bar below indicates species assignment alone for visual clarity (see legend). Mass spectrometry data is here depicted as a heatmap, where rows represent individual monoisotopic masses (deconvoluted protein masses) and columns individual strains (technical LC-MS replicates for each strain were merged to a single leaf in the horizontal dendrogram) of the study cohort. Data has been converted to a binary state, where presents of a protein mass in each strain (species) is encoded as 1 (red) and absents 0 (blue). The representation indicates proteoform overlap and non-overlap between strains among all species due to their closeness at species level. Unique proteoforms detected among individual species specifically enable the classification down to species level (Specific number of exclusive red blocks for a given taxon). Central red block of proteoforms is shared between the species of interest and is non-species specific (conserved). The dendrogram shows that the *M. bovis* and *M. bovis* BCG clinical isolates are split in two separate branches, allowing discrimination of these fundamentally different strains (non-BCG and BCG strains). Additional work is required to understand proteomic diversity of atypical isolates, considering that a reliable identification must ideally capture all clinically relevant variants of a given species as paramount criterion to microbial diagnostics.

among the *M. africanum* (sensu stricto) isolates. This misplaced isolate is obvious at the very left of the heatmap-depicted clustered monoisotopic masses (**Figure 2**). This result disagrees with our reference-based identification and can likely be explained by proteoforms which might be rarely expressed by atypical *M. tuberculosis* strains. This inconsistency will require further investigation with additional *M. tuberculosis* and *M. africanum* strains. Subsequently, the classification results returned from the training and test data definitions returned very high success rates for the clinically important species *M. tuberculosis* and *M. bovis* BCG, while *M. africanum* and *M. bovis* returned slightly inferior results (100% correct identification vs. 90% and 88% respectively). Reciprocally, identification success is lowered for *M. africanum*, by false hits against *M. bovis* but not *M. tuberculosis* and for *M. bovis* sensu stricto against *M. bovis BCG*. The results of the species prediction are given in **Table 1**. *M. microti* was excluded from the analysis due to representation of the type strain only (eg. training and test dataset as described under material and methods accordingly would be identical).

Based on the different expression of species-specific protein patterns, we were capable to differentiate the clinically most prevailing species within the *Mycobacterium tuberculosis* complex down to species level. Differential proteoforms may serve as potential biomarkers for identifying these microorganisms in patient samples in additional confirmatory studies using clinical specimens. These results outline the potential to the employed LC-MS technology, as a first-line platform in the rapid and accurate identification of *MTBC* species in routine clinical microbiological laboratories.

TABLE 1 | Classification success for identification of clinically prevalent *MTBC* species.

Species	N	Identification success (Top match only)	Combined top 3 matches for each data file
M. africanum	16	88%	41 hits to *M. africanum*, 7 hits to *M. bovis*
M. bovis	20	90%	56 hits to *M. bovis* 4 hits to *M. bovis* BCG
M. tuberculosis	22	100%	64 hits to *M. tuberculosis* 2 hits to *M. africanum*
M. bovis BCG	22	100%	66 hits to *M. bovis* BCG
Total	**80**	**95%**	

N refers to the total number of mass spectra measured for each species. Total identification success is presented as 'percent success' as a result to predict the target species with the employed algorithm. For each data file, the 3 closest matches were collected (additional and including the top match) if applicable, and the species results for these top 3 matches is displayed in the right-hand column. In all cases the best match was to another strain of the same species, but in some few cases the 2nd or 3rd best match was for a different species as detailed in the column on the right. In the analysis we used only the type-strain of the M. microti*, accordingly no species predictions are returned in this case as training and test data would be identical.*

DISCUSSION

In this study, we evaluated the resolution power of LC-MS as a novel method to delineate clinically relevant closely related *MTBC* species as a model system for challenging identifications. Rapid and accurate identification of microbial infections is essential for accurate patient supervision. Especially for *Mtb* infection, differentiation of *MTBC* species is very critical for the accurate disease diagnosis, starting drug therapy, to control the spread of disease, for public health surveillance and appropriate patient case management. *MTBC* infections have been one of the most important and common mycobacterial clinical pathogens, especially in immune deficient adults and pediatric patients. Among *MTBC* species, *Mycobacterium tuberculosis* is more predominant in clinical samples and environmental samples like water and soil which contributes almost exclusively to disseminated *MTBC* disease.

Acid-fast staining and microscopy as a routine technique was the most common and least expensive option for laboratory diagnosis of human tuberculosis. However, this technology has a low sensitivity and specificity and does not provide information on the identity of the pathogen. Comparatively rapid nucleic acid amplification test (NAAT) (Derese et al., 2012) and two-step PCR processes have been used for differentiation of *MTBC* species (Pinsky and Banaei, 2008; Pounder et al., 2010; Reddington et al., 2012; Nikam et al., 2013). However, these techniques fail to differentiate *MTBC* species, is more laborious and complexity of multiplex RT-PCR can be a problem. Routine laboratory culture, chemical testing procedures, and nested PCR targeting (Sinha et al., 2016) assays can differentiate *MTBC* members at the species level but the long identification process is not practical for rapid diagnosis of patients in need of immediate therapy. Alternatively, molecular methods such as GenoType MTBDRplus test (Hain Lifescience, Nehren, Germany) (Richter et al., 2004) or DNA probe assays (Kasai et al., 2000; Niemann et al., 2000) have been able to identify mycobacterial isolates as *MTBC* species, but lack capability to identify the isolate to the species level and limitation of it reliability on bacterial cultures to produce enough amount of bacterial DNA. Differentiation of *MTBC* species is possible based on intergenic spacers analysis in the genotyping of *M. tuberculosis* such as the exact tandem repeat D (ETR-D) (Frothingham and Meeker-O'Connell, 1998) and aliased mycobacterial interspersed repeat unit 04 (MIRU04) (Supply et al., 1997). And also, based on molecular methods such as the major polymorphism of tandem repeat (MPTR) sequencing (Frothingham, 1995), single nucleotide polymorphisms (SNP) in the *pncA* gene (Djelouadji et al., 2008), the *oxyR* locus (Sreevatsan et al., 1996), the detection of deleted regions (Somoskovi et al., 2008), the restriction fragment length polymorphism of the *hupB* gene (Prabhakar et al., 2004), *gyrB* gene based differentiation (Chimara et al., 2004; Arnold et al., 2005), and mycobacterial interspersed repetitive-unit-variable-number tandem-repeat (MIRU-VNTR) typing and spoligotyping (Godreuil et al., 2007). Previous methods could differentiate the *MTBC* at the species level but are often complicated by low sequence variability at the nucleotide level. However, these methods may have some limitations when encountered with rare species or atypical strain variants, and do not have the ability to differentiate all *MTBC* species such as *M. pinnipedii* and *M. microti* (Ayele et al., 2004). Such time-consuming and laborious methods hamper proper treatment of patients with respect to the different antibiotics and supportive treatments and are not practical for surveillance purposes. MALDI-TOF methods have been applied to mycobacterial (Mather et al., 2014) species identification and have shown to be a reliable technique in the routine laboratory. Although, MALDI-TOF for discrimination of mycobacterium is relatively rapid and reasonably accurate, however, this technique also could not differentiate *MTBC* species in clinical laboratories. Recently, a cheap and rapid new High Resolution Melting (HRM) assay for identification and differentiation of Mycobacterium tuberculosis complex samples was developed but it still had limitation to differentiate *M. bovis* from *M. bovis BCG* and *M. caprae* as well as *M. africanum* from *M. tuberculosis* (Landolt et al., 2019).

In contrast, in the present study, we demonstrated that ESI-Orbitrap LC-MS could be used for accurate identification of taxonomically complex microbial species. One of the advantages of using ESI is that it ionizes analytes to produce multiple charge states, bringing the mass to charge ratio of larger proteins into the window of the usual mass spectrometer range. These higher

mass proteins show increased discriminatory power for speciation between highly similar species which may be a reason for the improved success of this approach above other Mass Spectrometry approaches. While in this study protein identification was not carried out, the setup would allow the further characterization of the discriminatory proteins through a top-down proteomics workflow. These protein identifications if characterized as related to resistance or virulence could also have possible applications in routine clinical diagnostics (LeDuc et al., 2004). While novel diagnostic approaches employing complex LCMS technology might not be directly suitable and useful in developing countries, great benefit arises to many other countries and reference laboratories which will have access and funds to high resolution MS systems where the incidence of TB infection is still high.

ESI-LC-MS has been applied to study secretome, cell wall proteome, membrane proteome, and PTM profiling of *M. tuberculosis* (Ge et al., 2003; Gunawardena et al., 2013). However, no study has demonstrated the applicability of ESI-Orbitrap LC-MS in mycobacterial identification. Also, Dukik et al. demonstrated the use of ultra-high-resolution mass spectrometry technique for identification of closely related dermatophytes but no other report yet outlined this technique for microbial identification (Dukik et al., 2018). To the best of our knowledge, this is first study showing applicability of this technique for *MTBC* identification and discrimination at species level with very high accuracy in a very short time utilizing unique masses (protein profiles) from each species. Our present study was optimized to have an LC-MS analysis method of 5 minutes and demonstrates its potential for rapid diagnosis which could impact treatment times. This method is universally applicable and can be beneficial in the veterinary and other health care related applications for fast and precise testing. The methodology could serve as a tool in the differentiation of *MTBC* members and detection of transmission in captive and other animal populations. The *MTBC* consists of the closely related organisms *M. tuberculosis, M. africanum, M. bovis, M. bovis BCG*, and animal born zoonotic species rarely identified in patients. The accurate molecular species identification within the *MTBC* is paramount to guide public health and primary care decisions more effectively due to species specific epidemiology, partial specificity in their host spectra (e.g. zoonotic taxa), geographic prevalence and drug susceptibility. *M. tuberculosis* and *M. bovis* may highly differ in contact tracing. Treatment with pyrazinamide can be excluded in case of *M. bovis* or *M. bovis* BCG as they are naturally resistant to the drug. *Mycobacterium bovis* Calmette-Guerin (BCG) is a live, attenuated strain of *M. bovis*. It is widely used as a vaccine against tuberculosis worldwide, and BCG is very effective for the treatment of transitional cell carcinoma of the bladder. Typically, it may require months to years for physicians to identify patients being infected with BCG disease upon exposure. Also, *M. bovis* mostly causes infection in cattle, deer and other mammals but the consumption of unpasteurized infected cow milk or transmission from infectious tuberculosis patient harboring *M. bovis* can cause disseminated infection in humans. The distribution of the various species is as follows and may vary according to the patient population served: *M. tuberculosis* (95%), *M. bovis* (2%), *M. bovis BCG* (1.5%), and others (1.5%) (ARUP internal communication Mycobacteriology department; Incident rates 2020).

In this study, we show potential for utilizing LC-MS and algorithmic discrimination at the species level for *MTBC* species with high classification success for the clinically most relevant entities. This method offers the ability to generate classification models from large numbers of spectra in a relatively rapid and flexible way. The aim is to determine a common signature among spectra for each of the identified taxa in such a way that spectra of test isolates can be classified accurately. The utilized algorithm uses proteoforms in the approximate mass range of 5 to 40 kDa which were obtained from the mass spectra. A characteristic protein profile in this range provides enough information for the differentiation of various clinically relevant mycobacterial species and clinical isolates at least at species level with accuracy as high as 100% as shown in **Table 1**. While molecular taxonomy of mycobacterium is in general very dynamic, and species and subspecies (lineages) boundaries are evolving with advancement of laboratory technologies, our approach demonstrates the possibility to identify strains to their species by mass spectrometry in a method that matches their current genomic reference.

CONCLUSION

Whole-protein top-down LC-MS analysis has significant diagnostic potential because of its ability to detect proteins routinely in a wider mass range and the method flexibility which can be optimized to provide the necessary protein coverage, e.g. if needed even to discriminate below the species level i.e. at the lineage or strain level. The accurate determination of protein masses, separation of high numbers of individual proteins, and high-resolution enabling detection of single-amino-acid substitutions are responsible for this high performance. Our algorithms showed a potential to recognize individual strains that could be applied in epidemics or outbreak scenarios. This novel assay is the first to use LC-ESI-MS to accurately identify the *M. tuberculosis* complex to the species level. The assay can rapidly, precisely, and accurately discriminate *M. tuberculosis* complex. Most importantly it can discriminate among *M. tuberculosis* complex isolates to the species level. These species are closely related members of the *M. tuberculosis* complex but very diverse pathogenetically. Having an effective and accurate way to distinguish these taxa will help in understanding the epidemiological behavior of these pathogens with a goal of supporting the development of improved diagnostics and treatment. However, our analysis was limited to 7H11 agar medium only and not yet tested with liquid culture medium as well as Loewenstein-Jensen agar which need to be assessed in the future. Additional research is required in targeting a wider species and strain panel, including the entire *MTBC* and its rarer zoonotic taxa, a large sample size and fine-tuned protocols. Algorithmic improvements to increase and further test classification success and to provide confirmatory experimental data to this first proof of principle study splitting

clinically common species in the *M. tuberculosis* species complex will be required to underline the high potential of Orbitrap LCMS technology.

DATA AVAILABILITY STATEMENT

The raw data supporting the conclusions of this article will be made available by the authors, without undue reservation.

AUTHOR CONTRIBUTIONS

AOB and SS have drafted the work, AOB, SS, JF, JBS, and APB designed research, AOB performed experimental work, data acquisition, analysis, AOB and JBS conducted review and editing, JK and JBS performed interpretation of data and computational analysis used for the work, and JF and APB provided funding acquisition, project administration, and resources. All authors contributed to the article and approved the submitted version.

REFERENCES

Alexander, K. A., Laver, P. N., Michel, A. L., Williams, M., van Helden, P. D., Warren, R. M., et al. (2010). Novel Mycobacterium Tuberculosis Complex Pathogen, M. Mungi. *Emerg. Infect. Dis.* 16 (8), 1296–1299. doi: 10.3201/eid1608.100314

Andersen, A., and Brennan, P. (1994). "Proteins and Antigens of Mycobacterium Tuberculosis," in *Tuberculosis* American Society of Microbiology, Wiley Online Library. vol. 307-332. Ed. B. R. Bloom

Arnold, C., Westland, L., Mowat, G., Underwood, A., Magee, J., and Gharbia, S. (2005). Single-Nucleotide Polymorphism-Based Differentiation and Drug Resistance Detection in Mycobacterium Tuberculosis From Isolates or Directly From Sputum. *Clin. Microbiol. Infect.* 11 (2), 122–130. doi: 10.1111/j.1469-0691.2004.01034.x

Ayele, W. Y., Neill, S. D., Zinsstag, J., Weiss, M. G., and Pavlik, I. (2004). Bovine Tuberculosis: An Old Disease But a New Threat to Africa. *Int. J. Tuberc. Lung Dis.* 8 (8), 924–937.

Bhowmick, T., Ghosh, S., Dixit, K., Ganesan, V., Ramagopal, U. A., Dey, D., et al. (2014). Targeting Mycobacterium Tuberculosis Nucleoid-Associated Protein HU With Structure-Based Inhibitors. *Nat. Commun.* 5, 4124. doi: 10.1038/ncomms5124

Bloom, B. R., and Murray, C. J. (1992). Tuberculosis: Commentary on a Reemergent Killer. *Science* 257 (5073), 1055–1064. doi: 10.1126/science.257.5073.1055

Brock, I., Munk, M. E., Kok-Jensen, A., and Andersen, P. (2001). Performance of Whole Blood IFN-Gamma Test for Tuberculosis Diagnosis Based on PPD or the Specific Antigens ESAT-6 and CFP-10. *Int. J. Tuberc. Lung Dis.* 5 (5), 462–467.

Chen, J. H., Yam, W. C., Ngan, A. H., Fung, A. M., Woo, W. L., Yan, M. K., et al. (2013). Advantages of Using Matrix-Assisted Laser Desorption Ionization-Time of Flight Mass Spectrometry as a Rapid Diagnostic Tool for Identification of Yeasts and Mycobacteria in the Clinical Microbiological Laboratory. *J. Clin. Microbiol.* 51 (12), 3981–3987. doi: 10.1128/jcm.01437-13

Chimara, E., Ferrazoli, L., and Leão, S. C. (2004). Mycobacterium Tuberculosis Complex Differentiation Using Gyrb-Restriction Fragment Length Polymorphism Analysis. *Mem Inst Oswaldo Cruz* 99 (7), 745–748. doi: 10.1590/s0074-02762004000700014

DeGeorge, K. C., Holt, H. R., and Hodges, S. C. (2017). Bladder Cancer: Diagnosis and Treatment. *Am. Fam. Phys.* 96 (8), 507–514.

Derese, Y., Hailu, E., Assefa, T., Bekele, Y., Mihret, A., Aseffa, A., et al. (2012). Comparison of PCR With Standard Culture of Fine Needle Aspiration Samples in the Diagnosis of Tuberculosis Lymphadenitis. *J. Infect. Dev. Countries* 6 (1), 53–57. doi: 10.3855/jidc.2050

de Steenwinkel, J. E., de Knegt, G. J., ten Kate, M. T., van Belkum, A., Verbrugh, H. A., Kremer, K., et al. (2010). Time-Kill Kinetics of Anti-Tuberculosis Drugs, and Emergence of Resistance, in Relation to Metabolic Activity of Mycobacterium Tuberculosis. *J. Antimicrob. Chemother.* 65 (12), 2582–2589. doi: 10.1093/jac/dkq374

Djelouadji, Z., Raoult, D., Daffé, M., and Drancourt, M. (2008). A Single-Step Sequencing Method for the Identification of Mycobacterium Tuberculosis Complex Species. *PLoS Negl. Trop. Dis.* 2 (6), e253. doi: 10.1371/journal.pntd.0000253

Doig, C., Seagar, A. L., Watt, B., and Forbes, K. J. (2002). The Efficacy of the Heat Killing of Mycobacterium Tuberculosis. *J. Clin. Pathol.* 55 (10), 778–779. doi: 10.1136/jcp.55.10.778

Dukik, K., Freeke, J., Jamalian, A., van den Ende, B. G., Yip, P., Stephenson, J. L., et al. (2018). Ultra-High-Resolution Mass Spectrometry for Identification of Closely Related Dermatophytes With Different Clinical Predilections. *J. Clin. Microbiol.* 56 (7), 1–11. doi: 10.1128/jcm.00102-18

Frothingham, R. (1995). Differentiation of Strains in Mycobacterium Tuberculosis Complex by DNA Sequence Polymorphisms, Including Rapid Identification of M. Bovis BCG. *J. Clin. Microbiol.* 33 (4), 840–844. doi: 10.1128/jcm.33.4.840-844.1995

Frothingham, R., and Meeker-O'Connell, W. A. (1998). Genetic Diversity in the Mycobacterium Tuberculosis Complex Based on Variable Numbers of Tandem DNA Repeats. *Microbiol. (Reading)* 144 (Pt 5), 1189–1196. doi: 10.1099/00221287-144-5-1189

Gagneux, S., and Small, P. M. (2007). Global Phylogeography of Mycobacterium Tuberculosis and Implications for Tuberculosis Product Development. *Lancet Infect. Dis.* 7 (5), 328–337. doi: 10.1016/s1473-3099(07)70108-1

Ge, Y., El-Naggar, M., Sze, S. K., Oh, H. B., Begley, T. P., McLafferty, F. W., et al. (2003). Top Down Characterization of Secreted Proteins From Mycobacterium Tuberculosis by Electron Capture Dissociation Mass Spectrometry. *J. Am. Soc. Mass Spectrom.* 14 (3), 253–615. doi: 10.1016/s1044-0305(02)00913-3

Godreuil, S., Torrea, G., Terru, D., Chevenet, F., Diagbouga, S., Supply, P., et al. (2007). First Molecular Epidemiology Study of Mycobacterium Tuberculosis in Burkina Faso. *J. Clin. Microbiol.* 45 (3), 921–927. doi: 10.1128/jcm.01918-06

Gunawardena, H. P., Feltcher, M. E., Wrobel, J. A., Gu, S., Braunstein, M., and Chen, X. (2013). Comparison of the Membrane Proteome of Virulent Mycobacterium Tuberculosis and the Attenuated Mycobacterium Bovis BCG Vaccine Strain by Label-Free Quantitative Proteomics. *J. Proteome Res.* 12 (12), 5463–5474. doi: 10.1021/pr400334k

Gupta, R. S., Lo, B., and Son, J. (2018). Phylogenomics and Comparative Genomic Studies Robustly Support Division of the Genus Mycobacterium Into an Emended Genus Mycobacterium and Four Novel Genera. *Front. Microbiol.* 9, 67. doi: 10.3389/fmicb.2018.00067

Hesseling, A. C., Marais, B. J., Gie, R. P., Schaaf, H. S., Fine, P. E., Godfrey-Faussett, P., et al. (2007). The Risk of Disseminated Bacille Calmette-Guerin (BCG) Disease in HIV-Infected Children. *Vaccine* 25 (1), 14–18. doi: 10.1016/j.vaccine.2006.07.020

Hughes, R., Wonderling, D., Li, B., and Higgins, B. (2012). The Cost Effectiveness of Nucleic Acid Amplification Techniques for the Diagnosis of Tuberculosis. *Respir. Med.* 106 (2), 300–307. doi: 10.1016/j.rmed.2011.10.005

Kasai, H., Ezaki, T., and Harayama, S. (2000). Differentiation of Phylogenetically Related Slowly Growing Mycobacteria by Their Gyrb Sequences. *J. Clin. Microbiol.* 38 (1), 301–308.

Landolt, P., Stephan, R., and Scherrer, S. (2019). Development of a New High Resolution Melting (HRM) Assay for Identification and Differentiation of Mycobacterium Tuberculosis Complex Samples. *Sci. Rep.* 9 (1), 1850. doi: 10.1038/s41598-018-38243-6

Larsen, E. S., Joensen, U. N., Poulsen, A. M., Goletti, D., and Johansen, I. S. (2020). Bacillus Calmette-Guérin Immunotherapy for Bladder Cancer: A Review of Immunological Aspects, Clinical Effects and BCG Infections. *Apmis* 128 (2), 92–103. doi: 10.1111/apm.13011

LeDuc, R. D., Taylor, G. K., Kim, Y. B., Januszyk, T. E., Bynum, L. H., Sola, J. V., et al. (2004). Prosight PTM: An Integrated Environment for Protein Identification and Characterization by Top-Down Mass Spectrometry. *Nucleic Acids Res.* 32 (Web Server issue), W340–W345. doi: 10.1093/nar/gkh447

Lévesque, S., Dufresne, P. J., Soualhine, H., Domingo, M. C., Bekal, S., Lefebvre, B., et al. (2015). A Side by Side Comparison of Bruker Biotyper and VITEK MS: Utility of MALDI-TOF MS Technology for Microorganism Identification in a Public Health Reference Laboratory. *PLoS One* 10 (12), e0144878. doi: 10.1371/journal.pone.0144878

Lipworth, S., Jajou, R., de Neeling, A., Bradley, P., van der Hoek, W., Maphalala, G., et al. (2019). SNP-IT Tool for Identifying Subspecies and Associated Lineages of Mycobacterium Tuberculosis Complex. *Emerg. Infect. Dis.* 25 (3), 482–488. doi: 10.3201/eid2503.180894

Louw, G. E., Warren, R. M., Gey van Pittius, N. C., Leon, R., Jimenez, A., Hernandez-Pando, R., et al. (2011). Rifampicin Reduces Susceptibility to Ofloxacin in Rifampicin-Resistant Mycobacterium Tuberculosis Through Efflux. *Am. J. Respir. Crit. Care Med.* 184 (2), 269–276. doi: 10.1164/rccm.201011-1924OC

Mather, C. A., Rivera, S. F., and Butler-Wu, S. M. (2014). Comparison of the Bruker Biotyper and Vitek MS Matrix-Assisted Laser Desorption Ionization-Time of Flight Mass Spectrometry Systems for Identification of Mycobacteria Using Simplified Protein Extraction Protocols. *J. Clin. Microbiol.* 52 (1), 130–138. doi: 10.1128/jcm.01996-13

Mehaffy, M. C., Kruh-Garcia, N. A., and Dobos, K. M. (2012). Prospective on Mycobacterium Tuberculosis Proteomics. *J. Proteome Res.* 11 (1), 17–25. doi: 10.1021/pr2008658

Murdoch, L. E., Maclean, M., Endarko, E., MacGregor, S. J., and Anderson, J. G. (2012). Bactericidal Effects of 405 Nm Light Exposure Demonstrated by Inactivation of Escherichia, Salmonella, Shigella, Listeria, and Mycobacterium Species in Liquid Suspensions and on Exposed Surfaces. *Sci. World J.* 2012, 137805. doi: 10.1100/2012/137805

Niemann, S., Harmsen, D., Rüsch-Gerdes, S., and Richter, E. (2000). Differentiation of Clinical Mycobacterium Tuberculosis Complex Isolates by Gyrb DNA Sequence Polymorphism Analysis. *J. Clin. Microbiol.* 38 (9), 3231–3234. doi: 10.1128/jcm.38.9.3231-3234.2000

Nikam, C., Jagannath, M., Narayanan, M. M., Ramanabhiraman, V., Kazi, M., Shetty, A., et al. (2013). Rapid Diagnosis of Mycobacterium Tuberculosis With Truenat MTB: A Near-Care Approach. *PLoS One* 8 (1), e51121. doi: 10.1371/journal.pone.0051121

Peters, J. S., Nabila, I., Anzaan, D., Shuyi, M., David, R. S., Robin, M. W., et al. (2020). Genetic Diversity in Mycobacterium Tuberculosis Clinical Isolates and Resulting Outcomes of Tuberculosis Infection and Disease. *Annu. Rev. Genet.* 54 (1), 511–537. doi: 10.1146/annurev-genet-022820-085940

Pinsky, B. A., and Banaei, N. (2008). Multiplex Real-Time PCR Assay for Rapid Identification of Mycobacterium Tuberculosis Complex Members to the Species Level. *J. Clin. Microbiol.* 46 (7), 2241–2246. doi: 10.1128/jcm.00347-08

Pounder, J. I., Anderson, C. M., Voelkerding, K. V., Salfinger, M., Dormandy, J., Somoskovi, A., et al. (2010). Mycobacterium Tuberculosis Complex Differentiation by Genomic Deletion Patterns With Multiplex Polymerase Chain Reaction and Melting Analysis. *Diagn. Microbiol. Infect. Dis.* 67 (1), 101–105. doi: 10.1016/j.diagmicrobio.2009.12.014

Prabhakar, S., Mishra, A., Singhal, A., Katoch, V. M., Thakral, S. S., Tyagi, J. S., et al. (2004). Use of the Hupb Gene Encoding a Histone-Like Protein of Mycobacterium Tuberculosis as a Target for Detection and Differentiation of M. Tuberculosis and M. Bovis. *J. Clin. Microbiol.* 42 (6), 2724–2732. doi: 10.1128/jcm.42.6.2724-2732.2004

Reddington, K., Zumla, A., Bates, M., van Soolingen, D., Niemann, S., Barry, T., et al. (2012). Seektb, a Two-Stage Multiplex Real-Time-PCR-Based Method for Differentiation of the Mycobacterium Tuberculosis Complex. *J. Clin. Microbiol.* 50 (7), 2203–2206. doi: 10.1128/jcm.00718-12

Richter, E., Weizenegger, M., Fahr, A. M., and Rüsch-Gerdes, S. (2004). Usefulness of the Genotype MTBC Assay for Differentiating Species of the Mycobacterium Tuberculosis Complex in Cultures Obtained From Clinical Specimens. *J. Clin. Microbiol.* 42 (9), 4303–4306. doi: 10.1128/jcm.42.9.4303-4306.2004

Riojas, M. A., McGough, K. J., Rider-Riojas, C. J., Rastogi, N., and Hazbón, M. H. (2018). Phylogenomic Analysis of the Species of the Mycobacterium Tuberculosis Complex Demonstrates That Mycobacterium Africanum, Mycobacterium Bovis, Mycobacterium Caprae, Mycobacterium Microti and Mycobacterium Pinnipedii are Later Heterotypic Synonyms of Mycobacterium Tuberculosis. *Int. J. Syst. Evol. Microbiol.* 68 (1), 324–332. doi: 10.1099/ijsem.0.002507

Ritz, N., Tebruegge, M., Connell, T. G., Sievers, A., Robins-Browne, R., and Curtis, N. (2009). Susceptibility of Mycobacterium Bovis BCG Vaccine Strains to Antituberculous Antibiotics. *Antimicrob. Agents Chemother.* 53 (1), 316–318. doi: 10.1128/aac.01302-08

Scorpio, A., and Zhang, Y. (1996). Mutations in Pnca, a Gene Encoding Pyrazinamidase/Nicotinamidase, Cause Resistance to the Antituberculous Drug Pyrazinamide in Tubercle Bacillus. *Nat. Med.* 2 (6), 662–667. doi: 10.1038/nm0696-662

Sinha, P., Gupta, A., Prakash, P., Anupurba, S., Tripathi, R., and Srivastava, G. N. (2016). Differentiation of Mycobacterium Tuberculosis Complex From Non-Tubercular Mycobacteria by Nested Multiplex PCR Targeting IS6110, MTP40 and 32kd Alpha Antigen Encoding Gene Fragments. *BMC Infect. Dis.* 16, 123. doi: 10.1186/s12879-016-1450-1

Somoskovi, A., Dormandy, J., Rivenburg, J., Pedrosa, M., McBride, M., and Salfinger, M. (2008). Direct Comparison of the Genotype MTBC and Genomic Deletion Assays in Terms of Ability to Distinguish Between Members of the Mycobacterium Tuberculosis Complex in Clinical Isolates and in Clinical Specimens. *J. Clin. Microbiol.* 46 (5), 1854–1857. doi: 10.1128/jcm.00105-07

Somoskovi, A., Parsons, L. M., and Salfinger, M. (2001). The Molecular Basis of Resistance to Isoniazid, Rifampin, and Pyrazinamide in Mycobacterium Tuberculosis. *Respir. Res.* 2 (3), 164–168. doi: 10.1186/rr54

Sreevatsan, S., Escalante, P., Pan, X., Gillies, D. A., Siddiqui, 2. S., Khalaf, C. N., et al. (1996). Identification of a Polymorphic Nucleotide in Oxyr Specific for Mycobacterium Bovis. *J. Clin. Microbiol.* 34 (8), 2007–2010. doi: 10.1128/jcm.34.8.2007-2010.1996

Supply, P., Magdalena, J., Himpens, S., and Locht, C. (1997). Identification of Novel Intergenic Repetitive Units in a Mycobacterial Two-Component System Operon. *Mol. Microbiol.* 26 (5), 991–1003. doi: 10.1046/j.1365-2958.1997.6361999.x

WHO (2020). "*Global Tuberculosis Report* " Geneva: World Health Organization. (Accessed October 15). Available at: https://www.who.int/tb/publications/global_report/en/.

Conflict of Interest: Authors JF, JBS, and JK were employed by company Thermo Fisher Scientific.

The authors declare that this study received funding from Thermo Fisher Scientific. The funder was involved (equal partner) in the study design, assisting with providing tools and assistance in analyzing the data, and technical interpretation of results. The funder was not further involved in the collection, interpretation of data, the writing of this article (beyond assisting with technical details for the materials and methods and textual review) or the decision to submit it for publication.

frontiers in Cellular and Infection Microbiology

ORIGINAL RESEARCH
published: 06 July 2021
doi: 10.3389/fcimb.2021.687240

Developing Two Rapid Protein Extraction Methods Using Focused-Ultrasonication and Zirconia-Silica Beads for Filamentous Fungi Identification by MALDI-TOF MS

Ya-Ting Ning[1,2,3†], Wen-Hang Yang[1,2,3†], Wei Zhang[2,4], Meng Xiao[1,2,3], Yao Wang[1,3], Jing-Jia Zhang[1,3], Ge Zhang[1,3], Si-Meng Duan[1,3], Ai-Ying Dong[5], Da-Wen Guo[6], Gui-Ling Zou[7], Hai-Nan Wen[8], Yan-Yan Guo[9], Li-Ping Chen[10], Miao Chai[11], Jing-Dong He[12], Qiong Duan[13], Li-Xia Zhang[14], Li Zhang[1,3] and Ying-Chun Xu[1,3*]*

[1] Department of Clinical Laboratory, State Key Laboratory of Complex Severe and Rare Diseases, Peking Union Medical College Hospital, Chinese Academy of Medical Sciences and Peking Union Medical College, Beijing, China, [2] Graduate School, Chinese Academy of Medical Sciences and Peking Union Medical College, Beijing, China, [3] Beijing Key Laboratory for Mechanisms Research and Precision Diagnosis of Invasive Fungal Diseases, Beijing, China, [4] Clinical Microbiology Laboratory, The First Affiliated Hospital of Hebei North University, Zhangjiakou, China, [5] Department of Clinical Laboratory, North China University of Science and Technology Affiliated Hospital, Tangshan, China, [6] Department of Clinical Laboratory, The First Affiliated Hospital of Harbin Medical University, Harbin, China, [7] Department of Clinical Laboratory, The Fourth Affiliated Hospital of Harbin Medical University, Harbin, China, [8] Department of Laboratory, The Affiliated Hospital of Chengde Medical University, Chengde, China, [9] Department of Clinical Laboratory, Tangshan Worker's Hospital, Tangshan, China, [10] Department of Laboratory Medicine, Mudanjiang First People's Hospital, Heilongjiang, China, [11] Department of Clinical Laboratory, The First Hospital of Harbin, Harbin, China, [12] Department of Clinical Laboratory, Tianjin Chest Hospital, Tianjin, China, [13] Department of Clinical Laboratory, Jinling Province People's Hospital, Jinling, China, [14] Department of Clinical Laboratory, Shanxi Provincial People's Hospital, Taiyuan, China

Filamentous fungi identification by Matrix-assisted laser desorption ionization time-of-flight mass spectrometry (MALDI-TOF MS) has been challenging due to the lack of simple and rapid protein extraction methods and insufficient species coverage in the database. In this study, we created two rapid protein extraction methods for filamentous fungi: a one-step zirconia-silica beads method (ZSB) and a focused-ultrasonication method (FUS). The identification accuracy of two methods were evaluated with the VITEK MS, as well as number of spectra peaks and signal-to-noise ratio (S/N) with M-Discover 100 MALDI-TOF MS compared to the routine method. The better method was applied to build a filamentous fungi in-house spectra library for the M-Discover 100 MS, and then another one and routine method were performed in parallel to verify the accuracy and commonality of the in-house library. Using the two optimized methods, the dedicated operating time before MALDI-TOF MS analysis was reduced from 30 min to 7 (ZSB) or 5 (FUS) min per sample, with only a few seconds added for each additional strain. And both two methods identified isolates from most mold types equal to or better than the routine method, and the total correct identification rate using VITEK MS was 79.67, 76.42, and 76.42%, respectively. On the other hand, the two rapid methods generally achieved higher maximum and minimum S/N ratios with these isolates tested as compared to the

OPEN ACCESS

Edited by:
Yi-Wei Tang,
Cepheid, United States

Reviewed by:
Bryan Schmitt,
Indiana University Bloomington, United States
Xinxin Lu,
Capital Medical University, China

***Correspondence:**
Li Zhang
zhangli19870711@163.com
Ying-Chun Xu
xycpumch@139.com

[†]These authors have contributed equally to this work and share first authorship

Specialty section:
This article was submitted to Clinical Microbiology, a section of the journal Frontiers in Cellular and Infection Microbiology

Received: *29 March 2021*
Accepted: *14 June 2021*
Published: *06 July 2021*

Citation:
Ning Y-T, Yang W-H, Zhang W, Xiao M, Wang Y, Zhang J-J, Zhang G, Duan S-M, Dong A-Y, Guo D-W, Zou G-L, Wen H-N, Guo Y-Y, Chen L-P, Chai M, He J-D, Duan Q, Zhang L-X, Zhang L and Xu Y-C (2021) Developing Two Rapid Protein Extraction Methods Using Focused-Ultrasonication and Zirconia-Silica Beads for Filamentous Fungi Identification by MALDI-TOF MS. Front. Cell. Infect. Microbiol. 11:687240. doi: 10.3389/fcimb.2021.687240

routine method. Besides, the ZSB method produced overall mean of maximum and minimum S/N ratio higher than that by FUS. An in-house library of M-Discover MS was successfully built from 135 isolates from 42 species belonging to 18 genera using the ZSB method. Analysis of 467 isolates resulted in 97.22% correctly identified isolates to the species level by the ZSB method *versus* 95.50% by the routine method. The two novel methods are time- and cost-effective and allow efficient identification of filamentous fungi while providing a simplified procedure to build an in-house library. Thus, more clinical laboratories may consider adopting MALDI-TOF MS for filamentous fungi identification in the future.

Keywords: filamentous fungi, MALDI-TOF MS, protein extraction, sample processing, zirconia-silica beads, focused-ultrasonication, in-house library

INTRODUCTION

In recent years, fungi have come to pose a serious threat to immunocompromised patients with leukemia, AIDS, or receiving chemotherapy intervention, etc. (Enoch et al., 2006; Benedict et al., 2017; Bongomin et al., 2017). Even though *Candida* remains the leading invasive fungi pathogen, infections due to filamentous fungi are gradually rising with high mortality (Enoch et al., 2006; Liao et al., 2013; Benedict et al., 2017; Bongomin et al., 2017). However, appropriate treatment often varies by species, thus making rapid identification essential for accurate diagnosis and better outcomes (Brown et al., 2012). Conventional identification methods of filamentous fungi based on morphological traits are time-consuming and require extensive expertise training (Larone, 2011). Moreover, less common or non-sporulating molds are difficult to identify, and phylogenetically related species with similar morphological features are challenging to discriminate (Kozel and Wickes, 2014; Li et al., 2017; Luethy and Zelazny, 2018; Wickes and Wiederhold, 2018). Molecular identification is the gold standard method to identify the above strains, but is relatively expensive and requires specialized equipment which limits its routine use in clinical laboratories (Balajee et al., 2007; Samson et al., 2014; Wickes and Wiederhold, 2018).

Matrix-assisted laser desorption/ionization-time of flight mass spectrometry (MALDI-TOF MS) has emerged as a cost-effective and rapid alternative for mycobacterial, bacterial, and yeast identification (Seng et al., 2009; Fraser et al., 2016; Rodriguez-Sanchez et al., 2016). Currently, its use for the identification of filamentous fungi has gradually begun to be implemented in clinical microbiology laboratories, but has been hampered by commercial databases with limited coverage of filamentous fungi taxa and challenges of protein extraction to obtain good quality mass spectra for analysis (Welham et al., 2000; Cassagne et al., 2016; Santos et al., 2017). Building an in-house database that contains local or less common isolates is the most optimal way to overcome the deficiencies of commercial databases (Zvezdanova et al., 2019). At present, several in-house databases in the Bruker MALDI Biotyper (Bruker Daltonics, Germany) have been developed by laboratories, significantly increasing species-assignment of filamentous fungi (De Carolis et al., 2012; Becker et al., 2014; Gautier et al., 2014; Schulthess et al., 2014; Luethy and Zelazny, 2018; Zvezdanova et al., 2019).

Protein extraction is the most critical step of filamentous fungi identification by MALDI-TOF MS, but this process faces challenges due to the robust chitinous cell wall of filamentous fungi and necessitating protein extraction via a process usually initialized by cell homogenization (Shapaval et al., 2017; Krishnaswamy et al., 2019). Moreover, routine protein extraction methods in the manufacturer's instructions and laboratory-developed procedures involve multiple steps (i.e. wash, inactivation, chemical extraction) and require 30 min to over an hour to perform (Chakrabarti et al., 2015; Cassagne et al., 2016). Thus, a simpler and more rapid procedure for protein extraction is urgently needed to permit routine use of MALDI-TOF MS for filamentous fungi identification in clinical laboratories. Ultrasound disruption is a common mechanical cell homogenization method based on high shear force, applied successfully in MALDI-TOF MS for mycobacterial identification and LC-MS/MS (Klimek-Ochab et al., 2011; Adams et al., 2016). Adaptive focused acoustics *via* concentrated bursts of higher-frequency ultrasonic energy allows for rapid disruption of the cell wall and concomitant protein extraction into the extraction solution within minutes (Li et al., 2015; Adams et al., 2016). Another mechanical method is bead milling, such as through the use of zirconia-silica beads and zirconium beads (Krishnaswamy et al., 2019). Proteins are released by the action of circulating beads dispersed in the fluid (Doucha and Livansky, 2008; Klimek-Ochab et al., 2011).

To simplify and expedite the sample processing before the identification of filamentous fungi isolates by MALDI-TOF MS, we created two rapid protein extraction procedures: the one-step zirconia-silica beads (ZSB) method and the focused-ultrasonication method (FUS). In this study, we investigated the identification accuracy of two rapid sample processing methods in the VITEK MALDI-TOF MS system (bioMérieux, Marcy-l'Étoile, France), as well as number of mass peaks and signal-to-noise (S/N) ratio in M-Discover 100 MALDI-TOF MS (Zhuhai Meihua Medical Technology Co., Ltd., China) *versus* the routine method. Then according to the results, applied the better method as a means to build a filamentous fungi in-house spectra library for the M-Discover 100 MS. In addition, we evaluated the accuracy and

commonality of the in-house library using the new method consisting of building the database and the routine method.

METHODS AND MATERIALS

Isolates and Species Identification

A total of 602 non-duplicate mold isolates recovered from various clinical specimens of patients were under the China Hospital Invasive Fungal Surveillance Net–North China Program. Isolates were cultured on Sabouraud Dextrose Agar (SDA) plates (Becton Dickinson Microbiology Systems, Sparks, MD, USA) and incubated at 28°C for 2 to 5 days, and mycelia were collected for genomic DNA extraction. The internal transcribed spacer region was carried out as the primary sequencing gene for species level identification (Zvezdanova et al., 2019). The β-tubulin gene was employed additionally for the *Scedosporium/Pseudallescheria* spp., as well as the translation elongation factor 1-α gene for the *Fusarium* spp. (Gilgado et al., 2008; Wang et al., 2011). Sequencing data was analyzed using the National Center for Biotechnology Information (NCBI) or Mycobank database, and the results were accepted if homology >98% with >95% query coverage. One hundred twenty-three isolates belonging to 13 mold genera and 29 species were analyzed by VITEK MS to evaluate three protein extracting methods (**Table 1**). Another 135 clinical isolates were included in the in-house library of M-Discover 100

TABLE 1 | Identification of 123 clinical filamentous fungi isolates by VITEK MS using the routine method in comparison with two rapid methods.

Identification by DNA sequencing analysis	Reference spectra	Number	Routine method			ZSB method			FUS method		
			Correct ID	Incomplete ID	No ID	Correct ID	Incomplete ID	No ID	Correct ID	Incomplete ID	No ID
Aspergillus	**total**	**66**	**64**	**0**	**2**	**64**	**0**	**2**	**63**	**0**	**3**
*A. flavus**	√	10	10	0	0	10	0	0	10	0	0
A. fumigatus	√	10	9	0	1	10	0	0	10	0	0
A. lentulus	√	3	3	0	0	3	0	0	3	0	0
A. luchuensis	×	1	0	0	1	0	0	1	0	0	1
A. nidulans	√	10	10	0	0	10	0	0	8	0	2
A. niger	√	10	10	0	0	10	0	0	10	0	0
A. sydowii	√	1	1	0	0	1	0	0	1	0	0
A. terreus	√	10	10	0	0	10	0	0	10	0	0
*A. tubingensis**	√	10	10	0	0	9	0	1	10	0	0
*A. ustus**	√	1	1	0	0	1	0	0	1	0	0
Fusarium	**total**	**22**	**13**	**6**	**3**	**16**	**5**	**1**	**14**	**6**	**2**
F. incarnatum	×	1	0	1 (*Fch* complex)	0	0	0	1	0	0	1
F. proliferatum	√	6	1	2 (*Fve/pr*), 1 (*Fve*)	2	2	4 (*F. ve*)	0	1	3 (*Fve*), 1 (*Fve/pr*)	1
F. solani	√	9	9	0	0	9	0	0	9	0	0
F. verticillioides	√	6	3	1 (*F. ve/pr*), 1 (*F. pr*)	1	5	1 (*F. ve/pr*)	0	4	2 (*Fve/pr*)	0
Penicillium	**total**	**12**	**2**	**0**	**10**	**2**	**0**	**10**	**1**	**0**	**11**
P. chrysogenum	√	1	1	0	0	1	0	0	0	0	1
P. citrinum	√	1	1	0	0	1	0	0	1	0	0
P. oxalicum	×	10	0	0	10	0	0	10	0	0	10
Scedosporium	**total**	**5**	**3**	**0**	**2**	**4**	**0**	**1**	**4**	**0**	**1**
S. apiospermum	√	2	1	0	1	2	0	0	2	0	0
S. aurantiacum	×	1	0	0	1	0	0	1	0	0	1
S. boydii	√	2	2#	0	0	2#	0	0	2#	0	0
Others	**total**	**18**	**12**	**0**	**6**	**12**	**0**	**6**	**13**	**0**	**5**
Alternaria alternata	√	3	1	0	2	1	0	2	2	0	1
Beauveria bassiana	√	1	1	0	0	0	0	1	0	0	1
*Geotrichum candidum**	√	3	2	0	1	3	0	0	3	0	0
Mucor circinelloides	√	1	1	0	0	1	0	0	1	0	0
Rhizopus oryzae	√	2	2	0	0	2	0	0	2	0	0
Scopulariopsis brevicaulis	×	1	0	0	1	0	0	1	0	0	1
Sporothrix schenckii	√	1	1	0	0	1	0	0	1	0	0
Syncephalastrum racemosum	×	2	0	0	2	0	0	2	0	0	2
Trichoderma longibrachiatum	√	4	4	0	0	4	0	0	4	0	0
Total		**123**	**94**	**6**	**23**	**98**	**5**	**20**	**95**	**6**	**22**

*According to the specification of database v3.2, the proteomes of some species are so similar that it is difficult for VITEK MS to distinguish, such as *A. flavus* and *A. oryzae*, *A. calidoustus* and *A. ustus*, Geotrichum candidum and Geotrichum klebahnii, as well as *A. tubingensis* which shows "A. niger complex". Those results were all considered as "correct-ID".

VITEK MS identified *S. boydii* (Pseudallescheria boydii's asexual stage) as Pseudallescheria boydii. These results were considered as correct.

ID, identification; Fch, *F. chlamydosporum*; Fve, *F. verticillioides*; Fpr, *F. proliferatum*; Fve/pr, *F. verticillioides/proliferatum*.

TABLE 2 | List of isolates included in the in-house library of M-Discover 100 MS.

Identification by DNA sequencing analysis	Number of isolates
Aspergillus	
A. fumigatus	15
A. insuetus	2
A. japonicus	1
A. lentulus	1
A. luchuensis	3
A. nidulans	10
A. niger	15
A. oryzae	4
A. pseudoglaucus	1
A. ruber	1
A. sydowii	8
A. tamarii	3
A. terreus	12
A. tubingensis	15
A. uvarum	1
Penicillium	
P. chermesinum	1
P. citrinum	2
P. oxalicum	7
Scedosporium	
S. apiospermum	1
S. aurantiacum	1
S. boydii	1
Trichoderma	
T. longibrachiatum	1
T. asahii	2
T. coremiiforme	1
T. japonicum	1
Others	
Alternaria alternata	1
Arthrinium spp.	1
Beauveria bassiana	1
Doratomyces spp.	1
Exophiala dermatitidis	2
Geotrichum candidum	2
Monascus purpureus	1
Mucor circinelloides	3
Paecilomyces variotii	1
Phanerochaete chrysosporium	1
Rhizomucor pusillus	1
Rhizopus microsporus	4
Rhizopus oryzae	1
Scopulariopsis spp.	1
Syncephalastrum racemosum	2
Talaromyces funiculosus	1
Talaromyces stollii	1
Total	**135**

MS (**Table 2**); the remaining 467 isolates were analyzed using the in-house library coupled with the rapid method and routine method (**Table 3**).

Protein Extraction

The Routine Three-Step Method

Isolates were inoculated on SDA plates at 28°C for 3 days. The routine method for protein preparation was performed according to the manufacturer's instructions as described by Li et al. (Li et al., 2017). Briefly, one to two colonies (~OD_{600} of 2.0) were mixed with 900 µl ethanol and 300 µl distilled water, followed by centrifugation for 3 min at 13,800 g. The pellet was dried at room temperature (RT) for 5 min, and then re-suspended in 50–80 µl of 70% formic acid (FA). After an incubation of 5 min at RT, an equal volume of acetonitrile was added. Samples were incubated again at RT for 5 min and subsequently centrifuged at 13,800 g for 1 min.

One-Step Zirconia-Silica Beads Method (ZSB)

Rapid extraction of protein using the ZSB method was performed using the same cultures as the routine method. Approximately 1–2 cm^2 pieces of mold were removed from the agar and added to a 1.5 ml tube containing 30 µl of zirconia-silica beads with a diameter of 0.5 mm and 60 ul extraction solution (consisting of 30 ul acetonitrile and 30 ul FA). The tubes were vortexed for 5 min at RT, and then centrifuged for 1 min at 13,800 g.

Focused-Ultrasonication Method (FUS)

One to two colonies were added to a microtube containing 80 ul of extraction solution, and then processed in a precooled focused-ultrasonicator (Longlight Technology Co., Ltd, China) under the following conditions: pulse period of 500, pulse width of 250, running power of 100, running time of 60 s, and water temperature at 15°C.

Evaluation of Protein Extraction Methods

Two novel methods of protein extraction were evaluated in parallel with the routine method. One microliter of supernatant after treatment was transferred to the target plate and allowed to dry at RT before being overlaid with 1 ul of matrix solution (α-cyano-4-hydroxy-cinnamic acid). The acquisition and analysis of mass spectra were performed by VITEK MALDI-TOF MS using the Vitek MS database (MS-ID version v3.2). The results were interpreted referred the manufacturer's instructions. An isolate was considered correctly identified with an acceptable confidence value of 99.9%. Samples were analyzed in duplicates and repeated when there were discrepancies and isolates exhibited discrepant identification results. Results were compared with the sequencing-based identification results and grouped into four categories: a) correct identification: identical to sequencing results, b) incomplete identification (Incomplete ID): either only the genus level was correctly identified or more than one species was proposed and one was correct, c) misidentification (Mis-ID): none of the proposed species were correct, or d) no identification (no-ID).

Spectra were validated with 123 strains by M-Discover 100 MS. The number of peaks and S/N ratios were determined by using the program provided by M-Discover. The maximum (or minimum) S/N ratio is defined as the height of the highest (or lowest) mass peak above its baseline relative to the standard deviation of the noise.

In-House Database Construction and Clinical Isolates Identification

According to the evaluation results, we selected the more efficient method to build an in-house library for M-Discover 100 MS. One hundred thirty-five isolates were included in the in-house spectra library (**Table 2**) after following the manufacturer's instructions. Freshly prepared isolates were processed and spotted onto

TABLE 3 | 467 clinical filamentous fungi isolates identified by M-Discover 100 MS with the in-house library using the ZSB method in comparison with the routine method.

Identification by DNA sequencing analysis	Number	ZSB method								Routine method							
		Correct ID to Species Level				Only Correct ID to Genus Level		Mis ID		Correct ID to Species Level				Only Correct ID to Genus Level		Mis ID	
		Subtotal	≥90	90–60	≤60	Number	score	Number	score	Subtotal	≥90	90–60	≤60	Number	score	Number	score
Aspergillus																	
A. flavus/oryzae	63	63	55	8	0	0	–	0	–	63	46	15	2	0	–	0	–
A. fumigatus	184	184	180	4	0	0	–	0	–	183	179	3	1	1	–	0	–
A. lentulus	2	1	1	0	0	1	≤60	0	–	1	1	0	0	1	–	0	–
A. luchuensis	1	1	1	0	0	0	–	0	–	1	1	0	0	0	–	0	–
A. nidulans	20	20	19	1	0	0	–	0	–	20	17	3	0	0	–	0	–
A. niger	58	58	58	0	0	0	–	0	–	58	53	5	0	0	–	0	–
A. sydowii	1	1	0	1	0	0	–	0	–	1	0	1	0	0	–	0	–
A. terreus	32	32	27	5	0	0	–	0	–	32	27	5	0	0	–	0	–
A. tubingensis	36	35	35	0	0	1	≤60	0	–	35	32	3	0	1	≤60	0	–
A. ustus	1	1	1	0	0	0	–	0	–	1	1	0	0	0	–	0	–
Subtotal	**398**	**396**	**377**	**19**	**0**	**2**	**-**	**0**	**-**	**395**	**357**	**35**	**3**	**3**	**-**	**0**	**-**
Fusarium																	
F. moniliforme	5	4	3	1	0	1	90–60	0	–	4	2	2	0	1	90–60	0	–
F. proliferatum	6	6	0	6	0	0	–	0	–	4	0	2	2	1	90–60	1	≤60
F. solani	9	7	4	3	0	0	–	2	≤60	8	0	5	3	0	–	1	≤60
F. verticillioides	6	0	0	0	0	6	3(>90) 3(90–60)	0	–	0	0	0	0	6	2(>90) 3 (90–60) 1 (≤60)	0	–
Subtotal	**26**	**17**	**7**	**10**	**0**	**7**	**0**	**2**		**16**	**2**	**9**	**5**	**8**	**-**	**2**	**-**
Penicillium																	
P. chrysogenum	1	1	0	0	1	0	–	0	–	1	0	0	1	0	–	0	–
P. citrinum	1	1	1	0	0	0	–	0	–	1	1	0	0	0	–	0	–
P. oxalicum	16	16	16	0	0	0	–	0	–	16	15	1	0	0	–	0	–
Subtotal	**18**	**18**	**17**		**1**	**0**	**-**	**0**	**-**	**18**	**16**	**1**	**1**	**0**	**-**	**0**	**-**
Scedosporium																	
S. apiospermum	2	2	1	1	0	0	–	0	–	2	1	1	0	0	–	0	–
S. aurantiacum	1	1	1	0	0	0	–	0	–	1	1	0	0	0	–	0	–
S. boydii	2	2	2	0	0	0	–	0	–	2	2	0	0	0	–	0	–
Subtotal	**5**	**5**	**4**	**1**	**0**	**0**	**-**	**0**	**-**	**5**	**4**	**1**	**0**	**0**	**-**	**0**	**-**
Others																	
Alternaria alternata	3	3	3	0	0	0	–	0	–	2	0	2	0	0	–	1	≤60
Beauveria bassiana	1	1	0	1	0	0	–	0	–	0	0	0	0	0	–	1	≤60
Geotrichum candidum	3	3	3	0	0	0	–	0	–	3	3	0	0	0	–	0	–
Mucor circinelloides	1	1	1	0	0	0	–	0	–	1	1	0	0	0	–	0	–
Rhizopus oryzae	2	0	0	0	0	1	≤60	1	≤60	0	0	0	0	0	–	2	≤60
Scopulariopsis brevicaulis	1	1	1	0	0	0	–	0	–	1	1	0	0	0	–	0	–
Sporothrix schenckii	1	1	0	0	1	0	–	0	–	1	0	0	1	0	–	0	–
Syncephalastrum racemosum	2	2	1		1	0	–	0	–	1	1	0	0	0	–	1	≤60
Trichoderma longibrachiatum	4	4	4	0	0	0	–	0	–	1	1	0	0	3	90–60		–
Trichosporon asahii	2	2	1	1	0	0	–	0	–	2	2	0	0	0	–	0	–
Subtotal	**20**	**18**	**14**	**2**	**2**	**1**	**-**	**1**	**-**	**12**	**9**	**2**	**1**	**3**	**-**	**5**	**-**
Total	**467**	**454**	**419**	**32**	**3**	**10**	**-**	**3**	**-**	**446**	**388**	**48**	**10**	**14**	**-**	**7**	**-**

eight-well positions on the target plate. Each position was read three times. After excluding the spectra that were obviously abnormal with others, 20 to 24 replica spectra of each strain were added to the in-house library. To verify the accuracy and commonality of the in-house library, the remaining 467 isolates were analyzed. Following the instructions of M-Discover 100 MS, identification scores of ≥90 indicated species-level identification, scores of 60–90 indicated genus-level identification, and scores of ≤60 were considered as "not reliable" (NRI). If isolates exhibited discrepant identification results or produced low matches by M-Discover 100 MS analysis and sequencing analysis, identification by M-Discover 100 MS analysis for the isolates was repeated. In this study, results were compared at the species and genus level with those obtained by sequencing regardless of score values, and grouped into three categories: a) correct identification to species level, b) only correct identification to genus level, c) misidentification.

Statistical Analysis

Comparison for the identification rates of three protein extraction methods was performed using GraphPad Prism software. This software was also used to compare scores, the peak number, and S/N ratios between two groups *via* a paired t-test. $P < 0.05$ indicated a statistically significant difference (*p values < 0.05, **p values < 0.01, ***p values < 0.005, ****p values < 0.001).

RESULTS

Comparison of Identification Performance in VITEK MS

Table 1 demonstrates the performance of the VITEK MS system for identifying 123 filamentous fungi clinical isolates using the routine and two rapid methods. Among isolates that underwent repeat testing due to discrepancies with the sequencing results, the repeat and original results were consistent. Testing of clinical isolates with two rapid methods revealed significant time savings compared to the routine method. Following the routine procedure, each filamentous fungi isolate required at least 30 min of sample processing, while the ZSB and FUS method reduced the dedicated operating time to 7 or 5 min per sample, respectively, with only a few seconds added for each additional strain.

Applying the routine protein extraction method recommended by the manufacturer, VITEK MS correctly identified (species-level identification) 94 (76.42%) isolates, whereas 98 (79.67%) and 95 (76.42%) isolates by ZSB and FUS method, respectively. "Incomplete ID" results were produced by the routine and FUS methods for 6 (4.88%) isolates, and 5 isolates (4.07%) by the ZSB method, which all belonged to the *Fusarium* spp. None of isolates showed a "Mis-ID" result using all methods, while 23 (18.70%), 20 (16.26%) and 22 (17.89%) isolates had "no-ID" results by the routine, ZSB, and FUS methods. Of these "no-ID" isolates, 16 isolates belonging to six species were due to no reference spectra available in v3.2 database, except one *F. incarnatum* that was correctly identified to genus level as "*F. chlamydosporum complex*" by the routine method.

After excluding the isolates that lacked reference spectra, the success rate of identification by VITEK MS applying the routine, ZSB, or FUS method was 92.52% (99/107) *vs* 96.26% (103/107) *vs* 94.39% (94/107), and the accuracy was up to 100% for *Aspergillus*, *Penicillium*, *Scedosporium*, and other spp., except for *Fusarium* spp. with 72.22% (13/18), 76.19% (16/21), and 70.00% (14/20), respectively by three methods. The remaining 8 (8.75%), 4 (2.50%), and 6 (6.25%) isolates had "no-ID", respectively. Upon further analysis, for the *Fusarium* spp., the VITEK MS showed good ability to identify *F. solani* (100% accuracy rate by three methods), but could not accurately identify *F. proliferatum* and *F. verticillioides*. The identification ability for *F. proliferatum* and *F. verticillioides* by the ZSB method was 33.33% (1/6) and 83.33% (5/6) with none showing as "no-ID", followed by the FUS method showing 16.67% (1/6) and 66.67% (4/6) with only one *F. proliferatum* as "no-ID", and 16.67% (1/6) and 33.33% (2/6), with two *F. proliferatum* and one *F. verticillioides* showing as "no-ID" by the routine method. VITEK MS was unable to distinguish between the remaining *F. proliferatum* and *F. verticillioides*.

Overall, both ZSB and FUS methods identified isolates from each mold type equal to or better than the routine method without statistically significant differences.

Comparison of Spectral Characteristics in M-Discover 100 MS

Table S1 shows the number of peaks per strain by three methods. Overall, the number of peaks performed by the routine method was significantly higher than that of two rapid methods ($P < 0.0001$). Among the 123 isolates, the peak number of 28 strains extracted by ZSB was more than that extracted by routine method, and 6 strains were the same, mainly distributed in *Aspergillus terreus* and *A. tubingensis*. For FUS, 32 strains more than, while 12 strains equal to that of routine method, mainly distributed in *A. flavus*, *A. terreus*, and *A. tubingensis*. And the results of FUS were significantly higher than ZSB ($P = 0.0129$).

The minimum and maximum S/N ratios for each isolate are showed in **Figure 1**. Overall comparing with routine method, significant increase in minimum S/N ratios was noted for ZSB ($P < 0.0001$) and FUS ($P = 0.0041$) (**Figure 1A**). The mean ratio for each species that had two clinical isolates was higher for 16/18 species by ZSB and for 14/18 species by the FUS method, lower than the routine method for *A. terreus* and *A. tubingensis* by ZSB, and *A. flavus*, *A. lentulus*, *A. niger*, *A. terreus* by FUS. In addition, statistically higher minimum S/N ratios were obtained for *A. nidulans*, *F. solani*, *P. oxalicum*, and *T. longibrachiatum* by both two rapid methods, and *Alternaria alternata* and *S. apiospermum* only by ZSB as compared to the routine method.

As observed for the maximum S/N ratios, the two rapid method achieved higher overall mean ratio with the 123 isolates (1,784.1, 1,678.4, and 1,514.4 for the ZSB, FUS, routine method, respectively). Statistically higher maximum S/N ratios were obtained for *A. nidulans*, *A. tubingensis*, and *P. oxalicum* by

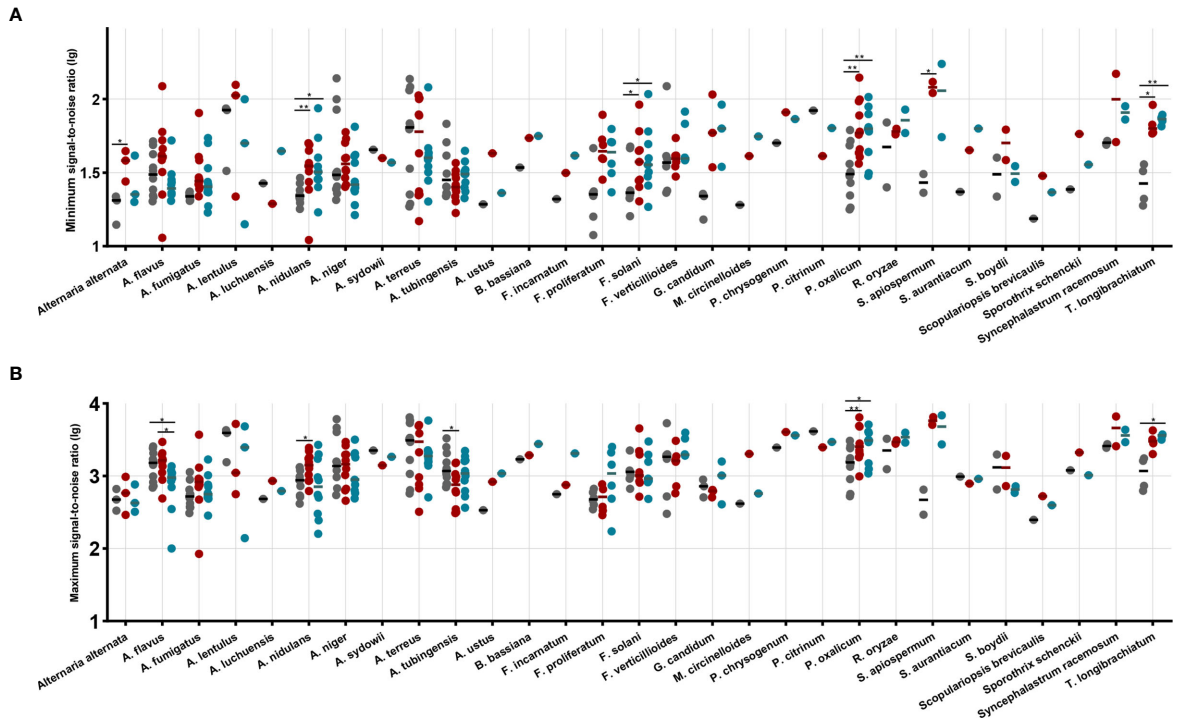

FIGURE 1 | The maximum signal-to-noise ratio **(A)** and the minimum signal-to-noise ratio **(B)** by species and by method performed. Each dot represents the signal-to-noise ratio (lg) for each isolate identification achieved by routine (black dots), ZSB (red dots), and FUS (blue dots) methods. Horizontal bars represent the mean ratio (lg) achieved by each method for each species including at least two isolates. A paired t-test was performed to analyze differences between each two groups, and statistical significance was defined by p values less than 0.05 (*$p < 0.05$, **$p < 0.01$).

ZSB, while for *A. flavus*, *P. oxalicum*, and *T. longibrachiatum* by FUS as compared to the routine method. The ZSB method produced overall mean ratio higher than that by FUS, and showed superior performance for *A. flavus* compared to FUS (**Figure 1B**).

Identification of Filamentous Fungi by In-House Library of M-Discover 100 MS Built by ZSB

According to the above evaluation results, we selected the ZSB method to build an in-house library for M-Discover 100 MS. From the 135 strains distributed by 42 species and 18 genera (**Table 2**), 2,960 reference spectra were successfully created.

Of the 467 clinical isolates tested, the implementation of the ZSB protein extraction method allowed the correct identification of 99.50% *Aspergillus*, 65.38% *Fusarium* (absent in the in-house library), 100% *Penicillium/Scedosporium*, 90% other molds, and 454/467 (97.22%) total clinical isolates by M-Discover 100 MS at the species level using the in-house library regardless of score values (**Table 3**). Among these 454 isolates, the scores were between 55.76 and 96.90 (median 92.6). A score of ≥90 was obtained for 419 isolates (92.30%), a score of 60–90 for 32 isolates (7.05%), and a score of ≤60 for 3 isolates (0.66%). Ten isolates (2.20%) were identified at the genus level. All *F. verticillioide* (n = 6) and one *F. moniliforme* were identified as *F. moniliforme* (n = 4)/*F. proliferatum* (n = 2, scores 60–90) and *F. proliferatum*; one *A. lentulus*, one *A. tubingensis*, and one *Rhizopus oryzae* were unreliably identified as *A. uvarum* (score 40.94), *A. niger* (score 52.25), and *R. baikonurensis* (score 43.41). In addition, two *F. solani* and one *R. oryzae* were completely misidentified as *Mycobacterium immunogenum/M. malmoense* and *Nocardia cyriacigeorgicascore* (all scores ≤60).

In contrast, when the routine method was coupled with the in-house library, the correct species-level identification rate was 99.74%%, 61.54%%, 100%, 60%, and 95.50% (n = 446, scores ≥90 for 388 isolates, 60–90 for 48 isolates, and ≤60 for 10 isolates) for *Aspergillus*, *Fusarium*, *Penicillium/Scedosporium*, other molds, and total isolates, respectively, and 3.00% (n = 14) to the genus level, thus demonstrating a 1.50% (n = 7, and all with NRI) discrepancy compared to molecular identification. There was no statistically significant difference between the routine and ZSB methods using the in-house library. However, the ability to identify the *Fusarium* spp. was relatively weak. Among 16/26 (61.54%) correctly identified *Fusarium* spp. isolates, only two *F. moniliforme* were completely identified with a high confidence level (score ≥90) and up to five isolates with NRI. In addition, compared to the ZSB method, the routine method was inferior for some rare species, including *Alternaria alternata*, *Beauveria bassiana*, *Rhizopus oryzae*, *Syncephalastrum racemosum*.

The distribution and mean scores for each species that was isolated at least twice from individual clinical samples are shown in **Figure 2**. When coupled with the M-Discover

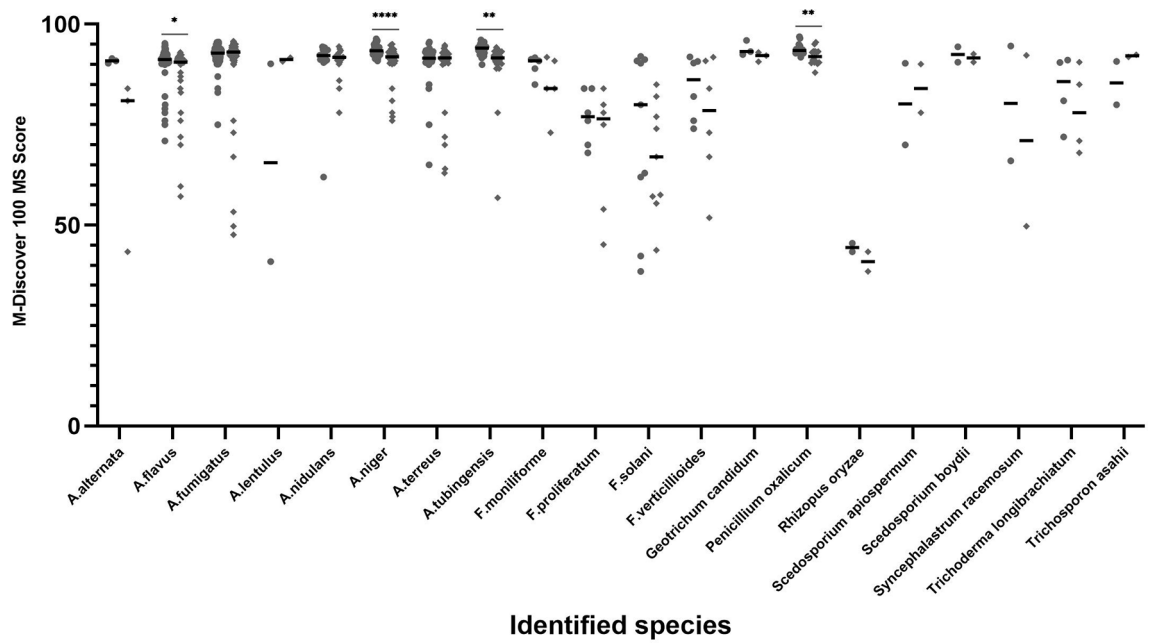

FIGURE 2 | Average score and distribution by M-Discover 100 with the in-house library by method performed. Each dot represents the score for each isolate identification achieved by the ZSB (round dots) and routine (diamond dots) methods. Horizontal bars represent the mean identification score achieved by each method for each species including at least two isolates. A paired t-test was performed to analyze differences between the ZSB method and the routine method, and statistical significance was defined by p values less than 0.05 (*$p < 0.05$, **$p < 0.01$, ****$p < 0.001$).

100 in-house library, the ZSB method showed comparable or higher maximum and mean scores for most species with the exception of *A. lentulus* and *Scedosporium apiospermum.* For the 20 species included, statistically significant differences were only observed in four species (*A. flavus*, *A. niger*, *A. tubinensis*, and *P. oxalicum*). From the point of the score classification, the species-level identification accuracy of strains with the identification score of ≥90 was 99.29% (419/422) provided by ZSB method and 99.49% (388/390) by the routine method. When the species-level cutoff value was artificially set to 60, the correct species-level identification rate was 98.47% (451/458) by ZSB and 98.20% (436/444) by routine method.

In addition, the use of the FUS method by the M-Discover 100 system simultaneously using the in-house library also showed good species-assignment of filamentous fungi (87.00%, 107/123), which was better than routine method (84.55%, 104/123), but inferior to the ZSB method (90.24%) (**Table S2**).

DISCUSSION

MALDI-TOF MS has gradually been popularized as an accurate, rapid and cost-effective method for routine identification of clinical filamentous fungi. However, unlike yeast and bacteria, routine clinical use for filamentous fungi is hindered by two main reasons: (i) insufficient filamentous fungi coverage in the commercial database (Schulthess et al., 2014; Li et al., 2017); (ii) prolonged testing time due to the multi-step protein extraction procedure.

To improve work efficiency, we created the one-step zirconia-silica beads method and focused-ultrasonication method for protein extraction. With the routine procedure, each filamentous fungi isolate required at least 30 min of sample processing before MALDI-TOF MS analysis (Luethy and Zelazny, 2018). The two optimized methods, however, negated the separate inactivation step without reducing the effect (no growth within 14 days after treated), while significantly reduced the dedicated operating time to 7 (ZSB) or 5 (FUS) min per sample, with only a few seconds added for each additional strain.

Of note, using the ZSB and FUS methods with the VITEK MS commercial database v3.2, all of the species resulted in comparable or better identification to the species level than the routine method, except for *A. nidulans*, *A. tubingensis*, and *Beauveria bassiana*. Both rapid methods can be utilized with the existing commercial database v3.2 in VITEK MS, without any required alterations of the database. Similar conclusions have been reported in another study by Luethy and Zelazny (2018). Their study evaluated the capacity of the zirconia-silica beads method combined the high-power bead-based homogenizer for the identification of molds using Bruker MALDI Biotyper, and reported more samples achieving clinically acceptable identification scores (≥2.00) than the routine method (63.0 *vs* 52.8%) (Adams et al., 2016; Luethy and Zelazny, 2018). Our optimized ZSB method provides significant cost savings in investment (no need for a

homogenizer) compared to Luethy's method without sacrificing identification effectiveness, while has been verified in two mass spectrometers. In addition, a previous study has proved that the FUS method can significantly increase the identification of mycobacteria by Bruker MALDI Biotyper (Adams et al., 2016). Combining the above two studies and our study, we believe our two rapid methods have universality in most mass spectrometer and species which identification hindered by difficulties related to peptide extraction due to the intrinsic characteristics of the cell. Future studies should be carried out to evaluate and optimize those methods for different mass spectrometers and for more species.

Although VITEK MS reliably identified various filamentous fungi by three methods, including *Aspergillus* and *Penicillium*, *Scedosporium*, and other species with a very low rate of misidentification that was not different from previous reports. For the *Fusarium* species, which tend to be multi-resistant and are the second most common filamentous fungi causing invasive fungal infections in immunocompromised patients, VITEK MS demonstrated a lower rate of correct identification to the species-level by all methods compared than to those in previous studies (100, 93.0, and 65.4%) (Heo et al., 2015; McMullen et al., 2016; Luethy and Zelazny, 2018; Rychert et al., 2018; Shin et al., 2021).

Given that all of the tested isolates in this study were from northern China, there may be intrinsic differences between the isolates included in the commercial database and those used in this study due to geographic variation (Adams et al., 2016). Specifically, *F. proliferatum* and *F. verticillioides* could not be distinguished by VITEK MS: further examination of the spectra obtained for these clinical isolates of two species revealed the closely related spectra pattern between them. Thus, it is necessary to increase the number of reference isolates in the database in order to distinguish between closely related species well (Lau et al., 2013).

On the other hand, we also evaluated the number of peaks and S/N ratios produced by three methods. Since the closed VITEK MS database, the spectra peak cannot be exported, we chose the peaks produced by the M-Discover 100 MS to spectrum analysis. Despite the less number of peaks generated, the two rapid methods generally achieved higher maximum and minimum S/N ratios with these isolates tested as compared to the routine method. It is worth noting that not all of these counted peaks are characteristic peaks identified by MS, thus this index may be not a good indicator of the quality of the extraction method. In addition, the ZSB method produced overall mean of maximum and minimum S/N ratio higher than that by FUS.

Evaluation of the rapid ZSB method not only revealed good applicability with the existing commercial database, but also demonstrated it can be a rapid and standardized protocol to construct an in-house library. In this study, we used the ZSB method as a protein extraction procedure to construct an in-house library in M-Discover 100 MS. The inclusion of 2,960 references from 42 species to our in-house database allowed the identification of 454 isolates at the species level (97.22%) using the ZSB method (**Table 3**), showing high correlation with DNA sequencing analysis regardless the score values. However, 10 isolates were identified only at the genus level and three completely misidentified, eleven of which were from four different species not available in the in-house database (*F. moniliforme*, *F. verticillioides*, *F. solani*, and *Rhizopus oryzae*). This highlights the necessity of adding endemic reference strains in the database in order to improve the identification capacity of MALDI-TOF MS. Besides, when lowering the species-level cutoff value to 60 in this study, the correct species-level identification rate showed a high robustness compared with that (≥90) in the manufacturer's instructions (98.47 *vs* 99.29%). Further research can be done to establish appropriate cutoff value to improve the capacity of MALDI-TOF MS for filamentous fungi.

This in-house library can be used with other protein methods. Although the identification accuracy using the in-house library of both routine and FUS methods were inferior to the ZSB method, there were no statistically significant differences between them. However, the percent of isolates with scores ≥90 and 60–90 as generated by the routine method was lower than the ZSB method, while statistically significant differences were observed in four species (*A. flavus*, *A. niger*, *A. tubinensis*, and *P. oxalicum*) (**Figure 2**). There are several possibilities for why fewer accurate identifications occurred. First, it is plausible that the ZSB method breaks the cell wall thoroughly and can achieve higher protein content than the routine method. Further verification, such as comparing protein concentrations and profile are needed according to Akhila's method (Krishnaswamy et al., 2019). Second, the spectra of the same strains had some differences produced by the ZSB and routine method, such as the number and relative position. Thus, the matching degree of the spectra by the routine method with the reference spectra by the ZSB method decreased slightly, resulting in lower scores.

This study has some limitations. First, the strains used in this study represent species typically encountered in northern China. And the *Aspergillus* species, along with *Fusarium* and *Penicillium* species, constitute over half of the tested isolates in this study. Thus, a more comprehensive list of filamentous fungi is needed and filamentous fungi species commonly encountered in other regions should be tested to further evaluate the two rapid methods. Second, the *Fusarium* species, the second most common strain in this study, was not added to the in-house library, while some common species had only one strain included in the in-house library. It is unknown whether geographic differences of the strains may result in variations in identification accuracy using the in-house library. Thus, updates to the M-Discover 100 in-house library are necessary to improve the identification ability.

CONCLUSION

MALDI-TOF MS is widely used for filamentous fungi identification under the condition that an efficient sample processing procedure is implemented and an abundant library is available. Two rapid protein extraction methods we created for filamentous fungi isolates that not only significantly reduced sample processing time but also demonstrated superior

maximum and minimum S/N ratio, and comparable or superior identification to the routine method when utilized with both the existing commercial database and the in-house library. Moreover, to our knowledge, this study represents the first implementation of the zirconia-silica beads method as the sample processing for building an in-house library in MALDI-TOF MS. We believe the advantages provided by the two rapid methods will attract more clinical laboratories to consider adopting MALDI-TOF MS for filamentous fungi identification.

DATA AVAILABILITY STATEMENT

The raw data supporting the conclusions of this article will be made available by the authors, without undue reservation.

ETHICS STATEMENT

The program was approved by the Human Research Ethics Committee of Peking Union Medical College Hospital (S-263).

AUTHOR CONTRIBUTIONS

Y-TN processed the experimental data, performed the analysis, drafted the manuscript, and revised the manuscript. W-HY, M-X, W-Y designed the study and revised the manuscript. W-Z, J-JZ, GZ, and S-MD carried out the experiments, performed protein extraction and MALDI-TOF MS identification. A-YD, D-WG, G-LZ, HNW, Y-YG, L-P C, MC, J-DH, and QD contributed to strain collection, performed DNA sequencing identification. LZ and YCX revised the manuscript, and involved in planning and supervised the work. All authors contributed to the article and approved the submitted version.

FUNDING

This work was supported by the National Major Science and Technology Project for the Control and Prevention of Major Infectious Diseases of China (nos. 2018ZX10712001 and 2020ZX1001015), Beijing Municipal Science and Technology Project (no. Z181100001618015), the National Natural Science Foundation of China (nos. 81802049 and 81971979), and Beijing Key Clinical Specialty for Laboratory Medicine - Excellent Project (no. ZK201000).

SUPPLEMENTARY MATERIAL

The Supplementary Material for this article can be found online at: https://www.frontiersin.org/articles/10.3389/fcimb.2021.687240/full#supplementary-material

REFERENCES

Adams, L. L., Dionne, K., Fisher, S., and Parrish, N. (2016). A Rapid, Standardized Protein Extraction Method Using Adaptive Focused Acoustics for Identification of Mycobacteria by MALDI-ToF Ms. *Diagn. Microbiol. Infect. Dis.* 86 (3), 284–288. doi: 10.1016/j.diagmicrobio.2016.06.001

Balajee, S. A., Houbraken, J., Verweij, P. E., Hong, S. B., Yaghuchi, T., Varga, J., et al. (2007). Aspergillus Species Identification in the Clinical Setting. *Stud. Mycol.* 59, 39–46. doi: 10.3114/sim.2007.59.05

Becker, P. T., de Bel, A., Martiny, D., Ranque, S., Piarroux, R., Cassagne, C., et al. (2014). Identification of Filamentous Fungi Isolates by MALDI-TOF Mass Spectrometry: Clinical Evaluation of an Extended Reference Spectra Library. *Med. Mycol.* 52 (8), 826–834. doi: 10.1093/mmy/myu064

Benedict, K., Richardson, M., Vallabhaneni, S., Jackson, B. R., and Chiller, T. (2017). Emerging Issues, Challenges, and Changing Epidemiology of Fungal Disease Outbreaks. *Lancet Infect. Dis.* 17 (12), e403–e411. doi: 10.1016/S1473-3099(17)30443-7

Bongomin, F., Gago, S., Oladele, R. O., and Denning, D. W. (2017). Global and Multi-National Prevalence of Fungal Diseases-Estimate Precision. *J. Fungi (Basel)* 3 (4), 57. doi: 10.3390/jof3040057

Brown, G. D., Denning, D. W., Gow, N. A., Levitz, S. M., Netea, M. G., and White, T. C. (2012). Hidden Killers: Human Fungal Infections. *Sci. Transl. Med.* 4 (165), 113r–165r. doi: 10.1126/scitranslmed.3004404

Cassagne, C., Normand, A. C., L'Ollivier, C., Ranque, S., and Piarroux, R. (2016). Performance of MALDI-TOF MS Platforms for Fungal Identification. *Mycoses* 59 (11), 678–690. doi: 10.1111/myc.12506

Chakrabarti, A., Bonifaz, A., Gutierrez-Galhardo, M. C., Mochizuki, T., and Li, S. (2015). Global Epidemiology of Sporotrichosis. *Med. Mycol.* 53 (1), 3–14. doi: 10.1093/mmy/myu062

De Carolis, E., Posteraro, B., Lass-Florl, C., Vella, A., Florio, A. R., Torelli, R., et al. (2012). Species Identification of Aspergillus, Fusarium and Mucorales With Direct Surface Analysis by Matrix-Assisted Laser Desorption Ionization Time-of-Flight Mass Spectrometry. *Clin. Microbiol. Infect.* 18 (5), 475–484. doi: 10.1111/j.1469-0691.2011.03599.x

Doucha, J., and Livansky, K. (2008). Influence of Processing Parameters on Disintegration of Chlorella Cells in Various Types of Homogenizers. *Appl. Microbiol. Biotechnol.* 81 (3), 431–440. doi: 10.1007/s00253-008-1660-6

Enoch, D. A., Ludlam, H. A., and Brown, N. M. (2006). Invasive Fungal Infections: A Review of Epidemiology and Management Options. *J. Med. Microbiol.* 55 (Pt 7), 809–818. doi: 10.1099/jmm.0.46548-0

Fraser, M., Brown, Z., Houldsworth, M., Borman, A. M., and Johnson, E. M. (2016). Rapid Identification of 6328 Isolates of Pathogenic Yeasts Using MALDI-ToF MS and a Simplified, Rapid Extraction Procedure That is Compatible With the Bruker Biotyper Platform and Database. *Med. Mycol.* 54 (1), 80–88. doi: 10.1093/mmy/myv085

Gautier, M., Ranque, S., Normand, A. C., Becker, P., Packeu, A., Cassagne, C., et al. (2014). Matrix-Assisted Laser Desorption Ionization Time-of-Flight Mass Spectrometry: Revolutionizing Clinical Laboratory Diagnosis of Mould Infections. *Clin. Microbiol. Infect.* 20 (12), 1366–1371. doi: 10.1111/1469-0691.12750

Gilgado, F., Cano, J., Gene, J., Sutton, D. A., and Guarro, J. (2008). Molecular and Phenotypic Data Supporting Distinct Species Statuses for Scedosporium Apiospermum and Pseudallescheria Boydii and the Proposed New Species Scedosporium Dehoogii. *J. Clin. Microbiol.* 46 (2), 766–771. doi: 10.1128/JCM.01122-07

Heo, M. S., Shin, J. H., Choi, M. J., Park, Y. J., Lee, H. S., Koo, S. H., et al. (2015). Molecular Identification and Amphotericin B Susceptibility Testing of Clinical Isolates of Aspergillus From 11 Hospitals in Korea. *Ann. Lab. Med.* 35 (6), 602–610. doi: 10.3343/alm.2015.35.6.602

Klimek-Ochab, M., Brzezinska-Rodak, M., Zymanczyk-Duda, E., Lejczak, B., and Kafarski, P. (2011). Comparative Study of Fungal Cell Disruption–Scope and Limitations of the Methods. *Folia Microbiol. (Praha)* 56 (5), 469–475. doi: 10.1007/s12223-011-0069-2

Kozel, T. R., and Wickes, B. (2014). Fungal Diagnostics. *Cold Spring Harb. Perspect. Med.* 4 (4), a19299. doi: 10.1101/cshperspect.a019299

Krishnaswamy, A., Barnes, N., Lotlikar, N. P., and Damare, S. R. (2019). An Improved Method for Protein Extraction From Minuscule Quantities of Fungal Biomass. *Indian J. Microbiol.* 59 (1), 100–104. doi: 10.1007/s12088-018-0752-y

Larone, D. H. (2011). *Medically Important Fungi: A Guide to Identification. 5th ed* (Washington, DC: ASM Press).

Lau, A. F., Drake, S. K., Calhoun, L. B., Henderson, C. M., and Zelazny, A. M. (2013). Development of a Clinically Comprehensive Database and a Simple Procedure for Identification of Molds From Solid Media by Matrix-Assisted Laser Desorption Ionization-Time of Flight Mass Spectrometry. *J. Clin. Microbiol.* 51 (3), 828–834. doi: 10.1128/JCM.02852-12

Liao, Y., Chen, M., Hartmann, T., Yang, R. Y., and Liao, W. Q. (2013). Epidemiology of Opportunistic Invasive Fungal Infections in China: Review of Literature. *Chin. Med. J. (Engl.)* 126 (2), 361–368. doi: 10.3760/cma.j.issn.0366-6999

Li, S., Plouffe, B. D., Belov, A. M., Ray, S., Wang, X., Murthy, S. K., et al. (2015). An Integrated Platform for Isolation, Processing, and Mass Spectrometry-Based Proteomic Profiling of Rare Cells in Whole Blood. *Mol. Cell Proteomics* 14 (6), 1672–1683. doi: 10.1074/mcp.M114.045724

Li, Y., Wang, H., Zhao, Y. P., Xu, Y. C., and Hsueh, P. R. (2017). Evaluation of the Bruker Biotyper Matrix-Assisted Laser Desorption/Ionization Time-of-Flight Mass Spectrometry System for Identification of Aspergillus Species Directly From Growth on Solid Agar Media. *Front. Microbiol.* 8, 1209. doi: 10.3389/fmicb.2017.01209

Luethy, P. M., and Zelazny, A. M. (2018). Rapid One-Step Extraction Method for the Identification of Molds Using MALDI-TOF Ms. *Diagn. Microbiol. Infect. Dis.* 91 (2), 130–135. doi: 10.1016/j.diagmicrobio.2018.01.015

McMullen, A. R., Wallace, M. A., Pincus, D. H., Wilkey, K., and Burnham, C. A. (2016). Evaluation of the Vitek Ms Matrix-Assisted Laser Desorption Ionization-Time of Flight Mass Spectrometry System for Identification of Clinically Relevant Filamentous Fungi. *J. Clin. Microbiol.* 54 (8), 2068–2073. doi: 10.1128/JCM.00825-16

Rodriguez-Sanchez, B., Ruiz-Serrano, M. J., Ruiz, A., Timke, M., Kostrzewa, M., and Bouza, E. (2016). Evaluation of MALDI Biotyper Mycobacteria Library v3.0 for Identification of Nontuberculous Mycobacteria. *J. Clin. Microbiol.* 54 (4), 1144–1147. doi: 10.1128/JCM.02760-15

Rychert, J., Slechta, E. S., Barker, A. P., Miranda, E., Babady, N. E., Tang, Y. W., et al. (2018). Multicenter Evaluation of the Vitek MS V3.0 System for the Identification of Filamentous Fungi. *J. Clin. Microbiol.* 56 (2), e01353-17. doi: 10.1128/JCM.01353-17

Samson, R. A., Visagie, C. M., Houbraken, J., Hong, S. B., Hubka, V., Klaassen, C. H., et al. (2014). Phylogeny, Identification and Nomenclature of the Genus Aspergillus. *Stud. Mycol.* 78, 141–173. doi: 10.1016/j.simyco.2014.07.004

Santos, C. R., Francisco, E., Mazza, M., Padovan, A. C. B., Colombo, A., and Lima, N. (2017). "Impact of MALDI-TOF MS in Clinical Mycology; Progress and Barriers in Diagnostics", in *Maldi-TOF and Tandem MS for Clinical Microbiology, 1st ed.* H. N. Shah and S. E. Gharbia, Eds.; (London, UK: John Wiley & Sons Ltd.) p. 211–230.

Schulthess, B., Ledermann, R., Mouttet, F., Zbinden, A., Bloemberg, G. V., Bottger, E. C., et al. (2014). Use of the Bruker Maldi Biotyper for Identification of Molds in the Clinical Mycology Laboratory. *J. Clin. Microbiol.* 52 (8), 2797–2803. doi: 10.1128/JCM.00049-14

Seng, P., Drancourt, M., Gouriet, F., La Scola, B., Fournier, P. E., Rolain, J. M., et al. (2009). Ongoing Revolution in Bacteriology: Routine Identification of Bacteria by Matrix-Assisted Laser Desorption Ionization Time-of-Flight Mass Spectrometry. *Clin. Infect. Dis.* 49 (4), 543–551. doi: 10.1086/600885

Shapaval, V., Moretro, T., Wold, A. A., Suso, H. P., Schmitt, J., Lillehaug, D., et al. (2017). A Novel Library-Independent Approach Based on High-Throughput Cultivation in Bioscreen and Fingerprinting by FTIR Spectroscopy for Microbial Source Tracking in Food Industry. *Lett. Appl. Microbiol.* 64 (5), 335–342. doi: 10.1111/lam.12691

Shin, J. H., Kim, S. H., Lee, D., Lee, S. Y., Chun, S., Lee, J. H., et al. (2021). Performance Evaluation of VITEK MS for the Identification of a Wide Spectrum of Clinically Relevant Filamentous Fungi Using a Korean Collection. *Ann. Lab. Med.* 41 (2), 214–220. doi: 10.3343/alm.2021.41.2.214

Wang, H., Xiao, M., Kong, F., Chen, S., Dou, H. T., Sorrell, T., et al. (2011). Accurate and Practical Identification of 20 Fusarium Species by Seven-Locus Sequence Analysis and Reverse Line Blot Hybridization, and an In Vitro Antifungal Susceptibility Study. *J. Clin. Microbiol.* 49 (5), 1890–1898. doi: 10.1128/JCM.02415-10

Welham, K. J., Domin, M. A., Johnson, K., Jones, L., and Ashton, D. S. (2000). Characterization of Fungal Spores by Laser Desorption/Ionization Time-of-Flight Mass Spectrometry. *Rapid Commun. Mass Spectrom.* 14 (5), 307–310. doi: 10.1002/(SICI)1097-0231(20000315)14:5<307::AID-RCM823>3.0.CO;2-3

Wickes, B. L., and Wiederhold, N. P. (2018). Molecular Diagnostics in Medical Mycology. *Nat. Commun.* 9 (1), 5135. doi: 10.1038/s41467-018-07556-5

Zvezdanova, M. E., Escribano, P., Ruiz, A., Martinez-Jimenez, M. C., Pelaez, T., Collazos, A., et al. (2019). Increased Species-Assignment of Filamentous Fungi Using MALDI-TOF MS Coupled With a Simplified Sample Processing and an in-House Library. *Med. Mycol.* 57 (1), 63–70. doi: 10.1093/mmy/myx154

Conflict of Interest: The authors declare that the research was conducted in the absence of any commercial or financial relationships that could be construed as a potential conflict of interest.

frontiers in Cellular and Infection Microbiology

ORIGINAL RESEARCH
published: 21 July 2021
doi: 10.3389/fcimb.2021.695134

Comprehensive Description of Pathogens and Antibiotic Treatment Guidance in Children With Community-Acquired Pneumonia Using Combined Mass Spectrometry Methods

Liying Sun[1,2†], Chi Zhang[1,2†], Shuhua An[3†], Xiangpeng Chen[4], Yamei Li[1,2], Leshan Xiu[1,2], Baoping Xu[5], Zhengde Xie[4] and Junping Peng[1,2*]*

[1] NHC Key Laboratory of Systems Biology of Pathogens, Institute of Pathogen Biology, Chinese Academy of Medical Sciences & Peking Union Medical College, Beijing, China, [2] Key Laboratory of Respiratory Disease Pathogenomics, Chinese Academy of Medical Sciences and Peking Union Medical College, Beijing, China, [3] Department of Respiratory Medicine, Hebei Children's Hospital, Hebei Medical University, Shijiazhuang, China, [4] Beijing Key Laboratory of Pediatric Respiratory Infection Diseases, Key Laboratory of Major Diseases in Children, Ministry of Education, National Clinical Research Center for Respiratory Diseases, Research Unit of Critical Infection in Children, Chinese Academy of Medical Sciences, 2019RU016, Laboratory of Infection and Virology, Beijing Pediatric Research Institute, Beijing Children's Hospital, Capital Medical University, National Center for Children's Health, Beijing, China, [5] National Clinical Research Center for Respiratory Diseases, Research Unit of Critical Infection in Children, Chinese Academy of Medical Sciences, 2019RU016, Respiratory Department, Beijing Children's Hospital, Capital Medical University, National Center for Children's Health, Beijing, China

The objective of this study was to evaluate the value of molecular methods in the management of community-acquired pneumonia (CAP) in children. Previously developed mass spectrometry (MS)-based methods combined with quantitative real-time PCR (combined-MS methods) were used to describe the aetiology and evaluate antibiotic therapy in the enrolled children. Sputum collected from 302 children hospitalized with CAP were analyzed using the combined-MS methods, which can detect 19 viruses and 12 bacteria related to CAP. Based on the results, appropriate antibiotics were determined using national guidelines and compared with the initial empirical therapies. Respiratory pathogens were identified in 84.4% of the patients (255/302). Co-infection was the predominant infection pattern (51.7%, 156/302) and was primarily a bacterial-viral mixed infection (36.8%, 111/302). Compared with that using culture-based methods, the identification rate for bacteria using the combined-MS methods (61.8%, 126/204) increased by 28.5% (p <0.001). Based on the results of the combined-MS methods, the initial antibiotic treatment of 235 patients was not optimal, which mostly required switching to β-lactam/β-lactamase inhibitor combinations or reducing unnecessary macrolide treatments. Moreover, using the combined-MS methods to guide antibiotic

OPEN ACCESS

Edited by:
Yang Zhang,
University of Pennsylvania,
United States

Reviewed by:
Hao Zhang,
University of Pennsylvania,
United States
Jaroslav Hrabak,
Charles University, Czechia

***Correspondence:**
Junping Peng
pengjp@hotmail.com
Zhengde Xie
xiezhengde@bch.com.cn

†These authors have contributed equally to this work

Specialty section:
This article was submitted to Clinical Microbiology, a section of the journal Frontiers in Cellular and Infection Microbiology

Received: 14 April 2021
Accepted: 15 June 2021
Published: 21 July 2021

Citation:
Sun L, Zhang C, An S, Chen X, Li Y, Xiu L, Xu B, Xie Z and Peng J (2021) Comprehensive Description of Pathogens and Antibiotic Treatment Guidance in Children With Community-Acquired Pneumonia Using Combined Mass Spectrometry Methods. Front. Cell. Infect. Microbiol. 11:695134. doi: 10.3389/fcimb.2021.695134

therapy showed potential to decrease the length of stay in children with severe CAP. For children with CAP, quantitative molecular testing on sputum can serve as an important complement to traditional culture methods. Early aetiology elucidated using molecular testing can help guide the antibiotic therapy.

Keywords: community-acquired pneumonia, respiratory pathogens, molecular testing, mass spectrometry, antibiotic therapy

HIGHLIGHTS

1) We used combined-MS methods to comprehensively analyze the etiology in children with CAP in North China;
2) Early etiology obtained using molecular testing in our study can be introduced to guide antibiotic therapy;
3) We provided valuable reference for the principles and practices of antibiotic stewardship in children hospitalized for CAP.

INTRODUCTION

Pneumonia is the predominant cause of infection-related deaths in young children, with approximately 0.9 million deaths annually in children younger than 5 years of age (Bryce et al., 2005, Liu et al., 2016). The infectious agents of community-acquired pneumonia (CAP) are diverse. Currently, clinical microbiology laboratories rely heavily on sputum culture; however, culture-based methods are time-consuming and less sensitive, which makes them less useful for timely diagnosis. Based solely on the results of culture, a precise microbiological diagnosis can be made in less than 15% of children hospitalized with CAP (Bradley et al., 2011). Owing to the limitations of culture-based methods, empirical antimicrobials are administered to patients who do not have a precise microbiological diagnosis. Such untargeted antibiotic selection or excessive use of antimicrobials is associated with increased antimicrobial resistance (Duong et al., 2018).

To comprehensively and rapidly identify the causative agents of CAP, new methods are urgently needed. Compared with traditional culture-based methods, molecular testing offers the following advantages: besides high sensitivity and shorter turnaround time, it has the superiority of detecting multiple pathogens, which can substantially improve identification efficiency. Molecular-based tests are also crucial for identifying respiratory viruses and atypical pathogens that require rigorous culture conditions, like *Legionella pneumophila*, *Bordetella pertussis*, *Mycoplasma pneumoniae*, and *Chlamydophila pneumoniae*. Currently, the most frequently used molecular-based method is real-time PCR; however, it can only detect a limited number of pathogens simultaneously (Caliendo, 2011). Therefore, when screening diverse candidate pathogens of CAP, multiple reactions are needed, which is time-consuming and labor intensive. To perform multiple reactions, a larger sample size is required, placing an additional burden on patients, especially children. To overcome these limitations, we developed two multiplex PCR coupled with matrix-assisted laser desorption ionisation-time of flight mass spectrometry (MALDI-TOF MS), common respiratory virus-mass spectrometry (CRV-MS), and bacterial pathogen-mass spectrometry (BP-MS).

The viral pathogen panel (CRV-MS) can simultaneously detect and identify 19 common respiratory virus types/subtypes, and the bacterial panel (BP-MS) can screen 12 bacterial pathogens associated with CAP (Zhang et al., 2015; Zhang et al., 2018). The CRV-MS and the BP-MS methods are therefore suitable for large-scale pathogen screening and epidemiological studies.

Here, we used the CRV-MS and BP-MS methods to detect pathogens in sputum from children hospitalized with CAP retrospectively. By comparing the results with those of the culture-based method, we evaluated the potential of combined-MS in improving the detection rate of pathogens and to guide initial antimicrobial therapy. Moreover, we described the aetiology of CAP in North China by analysing the results of combined-MS methods.

MATERIALS AND METHODS

Subjects

A total of 302 children hospitalized with CAP between January 2016 and December 2018 were included in this study. They were all younger than 16 and admitted to Beijing Children's Hospital (Beijing, China) and Children's Hospital of Hebei Province (Shijiazhuang, Hebei Province, China). CAP was diagnosed according to the Chinese national guidelines for the management of CAP in children, update 2013. All children had fever (body temperature ≥ 38°C), cough, tachypnoea, dyspnoea, chest retractions, abnormal auscultatory findings, and radiological evidence of CAP. The severity of CAP was also evaluated based on the same guidelines. Patient information on age, sex, length of stay (LOS), sputum culture results, empirical antibiotic prescription, or antibiotic administration before hospitalisation were retrospectively collected from electronic medical records. All enrolled patients were divided into five overlapping groups for different study aims (**Figure 1**). For sputum culture, only results obtained within 72 hours of the sampling time were included in subsequent analyses.

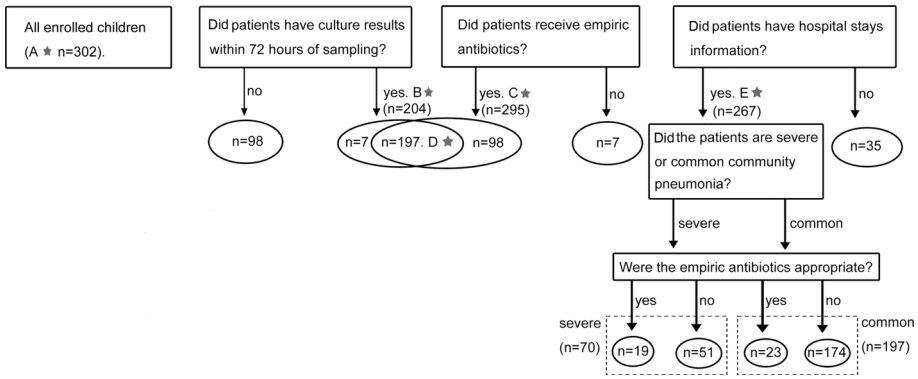

FIGURE 1 | Cases enrolment and study design. The numbers marked with a star referred to the sample size of five groups. **(A)** Results of combined-MS methods obtained from all 302 patients were used to define the etiology of CAP. **(B)** 204 cases with culture results within 72 hours of sampling were used to compare the performance of combined-MS methods and culture. **(C)** 295 cases with information of empirical antimicrobial therapy were used to study the value of combined-MS methods in guiding antimicrobial prescribing. **(D)** 197 cases with both information of culture and empirical antimicrobial therapy were used to investigate the impact of antibiotic usage on the performance of combined-MS methods and culture. **(E)** 267 patients with information of LOS were used to assess how antibiotic therapy affect LOS. LOS, length of stay.

Specimen Collection and Nucleic Acid Extraction

Sputum was collected within 72 hours of patient admission. Nebulisation was used for younger children. Induced sputum samples from the inhalation of hypertonic saline solution were collected by trained personnel according to standard operating procedures, as published previously (Lahti et al., 2009; Honkinen et al., 2012).

A total of 2 mL of sputum was obtained from each patient with sterility sputum aspiratory tubes and stored at -80°C. The nucleic acids of the viruses were extracted using QIAamp MinElute Virus Spin kits (QIAGEN, Hilden, Germany), and cDNA was synthesized using SuperScript First-Strand Synthesis System (Invitrogen, Carlsbad, CA, USA) according to the manufacturer's instructions. To extract bacterial DNA, 200 μL of sputum were centrifuged at 5000 × g for 10 min, and pellets resuspended in 150 μL enzyme cocktail containing 6 mg lysozyme, 30 U lysostaphin, 37.5 U mutanolysin, and 30U lyticase in lysis buffer of 20 mM Tris-HCl (pH 8), 2 mM EDTA, and 1.2% Triton. The mixture was incubated at 37°C for 30 min to lyse the cell walls of Gram-positive bacteria. DNA was then purified using the QIAamp DNA Mini Kit (Qiagen, Hilden, Germany) according to the manufacturer's instructions. Purified DNA was eluted in 200 μL nuclease-free water.

Cultural and Combined-MS Methods

Sputum culture and identification were performed using standard microbiological and biochemical methods.

The CRV-MS method can simultaneously identify 19 common respiratory viruses, including adenovirus (AdV), human enterovirus (EV), four human coronaviruses (HCoV-OC43, 229E, NL63, and HKU1), human bocavirus 1 (HBoV1), human metapneumoviruses A and B (HMPV-A and HMPV-B), human rhinovirus (HRV), influenza A viruses (IFV-A H1N1, and H3N2), influenza B viruses (IFV-B), parainfluenza virus types 1–4 (PIV1 to-4), and respiratory syncytial viruses A and B (RSV-A and RSV-B, respectively) (Jain, 2017). The BP-MS method can simultaneously identify 12 bacterial pathogens related to pneumonia, including *Legionella pneumophila*, *Bordetella pertussis*, *Mycoplasma pneumoniae*, *Chlamydophila pneumoniae*, *Haemophilus influenzae*, *Staphylococcus aureus*, *Moraxella catarrhalis*, *Klebsiella pneumoniae*, *Pseudomonas aeruginosa*, *Acinetobacter baumannii*, *Streptococcus pneumoniae*, and *Escherichia coli*. Detailed procedures for CRV-MS and BP-MS have been described previously (Zhang et al., 2015; Zhang et al., 2018).

Among the bacterial targets, *H. influenzae*, *S. aureus*, *M. catarrhalis*, *K. pneumoniae*, *P. aeruginosa*, *A. baumannii*, *S. pneumoniae*, and *E. coli* are commonly detected commensals of the respiratory tract, which may act as contaminants of the sputum (Apisarnthanarak and Mundy, 2005; Jain, 2017). As BP-MS is a qualitative method, positive results for the above bacteria were retested by quantitative real-time PCR to obtain their bacterial loads. Only bacteria with a load of $\geq 10^5$ CFU/mL can be regarded as a pathogen responsible for infection (combined-MS methods positive) (Gadsby et al., 2016). The assays used in the real-time methods refer to previous studies (Zhang et al., 2018).

Antibiotics Selected for Pathogen-Guided Therapy

According to the results of combined-MS methods, the right antibiotics were determined using the Children's Community Pneumonia Diagnosis and Treatment Guidelines (2013 revised) and revised World Health Organization (WHO) Classification and Treatment of Pneumonia in Children at Health Facilities: Evidence Summaries (see **Supplementary Material**, **Table S1**) (Subspecialty Group of Respiratory Diseases and Chinese Medical Association The Editorial Board, 2013; WHO, 2014).

Statistical Analysis

Categorical data were compared using the chi-squared (χ^2) or Fisher's exact tests. Paired proportions were compared using the McNemar test. Continuous variables were analyzed using the Shapiro-Wilk test for normality. Student's t-test and the Mann-Whitney U test were used to compare normally and non-normally distributed continuous variables, respectively. The above statistical analyses were performed with SPSS (Statistical Product and Service Solutions) software version 19, and a *P* value <0.05 was considered statistically significant.

RESULTS

General Characteristics of Patients Included

Among 302 included children, the median age was 1 year (range, 0.04-16 years), and 65.9% (199) were male (**Table 1**). Children were categorised into neonates (age < 1, 47.0%, 142), toddlers (1 ≤ age < 3, 23.9%, 72), pre-schoolers (3 ≤ age < 6, 8.6%, 26), and school-age children (6 ≤ age ≤ 16, 20.5%, 62, **Table 1**). Patients were divided into four groups based on sampling times: spring (26.5%, 80), summer (4.6%, 14), autumn (5.6%, 17), and winter (63.3%, 191).

Aetiology of CAP in Hospitalised Children Identified by Combined-MS Methods

Respiratory pathogens were identified in 84.4% of patients (255). Among them, 64.9% (196) were bacteria and 56.3% (170) were virus-positive. Specifically, RSV was the most common pathogen (26.5%, 80), followed by *H. influenzae* (22.2%, 67), *S. pneumoniae* (20.5%, 62), and *M. pneumoniae* (14.9%, 45, **Table 2**).

Mixed infection was the most frequent pattern in patients (51.7%, 156). Of 156 mixed infection cases, dual pathogen co-infection (57.0%, 89) was the most common, followed by triple (26.3%, 41), quadruple (11.5%, 18), and mixed-infection with more than four pathogens (5.1%, 8). Bacterial-viral mixed infection (36.8%, 111/302) was the primary co-infection pattern. *H. influenzae*/RSV (12.8%, 20/156) was the most common co-infection combination, followed by *S. pneumoniae*/*H. influenzae* (11.5%, 18/156) and *S. pneumoniae*/RSV (11.5%, 18/156). No pathogen was detected in 47 (15.6%, 47/302) specimens (**Figure 2**).

The predominant respiratory pathogens in children with CAP varied with age. RSV was the most frequently detected pathogen in children under age 3 (29.4%, 63/214), *H. influenzae* was found in children aged 3 to 6 (15.4%, 4/26), and *M. pneumoniae* was found in children aged 6 to 16 (24.2%, 15/62; **Figure 2B**). The primary pathogens changed with seasons. RSV was most commonly identified in both spring and winter (30%, 24/80; 27%, 52/191) and PIV and EV were most frequently detected in summer (21.4%, 3/14), and autumn (29.4%, 5/17), respectively. (**Figure 2C**). However, there was no statistically significant difference in mixed infection rates among the age groups or season ($P > 0.05$).

TABLE 1 | Characteristics of 302 included children.

Characteristics	N (%)
Sex	
Male	199 (65.9)
Female	103 (34.1)
Age (yr)	
Age < 1 (neonatal group)	142 (47.0)
1 ≤ age < 3 (toddler group)	72 (23.9)
3 ≤ age < 6 (preschool group)	26 (8.6)
6 ≤ age < 16 (school group)	62 (20.5)
Sampling time	
Spring (from March to May)	80 (26.5)
Summer (from June to August)	14 (4.6)
Autumn (from September to November)	17 (5.6)
Winter (from December to February)	191 (63.3)
Outcome	
Discharge	299 (99.01)
Death	3 (0.99)

TABLE 2 | Detection rate of common respiratory pathogens with combined-MS methods (n = 302).

Pathogens	N (%)
Any pathogen	255 (84.4)
Any bacteria	196 (64.9)
L. pneumophila	3 (1.0)
B. pertussis	10 (3.3)
M. pneumoniae	45 (14.9)
C. pneumonia	1 (0.3)
S. pneumoniae	62 (20.5)
H. influenzae	67 (22.2)
S. aureus	36 (11.9)
M. catarrhalis	25 (8.3)
P. aeruginosa	6 (2.0)
A. baumannii	7 (2.3)
K. pneumoniae	9 (3.0)
E. coli	10 (3.3)
Any virus	170 (56.3)
Human coronavirus (HCoV)	8 (2.7)
HCoV-229E	5 (1.7)
HCoV-HKU1	1 (0.3)
HCoV-NL63	0 (0)
HCoV-OC43	2 (0.7)
Adenovirus (AdV)	30 (9.9)
Enteroviruses (EV)	31 (10.3)
Human bocavirus (HBoV)	13 (4.3)
Human metapneumovirus (HMPV)	7 (2.3)
HMPV-A	6 (2.0)
HMPV-B	1 (0.3)
Human rhinovirus (HRV)	27 (8.9)
Influenza (IFV)	27 (8.9)
IFV-A-H1	13 (4.3)
IFV-A-H3	2 (0.7)
IFV-B	12 (4.0)
Parainfluenza virus (PIV)	12 (4.0)
PIV-1	1 (0.3)
PIV-2	0 (0)
PIV-3	11 (3.6)
PIV-4	0 (0)
Respiratory syncytial virus (RSV)	80 (26.5)
RSV-A	50 (16.6)
RSV-B	30 (9.9)

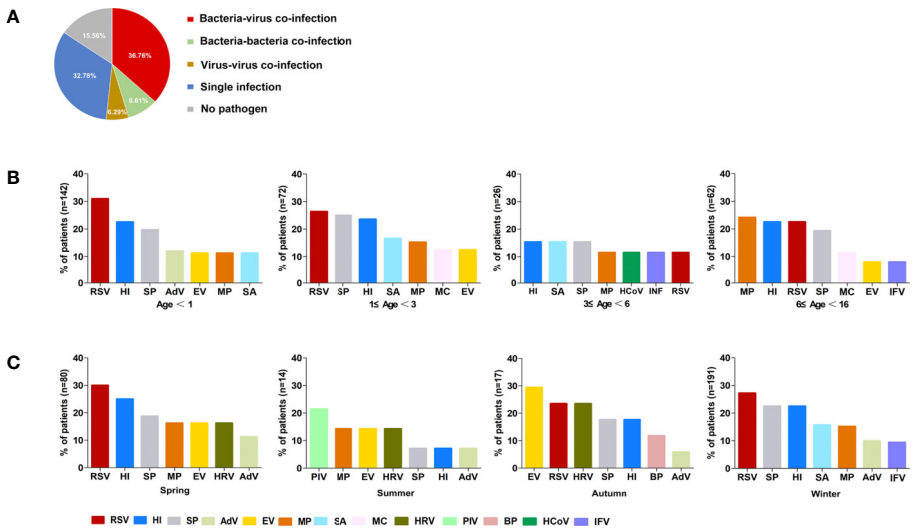

FIGURE 2 | The etiology of 302 included children defined by combined-MS methods. **(A)** The proportions of different patterns of infection. **(B)** Distribution of main pathogens in patients with different age groups. **(C)** Seasonal prevalence of main pathogens. RSV, respiratory syncytial virus; HI, *Haemophilus influenzae*; SP, *Streptococcus pneumoniae*; MP, *Mycoplasma pneumoniae*; SA, *Staphylococcus aureus*; EV, Enterovirus; AdV, Adenovirus; IFV, Influenza virus; HRV, Human rhinovirus; MC, *Moraxella catarrhalis*; PIV, Parainfluenza virus; BP, *Bordetella pertussis*; HCoV, Human coronavirus.

Comparison of Performance Between Culture-Based and Combined-MS Methods

The detection rate of ten culturable bacterial pathogens using combined-MS methods was significantly higher than that using sputum culture (61.8%, 126 versus 33.3%, 68, $P < 0.001$, **Table 3**) in 204 patients with culture-based detection information. Compared with culture-based methods, combined-MS methods detected more of the following pathogens: *S. pneumoniae* (6.9% vs. 20.6%, $P < 0.001$), *H. influenzae* (6.9% versus 23.1%, $P < 0.001$), *S. aureus* (6.9% versus 16.2%, $P < 0.001$),

TABLE 3 | Comparison of the performance between combined-MS methods and culture-based methods (n = 204).

	Combined-MS methods	Culture-based methods		*P* [b]
		Positive n (%) [c]	Negative n (%)	
Ten culturable pathogens [a]	Positive	63 (30.9)	63 (30.9)	*P* <0.001
	Negative	5 (2.4)	73 (35.8)	
S. pneumoniae	Positive	14 (6.9)	28 (13.7)	*P* <0.001
	Negative	0 (0)	162 (79.4)	
H. influenzae	Positive	13 (6.4)	34 (16.7)	*P* <0.001
	Negative	1 (0.5)	156 (76.5)	
S. aureus	Positive	12 (5.9)	21 (10.3)	*P* <0.001
	Negative	2 (1.0)	169 (82.8)	
M. catarrhalis	Positive	5 (2.5)	15 (7.4)	*P* <0.001
	Negative	0 (0)	184 (90.2)	
P. aeruginosa	Positive	4 (2.0)	1 (0.5)	*P* >0.05
	Negative	1 (0.5)	198 (97)	
A. baumannii	Positive	3 (1.5)	2 (1)	*P* >0.05
	Negative	2 (1)	197 (96.5)	
K. pneumoniae	Positive	4 (2.0)	3 (1.4)	*P* >0.05
	Negative	2 (1.0)	195 (95.6)	
E. coli	Positive	3 (1.5)	3 (1.5)	*P* >0.05
	Negative	1 (0.5)	197 (96.5)	
L. pneumophila	Positive	0 (0)	2 (1)	*P* >0.05
	Negative	0 (0)	202 (99.0)	
B. pertussis	Positive	0 (0)	2 (1)	*P* >0.05
	Negative	0 (0)	202 (99.0)	

[a]*Ten culturable pathogens included S. pneumoniae, H. influenzae, S. aureus, M. catarrhalis, P. aeruginosa, A. baumannii, K. pneumoniae, E. coli, L. pneumophila, and B. pertussis.* [b]*P values were calculated using the McNemar test.* [c]*The number and the percentage.*

and *M. catarrhalis* (2.5% versus 9.9%, $P < 0.001$, **Table 3**). For the other four pathogens, the detection rate of combined-MS methods was higher than that of culture-based methods, but the difference was not statistically significantly (**Table 3**, $P > 0.05$). In the other ten patients, bacteria not selected as targets of combined-MS methods were detected using culture-based methods (see **Supplementary Material**, **Table S2**).

Impact of Antibiotic Use on the Performance of Combined-MS Methods and Culture

Among 197 cases who received empirical antimicrobial therapy, the detection rate of ten culturable pathogens using combined-MS method was 60.9% (120), which was higher than the rate using culture (29.4%, 58, $P < 0.001$). The results showed that compared with culture, the impact of initial empirical antibiotic usage on bacterial detection was lower in combined-MS methods.

Using the Results of the Combined-MS Methods to Evaluate Initial Empirical Antibiotic Treatment

In 295 patients who received empirical antimicrobial therapy based on to the results of combined-MS methods, the initial antibiotic therapies of 235 patients were not optimal. Most class of antibiotics (39.0%, 115) needed to change and the number of antibiotics needed to decrease (36.9%, 109, **Table 4**). Changing the class of antibiotics mainly involved switching β-lactam (26.1%, 77) or macrolide antibiotics (8.5%, 25) to a β-lactam/β-lactamase inhibitor combinations. Decreasing the number of excessive antibiotics mainly referred to a reduction in the use of macrolide antibiotics (25.4%, 75) and β-lactam agents (10.2%, 30). The number of antibiotics needed to be increased in 11 patients (3.8%, 11) while 60 patients (20.3%, 60) needed no change.

TABLE 4 | Using the results of combined-MS methods to guide the antibiotic treatment (n = 295).

Antibiotics modify	N (%)
Change class	115 (39.0)
LA to LIC	77 (26.1)
MA to LIC	25 (8.5)
LIC to LA	4 (1.4)
MA to LA	3 (1.0)
LA to MA	3 (1.0)
LIC to MA	3 (1.0)
Decrease numbers	109 (36.9)
MA	75 (25.4)
LA	30 (10.2)
LIC	1 (0.3)
LIC+MA	2 (0.7)
LA+MA	1 (0.3)
Increase numbers	11 (3.8)
LIC	4 (1.4)
MA	3 (1.0)
Increase numbers and change class	
LA to LIC+MA	4 (1.4)
No change	60 (20.3)

LA, β-lactam; LIC, β-lactam/β-lactamase inhibitor combinations; MA, macrolides.

Assessment of LOS Affected by Antibiotic Therapy

Among 70 children with severe CAP, the mean LOS was significantly shorter for children who did not need to change antibiotic than those who needed therapy change (11.63 ± 0.95 days vs. 18.57 ± 1.97 days, $P = 0.037$). Additionally, in children with common CAP, the mean LOS was also shorter for those not needing therapy change than those who needed a change, though the difference was not statistically significant (11.83 ± 1.34 days versus 13.38 ± 2.20 days, $P = 0.79$).

DISCUSSION

This study demonstrated that molecular methods to identify infectious pathogens in children with CAP can significantly increase detection rates and molecular methods have the potential to guide antimicrobial selection. Our findings were consistent with a retrospective study conducted on hospitalised adults with CAP (Gadsby et al., 2016). As there are some differences in the aetiology, specimen collection, and antibiotic usage between children and adults, our study can specifically provide evidence for the diagnosis and management of childhood CAP.

It is thought that viruses play a more important role in childhood CAP, and in most studies, the identification rates of viruses are higher than those of bacteria (Johnson et al., 2008; Holter et al., 2015; Jain et al., 2015). However, the opposite was true in our study. *H. influenzae* and *S. pneumoniae* in particular ranked second and third most common pathogens, respectively, with identification rates over 20%. This detection rate was higher than in studies where bacteria were detected using culture and similar to studies that used molecular methods (Elemraid et al., 2013; Howie et al., 2014; Gadsby et al., 2016). Therefore, the detection of bacterial pathogens solely based on culture is difficult to comprehensively reveal the underlying causative pathogen spectrum, which would possibly result in underestimating the risk of bacterial infection following primary viral infection. Multiple-target detection techniques based on real-time PCR and metagenomic next-generation sequencing (mNGS), which have the ability to identify both viral and bacterial infections, can serve as quantitative and comprehensive means of diagnosis, and are ideal for prescribing proper treatment (Gadsby et al., 2015; Miao et al., 2018).

In China, pneumococcal conjugated vaccine (PCV) and *Haemophilus Influenzae* Type b (Hib) were introduced for private purchase against 13 serotypes of *S. pneumoniae* in 2008 and *H. influenzae* type B in 2000 respectively (Wagner et al., 2014). However, these two vaccines were not included in the national immunization program in China, and the proportions of age-appropriate vaccination coverage were critically low (Qu et al., 2017). In the present study, *S. pneumoniae* and *H. influenzae* have been shown the rather high detection rate in children with CAP of Beijing and Hebei. Taking into account the above situation, incorporating PCV and Hib into the free

immunization program in China would undoubtedly reduce the prevalence of these two agents and might play important roles in preventing childhood CAP.

Sputum samples are likely to be contaminated with upper airway flora, which might lead to false identification of the true pathogen. This is more likely to occur in patients taking antibiotics because antibiotics will inhibit the growth of the causative bacteria (Rodrigues and Groves, 2018). We speculate that this may be the reason why the results of culture were inconsistent with combined-MS methods in five specimens in this study. For other culture-positive samples, bacteria identified using culture were identical to those identified using combined-MS methods, which set a threshold as previously published for excluding the interference of bacteria colonizing (Gadsby et al., 2016). We therefore suggest that collecting induced sputum in children with CAP and analysing them with quantitative molecular bacterial testing can serve as an important complement to traditional culture methods.

By comparing the initial empirical antibiotic treatment with the pathogen-directed therapy guided by combined-MS methods, we found some useful evidence supporting the use of empirical antibiotics. First, *H. influenzae* was the most commonly identified bacterial pathogen in our study. β-lactam/β-lactamase inhibitor combinations are recommended as its first-line treatment. Therefore, it is recommended the original empirical therapy to be β-lactam/β-lactamase inhibitor combinations in most cases. Second, macrolides are frequently prescribed to children with CAP because of their long half-life and short duration of therapy (Blyth and Gerber, 2018). However, except for CAP caused by atypical pathogens, most macrolides are unnecessary, which was also the case in our study (25.4%) (Al-Niemat et al., 2014; Wunderink, 2018). Overuse of macrolides lead to an economic burden and an increase in macrolide resistance in respiratory pathogens (Gandra et al., 2014; Xiao et al., 2016; McEwen and Collignon, 2018). It is noteworthy that antimicrobial resistance is a crucial consideration when selecting antimicrobials. As the phenotypic characteristics, such as susceptibility, can only be identified using culture-based methods, which offers it irreplaceable advantages over molecular testing. A limitation of the combined-MS method described here was that it cannot provide information on antimicrobial resistance during bacteria detection. However, for multiplex PCR-MS platforms, screening multiple mutations associated with drug resistance is reasonably practicable. Therefore, in the follow-up study, an extra panel targeting resistance genes in key pathogens causative of bacterial pneumonia can be designed and included to complement the detection panel. Combing the positive microbiological identification and AMR profiles of the causative agents, empirical selection of antibiotics would be more effective and individualized.

DATA AVAILABILITY STATEMENT

The raw data supporting the conclusions of this article will be made available by the authors, without undue reservation.

ETHICS STATEMENT

This study was approved by Medical Ethics Committee of Beijing Children's Hospital, Capital Medical University. Written informed consent to participate in this study was provided by the participants' legal guardian/next of kin.

AUTHOR CONTRIBUTIONS

JP contributed to the development of the study design and the coordination of the execution of the study. ZX and JP coordinated the study and reviewed drafts of the manuscript. LS and CZ drafted the study protocol, analyzed the results, and drafted the manuscript. SA conducted to the experiment and assisted in writing the manuscript. XC, YL, LX, and BX helped to performed the experiments. All authors contributed to the article and approved the submitted version.

FUNDING

This work was funded by the Non-profit Central Research Institute Fund of Chinese Academy of Medical Sciences (2018PT51009, 2019PT310006 and 2019PT310029) and Key Technology R&D Program of China (2017 ZX10103004-004).

SUPPLEMENTARY MATERIAL

The Supplementary Material for this article can be found online at: https://www.frontiersin.org/articles/10.3389/fcimb.2021.695134/full#supplementary-material

REFERENCES

Al-Niemat, S. I., Aljbouri, T. M., Goussous, L. S., Efaishat, R. A., and Salah, R. K. (2014). Antibiotic Prescribing Patterns in Outpatient Emergency Clinics at Queen Rania Al Abdullah II Children's Hospital, Jordan 2013. *Oman Med. J.* 29 (4), 250–254. doi: 10.5001/omj.2014.67

Apisarnthanarak, A., and Mundy, L. M. (2005). Etiology of Community-Acquired Pneumonia. *Clin. Chest Med.* 26 (1), 47–55. doi: 10.1016/j.ccm.2004.10.016

Blyth, C. C., and Gerber, J. S. (2018). Macrolides in Children With Community-Acquired Pneumonia: Panacea or Placebo? *J. Pediatr. Infect. Dis. Soc.* 7 (1), 71–77. doi: 10.1093/jpids/pix083

Bradley, J. S., Byington, C. L., Shah, S. S., Alverson, B., Carter, E. R., Harrison, C., et al. (2011). The Management of Community-Acquired Pneumonia in Infants and Children Older Than 3 Months of Age: Clinical Practice Guidelines by the Pediatric Infectious Diseases Society and the Infectious Diseases Society of America. *Clin. Infect. Dis.* 53 (7), e25–e76. doi: 10.1093/cid/cir531

Bryce, J., Boschi-Pinto, C., Shibuya, K., Black, R. E., and WHO Child Health Epidemiology Reference Group. (2005). WHO Estimates of the Causes of Death in Children. *Lancet* 365 (9465), 1147–1152. doi: 10.1016/S0140-6736(05)71877-8

Caliendo, A. M. (2011). Multiplex PCR and Emerging Technologies for the Detection of Respiratory Pathogens. *Clin. Infect. Dis.* 52 (Suppl 4), S326–S330. doi: 10.1093/cid/cir047

Duong, V. T., Tuyen, H. T., Van Minh, P., Campbell, J. I., Phuc, H. L., Nhu, T. D. H., et al. (2018). No Clinical Benefit of Empirical Antimicrobial Therapy for Pediatric Diarrhea in a High-Usage, High-Resistance Setting. *Clin. Infect. Dis.* 66 (4), 504–511. doi: 10.1093/cid/cix844

Elemraid, M. A., Sails, A. D., Eltringham, G. J., Perry, J. D., Rushton, S. P., Spencer, D. A., et al. (2013). Aetiology of Paediatric Pneumonia After the Introduction of Pneumococcal Conjugate Vaccine. *Eur. Respir. J.* 42 (6), 1595–1603. doi: 10.1183/09031936.00199112

Gadsby, N. J., McHugh, M. P., Russell, C. D., Mark, H., Conway Morris, A., Laurenson, I. F., et al. (2015). Development of Two Real-Time Multiplex PCR Assays for the Detection and Quantification of Eight Key Bacterial Pathogens in Lower Respiratory Tract Infections. *Clin. Microbiol. Infect.* 21 (8), 788.e781–788.e713. doi: 10.1016/j.cmi.2015.05.004

Gadsby, N. J., Russell, C. D., McHugh, M. P., Mark, H., Conway Morris, A., Laurenson, I. F., et al. (2016). Comprehensive Molecular Testing for Respiratory Pathogens in Community-Acquired Pneumonia. *Clin. Infect. Dis.* 62 (7), 817–823. doi: 10.1093/cid/civ1214

Gandra, S., Barter, D. M., and Laxminarayan, R. (2014). Economic Burden of Antibiotic Resistance: How Much Do We Really Know? *Clin. Microbiol. Infect.* 20 (10), 973–980. doi: 10.1111/1469-0691.12798

Holter, J. C., Muller, F., Bjorang, O., Samdal, H. H., Marthinsen, J. B., Jenum, P. A., et al. (2015). Etiology of Community-Acquired Pneumonia and Diagnostic Yields of Microbiological Methods: A 3-Year Prospective Study in Norway. *BMC Infect. Dis.* 15, 64. doi: 10.1186/s12879-015-0803-5

Honkinen, M., Lahti, E., Osterback, R., Ruuskanen, O., and Waris, M. (2012). Viruses and Bacteria in Sputum Samples of Children With Community-Acquired Pneumonia. *Clin. Microbiol. Infect.* 18 (3), 300–307. doi: 10.1111/j.1469-0691.2011.03603.x

Howie, S. R., Morris, G. A., Tokarz, R., Ebruke, B. E., Machuka, E. M., Ideh, R. C., et al. (2014). Etiology of Severe Childhood Pneumonia in the Gambia, West Africa, Determined by Conventional and Molecular Microbiological Analyses of Lung and Pleural Aspirate Samples. *Clin. Infect. Dis.* 59 (5), 682–685. doi: 10.1093/cid/ciu384

Jain, S. (2017). Epidemiology of Viral Pneumonia. *Clin. Chest Med.* 38 (1), 1–9. doi: 10.1016/j.ccm.2016.11.012

Jain, S., Self, W. H., Wunderink, R. G., and CDC EPIC Study Team. (2015). Community-Acquired Pneumonia Requiring Hospitalization. *N Engl. J. Med.* 373 (24), 2382. doi: 10.1056/NEJMc1511751

Johnson, A. W., Osinusi, K., Aderele, W. I., Gbadero, D. A., Olaleye, O. D., and Adeyemi-Doro, F. A. (2008). Etiologic Agents and Outcome Determinants of Community-Acquired Pneumonia in Urban Children: A Hospital-Based Study. *J. Natl. Med. Assoc.* 100 (4), 370–385. doi: 10.1016/s0027-9684(15)31269-4

Lahti, E., Peltola, V., Waris, M., Virkki, R., Rantakokko-Jalava, K., Jalava, J., et al. (2009). Induced Sputum in the Diagnosis of Childhood Community-Acquired Pneumonia. *Thorax* 64 (3), 252–257. doi: 10.1136/thx.2008.099051

Liu, L., Oza, S., Hogan, D., Chu, Y., Perin, J., Zhu, J., et al. (2016). Global, Regional, and National Causes of Under-5 Mortality in 2000-15: An Updated Systematic Analysis With Implications for the Sustainable Development Goals. *Lancet* 388 (10063), 3027–3035. doi: 10.1016/S0140-6736(16)31593-8

McEwen, S. A., and Collignon, P. J. (2018). Antimicrobial Resistance: A One Health Perspective. *Microbiol. Spectr.* 6 (2), 1–26. doi: 10.1128/microbiolspec.ARBA-0009-2017

Miao, Q., Ma, Y., Wang, Q., Pan, J., Zhang, Y., Jin, W., et al. (2018). Microbiological Diagnostic Performance of Metagenomic Next-Generation Sequencing When Applied to Clinical Practice. *Clin. Infect. Dis.* 67 (suppl_2), S231–S240. doi: 10.1093/cid/ciy693

Qu, F., Weschler, L. B., Sun, Y., and Sundell, J. (2017). High Pneumonia Lifetime-Ever Incidence in Beijing Children Compared With Locations in Other Countries, and Implications for National PCV and Hib Vaccination. *PloS One* 12 (2), e0171438. doi: 10.1371/journal.pone.0171438

Rodrigues, C. M. C., and Groves, H. (2018). Community-Acquired Pneumonia in Children: The Challenges of Microbiological Diagnosis. *J. Clin. Microbiol.* 56 (3), e01318–17. doi: 10.1128/JCM.01318-17

Subspecialty Group of Respiratory Diseases, T.S.o.P., and Chinese Medical Association The Editorial Board, C.J.o.P. (2013). Guidelines for Management of Community Acquired Pneumonia in Children (the Revised Edition of 2013) (II). *Zhonghua Er Ke Za Zhi* 51 (11), 856–862. doi: 10.3760/cma.j.issn.0578-1310.2013.11.012

Wagner, A. L., Sun, X., Montgomery, J. P., Huang, Z., and Boulton, M. L. (2014). The Impact of Residency and Urbanicity on Haemophilus Influenzae Type B and Pneumococcal Immunization in Shanghai Children: A Retrospective Cohort Study. *PloS One* 9 (5), e97800. doi: 10.1371/journal.pone.0097800

World Health Organization. (2014). *Revised WHO Classification and Treatment of Pneumonia in Children at Health Facilities: Evidence Summaries* (Geneva: Switzerland). Available at: https://www.who.int/maternal_child_adolescent/documents/child-pneumonia-treatment/en/.

Wunderink, R. G. (2018). Guidelines to Manage Community-Acquired Pneumonia. *Clin. Chest Med.* 39 (4), 723–731. doi: 10.1016/j.ccm.2018.07.006

Xiao, Y., Wang, J., Shen, P., Zheng, B., Zheng, Y., and Li, L. (2016). Retrospective Survey of the Efficacy of Mandatory Implementation of the Essential Medicine Policy in the Primary Healthcare Setting in China: Failure to Promote the Rational Use of Antibiotics in Clinics. *Int. J. Antimicrob. Agents* 48 (4), 409–414. doi: 10.1016/j.ijantimicag.2016.06.017

Zhang, C., Xiao, Y., Du, J., Ren, L., Wang, J., Peng, J., et al. (2015). Application of Multiplex PCR Coupled With Matrix-Assisted Laser Desorption Ionization-Time of Flight Analysis for Simultaneous Detection of 21 Common Respiratory Viruses. *J. Clin. Microbiol.* 53 (8), 2549–2554. doi: 10.1128/JCM.00943-15

Zhang, C., Xiu, L., Xiao, Y., Xie, Z., Ren, L., and Peng, J. (2018). Simultaneous Detection of Key Bacterial Pathogens Related to Pneumonia and Meningitis Using Multiplex PCR Coupled With Mass Spectrometry. *Front. Cell Infect. Microbiol.* 8, 107. doi: 10.3389/fcimb.2018.00107

Conflict of Interest: The authors declare that the research was conducted in the absence of any commercial or financial relationships that could be construed as a potential conflict of interest.

frontiers in Cellular and Infection Microbiology

ORIGINAL RESEARCH
published: 26 July 2021
doi: 10.3389/fcimb.2021.634215

Mass Spectrometry Proteotyping-Based Detection and Identification of *Staphylococcus aureus*, *Escherichia coli*, and *Candida albicans* in Blood

*Nahid Kondori[1,2], Amra Kurtovic[2], Beatriz Piñeiro-Iglesias[2], Francisco Salvà-Serra[1,2,3,4], Daniel Jaén-Luchoro[1,3], Björn Andersson[5], Gelio Alves[6], Aleksey Ogurtsov[6], Annika Thorsell[7], Johannes Fuchs[7], Timur Tunovic[2], Nina Kamenska[8], Anders Karlsson[9], Yi-Kuo Yu[6], Edward R. B. Moore[1,2,3] and Roger Karlsson[1,2,9]**

[1] Department of Infectious Diseases, Sahlgrenska Academy, University of Gothenburg, Gothenburg, Sweden, [2] Department of Clinical Microbiology, Sahlgrenska University Hospital, Gothenburg, Sweden, [3] Culture Collection University of Gothenburg (CCUG), Sahlgrenska Academy of the University of Gothenburg, Gothenburg, Sweden, [4] Microbiology, Department of Biology, University of the Balearic Islands, Palma de Mallorca, Spain, [5] Bioinformatics Core Facility at Sahlgrenska Academy, University of Gothenburg, Gothenburg, Sweden, [6] National Center for Biotechnology Information (NCBI), Bethesda, MD, United States, [7] Proteomics Core Facility at Sahlgrenska Academy, University of Gothenburg, Gothenburg, Sweden, [8] Norra-Älvsborgs-Länssjukhus (NÄL), Trollhättan, Sweden, [9] Nanoxis Consulting AB, Gothenburg, Sweden

OPEN ACCESS

Edited by:
Yi-Wei Tang,
Cepheid, United States

Reviewed by:
Bryan Schmitt,
Indiana University Bloomington, United States
Abdullah Kilic,
Wake Forest University, United States

***Correspondence:**
Roger Karlsson
roger.karlsson@vgregion.se

Specialty section:
This article was submitted to Clinical Microbiology, a section of the journal Frontiers in Cellular and Infection Microbiology

Received: *27 November 2020*
Accepted: *09 July 2021*
Published: *26 July 2021*

Citation:
Kondori N, Kurtovic A, Piñeiro-Iglesias B, Salvà-Serra F, Jaén-Luchoro D, Andersson B, Alves G, Ogurtsov A, Thorsell A, Fuchs J, Tunovic T, Kamenska N, Karlsson A, Yu Y-K, Moore ERB and Karlsson R (2021) Mass Spectrometry Proteotyping-Based Detection and Identification of Staphylococcus aureus, Escherichia coli, and Candida albicans in Blood. Front. Cell. Infect. Microbiol. 11:634215. doi: 10.3389/fcimb.2021.634215

Bloodstream infections (BSIs), the presence of microorganisms in blood, are potentially serious conditions that can quickly develop into sepsis and life-threatening situations. When assessing proper treatment, rapid diagnosis is the key; besides clinical judgement performed by attending physicians, supporting microbiological tests typically are performed, often requiring microbial isolation and culturing steps, which increases the time required for confirming positive cases of BSI. The additional waiting time forces physicians to prescribe broad-spectrum antibiotics and empirically based treatments, before determining the precise cause of the disease. Thus, alternative and more rapid cultivation-independent methods are needed to improve clinical diagnostics, supporting prompt and accurate treatment and reducing the development of antibiotic resistance. In this study, a culture-independent workflow for pathogen detection and identification in blood samples was developed, using peptide biomarkers and applying bottom-up proteomics analyses, i.e., so-called "proteotyping". To demonstrate the feasibility of detection of blood infectious pathogens, using proteotyping, *Escherichia coli* and *Staphylococcus aureus* were included in the study, as the most prominent bacterial causes of bacteremia and sepsis, as well as *Candida albicans*, one of the most prominent causes of fungemia. Model systems including spiked negative blood samples, as well as positive blood cultures, without further culturing steps, were investigated. Furthermore, an experiment designed to determine the incubation time needed for correct identification of the infectious pathogens in blood cultures was performed. The results for the spiked negative blood samples showed that proteotyping was 100- to 1,000-fold more sensitive, in comparison with the MALDI-TOF MS-based approach. Furthermore, in the analyses of ten positive blood cultures each of *E. coli* and *S. aureus*, both the MALDI-TOF MS-based

and proteotyping approaches were successful in the identification of *E. coli*, although only proteotyping could identify *S. aureus* correctly in all samples. Compared with the MALDI-TOF MS-based approaches, shotgun proteotyping demonstrated higher sensitivity and accuracy, and required significantly shorter incubation time before detection and identification of the correct pathogen could be accomplished.

Keywords: blood-stream infections, proteotyping, MALDI-TOF MS, proteomics, bacteremia, fungemia, sepsis, rapid diagnostics of infectious diseases

INTRODUCTION

Blood stream infections (BSIs) are ranked as the third leading cause of health care-related infections (Seymour et al., 2016). BSIs are caused mainly by bacteria or fungi and are frequently derived from urinary tract or abdominal infections or community acquired pneumonia (Angus et al., 2001; Lagu et al., 2012). Common causative bacterial agents of BSIs include *Escherichia coli*, *Staphylococcus* spp., *Enterococcus* spp., *Streptococcus* spp., *Pseudomonas aeruginosa*, and *Klebsiella* spp. (Martinez and Wolk, 2016). The presence of *Candida* fungi in blood, referred to as, "candidemia", is also common in hospitalized patients (Alam et al., 2014; Klingspor et al., 2018). Most cases of candidemia are caused by five species: *Candida albicans*; *Candida glabrata*; *Candida parapsilosis*; *Candida tropicalis*; and *Candida krusei* (Pappas et al., 2003; Bassetti et al., 2013; Lindberg et al., 2019; Xiao et al., 2019). Among them, *C. albicans* is the most common fungus isolated from BSI in adults and children and is associated with high rates of mortality (Alam et al., 2014; Steinbach, 2016). Early identification of infectious strains and treatment with appropriate anti-microbial drugs are the keys to reducing morbidity and mortality associated with BSI (Metzgar et al., 2016; Tassinari et al., 2018), as BSI can lead to sepsis (Huerta and Rice, 2018), a serious and life-threatening condition of multiorgan failure, triggered by an uncontrolled host response to an infection (Singer et al., 2016). On a global scale, sepsis is one of the most predominant causes of death in hospitalized patients (Fleischmann et al., 2016a; Fleischmann et al., 2016b; Grumaz et al., 2016; Ibrahim et al., 2020), highlighting the importance of rapid diagnostics of BSIs.

The blood culture is still the "gold standard" for the diagnosis of patients with BSI (Mancini et al., 2010; Źródłowski et al., 2018; Ombelet et al., 2019). The identification of pathogenic microorganisms and antimicrobial susceptibility testing also generally relies on the cultivation and identification of pathogens from blood culture flasks (Opota et al., 2015). Positive blood cultures indicate a microbial growth (bacteria and/or fungi), whereas negative blood cultures indicate no microbial growth in the blood culture flasks. Completed routine identification may be achieved within two days but may take longer for infections by different species and different strains (Seng et al., 2009; Kirn and Weinstein, 2013; Nagy et al., 2018). Drawbacks exist in performing the cultivation step, including the time required for the culturing itself, as well as the fact that many blood cultures are inconclusive, in the sense that the bacteria or fungi from patient samples may not grow in the culture or cannot be recovered, *i.e.* false negative results (Murray and Masur, 2012; Skvarc et al., 2013; Sinha et al., 2018; Hazwani et al., 2020; Źródłowski et al., 2020). However, false negative blood cultures may result from the presence of antibiotics in the culture, originating from the patient blood, from infections caused by opportunistic microorganisms that grow poorly in standardized, automated, blood culture systems or that only few viable cells of the pathogen have been recovered from patient blood samples (Sinha et al., 2018). Furthermore, the success of recovery of microorganisms in cases of bacteremia has been shown to be linked to the volume of blood initially taken (Murray and Masur, 2012; Skvarc et al., 2013; Loonen et al., 2014; Opota et al., 2015; Henning et al., 2019). In some cases, however, it is not possible to recover large volumes of blood (Kirn and Weinstein, 2013), for example, from newborn infants at neonatal intensive care units, wherein culture-independent diagnostics methods, i.e., not relying on blood cultures, and thus not needing large volumes of patient blood, would be of utmost importance (Steinbach, 2016; Henning et al., 2019).

Recently, methods for detection of genetic material (Mancini et al., 2010; Skvarc et al., 2013; Gosiewski et al., 2014; Liesenfeld et al., 2014; van de Groep et al., 2018), as well as DNA-sequencing-based methods (Grumaz et al., 2016; Gosiewski et al., 2017; Watanabe et al., 2018; Grumaz et al., 2020), have been used for the detection of pathogens in blood. Serological methods, including detection of lipopolysaccharides for Gram-negative bacteria or galactomannan for fungi (Opal, 2010; Dickson and Lehmann, 2019), but also methods based on Gram-staining and fluorescence in-situ hybridization (FISH) have been successfully applied for direct detection of pathogens in blood (Gosiewski et al., 2014; Źródłowski et al., 2020). An advantage of these methods is that they do not rely on isolates

Abbreviations: AMR, Antimicrobial resistance; BSI, Bloodstream infection; CCUG, Culture Collection University of Gothenburg; CHCA, α-cyano-4-hydroxycinnamic acid; CRE, Carbapenem-Resistant Enterobacteriaceae; ESBL, Extended Spectrum β-Lactamase ; FISH, fluorescence *in-situ* hybridization; IVD *In Vitro* Diagnostics ; LC-MS/MS, liquid chromatography tandem mass spectrometry; MALDI-TOF, matrix assisted laser desorption/ionization time of flight; MS, mass spectrometry ; MiCld, Microorganism Classification and Identification; mmu, millimass units; OD, Optical Density; ON, overnight; PRM, parallel reaction monitoring; RUO, research use only; SDC, sodium deoxycholate; TCUP, Typing and Characterisation Using Proteomics; VIR, virulence; WHO, World Health Organization.

from blood cultures and can be used on samples where antibiotic treatment has been initiated (Źródłowski et al., 2018; Źródłowski et al., 2020). These procedures are efficient, although some of them are relatively expensive and not suitable for the routine in clinical laboratories with large numbers of samples (Mancini et al., 2010; Skvarc et al., 2013; Opota et al., 2015; Źródłowski et al., 2018; Briggs et al., 2021).

Matrix assisted laser desorption/ionization time of flight mass spectrometry (MALDI-TOF MS)-based identification of microorganisms has emerged as an alternative or a complement to the traditional phenotypic methods (Seng et al., 2009; Ferroni et al., 2010; Welker and Moore, 2011; Spanu et al., 2012; Kondori et al., 2015). The implementation of MALDI-TOF MS identification into the clinical routine laboratories has been successful due to several benefits, including ease-of-use, speed in obtaining results, low cost, as well as high resolution of species identifications, in most cases (Florio et al., 2018). However, generally, the approach includes a necessary cultivation step, although efforts are being made to implement short cultivations steps or perform direct MALDI-TOF MS-based identification from the positive blood cultures (Florio et al., 2018; Briggs et al., 2021). A direct analysis of a patient sample, however, relies on successful removal of human blood cells and plasma proteins, as these may hinder the identification of bacterial and fungal pathogens, which are present to a much lesser degree in a blood sample, compared with the cells and proteins of human origin.

Even though the "gold standard" of blood cultures is nowadays complemented by molecular methods and MALDI-TOF MS approaches, none of the current rapid diagnostic methodologies is able to provide broad-range species identification as well as results regarding antibiotic susceptibility in one single analysis (Briggs et al., 2021). Therefore, development of reliable and rapid analytical techniques for comprehensive diagnostics and characterizations of infectious bacteria is still essential.

In this study, we investigate the use of unique peptides and bottom-up proteomics for performing rapid diagnostics of infectious bacteria and fungi. "Bottom-up proteomics", as differentiated from "top-down proteomics", relies on digestion of proteins into peptides using proteolytic enzymes, such as trypsin, followed by separation of the complex mixture of peptides, using a separation step, typically liquid chromatography (LC) prior to ionization, fragmentation and identification of peptides by tandem mass spectrometry (MS/MS) (Karlsson et al., 2015). Bottom-up proteomic approaches have been employed to increase the discriminative power and resolution of closely related species, i.e., to strain-level typing (Dworzanski et al., 2006; Karlsson et al., 2012; Chenau et al., 2014; Semanjski and Macek, 2016; Chen et al., 2019; Karlsson et al., 2020). Such "proteotyping" approaches, using peptide biomarkers, enable differentiating, for instance, the taxonomically close species of *Streptococcus pneumoniae*, *Streptococcus pseudopneumoniae* and *Streptococcus mitis* of the Mitis group of the genus *Streptococcus* (Karlsson et al., 2018). To facilitate the identification of species-unique peptides, several different bioinformatics pipelines have been developed to highlight peptides unique for different taxonomic levels (Family, Genus, Species) (Boulund et al., 2017; Grenga et al., 2019; Pible et al., 2020), including the Microorganism Classification and Identification (MiCId), which was used in this study (Alves et al., 2018; Alves and Yu, 2020). The goal of this study was to detect and identify bacteria and fungi directly in a model system including spiked negative blood samples, as well as in positive blood cultures, without further cultivation, using liquid chromatography tandem mass spectrometry (LC-MS/MS) and species-unique peptide identification, *i.e.* shotgun proteotyping (Karlsson et al., 2015; Karlsson et al., 2017; Karlsson et al., 2018; Karlsson et al., 2020).

MATERIAL AND METHODS

Experimental Design

Four different experiments were included, briefly outlined in **Figure 1**. The first experiment was designed to investigate a proper workflow for reducing cells and proteins of host origin, and therefore various host depletion methods were tested (**Figure 1A**). The next experiment was focused on assessing the sensitivity of the shotgun proteotyping approach, as compared to the traditionally used MALDI-TOF MS-based identification. This was performed by adding known amounts of bacterial or fungal cells to negative blood samples (**Figure 1B**). In the third experiment, positive blood cultures derived from patient samples, were analyzed to assess the accuracy of the shotgun proteotyping approach (**Figure 1C**). Finally, in order to investigate the time needed for correct identification of the infectious pathogens in blood cultures, a low number of bacterial or fungal cells (1,000 or 10,000) was added to blood culture flasks followed by incubation in a blood culture cabinet, and at each hour, from 2 to 7 hours, plus overnight (ON), samples were taken for analysis (**Figure 1D**). An overnight (ON) incubation corresponds to an hour range of 15-18 hours.

Cultivation of Bacteria and Fungi

Bacterial and fungal strains were acquired from the Culture Collection University of Gothenburg (CCUG, www.ccug.se). *Staphylococcus aureus* and *Escherichia coli* were included as representative bacterial pathogens and *Candida albicans* was included as a representative fungal pathogen. *S. aureus* (CCUG 41582), *E. coli* (CCUG 49263) and *C. albicans* (CCUG 32723) were cultivated on Columbia agar supplemented with 5% of defibrinated horse blood (Substrate Unit, Department of Clinical Microbiology, Sahlgrenska University Hospital, Gothenburg, Sweden) and incubated at 37°C, for 24 hours.

Host Biomass Depletion Methods: Saponin, MolYsis, and Cytolysis

Three different methods for host biomass depletion of the samples were investigated: A cytolysis approach, a protocol using Saponin and the use of a commercial kit (MolYsis Kit™ Basic5, Molzym, GmbH & Co. KG, Bremen, Germany) with a modified protocol. The Cytolysis approach relies on osmotic

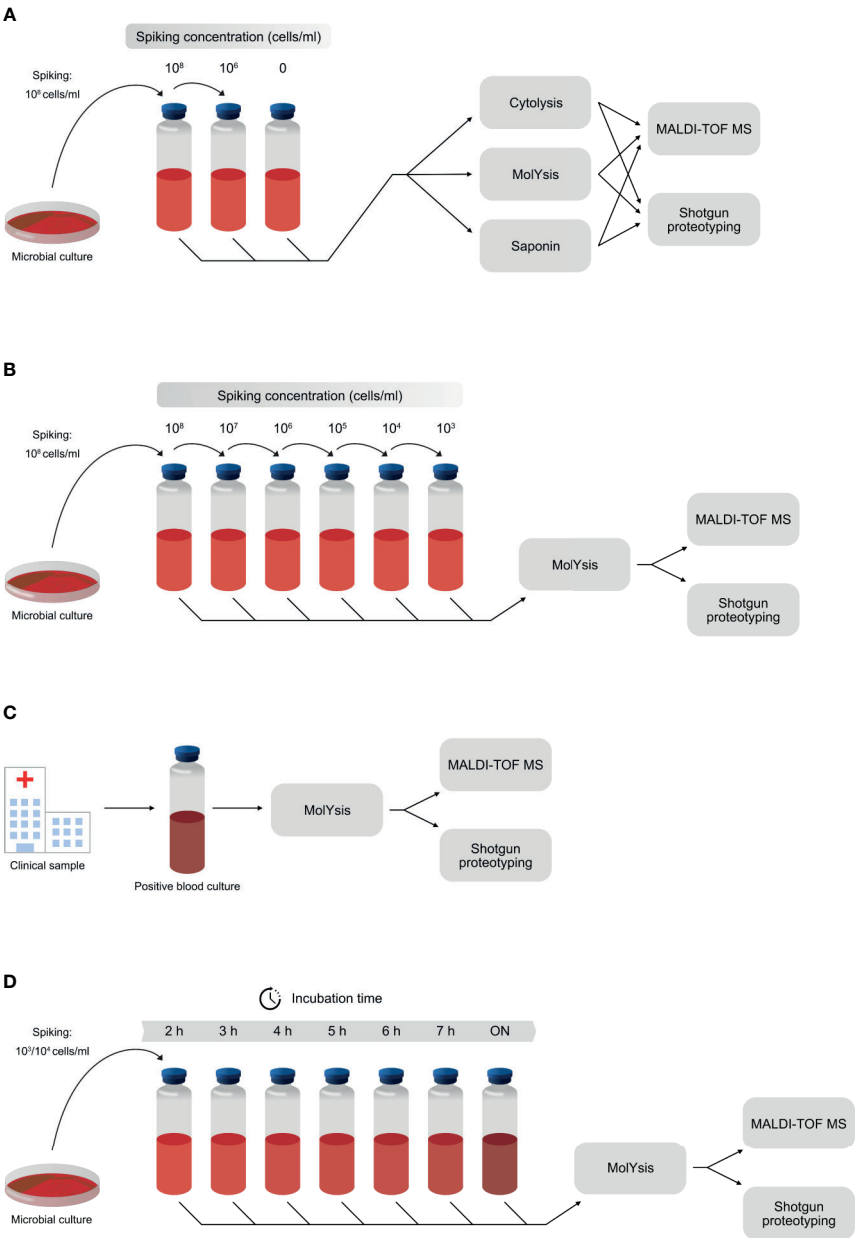

FIGURE 1 | The experimental design of the experiments included in the study. **(A)** Host depletion methods MolYsis, Saponin and Cytolysis were investigated by spiking negative blood with different numbers of cells from *S. aureus*. **(B)** Assessment of the sensitivity of shotgun proteotyping, compared with direct MALDI-TOF MS-based identification. Different numbers of cells were added to negative blood samples in the range of 1,000 cells/ml to 100 million cells/ml, and the samples were then analyzed by both methodologies. **(C)** Assessment of the accuracy of shotgun proteotyping and direct MALDI-TOF MS-based identification by analysis of positive blood cultures from the clinical routine laboratories. **(D)** Assessment of the incubation time needed for a positive identification of the correct species, using shotgun proteotyping and direct MALDI-TOF MS-based identification. A low number of cells (1,000 or 10,000) was added to negative blood samples, followed by incubation in a blood culture cabinet. Samples were taken after 2, 3, 4, 5, 6 and 7 hours of incubation, as well as after overnight (ON).

shock, lysis of human cells, but maintaining the integrity of bacterial and fungal cells, which are more resistant. The Saponin approach, which is used at the Department of Clinical Microbiology (Sahlgrenska University Hospital, Gothenburg, Sweden) for performing direct MALDI-TOF-MS-based analyses of blood samples, consists of adding a solution of saponin for lysis of host cells. The MolYsis kit has previously been used for identification of *S. aureus* in positive blood cultures (McCann and Jordan, 2014; Thoendel et al., 2016), for application of PCR-based methods. However, in the procedure, the first step of the MolYsis workflow entails selective lysis of human blood cells, whereby a pellet of bacteria or fungi is

achieved. The later steps of the procedure involve lysis of the cells and extraction of DNA, although, in this study, the MolYsis procedure was used only for removal of human cells and the generation of a pellet of bacteria or fungi, as described previously (Karlsson et al., 2020). The pellet of bacteria or fungi was then processed, using a separately developed protocol, as described.

MolYsis Clean-Up

The MolYsis™ Kit (Molzym, GmbH & Co. KG, Germany) was used, according to the manufacturer´s instructions, with some adjustments (Karlsson et al., 2020). After centrifugation at 12,000 x g for 5 minutes, the supernatant was discarded, and the pellet saved. MALDI-TOF MS was performed on the bacterial pellets. In cases where pellets were not large enough to be processed, they were dissolved in 5 µl of deionized water (W6-212 Water, Optima® LC/MS, Fisher Chemical), whereas the pellet for proteotyping was dissolved in 150 µl of PBS.

Saponin Clean-Up

An in-house Saponin clean-up method, modified from a protocol (Ferroni et al., 2010) was implemented. Saponin solution (200 µl of 5% solution in distilled water) was added to 1 ml of blood culture sample. The suspension was vortexed and then allowed to stand at room temperature for 5 minutes. The suspension was then centrifuged at 12,000 x g for 1 minute. The pellet was washed 3 times by resuspension with 1 ml distilled water and centrifugation at 12,000 x g for 5 minutes. The final supernatant was discarded, and the pellet was saved. MALDI-TOF MS was performed on the bacterial pellets. In cases where pellets were not large enough to be processed, they were dissolved in 5 µl of deionized water (W6-212 Water, Optima® LC/MS), while the pellet for proteotyping was dissolved in 150 µl of PBS.

Cytolysis Clean-Up

Cell lysis by osmotic shock (Cytolysis) was performed. The blood culture sample was centrifuged at 12,000 x g for 5 minutes. The supernatant was discarded, and 1 ml deionized water was added to resuspend the pellet, to create osmotic shock for the blood cells, lysing them, but leaving bacterial and fungal cells intact. Samples were centrifuged at 12,000 x g for 1 minute. The supernatant was discarded, and the pellet saved. MALDI-TOF MS was performed on the bacterial pellets. In cases where pellets were not large enough to be processed, they were dissolved in 5 µl of deionized water (W6-212 Water, Optima® LC/MS), while the pellet for proteotyping was dissolved in 150 µl of PBS.

The Sensitivities and Specificities of MALDI-TOF-MS and Shotgun Prototyping

Horse blood was spiked with bacterial or fungal cells in 10-fold dilutions, generating a range of cell concentrations from 0 to 100 million cells/ml, to assess the sensitivity of the MALDI-TOF MS and nanoLC-MS/MS shotgun proteotyping methods. The final concentrations of bacteria or fungi in blood ranged from 0 up to 10^8 cells/ml (0, 10, 100, 1,000, 10,000, 100,000, 1 million, 10 million, 100 million cells/ml).

Preparation of Samples Spiked With Bacterial or Fungal Cells

Bacterial and fungal biomass were collected from agar plates and resuspended in phosphate-buffered saline (PBS). Bacterial and fungal cell densities (Optical Density, OD) were measured by spectrophotometry (WPA CO 8000 Cell Density Meter, Biochrom Ltd. Cambridge, United Kingdom) at a wavelength of 600 nm. For each experiment, the same amounts of biomass were established, by adjusting the OD to 1.0 (OD = 1.0 corresponds to ~10^8 bacteria) in 1 ml of PBS. The biomass was washed with PBS three times by centrifuging the sample for 5 minutes at 12,000 x g, discarding the supernatant and resuspending the pellet in 1 ml of PBS. Finally, the biomass was centrifuged for 5 minutes at 12,000 x g and supernatant discarded. The pellet was resuspended in 100 µl PBS, which was added to 900 µl sterile horse blood, creating the first spiked sample of 1 ml blood containing 10^8 bacterial cells per ml. This procedure was followed to create samples containing bacterial/fungal cells with 10-fold serial dilutions of 0 cells/ml to 100 million cells/ml (10^8). The spiking procedure was performed by generating two samples in parallel. In the final step, the two samples were combined, vortexed and split, in order to ensure that the contents of each portion were as equivalent as possible, i.e., to ensure the same number of cells in each sample. One of the samples was used for MALDI-TOF MS analysis and the other for proteotyping by tandem nanoLC-MS/MS.

Incubation Time Required for Direct Identification of Bacteria and Fungi by MALDI-TOF MS or Shotgun Proteotyping

The kinetics of direct identifications of bacteria and fungi by MALDI-TOFMS or proteotyping were studied by incubation of bacteria and fungi at a final concentration of 1,000 cells/ml (or 10,000 cells/ml) in the blood culture flasks (BACT/ALERT®FA Plus Aerobic 30 ml, bioMérieux, Marcy l'Etoile, France). The blood cultures were incubated in a continuous monitoring blood culture system (CMBCS) with a colorimetric sensor (BacT/Alert®; bioMérieux, Marcy l'Etoile, France) (Kennedy et al., 1995). The samples were collected from the blood culture tubes at different time points after incubation [2 h, 3 h, 4 h, 5 h, 6 h, 7 h and overnight (ON)]. Prior to analysis, the samples were subjected to the MolYsis clean-up procedure. The samples for MALDI-TOF MS were stored at 2°C until analysis or, in the case of proteotyping, were stored at -20°C until analysis by tandem nanoLC-MS/MS for detection of microbial pathogen in blood samples.

Analysis of Positive Blood Cultures

Positive blood cultures with *E. coli* (n=10), *S. aureus* (n=10) and *C. albicans* (n=5) were included in this study. The samples were collected at the Department of Clinical Microbiology,

Sahlgrenska University Hospital in Gothenburg, Sweden. Only samples that were collected as part of the standard diagnostic protocols were included in this study; no additional or extra sampling from patients was carried out and no patient identifiable information was collected; hence, informed consent was not required. Blood cultures were incubated by means of a BacT/Alert continuous monitoring blood culture system (CMBCS) that detects bacterial or fungal growth. Bottles flagged as positive by the BacT/Alert system were sub-cultured and incubated at 37°C, under aerobic and anaerobic conditions, until positive growth or otherwise, for 7-10 days, and interpreted according to the standard protocols in the laboratory. Prior to proteotyping MS analysis, the samples were subjected to the MolYsis clean-up procedure.

Matrix Assisted Laser Desorption/ Ionization Time of Flight Mass Spectrometry (MALDI-TOF MS) Analysis

MALDI-TOF MS was performed on the bacterial pellets. In cases where pellets were not large enough to be processed, they were dissolved in 5 µl of deionized water (W6-212 Water, Optima® LC/MS). Each sample was spotted in four replicates on disposable target slides (VITEK® MS-DS slide, bioMérieux, France). After drying at room temperature, 1 µl of ready-to-use α-cyano-4-hydroxycinnamic acid (CHCA) matrix solution (VITEK® MS-CHCA, bioMérieux, France) was added and allowed to dry at room temperature. In the cases of Gram-positive bacteria (*S. aureus*) and fungi samples (i.e., *C. albicans*), prior to the addition of the CHCA matrix solution, 1 µl of a formic acid solution (70%, VITEK® MS-FA, bioMérieux, France) was added to the sample and allowed to dry at room temperature. Subsequently, the slides were placed in the MALDI-TOF MS (VITEK MS™ RUO v.3.0, bioMérieux, France) with standard settings for routine identification, in a mass range of 2 to 20 kDa, Research Use Only (RUO), to be analyzed. Controls in the slide were performed in each run with *E. coli* CCUG 10979. The resulting spectra were analyzed in the proprietary IVD (*In Vitro* Diagnostics) Knowledge Database v2 (bioMérieux, France).

Sample Preparation for Proteotyping

After the host biomass depletion methods (Saponin, Cytolysis or MolYsis), the pellets containing bacterial or fungal cells were resuspended in 150 µl of PBS. The cell suspensions were transferred to 200 µl vials containing glass beads (Sigma-Aldrich, G1145). The cells were lysed by bead-beating, using approx. 50 µl of acid-washed 150-212 µm glass beads in a 200 µl tube, with a TissueLyser (Qiagen, 85220) with the following settings: frequency 1/25 s and 5 minutes. The cell lysates were frozen at -20°C until analysis.

Digestion of Samples for Proteotyping Into Peptides

Samples were thawed and sodium deoxycholate (SDC, 5%) was added to a 1% final concentration. Trypsin (2 µg/ml, 100 µl ammonium bicarbonate, 20 mM pH 8) was added and samples were digested overnight (ON) at 37°C. SDC was removed by acidification with formic acid (neat; 2 µl to 100 µl sample) and the supernatant was stored in -20°C until analysis.

nanoLC-MS/MS Analysis of Proteotyping Samples

Peptide samples were desalted, using PepClean C18 spin columns (Thermo Fisher Scientific), according to the manufacturer's guidelines, prior to analysis on a Q Exactive HF mass spectrometer (Thermo Fisher Scientific) interfaced with Easy nLC 1200 liquid chromatography system (Thermo Fisher Scientific). Peptides were trapped on an Acclaim Pepmap 100 C18 trap column (100 µm x 2 cm, particle size 5 µm, Thermo Fischer Scientific) and separated on an in-house packed analytical column (75 µm x 300 mm, particle size 3 µm, Reprosil-Pur C18, Dr. Maisch), using a linear gradient from 7% to 35% B over 45 or 75 minutes, followed by an increase to 100% B for 5 minutes at a flow of 300 nL/minutes, where solvent A was 0.2% formic acid in water and solvent B was 0.2% formic acid, 80% acetonitrile in water. MS/MS analysis was performed in a data-dependent mode where the precursor ion mass spectra were acquired at a resolution of 60,000, *m/z* 400-1,600, and the Top10 most intense precursor ions, with charge states of 2 to 4, were selected for fragmentation. The isolation window was set to 1.2 Da, and MS2 spectra were recorded at a resolution of 30,000, *m/z* 200-2,000. Dynamic exclusion was set to 20 seconds and 10 ppm.

MiCId Bioinformatics Pipeline for Microorganism Classification and Identification

Microorganism Classification and Identification (MiCId) is a workflow designed for the identifications of microorganisms, proteins and estimations of microbial biomass in samples (Alves et al., 2016; Alves et al., 2018; Alves and Yu, 2020). For a rapid identification of microorganism, MiCId (version v.06.11.2020) workflow performs peptide identification by querying the MS/MS spectra in a peptide-centric database and assigns to every peptide a MS/MS spectrum-specific measure, namely, E- value (Alves et al., 2007; Alves et al., 2008; Alves and Yu, 2008; Alves et al., 2010). To provide microorganism identification significances, MiCId computes a weighted unified E-value by combining the spectrum-specific E-values of the identified peptides mappable to a given microorganism. For each identified microorganism, MiCId also computes a prior probability using a modified expectation-maximization method. The computed prior probabilities reflect the relative protein biomasses, due to the various reported microorganisms, in the sample. Assigning to microorganism accurate E-values along with the prior probability, MiCId provides users a measure suitable for controlling false positives (type I errors). In MiCId's default settings, microorganisms identified with E-values smaller or equal to 0.01 and with prior probability greater or equal to 0.01 are deemed true positives. Using these cut-off values allows users to control the false positive rate well below 5%.

Since peptides that are unique to a taxon at a given taxonomic level are often used as the main evidence for the presence of that

taxon, a false identification of such unique peptides can have undesirable consequence. To better control false microorganism identification, in addition to computing a unified E-value mentioned above, MiCId put an extra requirement for an identified peptide to qualify as an unique peptide. An identified unique peptide to a given taxon must have an E-value 10^{-4} or less aside from uniquely mappable to that taxon (Alves et al., 2018).

The database MiCId used to query MS/MS spectra comprises 3,887 organisms, including *Homo sapiens* and *Equus caballus*, covering 1,959 species. Protein sequences included in the database, for the 3,868 organisms (excluding *Shigella*), were downloaded (on April 27, 2020) from the National Center for Biotechnology Information (NCBI) at (ftp://ftp.ncbi.nlm.nih.gov/genomes/genbank/).

Supplementary Table 7S lists the microorganisms included. When performing database searches, up to two missed cleavage sites per peptide were allowed under the digestion rules of trypsin and Lys-C. The amino acid cysteine was kept unmodified. The mass error tolerance of 5 ppm was set for precursor ions and 20 ppm for product ions.

DATA AVAILABILITY

The mass spectrometry proteomics data have been deposited to the ProteomeXchange Consortium *via* the PRIDE (Perez-Riverol et al., 2019) partner repository with the dataset identifier, PXD023033.

RESULTS

Host Biomass Depletion Methods of Blood Samples

Three different host biomass depletion methods were employed on blood samples spiked with *S. aureus* (CCUG 41582), wherein the MolYsis™ kit was observed to reduce the number of peptides from horse blood origin (n= 17, 44 and 62 at 0, 10^6 and 10^8 cells respectively) while also recovering bacterial peptides (n=0, n=6 and n=415 from 0, 10^6 and 10^8 cells, respectively) (**Table 1**). The computed prior probabilities reflect the relative protein, due to the various reported (micro)organisms in the sample and can be used to assess the performance of the clean-up protocols. **Table 1** shows that, for the horse blood spiked samples with 10^6 and 10^8 cells/ml, the relative sample biomass for *S. aureus* are respectively around 25% and 93% *via* MolYsis, around 5% and 75% *via* Saponin, and around 0% and 60% *via* Cytolysis (**Table 1** and **Supplementary Table 1S**). MALDI-TOF MS (results not shown in the table) only identified *S. aureus* when 10^8 cells/ml were added to the blood samples.

The Sensitivities and Specificities of MALDI-TOF MS and Shotgun Proteotyping

The sensitivities and specificities of the proteotyping approach were investigated by adding (spiking) known amounts of bacterial or fungal cells, ranging from 0 to 100 million cells/ml to negative horse blood samples. The MALDI-TOF MS approach correctly identified the bacteria in the spiked samples containing the highest amounts of cells, i.e., 100 million cells/ml, but was not able to detect bacteria at 10 million cells/ml or less. In contrast, proteotyping was able to detect and identify species-unique peptides of the studied pathogens (*E. coli*, *S. aureus* and *C. albicans*) even down to spiked samples with as low as 10,000 cells/ml. Thus, proteotyping, was a 100- to 1,000-fold more sensitive in comparison of MALDI-TOF MS (**Table 2** and **Supplementary Table 2S**).

Analysis of Positive Blood Cultures

Samples from ten positive blood cultures from *E. coli* and *S. aureus* and five positive blood cultures from *C. albicans* were analyzed directly, without further culturing, using MALDI-TOF MS-based analysis and proteotyping. **Table 3** shows the identifications from the direct MALDI-TOF MS analyses, as well as the number of species-unique peptides found by the proteotyping analysis. Both protocols were able to identify the correct species in all ten samples with *E. coli*. However, MALDI-TOF MS was able to identify *S. aureus* in only four of the ten samples, whereas proteotyping was able to correctly identify *S. aureus* in all ten samples. *C. albicans* was not identified using the direct MALDI-TOF MS-based approach, however, proteotyping successfully identified the correct species in 4 out of the 5 samples (**Table 3**).

Incubation Time Required for Direct Identification of Bacteria and Fungi by MALDI-TOF MS or Proteotyping

Direct MALDI-TOF MS detected and identified *E. coli* in bacterial positive blood culture flasks after incubation overnight, however, *S. aureus* and *C. albicans* were not detected by MALDI-TOF MS in any of the blood cultures at any time after incubation (**Table 4**). Proteotyping was able to detect *S. aureus* after 7 hours of incubation, and for *E. coli* a correct identification could be achieved after only 5 hours of incubation. *C. albicans* was correctly identified by proteotyping after ON incubation (**Table 4** and **Supplementary Table 4S**).

DISCUSSION

Early recognition of BSIs is crucial for successful treatment of patients, before conditions worsen and, possibly, become fatal, by development of sepsis (Kumar et al., 2006; Loonen et al., 2014). Clinical manifestations of sepsis are variable, depending upon sites of infection and causative microorganisms, as well as underlying conditions of patients (Iskander et al., 2013; Huang et al., 2019; Özenci et al., 2019). Unfortunately, diagnosis of sepsis is complex and problematic, often delayed because early symptoms are not recognized; many symptoms are subtle and mimic other clinical conditions (Iskander et al., 2013). While sepsis may be identified by clinical signs and symptoms in a patient, no "gold standard" diagnostic test exists (Singer et al., 2016; Ibrahim et al., 2020).

TABLE 1 | Assessment of host biomass depletion methods prior to MS analyses.

Spiking concentration (cells/ml)	Host biomass depletion method	Taxa identified	Identification fraction	Average ln (E-value)	Average number of identified unique peptides	Average number of identified peptides	Average Prior
0	MolYsis kit	*H. sapiens*	1/1	-223	43	154	0.693
		E. caballus	1/1	-62.2	17	104	0.282
		S. aureus	0/1	–	–	–	–
	Saponin	*H. sapiens*	0/1	–	–	–	–
		E. caballus	1/1	-2440	663	1326	0.993
		S. aureus	0/1	–	–	–	–
	Cytolysis	*H. sapiens*	0/1	–	–	–	–
		E. caballus	1/1	-2780	786	1534	0.99
		S. aureus	0/1	–	–	–	–
10^6	MolYsis kit	*H. sapiens*	3/3	-214	41 ± 14	173 ± 34	0.351 ± 0.02
		E. caballus	3/3	-175	44 ± 4	172 ± 23	0.366 ± 0.07
		S. aureus	3/3	-122	6 ± 1.4	117 ± 39	0.25 ± 0.05
	Saponin	*H. sapiens*	0/1	–	–	–	–
		E. caballus	1/1	-2790	756	1722	0.937
		S. aureus	1/1	-146	10	134	0.0544
	Cytolysis	*H. sapiens*	0/1	–	–	–	–
		E. caballus	1/1	-2500	704	1295	0.989
		S. aureus	0/1	–	–	–	–
10^8	MolYsis kit	*H. sapiens*	3/3	-113	23 ± 5	118 ± 19	0.0199 ± 0.003
		E. caballus	3/3	-302	62 ± 13	187 ± 28	0.0521 ± 0.003
		S. aureus	3/3	-5090	415 ± 78	3394 ± 681	0.926 ± 0.005
	Saponin	*H. sapiens*	0/1	–	–	–	–
		E. caballus	1/1	-1800	443	1015	0.248
		S. aureus	1/1	-5140	426	3417	0.751
	Cytolysis	*H. sapiens*	0/1	–	–	–	–
		E. caballus	1/1	-2700	651	1300	0.399
		S. aureus	1/1	-3820	265	2271	0.599

MiCId identification results of horse blood samples spiked with 0, 10^6 and 10^8 cells of S. aureus and processed with three different host biomass depletion methods.

MALDI-TOF MS (results not shown in the table) identified S. aureus only when 10^8 cells/ml were added to the blood samples. In that case, the identification was successful with all three host biomass depletion methods. The denominator of the identification fraction shows the number of analyzed samples and the numerator shows the number of times each taxon has been identified; the number after "±" is the standard deviation (from triplicate analyses). For a taxon reported by MiCId, the "average number of identified peptides" records the average total number of identified peptides mappable to that taxon, while the "average number of identified unique peptides" sums to the total number of identified peptides satisfying the following two conditions simultaneously: these peptides must be unique to that taxon at a given taxonomic level and must have E-values that are 10^{-4} or less.

TABLE 2 | The sensitivity of the LC-MS/MS shotgun proteotyping protocol.

Spiked species	Taxa identified	Spiking concentration (cells/ml)			
		10^4	10^5	10^6	10^7
S. aureus	Species (*S. aureus*)	0/3	0/3	3/3	
	Genus (*Staphylococus*)	0/3	1/3	3/3	
	Family (*Staphylococcaceae*)	0/3	1/3	3/3	
	Order (Bacillales)	0/3	1/3	3/3	
	Class (Bacilli)	0/3	1/3	3/3	
	Phylum (Firmicutes)	0/3	2/3	3/3	
E. coli	Species (*E. coli*)	3/3	3/3	3/3	
	Genus (*Escherichia*)	3/3	3/3	3/3	
	Family (*Enterobacteriaceae*)	3/3	3/3	3/3	
	Order (Enterobacterales)	3/3	3/3	3/3	
	Class (Gammaproteobacteria)	3/3	3/3	3/3	
	Phylum (Proteobacteria)	3/3	3/3	3/3	
C. albicans	Species (*C. albicans*)	0/3	3/3	3/3	3/3
	Genus (*Candida*)	0/3	3/3	3/3	3/3
	Family (*Saccharomycetaceae*)	0/3	3/3	3/3	3/3
	Order (Saccharomycetales)	0/3	3/3	3/3	3/3
	Class (Saccharomycetes)	0/3	3/3	3/3	3/3
	Phylum (Ascomycota)	0/3	3/3	3/3	3/3

MiCId identification results of S. aureus, E. coli and C. albicans spiked at different concentrations in horse blood.
The number x/y in the table is the identification fraction, in which the denominator shows the number of samples containing the microorganism and the numerator is the number of times that microorganism is identified correctly. E. coli and S. aureus were analyzed through the concentration ranges of 10^3-10^6 cells/ml, whereas C. albicans was analyzed through concentration ranges of 10^3-10^7 cells/ml. MALDI-TOF MS (results not shown in the table) identified S. aureus, E. coli and C. albicans only when 10^8 cells/ml were added to the blood samples.

TABLE 3 | Comparison of identification accuracies of MALDI-TOF MS and shotgun proteotyping.

Species identified in the routine clinical laboratories	Sample ID	Shotgun proteotyping ID (MiCId)				Direct MALDI-TOF MS ID
		Species	Ln(E-value)	Number of identified unique peptides	Prior	
E. coli	E1	*E. coli*	-1.413e+02	3	6.356e-01	*E. coli*
	E2	*E. coli*	-3.877e+02	14	7.162e-01	*E. coli*
	E3	*E. coli*	-1.605e+02	3	3.976e-01	*E. coli*
	E4	*E. coli*	-3.024e+03	96	5.957e-01	*E. coli*
	E5	*E. coli*	-1.118e+02	2	3.694e-01	*E. coli*
	E6	*E. coli*	-2.224e+02	6	7.232e-01	*E. coli*
	E7	*E. coli*	-2.181e+03	68	9.299e-01	*E. coli*
	E8	*E. coli*	-4.306e+02	14	7.500e-01	*E. coli*
	E9	*E. coli*	-9.672e+02	30	7.335e-01	*E. coli*
	E10	*E. coli*	-7.703e+02	23	6.926e-01	*E. coli*
S. aureus	S1	*S. aureus*	-8.468e+01	11	4.528e-02	Negative
	S2	*S. aureus*	-3.991e+02	38	9.623e-02	Negative
	S3	*S. aureus*	-1.368e+03	113	3.798e-01	Negative
	S4	*S. aureus*	-2.098e+03	151	3.965e-01	*S. aureus*
	S5	*S. aureus*	-4.020e+03	303	6.842e-01	*S. aureus*
	S6	*S. aureus*	-8.035e+02	67	1.903e-01	Negative
	S7	*S. aureus*	-2.856e+02	20	9.698e-02	Negative
	S8	*S. aureus*	-8.655e+02	75	2.279e-01	*S. aureus*
	S9	*S. aureus*	-1.824e+02	25	6.388e-02	Negative
	S10	*S. aureus*	-3.495e+03	261	6.393e-01	*S. aureus*
C. albicans	C1	*C. albicans*	-9.763e+01	14	1.150e-01	Negative
	C2	*C. albicans*	-2.334e+02	26	3.706e-01	Negative
	C3	*C. albicans*	-1.896e+01	2	1.696e-02	Negative
	C4	*C. albicans*	-9.807e+01	10	6,586e-01	Negative
	C5	Negative	–	–	–	Negative

Results of analysis of ten positive blood cultures for E. coli and S. aureus and five for C. albicans, using MALDI-TOF MS and proteotyping. The identifications by MALDI-TOF MS, as well as the number of species-unique peptides are shown.

TABLE 4 | Incubation times for identifications by shotgun proteotyping.

Spiked species	Spiking concentration (cells/ml)	Taxa identified	Incubation time in blood culture cabinet						ON
			2 h	3 h	4 h	5 h	6 h	7 h	
E. coli	1,000	*E. coli*	0/2	0/2	0/2	**1/2**	**2/2**	**2/2**	**2/2**
		Escherichia	0/2	0/2	0/2	**1/2**	**2/2**	**2/2**	**2/2**
		Enterobacteriaceae	0/2	0/2	0/2	**1/2**	**2/2**	**2/2**	**2/2**
		Enterobacterales	0/2	0/2	0/2	**1/2**	**2/2**	**2/2**	**2/2**
		Gammaproteobacteria	0/2	0/2	0/2	**1/2**	**2/2**	**2/2**	**2/2**
		Proteobacteria	0/2	0/2	**1/2**	**1/2**	**2/2**	**2/2**	**2/2**
S. aureus	1,000	*S. aureus*	0/2	0/2	0/2	0/2	0/2	**1/2**	**2/2**
		Staphylococcus	0/2	0/2	0/2	0/2	0/2	**1/2**	**2/2**
		Staphylococcaceae	0/2	0/2	0/2	0/2	0/2	**1/2**	**2/2**
		Bacillales	0/2	0/2	0/2	0/2	0/2	**1/2**	**2/2**
		Bacilli	0/2	0/2	0/2	0/2	0/2	**1/2**	**2/2**
		Firmicutes	0/2	**1/2**	0/2	0/2	0/2	**1/2**	**2/2**
S. aureus	10,000	*S. aureus*	0/2	0/2	0/2	**2/2**	**2/2**	**2/2**	**2/2**
		Staphylococcus	0/2	0/2	0/2	**2/2**	**2/2**	**2/2**	**2/2**
		Staphylococcaceae	0/2	0/2	0/2	**2/2**	**2/2**	**2/2**	**2/2**
		Bacillales	0/2	0/2	0/2	**2/2**	**2/2**	**2/2**	**2/2**
		Bacilli	0/2	0/2	0/2	**2/2**	**2/2**	**2/2**	**2/2**
		Firmicutes	0/2	**1/2**	0/2	**2/2**	**2/2**	**2/2**	**2/2**
C. albicans	1,000	*C. albicans*	0/1	0/1	0/1	0/1	0/1	0/1	**2/2**
		Candida	0/1	0/1	0/1	0/1	0/1	0/1	**2/2**
		Saccharomycetaceae	0/1	0/1	0/1	0/1	0/1	0/1	**2/2**
		Saccharomycetales	0/1	0/1	0/1	0/1	0/1	0/1	**2/2**
		Saccharomycetes	0/1	0/1	0/1	0/1	0/1	0/1	**2/2**
		Ascomycota	0/1	0/1	0/1	0/1	0/1	0/1	**2/2**

Incubation time needed for accurate identifications of E. coli, S. aureus and C. albicans, using shotgun proteotyping after incubation of 1,000 (or 10,000) cells in negative blood samples and incubation in blood culture cabinets.

The number x/y in the table is the identification fraction, in which the denominator shows the number of samples containing the microorganism and the numerator is the number of times that microorganism is identified correctly at different taxonomic levels. In the analyses of S. aureus, a false positive identification at the Firmicutes level was observed in one of the duplicates at 3 h incubation.

Bold signifies a positive identification in at least one of the replicates.

Rapid diagnoses of bloodstream infections, helping physicians administer proper treatments, is essential for reducing mortality due to BSIs and sepsis, as well as reducing costs associated with hospitalized patients. Since bloodstream infections are most often caused by a single pathogenic species (monospecies infection), and only rarely caused by two or several pathogens (Bouza et al., 2013), efforts have been focused on being able to skip the isolation and sub-culturing steps and analyze the positive blood cultures directly (Ferroni et al., 2010; Stevenson et al., 2010; Radic et al., 2016; Salimnia et al., 2016; Florio et al., 2018; Briggs et al., 2021). However, the use of MALDI-TOF MS for identification of the pathogen requires in most cases, a pure culture isolate of the bacteria or fungi after observation of a positive blood culture in the cultivation step (Opota et al., 2015). Currently, blood cultures and PCR-based assays are the protocols used for detecting and identifying the agents responsible for bloodstream infections (Book et al., 2013). PCR-based gene-amplification methods are potentially faster, however, a disadvantage is that they require pre-defined targets, which is a not neglectable limitation since the range of unknown infectious agents is extensive. Furthermore, at the time of diagnosis, the responsible microorganisms may no longer be in the bloodstream or are otherwise not detectable with existing methods (Warhurst et al., 2015).

In this study, the concept of using shotgun proteotyping, i.e., bottom-up proteomics, and peptide biomarkers, for detection of bloodstream infectious pathogens, was investigated. The bioinformatics pipeline MiCId, was used for data evaluation and identification of taxonomically unique peptides (Alves et al., 2018). Shotgun proteotyping does not rely on the traditionally applied cultivation step to obtain a pure culture isolate, instead, the samples can be analyzed directly. A key step in the success of using mass spectrometry-based proteomics for discovery of pathogens directly in clinical samples, is the removal of human "contamination", such as blood cells and plasma proteins. The presence of these highly abundant proteins may hinder the detection and identification of peptides originating from the pathogens, which are present in much lower abundance in the samples. Different host biomass depletion methods were applied, i.e., clean-up by osmotic shock (Cytolysis), Saponin-based cell lysis protocol (Ferroni et al., 2010) and a commercial kit (MolYsis kit Basic5). The MolYsis kit not only facilitated the discovery of a high number of the bacterial peptides after the clean-up, but greatly reduced the number of peptides originating from host blood, compared to the other two approaches (**Table 1**). This agrees with earlier studies, where the MolYsis kit was used for identification of *S. aureus* in positive blood cultures (McCann and Jordan, 2014; Thoendel et al., 2016); therefore, the MolYsis kit with a modified protocol (Karlsson et al., 2020) was used as a host biomass depletion method throughout the experiments included in this study.

When blood samples spiked with cells of bacteria and fungi were analyzed with both MALDI-TOF MS and with

proteotyping, the MALDI-based approach was able to correctly identify the species when the highest numbers of cells were added to the blood sample (100 million cells), whereas the proteotyping approach was able to find species-unique peptides from as few as 10,000-100,000 cells, demonstrating a thousand-fold increase in the sensitivity. This was expected, since the MALDI-TOF MS identification needs a certain amount of biomass for the generation of good quality spectra, which can be matched against the spectral database. Analyses of positive blood cultures by proteotyping were able to correctly identify all the positive blood cultures, with high numbers of species-unique peptides from each sample. The MALDI-based approach was also able to identify all the positive blood cultures containing *E. coli*, but only 4 of 10 positive blood cultures were correctly identified for those containing *S. aureus*. This is in agreement with earlier studies, showing that the identification of Gram-positive bacteria, such as *S. aureus*, using direct MALDI-TOF MS-based identification (i.e., no isolation of bacteria by a sub-culture from the positive blood cultures) fails more often, thus producing false negatives, compared to the identifications of Gram-negative bacteria, including *E. coli* (Ferroni et al., 2010; Stevenson et al., 2010; Loonen et al., 2012; Kirn and Weinstein, 2013; Briggs et al., 2021). Interestingly, in general, a higher number of species-unique peptides was detected and identified for *S. aureus* compared to the *E. coli* in the ten positive blood cultures. The higher number of species-unique peptides most likely reflects the taxonomy of the two species, *S. aureus* being more separated from closely related species, and, thus, having a larger repertoire of species-unique peptides compared to *E. coli*, making it easier to identify a higher number of species-unique peptides (Boulund et al., 2017).

Proteotyping relies on the identification of unique peptides (at any taxonomic level) and thus rely on accurate and comprehensive, often manually curated databases. Falsely identified unique peptides thus have far-reaching adverse consequence. In this study, MiCId was used as a bioinformatics pipeline to minimize the need of human curation and intervention. As explained in the Materials and Methods section, MiCId demands a more stringent criterion (E-value < 10^{-4}) for qualifying unique peptides. This effectively removes false positives in terms of microorganism identification when only unique peptides will be employed for taxon identification. By limiting the count of unique peptides to those of high identification confidence, one may expect that the sensitivity in microorganism identification will drop. In other words, the occurrence of false negatives. MiCId mitigates this issue by offering the unified microorganism E-value that combines all identified peptides mappable to that microorganism, not just the unique peptides. This strengthen the signal of a microorganism if it is present in the sample, hence reduces the false negatives while controlling the false positives.

The analysis of positive blood cultures suspected to contain *C. albicans* were negative when analyzed by the direct MALDI-TOF MS-based method. This could be because *C. albicans* may be at a different growth state in the blood cultures, compared to when grown on agar medium. Therefore, protein expression levels might differ and, hence, the spectra generated might not match the spectra in the databases. Furthermore, a higher background of blood proteins of host origin, is expected from samples drawn from blood culture flasks, as compared to cultures grown on an agar plate. As this study was not focused on improving the MALDI-based approach, but rather to demonstrate the ability of proteotyping to correctly identify not only bacteria, but also fungi, no further efforts were performed to improve the results from the MALDI-based approach. The identification of fungi by MALDI-TOF MS-based methods often benefits from expanded extraction protocols, however, this was not implemented in this study, as it was not part of the clinical laboratory routine. Proteotyping was able to correctly identify 4 of the 5 samples included in the study. Further work is therefore necessary to optimize the sample clean-up step, and hence improve the accuracy in the proteotyping workflow for detection and identification of *C. albicans* in blood.

A clear difference was seen in both sensitivity and identification accuracy when comparing direct MALDI-TOF MS with shotgun proteotyping. Since it was suspected that lower numbers of bacterial and fungal cells (biomass) were needed for being able to correctly identify the infectious pathogens, an experiment was performed, to investigate if it was possible to reduce the time needed for performing a correct identification, i.e., even before the blood culture cabinets gave off an alarm. Generally, bacterial and fungal growth in blood culture flasks was detected after overnight incubation in blood culture cabinet (BacT/Alert®). Here, we studied the limit of detection and identification of bacterial and fungal growth in blood culture flasks, by incubating 1,000 cells/blood flask for 2, 3, 4, 5, 6 and 7 h incubation, as well as overnight (ON). The MALDI-TOF MS-based method was able to correctly identify *E. coli* only after ON incubation and was not able to identify *S. aureus* and *C. albicans*, even after ON incubation. On the other hand, proteotyping was able to identify *E. coli* even after 4-5 h of incubation, *S. aureus* at 7 h incubation, and *C. albicans* at the ON incubation (**Table 4**). The early identification of *E. coli* (4-5 hours), compared with *S. aureus* and *C. albicans* could, in these experiments, be explained by the shorter doubling time of *E. coli*, however further studies are required to pinpoint the influence of the growth rates of different species on the time needed for identification by proteotyping. Furthermore, since highly abundant housekeeping proteins are taxonomically more conserved within Families/Genera they are easier to detect compared to identifying lower abundant unique peptides at the species level. Therefore, species-unique peptides in combination with peptides on higher taxonomic levels should be used in the diagnosis. These peptides are shared by different species e.g. within the same genus, but still they will provide important information and strengthen the identification of the correct species and improves the sensitivity of the analysis. For example, an earlier detection of higher taxonomic level peptide biomarkers, e.g., *Enterobacteraceae*, would be of great value in reducing precious time spent for reaching a diagnosis during a suspected sepsis. In this study, an ON incubation was used for the digestion of proteins into peptides, although recently, it has

been shown that the digestion time required for processing samples in proteotyping workflows can be reduced to 15 minutes (Hayoun et al., 2019). The proteotypic workflow can also be optimized further by implementing a targeted LCMS approach of the proteotypic peptides using triple quadrupole MS instrumentation (already present in many clinical laboratories) eliminating the database matching step.

Typically, addressing bloodstream infection is done through treatment with broad-spectrum antibiotics (Kuti et al., 2008; Tassinari et al., 2018). The global range of bacteria resistant to multiple antibiotics, particularly pathogens of human diseases, presents major challenges for treatment and preventing the spread of infection. Without more effective diagnostic tools than what exists today, antimicrobial resistance (AMR) will continue to increase, and treatment options will be increasingly limited, with the establishment of so-called multi-resistant "superbugs", e.g., Extended Spectrum β-Lactamase (ESBL) and Carbapenem-Resistant Enterobacteriaceae (CRE). The World Health Organization (WHO) has predicted the advent of the post-antibiotic era, facing infections for which no antibiotic treatment will be available (Reardon, 2014) With this prognosis, there is an increasingly critical need to develop new, rapid and reliable methodologies for comprehensive diagnostics of infectious microorganisms and associated virulence and antimicrobial resistance (AMR), to guide more appropriate treatments of infections, reduce the risk of AMR development, prevent mortality and reduce costs associated with treatment and infection control.

The recent evolution of mass spectrometers, with high sensitivity, accuracy and resolution, in conjunction with improved chromatographic separation techniques, enables detection of almost the entire expressed proteome of a microorganism (Armengaud, 2013). A great advantage of the proteotyping approach is that, whereas other traditionally used methods in clinical microbiology diagnostics rely completely on a successful isolation of a pure culture (including MALDI-TOF MS), proteotyping is able to identify tens of thousands of peptides, all potential markers for species, strain, resistance and virulence traits, from the same sample in just one analysis. Hence, proteotyping can identify several different species (or even strains) in a patient sample with a co-infection of bacteria/fungi (Karlsson et al., 2012; Karlsson et al., 2015; Karlsson et al., 2018). The growing amount of genome sequence data enables accurate detection of a growing number and diversity of microorganisms, as well as deeper understanding of traits such as virulence and antimicrobial resistance (AMR). With such analytical means, it is feasible to determine directly, within a clinical sample, the species identity, the sub-species strain type and factors expressing virulence and AMR.

In further studies, peptide biomarkers for blood infectious bacteria or fungi, even on different taxonomical levels, will be investigated. The approach of exploiting those biomarkers as a rapid, accurate and sensitive alternative to traditional, often culture-based, protocols would also need to be investigated. The proteotyping workflow in this paper was applied to demonstrate the feasibility of using peptide biomarkers to detect bacteria and fungi in blood samples, using culture-independent tandem mass spectrometry analyses. Attention was given to optimizing the workflow to reduce cells and proteins of host origin, as well as assessing the sensitivity and accuracy compared to the commonly used MALDI-TOF MS-based identification. At this stage, less attention has been given to the time and cost of the analysis, using the proteotyping workflow. To transfer the peptide biomarker candidates into a clinical setting, especially the cost per sample would need to be specifically addressed, as well as the time required from sample preparation to analysis result. The sample preparation step and the digestion step, to produce the biomarker peptides, are steps in the workflow where there is plenty of potential for reducing the processing time. Indeed, the proteotyping workflow has been shown to be markedly reduced, in some settings, to only 30 minutes (Hayoun et al., 2019). Further optimization and time-saving may include targeted LCMS approaches using already existing triple quadrupole MS instrumentation in the clinic. Furthermore, alternative strategies to reduce the cost and time per sample may include utilization of the unique amino acid sequences of the biomarker peptides found by shotgun proteotyping, as the biomarker information also may hold potential to be transferred into other diagnostics approaches, such as ELISA-based assays or, as previously shown, MALDI-TOF MS (Mery et al., 2016). A key benefit of using proteomics-based methods compared to methods detecting genetic material is the information regarding expression. Further studies will focus on markers for antibiotic resistance and virulence, ideally information regarding species and strain identification will be provided at the same time as information regarding expression of resistance and virulence traits in one single direct analysis of a clinical sample, without any culturing (Charretier et al., 2015; Karlsson et al., 2015).

DATA AVAILABILITY STATEMENT

The datasets presented in this study can be found in online repositories. The names of the repository/repositories and accession number(s) can be found below: ProteomeXchange *via* the PRIDE database PXD023033.

ETHICS STATEMENT

Ethical review and approval was not required for the study on human participants in accordance with the local legislation and institutional requirements. Written informed consent for participation was not required for this study in accordance with the national legislation and the institutional requirements.

AUTHOR CONTRIBUTIONS

RK, AKa, AT, EM, and NKo designed research. AKu, BP-I, TT, NKa, AT, and JF performed research. RK, AKa, Y-KY, GA, and AO contributed new reagents/analytic tools. RK, AT, BP-I, FS-S,

DJ-L, JF, AK, Y-KY, GA, and AO analyzed data. All authors contributed to the article and approved the submitted version.

FUNDING

RK, FS-S, DJ-L, and EM acknowledge support from the European Commission 7th Framework Programme: "Tailored-Treatment", EU Grant Agreement No.: HEALTH-F3-602860-2013. Swedish Västra Götaland regional funding, project nos. ALFGBG-437221 supported RK, FS-S, EM, and ALFGBG-720761 supported RK, FS-S and EM. The Swedish Västra Götaland Region, FoU grant number VGFOUREG-665141 and Lab Medicine Project number 51060-6258 supported RK and EM. FS-S, DJ-L, and EM acknowledge support from the Swedish Västra Götaland Region, Lab Medicine Project number 51060-6268. FS-S and DJ-L were supported by stipends for Basic and Advanced Research from the Culture Collection of the University of Gothenburg (CCUG), through the Institute of Biomedicine, Sahlgrenska Academy, University of Gothenburg.

ACKNOWLEDGMENTS

The CCUG and the staff are acknowledged for providing reference strains and expert characterization and maintenance. The CCUG is supported by the Department of Clinical Microbiology, Sahlgrenska University Hospital and the Sahlgrenska Academy of the University of Gothenburg, Sweden. The staff of the Bacteriology laboratory of the Department of Clinical Microbiology of Sahlgrenska University Hospital are acknowledged for providing clinical samples and for expert identification analyses. We acknowledge the expertise and effort of the Proteomics Core Facility, Sahlgrenska Academy, University of Gothenburg.

SUPPLEMENTARY MATERIAL

The Supplementary Material for this article can be found online at: https://www.frontiersin.org/articles/10.3389/fcimb.2021.634215/full#supplementary-material

REFERENCES

Alam, M. Z., Alam, Q., Jiman-Fatani, A., Kamal, M. A., Abuzenadah, A. M., Chaudhary, A. G., et al. (2014). Candida Identification: A Journey From Conventional to Molecular Methods in Medical Mycology. *World J. Microbiol. Biotechnol.* 30, 1437–1451. doi: 10.1007/s11274-013-1574-z

Alves, G., Ogurtsov, A. Y., Wu, W. W., Wang, G., Shen, R.-F., and Yu, Y. K. (2007). Calibrating E-Values for MS2 Database Search Methods. *Biol. Direct* 2, 26. doi: 10.1186/1745-6150-2-26

Alves, G., Ogurtsov, A. Y., and Yu, Y. K. (2008). RAId DbS: Mass-Spectrometry Based Peptide Identification Web Server With Knowledge Integration. *BMC Genomics* 9, 505. doi: 10.1186/1471-2164-9-505

Alves, G., Ogurtsov, A. Y., and Yu, Y. K. (2010). RAId_aPS: MS/MS Analysis With Multiple Scoring Functions and Spectrum-Specific Statistics. *PloS One* 5 (11), e15438. doi: 10.1371/journal.pone.0015438

Alves, G., Wang, G., Ogurtsov, A. Y., Drake, S. K., Gucek, M., Sacks, D. B., et al. (2018). Rapid Classification and Identification of Multiple Microorganisms With Accurate Statistical Significance *via* High-Resolution Tandem Mass Spectrometry. *J. Am. Soc. Mass Spectrom.* 29 (8), 1721–1737. doi: 10.1007/s13361-018-1986-y

Alves, G., Wang, G., Ogurtsov, A. Y., Drake, S. K., Gucek, M., Suffredini, A. F., et al. (2016). Identification of Microorganisms by High Resolution Tandem Mass Spectrometry With Accurate Statistical Significance. *J. Am. Soc. Mass Spectrom.* 27 (2), 194–210. doi: 10.1007/s13361-015-1271-2

Alves, G., and Yu, Y. K. (2008). Statistical Characterization of a 1D Random Potential Problem With Applications in Score Statistics of MS-Based Peptide Sequencing. *Phys. A* 387 (26), 6538–6544. doi: 10.1016/j.physa.2008.08.024

Alves, G., and Yu, Y. K. (2020). Robust Accurate Identification and Biomass Estimates of Microorganisms via Tandem Mass Spectrometry. *J. Am. Soc. Mass Spectrom.* 31 (1), 85–102. doi: 10.1021/jasms.9b00035

Angus, D. C., Linde-Zwirble, W. T., Lidicker, J., Clermont, G., Carcillo, J., and Pinsky, M. R. (2001). Epidemiology of Severe Sepsis in the United States: Analysis of Incidence, Outcome, and Associated Costs of Care. *Crit. Care Med.* 29, 1303–1310. doi: 10.1097/00003246-200107000-00002

Armengaud, J. (2013). Microbiology and Proteomics, Getting the Best of Both Worlds! *Environ. Microbiol.* 15, 12–23. doi: 10.1111/j.1462-2920.2012.02811.x

Bassetti, M., Merelli, M., Righi, E., Diaz-Martin, A., Rosello, E. M., Luzzati, R., et al. (2013). Epidemiology, Species Distribution, Antifungal Susceptibility, and Outcome of Candidemia Across Five Sites in Italy and Spain. *J. Clin. Microbiol.* 51 (12), 4167–4172. doi: 10.1128/JCM.01998-13

Book, M., Lehmann, L. E., Zhang, X., and Stüber, F. (2013). Monitoring Infection: From Blood Culture to Polymerase Chain Reaction (PCR). *Best Pract. Res. Clin. Anaesthesiol.* 27 (2), 279–288. doi: 10.1016/j.bpa.2013.06.010

Boulund, F., Karlsson, R., Gonzales-Siles, L., Johnning, A., Karami, N., Al-Bayati, O., et al. (2017). Typing and Characterization of Bacteria Using Bottom-Up Tandem Mass Spectrometry Proteomics. *Mol. Cell Proteomics* 16 (6), 1052–1063. doi: 10.1074/mcp.M116.061721

Bouza, E., Burillo, A., Munoz, P., Guinea, J., Marin, M., and Rodriguez-Creixems, M. (2013). Mixed Bloodstream Infections Involving Bacteria and Candida Spp. *J. Antimicrob. Chemother.* 68 (8), 1881–1888. doi: 10.1093/jac/dkt099

Briggs, N., Campbell, S., and Gupta, S. (2021). Advances in Rapid Diagnostics for Bloodstream Infections. *Diagn. Microbiol. Infect. Dis.* 99 (1), 115–219. doi: 10.1016/j.diagmicrobio.2020.115219

Charretier, Y., Dauwalder, O., Franceschi, C., Degout-Charmette, E., Zambardi, G., Cecchini, T., et al. (2015). Rapid Bacterial Identification, Resistance, Virulence and Type Profiling Using Selected Reaction Monitoring Mass Spectrometry. *Sci. Rep.* 5, 139–144. doi: 10.1038/srep13944

Chenau, J., Fenaille, F., Caro, V., Haustant, M., Diancourt, L., Klee, S. R., et al. (2014). Identification and Validation of Specific Markers of Bacillus Anthracis Spores by Proteomics and Genomics Approaches. *Mol. Cell. Proteomics* 13 (3), 716–732. doi: 10.1074/mcp.M113.032946

Chen, S. H., Parker, C. H., Croley, T. R., and McFarland, M. A. (2019). Identification of Salmonella Taxon-Specific Peptide Markers to the Serovar Level by Mass Spectrometry. *Anal. Chem.* 91 (7), 4388–4395. doi: 10.1021/acs.analchem.8b04843

Dickson, K., and Lehmann, C. (2019). Inflammatory Response to Different Toxins in Experimental Sepsis Models. *Int. J. Mol. Sci.* 20 (18), 4341. doi: 10.3390/ijms20184341

Dworzanski, J. P., Deshpande, S. V., Chen, R., Jabbour, R. E., Snyder, A. P., Wick, C. H., et al. (2006). Mass Spectrometry-Based Proteomics Combined With Bioinformatic Tools for Bacterial Classification. *J. Proteome Res.* 5 (1), 76–87. doi: 10.1021/pr050294t

Ferroni, A., Suarez, S., Beretti, J. L., Dauphin, B., Bille, E., Meyer, J., et al. (2010). Real-Time Identification of Bacteria and Candida Species in Positive Blood Culture Broths by Matrix-Assisted Laser Desorption Ionization-Time of Flight Mass Spectrometry. *J. Clin. Microbiol.* 48 (5), 1542–1548. doi: 10.1128/JCM.02485-09

Fleischmann, C., Scherag, A., Adhikari, N. K. J., Hartog, C. S., Tsaganos, T., Schlattmann, P., et al. (2016a). Assessment of Global Incidence and Mortality of Hospital-Treated Sepsis Current Estimates and Limitations. *Am. J. Respir. Crit. Care Med.* 193, 259–272. doi: 10.1164/rccm.201504-0781OC

Fleischmann, C., Thomas-Rueddel, D. O., Hartmann, M., Hartog, C. S., Welte, T., Heublein, S., et al. (2016b). Hospital Incidence and Mortality Rates of Sepsis. *Dtsch. Arztebl. Int.* 113 (10), 159–166. doi: 10.3238/arztebl.2016.0159

Florio, W., Tavanti, A., Barnini, S., Ghelardi, E., and Lupetti, A. (2018). Recent Advances and Ongoing Challenges in the Diagnosis of Microbial Infections by MALDI-TOF Mass Spectrometry. *Front. Microbiol.* 9, 1097. doi: 10.3389/fmicb.2018.01097

Gosiewski, T., Flis, A., Sroka, A., Kedzierska, A., Pietrzyk, A., Kedzierska, J., et al. (2014). Comparison of Nested, Multiplex, qPCR; FISH; SeptiFast and Blood Culture Methods in Detection and Identification of Bacteria and Fungi in Blood of Patients With Sepsis. *BMC Microbiol.* 14, 313. doi: 10.1186/s12866-014-0313-4

Gosiewski, T., Ludwig-Galezowska, A. H. H., Huminska, K., Sroka-Oleksiak, A., Radkowski, P., Salamon, D., et al. (2017). Comprehensive Detection and Identification of Bacterial DNA in the Blood of Patients With Sepsis and Healthy Volunteers Using Next-Generation Sequencing Method - the Observation of DNAemia. *Eur. J. Clin. Microbiol. Infect. Dis.* 36 (2), 329–336. doi: 10.1007/s10096-016-2805-7

Grenga, L., Pible, O., and Armengaud, J. (2019). Pathogen Proteotyping: A Rapidly Developing Application of Mass Spectrometry to Address Clinical Concerns. *Clin. Mass Spectrom.* 14, A, 9–17. doi: 10.1016/j.clinms.2019.04.004

Grumaz, C., Hoffmann, A., Vainshtein, Y., Kopp, M., Grumaz, S., Stevens, P., et al. (2020). Rapid Next-Generation Sequencing-Based Diagnostics of Bacteremia in Septic Patients. *J. Mol. Diagn.* 22 (3), 405–418. doi: 10.1016/j.jmoldx.2019.12.006

Grumaz, S., Stevens, P., Grumaz, C., Decker, S. O., Weigand, M. A., Hofer, S., et al. (2016). Next-Generation Sequencing Diagnostics of Bacteremia in Septic Patients. *Genome Med.* 8 (1):73. doi: 10.1186/s13073-016-0326-8

Hayoun, K., Gouveia, D., Grenga, L., Pible, O., Armengaud, J., and Alpha-Bazin, B. (2019). Evaluation of Sample Preparation Methods for Fast Proteotyping of Microorganisms by Tandem Mass Spectrometry. *Front. Microbiol.* 10, 1985. doi: 10.3389/fmicb.2019.01985

Hazwani, T. R., Kazzaz, Y. M., Alsugheir, S., Aldelaijan, S., Alsugheir, F., Alali, H., et al. (2020). Association Between Culture-Negative Versus Culture-Positive Sepsis and Outcomes of Patients Admitted to the Pediatric Intensive Care Unit. *Cureus* 12 (8), e9981. doi: 10.7759/cureus.9981

Henning, C., Aygül, N., Dinnétz, P., Wallgren, K., and Özenci, V. (2019). Detailed Analysis of the Characteristics of Sample Volume in Blood Culture Bottles. *J. Clin. Microbiol.* 57 (8), e00268–e00219. doi: 10.1128/JCM.00268-19

Huang, M., Cai, S., and Su, J. (2019). The Pathogenesis of Sepsis and Potential Therapeutic Targets. *Int. J. Mol. Sci.* 20 (21), 5376. doi: 10.3390/ijms20215376

Huerta, L., and Rice, T. (2018). Pathologic Difference Between Sepsis and Bloodstream Infections. *J. Appl. Lab. Med.* 3 (4), 654–663. doi: 10.1373/jalm.2018.026245

Ibrahim, Z. M., Wu, H., Hamoud, A., Stappen, L., Dobson, R., and Agarossi, A. (2020). On Classifying Sepsis Heterogeneity in the ICU: Insight Using Machine Learning. *J. Am. Med. Inf. Assoc.: JAMIA* 27 (3), 437–443. doi: 10.1093/jamia/ocz211

Iskander, K. N., Osuchowski, M. F., Stearns-Kurosawa, D. J., Kurosawa, S., Stepien, D., Valentine, C., et al. (2013). Sepsis: Multiple Abnormalities, Heterogeneous Responses, and Evolving Understanding. *Physiol. Rev.* 93 (3), 1247–1288. doi: 10.1152/physrev.00037.2012

Karlsson, R., Davidson, M., Svensson-Stadler, L., Karlsson, A., Olesen, K., Carlsohn,, et al. (2012). Strain-Level Typing and Identification of Bacteria Using Mass Spectrometry-Based Proteomics. *J. Proteome Res.* 11 (5), 2710–2720. doi: 10.1021/pr2010633

Karlsson, R., Gonzales-Siles, L., Boulund, F., Lindgren, Å., Svensson-Stadler, L., Karlsson, A., et al. (2017). "Proteotyping: Tandem Mass Spectrometry Shotgun Proteomic Characterization and Typing of Pathogenic Microorganisms," in *MALDI-TOF and Tandem MS for Clinical Microbiology, vol. 16.* (Chichester, United Kingdom: John Wiley and Sons Ltd), 419–450. doi: 10.1002/9781118960226.ch16

Karlsson, R., Gonzales-Siles, L., Boulund, F., Svensson-Stadler, L., Skovbjerg, S., Karlsson, A., et al. (2015). Proteotyping: Proteomic Characterisation, Classification and Identification of Microorganisms – A Prospectus. Minireview in Special Issue "Taxonomy of the 21st Century". *Syst. Appl. Microbiol.* 38 (4), 246–257. doi: 10.1016/j.syapm.2015.03.006

Karlsson, R., Gonzales-Siles, L., Gomila, M., Busquets, A., Salvà-Serra, F., Jaén-Luchoro, D., et al. (2018). Proteotyping Bacteria: Characterization, Differentiation and Identification of Pneumococcus and Other Species Within the Mitis Group of the Genus Streptococcus by Tandem Mass Spectrometry Proteomics. *PloS One* 13 (12), e0208804. doi: 10.1371/journal.pone.0208804

Karlsson, R., Thorsell, A., Gomila, M., Salvà-Serra, F., Jakobsson, H. E., Gonzales-Siles, L., et al. (2020). Discovery of Species-Unique Peptide Biomarkers of Bacterial Pathogens by Tandem Mass Spectrometry-Based Proteotyping. *Mol. Cell. Proteomics* 19 (3), 518–528. doi: 10.1074/mcp.RA119.001667

Kennedy, G. T., Barr, J. G., and Goldsmith, C. (1995). Detection of Bacteraemia by the Continuously Monitoring BacT/Alert System. *J. Clin. Pathol.* 48 (10), 912–914. doi: 10.1136/jcp.48.10.912

Kirn, T. J., and Weinstein, M. P. (2013). Update on Blood Cultures: How to Obtain, Process, Report, and Interpret. *Clin. Microbiol. Infect.* 19 (6), 513–520. doi: 10.1111/1469-0691.12180

Klingspor, L., Ullberg, M., Rydberg, J., Kondori, N., Serrander, L., Swanberg, J., et al. (2018). Epidemiology of Fungaemia in Sweden: A Nationwide Retrospective Observational Survey. *Mycoses* 61 (10), 777–785. doi: 10.1111/myc.12816

Kondori, N., Erhard, M., Welinder-Olsson, C., Groenewald, M., Verkley, G., and Moore, E. R. (2015). Analyses of Black Fungi by Matrix-Assisted Laser Desorption/Ionization Time-Of-Flight Mass Spectrometry (MALDI-TOF MS): Species-Level Identification of Clinical Isolates of Exophiala Dermatitidis. *FEMS Microbiol. Lett.* 362 (1), 1–6. doi: 10.1093/femsle/fnu016

Kumar, A., Roberts, D., Wood, K. E., Light, B., Parrillo, J. E., Sharma, S., et al. (2006). Duration of Hypotension Before Initiation of Effective Antimicrobial Therapy is the Critical Determinant of Survival in Human Septic Shock. *Crit. Care Med.* 34 (6), 1589–1596. doi: 10.1097/01.CCM.0000217961.75225.E9

Kuti, E. L., Patel, A. A., and Coleman, C. I. (2008). Impact of Inappropriate Antibiotic Therapy on Mortality in Patients With Ventilator-Associated Pneumonia and Blood Stream Infection: A Meta-Analysis. *J. Crit. Care* 23 (1), 91–100. doi: 10.1016/j.jcrc.2007.08.007

Lagu, T., Rothberg, M. B., Shieh, M. S., Pekow, P. S., Steingrub, J. S., and Lindenauer, P. K. (2012). Hospitalizations, Costs, and Outcomes of Severe Sepsis in the United States 2003 to 2007. *Crit. Care Med.* 40, 754–761. doi: 10.1097/CCM.0b013e318232db65 Erratum in: Crit Care Med. 2012, 40(10), 2932.

Liesenfeld, O., Lehman, L., Hunfeld, K. P., and Kost, G. (2014). Molecular Diagnosis of Sepsis: New Aspects and Recent Developments. *Eur. J. Microbiol. Immunol. (Bp).* 4 (1), 1–25. doi: 10.1556/EuJMI.4.2014.1.1

Lindberg, E., Hammarström, H., Ataollahy, N., and Kondori, N. (2019). Species Distribution and Antifungal Drug Susceptibilities of Yeasts Isolated From the Blood Samples of Patients With Candidemia. *Sci. Rep.* 9, (1), 3838. doi: 10.1038/s41598-019-40280-8

Loonen, A. J. M., Jansz, A. R., Stalpers, J., Wolffs, P. F. G., and van den Brule, A. J. C. (2012). An Evaluation of Three Processing Methods and the Effect of Reduced Culture Times for Faster Direct Identification of Pathogens From BacT/ALERT Blood Cultures by MALDI-TOF MS. *Eur. J. Clin. Microbiol. Infect. Dis.* 31 (7), 1575–1583. doi: 10.1007/s10096-011-1480-y

Loonen, A. J. M., Wolffs, P. F. G., Bruggeman, C. A., and van den Brule, A. J. C. (2014). Developments for Improved Diagnosis of Bacterial Bloodstream Infections. *Eur. J. Clin. Microbiol. Infect. Dis.* 33, 1687–1702. doi: 10.1007/s10096-014-2153-4

Mancini, N., Carletti, S., Ghidoli, N., Cichero, P., Burioni, R., and Clementi, M. (2010). The Era of Molecular and Other Non-Culture-Based Methods in Diagnosis of Sepsis. *Clin. Microbiol. Rev.* 23 (1), 235–251. doi: 10.1128/CMR.00043-09

Martinez, R. M., and Wolk, D. M. (2016). Bloodstream Infections. *Microbiol. Spectr.* 4 (4). doi: 10.1128/microbiolspec.DMIH2-0031-2016

McCann, C. D., and Jordan, J. A. (2014). Evaluation of MolYsis™ Complete5 DNA Extraction Method for Detecting Staphylococcus Aureus DNA From Whole Blood in a Sepsis Model Using PCR/Pyrosequencing. *J. Microbiol. Methods* 99, 1–7. doi: 10.1016/j.mimet.2014.01.013

Mery, A., Sendid, B., François, N., Cornu, M., Poissy, J., Guerardel, Y., et al. (2017). Application of Mass Spectrometry Technology to Early Diagnosis of Invasive Fungal Infections. *J. Clin. Microbiol.* 54, 2786–2797. doi: 10.1128/JCM.01655-16

Metzgar, D., Frinder, M. W., Rothman, R. E., Peterson, S., Carroll, K. C., Zhang, S. X., et al. (2016). The IRIDICA BAC BSI Assay: Rapid, Sensitive and Culture-Independent Identification of Bacteria and Candida in Blood. *PloS One* 11 (7), e0158186. doi: 10.1371/journal.pone.0158186

Murray, P. R., and Masur, H. (2012). Current Approaches to the Diagnosis of Bacterial and Fungal Bloodstream Infections in the Intensive Care Unit. *Crit. Care Med.* 40 (12), 3277–3282. doi: 10.1097/CCM.0b013e318270e771

Nagy, E., Boyanova, L., and Justesen, U. S. (2018). ESCMID Study Group of Anaerobic Infections. How to Isolate, Identify and Determine Antimicrobial Susceptibility of Anaerobic Bacteria in Routine Laboratories. *Clin. Microbiol. Infect.* 24 (11), 1139–1148. doi: 10.1016/j.cmi.2018.02.008

Ombelet, S., Barbé, B., Affolabi, D., Ronat, J. B., Lompo, P., Lunguya, O., et al. (2019). Best Practices of Blood Cultures in Low- and Middle-Income Countries. *Front. Med.* 6, 131. doi: 10.3389/fmed.2019.00131

Opal, S. M. (2010). Endotoxins and Other Sepsis Triggers. *Contrib. Nephrol.* 167, 14–24. doi: 10.1159/000315915

Opota, O., Croxatto, A., Prod'hom, G., and Greub, G. (2015). Blood Culture-Based Diagnosis of Bacteraemia: State of the Art. *Clin. Microbiol. Infect.* 21 (4), 313 – 322. doi: 10.1016/j.cmi.2015.01.003

Özenci, V., Klingspor, L., Ullberg, M., Chryssanthou, E., Denning, D. W., and Kondori, N. (2019). Estimated Burden of Fungal Infections in Sweden. *Mycoses* 62 (11), 1043–1048. doi: 10.1111/myc.12981

Pappas, P. G., Rex, J. H., Lee, J., Hamill, R. J., Larsen, R. A., Powderly, W., et al. (2003). A Prospective Observational Study of Candidemia: Epidemiology, Therapy, and Influences on Mortality in Hospitalized Adult and Pediatric Patients. *Clin. Infect. Dis.* 37 (5), 634–643. doi: 10.1086/376906

Perez-Riverol, Y., Csordas, A., Bai, J., Bernal-Llinares, M., Hewapathirana, S., Kundu, D. J., et al. (2019). The PRIDE Database and Related Tools and Resources in 2019: Improving Support for Quantification Data. *Nucleic Acids Res.* 47 (D1), D442–D450. doi: 10.1093/nar/gky1106

Pible, O., Allain, F., Jouffret, V., Culotta, K., Miotello, G., and Armengaud, J. (2020). Estimating Relative Biomasses of Organisms in Microbiota Using "Phylopeptidomics". *Microbiome* 8, 30. doi: 10.1186/s40168-020-00797-x

Radic, M., Goic-Barisic, I., Novak, A., Rubic, Z., and Tonkic, M. (2016). Evaluation of PNA FISH® Yeast Traffic Light in Identification of Candida Species From Blood and non-Blood Culture Specimens. *Med. Mycol.* 54 (6), 654–658. doi: 10.1093/mmy/myw012

Reardon, S. (2014). WHO Warns Against "Post-Antibiotic" Era. *Nat. News*. doi: 10.1038/nature.2014.15135

Salimnia, H., Fairfax, M. R., Lephart, P. R., Schreckenberger, P., DesJarlais, S. M., Johnson, J. K., et al. (2016). Evaluation of the FilmArray Blood Culture Identification Panel: Results of a Multicenter Controlled Trial. *J. Clin. Microbiol.* 54 (3), 687–698. doi: 10.1128/JCM.01679-15

Semanjski, M., and Macek, B. (2016). Shotgun Proteomics of Bacterial Pathogens: Advances, Challenges and Clinical Implications. *Expert Rev. Proteomics* 13 (2), 139–156. doi: 10.1586/14789450.2016.1132168

Seng, P., Drancourt, M., Gouriet, F., La Scola, B., Fournier, P. E., Rolain, J. M., et al. (2009). Ongoing Revolution in Bacteriology: Routine Identification of Bacteria by Matrix-Assisted Laser Desorption Ionization Time-Of-Flight Mass Spectrometry. *Clin. Infect. Dis.* 49 (4), 543–551. doi: 10.1086/600885

Seymour, C. W., Liu, V. X., Iwashyna, T. J., Brunkhorst, F. M., Rea, T. D., Scherag, A., et al. (2016). Assessment of Clinical Criteria for Sepsis: For the Third International Consensus Definitions for Sepsis and Septic Shock (Sepsis-3). *JAMA* 315 (8), 762–774. doi: 10.1001/jama.2016.0288

Singer, M., Deutschman, C. S., Seymour, C. W., Shankar-Hari, M., Annane, D., Bauer, M., et al. (2016). The Third International Consensus Definitions for Sepsis and Septic Shock (Sepsis-3). *JAMA* 315 (8), 801–810. doi: 10.1001/jama.2016.0287

Sinha, M., Jupe, J., Mack, H., Coleman, T. P., Lawrence, S. M., and Fraley, S. I. (2018). Emerging Technologies for Molecular Diagnosis of Sepsis. *Clin. Microbiol. Rev.* 31 (2), e00089–e00017. doi: 10.1128/CMR.00089-17

Skvarc, M., Stubljar, D., Rogina, P., and Kaasch, A. J. (2013). Non-Culture-Based Methods to Diagnose Bloodstream Infection: Does It Work? *Eur J. Microbiol. Immunol. (Bp)* 3 (2), 97–104. doi: 10.1556/EuJMI.3.2013.2.2

Spanu, T., Posteraro, B., Fiori, B., D'Inzeo, T., Campoli, S., Ruggeri, A., et al. (2012). Direct Maldi-Tof Mass Spectrometry Assay of Blood Culture Broths for Rapid Identification of Candida Species Causing Bloodstream Infections: An Observational Study in Two Large Microbiology Laboratories. *J. Clin. Microbiol.* 50 (1), 176–179. doi: 10.1128/JCM.05742-11

Steinbach, W. J. (2016). Pediatric Invasive Candidiasis: Epidemiology and Diagnosis in Children. *J. fungi (Basel Switzerland)* 2 (1), 5. doi: 10.3390/jof2010005

Stevenson, L. G., Drake, S. K., and Murray, P. R. (2010). Rapid Identification of Bacteria in Positive Blood Culture Broths by Matrix-Assisted Laser Desorption Ionization-Time of Flight Mass Spectrometry. *J. Clin. Microbiol.* 48 (2), 444–447. doi: 10.1128/JCM.01541-09

Tassinari, M., Zannoli, S., Farabegoli, P., Pedna, M. F., Pierro, A., Mastroianni, A., et al. (2018). Rapid Diagnosis of Bloodstream Infections in the Critically Ill: Evaluation of the Broad-Range PCR/ESI-MS Technology. *PloS One* 13 (5), e0197436. doi: 10.1371/journal.pone.0197436

Thoendel, M., Jeraldo, P. R., Greenwood-Quaintance, K. E., Yao, J. Z., Chia, N., Hanssen, A. D., et al. (2016). Comparison of Microbial DNA Enrichment Tools for Metagenomic Whole Genome Sequencing. *J. Microbiol. Methods* 127, 141–145. doi: 10.1016/j.mimet.2016.05.022

van de Groep, K., Bos, M. P., Savelkoul, P., Rubenjan, A., Gazenbeek, C., Melchers, W., et al. (2018). Development and First Evaluation of a Novel Multiplex Real-Time PCR on Whole Blood Samples for Rapid Pathogen Identification in Critically Ill Patients With Sepsis. *Eur. J. Clin. Microbiol. Infect. Dis.: Off. Publ. Eur. Soc. Clin. Microbiol.* 37 (7), 1333–1344. doi: 10.1007/s10096-018-3255-1

Warhurst, G., Dunn, G., Chadwick, P., Blackwood, B., McAuley, D., Perkins, G. D., et al. (2015). Rapid Detection of Health-Care-Associated Bloodstream Infection in Critical Care Using Multipathogen Real-Time Polymerase Chain Reaction Technology: A Diagnostic Accuracy Study and Systematic Review. *Health Technol. Assess.* 19 (35), 1–142. doi: 10.3310/hta19350

Watanabe, N., Kryukov, K., Nakagawa, S., Takeuchi, J. S., Takeshita, M., Kirimura, Y., et al. (2018). Detection of Pathogenic Bacteria in the Blood From Sepsis Patients Using 16s rRNA Gene Amplicon Sequencing Analysis. *PloS One* 13 (8), e0202049. doi: 10.1371/journal.pone.0202049

Welker, M., and Moore, E. R. B. (2011). Applications of Whole-Cell Matrix-Assisted Laser-Desorption/Ionization Time-Of-Flight Mass Spectrometry in Systematic Microbiology. *Syst. Appl. Microbiol.* 34 (1), 2–11. doi: 10.1016/j.syapm.2010.11.013

Xiao, Z., Wang, Q., Zhu, F., and An, Y. (2019). EpidemiologySpecies Distribution, Antifungal Susceptibility and Mortality Risk Factors of Candidemia Among Critically Ill Patients: A Retrospective Study From 2011 to 2017 in a Teaching Hospital in China. *Antimicrobial. Resist. Infect. Control* 8, 89. doi: 10.1186/s13756-019-0534-2

Źródłowski, T. W., Jurkiewicz-Badacz, D., Sroka-Oleksiak, A., Salamon, D., Bulanda, M., and Gosiewski, T. (2018). Comparison of PCR, Fluorescent in Situ Hybridization and Blood Cultures for Detection of Bacteremia in Children and Adolescents During Antibiotic Therapy. *Pol. J. Microbiol.* 67 (4), 479–486. doi: 10.21307/pjm-2018-056

Źródłowski, T., Sobońska, J., Salamon, D., McFarlane, I. M., Ziętkiewicz, M., and Gosiewski, T. (2020). Classical Microbiological Diagnostics of Bacteremia: Are the Negative Results Really Negative? What Is the Laboratory Result Telling Us About the "Gold Standard"? *Microorganisms* 8 (3), 346. doi: 10.3390/microorganisms8030346

Conflict of Interest: Authors AKa and RK are affiliated to a company, Nanoxis Consulting AB. The Company did not have influence on the collection, analysis, or interpretation of data, the writing of the paper, or the decision to submit for publication.

The remaining authors declare that the research was conducted in the absence of any commercial or financial relationships that could be construed as a potential conflict of interest.

Publisher's Note: All claims expressed in this article are solely those of the authors and do not necessarily represent those of their affiliated organizations, or those of the publisher, the editors and the reviewers. Any product that may be evaluated in this article, or claim that may be made by its manufacturer, is not guaranteed or endorsed by the publisher.

frontiers in Cellular and Infection Microbiology

BRIEF RESEARCH REPORT
published: 19 August 2021
doi: 10.3389/fcimb.2021.705468

Linking inherent O-Linked Protein Glycosylation of YghJ to Increased Antigen Potential

Mette Thorsing[1], *Thøger Jensen Krogh*[1], *Lars Vitved*[2], *Arkadiusz Nawrocki*[3], *Rikke Jakobsen*[1], *Martin R. Larsen*[3], *Subhra Chakraborty*[4], *A. Louis Bourgeois*[5], *Ann Zahle Andersen*[1] *and Anders Boysen*[1]*

[1] GlyProVac LLC, Odense, Denmark, [2] Department of Cancer and Inflammation Research, University of Southern Denmark, Odense, Denmark, [3] Department of Biochemistry and Molecular Biology, University of Southern Denmark, Odense, Denmark, [4] Center for Immunization Research, Johns Hopkins Bloomberg School of Public Health, Baltimore, MD, United States, [5] Center for Vaccine Innovation and Access, PATH, Washington, DC, United States

OPEN ACCESS

Edited by:
Di Xiao,
National Institute for Communicable Disease Control and Prevention (China CDC), China

Reviewed by:
Felipe Del Canto,
University of Chile, Chile
Astrid Maria Von Mentzer,
University of Gothenburg, Sweden
Frederick Kuhlmann,
Washington University in St. Louis, United States

***Correspondence:**
Anders Boysen
Boysen@glyprovac.com

Specialty section:
This article was submitted to Clinical Microbiology, a section of the journal Frontiers in Cellular and Infection Microbiology

Received: 05 May 2021
Accepted: 23 July 2021
Published: 19 August 2021

Citation:
Thorsing M, Krogh TJ, Vitved L, Nawrocki A, Jakobsen R, Larsen MR, Chakraborty S, Bourgeois AL, Andersen AZ and Boysen A (2021) Linking inherent O-Linked Protein Glycosylation of YghJ to Increased Antigen Potential. Front. Cell. Infect. Microbiol. 11:705468. doi: 10.3389/fcimb.2021.705468

Enterotoxigenic Escherichia coli (ETEC) is a WHO priority pathogen and vaccine target which causes infections in low-income and middle-income countries, travelers visiting endemic regions. The global urgent demand for an effective preventive intervention has become more pressing as ETEC strains have become increasingly multiple antibiotic resistant. However, the vaccine development pipeline has been slow to address this urgent need. To date, vaccine development has focused mainly on canonical antigens such as colonization factors and expressed toxins but due to genomic plasticity of this enteric pathogen, it has proven difficult to develop effective vaccines. In this study, we investigated the highly conserved non-canonical vaccine candidate YghJ/SslE. Using the mass spectrometry-based method BEMAP, we demonstrate that YghJ is hyperglycosylated in ETEC and identify 54 O-linked Set/Thr residues within the 1519 amino acid primary sequence. The glycosylation sites are evenly distributed throughout the sequence and do not appear to affect the folding of the overall protein structure. Although the glycosylation sites only constitute a minor subpopulation of the available epitopes, we observed a notable difference in the immunogenicity of the glycosylated YghJ and the non-glycosylated protein variant. We can demonstrate by ELISA that serum from patients enrolled in an ETEC H10407 controlled infection study are significantly more reactive with glycosylated YghJ compared to the non-glycosylated variant. This study provides an important link between O-linked glycosylation and the relative immunogenicity of bacterial proteins and further highlights the importance of this observation in considering ETEC proteins for inclusion in future broad coverage subunit vaccine candidates.

Keywords: Enterotoxigenic *Escherichia coli*, immunogenicity, vaccine development, mass spectrometry, protein glycosylation, sub-unit vaccines, YghJ, SslE

INTRODUCTION

Whereas an increase in the availability of resources such as clean water and professional healthcare has significantly decreased the mortality from *E. coli* infections in low and middle-income countries (LMICs), the number of non-fatal infections remains high and so does the cost of these infections to societies in low-resource settings due to childhood stunting and delays in cognitive development as well as increased risk of dying from other infectious diseases (Anderson et al., 2019; Khalil et al., 2021). In addition, *enterotoxigenic Escherichia coli* (ETEC) globally continues to cause severe diarrhea and death in high risk patient groups, including older individuals (Poolman and Anderson, 2018) and is the most common cause of diarrhea in travelers to endemic regions (Olson et al., 2019).

E. coli remains a World Health Organization (WHO) priority pathogen and vaccine target given its high burden and the increasing emergence of Extended-spectrum β-lactamase producing Enterobacteriaeceae including ESBL-ETEC (Shrivastava et al., 2018; Tacconelli et al., 2018). In a recent report, the Wellcome Trust and Boston Consulting Group recommend that vaccine development for enteric *E. coli* including ETEC be accelerated due to the increasing antimicrobial resistance (AMR) threat (Wellcome Trust, 2019) and this recommendation was repeated in the WHO Action Framework: Leveraging Vaccines to Reduce Antibiotic Use and Prevent Antimicrobial Resistance (World Health Organization, 2020). In striking contrast to the increasing need for therapeutic interventions, the *E. coli* vaccine pipeline is limited to only 16 vaccine candidates, ten of which are in the research/preclinical phase. Thus, whereas ETEC is a global challenge, both the commercial and academic *E. coli* vaccine pipeline remains inadequate (Barry et al., 2019; Theuretzbacher et al., 2019; Bekeredjian-Ding et al., 2020; Giersing, 2020).

The traditional canonical antigens of ETEC include colonization factors and secreted toxins. Past efforts in *E. coli* vaccine development have focused mainly on these important virulence factors. However, *E. coli* displays huge genomic plasticity, resulting in large variations in virulence factors with each pathotype within the species, which hinders the development of a vaccine with broad coverage based on these canonical antigens (Turner et al., 2006; Moriel et al., 2012; Nesta and Pizza, 2018). With an increased understanding of the complexity of *E. coli* pathogenesis, significant efforts have been devoted to the discovery and characterization of novel non-canonical antigens (Roy et al., 2010; Fleckenstein et al., 2014; Chakraborty et al., 2016). These antigens form a group of molecular entities identified to be relevant for either pathogenesis, immunology or vaccinology.

One of the non-canonical antigens, which has received significant attention, is YghJ, also known as SslE (Nesta et al., 2014; Chakraborty et al., 2018). YghJ is a secreted and broadly conserved metalloprotease within the pathogenic *E. coli* family (Luo et al., 2014). During the early stages of infection, YghJ degrades the protective intestinal mucin layer, facilitating access to the epithelial cell surface and colonization, as well as toxin delivery. Moreover, proteomic and transcriptomic analyses show that YghJ is immunogenic in both animals and humans and that expression increases upon adherence to host cells (Roy et al., 2010; Kansal et al., 2013; Chakraborty et al., 2018). From the host's perspective, it has been demonstrated that YghJ from *E. coli* strains associated with neonatal sepsis not only causes *in vitro* stimulation of proinflammatory cytokines in a human intestinal epithelial cell line, but also induces damage to mouse ileal tissues *in vivo* (Tapader et al., 2016; Tapader et al., 2017). Lastly, immunization with YghJ has been shown to confer some protection in animals against extraintestinal pathogenic *E. coli* bacteremia (Moriel et al., 2010), uropathogenic *E. coli* pyelonephritis, ETEC colonization of caecum and *E. coli* caused sepsis (Nesta et al., 2014). In addition to academic interest, YghJ has also been pursued commercially by Novartis and later Glaxo Smith Kline (Moriel et al., 2010; Serino et al., 2010; Nesta et al., 2014). However, despite the continuous attention on YghJ in ETEC controlled human infection model (CHIM) studies and the established role of YghJ as an important factor in effective intestinal colonization (Fleckenstein et al., 2014; Chakraborty et al., 2018; Mirhoseini et al., 2018; Nesta and Pizza, 2018; Vedøy et al., 2018), YghJ has, to the best of our knowledge, not progressed as a vaccine candidate antigen beyond early animal challenge studies.

With the discovery and identification of O-linked glycosylated proteins, an extra layer of complexity has been added to bacterial pathogenesis. O-linked protein glycosylation, the addition of glycans to either Serine (Ser) or Threonine (Thr) amino acid residues, is well documented in diverse Gram-negative bacterial species such as *Neisseria gonorrhoeae*, *Burkholderia cenocepacia*, *Acinetobacter baumannii*, *Pseudomonas aeruginosa* as well as *E. coli* (Benz and Schmidt, 2001; Castric et al., 2001; Vik et al., 2009; Iwashkiw et al., 2012; Lithgow et al., 2014). The species-specific glycans used for protein glycosylation are remarkably diverse but nevertheless important as their loss results in reduced virulence potential, reduced fitness and altered biophysical properties of e.g. adhesins (Knudsen et al., 2008; Faulds-Pain et al., 2014; Schäffer and Messner, 2017; Mohamed et al., 2019). Furthermore, protein glycosylation also appear to increase the antigenic variation in order to evade the immune system of the host (Gault et al., 2015). The most comprehensive O-linked protein glycosylation studies include high-throughput mass spectrometry and the dedicated glycoproteomics technique termed BEMAP (β-elimination of O-linked carbohydrate modifications, Michael addition of 2-Aminoethyl phosphonic acid) (Boysen et al., 2016; Scott, 2019). The BEMAP technique (patent US 10,647,749 B2) can be employed to map O-linked glycoproteins from any biological source and was developed with the intention to identify and expand the repertoire of glycosylated proteins linked to ETEC pathophysiology. Using BEMAP, more than 140 glycoproteins associated with the outer membrane fraction and outer membrane vesicles were previously identified in *E. coli* K-12 and ETEC H10407 and a potential link between pathogenesis and O-linked glycosylation was discussed (Boysen et al., 2016). This was based on the remarkable finding that protein glycosylations were only found in the pathogenic ETEC strain despite that most of the identified glyco-proteins were conserved on a protein level

between ETEC and the commensal *E. coli* K-12. In addition, it was observed that the majority of canonical as well as non-canonical ETEC virulence factors were glycosylated, including YghJ.

In the present study we have further investigated the extent of YghJ glycosylation and coupled this inherent O-linked protein glycosylation to an increased antigenic potential of YghJ. We have expressed and purified glycosylated YghJ from the canonical ETEC strain H10407 and performed an in depth BEMAP analysis to identify glycosylated Ser/Thr residues. Using BEMAP, we identified 54 modified residues within this 1519 amino acid protein. To obtain a control protein for the investigation of the potential impact of O-linked glycosylation on protein immunogenicity we over-expressed and purified a non-glycosylated version of YghJ. This control antigen was overexpressed from a K-12 MG1655Δ*hldE* genetic background and the absence of O-linked glycosylation was confirmed using BEMAP. In pathogenic *E. coli*, HldE catalyzes the biosynthesis of ADP-activated heptose precursor units which are used in protein glycosylation (Benz and Schmidt, 2001; Nakao et al., 2012). Therefore, with the deletion of hldE, the expression strain loses its ability to add heptose glycans to YghJ.

To examine the difference in immune response towards glycosylated YghJ and the non-modified protein variant subsequent to ETEC infection, serum isolated from pre- and post H10407 challenged volunteers was used in ELISA experiments (Chakraborty et al., 2016). Both glycosylated YghJ and non-glycosylated YghJ were recognized by sera from patients prior to infection (day 0). Importantly, the increase in recognition of glycosylated YghJ from days 0 to day 7 and 28 post infection was significantly greater than recognition of non-modified YghJ variant at both time points.

The current study shows that the bacterial mucinase YghJ is a hyper O-glycosylated protein. We also show that antibodies from patients exposed to ETEC infections predominantly recognize glycosylated over non-glycosylated YghJ which points to increased immunogenicity of glycosylated YghJ compared to the non-glycosylated antigen. The current study therefore highlights the importance of considering O-linked glycosylation when considering the role of bacterial proteins in pathogenic evolution but also from the perspective of antigen discovery and the development of effective and more broadly protective vaccines.

MATERIALS AND METHODS

Bacterial Strains and Culture Conditions

Strains were grown in Luria Bertani (LB) (Sambrook and Green, 2012) or M9 minimal medium (Boysen et al., 2010) supplemented with 0.4% glucose and 0.2% casamino acids. Cells used for electroporation were grown in Super Optimal Broth (SOB) and Super Optimal Broth with Catabolite repression (SOC) (Hanahan, 1983). Protein expression was induced from the $P_{A1/04/03}$ promoter by 1 mM isopropyl-β-d-thiogalactopyranoside (IPTG). When required, the media was supplemented with either 40 μg/ml Kanamycin or 30 μg/ml Chloramphenicol. Strains and plasmids are listed in **Supplementary Table S1** and primers are listed in **Supplementary Table S2**.

DNA Manipulations

The Datsenko and Wanner system and primers JMJ388 and JMJ389 were used to delete *hldE* in MG1655 (Datsenko and Wanner, 2000). The *hldE* gene plays a role in the biosynthesis of ADP-activated heptose units required for post-translational protein heptosylation (Benz and Schmidt, 2001; Nakao et al., 2012). Candidate clones were selected, isolated and tested by PCR using the primer pairs JMJ390+JMJ391 and JMJ390+JMJ99.

To isolate glycosylated YghJ, a 3xFLAG epitope tag was added to the *yghJ* gene on the ETEC H10407 chromosome as described by Uzzau et al. (2001). In brief, a PCR product generated using pSUB11 as template and the primer pairs GPV18+GPV19 was electroporated into *E. coli* H10407. Transformants were selected on LB agar plates containing 40 μg/ml kanamycin. The primer pairs GPV16+GPV17 as well as GPV67+GPV147 were used to verify H10407*yghJ* 3xFLAG. The construct was verified by sequencing.

To isolate a non-glycosylated YghJ protein version, a 3xFLAG epitope tag was added to the *yghJ* gene and put under an IPTG inducible promoter for expression in a MG1655Δ*hldE* mutant strain background. Briefly described, An IPTG inducible promoter and the 3xFLAG epitope was added to the *yghJ* gene in two steps. First, the primers GPV95 and GPV97 were used to generate a PCR product using chromosomal DNA from the ETEC H10407*yghJ* 3xFLAG strain as template. In the second step, GPV96 and GPV97 were used to generate a PCR product that was digested with XhoI and XbaI and subsequently ligated into pXG-0. This generated pGPV104. pGPV104 was verified by sequencing before transformation into the MG1655Δ*hldE* mutant strain background.

Protein Purification

Glycosylated YghJ 3xFLAG was isolated from the ETEC H10407*yghJ* strain grown in M9 minimal medium supplemented with 0.2% glucose and 0.4% casamino acid and 40 μg/ml kanamycin. The culture was grown to OD_{600} = 2.5 at 37°C after which it was harvested. The culture supernatant was sterile filtered (0.22μm pore size), NaCl and Triton X-100 was added to obtain a final concentration of 200 mM and 0.01%, respectively. Anti-FLAG M2 affinity agarose gel beads (SigmaAldrich; A2220) was used to capture the 3xFLAG epitope. Isolated FLAG affinity agarose beads were washed twice with FLAG Sup wash buffer I (400 mM NaCl, 0.1% Triton X-100, 1 mM EDTA in PBS buffer pH 7.6) and once with FLAG Sup buffer II (400 mM NaCl, 0.01% Triton X-100, 1 mM EDTA in PBS buffer pH 7.6). Elution was accomplished with Elution buffer (500 mM Arginine, 500 mM NaCl, pH = 3.5). Eluate fractions were spin filter concentrated before dialyzed against PBS at 4°C over night in a cold room.

Non-glycosylated YghJ 3xFLAG was isolated from the MG1655Δ*hldE*/pGPV104 strain grown in LB medium supplemented with 40 μg/ml Chloramphenicol. The culture was grown to OD_{600} = 2.5 at 37°C after which it was harvested by centrifugation. Cell pellets were collected and 500 μg DNaseI was added before the sample was lysed three times in a French Press at 2.2 kbar. The lysate was cleared by ultracentrifugation at 125.000 x g at 4°C for three hours in a Beckman SW 32 Ti rotor.

Sample volume was increased to 1 L and NaCl, Triton X-100 and EDTA was added to obtain a final concentration of 600 mM, 0.01% and 1 mM, respectively. Anti-FLAG M2 affinity agarose gel beads was added to the supernatant and incubated with shake at 4°C O/N in a cold room. FLAG affinity agarose beads were isolated, washed, eluted and dialyzed as described above.

BEMAP and Mass Spectrometry Assisted Identification of Glycosylated Ser/Thr Residues

The BEMAP analysis was carried out as previously described (Boysen et al., 2016). A total of 40 μg protein was used as input to identify glycosylated YghJ Ser/Thr residues. As described in detail in (Boysen et al., 2016), raw data was generated on LTQ Orbitrap Velos, Orbitrap Velos Pro or Q-Exactive Plus mass spectrometers (Thermo Fisher Scientific, Bremen, Germany). Data was processed with Proteome Discoverer (Version 1.4.1.14, Thermo Fisher Scientific) and subjected to database searching using an in-house Mascot server (Version 2.2.04, Matrix Science Ltd., London, UK). Database searches were performed as previously described (Boysen et al., 2016). The mass spectrometry proteomics data have been deposited to the ProteomeXchange Consortium via the PRIDE (Perez-Riverol et al., 2019) partner repository with the dataset identifier PXD025876.

Experimental Human Challenge Study

In a dose descending experimental challenge model, healthy American adult volunteers were challenged with an ETEC strain H10407 in 3 cohorts in an in-patient unit at Johns Hopkins University as described before (Chakraborty et al., 2016). Samples from cohort 2, where volunteers were challenged with 10^7 CFU of ETEC, were used in this study. Subjects were excluded if they had significant medical problems; if an HIV-1, hepatitis B, or hepatitis C test was positive; or if they had traveled to countries where ETEC or cholera infection is endemic within two years prior to receipt of investigational agent. After challenge, subjects were monitored for signs and symptoms of enteric illness. All the subjects were treated with antibiotics 120 hours (5 days) after challenge, or earlier if required because of the diarrhea illness according to the clinical protocol. Diarrhea was classified as mild (1 to 3 diarrheal stools totaling 200 to 400 g/24 h), moderate (4 to 5 diarrheal stools or 401 to 800 g/24 h), or severe (6 or more diarrheal stools or ≥800 g/24 h). No diarrhea was defined as no loose stool observed. The volunteers challenged with $2x10^7$ dose resulted in attack rate of 67%.

ELISA Experiment

96-well Maxisorb ELISA plates (Nunc, Denmark) were coated overnight at 4°C with glycosylated and non-glycosylated YghJ (2.5 μg/mL) in phosphate buffered saline (PBS). Plates were washed twice and blocked with PBS containing 0.05% Tween 20 for 15 min before the human serum samples (PBS containing 0.05% Tween 20 and 3% skimmed milk), from the experimental challenge model described above, were added to the plate. Each serum sample was two-fold serial diluted in 11 wells starting with a dilution factor of 25. The twelfth well was used for background determination (no serum). All three sera from each patient were analyzed on the same plate. After 1 hr of incubation with serum, the plates were washed 3 times with phosphate buffered saline (PBS) containing 0.05% Tween 20. Secondary polyclonal rabbit anti-Human IgG/A/M (DAKO P0212) HRP conjugated antibody was diluted x1000 and added to all wells in the plates. The plates were washed as described above before the signal strength was detected using TMB X-tnd (Kementec cat. no. 5280) and a Molecular Devices microplate reader set at 450nm. SoftMax Pro 7 software was used to fit measured intensity values (arbitrary units) as a function of serum concentration. Endpoint titers at 0.4 units above background were read from the fitted curve as described in Chakraborty et al., 2019 (Chakraborty et al., 2019).

SDS-PAGE and Western Blots

Denaturing Western blotting was used to detect YghJ protein secreted to the culture supernatant as well as for the analysis of purified glycosylated YghJ and non-glycosylated YghJ. YghJ protein samples were boiled and run on PAGE gels as described in (Boysen et al., 2010). After the transfer, the membrane was blocked with 1% skimmed milk in PBS buffer with 0.05% Tween-20 for 1 hour. When analyzing human serum samples, the membrane was blocked with 3% skimmed milk in PBS buffer with 0.05% Tween-20 for 1 hour. Both primary and secondary antibodies were diluted into 1% skimmed milk in PBS buffer with 0.05% Tween-20. Incubation times were 1 hour. The antibodies were diluted as shown in **Supplementary Table S3**. Blots were developed using Immobilon Forte Western HRP substrate (Millipore). The signal was detected using an Amersham Imager 680 (Cytivalifesciences).

Native Western blotting was used to detect purified glycosylated YghJ and non-glycosylated YghJ. Briefly described, YghJ protein was mixed 1x SDS native loading buffer (60 mM Tris-HCl, pH 6.8, 10% glycerol, 0.005% bromphenol blue) at room temperature before loading onto a NUPAGE 4-12% Bis-Tris Gels (Invitrogen). Proteins were separated in a native MES buffer (50mM MES, 50mM Tris Base, 0.01% SDS, pH 7.3) after which they were transferred to a PVDF membrane as described above. The YghJ specific signal was obtained as described above.

Statistical Analysis

For preparation of graphs and statistical analysis, we used Prism, version 6.07 (GraphPad Software, San Diego, CA). To test for differences in YghJ specific antibody levels in serum samples, between day 0 and day 7 as well as day 0 and day 28, we used Wilcoxon signed rank test. Minimum p-values, for which the null hypothesis was rejected, were reported. P-values ≤ 0.05 were considered significant.

RESULTS

BEMAP Reveals Extensive YghJ O-Linked Protein Glycosylation

We have previously established a catalogue of O-linked glycosylated proteins in ETEC strain H10407 (Boysen et al., 2016; Maigaard Hermansen et al., 2018). More than 200 proteins

were found to be modified and >800 specific glycosylated Ser/Thr residues were identified in the screening. Among these, the non-canonical antigen YghJ was found to be modified at four sites (Boysen et al., 2016). In the current study YghJ was affinity purified using a 3xFLAG epitope tag added to the C-terminus of the protein (Uzzau et al., 2001). Under standard laboratory conditions, ETEC secretes enzymatically active YghJ into the growth medium (Luo et al., 2014), thus, to ensure that only fully processed and modified YghJ was analyzed by BEMAP, we purified the exported protein from the culture supernatant. With an input of 40 μg purified YghJ, 28 peptides which contained a total of 54 glycosylated residues were identified using the BEMAP protocol, see **Table 1**.

Thus, whereas the previous screening revealed four glycosylated sites in YghJ, our in depth analysis shows that approximately 25% of all the Ser/Thr residues in YghJ are O-linked glycosylated. When assigning the glycosylation site to the primary sequence of YghJ, the modifications were more or less evenly distributed throughout the protein. We next investigated if the O-glycosylation sites were randomly distributed within the protein structure or if they clustered into particular spatial regions, which could be of biological importance. Unfortunately, an YghJ crystal structure remains to be resolved. However, we used the Protein Homology/analogY Recognition Engine (Phyre2) to generate a 3D model of the protein. The algorithm was able to assign a structure to the last 500 aa of the protein and we visualized the structural position of the O-glycosylation sites by highlighting sugar-modified residues within the structures, see **Supplementary Figure S1**. We found that in general, the glycosylation sites were surface exposed and located in unstructured regions on the protein. In previous studies it has been speculated that the spatial arrangement of the glycosylated residues could be a mode to scramble the surface structure in order to evade recognition by the immune system (Gault et al., 2015). Based on the Phyre2 model prediction and the location of the glycans, it is possible that the YghJ modifications serve the same immunologic purpose.

Purification and Characterization of Glycosylated and Non-Glycosylated YghJ

The extensive O-linked protein glycosylation observed in ETEC indicates a role for these modifications in normal cellular physiology in addition to virulence (Boysen et al., 2016; Maigaard Hermansen et al., 2018). We speculated if this abundant but overlooked type of protein modification for example could influence protein conformation. To examine this, we first purified and characterized a glycosylated and non-glycosylated version of YghJ. As for the BEMAP analysis, glycosylated YghJ was isolated from the ETEC culture supernatant. In contrast, the non-glycosylated YghJ version was ectopically expressed, and affinity purified from a commensal *E. coli* MG1655Δ*hldE* mutant background. Pathogenic *E. coli* uses mono heptoses for protein glycosylation and the synthesis of these glycans depends on the *hldE* gene (Benz and Schmidt, 2001; Nakao et al., 2012; Boysen et al., 2016). Therefore, with the deletion of *hldE*, the expression strain would lose its ability to modify YghJ with this type of glycan. To

TABLE 1 | BEMAP analysis of glycosylated YghJ. YghJ was digested with Trypsin and O-linked glycosylated peptide sequences were identified using BEMAP in combination with mass spectrometry.

start	end	Sequence	Site#	Site#	Site#	Site#	Site#	Site#	Site#
91	101	TGYLTLGGsQR	99						
102	143	VtGAtCNGEssDGFtFKPGEDVtCVAGNtTIATFNTQSEAAR	103	106	111	112	116	124	130
169	199	SNAVSLVTsSNsCPANtEQVCLtFSSVIESK	177	180	185	191			
218	231	LVNEEVENNAAtDK	229						
355	364	YsttGQNNtR	356	357	358	363			
419	435	ElDtAICAKTDGCNEAR	422						
428	442	tDGCNEARWFsLttR	428	438	440	441			
456	468	LWGVDTNYKSVsK	467						
469	486	FHVFHDStNFYGsTGNAR	476	481					
487	504	GQAVVNIsNAAFPILMAR	494						
588	609	DGQCtLNsDPDDMKNFMENVLR	592	595					
610	615	YLsnDR	612						
622	636	ssMtVGTNLEtVYFK	622	623	625	632			
720	734	GGsVLIMENVMSNLK	722						
735	743	EEsAsGFVR	739						
757	769	sVVnNDPQGYPDR	757						
818	830	LEVAsWQEEVEGK	822						
845	853	TPEsLAAAK	848						
909	922	AMLQAADLGtNIQR	918						
923	935	LYQHELYFRtNGR	932						
1000	1015	KsLIDNKMIYGEEssK	1001	1013	1014				
1016	1034	AGMMNPsYPLNYMEKPLTR	1022						
1048	1075	VDVEKYPGVVNtNGEtVtQNINLYSAPTK	1059	1063	1065				
1101	1120	StVPVtVTVALADDLtGREK	1102	1106	1116				
1134	1142	tYDLKANDK	1134						
1134	1146	TYDLKANDKVtFK	1144						
1341	1362	VADDITVAPEYLEEsNGQAWAR	1355						
1418	1431	ARGDEVsNDKFGGK	1424						

The start and end position of each of the 28 peptide sequences within YghJ are listed, as well as the specific residue number which is modified. Lower case s or t indicate modified residue.

assess the conformation of glycosylated YghJ and the non-glycosylated counterpart, the linear and native structure of both proteins were compared using reducing and native PAGE analysis, respectively. As shown in **Figure 1**, several bands carrying the FLAG-tag were identified for both glycosylated and non-glycosylated YghJ. These bands reflect degradation of the proteins during the purification process. It is observed that both proteins displayed similar migration patterns and the degradation fragments were of equal sizes. Next, we verified the non-modified state of YghJ isolated from the MG1655Δ*hldE* expression strain, using 40 μg purified protein as input to a BEMAP analysis. No modified sites were identified (data not shown). Based on the PAGE analysis and BEMAP, we conclude that our purification approach allows us to isolate glycosylated YghJ as well as a non-glycosylated version. In addition, the modifications do not appear to dramatically influence the overall protein structure, but it is possible that the glycosylation could induce local conformational changes throughout YghJ (Shental-Bechor and Levy, 2008).

YghJ Glycosylation Is Associated With Increased Recognition by Human Immune Response

The controlled human infection model (CHIM) has advanced the understanding of ETEC pathogenesis, assisted in characterizing the gut mucosal immune system and aided the search for candidate vaccine antigens, as well as evaluating early candidates in Phase 1/2/2B clinical trials (Chakraborty et al., 2016; Chakraborty et al., 2018; Vedøy et al., 2018). In this study we use sera from the CHIM study to investigate the human YghJ-specific immune response following infection (Chakraborty et al., 2015). Only individuals which experienced a moderate to severe diarrhea when ingesting ETEC were included in this analysis.

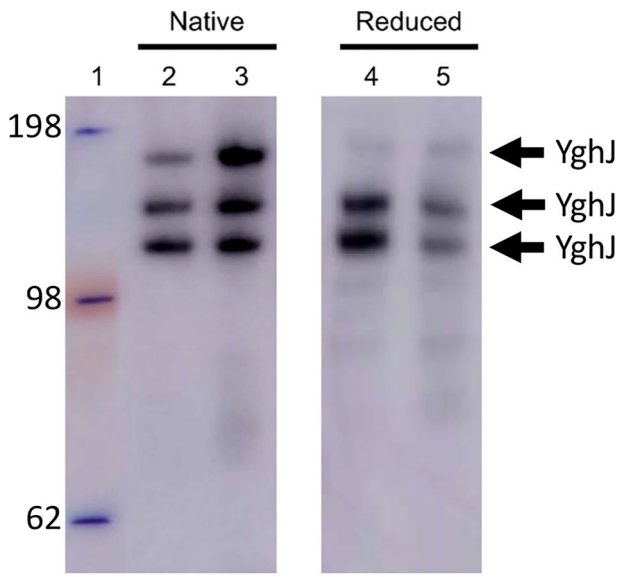

FIGURE 1 | Western blot analysis of purified glycosylated and non-glycosylated YghJ. Glycosylated and non-glycosylated YghJ was loaded onto a PAGE gel and run under either non-reducing (left panel) or reducing conditions (right panel) to assess the linear and native protein conformations. Molecular weight marker (kDa) was loaded in lane 1. Glycosylated YghJ was loaded in lanes 2 and 4 whereas the non-glycosylated protein variant was loaded in lanes 3 and 5. Chicken anti-FLAG antibodies (diluted x4.000) and HRP conjugated rabbit Anti-Chicken IgY (diluted x5.000) were used to visualize YghJ.

As shown above, the 1519 amino acid protein YghJ is glycosylated at 54 different Ser/Thr residues. Therefore, these glycan-peptide epitopes constitute only a fraction of YghJ epitopes presented to the immune system during infection. Nevertheless, we speculated whether the ingestion of ETEC and thus an exposure to glycosylated YghJ would raise an immune response, which differed in recognition compared to the non-glycosylated protein variant. Specifically, we investigated the difference between antibodies recognizing the glycosylated YghJ as compared to the non-glycosylated variant using 17 serum samples from the CHIM study. In order to quantitatively assess the immune response, we conducted ELISA experiments. Serum isolated from the individuals before infection (Day 0), after 7 days (Day 7) and 28 days (Day 28) post infection was used as input for the analysis. The relative serum antibody response towards the glycosylated and non-glycosylated antigen is shown in **Figures 2A, B**. As shown in **Figure 2C**, we have plotted the relative increase in immune response towards the two antigens by comparing the Day 0 samples to either Day 7 or the Day 28 samples in a patient by patient manner. In our analysis, serum samples withdrawn from patients on Day 7 showed a significantly stronger response ($p = 0.0003$) towards the glycosylated YghJ (+glyco) compared to the non-modified protein variant (-glyco) with calculated medians of 2.3 and 1.3, respectively. The response towards glycosylated YghJ and the non-modified protein variant became even more pronounced on Day 28 ($p = 0.0001$). The patient-to-patient variability in antibodies recognizing glycosylated YghJ increased and the median rose from 2.3 to 3.0. On the other hand, the level of patient antibodies recognizing non-glycosylated YghJ was more uniformly distributed and the median increased modestly from 1.3 to 1.6.

To ensure that serum ELISA signal depended only on YghJ recognizing antibodies, two control experiments were performed. In one control experiment we used Western blotting and serum samples from three patients to probe for glycosylated YghJ to determine if co-purified contaminants had contributed to the ELISA signals. In this analysis, we detected one specific YghJ signal suggesting our results exclusively are based on antibodies recognizing our antigen (**Supplementary Figures S2** and **S3**). In another control experiment ELISA plates were coated with a nonsense protein and the serum response measured. Only low titers, with no correlation to sample day were observed, supporting that we have measured an YghJ-specific antibody response in our experimental setup (data not shown).

Remarkably, even though the protein glycosylation only constitutes a minor fraction of all the possible epitopes, our ELISA results show that the immune response towards glycosylated YghJ is stronger than that of the non-glycosylated protein variant. These results assign a clear role to protein glycosylation in the immune response against the YghJ antigens, both natural and recombinant.

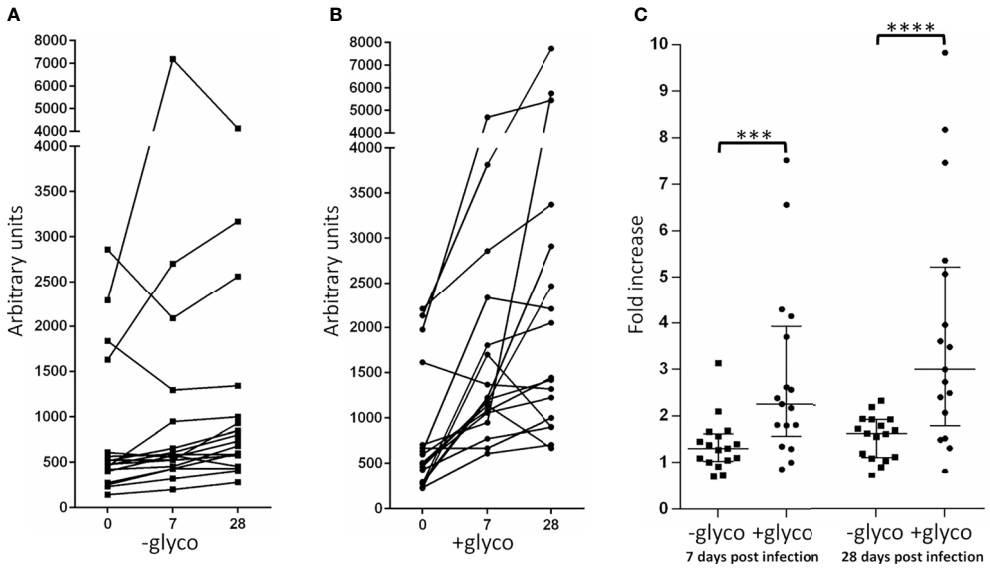

FIGURE 2 | ELISA experiment using 17 serum samples from a controlled human infection model (CHIM) study showing the relative immune response towards glycosylated YghJ (+glyco) and the non-glycosylated protein variant (-glyco). **(A)** Arbitrary anti non-glycosylated YghJ IgG/A/M antibody levels in serum 0, 7 and 28 days after ETEC ingestion is shown. **(B)** Arbitrary anti glycosylated YghJ IgG/A/M antibody levels in serum 0, 7 and 28 days after ETEC ingestion is shown. **(C)** The ratio between measured endpoint titers obtained at Day 0 and Day 7 as well as Day 0 and Day 28 for antibodies that bound –glyco (squares) or +glyco (circles) was calculated and plotted. A Wilcoxon matched-pairs signed rank test was performed to evaluate significant differences in the immune response towards glycosylated and non-glycosylated YghJ. ***P = 0.0003. ****P < 0.0001. Median with interquartile range for each data set is indicated.

DISCUSSION

BEMAP is a sensitive, selective and robust method which enables the identification of O-linked glycosylated sites in proteins (Boysen et al., 2016). When screening for glycosylated proteins in ETEC H10407, four glycosylated YghJ Ser/Thr sites were initially identified within the 1519 amino acid sequence. In this study, we have used BEMAP to further study glycosylated YghJ purified from ETEC H10407. As shown in **Table 1**, our analysis increases the number of identified sites from four to a total of 54 and we conclude that YghJ is hyperglycosylated. The macro heterogeneity, or glycan site occupancy, for each Ser/Thr residue within YghJ remains to be determined but we speculate that the site variation may be just as significant as observed in the Eukaryotic domain (Čaval et al., 2021). The BEMAP method can only determine if a site is modified or not. Therefore, if the site occupancy varies, it is possible that even more sites may be identified if more protein is analyzed and/or the sensitivity of the used MS instrument is increased. Based on the results presented here, we have firmly established that YghJ is hyperglycosylated and our observations indicate that this non-canonical ETEC antigen should be added to the growing list of modified bacterial proteins with potential vaccine importance. Moreover, as demonstrated with YghJ, we highlight that the BEMAP method has the potential to reveal novel insights into proteins already extensively characterized (Luo et al., 2014; Nesta et al., 2014).

Post translational protein modifications in the prokaryotic world have until recently been regarded as rare and exotic. However, increasing efforts are being dedicated to understanding the functions and benefit of protein glycosylation in the context of immunogenicity. Some studies have for example demonstrated that the glycosylation mask the surface of the protein or even forms a glycan-shield in order to avoid recognition by the immune system of the host (Gault et al., 2015; Walls et al., 2016). The mapping of the glycosylated residues onto a Phyre2 based 3D model (Kelley et al., 2015) of YghJ (**Supplementary Figure S1**) reveals extensive surface exposure of the glycans. Therefore one could imagine a similar role for YghJ protein glycosylation. This hypothesis, however, is rejected by our data presented in **Figure 2**, showing that YghJ glycosylation increases the overall immunogenicity of the protein although they only constitute a small fraction of all the available epitopes.

In this study, we have preliminarily investigated if these modifications induce topology changes of YghJ by comparing the native and denatured conformation of the protein. As presented in **Figure 1**, the PAGE analysis did not reveal any detectable differences between glycosylated YghJ and the non-modified protein variant when examined under the different experimental conditions. This indicates, that if the glycosylation does induce conformational changes in YghJ, they are local. However, the data does not exclude the possibility that O-linked glycosylation serves to influence folding kinetics, protein stability or contributes to protein function as seen with other glycoproteins (Knudsen et al., 2008; Shental-Bechor and Levy, 2008).

Despite an increasingly important unmet public health need, there is still a large number of important bacterial pathogens such as ETEC where the first effective vaccine has yet to enter the market. The evidence of widespread bacterial O-linked protein glycosylation and the impact of these modifications on function

and immunogenicity is accumulating at an increasing rate. We speculate that the failure to produce safe and high efficacy subunit vaccines targeting bacterial pathogens may in part be associated with absence of immunologically important O-linked glycosylations in the final protein antigen formulation. The absence of these glycosylations could for example arise if protein antigens are produced in an *E. coli* K-12 background. In a previous study we identified cell surface-associated glycoproteins from ETEC and *E. coli* K-12 (Boysen et al., 2016). Here we observed that the majority of the ETEC glycoproteins were conserved in both strains but nevertheless were only glycosylated in the pathogens. This suggests that antigen expression in *E. coli* K-12 will result in little or no protein glycosylation at all. As described, all CHIM patients carried antibodies against YghJ on day 0 and 67% of the enrolled patients became ill when exposed to a dose of ETEC. This suggests that prior exposure to *E. coli* did not raise antibodies against YghJ or any other *E. coli* antigen, associated with cross-protection against ETEC. This lack of protection may be a matter of antibody threshold levels. It has previously been reported, that the higher the baseline level of serum IgA and IgG against ETEC in unvaccinated individuals, the lower the incidence of moderate to severe illness (McKenzie et al., 2008). With this study, using serum from an ETEC controlled human infection study, we have provided an important link between protein glycosylation and the immunogenicity on an established and well investigated non-canonical ETEC antigen. It is possible that YghJ could show the same level of cross-protection as demonstrated in *Shigella* using the conserved protein outer membrane protein PSSP-1 (Kim et al., 2018). Future investigations will include specific epitope analyses of the glycosylated YghJ and the non-modified protein variant to further study the antigenic potential of O-linked glycosylation. We believe that the increased immunogenicity of glycosylated YghJ compared to the non-modified protein variant will prove to be a distinguishing factor impacting on the ability of this protein to induce protective immune responses and thus enhance its potential as a non-canonical antigen component of future diarrheagenic and uropathogenic *E. coli* vaccines.

DATA AVAILABILITY STATEMENT

The datasets presented in this study can be found in online repositories. The names of the repository/repositories and accession number(s) can be found below: ProteomeXchange, PXD025876.

ETHICS STATEMENT

The studies involving human participants were reviewed and approved by The CHIMs study with H01047 was conducted under BB-IND-12,243 at the Center for Immunization Research (CIR) and the Johns Hopkins Bloomberg School of Public Health (JHBSPH), Baltimore, MD, USA. Ethic approval to conduct the study was provided by the Western Institutional Review Board (WIRB) (Olympia, WA) for JHBSPH and PATH and by the Institutional Biosafety Committee of the Johns Hopkins Medical Institutions. The patients/participants provided their written informed consent to participate in this study.

AUTHOR CONTRIBUTIONS

MT, LV, ML, AA and AB conceived and designed the experiments. MT, SC, ALB, AA and AB wrote the manuscript. MT, TK, AN, SC, ALB, AA and AB analyzed the data. MT and RJ purified protein for all experiments. SC and ALB supplied the CHIMs serum samples. MT and RJ performed PAGE experiments. LV and AB performed ELISA. AN, ML and AB performed mass spectrometry analyses. All authors contributed to the article and approved the submitted version.

FUNDING

This work was supported, in whole or in part, by the Innovation Fund Denmark grant 7041-00220 and Bill & Melinda Gates Foundation grant OPP1112376. Under the grant conditions of the Foundation, a Creative Commons Attribution 4.0 Generic License has already been assigned to the Author Accepted Manuscript version that might arise from this submission.

SUPPLEMENTARY MATERIAL

The Supplementary Material for this article can be found online at: https://www.frontiersin.org/articles/10.3389/fcimb.2021.705468/full#supplementary-material

REFERENCES

Anderson, J. D., Bagamian, K. H., Muhib, F., Amaya, M. P., Laytner, L. A., Wierzba, T., et al. (2019). Burden of Enterotoxigenic Escherichia Coli and Shigella non-Fatal Diarrhoeal Infections in 79 Low-Income and Lower Middle-Income Countries: A Modelling Analysis. *Lancet Glob. Heal.* 7 (3), e321–e330. doi: 10.1016/S2214-109X(18)30483-2

Barry, E., Cassels, F., Riddle, M., Walker, R., and Wierzba, T. (2019). Vaccines Against Shigella and Enterotoxigenic Escherichia Coli: A Summary of the 2018 VASE Conference. *Vaccine* 37 (34), 4768–4774. doi: 10.1016/j.vaccine.2019.02.070

Bekeredjian-Ding, I., Delany-Moretlwe, S., Fritzell, B., Kang, G., Karron, R., Kaslow, D., et al. (2020). WHO Product Development for Vaccines Advisory Committee (PDVAC) Virtual Consultation 4: Update on Development of Enterotoxigenic E.coli (ETEC) Vaccines 18 June 2020. *Prod. Dev. Vaccines Advis. Commun.* 0 (0), 1–15.

Benz, I., and Schmidt, M. A. (2001). Glycosylation With Heptose Residues Mediated by the Aah Gene Product is Essential for Adherence of the AIDA-I Adhesin. *Mol. Microbiol.* 40 (6), 1403–1413. doi: 10.1046/j.1365-2958.2001.02487.x

Boysen, A., Moller-Jensen, J., Kallipolitis, B., Valentin-Hansen, P., and Overgaard, M. (2016). A Novel Mass Spectrometric Strategy 'Bemap' Reveals Extensive O-Linked Protein Glycosylation in Enterotoxigenic Escherichia Coli. *Sci. Rep.* 6, 32016. doi: 10.1038/srep32016

Boysen, A., Moller-Jensen, J., Kallipolitis, B., Valentin-Hansen, P., and Overgaard, M. (2010). Translational Regulation of Gene Expression by an Anaerobically Induced Small Non-Coding RNA in Escherichia Coli. *J. Biol. Chem.* 285 (14), 10690–10702. doi: 10.1074/jbc.M109.089755

Castric, P., Cassels, F. J., and Carlson, R. W. (2001). Structural Characterization of the Pseudomonas Aeruginosa 1244 Pilin Glycan. *J. Biol. Chem.* 276 (28), 26479–26485. doi: 10.1074/jbc.M102685200

Čaval, T., Heck, A. J. R., and Reiding, K. R. (2021). Meta-Heterogeneity: Evaluating and Describing the Diversity in Glycosylation Between Sites on the Same Glycoprotein. *Mol. Cell. Proteomics.* 20, 1–14. doi: 10.1074/MCP.R120.002093

Chakraborty, S., Brubaker, J., Harro, C., Weirzba, T., and Sack, D. (2019). Development of a Novel Multiplex Electrochemiluminescent-Based Immunoassay to Aid Enterotoxigenic Escherichia Coli Vaccine Development and Evaluations. *J. Immunol. Methods* 470, 6–14. doi: 10.1016/j.jim.2019.04.003

Chakraborty, S., Brubaker, J., Harro, C., Weirzba, T., and Sack, D. (2015). Characterization of Mucosal Immune Responses to Enterotoxigenic Escherichia Coli Vaccine Antigens in a Human Challenge Model: Response Profiles After Primary Infection and Homologous Rechallenge With Strain H10407. *Clin. Vaccine Immunol.* 23 (1), 55–64. doi: 10.1128/CVI.00617-15

Chakraborty, S., Harro, C., DeNearing, B., Ram, M., Feller, A., Cage, A., et al. (2016). Characterization of Mucosal Immune Responses to Enterotoxigenic Escherichia Coli Vaccine Antigens in a Human Challenge Model: Response Profiles After Primary Infection and Homologous Rechallenge With Strain H10407. *Clin. Vaccine Immunol.* 23 (1), 55–64. doi: 10.1128/CVI.00617-15

Chakraborty, S., Randall, A., Vickers, T. J., Molina, D., Harro, C. D., DeNearing, B., et al. (2018). Human Experimental Challenge With Enterotoxigenic Escherichia Coli Elicits Immune Responses to Canonical and Novel Antigens Relevant to Vaccine Development. *J. Infect. Dis.* 218 (9), 1436–1446. doi: 10.1093/infdis/jiy312

Datsenko, K. A., and Wanner, B. L. (2000). One-Step Inactivation of Chromosomal Genes in Escherichia Coli K-12 Using PCR Products. *Proc. Natl. Acad. Sci. U. S. A.* 97 (12), 6640–6645. doi: 10.1073/pnas.120163297

Faulds-Pain, A., Twine, S. M., Vinogradov, E., Strong, P. C. R., Dell, A., Buckley, A. M., et al. (2014). The Post-Translational Modification of the Clostridium Difficile Flagellin Affects Motility, Cell Surface Properties and Virulence. *Mol. Microbiol.* 94 (2), 272–289. doi: 10.1111/mmi.12755

Fleckenstein, J., Sheikh, A., and Qadri, F. (2014). Novel Antigens for Enterotoxigenic Escherichia Coli Vaccines. *Expert Rev. Vaccines* 13 (5), 631–639. doi: 10.1586/14760584.2014.905745

Gault, J., Ferber, M., Machata, S., Imhaus, A. F., Malosse, C., Charles-Orszag, A., et al. (2015). Neisseria Meningitidis Type IV Pili Composed of Sequence Invariable Pilins Are Masked by Multisite Glycosylation. *PLoS Pathog.* 11 (9), e1005162. doi: 10.1371/journal.ppat.1005162

Giersing, B. (2020). DRAFT WHO Preferred Product Characteristics for Vaccines Against Enterotoxigenic Escherichia Coli no. May

Hanahan, D. (1983). Studies on Transformation of Escherichia Coli With Plasmids. *J. Mol. Biol.* 166, 557–580. doi: 10.1016/S0022-2836(83)80284-8

Iwashkiw, J. A., Seper, A., Weber, B. S., Scott, N. E., Vinogradov, E., Stratilo, C., et al. (2012). Identification of a General O-Linked Protein Glycosylation System in Acinetobacter Baumannii and its Role in Virulence and Biofilm Formation. *PLoS Pathog.* 8 (6), e1002758. doi: 10.1371/journal.ppat.1002758

Kansal, R., Rasko, D. A., Sahl, J. W., Munson, G. P., Roy, K., Luo, Q., et al. (2013). Transcriptional Modulation of Enterotoxigenic Escherichia Coli Virulence Genes in Response to Epithelial Cell Interactions. *Infect. Immun.* 81 (1), 259–270. doi: 10.1128/IAI.00919-12

Kelley, L. A., Mezulis, S., Yates, C. M., Wass, M. N., and Sternberg, M. J. (2015). The Phyre2 Web Portal for Protein Modeling, Prediction and Analysis. *Nat. Protoc.* 10, 845–858. doi: 10.1038/nprot.2015-053

Khalil, I., Walker, R., Porter, C. K., Muhib, F., Chilengi, R., Cravioto, A., et al. (2021). Enterotoxigenic Escherichia Coli (ETEC) Vaccines: Priority Activities to Enable Product Development, Licensure, and Global Access. *Vaccine* xxxx. doi: 10.1016/j.vaccine.2021.04.018

Kim, M. J., Moon, Y. H., Kim, H. J., Rho, S., Shin, Y. K., Song, M., et al. (2018). Cross-Protectiveshigella Whole-Cell Vaccine With a Truncated O-Polysaccharide Chain. *Front. Microbiol.* 9, 2609. doi: 10.3389/fmicb.2018.02609

Knudsen, S. K., Stensballe, A., Franzmann, M., Westergaard, U. B., and Otzen, D. E. (2008). Effect of Glycosylation on the Extracellular Domain of the Ag43 Bacterial Autotransporter: Enhanced Stability and Reduced Cellular Aggregation. *Biochem. J.* 412 (3), 563–577. doi: 10.1042/BJ20071497

Lithgow, K. V., Scott, N. E., Iwashkiw, J. A., Thomson, E. L., Foster, L. J., Feldman, M. F., et al. (2014). A General Protein O-Glycosylation System Within the Burkholderia Cepacia Complex is Involved in Motility and Virulence. *Mol. Microbiol.* 92 (1), 116–137. doi: 10.1111/mmi.12540

Luo, Q., Kumar, P., Vickers, T. J., Sheikh, A., Lewis, W. G., Rasko, D. A., et al. (2014). Enterotoxigenic Escherichia Coli Secretes a Highly Conserved Mucin-Degrading Metalloprotease to Effectively Engage Intestinal Epithelial Cells. *Infect. Immun.* 82 (2), 509–521. doi: 10.1128/IAI.01106-13

Maigaard Hermansen, G. M., Boysen, A., Krogh, T. J., Nawrocki, A., Jelsbak, L., and Moller-Jensen, J. (2018). HldE Is Important for Virulence Phenotypes in Enterotoxigenic Escherichia Coli. *Front. Cell Infect. Microbiol.* 8, 253. doi: 10.3389/fcimb.2018.00253

McKenzie, R., Darsley, M., Thomas, N., Randall, R., Carpenter, C., Forbes, E., et al. (2008). A Double-Blind, Placebo-Controlled Trial to Evaluate the Efficacy of PTL-003, an Attenuated Enterotoxigenic E. Coli (ETEC) Vaccine Strain, in Protecting Against Challenge With Virulent ETEC. *Vaccine* 26 (36), 4731–4739. doi: 10.1016/j.vaccine.2008.06.064

Mirhoseini, A., Amani, J., and Nazarian, S. (2018). Review on Pathogenicity Mechanism of Enterotoxigenic Escherichia Coli and Vaccines Against it. *Microb. Pathog.* 117, 162–169. doi: 10.1016/j.micpath.2018.02.032

Mohamed, Y. F., Scott, N. E., Molinaro, A., Creuzenet, C., Ortega, X., Lertmemongkolchai, G., et al. (2019). A General Protein O-Glycosylation Machinery Conserved in Burkholderia Species Improves Bacterial Fitness and Elicits Glycan Immunogenicity in Humans. *J. Biol. Chem.* 294 (36), 13248–13268. doi: 10.1074/jbc.RA119.009671

Moriel, D. G., Bertoldi, I., Spagnuolo, A., Marchi, S., Rosini, R., Nesta, B., et al. (2010). Identification of Protective and Broadly Conserved Vaccine Antigens From the Genome of Extraintestinal Pathogenic Escherichia Coli. *Proc. Natl. Acad. Sci. U. S. A.* 107 (20), 9072–9077. doi: 10.1073/pnas.0915077107

Moriel, D. G., Rosini, R., Seib, K. L., Serino, L., Pizza, M., and Rappuoli, R. (2012). Escherichia Coli: Great Diversity Around a Common Core. *MBio* 3 (3), 6–8. doi: 10.1128/mBio.00118-12

Nakao, R., Ramstedt, M., Wai, S. N., and Uhlin, B. E. (2012). Enhanced Biofilm Formation by Escherichia Coli LPS Mutants Defective in Hep Biosynthesis. *PLoS One* 7 (12), e51241. doi: 10.1371/journal.pone.0051241

Nesta, B., Valeri, M., Spagnuolo, A., Rosini, R., Mora, M., Donato, P., et al. (2014). SslE Elicits Functional Antibodies That Impair In Vitro Mucinase Activity and In Vivo Colonization by Both Intestinal and Extraintestinal Escherichia Coli Strains. *PloS Pathog.* 10, 1–12. doi: 10.1371/journal.ppat.1004124

Nesta, B., and Pizza, M. (2018). Vaccines Against Escherichia Coli. *Curr. Top. Microbiol. Immunol.* 416, 213–242. doi: 10.1007/82_2018_111

Olson, S., Hall, A., Riddle, M. S., and Porter, C. K. (2019). Travelers' Diarrhea: Update on the Incidence, Etiology and Risk in Military and Similar Populations - 1990-2005 Versus 2005-2015, Does a Decade Make a Difference? *Trop. Dis. Travel Med. Vaccines* 5 (1), 1–15. doi: 10.1186/s40794-018-0077-1

Perez-Riverol, Y., Csordas, A., Bai, J., Bernal-Llinares, M., Hewapathirana, S., Kundu, D. J., et al. (2019). The PRIDE Database and Related Tools and Resources in 2019: Improving Support for Quantification Data. *Nucleic Acids Res* 47, D442–D450. doi: 10.1093/nar/gky1106

Poolman, J. T., and Anderson, A. S. (2018). Escherichia Coli and Staphylococcus Aureus: Leading Bacterial Pathogens of Healthcare Associated Infections and Bacteremia in Older-Age Populations. *Expert Rev. Vaccines* 17 (7), 607–618. doi: 10.1080/14760584.2018.1488590

Roy, K., Bartels, S., Qadri, F., and Fleckenstein, J. M. (2010). Enterotoxigenic Escherichia Coli Elicits Immune Responses to Multiple Surface Proteins. *Infect. Immun.* 78 (7), 3027–3035. doi: 10.1128/IAI.00264-10

Sambrook, J., and Green, M. R. (2012). *Molecular Cloning: A Laboratory Manual. 4th ed* Vol. 3 (New York: Cold Spring Harbor Laboratory Press).

Schäffer, C., and Messner, P. (2017). Emerging Facets of Prokaryotic Glycosylation. *FEMS Microbiol. Rev.* 41 (1), 49–91. doi: 10.1093/femsre/fuw036

Scott, N. E. (2019). Expanding Our Understanding of the Role of Microbial Glycoproteomes Through High-Throughput Mass Spectrometry Approaches. *Glycoconj. J.* 36, 259–266. doi: 10.1007/s10719-019-09875-1

Serino, L., Pizza, M., Gomes Moriel, D., and Fontana Maria, R. (2010). Escherichia Coli Immunogens With Improved Solubility. 1–29. WO 2009/104092.

Shental-Bechor, D., and Levy, Y. (2008). Effect of Glycosylation on Protein Folding: A Close Look at Thermodynamic Stabilization. *Proc. Natl. Acad. Sci. U. S. A.* 105 (24), 8256–8261. doi: 10.1073/pnas.0801340105

Shrivastava, S. R., Shrivastava, P. S., and Ramasamy, J. (2018). World Health Organization Releases Global Priority List of Antibiotic-Resistant Bacteria to Guide Research, Discovery, and Development of New Antibiotics. *JMS J. Med. Soc* 32 (1), 76–77. doi: 10.4103/jms.jms_25_17

Tacconelli, E., Carrara, E., Savoldi, A., Harbarth, S., Mendelson, M., Monnet, D. L., et al. (2018). Discovery, Research, and Development of New Antibiotics: The WHO Priority List of Antibiotic-Resistant Bacteria and Tuberculosis. *Lancet Infect. Dis.* 18 (3), 318–327. doi: 10.1016/S1473-3099(17)30753-3

Tapader, R., Bose, D., and Pal, A. (2017). YghJ, the Secreted Metalloprotease of Pathogenic E. Coli Induces Hemorrhagic Fluid Accumulation in Mouse Ileal Loop. *Microb. Pathog.* 105, 96–99. doi: 10.1016/j.micpath.2017.02.020

Tapader, R., Bose, D., Basu, P., Mondal, M., Mondal, A., Chatterjee, N. S., et al. (2016). Role in Proinflammatory Response of YghJ, a Secreted Metalloprotease From Neonatal Septicemic Escherichia Coli. *Int. J. Med. Microbiol.* 306 (7), 554–565. doi: 10.1016/j.ijmm.2016.06.003

Theuretzbacher, U., Outterson, K., Engel, A., and Karlén, A. (2019). The Global Preclinical Antibacterial Pipeline. *Nat. Rev. Microbiol.* 2019, 1–11. doi: 10.1038/s41579-019-0288-0

Turner, S. M., Chaudhuri, R. R., Jiang, Z. D., DuPont, H., Gyles, C., Penn, C. W., et al. (2006). Phylogenetic Comparisons Reveal Multiple Acquisitions of the Toxin Genes by Enterotoxigenic Escherichia Coli Strains of Different Evolutionary Lineages. *J. Clin. Microbiol.* 44 (12), 4528–4536. doi: 10.1128/JCM.01474-06

Uzzau, S., Figueroa-Bossi, N., Rubino, S., and Bossi, L. (2001). Epitope Tagging of Chromosomal Genes in Salmonella. *Proc. Natl. Acad. Sci. U.S.A.* 98 (26), 15264–15269. doi: 10.1073/pnas.261348198

Vedøy, O. B., Hanevik, K., Sakkestad, S. T., Sommerfelt, H., and Steinsland, H. (2018). Proliferation of Enterotoxigenic Escherichia Coli Strain TW11681 in Stools of Experimentally Infected Human Volunteers. *Gut Pathog.* 10 (1), 1–8. doi: 10.1186/s13099-018-0273-6

Vik, Å., Aas, F. E., Anonsen, J. H., Bilsborough, S., Schneider, A., Egge-Jacobsen, W., et al. (2009). Broad Spectrum O-Linked Protein Glycosylation in the Human Pathogen Neisseria Gonorrhoeae. *Proc. Natl. Acad. Sci. U. S. A.* 106 (11), 4447–4452. doi: 10.1073/pnas.0809504106

Walls, A. C., Tortorici, M. A., Frenz, B., Snijder, J., Li, W., Rey, F. A., et al. (2016). Glycan Shield and Epitope Masking of a Coronavirus Spike Protein Observed by Cryo-Electron Microscopy. *Nat. Struct. Mol. Biol.* doi: 10.1038/nsmb.3293

Wellcome Trust. (2019). Vaccines to Tackle Drug Resistant Infections An Evaluation of R&D Opportunities.

World Health Organization. (2020). Leveraging Vaccines to Reduce Antibiotic Use and Prevent Antimicrobial Resistance: An Action Framework.

Conflict of Interest: AB and ML are listed as inventors on patent applications relating to WO 2017/059864 related to the glycosylated YghJ protein held by University of Southern Denmark and Aarhus University. AB, ML and AA have a financial interest in GlyProVac ApS, which has licensed exclusively the IP stated above. AB is the scientific founder, shareholder, and a member of the board. AA is co- founder, shareholder, and a member of the board. ML is a shareholder. AB, AA, MT, TK, and RJ are all employees of GlyProVac ApS.

The remaining authors declare that the research was conducted in the absence of any commercial or financial relationships that could be construed as a potential conflict of interest.

Publisher's Note: All claims expressed in this article are solely those of the authors and do not necessarily represent those of their affiliated organizations, or those of the publisher, the editors and the reviewers. Any product that may be evaluated in this article, or claim that may be made by its manufacturer, is not guaranteed or endorsed by the publisher.

frontiers in Cellular and Infection Microbiology

ORIGINAL RESEARCH
published: 21 September 2021
doi: 10.3389/fcimb.2021.734578

Strategies for Rapid Identification of *Acinetobacter baumannii* Membrane Proteins and Polymyxin B's Effects

*Yun Lu, Xinxin Hu, Tongying Nie, Xinyi Yang, Congran Li and Xuefu You**

Beijing Key Laboratory of Antimicrobial Agents, Institute of Medicinal Biotechnology, Chinese Academy of Medical Sciences and Peking Union Medical College, Beijing, China

Acinetobacter baumannii, especially multidrug resistant *Acinetobacter baumannii*, is a notable source of pressure in the areas of public health and antibiotic development. To overcome this problem, attention has been focused on membrane proteins. Different digestion methods and extraction detergents were examined for membrane proteome sample preparation, and label-free quantitative and targeted proteome analyses of the polymyxin B-induced *Acinetobacter baumannii* ATCC 19606 membrane proteome were performed based on nano LC-MS/MS. Ultracentrifugation of proteins at a speed of 150,000×*g*, digestion by trypsin, filter-aided sample preparation, and detergents such as lauryldimethylamine-N-oxide were proved as a fast and effective way for identification of membrane proteome by nano LC-MS/MS. Upon treatment with polymyxin B, expression levels of 15 proteins related to membrane structure, transporters, cell surface, and periplasmic space were found to be significantly changed. Furthermore, targeted proteome was also used to confirm these changes. A relatively rapid membrane proteome preparation method was developed, and a more comprehensive view of changes in the *Acinetobacter baumannii* membrane proteome under polymyxin B pressure was obtained.

Keywords: ***Acinetobacter baumannii*, membrane proteome, polymyxin B, detergents, LC-MS/MS**

OPEN ACCESS

Edited by:
Yi-Wei Tang,
Cepheid, United States

Reviewed by:
Arryn Craney,
Weill Cornell Medical Center, United States
Xiaojie Chu,
University of Pittsburgh, United States

***Correspondence:**
Xuefu You
xuefuyou@imb.pumc.edu.cn

Specialty section:
This article was submitted to Clinical Microbiology, a section of the journal Frontiers in Cellular and Infection Microbiology

Received: *01 July 2021*
Accepted: *30 August 2021*
Published: *21 September 2021*

Citation:
Lu Y, Hu X, Nie T, Yang X, Li C and You X (2021) Strategies for Rapid Identification of Acinetobacter baumannii Membrane Proteins and Polymyxin B's Effects. Front. Cell. Infect. Microbiol. 11:734578. doi: 10.3389/fcimb.2021.734578

INTRODUCTION

Acinetobacter baumannii (*A. baumannii*) is a Gram-negative bacterium that can cause serious nosocomial infection (Lin and Lan, 2014) and has developed extensive antimicrobial resistance with a high mortality rate (Vazquez-Lopez et al., 2020). The World Health Organization (WHO) reported that *A. baumannii* was one of the most serious ESKAPE organisms (*Enterococcus faecium*, *Staphylococcus aureus*, *Klebsiella pneumoniae*, *A. baumannii*, *Pseudomonas aeruginosa*, and *Enterobacter cloacae*) which could effectively escape the actions of antibacterial drugs (Boucher et al., 2009). With the increase in multidrug resistance (MDR), *A. baumannii* showed resistance to many first-line antibiotics, even colistin and polymyxin B (Olaitan et al., 2014).

In bacteria, approximately 20% to 30% of all genes encode membrane proteins. Membrane proteins play vital roles not only in defense and immunity but also in essential physiological functions, such as the generation or conversion of energy, the import or export of metabolites, the extrusion of toxic substances or antibiotics, and the homeostasis of metal ions (Ansgar and Dirk, 2010).

Many membrane proteins were found to be related to drug resistance or potential therapeutic targets, such as OmpA in *A. baumannii* (Bunpa et al., 2020).

In the past few decades, attention has been given to the bacterial membrane proteins, and proteome techniques for the detection of membrane proteins have been developed to help to identify the classes of proteins. Previous studies reported that the use of SDS-PAGE and LC-MS/MS to separate and detect bacterial membrane proteins (Ghosh et al., 2008) and 135 membrane proteins and 23 periplasmic proteins in *A. baumannii* ATCC 19606 were identified (De et al., 2011). Then two-dimensional gel electrophoresis (2-DE) was used to improve the separation efficiency, and 29 major protein spots were selected for MS analysis (Cordwell, 2006; Marti et al., 2006). In recent years, with the improvement of mass spectrometry, shotgun proteomics based on peptide detection combined with quantitative methods has been developed and widely used in protein identification and the comparison of protein expression levels (Boumediene and Boris, 2015). Currently, the quality and quantity of protein identification are further improved with the optimization of sample preparation methods such as filter-aided sample preparation (FASP), and the emergence of high-resolution mass spectrometers.

However, apart from the promotion of equipment and methods for detection, efficient and effective membrane protein extraction methods are essential for membrane peptide/protein identification. Characterization of the membrane proteome is challenging due to the hydrophobic nature of membrane proteins. Techniques such as density gradient centrifugation and ultracentrifugation have also been developed to separate membrane complexes (Papanastasiou et al., 2016). Amphiphilic molecules, such as detergents, are the main reagents used to extract membrane proteins, which can replace and imitate the stabilizing properties of natural phospholipids to avoid irreversibly disrupting the protein structure (Gao et al., 2017). According to the characteristics of their polar groups, detergents are generally divided into ionic, nonionic, and zwitterionic categories (Liu et al., 2015). Various studies have evaluated the effectiveness of extraction for targeted membrane proteins (Arachea et al., 2012). However, there are no guidelines that can recommend which detergent is the most effective for extracting a given protein class or total proteome from the membrane. Therefore, although the use of detergent-based proteomics analysis has produced a large amount of useful data, there is still an urgent need for novel methods that are effective for the overall membrane proteome and are not affected by detergent side effects. In our study, we evaluated the effectiveness of different digestion enzymes, digestion conditions, and detergents [ionic (sodium deoxycholate, SDC), nonionic (dodecyl-b-D-maltoside, DDM, or n-octyl-b-D-glucoside, OG), and zwitterionic detergents (lauryldimethylamine-N-oxide, LDAO or 3-[(3-cholamidopropyl)dimethylammonio]-1-propanesulfonate, CHAPS)] in *A. baumannii* membrane proteome analysis by nano LC-high resolution MS and developed an effective and rapid workflow for *A. baumannii* membrane proteome analysis.

Polymyxins have been treated as a last choice for the therapy of serious infections caused by multidrug-resistant Gram-negative bacteria, particularly *A. baumannii* (Nang et al., 2021). Many studies have focused on the mechanism of polymyxins in bacteria, and some have elucidated the molecular and chemical interactions between polymyxins and lipopolysaccharide structure (Ayoub Moubareck, 2020). However, there is little research observing the effect of polymyxin B on *A. baumannii* from the perspective of the whole membrane proteome by high-resolution MS. Thus, in our study, label-free quantitative proteome and parallel reaction monitoring (PRM) targeted proteome were used to explore the differentially expressed membrane proteins in polymyxin B treated *A. baumannii* ATCC 19606.

MATERIAL AND METHODS

Bacterial Strains and Materials

Acinetobacter baumannii (*A. baumannii*) ATCC19606 was purchased from American Type Culture Collection (ATCC) (Manassas, USA). OG, LDAO, DDM, CHAPS, and SDC were purchased from Sigma-Aldrich (St. Louis, MO). Trypsin Gold, Mass Spectrometry Grade, and Trypsin/Lys-C Mix, Mass Spec Grade, were purchased from Promega (WI, USA). Nanosep® Centrifugal Devices with Omega™ Membrane 10K were purchased from Pall Nanosep (Ann Arbor, MI).

Cell Culture and Sample Preparation

A. baumannii ATCC19606 was cultivated in Luria–Bertani (LB) broth at 37°C with shaking (220 rpm) until OD600 reached 0.6. Bacterial cells were harvested by centrifugation at 4,000×*g* for 10 min and washed with 0.85% NaCl. Bacterial precipitation was frozen at -80°C until use. *A. baumannii* cells were resuspended in Na_2CO_3 buffer (0.1 M) for sonication at 4°C. Cell debris was removed by centrifugation (12,000×*g* for 10 min, 4°C). Supernatants were transformed into thick-walled tube and ultracentrifuged at 50,000 or 150,000×*g* for 30 min. The previous steps were repeated twice to wash off non-membrane proteins as much as possible. Then, the detergents (4% CHAPS, 1% DDM, 2% SDC, 0.5% OG, and 1% LDAO) were added and incubated at 4°C overnight, after which ultracentrifugation was performed at 50,000×*g* for 30 min. Suspensions were collected for peptide preparation. After reduction by 10 mM dithiothreitol (DTT) at 95°C for 5 min, proteins were precipitated by frozen acetone and stored at -20°C for 30 min. Then, the precipitate was redissolved by 50 mM ammonium bicarbonate, then digested in solution by sequencing grade trypsin (1:50 w/w, Promega, Madison, WI) or trypsin/Lys-C Mix (1:25 w/w, Promega, Madison, WI) overnight at 37°C. For the FASP method, precipitate redissolved by 50 mM ammonium bicarbonate were transfer on ultrafiltration tube, centrifuged at 14,000×*g* for 30 min. Digestions were performed by microwaving for 2 min and then overnight at 37°C in 50 μl 50 mM ammonium bicarbonate with trypsin or trypsin/Lys-C Mix. Last, the sample was desalted by C18 reverse-phase Tips (ReproSil-Pur Basic C18, 5 μm, Dr. Maisch GmbH). For the study on *Acinetobacter baumannii* treated with polymyxin B,

A. baumannii ATCC19606 was cultivated until OD600 reached 0.5, then polymyxin B was added (0.5 μg·ml^{-1}) and bacteria were cultivated at 37°C for 1.5 h. Four biological replicates were performed, and both control and treatment groups were collected and lysed. Ultracentrifugation of proteins at a speed of 150,000×*g*, digestion by trypsin, filter-aided sample preparation, and lauryldimethylamine-N-oxide were used for membrane peptide acquisition.

Nano LC–MS/MS and Data Acquired

Samples were analyzed on a Thermo Scientific Orbitrap Fusion Lumos platform. The trap and separation columns along with the composition of solvent buffer A and B used in nano LC were the same as previously reported (Lu et al., 2021). Furthermore, a 75-min elution method was set as follows; the gradient started from 10% of solvent buffer B (80% acetonitrile with 0.1% formic acid) and then from 10% to 13% of solvent buffer B for 4 min. The gradient rose from 13% to 29% of solvent buffer B for 48 min and from 29% to 37% for 14 min. Ultimately, the gradient ascended to 100% of buffer B and was maintained for 9 min. The scan parameters of MS1 and MS2 were set as previously reported (Lu et al., 2021) with high energy collision-induced dissociation (HCD) as the activation type and Orbitrap as the detector. Data-dependent acquired data with four biological replicates were collected and searched against the *Acinetobacter baumannii* ATCC 19606 database downloaded from UniProt. The search parameters were set as previously reported (Lu et al., 2021), and the FDR was limited to a maximum of 0.01. Protein identification and label-free quantification (LFQ) analysis were all analyzed by Thermo Scientific™ Proteome Discoverer™ version 2.2 (PD2.2). The nano LC-MS/MS proteomics data have been deposited to the ProteomeXchange Consortium *via* the PRIDE (Perez-Riverol et al., 2019) partner repository with the dataset identifier PXD026714.

Bioinformatics Analysis

The counts of protein groups, peptide groups, PSMs, and MS/MS spectra were analyzed by PD 2.2, comparison between groups were performed by t test or one-way ANOVA. Venn analysis was used to compare the efficiency of different enzyme digestion methods to identify proteins. GRAVY and amino acid components were used to evaluate the peptides identified by different detergents used in extraction (Gao et al., 2017). For polymyxin B-induced *A. baumannii* ATCC19606, label-free quantitative analysis was performed as previously reported (Lu et al., 2021). In brief, missing value processing, CV limitation, and hypothetical tests were applied and proteins with fold change >1.5 and $p < 0.05$ were considered significantly changed. Differentially expressed proteins were annotated and clustered for enrichment by the Gene Ontology enrichment tool. In view of the lack of the *A. baumannii* ATCC19606 KEGG database, the database of *A. baumannii* AYE was used as both the GO annotation and KEGG pathway databases were relatively complete. The KEGG pathway database of *A. baumannii* AYE was used to aid in discovering the affected pathways under polymyxin B pressure.

Targeted Proteome Analysis

PRM, a targeted proteome method that can be performed by the nano LC-Orbitrap Fusion Lumos platform, was employed to verify the differentially expressed proteins. The extraction and preparation methods were the same with the label-free proteome analysis, and four biological replicates were generated. More than two peptides were selected for each protein, and peptides with missed cleavage sites and amino acid residues susceptible to modification such as M were excluded. Parameters of peptides (retention time, precursor m/z, and charge state) were exported by Skyline software according to the previous data-dependent acquisition (DDA) experiments. Moreover, the nano LC parameters were the same with that previously described. PRM was monitored by an Orbitrap detector, and a 0.7-m/z isolation window was used, as previously reported (Lu et al., 2021). PRM results were analyzed by Skyline with DDA results served as spectral library. Peptides were selected by t test with p-value < 0.05 and fold change >1.5.

RESULTS

Effects of Ultracentrifugation and Digestion Enzymes on Membrane Protein Identification

As shown in **Figure 1**, the number of protein groups, peptide groups, PSM, and MS/MS spectra at the speed of 150,000×*g* were higher than those obtained at 50,000×*g*. For membrane protein identification, there were 241 proteins common across the two groups, and 4 exclusive to the 50,000×*g* group and 19 exclusive to the 150,000×*g* group (**Supplementary Table 1**). Digestion in solution by trypsin was less effective than digestion on the membrane by trypsin with fewer protein groups, peptide groups, peptide spectrum match (PSM), and MS/MS spectrum (**Figure 2A**). Interestingly, the addition of LysC did not improve the digestion quality and quantity. Then, membrane proteins identified in different groups were compared to obtain the counts of overlap (**Figure 2B** and **Supplementary Tables 2–4**).

Detergent Efficiencies of Membrane Protein and Peptide Identification

We investigated the performances of different detergents including CHAPS, DDM, SDC, LDAO, and OG for membrane protein lysis and extraction. First, as shown in **Figure 3A**, the number of protein groups, peptide groups, and PSM of the LDAO group were highest among the five groups, and the number of MS/MS spectra in the DDM group was highest. Then, the membrane proteins identified in different groups were compared to acquire the numbers of overlaps (**Figure 3B**), 339 membrane proteins were identified in LDAO group, while 269, 330, 335, and 326 membrane proteins were identified in CHAPS, DDM, DOC, and OG groups, respectively (**Supplementary Table 5**). We further compared the amino acid distribution and grand average of hydropathy (GRAVY) scores, and the curves of amino acid distribution curves were similar among

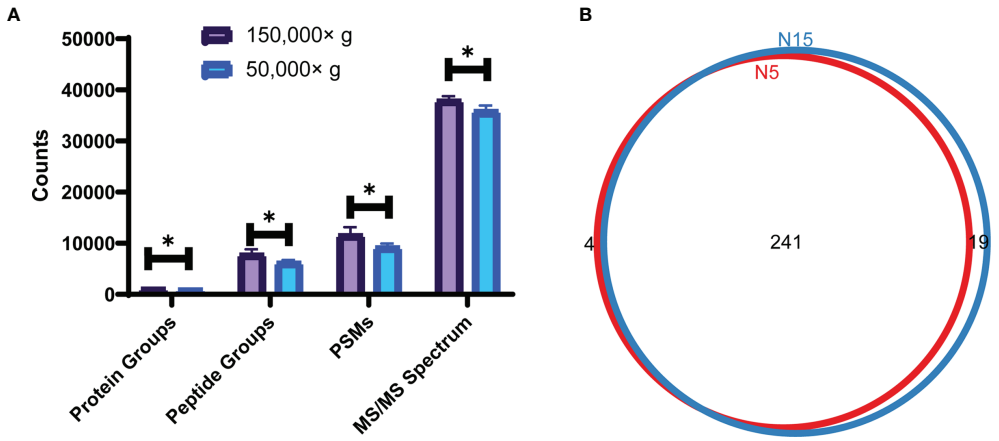

FIGURE 1 | Analysis results for ultracentrifugation at the speed of 150,000×g and 50,000×g **(A)** The counts of total protein groups, peptide groups, PSM, and MS/MS spectrum at speeds of 150,000×g and 50,000×g; comparison between groups was performed by t test, (*) $p < 0.05$. **(B)** Venn plot of membrane proteins identified at speeds of 150,000×g(N15) and 50,000×g(N5).

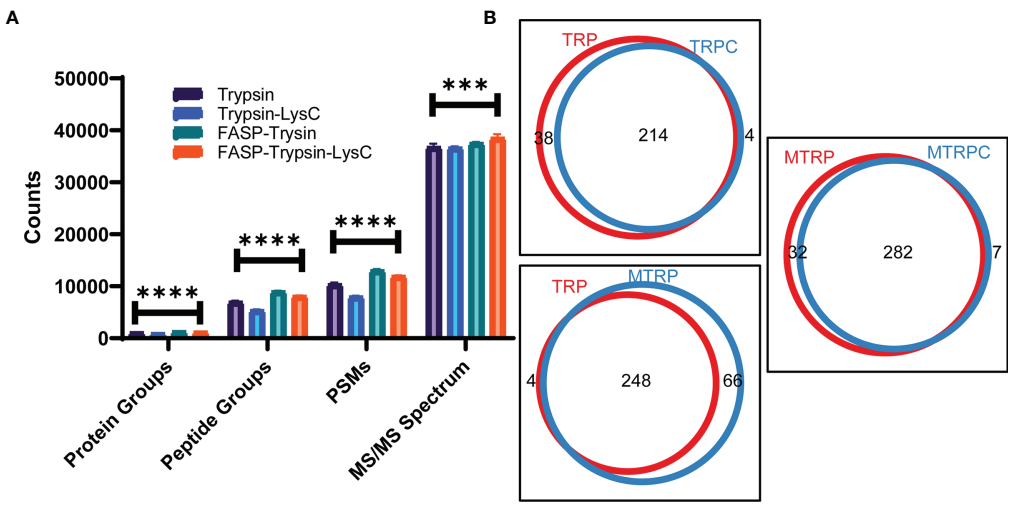

FIGURE 2 | Analysis results for different digestion methods. **(A)** Counts of total protein groups, peptide groups, PSM, and MS/MS spectrum of trypsin and trypsin-LysC digestion in solution or by FASP; comparison between groups was performed by one-way ANOVA, (***) $p < 0.001$, (****) $p < 0.0001$. **(B)** Venn plot of membrane proteins identified of trypsin (TRP) and trypsin-LysC digestion (TRPC) in solution or trypsin (MTRP) and trypsin-LysC digestion (MTRPC) by FASP.

groups (**Figure 3C**). Hydrophobic peptides (peptides with positive GRAVY values) and hydrophilic peptides (peptides with negative GRAVY values) were identified and classified, as shown in **Figure 3D**. All groups showed a higher proportion of hydrophilic peptides. Interestingly, the curves of the GRAVY score for DDM and SDC were similar, while that of LDAO was the highest.

Comparative Membrane Proteomics Under Polymyxin B Pressure

Optimized membrane protein extraction and peptide preparation methods were applied to the proteome analysis of polymyxin B-induced *A. baumannii* ATCC 19606. A previous study has found that polymyxin B inhibited *A. baumannii* ATCC 19606 at a minimum inhibitory concentration (MIC) of 1 $\mu g \cdot ml^{-1}$ (Cui et al., 2020). In our study, a sublethal concentration of polymyxin B (0.5 $\mu g \cdot ml^{-1}$) was used and four biological replicates were performed. In total, 2,000 proteins were identified with a cutoff of FDR <0.01 (**Supplementary Table 6**). Proteins with a CV value greater than 30% and a large proportion of missing values were excluded, and 421 membrane proteins (**Supplementary Table 7**) including membrane structure proteins and proteins located in the cell surface or periplasmic space and transporter were identified in both groups. Good repeatability was

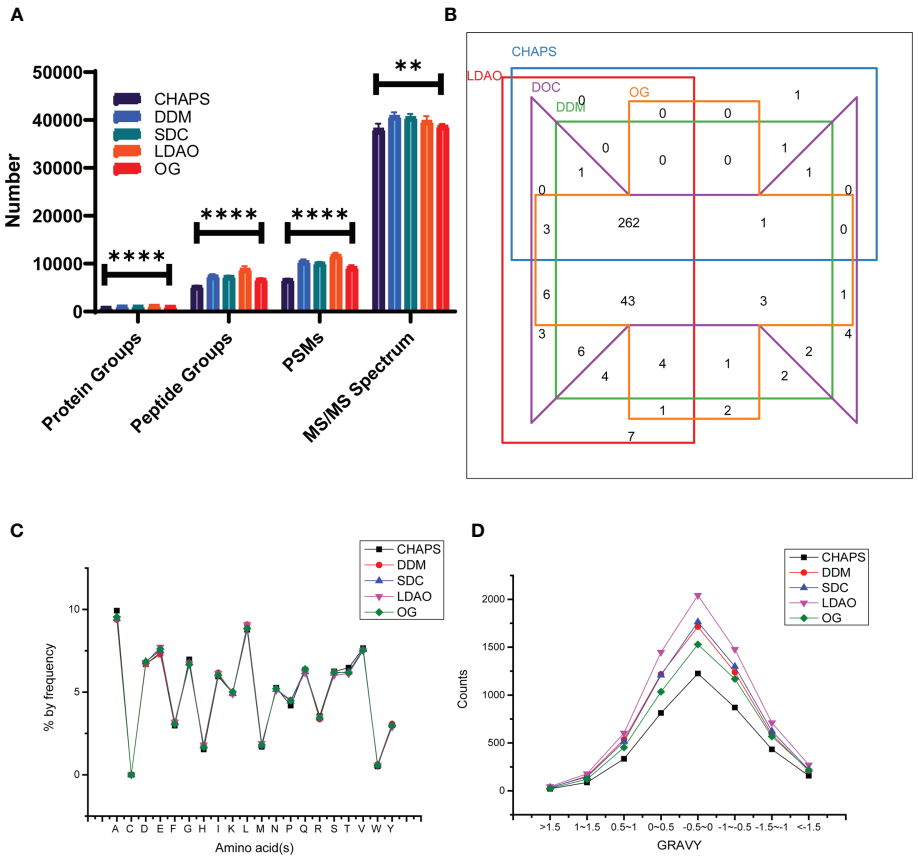

FIGURE 3 | The performances of CHAPS, DDM, SDC, LDAO, and OG for membrane protein lysis and extraction. **(A)** The identified counts of total protein groups, peptide groups, PSM, and MS/MS spectrum using different detergents; comparison between groups was performed by one-way ANOVA, (**) $p < 0.01$, (****) $p < 0.0001$. **(B)** Venn plot of membrane proteins identified using different detergents. **(C)** Amino acid distribution of peptides identified using different detergents. **(D)** GRAVY values of peptides identified using different detergents.

verified by linear correlations with $R^2 > 0.9$ (**Supplementary Figure 1**). The expression levels of 15 membrane proteins were identified as significantly changed under polymyxin B pressure (**Figure 4A**) based on a max fold change > 1.5 and adjusted p value ($p < 0.05$). The expression levels of 11 membrane-related proteins reduced while 4 proteins increased under polymyxin B pressure.

All 15 significantly changed membrane proteins (**Supplementary Table 8**) were analyzed by gene ontology (GO) annotation enrichment and Kyoto Encyclopedia of Genes and Genomes (KEGG) pathway enrichment. As shown in **Supplementary Figure 2**, most of the enriched proteins were related to transport, localization, cellular anatomical entity, membrane, binding, etc. Due to the lack of the KEGG pathway database of *A. baumannii* ATCC19606, we aligned all the proteins to *A. baumannii* strain AYE to perform the KEGG pathway enrichment. According to the analysis results, D0CAD3 and D0C805 were involved in the ABC transporter pathway while D0CBP8 and D0C805 were involved in the two-component system pathway, indicating the extensive effects of polymyxin B on the membrane proteins of *A. baumannii* ATCC19606. We further quantified 5 proteins with 15 peptides (**Supplementary Table 9**, **Figure 4B**) as significantly differentially expressed proteins (p value < 0.05 and fold change >1.5) by PRM targeted proteomics.

Discussion

Recently, given the confirmation of the roles of cell membrane proteins in bacterial survival, defense, immunity, and drug resistance, interest has been focused on bacterial cell membrane proteins (Ansgar and Dirk, 2010). However, the complexity and specificity of membrane protein structures limit the extraction efficiency, and effective methods need to be developed. Moreover, the low abundance of membrane proteins and separation methods such as 1-DE or 2-DE has led to a limited number of identified proteins (Cordwell, 2006). As quantitative proteomics based on LC-high resolution MS has been widely used in studies related to pathogenic microorganism, compatible bacterial membrane extraction and preparation methods need to be developed.

In our study, ultracentrifugation combined with Na_2CO_3 was used to separate membrane proteins (Zhang et al., 2008). The extraction efficiency of proteins and peptides at a speed of

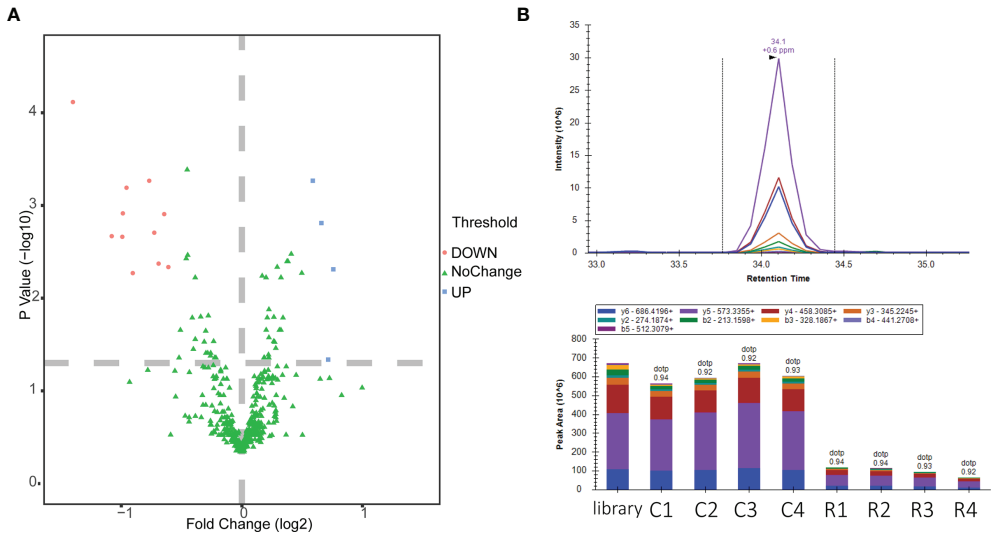

FIGURE 4 | Label-free quantitative analysis of polymyxin B-induced *(A) baumannii* ATCC19606. **(A)** Volcano plot of scaled values for proteins. Red indicates upregulation, and green indicates downregulation. **(B)** Chromatogram of PRM fragment ions for VLDLAVR and the peak area comparison of polymyxin B-treated and untreated groups. Control groups: C1, C2, C3, and C4; polymyxin B-treated groups: R1, R2, R3, and R4.

150,000×*g* was much higher than that at a speed of 50,000×*g*. Different protein digestion methods were also verified, and the digestion efficiency of by the FASP method was much higher than that of the in-solution digestion. Moreover, although studies have determined that LysC could help improve the digestion efficiency of the total proteins (Hakobyan et al., 2019), for membrane proteins, LysC decreased the digestion efficiency of both the FASP and in-solution digestion methods. We further classified the proteins by GO annotation enrichment. A total of 245 and 260 membrane proteins were obtained separately at speeds of 50,000×*g* and 150,000×*g*, respectively. A total of 252, 218, 314, and 289 membrane proteins were acquired separately for the trypsin (in solution), trypsin-LysC (in solution), trypsin-FASP, and trypsin-LysC-FASP methods, respectively.

Detergents are commonly used in membrane protein extraction. DDM is a mild detergent with the ability to purify membrane proteins and solubilize hydrophobic proteins without changing their structures (Liu et al., 2015; Lu et al., 2021). SDC, which is friendly to trypsin and can be removed easily from the peptides solution, demonstrated good ability in membrane protein extraction (Moore et al., 2016). CHAPS, LDAO, and OG were commonly used in proteome extraction (Arachea et al., 2012). In our study, we evaluated the extraction efficiencies of CHAPS, DDM, SDC, LDAO, and OG on the *A. baumannii* membrane proteome. To be consistent, all detergents were removed by acetone precipitation. As shown in **Figure 3A**, the extraction efficiencies of DDM, SDC, and LDAO were much higher than those of CHAPS and OG. Peptides identified in five groups were also analyzed. Amino acid distributions of the five groups were similar. For GRAVY values, as shown in **Figure 3D**, the peptides were mainly distributed in three sections: (−1.0, −0.5], (−0.5, 0], and (0, 0.5]. The range of the peptides identified indicated that both hydrophobicity and hydrophilicity could be identified by the five detergents. The counts of peptides obtained with LDAO were highest in all sections, which suggested that LDAO was the most efficient detergent. According to the GO enrichment results, 269, 330, 335, 339, and 326 membrane proteins were acquired separately for CHAPS, DDM, SDC, LDAO, and OG, indicating the different extraction abilities of the membrane proteins of the five detergents. Previous studies have reported that DDM is a detergent that has little influence on the enzyme activity and does not need to be removed from samples for proteomic analysis (Liu et al., 2015). Furthermore, SDC can precipitate in 1% formic acid (Lu et al., 2021), which can be easily separated from the peptide buffer. In view of the peptide loss that may be caused by detergent removal, SDC and DDM can also be considered as preferred detergents for the extraction of membrane proteins.

As the last-resort antibiotics for the treatment of MDR Gram-negative bacteria, polymyxin B has received notable attention. Previous studies have reported partial mechanisms of action of polymyxin B on Gram-negative bacteria, such as binding to LPS and oxidative bursts. Recently, outer membrane vesicles (OMVs) released from *A. baumannii* were reported as decoys against polymyxin B, whose production is linked to membrane-linkage proteins (Park et al., 2021). However, the mechanism of action of polymyxin B in *A. baumannii*, which can live without LPS, still needs to be explored. In our research, the membrane proteome changes of polymyxin B-induced *A. baumannii* ATCC 19606 were studied based on nano LC combined with high-resolution MS. Compared to the control group, 15 significantly differentially expressed proteins were

acquired and clustered by bioinformatics methods. Among the 15 membrane proteins, the reduced expression of SurA (D0C7T2), which is important for the biogenesis of β-barrel outer membrane proteins (OMPs), would damage the homeostasis and functions of the cell envelope (Behrens-Kneip, 2010; Humes et al., 2019). The expression level of OmpA family protein (D0C8N6), a major component of OMPs, is suppressed, which interrupts bacterial antibiotic resistance, infection, and immunomodulation (Bunpa et al., 2020). What is more, OmpA was reported to be identified in the colistin-resistant *Enterobacter asburiae* (Ayoub Moubareck, 2020), indicating the potential important roles of OmpA in the mechanism of actions and resistance development. The reduced expression level of glutamate/aspartate transport system permease protein GltK(D0C805) will affect the glutamate/aspartate uptake and metabolism and bile resistance (Zhang et al., 2013). The reduced expression level of CsgG (D0CE32) lowers the curli biogenesis and affects the biofilm formation (Zhang et al., 2020). The suppressed expression level of the TonB-dependent siderophore receptor (D0CC21) affects iron ion homeostasis (Fujita et al., 2019). Moreover, the downregulation of putative ATP synthase F0 (D0C7A7), C4-dicarboxylate transporter (D0CF35), and carbonate dehydratase (D0CCK7) influences the membrane transport, energy consume and metabolism. The reduced expression levels of two proteins, which were located in periplasmic space (D0CBP8, periplasmic serine endoprotease DegP-like; D0CBL3, Tol-Pal system protein TolB) (**Supplementary Table 8**), indicated the destruction of the periplasmic space. Moreover, the reduced expression level of tolB affects the Tol-Pal system, secretion of EspA/B, and infection (Hirakawa et al., 2020). Interestingly, the expression levels of three proteins increased in the polymyxin B-treated group, including signal peptide peptidase SppA (D0CBY0), GTPase Era (D0CBQ4), and MacB (D0CAD3), part of the MacAB-TolC complex. A previous study suggested that R-LPS, which can be bound by polymyxin B, is a physiological substrate of MacAB-TolC (Lu and Zgurskaya, 2013). However, due to the imperfect KEGG pathway database (*A. baumannii* strain AYE), only D0CAD3 and D0C805 were involved in the ABC transporter pathway while D0CBP8 and D0C805 were involved in the two-component system pathway. The upstream and downstream genes of the pathway are currently not annotated in the *A. baumannii* ATCC 19606 genome, which hindered us from further verifying the pathway affected by polymyxin B.

In general, the membrane proteome based on nano LC-MS/MS is an effective tool for research related to membrane proteins. As mentioned above, we developed a relatively rapid membrane protein extraction and preparation method, but there were still many non-membrane proteins mixed in, partially because of the super-high identification ability of high-resolution MS. According to the label-free results, the abundance of membrane-related proteins is about 50% of the total abundance of each group. The purity can meet the needs of the proteome analysis at present, but better extraction methods should be explored. Moreover, our study found that polymyxin B could decrease the expression of many membrane proteins, including inner, outer, and trans-membrane proteins, which provided new evidence for the mechanism of actions of polymyxin B on the *A. baumannii* ATCC 19606 membrane. In turn, the discovery of targets will further promote the development of new antibiotics.

In summary, a relatively rapid membrane proteome sample preparation method of *A. baumannii* was built and applied for nano LC-MS/MS analysis. Through optimized quantitative membrane proteome analysis, 15 membrane proteins were found to be significantly changed under the pressure of polymyxin B, which gives us a better understanding of the role of polymyxin B and can help us further discover the mechanism of action of polymyxin B from the perspective of membrane proteins.

DATA AVAILABILITY STATEMENT

The data presented in the study are deposited in the PRIDE repository, accession number PXD026714. The names of the repository/repositories and accession number(s) can be found in the article/**Supplementary Material**.

AUTHOR CONTRIBUTIONS

Conceptualization, XFY and YL. Methodology, YL. Software, YL. Validation, YL and TN. Resources, XH. Data curation, YL. Writing—original draft preparation, YL. Writing—review and editing, XFY, XYY, and CL. Visualization, YL. Supervision, XH. Project administration, XFY. funding acquisition, XFY and YL. All authors contributed to the article and approved the submitted version.

FUNDING

This research was funded by the National Natural Science Foundation of China (grant numbers 81803593, 81621064), the CAMS Initiative for Innovative Medicine (grant number 2016-I2M-3-014), the National Mega-project for Innovative Drugs (grant number 2019ZX09721001), the MOST/MOF Funds for the National Science and Technology Resource Sharing Service Platform, China (2019-194-NPRC), and the Fundamental Research Funds for the Central Universities (grant number 3332018094).

SUPPLEMENTARY MATERIAL

The Supplementary Material for this article can be found online at: https://www.frontiersin.org/articles/10.3389/fcimb.2021.734578/full#supplementary-material

REFERENCES

Ansgar, P., and Dirk, W. (2010). Bacterial Membrane Proteomics. *Proteomics* 8 (19), 4100–4122. doi: 10.1002/pmic.200800273

Arachea, B. T., Sun, Z., Potente, N., Malik, R., Isailovic, D., and Viola, R. E. (2012). Detergent Selection for Enhanced Extraction of Membrane Proteins. *Protein Expr. Purif.* 86 (1), 12–20. doi: 10.1016/j.pep.2012.08.016

Ayoub Moubareck, C. (2020). Polymyxins and Bacterial Membranes: A Review of Antibacterial Activity and Mechanisms of Resistance. *Membranes (Basel)* 10 (8), 181. doi: 10.3390/membranes10080181

Behrens-Kneip, S. (2010). The Role of SurA Factor in Outer Membrane Protein Transport and Virulence. *Int. J. Med. Microbiol.* 300 (7), 421–428. doi: 10.1016/j.ijmm.2010.04.012

Boucher, H. W., Talbot, G. H., Bradley, J. S., Edwards, J. E., Gilbert, D., Rice, L. B., et al. (2009). Bad Bugs, No Drugs: No ESKAPE! An Update From the Infectious Diseases Society of America. *Clin. Infect. Dis.* 48 (1), 1–12. doi: 10.1086/595011

Boumediene, S., and Boris, M. (2015). Global Analysis of Bacterial Membrane Proteins and Their Modifications. *Int. J. Med. Microbiol. JMM* 305 (2), 203–208. doi: 10.1016/j.ijmm.2014.12.017

Bunpa, S., Chaichana, N., Teng, J. L. L., Lee, H. H., Woo, P. C. Y., Sermwittayawong, D., et al. (2020). Outer Membrane Protein A (OmpA) Is a Potential Virulence Factor of Vibrio Alginolyticus Strains Isolated From Diseased Fish. *J. Fish Dis.* 43 (2), 275–284. doi: 10.1111/jfd.13120

Cordwell, S. J. (2006). Technologies for Bacterial Surface Proteomics. *Curr. Opin. Microbiol.* 9 (3), 320–329. doi: 10.1016/j.mib.2006.04.008

Cui, A. L., Hu, X. X., Chen, Y., Jin, J., Yi, H., Wang, X. K., et al. (2020). Design, Synthesis, and Bioactivity of Cyclic Lipopeptide Antibiotics With Varied Polarity, Hydrophobicity, and Positive Charge Distribution. *ACS Infect. Dis.* 6 (7), 1796–1806. doi: 10.1021/acsinfecdis.0c00056

De, E., Cosette, P., Coquet, L., Siroy, A., Alexandre, S., Duncan, A., et al. (2011). Membrane Proteomes of Pseudomonas Aeruginosa and Acinetobacter Baumannii. *Pathol. Biol. (Paris)* 59 (6), e136–e139. doi: 10.1016/j.patbio.2009.10.005

Fujita, M., Mori, K., Hara, H., Hishiyama, S., Kamimura, N., and Masai, E. (2019). A TonB-Dependent Receptor Constitutes the Outer Membrane Transport System for a Lignin-Derived Aromatic Compound. *Commun. Biol.* 2, 432. doi: 10.1038/s42003-019-0676-z

Gao, J., Zhong, S., Zhou, Y., He, H., Peng, S., Zhu, Z., et al. (2017). Comparative Evaluation of Small Molecular Additives and Their Effects on Peptide/Protein Identification. *Anal. Chem.* 89 (11), 5784–5792. doi: 10.1021/acs.analchem.6b04886

Ghosh, D., Beavis, R. C., and Wilkins, J. A. (2008). The Identification and Characterization of Membranome Components. *J. Proteome Res.* 7 (4), 1572–1583. doi: 10.1021/pr070509u

Hakobyan, A., Schneider, M. B., Liesack, W., and Glatter, T. (2019). Efficient Tandem LysC/Trypsin Digestion in Detergent Conditions. *Proteomics* 19 (20), e1900136. doi: 10.1002/pmic.201900136

Hirakawa, H., Suzue, K., Takita, A., Awazu, C., Kurushima, J., and Tomita, H. (2020). Roles of the Tol-Pal System in the Type III Secretion System and Flagella-Mediated Virulence in Enterohemorrhagic Escherichia Coli. *Sci. Rep.* 10 (1), 15173. doi: 10.1038/s41598-020-72412-w

Humes, J. R., Schiffrin, B., Calabrese, A. N., Higgins, A. J., Westhead, D. R., Brockwell, D. J., et al. (2019). The Role of SurA PPIase Domains in Preventing Aggregation of the Outer-Membrane Proteins Tompa and OmpT. *J. Mol. Biol.* 431 (6), 1267–1283. doi: 10.1016/j.jmb.2019.01.032

Lin, M. F., and Lan, C. Y. (2014). Antimicrobial Resistance in Acinetobacter Baumannii: From Bench to Bedside. *World J. Clin. Cases* 2 (12), 787–814. doi: 10.12998/wjcc.v2.i12.787

Liu, J., Wang, F., Mao, J., Zhang, Z., Liu, Z., Huang, G., et al. (2015). High-Sensitivity N-Glycoproteomic Analysis of Mouse Brain Tissue by Protein Extraction With a Mild Detergent of N-Dodecyl Beta-D-Maltoside. *Anal. Chem.* 87 (4), 2054–2057. doi: 10.1021/ac504700t

Lu, Y., Pang, J., Wang, G., Hu, X., and You, X. (2021). Quantitative Proteomics Approach to Investigate the Antibacterial Response of Helicobacter Pylori to Daphnetin, a Traditional Chinese Medicine Monomer. *RSC Adv.* 11 (4), 2185–2193. doi: 10.1039/D0RA06677J

Lu, S., and Zgurskaya, H. I. (2013). MacA, a Periplasmic Membrane Fusion Protein of the Macrolide Transporter MacAB-TolC, Binds Lipopolysaccharide Core Specifically and With High Affinity. *J. Bacteriol.* 195 (21), 4865–4872. doi: 10.1128/JB.00756-13

Marti, S., Sanchez-Cespedes, J., Oliveira, E., Bellido, D., Giralt, E., and Vila, J. (2006). Proteomic Analysis of a Fraction Enriched in Cell Envelope Proteins of Acinetobacter Baumannii. *Proteomics* 6 (Suppl 1), S82–S87. doi: 10.1002/pmic.200500323

Moore, S. M., Hess, S. M., and Jorgenson, J. W. (2016). Extraction, Enrichment, Solubilization, and Digestion Techniques for Membrane Proteomics. *J. Proteome Res.* 15 (4), 1243–1252. doi: 10.1021/acs.jproteome.5b01122

Nang, S. C., Azad, M. A. K., Velkov, T., Zhou, Q. T., and Li, J. (2021). Rescuing the Last-Line Polymyxins: Achievements and Challenges. *Pharmacol. Rev.* 73 (2), 679–728. doi: 10.1124/pharmrev.120.000020

Olaitan, A. O., Morand, S., and Rolain, J. M. (2014). Mechanisms of Polymyxin Resistance: Acquired and Intrinsic Resistance in Bacteria. *Front. Microbiol.* 5, 643. doi: 10.3389/fmicb.2014.00643

Papanastasiou, M., Orfanoudaki, G., Kountourakis, N., Koukaki, M., Sardis, M. F., Aivaliotis, M., et al. (2016). Rapid Label-Free Quantitative Analysis of the E. Coli BL21(DE3) Inner Membrane Proteome. *Proteomics* 16 (1), 85–97. doi: 10.1002/pmic.201500304

Park, J., Kim, M., Shin, B., Kang, M., Yang, J., Lee, T. K., et al. (2021). A Novel Decoy Strategy for Polymyxin Resistance in Acinetobacter Baumannii. *Elife* 10, e66988. doi: 10.7554/eLife.66988

Perez-Riverol, Y., Csordas, A., Bai, J., Bernal-Llinares, M., Hewapathirana, S., Kundu, D. J., et al. (2019). The PRIDE Database and Related Tools and Resources in 2019: Improving Support for Quantification Data. *Nucleic Acids Res.* 47 (D1), D442–D450. doi: 10.1093/nar/gky1106

Vazquez-Lopez, R., Solano-Galvez, S. G., Juarez Vignon-Whaley, J. J., Abello Vaamonde, J. A., Padro Alonzo, L. A., Rivera Resendiz, A., et al. (2020). Acinetobacter Baumannii Resistance: A Real Challenge for Clinicians. *Antibiotics (Basel)* 9 (4), 205. doi: 10.3390/antibiotics9040205

Zhang, X., Bierschenk, D., Top, J., Anastasiou, I., Bonten, M. J., Willems, R. J., et al. (2013). Functional Genomic Analysis of Bile Salt Resistance in Enterococcus Faecium. *BMC Genomics* 14, 299. doi: 10.1186/1471-2164-14-299

Zhang, L., Jia, X., Liu, X., Sheng, T., Cao, R., He, Q., et al. (2008). Dataset of the Plasma Membrane Proteome of Nasopharyngeal Carcinoma Cell Line HNE1 for Uncovering Protein Function. *Acta Biochim. Biophys. Sin. (Shanghai)* 40 (1), 55–70. doi: 10.1111/j.1745-7270.2008.00374.x

Zhang, M., Shi, H., Zhang, X., Zhang, X., and Huang, Y. (2020). Cryo-EM Structure of the Nonameric CsgG-CsgF Complex and Its Implications for Controlling Curli Biogenesis in Enterobacteriaceae. *PloS Biol.* 18 (6), e3000748. doi: 10.1371/journal.pbio.3000748

Conflict of Interest: The authors declare that the research was conducted in the absence of any commercial or financial relationships that could be construed as a potential conflict of interest.

Advantages of publishing in Frontiers

OPEN ACCESS
Articles are free to read for greatest visibility and readership

FAST PUBLICATION
Around 90 days from submission to decision

HIGH QUALITY PEER-REVIEW
Rigorous, collaborative, and constructive peer-review

TRANSPARENT PEER-REVIEW
Editors and reviewers acknowledged by name on published articles

Frontiers
Avenue du Tribunal-Fédéral 34
1005 Lausanne | Switzerland

Visit us: www.frontiersin.org
Contact us: frontiersin.org/about/contact

REPRODUCIBILITY OF RESEARCH
Support open data and methods to enhance research reproducibility

DIGITAL PUBLISHING
Articles designed for optimal readership across devices

FOLLOW US
@frontiersin

IMPACT METRICS
Advanced article metrics track visibility across digital media

EXTENSIVE PROMOTION
Marketing and promotion of impactful research

LOOP RESEARCH NETWORK
Our network increases your article's readership